MODERN PATHOLOGY

ABSTRACTS

HEMATOPATHOLOGY
(1316-1502)

USCAP 109TH ANNUAL MEETING
2020
EYES ON YOU

FEBRUARY 29-MARCH 5, 2020

LOS ANGELES CONVENTION CENTER
LOS ANGELES, CALIFORNIA

EDUCATION COMMITTEE

ABSTRACT REVIEW BOARD

1316 Next Generation Sequencing as Diagnostic Aid in Discriminating Non-Neoplastic Cytopenias from Myelodysplastic Syndrome

Sohaib Abu-Farsakh[1], Aaron Phelan[1], Mohammad Eldomery[2], Shanxiang Zhang[2], Magdalena Czader[3]
[1]Indiana University School of Medicine Department of Pathology and Laboratory Medicine, Indianapolis, IN, [2]Indiana University School of Medicine, Indianapolis, IN, [3]Indiana University, Indianapolis, IN

Disclosures: Sohaib Abu-Farsakh: None; Aaron Phelan: None; Mohammad Eldomery: None; Shanxiang Zhang: None; Magdalena Czader: None

Background: Patients with cytopenias and clinical suspicion of myelodysplastic syndrome frequently have additional comorbidities associated with bone marrow dysplasia. In these patients, diagnosis of MDS may be challenging, particularly when bone marrow shows no increase in blasts or defining abnormal karyotype. Somatic mutations can occur in healthy individuals, therefore, a contribution of NGS to a diagnosis of MDS remains to be determined. To better define diagnostic utility of NGS, we studied patients with documented non-neoplastic cytopenias (NNC) and compared findings to a low- and high-risk (LR- and H

Design: The study included 94 cytopenic patients with complete clinical and bone marrow evaluation. 58 patients had NNC, and 21 and 15 were diagnosed with LR- and HR-MDS, respectively. The median age of all patients was 69 years (range 25-91). NGS was performed on bone marrow samples using the FOUNDATIONONE®HEME panel including testing of entire coding regions of 406 genes and select introns of 31 genes.

Row Labels	ICOS	PD1	CXCL-13	BCl-6	CD10	Total # Cases
Angioimmunoblastic T-cell Lymphoma (Expression in Lymphoma Cells)						19
Strong positive	84% (16)	63% (12)	84% (16)	37% (7)	47% (9)	
Scattered/weak	5% (1)	10% (2)	16% (3)	26% (5)	32% (6)	
Negative	10% (2)	26% (5)	0% (0)	37% (7)	21% (4)	
Peripheral T-Cell Lymphoma (Expression in Lymphoma Cells)						8
Strong positive	37% (3)	0% (0)	50% (4)	0% (0)	0% (0)	
Scattered/weak	37% (3)	25% (2)	38% (3)	50% (4)	50% (4)	
Negative	25% (2)	75% (6)	13% (1)	50% (4)	50% (4)	
T-Cell/Histiocyte-Rich B-Cell Lymphoma (Average Expression % in Background T Lymphocytes), (average, (min-max))	9.5% (0%-50%)	43.7% (0%-95%)	14.4% (0%-60%)	-	-	10
Paracortical Hyperplasia (Expression In Paracortical Areas)						31
Positive	29% (9)	3% (1)	0% (0)	10% (3)	3% (1)	
Negative	70% (22)	96% (30)	100% (31)	90% (28)	97% (30)	
Progressive Transformation of Germinal Centers (Expression in Transformed Nodules)						5
Positive	100% (5)	100% (5)	100% (5)	100% (5)	100% (5)	
Negative	0% (0)	0% (0)	0% (0)	0% (0)	0% (0)	
Reactive Lymphoid Hyperplasia (Expression in Hyperplastic GCs)						10
Positive	100% (10)	100% (10)	100% (10)	100% (10)	100% (10)	
Negative	0% (0)	0% (0)	0% (0)	0% (0)	0% (0)	

Results: 47% NNC patients, 86% LR-MDS and 80% HR-MDS patients showed at least one pathogenic mutation. The average number of pathogenic mutations was 0.67, 1.38 and 1.93 for NNC, LR- and HR-MDS, respectively. The most frequently mutated genes were *TP53* (19 cases) and *SF3B1* (13 cases). *TP53* mutations were seen in 4 NNC cases (median VAF 3.68%), 2 LR-MDS (median VAF 5.92%), and 12 HR-MDS (median VAF 27.09%). The difference among *TP53* VAF in 3 patient groups was statistically significant ($p<0.05$). Additional NNC patient showed *TP53* mutation at VAF 47.62%, this mutation was questioned to represent variant of unknown significance. *SF3B1* mutations were seen in 2 NNC (median VAF 2.84%, range 1.45-4.22) and 11 LR-MDS (median VAF 39.33%, 9.21-49.69). *AXL1* VAF were lower in NNC patients than in MDS, however there were only 2 mutations in MDS group. VAF for other frequently mutated genes, *SRSF2*, *DNMT3A* and *TET2* showed a significant overlap between NNC and MDS patients. All but 11 mutations seen in NCC patients were reported in myeloid neoplasms.

Conclusions: Patients with NNC have lower number of mutations than seen in LR- and HR-MDS, however specific mutations are similar in both groups. Therefore, review of VAF may be more useful when considering a diagnosis of MDS. Diagnostic VAF threshold may differ for individual genes as shown for *TP53* and *SF3B1*. Select genes (*DNMT3A*, *TET2* and *SRSF2*) showed highly variable VAF in NNC group and therefore are less likely to be diagnostically useful.

1317 Patterns of Expression of PD-1, CXCL13, ICOS, CD10, and BCL-6 in Angioimmunoblastic T-cell Lymphoma (AITL), Peripheral T-Cell Lymphoma (PTCL), T-Cell/Histiocyte-Rich B-Cell Lymphoma (TCHRBCL), Paracortical Hyperplasia, Progressive Transformation of Germinal Centers (PTGC), and Reactive Follicular Hyperplasia

Ibrahim Abukhiran[1], Carol Holman[2], Sergei Syrbu[2]
[1]University of Iowa Hospitals and Clinics, Iowa City, IA, [2]University of Iowa, Iowa City, IA

Disclosures: Ibrahim Abukhiran: None; Carol Holman: None

Background: Angioimmunoblastic T-cell lymphoma and a recently recognized subset of Peripheral T-cell lymphoma are of a follicular helper T-cells (TFH) origin and they are diagnostically challenging due to histologic and immunophenotypic overlap with reactive lymphoid proliferations. Although PD-1 has been rendered a useful marker in the diagnosis of AITL, the differential expression of TFH-associated markers between benign and malignant lymphoid proliferations has not been well studied.

Design: We identified cases of angioimmunoblastic T-cell lymphoma (n=19), peripheral T-cell lymphoma (n=8), T-cell/histiocyte-rich B-cell lymphoma (n=10), paracortical hyperplasia (n=31), progressive transformation of germinal centers (n=5), and reactive follicular hyperplasia (n=10). Immunohistochemical staining for PD-1, CXCL13, ICOS, CD10, BCL-6, FOXP3 was done on whole tissue sections. Pattern and extent of staining was recorded and given one of the following categories: strong positive, scattered/weak staining, or negative. For TCHRBCL, the percentage of positive cells in the background T cells was estimated.

Results: Both CXCL13 and ICOS had a similar positivity rate (84%) in AITL, which was higher than the PD-1 (63%), CD10 (47%), and BCL-6 (37%). However, PD-1, CD10, and BCL-6 were more specific to AITL as the strong positivity rates in peripheral T-cell lymphoma were 0%. PD-1, CXCl13, and ICOS were all expressed in the background T-cells of TCHRBCL in the following descending order: 43.7%, 14.4%, 9.5%, respectively. In reactive lymph nodes with paracortical expansion, expression was seen most frequently with ICOS (29%) followed by BCL-6 (10%), PD-1 (3%), CD10 (3%), and was not seen with CXCL13. As expected, all markers were expressed in germinal centers of reactive follicular hyperplasia and in the transformed nodules in cases with progressive transformation of germinal centers.

Conclusions: Although ICOS and CXCL13 are more sensitive, PD-1, BCl-6, and CD10 are more specific in establishing the diagnosis AITL over PTCL. ICOS, PD-1, BCL-6, and CD10 can be expressed in the benign lymph nodes with paracortical expansion. ICOS, PD-1, and CXCL13 were all expressed with different extents (with PD-1 being the highest) in the background T cells of TCHRBCL. Hence, TFH-associated markers should be reviewed with caution before a definitive diagnosis (reactive versus neoplastic) is established, particularly when dealing with core needle biopsies.

1318 Pathway to CNS Metastasis for Diffuse Large B-cell Lymphoma: Why it Matters Where You Come From

Aadil Ahmed[1], Don Nguyen[2], Mina Xu[2]
[1]Yale University School of Medicine, New Haven, CT, [2]Yale University, New Haven, CT

Disclosures: Aadil Ahmed: None; Don Nguyen: *Grant or Research Support*, AstraZeneca; *Grant or Research Support*, Leidos; Mina Xu: None

Background: Diffuse Large B-cell Lymphomas (DLBCL) arising from extranodal organs account for approximately 30% of all cases and are clinically presumed to be at higher risk for CNS involvement. Recently published studies revealed that B lymphoblastic leukemia cells appear to spread to CNS via alpha-6 integrin (a6i) [PMID 30022166]. We aim to 1. demonstrate the relative risk of CNS involvement by primary site of disease, 2. show the percentage of tumors that demonstrate parenchymal brain involvement and 3. assess for potential role of adhesion molecules such as a6i in CNS metastasis.

Design: A retrospective review of DLBCL biopsies with paired CSF cytology was performed. All initial diagnostic biopsies with available CSF specimens were reviewed for the study by 2 hematopathologists. Four cohorts were used for the study: extranodal DLBCL with positive CSF, nodal DLBCL with positive CSF, extranodal DLBCL with negative CSF, nodal DLBCL with negative CSF. Biopsies were stained with anti-a6i and other potential targets by immunohistochemistry.

Results: A total of 1185 DLBCLs of which 182 cases had concomitant CSF were identified. Of these, 140 had negative CSF, 26 had positive CSF (13/26, 50% with histologic diagnosis of parenchymal disease) and 14 were "atypical." An over-representation of extranodal lymphomas (19 of 26, 73%) with a predominance of lymphomas that originate in the facial area (n=9), stomach (n=4), breast (n=2), testis

(n=2) and one each from heart and spleen was found. Anti-a6i was essentially negative in lymphoma cells in the control group (19 of 20, 95%) whereas 4 of 19 extranodal cases with CNS metastasis were positive (21%).

Conclusions: Our results show an overall 2% risk of CNS involvement with highest risk identified in extranodal and in particular facial-area DLBCLs. The results of a6i expression suggests the involvement of the integrin-laminin pathway in CNS infiltration by lymphoma cells, particularly those of extranodal origin. Along with the assessment of other proteins of interest and extending to a larger validation set, our preliminary findings point to a possible new biomarker. Our results can lead to therapeutic considerations of PI3Kδ inhibitor and/or a6i-neutralizing antibodies in this clinical context.

1319 Assessment of Ki67 Proliferation Index in Mantle Cell Lymphoma with Digital Image Analysis

Fahad Ahmed[1], Yuan Ji[2], Philippa Li[3], Kai Fu[2], Guohua Yu[4], Hongxia Cheng[5], Mina Xu[3], David Rimm[1], Zenggang Pan[1]
[1]Yale School of Medicine, New Haven, CT, [2]University of Nebraska Medical Center, Omaha, NE, [3]Yale University, New Haven, CT, [4]Yantai Yuhuangding Hospital, Yantai, Shandong, China, [5]Provincial Hospital Affiliated to Shandong University, Jinan, Shandong Province, China

Background: Mantle cell lymphoma (MCL) accounts for 5%-6% of non-Hodgkin lymphoma. It is associated with heterogeneous clinical outcome, ranging from indolent to aggressive with a median overall survival (OS) of 3-5 years. Ki67 immunostaining is commonly utilized to assess the proliferation index of MCL (cut-off ≥30%), which aids in predication of prognosis and selection of therapeutic regimens in clinical practice. However, the current "eyeballing" method has a high inter-observer variability and often results in over-estimation. Here, we evaluate an automated method to measure Ki67 expression using the QuPath Digital Imaging Analysis (DIA).

Design: A total of 69 MCLs were collected, and all cases were initially diagnosed with no prior treatment. The original slides were reviewed to confirm the diagnosis and to select cases with sufficient tissue. A tissue microarray (TMA) block was constructed with two 1.0 mm cores for each case. Immunohistochemical stain was performed using Ki67 antibody (Clone MIB-1, DAKO) on the TMA slide. The stained slide was then scanned using the Aperio scanner, which was analyzed using QuPath to count the positive cells. The cut-off point was determined with the X-Tile software (Camp et al, CCR 2004), the SPSS version 26 was used to construct survival curves, and the log-rank test was performed to calculate the *p*-value.

Results: The 69 cases included 52 males and 17 females, with a median age of 68 years (range 37-92). The overall median survival was 35 months (range 1-213). For each case, the proliferation index was assessed using the Ki67-positive cells over all the cells in the cores (Figures 1A and 1B), and an average percentage was calculated from the two cores (Figure 1C). The optimal cut-off point for the Ki67 proliferation index was 31.9% using X-Tile, which was very close to the 30% cut-off in the clinical practice. Therefore, we adopted the same cutoff of 30% for comparison of OS. In our study, the patients with lower Ki67 proliferation index of <30% was associated with a significantly better OS than those >30% (p-value <0.0001; Figure 1D).

Figure 1 - 1319
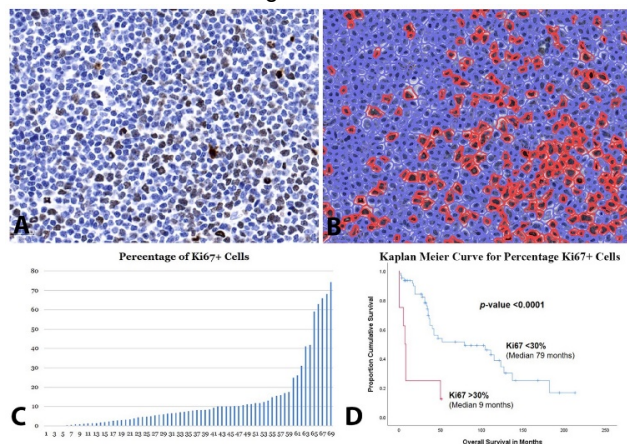
Figure 1. (**A**) Ki67. (**B**) Evaluation of Ki67+ cells using AuPath, red circle = positive cells, blue circle = negative cells. (**C**) Percentage of Ki67+ cells in all cases. (**D**) Overall survivals based on the 30% cut-off of Ki67+ cells.

Conclusions: QuPath DIA is a very promising tool to measure Ki67 proliferation index in MCL, and it accurately separated the patient groups with significantly different OS. Further studies will be performed with large cohorts to validate this assay.

1320 Wnt/β-catenin Signaling in Plasmablastic Lymphoma (PBL) Remains "In Check" through High Expression of Wnt/β-catenin Inhibitors

Ariz Akhter[1], Ghaleb Elyamany[2], Rasha ElGamal[3], Meer-Taher Shabani-Rad[4], Adnan Mansoor[1]
[1]University of Calgary, Calgary, AB, [2]Prince Sultan Military Medical City, Riyadh, Saudi Arabia, [3]Calgary, AB, [4]Division of Hematopathology, University of Calgary, Calgary, AB

Disclosures: Ariz Akhter: None; Ghaleb Elyamany: None; Rasha ElGamal: None; Adnan Mansoor: None

Background: High expression of Wnt/β-catenin signaling molecules exert an important role in the advancement of multiple myeloma (MM) and resistance to chemotherapy. Currently, targeted therapies against dysregulated Wnt/β-catenin signaling are being evaluated as adjuvant therapy in MM with beneficial results. The role of *Wnt/β-catenin* signaling network in the development and progression of aggressive B-cell- lymphoma is emerging. In diffuse large B-cell lymphoma (DLBCL), modulation of Wnt signaling has been reportedly linked with poor prognosis through high expression of FOXP1. Plasmablastic lymphoma is a rare but distinct aggressive B-cell lymphoma with overlapping features between DLBCL and MM. Wnt / β-catenin signaling in PBL has not been completely examined. We studied the expression pattern of Wnt/β-catenin signaling molecules in a series of PBL (EBV+ & EBV-) and compared it against well-defined activated DLBCL(ABC-DBCL) samples.

Design: Thirty-one PBL and 18 ABC-DLBCLs were assessed. RNA from formalin fixed paraffin embedded diagnostic tissue were subject to expression evaluation of key Wnt/β-catenin molecules utilizing nCounter platform (NanoString technologies). Principle component analysis (PCA) and hierarchical clustering were performed employing Qlucore Omics Explorer software. Differential expression of significance was defined as genes having minimum of 2.5-fold change with $p<0.01$ and false discovery rate (q value) of <0.05.

Results: We identified distinct differential expression of mRNA related to Wnt/β-catenin signaling between ABC-DLBCL and PBL (Figure1). Expression of Wnt/β-catenin signaling inhibitors (CXXC4; SFRP2; DKK1) were significantly higher among PBL compared to ABC-DLBCL (9.6 to 3.4-fold difference) (Table1). Molecules linked with Wnt/β-catenin signaling activation were elevated in PBL as compared to ABC-DLBCL.

Gene	p-value	q-value	Fold change
CXXC4*	0.0000	0.0000	9.6535
SFRP2*	0.0019	0.0087	8.4264
WNT5B#	0.0002	0.0011	6.4668
PLCB1#	0.0000	0.0000	5.7222
CCND2 @	0.0000	0.0000	4.3242
FZD3#	0.0000	0.0000	3.9089
DKK1*	0.0008	0.0046	3.4522
WNT10B#	0.0028	0.0119	3.4135
WNT5A *	0.0077	0.0284	3.3874
MYC@	0.0002	0.0011	2.9380
FOSL1@	0.0003	0.0020	2.9154
CCND3 @	0.0000	0.0003	0.4227
PRKCB	0.0005	0.0028	0.3635
NKD1*	0.0001	0.0009	0.3058
MMP7	0.0005	0.0029	0.1494
NFATC1	0.0000	0.0000	0.0973

- Wnt inhibitors # Wnt ligands @ Wnt targets

Figure 1 - 1320
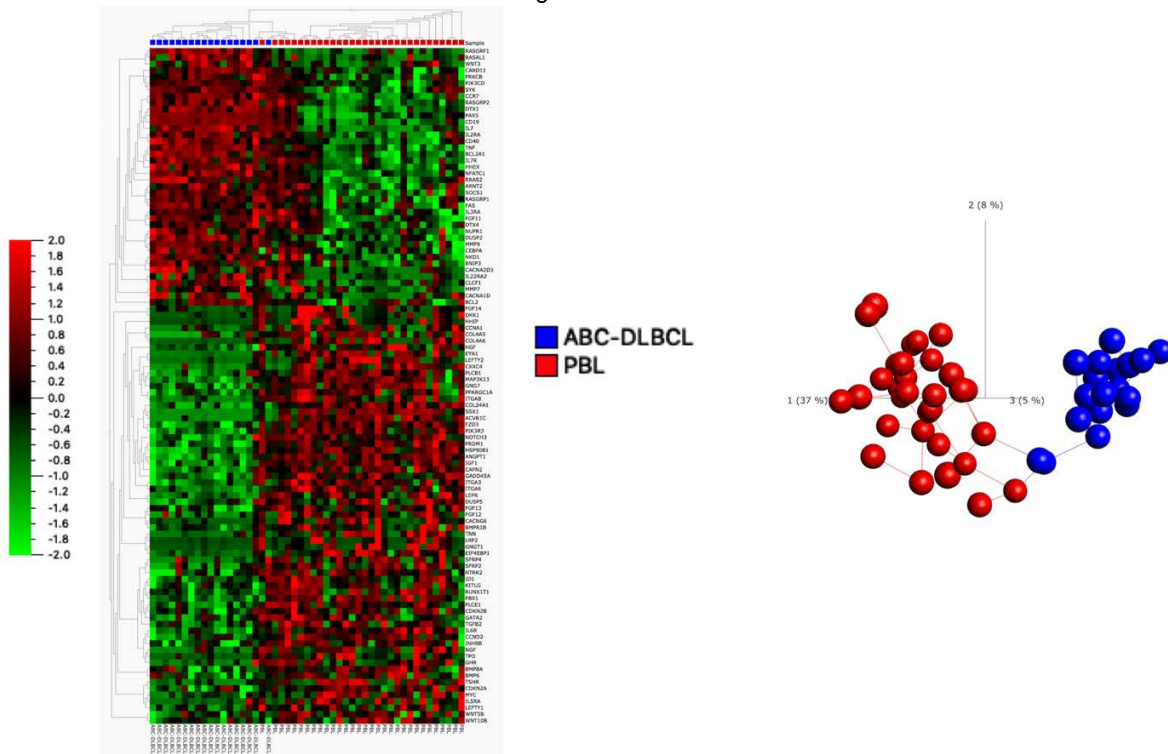
Conclusions: Our data suggest that in contrast to myeloma, the Wnt/β-catenin signaling in plasmablastic lymphoma is well balanced, may be due to high expression of Wnt inhibitors. Wnt/β-catenin signaling molecules were significantly quiescent in ABC-DLBCL samples examined.

1321 "Losing the Brakes" - Suppressed Inhibitors are Another Possible Mechanism of Uncontrolled Wnt Signaling in Old Age AML and a Potential for Targeted Therapy

Ariz Akhter[1], Ghaleb Elyamany[2], Meer-Taher Shabani-Rad[3], Adnan Mansoor[1]
[1]University of Calgary, Calgary, AB, [2]Prince Sultan Military Medical City, Riyadh, Saudi Arabia, [3]Division of Hematopathology, University of Calgary, Calgary, AB

Disclosures: Ariz Akhter: None; Ghaleb Elyamany: None; Adnan Mansoor: None

Background: *Wnt* signaling is critical for normal hematopoiesis, while dysregulated *Wnt* signal transduction is implicated in initiation and propagation of AML, where it exerts poor prognosis. In mouse models, epigenetic inactivation of *Wnt* inhibitors by CpG island methylation is considered central to *Wnt* hyperactivity in AML; thus, paving the pathway for *Wnt* inhibitor molecules as possible targeted therapy. In recent studies, dysregulated *Wnt* signaling have also been linked to the accelerated aging. Since, AML is a disease of senior years and old age (> 60 yrs.) denotes a poor prognostic factor; we hypothesized age related differential activity of *Wnt* signaling in AML patients. To this effect, we probed expression of *Wnt* signaling molecules in a series of pediatric AML (<18 yrs.) and compared it AML in old age (>60 yrs.).

Design: RNA from formalin fixed paraffin embedded bone marrow tissue at diagnosis (n=101) were subjected to expression evaluation of key Wnt/β-catenin molecules utilizing nCounter platform (NanoString technologies). Principle component analysis (PCA) and hierarchical clustering were performed employing Qlucore Omics Explorer software. Differential expression of significance was defined as genes having minimum of 2.5-fold change with p<0.01 and false discovery rate (q value) of <0.05.

Results: 34 pediatric AML (<18 yrs.) and 34 old-age AML (>60 yrs.) were identified in this cohort. In general, distinct mRNA expression pattern was noted between these two age groups (Fig 1). In *Wnt* signaling; we ascertained that inhibitors (CXXR, DKK1-4, SFRP1-4,SOST and WIFI) were suppressed in old age-AML compared to pediatric AML (Table1). *Wnt* target genes (MYC; MYB, RUNX1) showed upregulations in old age AML.

Genes	p-value	q-value	Fold change
AXIN2	1.38E-05	4.98E-05	3.1
CXXC4	1.74E-07	1.08E-06	3.5
DKK1	8.87E-07	4.96E-06	4.7
DKK2	0.008930	0.012775	2.5
DKK4	0.000645	0.001336	3.1
SFRP1	2.82E-06	1.27E-05	4.3
SFRP2	7.48E-10	1.04E-08	9.2
SFRP4	2.52E-05	8.32E-05	4.5
SKP1	0.005169	0.008091	0.3
SOST	6.67E-06	2.56E-05	4.5
WIF1	0.005997	0.008683	2.6
WNT5A	0.000274	0.000636	2.5

Figure 1 - 1321
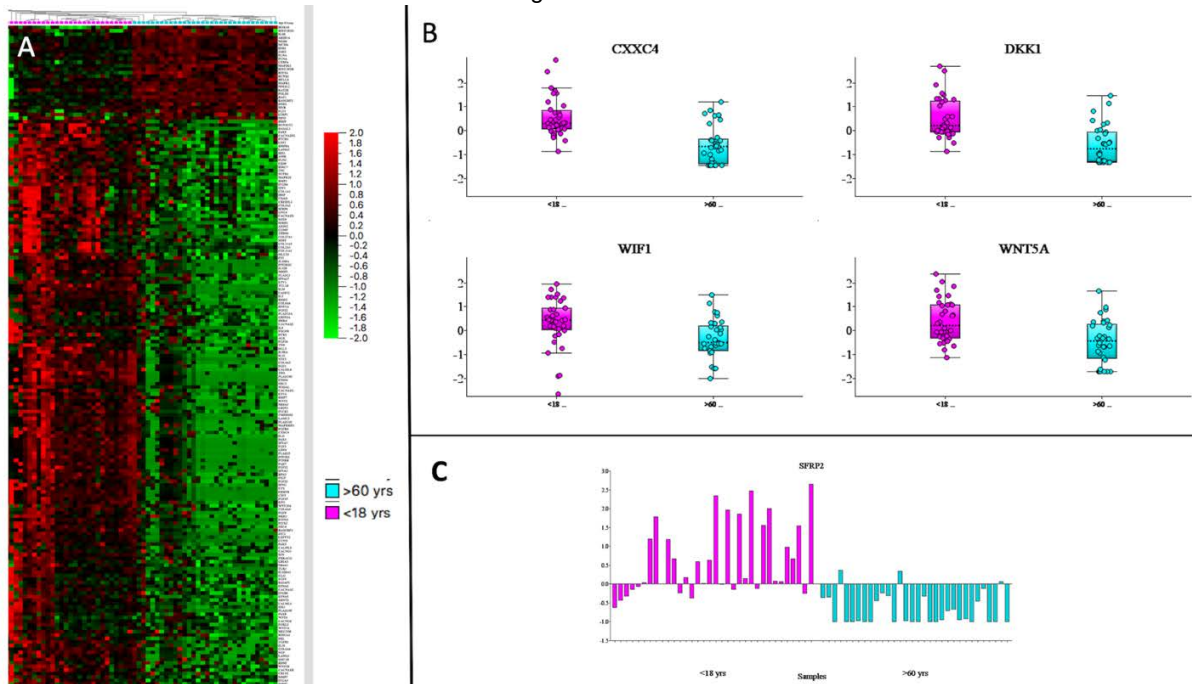
Conclusions: Our data denote through comparative analysis that suppression of inhibitors (either through mutation or hypermethylation) is a contributing factor in *Wnt* signaling hyperactivity in old age AML, hence *Wnt* inhibitors can be used as a potential targeted therapy.

1322 MRD Testing in Plasma Cell Myeloma: Is Next Generation Multi-Color Flow Cytometry Alone Sufficient?

Yahya Al-Ghamdi[1], Susan Mathew[2], Julia Geyer[2], Cara Rosenbaum[3], Adriana Rossi[3], Wayne Tam[2], Ruben Niesvizky[3], Amy Chadburn[4]

[1]New York-Presbyterian/Weill Cornell Medicine, New York, NY, [2]Weill Cornell Medicine, New York, NY, [3]Division of Hematology & Medical Oncology, New York-Presbyterian Hospital/Weill Cornell Medicine, New York, NY, [4]Weill Cornell Medical College, New York, NY

Disclosures: Yahya Al-Ghamdi: None; Susan Mathew: None; Julia Geyer: None; Cara Rosenbaum: None; Ruben Niesvizky: *Consultant*, Celgene; *Consultant*, Takeda; *Consultant*, Janssen; Amy Chadburn: None

Background: Minimal residual disease (MRD) negativity in plasma cell myeloma (PCM) is associated with better progression free and overall survival. While next generation multi-color flow cytometry (FC) is sensitive in detecting MRD, due to sampling, disease multifocality and poor plasma cell (PC) viability, it is not clear if one or several tests are required to determine MRD status in PCM patients.

Design: 59 bone marrow (BM) samples of 55 variably treated patients (35M, 20F; 46-80 years) were studied by FC, immunohistochemistry (IHC) and FISH for MRD. Only BMs with BCL1+ or CD56+ neoplastic PCs were included. MRD-FC used EuroFlow 8-color panels,

with collection of >1 million events (analytic sensitivity 0.01%). The PCM-FISH panel (CDKN2C, CKS1B, D5S23/D5S721, CEP 9, D13S319/13q14, D15Z4 - CEP15, TP53, CCND1-IGH) was done on CD138 enriched BM cells. IHC for CD56, BCL1, MUM1+CD56 and/or BCL1+CD138 was done on Bouins fixed decalcified BM core or formalin fixed clot sections. SPEP/SIFE results at MRD testing were collected (MRD-SPEP).

Results: 34 patients had disease, 17 were in remission and 4 had unclear disease status <1 -21 mo after MRD testing. 16/59 (27%) cases were MRD-FC+, 22/40 (55%) were MRD-IHC+, 19/51(37%) were MRD-FISH+ and 46% were MRD-SPEP+. At follow-up, 87% of MRD-FC, 77% MRD-IHC, 88% MRD-FISH and 88% MRD-SPEP positive cases compared to 57%, 46%, 51%, 46% of MRD-negative cases by FC, IHC, FISH, SPEP, respectively, had disease. MRD detection sensitivity ranged from 38% (FC) to 70% (IHC). MRD-FC had the highest specificity (94%) and PPV (93%), but all modalities were >75% for both. Combining FC with other techniques (all positive or all negative results) raised sensitivity (50-65%) and specificity remained high (>90%). The PPV, except for FC+IHC (50%), was >85% when combining 2 or 3 techniques (all positive or all negative results). When combining 2 techniques with any positive result, the sensitivity was highest for FC+FISH (95%) with the highest sensitivity and PPV for FC+SPEP (>80%). When any of the 4 tests was positive, the sensitivity was 85%, specificity was 72% and PPV was 85%. MRD positivity concordance was the highest between FC and FISH (63%; p<0.001) and the lowest between FC and IHC (29%; p=0.024).

Conclusions: MRD testing for PCM by multicolor FC alone, while specific, may not be as sensitive as other common techniques. Combining MRD-FC with another technique (IHC, FISH or SPEP) results in high specificity, sensitivity and PPV in identifying MRD in treated PCM patients.

1323 Intra-axial Versus Extra-axial Distribution of CNS Lymphoma and its Correlation with Phenotypic Markers

Feras Ally[1], Joo Song[2], Jasmine Zain[3], Ammar Chaudhry[4]
[1]City of Hope National Medical Center, Arcadia, CA, [2]City of Hope Medical Center, Duarte, CA, [3]COH, [4]City of Hope National Medical Center, Duarte, CA

Disclosures: Feras Ally: None; Joo Song: None

Background: Central nervous system (CNS) lymphoma is a rare aggressive disease which can be divided into primary CNS lymphoma (PCNS) versus secondary involvement of the CNS in systemic lymphoma. Pathology-radiology correlation is often needed to accurately stage these entities. We aim to assess whether tumor location can help differentiate between different types of lymphoma.

Design: In this single-institution IRB approved retrospective study, we reviewed 42 cases of CNS lymphoma (26 males, 16 females). Inclusion criteria required MRI (1.5Tesla or 3.0Tesla) of the brain and time-concordant histopathologic evaluation (i.e. MRI obtained within 72 hours of histologic evaluation) confirming diagnosis of CNS lymphoma. We identified a cohort of 16 patients with a diagnosis of primary CNS large B-cell lymphoma and 3 patients with T-cell lymphoma. All diagnoses were confirmed by evaluating biopsies through morphological and immunohistochemical analysis. All MRI studies included has T1-weighted pre- and post-contrast images, T2-weighted images and diffusion weighted images.

Results: Mean patient age of diagnosis was 57 (22-91) in B-cell lymphoma while mean age of diagnosis for T-cell lymphoma was 43 (20-59). All cases of CNS lymphoma (B- and T-cell) demonstrated enhancement on the post-contrast series. All T-cell lymphoma lesions were intra-axial and demonstrated homogeneous enhancement. Meanwhile, B-cell lymphomas demonstrated variable pattern of enhancement (homogenous enhancement, reticulonodular pattern, subcortical U-fiber enhancement, peripheral enhancement). 80% (4/5) patients tested for MYC alterations demonstrated peripheral enhancement. 70% (7/10) tested for BCL2 expression demonstrated homogenous enhancement; while BCL2 & MYC dual-expression was noted in the remaining 30% (3/10) with MRI showing peripheral enhancement. Both B- and T-cell lymphomas demonstrated variable degree of restricted diffusion (ADC range: 292-980). 84.2% (16/19) of the cases were intra-axial while 15.2 (3/19) were extra-axial (all of which were B-cell lymphoma).

Figure 1 - 1323
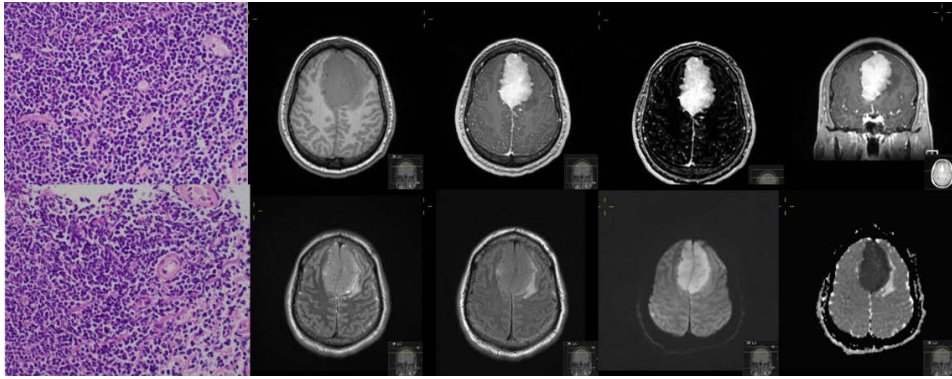
Figure 2 - 1323
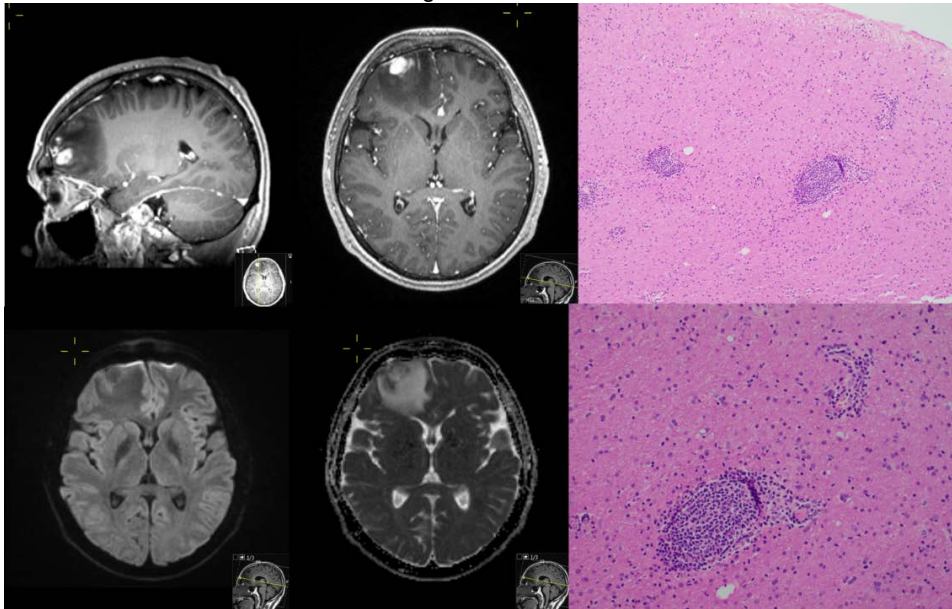
Conclusions: Our study shows all lymphomas enhance with variable degree of restricted diffusion and most are intra-axial in location. All extra-axial lymphomas were of the B-cell type. Patients with Myc-alterations showed peripheral enhancement, isolated BCL2 expressed tumors showed homogeneous enhancement, while dual-expression of BCL2-MYC showed peripheral enhancement.

1324 Minimal Residual Disease Detection in NPM1-Mutated AML: Correlation of NPM1 Immunohistochemical Staining with Flow Cytometry Detection

Erin Alston[1], Geraldine Pinkus[1], David Dorfman[1], Sanjay Patel[2], Olga Weinberg[3]
[1]Brigham and Women's Hospital, Boston, MA, [2]Weill Cornell Medical College, New York, NY, [3]Children's Hospital Boston, Boston, MA

Disclosures: Erin Alston: None; Geraldine Pinkus: None; David Dorfman: None; Sanjay Patel: None; Olga Weinberg: None

Background: The detection of minimal residual disease (MRD) in patients with nucleophosmin (*NPM1*)- mutated acute myelogenous leukemia (AML) is predictive of poor outcome. However, in these patients, MRD assessment for remission can be difficult given frequent lack of CD34 expression. We have previously shown that detection of mutant NPM1 protein by immunohistochemistry (IHC) correlates with molecular MRD. MRD can also be assessed by flow cytometry and relies on "difference from normal" antigen expression to detect abnormal clusters of cells of any cell line or maturity. In this study, we examined the concordance between NPM1 IHC and flow cytometry for MRD detection.

Design: We identified 20 *NPM1*-mutated AML cases with molecular (NGS [non-MRD]), cytogenetic, and flow cytometry data at diagnosis and post-induction (PI). Corresponding bone marrow tissue was stained using an NPM1 mutant protein-specific antibody. NPM1 IHC staining was analyzed and quantified (positive: negative cells, 200 total).

Results: In addition to *NPM1*, other common mutations at diagnosis included *DNMT3A* (12/20, 60%), *IDH1* (10/20, 50%) and *PTPN11* (6/20, 30%). Cytogenetic analysis at diagnosis showed that 17/20 (85%) cases had normal karyotype. NPM1 IHC was positive PI in 4/20 (20%) cases while flow cytometry MRD was positive in 3/20 (15%); each of these were also positive for NPM1 IHC. Concordance between PI NPM1 IHC and flow cytometry was high (19/20, 95%, CI 75.13%-99.87%), and in concordant cases, number of NPM1 positive cells detected on IHC correlated with blasts on flow cytometry results. Mutant *NPM1* DNA was detected PI in all seven cases with available NGS data; all seven were also positive by flow and NPM1 IHC. 2/4 IHC-positive cases had residual disease identified by morphologic evaluation (>5% blasts). In the 2/4 IHC-positive, morphologically-negative cases, flow MRD detected abnormal myeloblasts with phenotypes that differed from those seen at diagnosis (4.1% and 1.8%, respectively; CD34 negative to positive in both); the patient with 4.1% myeloblasts subsequently relapsed. The number of CD117-positive cells by IHC (retrospectively performed) also correlated with the number by NPM1 IHC. The number of positive cells correlated with flow cytometry results.

Conclusions: Our findings indicate that NPM1 IHC analysis for MRD detection is highly concordant with flow cytometry. In the setting of *NPM1* mutated AML, IHC represents a sensitive, fast, inexpensive, and accessible method for detecting MRD.

1325 A Clinicopathologic Study of RUNX1 Mutated MDS and MDS/MPN
Barina Aqil[1], Madina Sukhanova[2], Lawrence Jennings[3], Juehua Gao[4]
[1]Northwestern University Feinberg School of Medicine, Woodridge, IL, [2]Northwestern University Feinberg School of Medicine, Chicago, IL, [3]Northwestern University Feinberg School of Medicine, Hinsdale, IL, [4]Northwestern Memorial Hospital, Chicago, IL

Disclosures: Barina Aqil: None; Madina Sukhanova: None; Lawrence Jennings: None; Juehua Gao: None

Background: RUNX1 mutation has been identified in AML, MDS, and MDS/MPN. De novo AML with RUNX1 mutation is a provisional entity in the WHO classification associated with an adverse prognosis and frequent trisomies (+8, +13) and mutations in the spliceosome and chromatin modifiers. The clinicopathologic features of RUNX1 mutated MDS or MDS/MPN are less well characterized.

Design: We retrospectively identified 15 cases, which comprised of 11 MDS cases and 4 MDS/MPN cases. The cases were studied with regard to morphology, cytogenetic, molecular and clinical parameters.

Results: Our cohort consists of 6 female and 9 males, ranging from 32 to 84 years old (median 70). 3 cases of (27%) MDS patient present with pancytopenias including 2 cases with isolated thrombocytopenias. 2 of 4 cases of MDS/MPN present with leukocytosis and splenomegaly. The 11 cases of MDS include 7 MDS-excess blasts, and 4 MDS with multilineage dysplasia. The MDS/MPN cases consist of 3 cases of CMML and 1 case of atypical CML. The most common cytogenetic abnormalities are +8 (45%) and deletion 7q (20%). 3 cases (20%) have complex karyotype. All patients have at least one additional mutation besides the RUNX1 mutation. The highest mutation frequency besides RUNX1 mutations is observed for SRSF2, SF3B1 (spliceosome, 67%), ASXL1, EZH2, SETBP1 (chromatin modifiers, 60%), TET2, IDH1 (DNA methylation, 40%), FLT3, CBL1, NRAS, KIT (signaling transduction, 27%) and ETV6, GATA2, IKZF1 (transcription factors, 17%). RUNX1 variant allele frequency range from 4.8% to 51.7%. TP53 mutation is present in 4 cases. 2 cases (13%) demonstrated evolving acute leukemia. 3 cases of MDS transformed into acute myeloid leukemia. The majority of the patients had persistent disease (80%), some with relapses even after transplant (13%). 5 patients died of the disease. Two of the patient's with RUNX1 and TP53 mutations had a rapid clinical course and died from AML.

Conclusions: *RUNX1* mutated MDS and MDS/MPN often present with increased blasts and frequent transformation to AML, particularly those with TP53 mutations. These cases demonstrate high frequencies of +8 and mutations in the spliceosome and chromatin modifiers, suggesting tendency of developing to secondary AML genetically similar to de novo AML with mutated RUNX1.

1326 Further Evaluation of MEF2b Expression in Mantle Cell Lymphoma
Nicholas Barasch[1], Steven Swerdlow[2], Erika Moore[3]
[1]University of Pittsburgh Medical Center, Pittsburgh, PA, [2]University of Pittsburgh School of Medicine, Pittsburgh, PA, [3]University of Pittsburgh, Pittsburgh, PA

Disclosures: Nicholas Barasch: None; Steven Swerdlow: None; Erika Moore: None

Background: MEF2B is a transcriptional activator that directly modulates the expression of BCL6 in germinal center (GC) B-cells. Unexpectedly, as part of a prior study of MEF2B, we found most mantle cell lymphomas (MCL) were MEF2B+ with a single exception. We sought to further investigate the proportion of MEF2B negative MCL and, given the heterogeneity we now recognize in MCL, assess whether there are any clinicopathologic associations with these cases.

Design: 35 cyclin D1+ MCL were evaluated from multiple sites: bone marrow (10), lymph node (12), colon (5), oral/nasal cavity (3), stomach (2), parotid (2), and terminal ileum (1). Morphologic subtype was assessed and immunohistochemistry (IHC) performed for MEF2B, SOX11, CD5, cyclin D1, CD20 and/or PAX5, and Ki67. Select cases also had *TP53* mutation analysis, P53 IHC, flow cytometric studies, and/or cytogenetic studies.

Results: MEF2B was negative in 3/35 cases (9%) and positive in the remainder (Figure 1 and 2) (Table 1). 31/35 were classic MCL while 4 were blastoid. Of the 3 MEF2B negative MCL, 2 were in LN and 1 was in BM. Only 1/3 was also SOX11 negative, 1/3 CD5 negative, 1/3 blastoid and 2/2 had a *TP53* aberration. Comparison with the MEF2B+ cases is in Table 1. 1/2 non-blastoid MEF2B negative MCL had a high Ki-67.

Table 1: Characteristics of MEF2B+ vs MEF2B negative MCL		
	MEF2B Positive (n=32)	**MEF2B Negative (n=3)**
SOX11+/±	30/31 (97%)	2/3 (66%)
SOX11 Neg	1/31 (3%)	1/3 (33%)
Cyclin D1+	32/32 (100%)	3/3 (100%)
CD5+/±	28/31 (90%)	2/3 (66%)
Ki67 >30%	5/32 (16%)	2/3 (66%)
TP53 abnormality (high IHC, del, or mutations)	0/6 (0%)	2/2 (100%)
Blastoid Morphology	3/32 (9%)	1/3 (33%)

Figure 1 - 1326

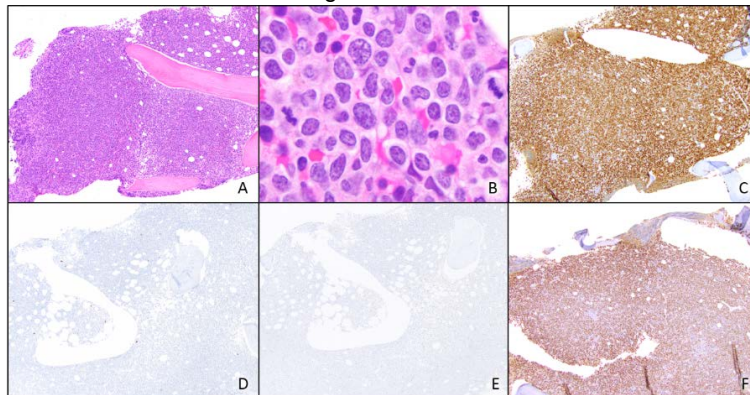Figure 1: MEF2B Negative Mantle Cell Lymphoma, Blastoid Variant. A. H&E 10x, B. H&E 100x, the lymphoma cells are positive for cyclin D1 (C) and negative for SOX11(D) and MEF2B (E). P53 (F) is strongly expressed.
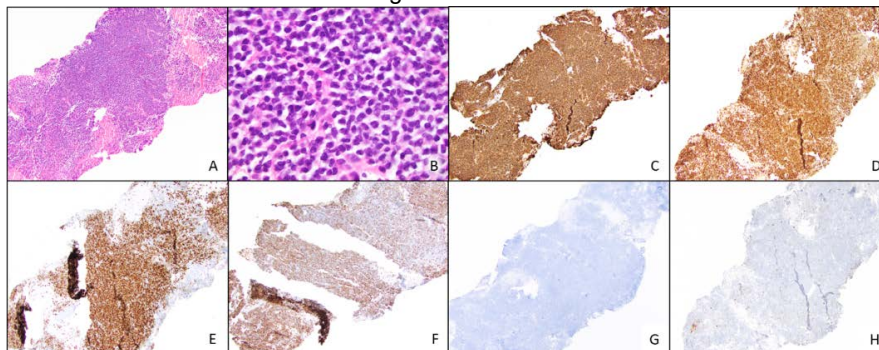
Figure 2 - 1326

Figure 2. MEF2B Positive Mantle Cell Lymphoma. A. H&E 10x, B. H&E 100x, the lymphoma cells are positive for CD20 (C), cyclin D1 (D), SOX11 (E), MEF2B (F) and negative for CD10 (G) and BCL6 (H).

Conclusions: These results further confirm that MEF2B negativity in MCL is rare. While the MEF2B negative cases may have some distinctive features, such as frequent *TP53* aberrations or a high Ki-67, ongoing evaluation of additional cases will be required to determine if any possible differences are statistically significant. Furthermore, while it remains to be established whether the MEF2B antibody is positive in MCL because of MEF2B expression versus a cross reactivity, characterization of the cases that lack staining with this antibody remains an area of interest.

1327 NF1-Mutated MDS: A Single Institution's Retrospective Study

Liron Barnea Slonim[1], Juehua Gao[2], Lawrence Jennings[3], Madina Sukhanova[4]
[1]Chicago, IL, [2]Northwestern Memorial Hospital, Chicago, IL, [3]Northwestern University Feinberg School of Medicine, Hinsdale, IL, [4]Northwestern University Feinberg School of Medicine, Chicago, IL

Disclosures: Liron Barnea Slonim: None; Juehua Gao: None; Lawrence Jennings: None; Madina Sukhanova: None

Background: Neurofibromin, the product of the *NF1* gene, is a negative regulator of RAS signaling. Children with neurofibromatosis-1 have increased risk of juvenile myelomonocytic leukemia. *NF1* mutations have been found in adult patients with myelodysplastic syndromes (MDS) and acute myeloid leukemia (AML) and are associated with lower complete remission (CR) and overall survival in younger AML patients. To our knowledge, thorough characterization of clinicopathologic, prognostic and somatic mutational background of *NF1*-mutated myeloid neoplasms, specifically MDS, has not been done. The goal of this study is to characterize the genomic and clinicopathologic features of *NF1*-mutated MDS.

Design: We retrospectively reviewed next generation sequencing results for 702 patients with myeloid neoplasms and identified 6 MDS patients with *NF1* mutations. Clinicopathologic and genetic data were reviewed.

Results: Our cohort consists of 3 males and 3 female patients, median age at 70 years (range 66-76) diagnosed with MDS: 2 MDS cases with isolated del(5q), 1 MDS case with single lineage dysplasia, 2 MDS cases with multilineage dysplasia, and 1 MDS case with excess blasts 1. All MDS patients had megakaryocytic dysplasia. Only 1/6 had increased marrow blasts counts (>5%). None of the patients had complex karyotypes, 1/6 had a normal karyotype and others had cytogenetic abnormalities belonging to the good and intermediate groups of the Comprehensive Cytogenetic Scoring System (CCSS) for MDS.1 Variant allele frequencies of NF1 mutations in 4/6 cases were close to 50% (range 44-53%), raising the possibility of germline origin and possible predisposition to myeloid neoplasm. Somatic mutational landscape of *NF1*-mutated MDS cases revealed an average of 2 accompanying mutations (range 1-3) in either *KIT, DNMT3A, IDH1, SF3B1, PRPF8, TET2, SRSF2, ASXL1, SETBP1*. All MDS patients showed persistent disease despite standard treatment and 2/6 received a stem cell transplant for refractory disease. 2/6 progressed to AML and 3/6 died of disease within 4-15 years after diagnosis.

Figure 1 - 1327
Table 1. MDS Patients with Mutated NF1

Study case	Age at diagnosis, Gender	Diagnosis	CBC	NF1 variant/VAF(%)	Other genes/VAF(%)	Dysplastic lineages	Conventional cytogenetics	Response (Remission Y/N)	Stem Cell Transplant (Y/N and date)	Last follow up status
1	66, F	MDS with isolated del(5q)	N/A	c.5624C>A (p.S1875*)/50.6%	TP53: c.542G>C (p.R181P)/5.10%; CALR: c.170A>G (p.Y57C)/48.80%	Erythroid and Megakaryocytic	46,XX,del(5)(q22q35)[17/46,XX[3]	N	Y	Progressed to AML, deceased
2	68, M	MDS-MLD	Neutropenia, anemia and throbocytopenia	c.3436G>A (p.V1146I)/53.1%	KIT: c.148G>T (p.V50L)/52.10%	Erythroid and Megakaryocytic	47,XY,+8,del(20)(q11.2q13.3)[10]/46,XY[10]	N	Y	Alive, relapse of MDS
3	67, M	MDS with isolated del(5q)	Anemia and thrombocytopenia	c.7718G>A (p.R2594H)/44.2%	DNMT3A: c.2657A>G (p.Q886R)/41.20%	Megakaryocytic	46,XY,del(5)(q15q33),del(13)(q12q14)[12]/46,XY[8]	N	N	Alive, persistant MDS
4	74, M	MDS-SLD	Neutropenia and thrombocytopenia	c.5087T>C (p.L1696P)/52%	IDH1: c.394C>T (p.R132C)/47.6%; SF3B1: c.1874G>T (p.R625L)/18.3%; PRPF8: c.4792G>A (p.D1598N)/4.4%	Megakaryocytic	N/A	N	N	Deceased
5	72, F	MDS-MLD	Neutropenia and thrombocytopenia	p.K1444E/NA	TET2 /NA; SRSF2/NA	Erythroid and Megakaryocytic	46,XX[20]	N	N	Progressed to AML, deceased
6	76, F	MDS-EB1	Anemia and neutropenia	c.101delT (p.V34Afs*10)/5%	ASXL1: c.2077C>T (p.R693*)/3.3%; SRSF2: c.284C>A (p.P95H)/42.2%; SETBP1: c.2608G>A (p.G870S)/3.3%	Erythroid and Megakaryocytic	47,XX,+8[1]/46,XX[2]	N	N	Alive, persistant MDS

AML, acute myeloid leukemia; MDS, myelodysplastic syndrome; MDS-EB1, myelodysplastic syndrome with excess blasts; MDS-MLD, myelodysplastic syndrome with multilineage dysplasia; MDS-SLD, myelodysplastic syndrome with single lineage dysplasia; VAF, variant allele frequency

Conclusions: Although our cohort of MDS cases is small, all cases revealed uniform favorable characteristics; however, despite the good to intermediate risk cytogenetics and low mutational burden, the clinical course was rather aggressive. *NF1* may function as a driver mutation, given higher variant allele frequency. The discrepancy between favorable cytogenetics in *NF1*-mutated MDS and poor prognosis prompts further investigation of the role of *NF1* in MDS.

1328 GATA3 Expression and Ki67 Proliferation Index as Diagnostic Tools in Mycosis Fungoides and its Mimickers

Pukhraz Basra[1], David Gajzer[1], Lubomir Sokol[2], Ling Zhang[3], Xiaohui Zhang[4]
[1]H. Lee Moffitt Cancer Center & Research Institute, University of South Florida, Tampa, FL, [2]H. Lee Moffitt Cancer Center & Research Institute, [3]Tampa, FL, [4]Moffitt Cancer Center, Tampa, FL

Disclosures: Pukhraz Basra: None; David Gajzer: None; Ling Zhang: None; Xiaohui Zhang: None

Background: Mycosis fungoides (MF) is a neoplasm of CD4+ helper T (Th) lymphocytes with dysregulation of Th1 and Th2 immunity. Mycosis fungoides without or with large cell transformation (MF-LCT) has significant morphologic overlap with other lymphocytic dermatologic entities such as reactive dermatoses and CD30+ lymphoproliferative disorders (CD30+ LPDs). Histological differentiation between these entities sometimes presents a diagnostic challenge. GATA3 is a transcription factor involved in Th2 cell differentiation, and there have been conflicting studies regarding the value of GATA3 in making differential diagnosis of the cutaneous T cell lymphomas include MF and its mimickers.

Design: We investigated the expression of GATA3 and Ki67 proliferation index in MF and its reactive and neoplastic mimics. Immunohistochemical staining for GATA3 (#5852, Cell Signaling Technologies, Danvers, MA) and Ki67 was performed on MF (n = 16), MF with LCT (n = 14), CD30+ LPDs (n = 12) and reactive dermatoses (n = 10). The percentage and intensity of GATA3 staining in the lymphoid populations was assessed by 500 cell count morphometric analysis. Intensity of GATA3 staining was graded on a scale of 1-5 (1= weak, 2= weak – moderate, 3= moderate, 4= moderate – strong, 5= strong).

Results: Reactive dermatoses showed predominantly low and moderate GATA3 expression with a distinctively low Ki67 proliferation index. In contrast, neoplastic T cells in MF showed increased GATA3 expression and a relatively low proliferation index. MF with LCT showed significantly increased GATA3 expression with moderate to strong intensity and a relatively high proliferation index. CD30+ LPDs had weak to moderate GATA3 expression with a relatively high proliferation index. The differences between reactive dermatoses and MF or MF with LCT, between MF and CD30+ LPDs, and between MF with LCT and CD30+ LPDs were statistically significant ($p<0.05$).

Table 1. GATA3 Expression and Ki67 Proliferation Index in Mycosis Fungoides and its Mimickers

Disease Process	N of Cases	GATA3 Positive Rate (%)	GATA3 Intensity Mean (range)	Ki67 Mean (range)(%)	GATA3 p-value
MF	16	59±14	3 (1-5)	13 (1-50)	0.011, when compared with RD* 0.118, when compared with MF with LCT 0.012, when compared with CD30+ LPD*
MF with LCT	14	70±24	4 (1-5)	58 (10-90)	0.003, when compared with CD30+ LPD*
CD30+ LPDs	12	39±25	2 (1-3)	52 (10-90)	
Reactive Dermatoses	10	38±23	3 (2-5)	8 (1-25)	0.005, when compared with MF with LCT* 0.961, when compared with CD30+ LPD

MF: Mycosis fungoides; MF with LCT: Mycosis fungoides with large cell transformation; CD30+ LPDs: CD30 positive lymphoproliferative disorders; RD: Reactive dermatoses

*. $p<0.05$, GATA3 positive rates were compared using independent samples t test.

Conclusions: A high GATA3 expression with weaker intensity and low proliferation index supports the diagnosis of MF over reactive dermatoses. A higher GATA3 expression with stronger intensity supports MF with LCT over CD30+ LPDs. CD30+ LPDs and reactive dermatoses have relatively lower and weaker GATA3 expression. These features may assist in differentiating the cutaneous lymphoproliferative disorders when morphologically they appear similar.

1329 Interobserver Variation in Morphologic Classification of Aggressive B-Cell Lymphoma: Considerations for Diagnosis of High-Grade B-Cell Lymphoma Not Otherwise Specified

Christopher Batuello[1], David Head[2], Ridas Juskevicius[2], Emily Mason[2], Kelley Mast[2], Claudio Mosse[3], Adam Seegmiller[2], Aaron Shaver[2], Mary Ann Arildsen[2], Dale Plummer[2], William Dupont[4], Tarsheen Sethi[2], Nishitha Reddy[2], Alexandra Kovach[2]
[1]Vanderbilt University, Spring Hill, TN, [2]Vanderbilt University Medical Center, Nashville, TN, [3]Vanderbilt University, Nashville, TN, [4]Vanderbilt University School of Medicine, Nashville, TN

Disclosures: Christopher Batuello: None; David Head: None; Ridas Juskevicius: None; Emily Mason: None; Kelley Mast: None; Claudio Mosse: None; Adam Seegmiller: None; Aaron Shaver: None; Mary Ann Arildsen: None; Dale Plummer: None; William Dupont: None; Tarsheen Sethi: None; Nishitha Reddy: None; Alexandra Kovach: None

Background: "High-grade B-cell lymphoma, not otherwise specified (HBCL-NOS)," introduced in the 2017 WHO Classification, is intended to signify rare lymphomas without MYC and BCL2 and/or BCL6 rearrangements ("double" or "triple hit", HBCL-DH) and with non-standardized morphologic and immunophenotypic (IP) features between diffuse large B-cell lymphoma (DLBCL) and Burkitt lymphoma (BL), which may behave more aggressively than DLBCL. Assignment of DLBCL-, BL-, intermediate (DLBCL/BL)- or blastoid-like morphologic features, integrated with IP and cytogenetic (CG) data, strongly informs the final diagnosis, particularly in HBCL-NOS where the diagnosis may hinge on morphology. This study aims to quantify interobserver variation in morphologic classification of aggressive B-cell lymphomas to shed light on variation in diagnosis of HGBCL-NOS.

Design: Eight academic hematopathologists (observers) with variable experience (range: 3-46 years) independently reviewed 53 archival H&E-stained tissue sections (1 slide/case), using criteria from routine practice and blinded to original diagnoses [HBCL-NOS (6), HBCL-DH (9), DLBCL-NOS (23), BL (5), or lymphoblastic lymphoma (LBL, 10)], and assigned each to 1 of 4 morphologic categories: DLBCL, DLBCL/BL, BL, or blastoid. Weighted kappa coefficients (κ) for interobserver variability among multiple readers were calculated.

Results: Overall interobserver agreement was fair ($\kappa=0.29$); 4 cases (8%) showed complete agreement among the 8 observers (3 DLBCL, 1 BL), 13 (25%) among at least 7 (10 DLBCL, 1 BL, 1 DLBCL/BL, 1 blastoid), and 21 (40%) among at least 6 (13 DLBCL, 2 BL, 3 DLBCL/BL, 4 blastoid). Agreement between each pair of observers (Table 1) ranged from slight to substantial (κ: 0.18-0.64), and agreement between each observer's diagnoses and majority diagnoses from moderate to substantial (κ: 0.41-0.74).

Figure 1 - 1329

Figure 1.

Overall morphologic agreement between each pair of observers (κ)

Observer	1	2	3	4	5	6	7
2	0.26						
3	0.44	0.27					
4	0.23	0.36	0.21				
5	0.64	0.25	0.36	0.33			
6	0.31	0.39	0.33	0.18	0.41		
7	0.39	0.41	0.32	0.23	0.46	0.48	
8	0.46	0.26	0.35	0.31	0.55	0.36	0.43

Figure 2 - 1329

Figure 2.

Overall morphologic agreement between each observer's and majority diagnoses

Observer	1	2	3	4	5	6	7	8
K	0.63	0.48	0.41	0.46	0.74	0.52	0.63	0.58

Conclusions: Interobserver agreement among academic hematopathologists in assigning DLBCL-, BL-, DLBCL/BL- and blastoid-like morphologic features to aggressive B-cell lymphomas appears fair, which is comparable to κ-based morphology studies in other pathology subspecialties. Accuracy of WHO classification may be strengthened by multiple observations (i.e. additional opinions), particularly in the absence of diagnostic IP and CG data. Ongoing studies using our cohort include assessment of intraobserver agreement, interobserver agreement following consensus review of morphologic definitions, and interobserver agreement within each morphologic category.

1330 Flow Cytometric Evaluation of TRBC1 Expression in Tissue Specimens and Body Fluids is a Novel, Sensitive and Specific Method for Assessment of T-Cell Clonality and Diagnosis of T-Cell Neoplasms

Holly Berg[1], Min Shi[1], Pedro Horna[1], Dragan Jevremovic[1], Heidi Corley[1], Gregory Otteson[1], Horatiu Olteanu[1]
[1]Mayo Clinic, Rochester, MN

Disclosures: Holly Berg: None; Min Shi: None; Pedro Horna: None; Dragan Jevremovic: None; Heidi Corley: None; Gregory Otteson: None; Horatiu Olteanu: None

Background: Flow cytometric detection of T-cell clonality is challenging. The current available methodology for T-cell receptor (TCR) Vβ repertoire evaluation is a complex assay and has limited sensitivity especially for low-level disease. Therefore, there is an unmet need for a reliable, simple and rapid assay to identify T-cell clonality. The rearrangement of the *TCRB* gene involves the random and mutually exclusive utilization of one of two constant β chain genes (*TRBC1* and *TRBC2*), analogous to the kappa and lambda gene utilization by B cells. Here, we use a single TRBC1 antibody, in conjunction with other T-cell associated markers, to detect T-cell clonality in tissue biopsies and body fluids.

Design: 131 tissue/body fluid specimens from 42 patients with a definitive diagnosis of a T-cell neoplasm and 89 patients with no T-cell malignancy were analyzed. Medical record data including morphologic pathology reports; molecular, cytogenetic and other laboratory results; clinical notes and imaging studies were reviewed to identify these patients. Flow cytometry was performed with a tissue antibody panel, including a T-cell tube (CD2/CD3/CD4/CD5/CD7/CD8/CD45/TCRγδ/TRBC1). TRBC1 expression was assessed on normal and aberrant T-cell subsets. Restricted (monotypic) TRBC1 expression was defined when present on > 90% or <10% of a distinct T-cell cluster.

Results: Specimens comprised lymph nodes (n=89), tonsil (n=2), other tissue (n=18), spleen (n=9), peritoneal fluid (n=4), pleural fluid (n=7), and CSF (n=2), and were obtained from 56 M and 64 F (median age=47 years; range, 5-92). Patients had a diagnosis of benign/lymphoid hyperplasia (n=67), B-cell lymphoma (n=14), peripheral T-cell lymphoma (n=30), mycosis fungoides (n=6), hepatosplenic T-cell lymphoma (n=1), T-lymphoblastic lymphoma (n=4), T-PLL (n=1), and thymoma/thymic hyperplasia (n=8). We examined TRBC1 expression on neoplastic T-cell populations identified based on their immunophenotypic aberrancies, and monotypic TRBC1 expression was identified in all 42 known T-cell lymphoma cases. We applied a similar gating strategy to the 89 cases without T-cell neoplasms, and arbitrarily dissected T-cell populations into immunophenotypic distinct subsets; of these, we found that all cases revealed an expected polytypic TRBC1 expression in all subsets (Table 1).

Table 1. TRBC1 expression in neoplastic vs. non-neoplastic T cells. The percentage of TRBC1-positive and/or TRBC1-negative T cells within different subsets is shown.				
	CD4(+)		CD8(+)	
T-cell neoplasms	%TRBC1 (+)	%TRBC1(-)	%TRBC1 (+)	%TRBC1(-)
Mean	97.42	2.784	97.99	1.953
Median	99.16	1.795	98.78	1.290
5th Percentile	91.61	0.1400	93.52	0.0
95th Percentile	99.91	9.380	99.94	9.380
No T-cell malignancy				
Mean	43.46	56.54	37.58	62.42
Median	44.33	55.68	38.69	61.32
5th Percentile	36.11	50.11	25.65	53.93
95th Percentile	49.89	63.89	46.07	74.35

Conclusions: Single TRBC1 antibody detection of T-cell clonality by flow cytometry is a highly sensitive and specific, rapid and robust assay that could be routinely utilized in clinical practice.

1331 The Presence of Hodgkin/Reed Sternberg Cells in Follicular Lymphoma. Clinical and Biological Relevance

Isabel Betancor Fernandez[1], Anabel Antonio da Conceiçao[2], Álvaro Trascasa Caño[2], Sonia Garcia-Hernandez[3], Gabriel Olmedilla[4], Adel Aboumar[5], Pilar Blanco Puente[6], María Begoña Iglesias Rodríguez[7], Carlos Santonja[2], Miguel Angel Piris Pinilla[2], Socorro María Rodríguez Pinilla[8]
[1]Hospital Universitario de Canarias, San Cristóbal de La Laguna, Santa Cruz de Tenerife, Spain, [2]Fundación Jiménez Díaz, Madrid, Spain, [3]Hospital Universitario de Canarias, La Laguna, Santa Cruz Tenerife, Spain, [4]Hospital Universitario La Paz, Madrid, Spain, [5]Hospital General Universitario de Elda, Alicante, Spain, [6]Hospital Lucus Augusti, Lugo, Spain, [7]Hospital Álvaro Cunqueiro, Vigo, Vigo, Spain, [8]Hospital Fundación Jiménez Díaz, Madrid, Spain

Disclosures: Isabel Betancor Fernandez: None; Anabel Antonio da Conceiçao: None; Álvaro Trascasa Caño: None; Sonia Garcia-Hernandez: None; Gabriel Olmedilla: None; María Begoña Iglesias Rodríguez: None; Carlos Santonja: None; Miguel Angel Piris Pinilla: None; Socorro María Rodríguez Pinilla: None

Background: Hodgkin/Reed Sternberg cells (HRSc) can be rarely found in cases diagnosed of follicular lymphomas. Whether these cases represent composite Hodgkin/follicular lymphoma or just a marker of progression is still a matter of debate and remains to be elucidated.

Design: Follicular lymphoma reports signed out in a single institution over three years (2017-2019) were studied looking for the presence of CD30-positive HRS cells. Eleven samples from six patients were selected. Morphology, immunophenotype and BCL2, BCL6, C-MYC rearrangements were reviewed. Clinical data at diagnosis and follow-up were retrieved.

Results: HRS cells were found in the initial diagnostic sample (four cases) or in follow-up samples (2 cases), clinically interpreted as relapses. Three cases were diagnosed as composite neoplasms, diagnosed as such based on a biphasic microscopic appearance. Areas

with HRS cells surrounded by its usual microenvironment (lymphocytes, eosinophiles and histiocytes) were in these cases combined with others with follicular growth pattern and centrocytic-centroblastic cytology. One of these cases was EBV (EBER ISH) focally positive.

The remaining three cases were diagnosed as follicular lymphoma with HRS cells.

FL samples showed a classic immunophenotype (CD10, BCL6 positivity) and presence of t14;18 in 5/6 cases. HRS cells showed in all cases CD30 and CD15 positivity with a weak PAX5 staining. HRS cells also showed t14;18 in the 3 investigated cases, shared on both follicular and classical Hodgkin looking areas. Four of the samples showed strong P53 expression on HRS cells.

Conclusions: Composite follicular lymphoma/classical Hodgkin lymphomas cases might represent different phenotypic counterparts of a single evolving neoplasm. P53 expression and shared Bcl2 translocations, found in both compartments support a common origin for both neoplasms. Ongoing NGS analyses are expected to clarify whether the cells from follicular and classical Hodgkin looking areas share additional molecular alterations.

1332 CD19 Expression and its Immunophenotypic and Molecular Cytogenetic Associations in Acute Myeloid Leukemia

Shweta Bhavsar[1], Sarika Jain[2], Svetlana Yatsenko[3], Steven Swerdlow[4], Nidhi Aggarwal[5]
[1]University of Pittsburgh Medical Center, Pittsburgh, PA, [2]University of Mississippi Medical Center, Madison, MS, [3]University of Pittsburgh, Pittsburgh, PA, [4]University of Pittsburgh School of Medicine, Pittsburgh, PA, [5]University of Pittsburgh, School of Medicine, Pittsburgh, PA

Disclosures: Shweta Bhavsar: None; Sarika Jain: None; Svetlana Yatsenko: None; Steven Swerdlow: None; Nidhi Aggarwal: None

Background: Aberrant CD19 expression is commonly seen in acute myeloid leukemia (AML) with t(8;21)(q22;q22.1); however, AMLs lacking this gene rearrangement occasionally express CD19. We studied the incidence of CD19 expression in all AMLs and their clinical, immunophenotypic and molecular/cytogenetic associations, to address its expression in the non-t(8;21) setting for accurate classification and because of recent interest in the use of CD19 as a potential therapeutic target.

Design: Blasts in 661 consecutive AMLs (1/2014 - 6/2019) were evaluated for CD19 expression by flow cytometry (FC). Clinical features, FC, classical cytogenetics (CCG), FISH, custom 4X180K CGH+SNP microarray (Agilent Technologies) (on a subset of cases), next generation sequencing (NGS) studies (myeloid panel of ≥37 genes, Illumina MiSeq) and Sanger for *CEBPA* were evaluated for all CD19+ AMLs and 103 CD19- AMLs (controls).

Results: 42/661 AML (6.4%) had CD19 expression on at least a subset of the blasts [ranging from 2 to 90% blasts, distinct subset (14/42) or variable expression (28/42)]. The CD19+ cases included AML with t(8;21)(n=15), AML with mutated *NPM1* (8) and AML with mutated *RUNX1* (6) (WHO 2016 classification). *RUNX1* aberrations (t(8;21)=16 (including 1 therapy related AML), *RUNX1* mutations=9 and variant *RUNX1* translocations=3) were the most common genetic abnormality in the CD19+ AML group (26/42), significantly more common than in the CD19- group (p=<0.0001). 2/3 cases with variant *RUNX1* translocations also had a *RUNX1* mutation. *FLT3* mutations were significantly more common in CD19+ AMLs (16/33) versus 16/103 in CD19- AML (p=0.0003) (Fig.1). All the CD19+ AMLs with *NPM1* mutation also had a *FLT3* mutation. All the *RUNX1* rearranged cases were CD19+ (n=19) as were 41% (9/22) of the *RUNX1* mutated AMLs. 50% (8/16) of the CD19+ AMLs showed aberrant expression of at least 1 other B-cell marker by FC (CD22 and/or CD79a). 19/41 CD19+ cases also showed TdT expression (including all *RUNX1* mutated cases). CD56 expression was seen in 10/15 AMLs with t(8;21), but was negative in all AMLs with *RUNX1* mutations (CD19+ and control groups). CD7 was expressed in 8/8 CD19+ *NPM1* mutated AMLs compared to only 1/15 AML with t(8;21).

Figure 1 - 1332
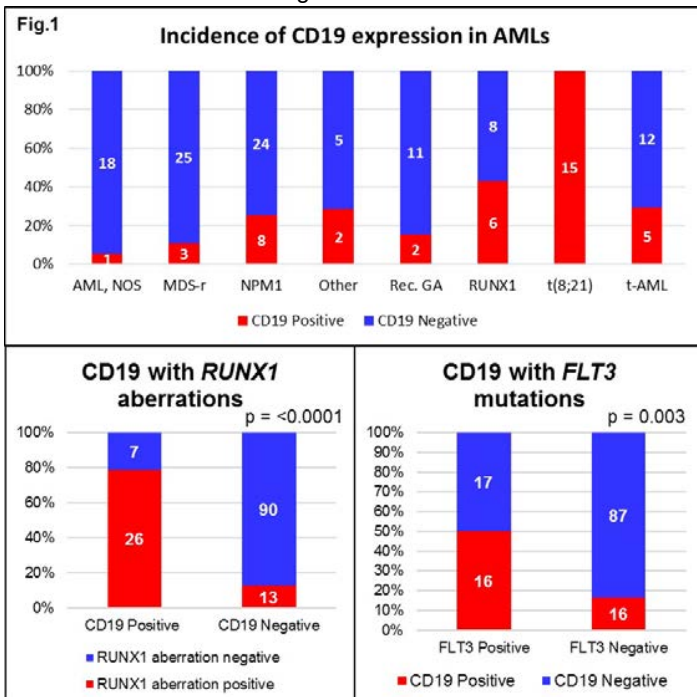
Figure 2 - 1332
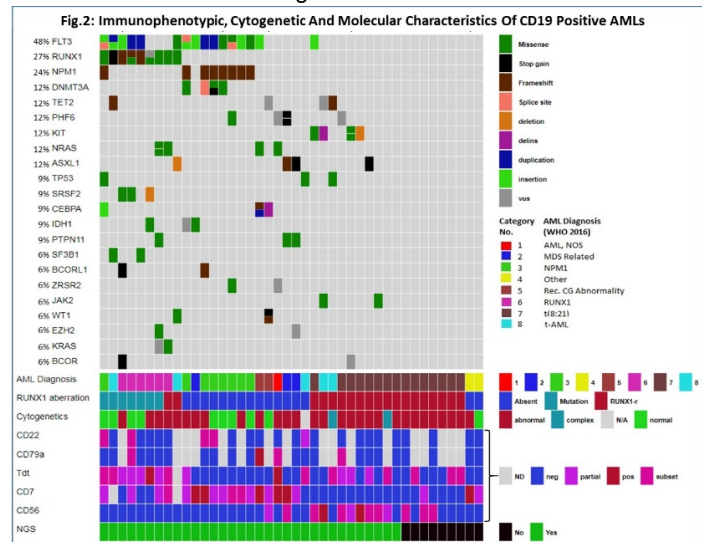
Conclusions: CD19 is expressed in at least a subset of blasts in ~6.4% of AMLs that are enriched in those with *RUNX1* aberrations and *FLT3* mutations. These cases also highlight that AMLs expressing CD19 can show expression of other B-cell antigens and must not be misdiagnosed as mixed phenotype acute leukemias.

1333 Potential Therapeutic Use of Elotuzumab in Primary Mediastinal B-cell Lymphoma

Juraj Bodo[1], Aaron Gruver[2], Xiaoxian Zhao[1], Timothy Holzer[2], Philip Ebert[2], Lisa Durkin[1], Andrew Schade[3], Eric Hsi[1]
[1]Cleveland Clinic, Cleveland, OH, [2]Eli Lilly & Co., Indianapolis, IN, [3]Eli Lilly & Co., Fishers, IN

Disclosures: Juraj Bodo: None; Aaron Gruver: None; Xiaoxian Zhao: None; Timothy Holzer: None; Philip Ebert: None; Lisa Durkin: None; Andrew Schade: None; Eric Hsi: *Consultant*, Seattle Genetics; *Consultant*, Jazz Pharmaceticals; *Grant or Research Support*, Eli Lilly; *Grant or Research Support*, Abbvie; *Grant or Research Support*, Cellerant

Background: Primary mediastinal B-cell lymphoma (PMBCL) is non-Hodgkin lymphoma bearing the closest pathological resemblance to nodular sclerosis Hodgkin's lymphoma (NSHL) and mediastinal gray zone lymphoma (GZL). It has been associated with good outcome, although treatment with chemotherapy combined with the use of mediastinal radiation brings a high risk of secondary tumors and other complications. This warrants the search for more specific and less toxic therapies. Elotuzumab is a monoclonal antibody recognizing SLAMF7 molecule (CD319, CS1) and is approved for the treatment of multiple myeloma. Our study evaluates the expression of SLAMF7 in PMBCL and explores therapeutic potential of elotuzumab in this disease.

Design: Targeted RNA sequencing was used to discover SLAMF7 expression in PMBCL samples. Immunohistochemistry (IHC) served to further investigate and confirm SLAMF7 expression in 21 PMBCL samples. The SLAMF7 immunostaining was compared to the staining of NSHL and GZL samples. Elotuzumab-mediated antitumor cell activity was tested *in vitro* using flow cytometric antibody-dependent cellular cytotoxicity (ADCC) assays with isolated normal PBMCs as effectors and Karpas 1106P as target in 1:100 ratio.

Results: SLAM family receptors are involved in the immunomodulation of both innate and adaptive immune response. RNA sequencing revealed high expression of SLAMF7 in 8/9 of PMBCL samples. Interestingly, the expression strongly correlated with the expression of immunosuppressive receptor IL-10RA (R = 0.82, *p* = 0.007). Flow cytometric analysis of Karpas 1106P detected SLAMF7 expression on the surface of these cells. The presence and localization of SLAMF7 molecule was further confirmed in 76% (16/21) of PMBCL cases by IHC. Anti-SLAMF7 antibody (clone 3B3) immunostaining showed membrane staining of lymphoma cells. This was in contrast with NSHL and GZL cases, where SLAMF7 was expressed in 2/19 and 1/5 cases, respectively. Elotuzumab exhibited a significant *in vitro* ADCC activity using Karpas1106P cells. Compared to the IgG1 control, elotuzumab treatment increased the ADCC of tumor cells from 20% to 37% (17.2 ± 0.7% increase).

Conclusions: In comparison to NSHL and GZL, SLAMF7 is expressed in the majority of PMBCL samples. Our study suggests that SLAMF7 is a potential therapeutic target in this disease and could be investigated for use with standard therapy or with new immunotherapy such as pembrolizumab.

1334 Plasma Cell Count Performed on CD138-Stained Tissue is Superior to Differential Count on Aspirate Smear: A Method Comparison Between Pathologist Estimate, Whole Slide Imaging, and Differential Count

Kelly Bowers[1], Mikhail Kovalenko[2], Megan Lee[3], Dmitriy Shin[4], Katsiaryna Laziuk[4], Richard Hammer[2]
[1]University of Missouri, Columbia, Columbia, MO, [2]University of Missouri, Columbia, MO, [3]University of Missouri School of Medicine, Columbia, MO, [4]Columbia, MO

Disclosures: Kelly Bowers: None; Mikhail Kovalenko: None; Megan Lee: None; Dmitriy Shin: None; Katsiaryna Laziuk: None; Richard Hammer: *Advisory Board Member*, Roche

Background: Plasma cell counts are an important measure for the clinical care of plasma cell neoplasms. Traditionally, these are obtained via a manual count of 500-cells on a bone marrow aspirate; however, this method is prone to sampling error and inter/intra-observer variability. CD138 is an adhesion molecule found on plasma cells and can facilitate estimation of plasma cells. In this study, we compare whole slide imaging (WSI) analysis and hematopathologist estimation of CD138-stained tissue as alternative methods for obtaining plasma cell percentages.

Design: Retrospective chart review (2015-2016) for bone marrow specimens with a CD138-immunostain revealed (n = 155) 114 trephine biopsies and 41 clots. Aspirate counts performed by lab technologists were obtained from the bone marrow pathology reports. CD138-stained slides were scanned by Leica Aperio ScanScope and analyzed with the Aperio positive pixel-count, a free FDA cleared image analysis algorithm. CD138-positivity was estimated microscopically by two expert hematopathologists. These were recorded independently then averaged for statistical analysis against the other methods.

Results: CD138-stained pathologist estimate compared to the aspirate count had the highest correlation (r = 0.801) with high correlation (r = 0.942) between the two hematopathologists. The lowest correlation (r = 0.599) was seen in WSI analysis compared to aspirate count. Review of WSI color maps showed variable positivity, with a "halo effect" surrounding cells, causing overestimation (24.4% WSI vs 8.3% aspirate count, p = < 0.001). WSI analysis was repeated on a manually-selected, artifact-free, area of the tissue, which improved the correlation of WSI compared to aspirate count (r = 0.837) and compared to pathologist estimate (r = 0.900).

Table 1: Comparison of Methods for Plasma Cell Count

	Mean ± SD	Difference of Means ± SD	(t) value Statistic	(p) value†		Pearson coeff. (r value)	(p) value‡
Versus Gold Standard Method							
Aspirate count	8.285 ± 17.5	-10.768 ± 17.0	-7.847	<0.001		0.801	<0.001
CD138 pathologist estimate	19.054 ± 27.5						
Aspirate count	8.285 ± 17.5	-16.119 ± 15.3	-13.068	<0.001		0.599	<0.001
CD138 WSI entire slide	24.404 ± 16.6						
Aspirate count	8.285 ± 17.5	-21.347 ± 16.0	-16.536	< 0.001		0.726	<0.001
CD138 WSI selected slide	29.632 ± 23.3						
Comparison Between Methods							
CD138 pathologist estimate	19.054 ± 27.5	4.980 ± 19.4	3.195	0.002		0.728	<0.001
CD138 WSI entire slide	24.404 ± 16.6						
CD138 pathologist estimate	19.054 ± 27.5	10.481 ± 12.2	10.667	<0.001		0.900	<0.001
CD138 WSI selected slide							

	29.632 ± 23.3					
Comparison Within Methods						
CD138 estimate pathologist #1	21.842 ± 31.3	4.809 ± 11.4	5.263	< 0.001	0.942	<0.001
CD138 estimate pathologist #2	17.030 ± 25.1					
CD138 WSI entire slide	24.404 ± 16.6	-5.501 ± 13.2	-5.177	<0.001	0.837	<0.001
CD138 WSI selected slide	29.632 ± 23.3					

Mean ± SD: average plasma cell counts of each method ± standard deviation of the average; **Mean difference ± SD**: average difference between the methods ± standard deviation of the average.

† t-value and p-value obtained with paired T-test

‡ r-value (pearson's coefficient) and p-value obtained by two-tailed Pearson's Correlation

Conclusions: CD138-stained tissue is an accurate and objective method for quantifying plasma cells and is superior to aspirate count. CD138-stained hematopathologist estimation of plasma cells is fast, accurate, and reproducible. In contrast, WSI analysis was slower and more variable, likely due to variation in staining or tissue quality causing impaired pixel interpretation. Once refined, WSI algorithms can be integrated into workflow to improve efficiency and accuracy of pathology results. This study confirms hematopathologist estimation of CD138-stained bone marrow tissue as an efficient and accurate method for plasma cell quantification, which improves patient care through appropriate diagnosis and treatment monitoring.

1335 Geospatial Analysis of Socioeconomic Disparity and Patterns of Leukemia Incidence and Distribution in the United States

Kelly Bowers[1], Summer Jensen[2], Timothy Haithcoat[1], Eileen Avery[2], Chi-Ren Shyu[1], Richard Hammer[2]
[1]University of Missouri, Columbia, Columbia, MO, [2]University of Missouri, Columbia, MO

Disclosures: Kelly Bowers: None; Summer Jensen: None; Timothy Haithcoat: None; Eileen Avery: None; Chi-Ren Shyu: None; Richard Hammer: *Advisory Board Member*, Roche

Background: Leukemias are a heterogeneous group of diseases with increasing incidence and limited literature exists on etiology, epidemiology and risk factors of the diverse subtypes. Race, poverty, accessibility, and other aspects of socioeconomic status (SES) have a well-documented role in health; however, recent studies show income inequality and health disparities continue to worsen in the United States. In this study, we utilize geospatial tools to investigate leukemia subtype variation within and between areas of socioeconomic disparity.

Design: Using U.S. Surveillance, Epidemiology and End Results (SEER-21) data from 2000-2016, age-adjusted incidence rates (AAIR) across 727 counties in 14 states for 77 different types of leukemia were analyzed against five county-level SES measures: Gini coefficient, income inequality ratio (80th to 20th percentile), residential segregation, CDC social vulnerability index, and rural-urban continuum. We used ArcGIS® software to identify statistically significant spatial clusters of high and low SES disparity. We examined these areas for patterns of leukemia incidence and distribution as well as standard demographic and descriptive variables.

Results: Analysis found multiple statistically significant areas of SE disparity, all of which had significant differences in leukemia incidence rate. Gini coefficient and income inequality ratio had the highest number, 37 and 38 types of leukemia respectively, and were the most disparate of the SES measures; followed by the social vulnerability index and residential segregation measures with 31 significant associations. Lastly, 24 types varied with rurality, particularly within myeloid and monocytic subtypes. Other SES trends were noted in hypodiploid B-Acute Lymphoblastic Leukemia, Hairy Cell Leukemia, Myeloproliferative Neoplasms, and multiple T-cell leukemias.

Conclusions: To our knowledge, this is the first comprehensive analysis comparing SES disparity and AAIR across all leukemia types. Our findings supported recent literature on the growing disparities of income and health equity in the United States. This study leveraged geospatial tools to model multifactorial big data, which is a powerful tool for elucidating patterns disease. However, limitations and biases include registry-based data, extrapolating population level socioeconomic disparities, and our evolving classification of leukemias. Our findings are a starting point but more research is needed to investigate how SES specifically relates to leukemia risk and outcomes.

1336 T-cell Prolymphocytic Leukemia Uniformly Expresses T-Cell Transcription Factor GATA3, Similar to T-Lymphoblastic Leukemia/Lymphoma, and in Contrast to Peripheral T-Cell Lymphomas

Ian Brain[1], David Dorfman[2], Winston Lee[3]
[1]Hamilton, ON, [2]Brigham and Women's Hospital, Boston, MA, [3]University of Michigan, Ann Arbor, MI

Disclosures: Ian Brain: None; David Dorfman: None; Winston Lee: None

Background: GATA3 plays a role in early T-cell development, and is uniformly expressed by cortical thymocytes. Previously we found that it is uniformly expressed by acute leukemias with T-cell differentiation. T-bet, the other T-cell transcription factor that controls Th1/Th2 T-cell fate, is not expressed in cortical thymocytes or acute leukemias with T-cell differentiation. C-MYC expression is associated with GATA3 expression in these acute leukemias, and may contribute to leukemogenesis. Recently, GATA3 and T-bet were found to be expressed in subsets of cases of several types of peripheral T-cell lymphoma, including anaplastic large cell lymphoma (ALCL) and peripheral T-cell lymphoma, NOS (PTCL-NOS). However, T-cell prolymphocytic leukemia (T-PLL), a rare T-cell leukemia thought to have a mature (post-thymic) immunophenotype and an aggressive clinical course, has not been examined for expression of GATA3 and T-bet.

Design: Twenty-eight cases of T-PLL were examined for nuclear expression of GATA3 and T-bet by immunohistochemical staining of formalin-fixed paraffin-embedded tissue, along with 28 cases of ALK-positive ALCL, 38 cases of ALK-negative ALCL, and 30 cases of PTCL-NOS.

Results: Cases of T-PLL were uniformly positive for GATA3 expression, including cases that were CD4+/CD8-, CD4-/CD8+, and CD4+/CD8+. A subset (7/28) were positive for T-bet. C-MYC expression correlated with GATA3 expression (68%; 19/28 cases). In contrast, a minority of cases of ALK+ ALCL (2/28), ALK- ALCL (20/38) and PTCL-NOS (13/30) were positive for GATA3, as previously reported, and a minority of these cases were positive for T-bet, with a smaller minority of cases exhibiting coexpression of GATA3 and T-bet.

Conclusions: T-PLL uniformly expresses GATA3 and is negative for T-bet expression, similar to acute leukemias with T-cell differentiation, and in contrast to PTCLs. C-MYC expression correlates with GATA3 expression in T-PLL, similar to acute leukemias with T-cell differentiation, and likely plays a role in disease pathogenesis, as suggested by previous studies showing gain of MYC in the majority of T-PLL cases. Our GATA3 findings also suggest that T-PLL corresponds to an intermediate state of T-cell development, as previously postulated based on relative expression levels of CD7 and CD3.

1337 CNS Lymphoproliferative Lesions – Evidence for Potential Therapeutic Agents in the Immunosuppressed

Miguel Cantu[1], Genevieve Crane[1], Samuel Yamshon[1], Sarah Rutherford[1], Amy Chadburn[2]
[1]New York-Presbyterian/Weill Cornell Medical Center, New York, NY, [2]Weill Cornell Medical College, New York, NY

Disclosures: Miguel Cantu: None; Genevieve Crane: None; Amy Chadburn: None

Background: Immunosuppressed patients, including those who are post-transplant or HIV+, are at high risk of CNS lymphoproliferative disease (LPD), which are usually Epstein Barr virus (EBV) positive. An in-depth evaluation of CNS lesions in the setting of immune suppression (PTLD or HIV) compared to primary CNS lymphomas (PCNSL) in immunocompetent patients has not been done. This may be of particular relevance in light of new immune-modulating and anti-viral agents.

Design: 42 CNS-LPDs were identified: 16 PTLDs (2005-2019; 13.3% of PTLDs in our institution), 8 HIV-LPDs (1997-2019; absolute CD4 count 1-70 cells/uL) and 18 immunocompetent PCNSLs (2014-2019). IHC was performed on FFPE tissues to assess cell of origin (COO; 41 cases; CD20, CD3, CD10, BCL6, MUM1, Hans criteria), plasma cell differentiation (39 cases; tumor suppressor BLIMP1/PRDM1) and immune regulation (39 cases: PDL-1). EBV status was determined by EBER ISH and IHC for LMP1 (latency II/III), EBNA2 (latency III) and BZLF1 (lytic) stages. All lesions were classified according to the 2017 WHO.

Results: All PTLD, HIV, and PCNSLs were of B cell origin. All PTLDs and HIV lesions were EBV+ and all PCNSL were EBV-. All PTLDs were polymorphic (Poly). BLIMP1 expression was >20% in all 6 PTLDs with lytic EBV infection (BZLF+ cells; all latency III), but was only weakly expressed or negative in BZLF negative PTLDs (5 latency II, 4 latency III) and in all HIV-LPDs. BLIMP1 expression did not correlate with PDL1 expression in the PTLDs or HIV cases. However, PTLDs with lytic EBV infection appeared to survive somewhat longer (6 mo vs. 2 mo) than the BZLF negative PTLDs or HIV cases. BZLF was positive in only 2 HIV-LPDs, including 1 polymorphic lesion patient who is still alive. PDL1 expression was more frequent in the HIV-LPDs and PTLDs, all EBV+ (75%), compared to the EBV negative PCNSLs (27%).

	Median Age (range)	Morphology	EBV Latency (LMP1/EBNA2)	Lytic (BZLF1)	GCB vs. non-GCB	BLIMP1 (cases)	PDL1 (cases)	Death (median time)
PTLD* **(N=16)**	58 years (8-74 years)	Poly =100%	latency II = 33% latency III = 67%	Focal Positive 40% (6/15)	non-GCB 100%	Focal Positive 80% (12/15)	Positive 93% (14/15)	81% (2.9 mo)
HIV-LPD* **(N=8)**	37.5 years (27-53 years)	Poly =25% DLBCL = 75%	latency III = 100%	Focal Positive 33% (2/6)	non-GCB 100%	Focal Positive 100% (6/6)	Positive 83% (5/6)	75% (1.5 mo)
PCNSL **(N=18)**	75.5 years (22-88 years)	DLBCL = 100%	NA	NA	GCB 17% non-GCB 83%	Focal Positive 61% (11/18)	Positive 89% (16/18)	44% (4 mo)

Table 1: Summary of Results

*1 PTLD and 2 HIV-LPDs had insufficient material for all studies.

Conclusions: CNS-LPDs are aggressive lesions. In immunosuppressed patients they are primarily EBV+, despite better therapies. Higher levels of PDL1 in HIV-LPDs and PTLDs were seen compared to PCNSL. Better survival was seen in patients with BLIMP1 expression and lytic EBV infection. As these lesions in the HIV+ and post-transplant settings are all LMP1+ (EBV latency II/III), which promotes PDL1 expression, anti-PDL1 therapy may be useful in these rapidly fatal lesions. Targeting latency III miRNAs that inhibit BLIMP1/PRDM1 may allow EBV+ cells to progress to the lytic stage, resulting in lesions that could potentially respond to antivirals like acyclovir.

1338   Double Fluorescence Probe In Situ Hybridization Approach to Detect MYC Rearrangements in Diffuse Large B-cell Lymphomas

Natalia Castrejón[1], Cindy Gabriela Fernández Diaz[2], Alfredo Rivas-Delgado[1], Marta Marginet[3], Antonio Pozo[3], Elías Campo[1], Olga Balagué[4]
[1]Hospital Clinic Barcelona, University of Barcelona, Barcelona, Spain, [2]Department of Pathology, Hospital Clinic, Barcelona, Spain, [3]Hospital Clinic, Barcelona, Spain, [4]Hospital Clinic of Barcelona, Barcelona, Spain

Disclosures: Natalia Castrejón: None; Cindy Gabriela Fernández Diaz: None; Antonio Pozo: None; Olga Balagué: None

Background: *MYC* rearrangement (*MYC*-R) confers poor prognosis to Diffuse large B-cell lymphomas (DLBCL), especially when is associated with *BCL2* and/or *BCL6*-R in Double (DH) or Triple hit lymphomas (TH). Fluorescence in situ hybridization (FISH) is the gold standard to detect *MYC, BCL2* and *BCL6*-R. Break apart probes (BAP) are the most widely used approach to identify these aberrations. However, due to variable breakpoints of *MYC* in DLBCL some cases may be overlooked. The correlation between MYC protein expression using immunohistochemistry (IHC) and *MYC*-R is variable in the reported studies. The aims of this study are to investigate the rate of unidentified *MYC*-R with a BAP, the role of IHC to identify those cases and the relevance of *MYC* partner in the outcome of the patients in a series of routinely diagnosed DLBCL and High-grade lymphomas (HGBL)

Design: 115 DLBCL and 23 HGBL routinely diagnosed between 2015 and 2019 were included. MYC, BCL2 expression, and Ki67proliferation index were also evaluated. Cases were classified for their cell of origin using IHC and gene expression profiling.

MYC, *BCL2* and *BCL6*-R were investigated using FISH BAP in all cases. Dual color-dual fusion probes (DCDFP) for IGH-*MYC*, *IG kappa (IGK)-MYC* and *IG lambda (IGL)-MYC* were performed in 40 cases

Results: 52/138 (38%) cases expressed MYC, BAP detected 29/52 (56%) MYC-R. 12 cases were DH, 4 with DLBCL morphology. DCDFP in rearranged cases showed 22/29 (76%) IG partners (19 with IGH, 2 with IGK and 1 with IGL). In MYC expressing cases lacking MYC-R with BAP, DCDFP identified 6/11 (55%) MYC-R, one was a DH.

In MYC negative cases, BAP detected 10/86 (12%) MYC-R, 4 were DH and DCDFP demonstrated IG as the most common partner (88%). When MYC was rearranged with IG, a tendency to high grade morphology and shorter overall survival (OS) was observed compared to MYC-R cases with non-IG partner (non-statistically significant probably due to the limited number of cases)

Conclusions: Not all *MYC*-R cases are captured by routinely used BAP FISH. The use of DCDFP identifies a number of *MYC*-R missed with BAP, and reclassified the cases as DH/TH. The presence of *BCL2* and or *BCL6*-R in a case without *MYC*-R by BAP should prompt further investigation with DCDFP. MYC expression is not a good surrogate for the presence of the rearrangement, since at least 12% of cases would be missed; however positive cases should be further investigated with DCDFP. This approach also allows the recognition of the *MYC* partner which may have prognostic impact

1339 Breast Implant Associated Anaplastic Large Cell Lymphoma Diagnosis: Role of Flow Cytometry Studies

Alexander Chan[1], Mikhail Roshal[1], Qi Gao[1], Oscar Lin[1]
[1]Memorial Sloan Kettering Cancer Center, New York, NY

Disclosures: Alexander Chan: None; Mikhail Roshal: None; Qi Gao: None; Oscar Lin: None

Background: Breast implant-associated anaplastic large cell lymphoma (BIA-ALCL) was accepted as a distinct entity in 2016. The most common presentation of BIA-ALCL is a large spontaneous periprosthetic fluid collection occurring on average 7 to 10 years following implantation with a textured surface breast implant. Fine needle aspiration and evaluation of the implant capsule are the optimal methods to evaluate for BIA-ALCL. Specimens should be sent for cell morphology evaluation by cytology, CD30 immunohistochemistry, and flow cytometry (FC) for evaluation, quantification, and characterization of T cells within the specimen. Although FC studies have been included the proposed diagnostic workup, most studies using FC have been small case reports and its role in the diagnosis of BIA-ALCL has not been well evaluated. We analyzed a large series of peri-implant fluid and tissue that was worked up by FC to rule out BIA-ALCL.

Design: The FC studies from peri-implant fluid collections and/or peri-implant capsular tissue biopsied or resected in a major cancer center for 4 years were analyzed. A minimum panel of antibodies including pan T cell markers CD2, CD3, CD4, CD5, CD7, CD8, CD30, CD45, CD56, and CD279 were evaluated by FC studies for expression and intensity. The findings were correlated with the results obtained from the concurrent cytology or histology diagnosis and the immunohistochemical studies performed. Sensitivity and specificity of the FC studies were calculated using cytology and histology diagnosis as the gold standard.

Results: A total of 70 FC specimens were reviewed. Forty-nine FC cases with no abnormal population suggestive of BIA-ALCL had concordant benign cytology/histology diagnosis. All 15 cases with an abnormal population suggestive of BIA-ALCL had confirmed BIA-ALCL on the cytology or histology sections. FC did not demonstrate the presence of an abnormal population in 6 BIA-ALCL cases, two of them had a low cellularity. The sensitivity of FC for BIA-ALCL was 72% with a specificity of 100%.

Conclusions: FC is a highly specific test in the detection of BIA-ALCL. The presence of an abnormal population on FC studies is diagnostic of BIA-ALCL; however, in the absence of an abnormal population detected by FC, immunohistochemical studies are indicated in the cytology and/or histology specimens to rule out BIA-ALCL.

1340 Gene Expression Profiling of Large B-Cell Lymphoma Presenting Initially in Bone Marrow, Liver and Spleen

Kung-Chao Chang[1], L. Jeffrey Medeiros[2]
[1]National Cheng Kung University and Hospital, Tainan, TW, Taiwan, [2]The University of Texas MD Anderson Cancer Center, Houston, TX

Disclosures: Kung-Chao Chang: None; L. Jeffrey Medeiros: None

Background: Diffuse large B-cell lymphoma (DLBCL) is the most common type of non-Hodgkin lymphoma worldwide, accounting for about 40% of all lymphoma cases. We previously identified a distinct type of DLBCL presenting initially in *b*one marrow, *l*iver and *s*pleen without lymphadenopathy, referred to as "BLS-type" DLBCL, which is aggressive clinically with early mortality and is frequently associated with hemophagocytic syndrome. The enigmatic tumorigenesis and molecular mechanisms of BLS-type DLBCL warrant clarification.

Design: Our specific aims are as follows: (1) to get characteristic genes by gene expression profiling in BLS-type LBCL; (2) to test the prognostic and clinical roles of stem cell markers in BLS-type and conventional type DLBCL; (3) to test the functions of stem cell markers *in vitro* by transfecting or knocking down stem cell (HOXA9 and NANOG) genes in DLBCL cell lines to see the effects on cell survival, cell proliferation and colony forming ability; (4) to test the *in vivo* tumor-forming ability of stem cell markers by tail vein injections of cell lines with differential expression of stem cell markers; and (5) to test if chemotaxis (CCR6) plays a role in cell migration *in vitro*.

Results: We found higher expression of the stem cell markers HOXA9 and NANOG, as well as BMP8B, CCR6 and S100A8 in BLS-type than in conventional DLBCL. We further validated expression of these markers in a large cohort of DLBCL cases including BLS-type DLBCL and found that expression of HOXA9 and NANOG correlated with inferior outcome and poor prognostic parameters. Functional studies with gene-overexpressing and -silenced DLBCL cell lines showed that expression of NANOG *and HOXA9* promoted cell viability and inhibited apoptosis through suppression of G2 arrest *In vitro* and enhanced tumor formation and hepatosplenic infiltration in a tail-vein-injected mouse model. Additionally, *HOXA9*-transfected tumor cells showed significantly increased soft-agar clonogenic ability. Interestingly, B cells with higher CCR6 expression revealed a higher chemotactic migration for CCL20.

Conclusions: Taken together, our findings support the concept that tumor or precursor cells of BLS-type DLBCL are attracted by chemotaxis and home to the bone marrow, where the microenvironment promotes the expression of stem cell signatures and clinical aggressiveness of DLBCL.

1341 Relative Frequency and Histopathologic Characteristics of MYC Rearranged Follicular Lymphoma

Shweta Chaudhary[1], Noah Brown[2], Joo Song[3], Jerry Wong[4], Lin Yang[5], Pamela Skrabek[6], Michel Nasr[7], Lindsay Kochan[1], Jie Li[8], Dennis Weisenburger[9], Anamarija Perry[2]
[1]Michigan Medicine, University of Michigan, Ann Arbor, MI, [2]University of Michigan, Ann Arbor, MI, [3]City of Hope Medical Center, Duarte, CA, [4]Roswell Park Comprehensive Cancer Center, Buffalo, NY, [5]Cancer Care Manitoba, Winnipeg, MB, [6]CancerCare Manitoba, Winnipeg, MB, [7]SUNY Upstate Medical University, Syracuse, NY, [8]University of Manitoba, Winnipeg, MB, [9]City of Hope National Medical Center, Duarte, CA

Disclosures: Shweta Chaudhary: None; Noah Brown: None; Joo Song: None; Jerry Wong: None; Lin Yang: None; Pamela Skrabek: None; Michel Nasr: None; Lindsay Kochan: None; Jie Li: None; Dennis Weisenburger: None; Anamarija Perry: None

Background: Follicular lymphoma (FL) accounts for 20-30% of all non-Hodgkin lymphomas in the Western world, with a highly variable prognosis and a 5-year overall survival rate ranging from 53-90%, depending on the risk factors. *MYC* rearrangement is a relatively rare genetic abnormality in FL with only a small number of cases reported in the literature. Therefore, we evaluated the relative frequency of *MYC* rearrangement in a large FL cohort from two institutions and studied the histopathologic characteristics of these cases.

Design: The study included 576 cases of FL from 2 institutions - University of Michigan (448 cases) and City of Hope National Medical Center (128 cases) from the period of 1991 to 2011. FISH studies for *MYC* rearrangement were performed on tissue microarrays. Cases positive for *MYC* rearrangement (break apart probe) were evaluated for *IGH/BCL2* rearrangement (dual color, dual fusion probe) by FISH. In cases that were negative for *IGH/BCL2* rearrangement, FISH for *BCL6* rearrangement (break apart probe) was performed. Furthermore, all cases were graded and immunohistochemical stains for CD10, BCL6, BCL2, and C-MYC protein expression were performed and scored.

Results: FISH studies for *MYC* rearrangement were successfully performed and scored on 429/576 cases and 10 cases (2.3%) were positive for rearrangement. The average number of *MYC* rearranged cells was 66.3% (range, 33-82%). In the 10 positive cases, the median age was 73.5 years (range, 39-87 years), with a male-to-female ratio of 4:1. Histologically, 6/10 cases were grade 1-2/3, and 4 cases were grade 3A. One grade 3A case had a minor component of diffuse large B-cell lymphoma. By immunohistochemistry, 9 cases were CD10+ (no tissue on 1 case), all cases were BCL6+, and 9/10 cases were BCL2+. C-MYC protein staining was low in all cases and 5% on average (range, 5-20%). *IGH/BCL2* rearrangement was detected in 6/9 cases evaluated, whereas *BCL6* rearrangement was detected in one of the three *IGH/BCL2*-negative cases.

Conclusions: *MYC* rearrangement is uncommon in FL, with a relative frequency of 2.3% in our study, and is mostly found in older patients. These cases exhibit a typical FL immunophenotype (CD10+, BCL6+, BCL2+) and *MYC* rearrangement does not appear to correlate with histologic grade. Despite the presence of *MYC* rearrangement, C-MYC protein expression was low in all the cases. Most cases, as expected in FL also have *IGH/BCL2* rearrangement. In summary, *MYC* rearranged FL cases do not appear to have specific histologic characteristics.

1342 PD-L1 is Highly Expressed in ALK-Positive Large B-Cell Lymphoma

Po-Han Chen[1], Ji Yuan[2], Qian-Yun Zhang[3], Huan-You Wang[4], Zenggang Pan[5]
[1]Yale School of Medicine, New Haven, CT, [2]University of Nebraska Medical Center, Omaha, NE, [3]Albuquerque, NM, [4]University of California San Diego, La Jolla, CA, [5]Yale University School of Medicine, New Haven, CT

Disclosures: Po-Han Chen: None; Ji Yuan: None; Huan-You Wang: None; Zenggang Pan: None

Background: ALK-positive large B-cell lymphoma (ALK-LBCL) is a rare, aggressive subtype of diffuse large B-cell lymphoma (DLBCL), with a median overall survival of ~22 months. Therefore, an effective alternative therapy is needed. Recently, immunotherapies targeting the immune checkpoint molecules (particularly PD-1 and PD-L1) have been promising in treating solid tumors, including non-small cell lung cancer. Particularly, tumoral expression of PD-L1 is a key biomarker to identify the patients who may have an enhanced response to PD1 and PD-L1 blockade. Recent studies have shown that PD-L1 expression is significantly higher in ALK+ anaplastic large-cell lymphoma (ALCL) than ALK-negative ALCL (Mod Pathol. 2019 Aug 5), which prompted us to investigate the expression of PD-L1 in ALK-LBCL for potential alternative therapies.

Design: Eleven cases of ALK-LBCL were collected from our institutions. The clinicopathologic characteristics were reviewed and the diagnoses were confirmed by necessary immunohistochemical stains. PD-L1 antibody (Ventana, SP263) was stained and the expression was evaluated based on the intensity (0, negative; 1+, weak; 2+, moderate; and 3+, strong) and the percentage of positive lymphoma cells.

Results: The 11 patients included 9 males and 2 females with a median age of 41.5 years (range 22-79). Nine of 11 cases occurred in the lymph nodes, and the remaining 2 were from submandibular soft tissue and nasopharynx, respectively. The lymphoma cells showed a diffuse infiltrative or sinusoidal in the lymph nodes, with plasmablastic and/or immunoblastic cytology (Fig. 1A). ALK was positive in all 11 cases with a characteristic cytoplasmic dotted pattern (Fig. 1B). The lymphoma cells also expressed CD45 (11/11), BOB.1 (7/7), OCT2 (7/7), CD138 (8/10), and EMA (7/11). However, the pan-B cell markers were mostly negative, including CD20 (0/10), CD79a (2/9), and PAX5 (2/8). Other negative stains included CD3 (0/11), CD30 (0/10), and EBER-ISH (0/7). For PD-L1 expression, 9 of 11 cases (82%)

were positive, including 2 cases with 3+ 100%, 1 case 2+ 100%, 3 cases 2+-3+ 75%, 2 cases 2+-3+ 50%, and 1 case 1+-2+ 30% (Figs 2A to 2C).
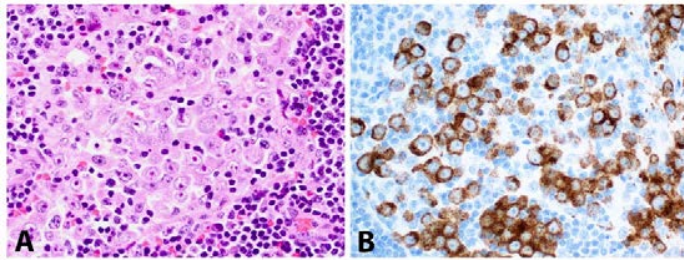
Figure 1 - 1342

Figure 1. A case of ALK-LBCL with a sinusoidal infiltration (A) and characteristic cytoplasmic dotted expression of ALK (B).
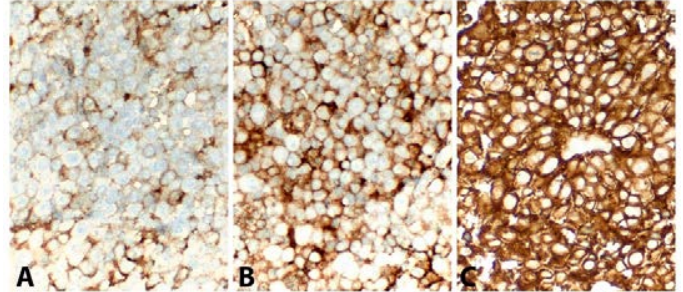
Figure 2 - 1342

Figure 2. PD-L1 expression. (A) 1+, weak; (B) 2+, moderate; and (C) 3+, strong.

Conclusions: ALK-LBCL is mostly positive for PD-L1, in contrast to the low expression in the conventional DLBCL (ranging from 0.8% to 36%), which indicates the potential application of anti-PD-L1 monoclonal antibody in treating this aggressive lymphoma.

1343   Quantitative Imaging of Drug-Selective Chromatin Topological Domains in Hematologic Malignancies: Towards Next Generation Digital Pathology and RNA Epigenomics
Jason Cheng[1], Shaun Wood[2], Li Cheng[2], Richard Larson[1], James Vardiman[1]
[1]The University of Chicago, Chicago, IL, [2]Department of Pathology, University of Chicago, Chicago, IL

Disclosures: Jason Cheng: None; Shaun Wood: None; Richard Larson: None

Background: Drug selectivity and resistance is a major obstacle to successful epigenetic therapy in patients with hematologic malignancies and other cancers. No reliable tools have been developed to predict and/or to overcome epigenetic drug resistance in clinical settings. We recently discovered that RNA and its modifying enzymes, RNA cytosine methyltransferases (RCMTs), can shape genomic DNA into unique chromatin functional domains/topologically associated domains (CFD/TAD) that regulate the response and resistance to the epigenetic drug azacitidine (5-azacytidine, 5-AZA) in leukemia cells (Cheng, J.X. et al. Nature Communications 9, 1163, 2018). This study is an extension of the discovery of 5-AZA-sensitive/resistant CFD/TAD and aims to quantitatively image drug- and lineage–specific CFD/TAD in normal and diseased bone marrows (BM) with novel molecular imaging techniques.

Design: Normal BM cells, various lineage leukemia cell lines, drug-sensitive and drug–resistant myeloid leukemia cell lines as well as clinical MDS/AML BM cells are used in this study. Novel quantitative imaging techniques, including 5-ethynyl uridine (EU) nascent RNA-clicking chemistry STED microscopy (EUNRC/STEDM) and proximity ligation and rolling circle amplification (PL-RCA) are used.

Results: By using novel quantitative imaging techniques, including EUNRC/STEDM and PL-RCA, we demonstrate quantitatively and qualitatively different drug-selective changes in CFD/TAD in various lineage leukemia cells. More specifically, in drug-sensitive leukemia cells, hnRNPK, a conserved RNA-binding protein, interacts with a specific set of RCMTs and other co-factors to recruit elongating RNA polymerase II (RNAPII) to nascent RNAs to form a unique active CFD/TAD. A marked increase in such unique hnRNPK-mediated CFD/TAD predicts the drug responsiveness. In contrast, drug-resistant leukemia cells have a distinctly different active CFD/TAD on nascent RNAs, which is composed of a different set of RCMTs and elongating RNAPII and correlates with drug resistance in leukemia cells.

Conclusions: This study provides digitalized imaging data of drug-selective chromatin structures and RNA epigenetics in normal BM cells and hematologic malignancies, which is a crucial step toward artificial intelligence (AI) prediction of drug response and resistance and the next generation digital Pathology.

1344   Clinical, Pathological, Genetic Features and Differential Diagnosis of EBV Positive Plasmacytoma
Jinjun Cheng[1], Liqiang Xi[1], Svetlana Pack[2], Hao-Wei Wang[3], Mark Raffeld[4], Elaine Jaffe[1], Stefania Pittaluga[5]
[1]National Cancer Institute, National Institutes of Health, Bethesda, MD, [2]NIH, Bethesda, MD, [3]Bethesda, MD, [4]National Cancer Institute, Bethesda, MD, [5]National Institutes of Health, Washington, DC

Disclosures: Jinjun Cheng: None; Liqiang Xi: None; Svetlana Pack: None; Hao-Wei Wang: None; Mark Raffeld: None; Elaine Jaffe: None; Stefania Pittaluga: None

Background: EBV positive plasmacytoma is a rare plasma cell neoplasm, and its relationship to plasmablastic lymphoma (PBL) and is unknown.

Design: We identified 10 EBV-pos plasmacytomas from our archives between 2000 and 2019. Immunohistochemical stains (LMP1, MYC, CD20, CD3, CD138, CD79, CD56, Cyclin D1, CD117, Kappa, Lambda, IgA, IgG, IgD, IgG4, IgM, MIB1), and FISH for *MYC* with break apart and confirmatory IGH/MYC fusion probes were performed. Cases were compared to 26 EBV-neg plasmacytomas, 32 EBV-pos PBLs, and 17 EBV-neg PBLs. (Table 1).

Results: Ten EBV-pos plasmacytomas (4 male/6 females; median age: 44 years, range 6-65) were identified. Underlying immune deficiency was evident in 7/10 cases. All but one EBV-pos plasmacytoma case was analyzed at diagnosis, and nine out of ten patients presented with a single non-bulky lesion (9/10, 90%), involving nasal or oral cavity (4/10, 40%), lymph node or tonsil or spleen* (3/10, 30%), bone (2/10, 20%) and parotid gland (1/10, 10%). In contrast to PBLs, which commonly affected the GI tract, GI tract involvement was absent in both EBV-pos and EBV-neg plasmacytoma. Histological features were similar to EBV-neg plasmacytomas including predominance of mature plasma cells (8/10, 20%), low mitotic activity (8/10, 80%), and occasional necrosis (2/10, 20%). By IHC, EBV-pos plasmacytomas were usually positive for CD79a or CD138, but rarely positive for CD56 (1/6, 17%), or MYC (1/10, 10%); all were CD20 negative. LMP1 was negative in all subgroups. All EBV-pos plasmacytomas showed light chain restriction, in contrast to EBV-pos PBLs, in which Ig expression was seen in only 65% (15/23). Two EBV-pos plasmacytomas contained a plasmablastic component (<30% of total tumor cells) with a relatively high Ki-67 proliferation rate. One of the two was positive for IGH/MYC translocation limited to the plasmablastic component only. All remaining cases were negative for *MYC* gene rearrangement and MYC immunostain. Clinically, both cases presented with a single lesion, with negative staging and bone marrow biopsy, good response to local excision or radiation and no recurrence or relapse (follow-up; 10 and 6 months respectively).

	EBV+ Plasmacytoma	EBV-Plasmacytoma	EBV+ Plasmablastic lymphoma	EBV-Plasmablastic lymphoma
No of cases	10	26	32	17
M:F ratio	4:6	19:7	27:4	13:4
Median age, y (range)	44 (6-65)	42 (4-87)	47 (11-83)	56 (18-88)
Clinical stage				
Single lesion	9/10 (90%)	24/26 (92%)	25/32 (78%)	12/17 (70%)
Multiple lesions	1/10 (10%)	2/26 (8%)	7/32 (22%)	5/17 (30%)
Sites of involvement				
Lymphoid tissue (lymph node/spleen/tonsil)	3 (30%)	14/26 (54%)	4/32 (12.5%)	4/17 (24%)
Nasal /oral cavity	4 (40%)	6/26 (23%)	13/32 (41%)	3/17 (18%)
Lower GI tract	0 (0%)	0/26 (0%)	10/32 (31%)	7/17 (41%)
Others (Bone, skin, brain)	3 (30%)	6/26 (23%)	5/32 (16%)	4/17 (24%)
Immunosuppression history				
HIV positive	3	2	21	4
Other abnormal Immune Status	4	11	4	3
Immunohistochemical stains and FISH				
CD20	0/10 (0%)	1/25 (4%)	1/32 (3%)	1/17 (6%)
CD79a	8/9 (89%)	11/12 (92%)	11/22 (50%)	6/11 (55%)
CD138	8/10 (80%)	20/20 (100%)	24/28 (86%)	9/11 (82%)
CD56	1/6 (17%)	3/9 (33%)	5/24 (21%)	2/11 (18%)
Monotypic Ig	10/10 (100%)	24/24 (100%)	15/23 (65%)	14/14 (100%)
EBER ISH	100%	0%	100%	0%
LMP1	0/10 (0%)	N/A	0/10 (0%)	N/A
MYC IHC	1/10 (10%)	1/10 (10%)	6/9 (67%)	5/8 (63%)
FISH MYC Pos	1/7 (15%)	1/7 (15%)	14/20 (70%)	12/16 (75%)

Conclusions: EBV-pos plasmacytoma is a rare neoplasm, and shows overlapping features with EBV-neg plasmacytoma and PBL.

1345   Germline Variants of HAVCR2 in a North American Consult Practice Cohort of Subcutaneous Panniculitis-like T-cell Lymphoma

Jinjun Cheng[1], Liqiang Xi[1], Yoon Jang[1], Hao-Wei Wang[2], Stefania Pittaluga[3], Elaine Jaffe[1], Mark Raffeld[4]
[1]National Cancer Institute, National Institutes of Health, Bethesda, MD, [2]Bethesda, MD, [3]National Institutes of Health, Washington, DC, [4]National Cancer Institute, Bethesda, MD

Background: Subcutaneous panniculitis-like T-cell lymphoma (SPTCL) is a rare neoplasm of mature cytotoxic T cells with an αβ phenotype. The clinical and pathological features overlap with lobular panniculitis and other cutaneous T-cell lymphomas with panniculitis features. Recently, HAVCR2 germline variants (Y82C and I97M) have been linked to SPTCL patients of Southeast Asian ethnicity.

Design: We identified 33 SPTCL cases in the pathology archives between 2000 and 2019; Ethnicities included 4 Southeast Asian, 8 African American, 3 Caucasian, 3 Hispanic, 1 American Indian, 14 unknown. 16 cases of lobular panniculitis were identified as controls. All available H&E slides and immunohistochemical stains were reviewed, as well as results of PCR for T-cell receptor (TCR) gene rearrangement. Droplet digital PCR assays for HAVCR2 variants Y82C and I97M were custom designed and performed in 46 cases with available material. Clinical history provided at the time of case submission was recorded.

Results: A total of 6/33 patients were found to have germline HAVCR2 Y82C variants (4 homozygous and 2 heterozygous). HAVCR2 I97M germline variants were not detected. All HAVCR2 Y82C variants occurred in the 4 patients of Southeast Asian where ethnicity was recorded. HAVCR2 Y82C variants were not present in any of the identified non - Asian patients. Two (33%) SPTCL patients with HAVCR2 Y82C variants presented with clinical hemophagocytic lymphohistiocytosis (HLH). Only one of 27 (4%) cases without these variants presented with HLH. Otherwise, there was no significant difference in clinical presentation, morphology and immunophenotypical features between the two groups of SPTCL patients. Additional screening for HAVCR2 germline variants in 16 cases of lobular panniculitis was positive for HAVCR2 Y82C homozygous variants in one case from a patient of Southeast Asian ethnicity with a diagnosis of "atypical lobular panniculitis", in which TRG PCR and morphology were insufficient for a diagnosis of SPTCL.

Conclusions: A subset of North American SPTCL patients contain HAVCR2 germline variants. These patients were exclusively of Southeast Asian ethnicity, when patient origin was known. The presence of HAVCR2 mutation in one case of lobular panniculitis suggests that HAVCR2 germline variants, while characteristic of SPTCL, may not be diagnostic for SPTCL in the setting of panniculitis.

1346 Pure Red Cell Aplasia in Patients with Germline Mutations in AIRE and APECED

Jinjun Cheng[1], Monica Schmitt[2], Elise Ferre[2], Bhavisha Patel[3], Weixin Wang[4], Stefania Pittaluga[5], Raul Braylan[6], Neal Young[7], Michail Lionakis[2], Katherine Calvo[8]
[1]National Cancer Institute, National Institutes of Health, Bethesda, MD, [2]Fungal Pathogenesis Section, LCIM, National Institute of Allergy and Infectious Diseases (NIAID), National Institutes of Health (NIH), Bethesda, MD, [3]National Institute of Allergy and Infectious Diseases (NIAID), National Institutes of Health (NIH), Bethesda, MD, [4]Clinical Center/NIH, Bethesda, MD, [5]National Institutes of Health, Washington, DC, [6]Hematology Section, Department of Laboratory Medicine, Clinical Center, National Institutes of Health, Bethesda, MD, [7]Cell Biology Section, National Heart Lung and Blood Institute (NHLBI), NIH, Bethesda, MD, [8]National Institutes of Health, Bethesda, MD

Background: Autoimmune polyendocrinopathy-candidiasis-ectodermal dystrophy (APECED), is a monogenic autosomal recessive disorder caused by AIRE mutations. Herein we report multiple cases of pure red cell aplasia (PRCA) in in patients with APECED.

Design: 5 out of 100 patients with APECED developed severe anemia and underwent bone marrow biopsy evaluation with flow cytometry (FC), cytogenetic, and molecular studies.

Results: Median age was 34 years (range 18-59), 3 females and 2 males. Common marrow features with markedly decreased to absent erythroid precursors with maturation arrest indicative of pure red cell aplasia (PRCA). Myelopoiesis and megakaryopoiesis was intact. Marrow cellularity was variable. There was no evidence of dysplasia and no increased in blasts. CD71 immunohistochemistry (IHC) stains from 4/5 patients confirmed absence of erythropoiesis. IHC for CD3 showed increased interstitial T cell infiltrates with predominance of CD8 positive T-cells in 5/5 (100%) marrows. CD20 showed markedly decreased to absent B cells. CD138 showed few plasma cells. Cytogenetic analysis was normal in all cases. FC of BM was done on 4 marrows and showed expansion of T cells expressing CD3 and CD8, +/- CD57 representing 71%, 45.3%, 33.8%, and 10.5% of lymphocytes. T cell clonality by PCR was positive in all cases. Abnormal B cell maturation was seen with markedly decreased mature B cells. Peripheral blood (PB) FC showed severe B lymphopenia, and reversed CD4:CD8 ratios in half of cases (2/4). PB screening for T-LGL showed aberrantly increased cytotoxic T cells in 4 out of 5 patients. PNH screening by FC was negative. Other abnormal laboratory parameters included hypogammaglobulinemia (1/4), low reticulocyte account (3/4), neutropenia (1/5), thrombocytopenia (2/5), and lymphopenia (1/5). Iron studies were unremarkable. Erythropoietin was increased (2 out of 2). Several patients achieved transfusion independence with erythroid reconstitution and decrease in LGLs with immunosuppressive therapy.

Conclusions: PRCA is a rare hematologic disease that can manifest in the setting of APECED and autoimmunity and responds to immunosuppression. The BM findings suggest that clonal T-LGL populations may play a role the etiology of PRCA in APECED.

1347 Nationwide Trends of Hematopoietic Stem Cell Transplantation in the Inpatient Setting in the United States, 2010-2014

Saurav Chopra[1], Carol Holman[2], Annette Schlueter[1]
[1]University of Iowa Hospitals and Clinics, Iowa City, IA, [2]University of Iowa, Iowa City, IA

Disclosures: Saurav Chopra: None; Carol Holman: None; Annette Schlueter: None

Background: Hematopoietic stem cell transplantation (HSCT) is an established therapy for various malignant and other high-risk hematologic conditions. The use of HSCT has steadily increased over time with the advent of alternative graft sources and technical advances in the transplant regimens and supportive care. We aimed to assess the nationwide practices and temporal trends in the use of HSCT for common diagnostic indications in the inpatient setting.

Design: Data for the study were drawn from the National Inpatient Sample, the largest all-payer inpatient database in the US. Diagnostic conditions and HSCT were identified using the International Classification of Diseases, 9th Revision diagnoses and procedure codes. Sampling weights were applied to generate nationally representative estimates. Primary admitting diagnosis was recorded for all hospitalizations with HSCT. The Cochran-Armitage test was used to estimate the linear temporal trends for specific diagnoses. Univariate analysis was used to analyze the hospital level characteristics associated with HSCT.

Results: From 2010-2014, HSCT was performed in 87,002 hospitalizations (mean±SD age: 47.1±20.3 years; female 40.8%; pediatric 13.9%). Average time from admission to HSCT was 6.5 days (range: -4 to 210 days). Various primary diagnostic indications for HSCT are shown in Table 1. Figure 1 shows the temporal trends in the proportion of hospitalizations with HSCT for different diagnoses. During the study period, there was an overall increase in the utilization of HSCT among the hospitalizations for malignant and non-malignant hematologic conditions, while there was a decline among the hospitalizations for non-hematologic malignancies. HSCT was more commonly performed in the urban teaching and government owned hospitals (Figure 2). Hospitalizations with HSCT had significantly longer length of stay and higher hospital charges as compared to the corresponding admissions without HSCT (mean difference: 18.1 days & $237,442; p<0.001).

Rank	Diagnosis	N	%
Table 1. Most common primary admission diagnoses for hospitalizations with hematopoietic stem cell transplantation (HSCT), 2010 - 2014			
Hematologic malignancies			
I	**Multiple Myeloma**	**24,175**	**27.79**
II	**Acute myeloid leukemias**	**13,520**	**15.55**
	Acute myeloid leukemia	13,404	15.41
	Myeloid sarcoma	45	0.05
	Acute erythroid leukemia	38	0.04
	Acute megakaryoblastic leukemia	33	0.04
III	**Other lymphoma with extra-nodal involvement**	**7,413**	**8.52**
IV	**Mature B-cell neoplasms**	**6,737**	**7.74**
	Mantle cell lymphoma	2,813	3.23
	Follicular lymphoma	1,613	1.85
	Chronic lymphocytic lymphoma/leukemia	1,313	1.51
	Diffuse large B-cell lymphoma	395	0.45
	Burkitt's lymphoma	189	0.22
	Primary CNS lymphoma	172	0.20
	Marginal zone lymphoma	134	0.15
	Waldenstrom Macroglobulinemia	108	0.12
V	**Acute lymphoblastic leukemia**	**5,301**	**6.09**
VI	**Hodgkin's lymphoma**	**4,578**	**5.26**
VII	**Myelodysplastic syndrome**	**3,502**	**4.03**
VIII	**T-cell neoplasms**	**2,082**	**2.39**
	Mycosis Fungoides	818	0.94
	Peripheral T-cell lymphoma	754	0.87
	Anaplastic large cell lymphoma	490	0.56
	Sezary syndrome	20	0.02
IX	**Myeloproliferative neoplasms**	**1,745**	**2.01**
	Chronic myeloid leukemia	1,518	1.75
	Myelofibrosis	153	0.18
	Polycythemia vera	74	0.09
X	**Other hematologic malignancies**	**826**	**0.95**
IV	**Other/unspecified myeloid leukemia**	**72**	**0.08**
Non-hematologic malignancies			
	Total	**2,886**	**3.32**
I	Brain tumor	1,757	2.02
II	Testicular neoplasm	969	1.11
III	Pineal gland tumor	160	0.18
Inherited/congenital disorders			
	Total	**1,287**	**1.48**
I	Sickle cell anemia	475	0.55

		N	%
II	Severe combined immunodeficiency	254	0.29
III	Thalassemia	188	0.22
IV	Mucopolysaccharidosis	99	0.11
V	Wiskott–Aldrich syndrome	81	0.09
VI	Leukodystrophy	60	0.07
VII	Peroxisomal disorders	50	0.06
VIII	Congenital neutropenia	30	0.03
IX	Congenital thrombocytopenic purpura	20	0.02
X	Deficiency of cell immunity NOS	15	0.02
XI	Genetic anomaly in leukocytes	15	0.02
Miscellaneous			
	Total	**2,834**	**3.26**
I	Aplastic anemia	1,525	1.75
II	Amyloidosis	943	1.08
III	Hemophagocytic lymphohistiocytosis	261	0.30
IV	Systemic sclerosis	55	0.06
V	Common variable immune deficiency	20	0.02
VI	Immune deficiency NOS	15	0.02
VII	Osteopetrosis	15	0.02
Others		**10,044**	**11.54**
	Total HSCT cases	**87,002**	**100%**
N: number of hospitalizations for each diagnosis with stem cell transplantation. %: percentage of each diagnosis relative to all admissions with HSCT (87,002).			
CNS: central nervous system; NOS: not otherwise specified			

Figure 1 - 1347

Figure 1. Yearly trends of inpatient hematopoietic stem cell transplantation for different diagnoses

Diagnosis	2010	2011	2012	2013	2014	P-trend
Acute myeloid leukemias	13.7	11.8	13.0	13.9	14.4	<0.001
Myeloproliferative neoplasms	8.4	6.1	9.0	8.1	8.4	0.146
Myelodysplastic syndrome	5.5	5.1	6.9	9.2	10.0	<0.001
Acute lymphoblastic leukemia	11.1	10.5	10.5	11.0	11.0	0.99
Multiple Myeloma	25.5	22.0	27.1	29.5	29.6	<0.001
Mature B-cell neoplasms	9.5	9.0	10.3	10.3	9.0	0.570
T-cell neoplasms	9.9	10.5	13.7	13.9	15.4	<0.001
Hodgkin's lymphoma	21.5	15.6	21.7	23.5	21.5	<0.001
Non-hematologic malignancies	2.3	1.5	1.3	1.3	1.3	<0.001
Sickle cell anemia	0.1	0.2	0.1	0.1	0.1	0.062
Thalassemia	0.2	0.8	0.8	0.3	1.7	<0.001
SCID	33.3	23.7	32.4	37.1	40.0	0.048
Aplastic anemia	2.8	2.2	6.9	9.3	8.6	<0.001
Amyloidosis	8.1	4.0	6.2	6.4	7.1	0.514
HLH	15.0	8.3	13.3	10.8	5.4	<0.001

Above data are represented as percentage of hospitalizations with HSCT relative to all admissions with each respective diagnosis.
P-trend: P-value of trend; SCID: severe combined immunodeficiency; HLH: hemophagocytic lymphohitiocytosis, AML: acute myeloid leukemia; MDS: myelodysplastic syndrome

Figure 2 - 1347

Figure 2. Hospital level characteristics associated with HSCT		
Characteristics	Odds Ratio (95% CI)	P-value
Location/Teaching status		
Rural	Reference	
Urban non-teaching	0.53 (0.17 − 1.64)	0.269
Urban teaching	22.98 (9.00 − 58.70)	<0.001
Bed-size		
Small	Reference	
Medium	0.25 (0.16 − 0.39)	<0.001
Large	0.86 (0.57 − 1.29)	0.467
Region		
NE	Reference	
Midwest	1.06 (0.73 − 1.55)	0.747
South	0.65 (0.44 − 0.93)	0.019
West	0.98 (0.65 − 1.48)	0.936
Hospital control		
Government	Reference	
Private nonprofit	0.75 (0.57 − 0.99)	0.046
Private investor-own	0.48 (0.26 − 0.90)	0.022
CI: confidence intervals; NE North-East		

Conclusions: This study provides an update on the nationwide practices in the use of HSCT in the inpatient setting with a focus on recent temporal trends for different diagnoses. Stem cell transplantation remains a resource intensive procedure and its utilization in the inpatient setting continues to increase, despite the growing evidence supporting its safety in the outpatient setting.

1348 ERBB(HER3/4)-NRG1 Receptor-Ligand Expression May Promote Chronic Lymphocytic Leukemia Cell Viability

Charles Chu[1], Kyu Kwang Kim[2], Mary Georger[3], Omar Aljitawi[4], Clive Zent[5], Andrew Evans[5]
[1]Wilmot Cancer Institute, University of Rochester Medical Center, Rochester, NY, [2]Division of Gynecologic Oncology, Department of Obstetrics and Gynecology, Wilmot Cancer Institute, University of Rochester Medical Center, Rochester, NY, [3]Wilmot Cancer Institute Histopathology Core, University of Rochester Medical Center, Rochester, NY, [4]Division of Hematology/Oncology and Bone Marrow Transplant Program, Department of Medicine, Wilmot Cancer Institute, University of Rochester Medical Center, Rochester, NY, [5]University of Rochester Medical Center, Rochester, NY

Disclosures: Charles Chu: *Grant or Research Support*, Acerta Pharma / AstraZeneca; *Stock Ownership*, Pfizer; Kyu Kwang Kim: None; Mary Georger: None; Omar Aljitawi: None; Clive Zent: *Grant or Research Support*, Acerta/AstraZeneca; Andrew Evans: None

Background: Targeting chronic lymphocytic leukemia/small lymphocytic lymphoma (CLL/SLL) through tyrosine kinase inhibitor (TKI) therapy has proven highly effective. The degree to which parallel kinase pathways may contribute to CLL cell viability, and the degree to which off-target effects by "specific" TKIs contributes to the efficacy of treatment is still unclear. Members of the ErbB/HER protein tyrosine kinase family (ErbB/HER1-4) function as homo- and heterodimer receptors that bind a diverse number of ligands to regulate cell growth and survival in a variety of cancer and tissue types. In particular, NRG1 is a specific ligand for HER3 and HER4. We sought to determine if signaling through ErbB/HER family members may contribute to CLL cell viability.

Design: Comparative effects of various TKI inhibitors on primary CLL cell viability was assessed by in-vitro culture with different drugs, including Bruton tyrosine kinase (BTK) inhibitor ibrutinib and Erb/HER kinase family inhibitor afatinib. Protein expression of select ErbB family members, namely HER3 and HER4, as well as corresponding ligand NRG1, was examined in up to 10 primary cases of CLL by western blot (from fresh viable cells) and/or immunohistochemistry (IHC) (from formalin fixed paraffin embedded tissue), and compared to normal lymphoid and bone marrow controls.

Results: In head-to-head comparison of primary CLL in-vitro cell culture in the presence of TKI drugs, afatinib showed 20-fold more potent inhibition of cell viability than ibrutinib as measured by chemiluminescent cell viability assay (IC50 of 0.5uM versus 10uM) (Figure 1).

Western blot demonstrated low level expression of full length HER3, low level expression of lower molecular weight HER4 (consistent with the activated intracellular domain cleavage product), and strong expression of lower molecular weight NRG1 ligand in primary CLL cells. Expression of HER3 and NRG1 was validated with IHC testing of 10 diagnostic CLL/SLL tumor biopsies. HER3 showed moderate polarized membranous expression in CLL tissue samples, and NRG1 expression was diffusely strong in a membranous/cytoplasmic pattern, both increased as compared to normal lymphoid tissue (Figure 2).
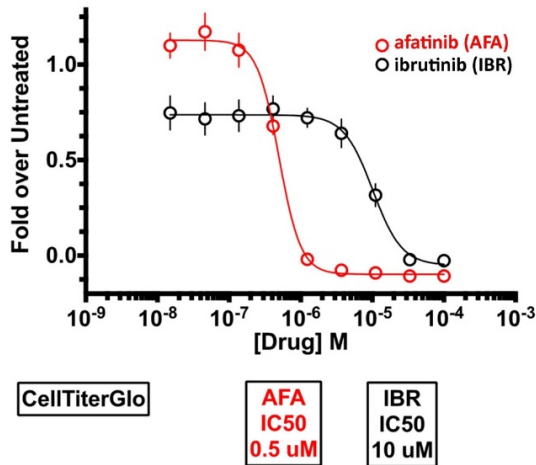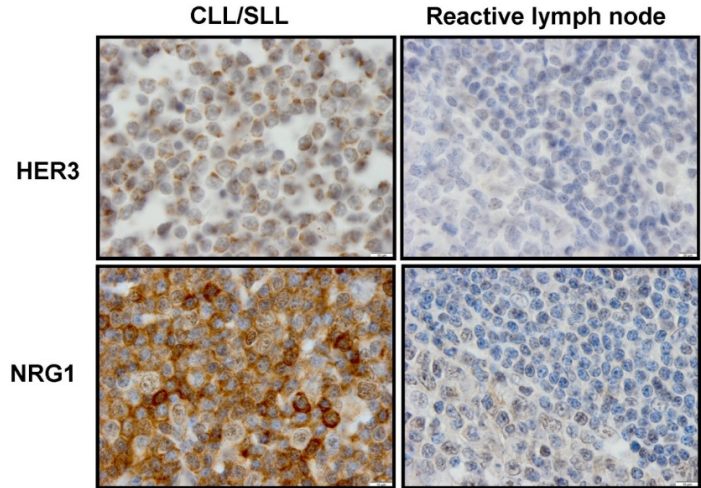
Figure 1 - 1348

Figure 2 - 1348

Conclusions: Alternative TKI activity may play an important role in CLL viability. ErbB/HER family members HER3/4 and their corresponding ligand NRG1 are expressed in CLL, and may be valuable target for future study of specific inhibitor therapy.

1349 Monomorphic Epitheliotropic Intestinal T-cell Lymphoma is the most Frequent Type of Primary Intestinal T-cell Lymphoma in Taiwan and is Frequently Associated with SEDT2 and STAT5B Mutations

Shih-Sung Chuang[1], Chang-Tsu Yuan[2], Kung-Chao Chang[3], Ren Ching Wang[4], Bo-Jung Chen[5], Shih-Yao Lin[6], Wen-Yu Chuang[7], Jen-Fan Hang[6]
[1]Chi Mei Medical Center, Tainan, Taiwan, Taiwan, [2]Taipei, Taiwan, [3]National Cheng Kung University and Hospital, Tainan, TW, Taiwan, [4]Taichung Veterans General Hospital, Taichung, Taiwan, [5]Shuang-Ho Hospital, Taipei Medical University, New Taipei City, Taiwan, [6]Taipei Veterans General Hospital, Taipei, Taiwan, [7]Taoyuan, Taiwan

Disclosures: Shih-Sung Chuang: None; Chang-Tsu Yuan: None; Kung-Chao Chang: None; Ren Ching Wang: None; Bo-Jung Chen: None; Shih-Yao Lin: None; Wen-Yu Chuang: None; Jen-Fan Hang: None

Background: Primary intestinal T-cell lymphoma (PITL) is rare with poor prognosis. In the 2017 WHO classification, classical enteropathy-associated T-cell lymphoma (EATL) was celiac disease-associated. Type II EATL in the 2008 WHO classification was renamed as monomorphic epitheliotropic intestinal T-cell lymphoma (MEITL), comprising of monomorphic medium-sized cells with expression of CD8, CD56, and cytotoxic markers. In additional, extranodal NK/T-cell lymphoma, nasal type (ENKTL), anaplastic large cell lymphoma (ALCL), and peripheral T-cell lymphoma-not otherwise specified (PTCL-NOS) may also occur primarily in the intestine. However, there are borderline cases with variable nuclear size and atypical phenotype not fitting into MEITL. The molecular features of PITL cases have not been fully elucidated. The aims of this study were to better characterize PITL in Taiwan based on the clinicopathological and molecular features, particularly those with borderline features, and to identify potential therapeutic targets.

Design: PITL cases were collected from multiple institutions in Taiwan and diagnosed according to the 2017 WHO classification. Those cases with pleomorphic cellular component and/or atypical immunophenotype for MEITL were categorized as borderline. We performed immunohistochemistry and *in situ* hybridization for EBV, and targeted next-generation sequencing for the whole coding regions of *SEDT2* and hotspot mutations of *STAT3, STAT5B, JAK1, JAK3, GNAI2, KRAS, NRAS*, and *BRAF*.

Results: A total of 59 PITL cases were recruited, including 36 MEITL, 8 PITL-NOS, 8 borderline, 4 ENKTL, and 3 ALCL. The clinicopathological and molecular findings are summarized in Table 1.

Table 1. The clinicopathological and molecular findings of PITL in Taiwan

	MEITL	PTCL-NOS	Borderline	ENKTL	ALCL
No.	36	8	8	4	3
Median age (range)	60 (34-91)	65 (25-83)	49 (23-64)	51 (44-63)	57 (10-65)
Sex, no. (M/F)	24/12	4/4	5/3	2/2	3/0
Site, no.					
small bowel	29	6	6	1	3
colon	0	1	2	1	0
both	2	1	0	1	0
not available	5	0	0	1	0
Perforation, no. (%)	26 (72%)	2 (25%)	7 (88%)	2 (50%)	1 (33%)
Overall survival (OS) rate					
1y, %	40	57	42.9	0	50
3y, %	16	14	0	0	50
Mutation, no. (%)					
SEDT2	32 (89%)	4 (50%)	5 (63%)	0 (0%)	1 (33%)
STAT3	0 (0%)	0 (0%)	0 (0%)	3 (75%)	2 (67%)
STAT5B	26 (72%)	2 (25%)	2 (25%)	0 (0%)	1 (33%)
JAK3	13 (36%)	0 (0%)	5 (63%)	0 (0%)	0 (0%)
GNAI2	5 (14%)	0 (0%)	1 (13%)	0 (0%)	0 (0%)
KRAS	6 (17%)	2 (25%)	2 (25%)	0 (0%)	0 (0%)
NRAS	2 (6%)	0 (0%)	0 (0%)	0 (0%)	0 (0%)
BRAF	1 (3%)	0 (0%)	0 (0%)	0 (0%)	0 (0%)

Conclusions: MEITL was the most common type of PITL in Taiwan and was frequently associated with bowel perforation, and mutations at the *SEDT2* (89%) and *STAT5B* (72%) loci. Therapeutic agents targeting these genes might be beneficial to prolong survival of MEITL patients. The borderline cases shared both the molecular changes of MEITL and PTCL-NOS, yet with the highest mutation rate at JAK3 (63%) among all groups. More histopathological, immunohistochemical, and molecular studies, and possibly including artificial intelligence methods to measure the nuclear size and shape of the neoplastic cells, are warranted to characterize the nature of such cases.

1350 Molecular and Survival Characteristics of Therapy Related Myeloid Neoplasms with Favorable Recurrent Cytogenetics
Jessica Corean[1], Kristin Karner[1]
[1]University of Utah, Salt Lake City, UT

Disclosures: Jessica Corean: None; Kristin Karner: None

Background: Therapy related myeloid neoplasm (t-MN) is defined as a late complication in patients treated with cytotoxic chemotherapy or radiation for a prior neoplastic or non-neoplastic disorder. This diagnosis typically has poor prognosis, complex cytogenetic findings, and resistance to typical therapy. Within t-MN, a subset of patients have favorable recurrent cytogenetics (RC) including t(15;17), t(8;21), and inv(16)/ t(16;16). In the usual de novo presentation, these findings correlate with good prognosis and define an AML even if the blast count is less than 20%. Here we identify cases of t-MN with recurrent cytogenetic (t-MN with RC), and aim to assess their clinical, prognostic and molecular differences from usual cases of t-MN.

Design: We retrospectively identified patients diagnosed with AML or t-MN, reviewed clinical history, and gathered molecular and cytogenetic data at the time of diagnosis. Favorable recurrent cytogenetics for AML was defined as t(15;17), t(8;21), or inv(16)/t(16;16).

Results: We identified 41 patients who met criteria as follows: 5 therapy-related myeloid neoplasm with favorable recurrent cytogenetics, 18 in a therapy related myeloid neoplasm and 18 de novo, favorable recurrent cytogenetic AML (AML with RC) cohorts. The overall survival difference between t-MN and the t-MN with RC was statistically significant (p value is .025 based on the Mann-Whitney test).

	Therapy related with favorable recurrent cytogenetics (t-MN with RC)	Therapy related MN (t-MN)	De novo favorable cytogenetics AML (AML with RC)
Patients, n	5	18	18
Age (years), range (mean)	54-72 (66)	30-89 (63)	20-72(49)
Sex (female: male)	4:1	9:9	8:10
Prior solid tumor malignancy n (%)	4 (80%)	6 (33%)	NA
Prior hematologic malignancy n (%)	1 (20%)	12 (67%)	NA
Length of time from prior malignancy to hematologic malignancy (years)	5.5	6	NA
Alive, n	2	8	14
Deceased, n	3	10	4
Overall survival from myeloid diagnosis to present time or death (months)	39.3*	11.9*	37.1
Molecular findings (Next generation sequencing myeloid panel)			
Number of variants, range, (mean)	1-4 (3)	0-5 (2)	1-5 (2)
Most frequent variants	KIT (3/4, 75%)	TP53 (6/18, 33%)	KIT (9/18, 50%)
	NRAS (3/4, 75%)	ASXL1 (6/18, 33%)	FLT3 (4/18, 22%)
	KRAS (2/4, 50%)	DNMT3A (3/18, 17%) U2AF1 (3/18, 17%)	ASXL1 (3/18, 17%)

*$p<0.05$ significant difference in overall survival in t-MN and t-MN with RC, based on Mann-Whitney test

Conclusions: Overall, our cohorts of t-MN and t-MN with RC are similar in age, whereas the AML with RC are younger. AML with RC and t-MN with RC had similar overall survival rates, while the t-MN cohort had the worst survival. This difference between t-MN with RC and t-MN overall survival is statistically significant. The molecular findings between AML with RC and t-MN with RC are similar, with KIT mutations being the most common and similar time to death in KIT positive patients. TP53 was the most common mutation in t-MN with time to death shorter than the remaining cohort. This small data set suggests that t-MN with RC follow a different pathway from t-MN with a distinctly different molecular profile and better prognostic outcome that behaves more like AML with RC.

1351 Significance of Low Blast Counts and KIT Mutations in Acute Myeloid Leukemia with t(8;21)(q22;q22.1); RUNX1-RUNX1T1

Claudiu Cotta[1], Karl Theil[1]
[1]Cleveland Clinic, Cleveland, OH

Disclosures: Claudiu Cotta: None; Karl Theil: None

Background: Acute myeloid leukemia with t(8;21)(q22;q22.1); *RUNX1-RUNX1T1* is diagnosed on specimens with the translocation regardless of blast counts. The origin of this exception from the usual requirement for 20% blasts in AML is blurry and there are no reliable studies of the clinical presentation and outcomes of AML t(8;21) with less than 20% blasts. Mutations of KIT have been described as poor prognostic markers in AML t(8;21), but data generated by different groups do not allow a definitive conclusion and there is a discrepancy between the significance attached to KIT mutations in USA vs. Europe. This study investigates whether t(8;21) cases with <20% blasts should be classified as AML and attempts to clarify the significance of CD117 mutation in a large series of AML t(8;21) diagnosed and treated in the same institution in the USA.

Design: From August 1997 to November 2016, 50 cases of AML t(8;21) were identified in the archives of the Cytogenetics Laboratory, 33 females and 17 adults. 2 patients were children, aged 7 and 11 and 48 were adults. All patients were treated in the same institution and the outcomes were documented and survival was quantified in months. When available, KIT mutation status was also documented.

Results: Of the 50 patients with AML t(8;21), 6 (12%, 2 males and 4 females, all adults) had less than 20% blasts at diagnosis. Of the 4 cases with known KIT status, 1 was positive and 3 were negative. Surprisingly, the survival curve points to a poorer prognosis of these patients when compared to the group with >20% (Fig. 1, median survival 25 vs. 164 months), even if statistical significance was not

reached. Of the 23 patients for which the KIT mutation status was known, 8 (35%) were positive. The survival of the positive patients was significantly poorer (p=0.037, median survival 25 months vs. not reached) (Fig 2).
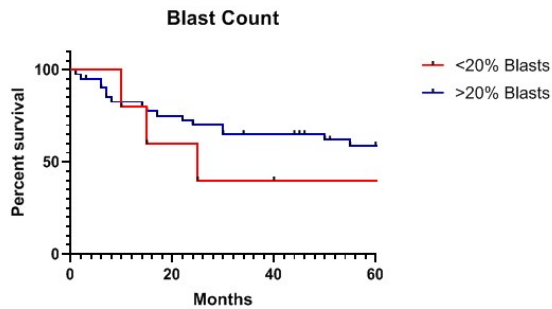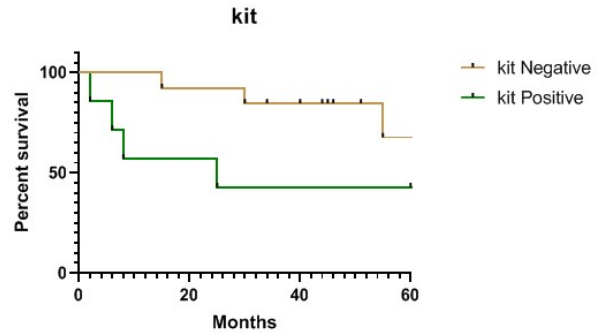
Figure 1 - 1351

Figure 2 - 1351

Conclusions: The poor prognosis of the patients with less than 20% blasts supports the classification of these cases as AML. The explanation for this finding is not obvious and requires further investigation. KIT mutations have been identified in a proportion similar to that reported in the literature. The favorable prognosis of the KIT non-mutated cases was confirmed. There was no evidence of a higher frequency of KIT mutations in cases with less than 20% blasts to account for the poor prognosis.

1352 A New Proficiency Testing Program for the Flow Cytometric Analysis of Plasma Cell Neoplasms: Design and Preliminary Results

David Dorfman[1], Christine Bashleben[2], Jolene Cardinali[3], Meghan Hupp[4], William Karlon[5], Michael Keeney[6], Catherine Leith[7], Claire Murphy[8], Vinodh Pillai[9], Flavia Rosado[10], Adam Seegmiller[11], Michael Linden[12]
[1]Brigham and Women's Hospital, Boston, MA, [2]College of American Pathologists, Northfield, IL, [3]Hartford Hospital, Hartford, CT, [4]University of Minnesota, Minneapolis, MN, [5]University of California San Francisco, San Francisco, CA, [6]London Health Sciences Center, London, ON, [7]University of Wisconsin, Madison, WI, [8]Summit Pathology, Loveland, CO, [9]The Children's Hospital of Philadelphia, Penn Valley, PA, [10]University of Texas Southwestern, Dallas, TX, [11]Vanderbilt University Medical Center, Nashville, TN, [12]University of Minnesota Medical Center, Minneapolis, MN

Disclosures: David Dorfman: None; Christine Bashleben: None; Jolene Cardinali: None; Meghan Hupp: None; William Karlon: *Employee*, Genentech/Roche; *Employee*, UCSF; Michael Keeney: None; Catherine Leith: None; Claire Murphy: None; Vinodh Pillai: None; Flavia Rosado: None; Adam Seegmiller: None; Michael Linden: None

Background: The CAP Diagnostic Immunology and Flow Cytometry Committee designed and implemented a new plasma cell neoplasia flow cytometry proficiency testing (PT) program, to allow labs to monitor and assess their performance compared with a peer group. Here we report the results from the first 2 years of this program.

Design: PT program participants were sent two sets of challenges per year, with clinical, lab, and morphologic findings, each including a "wet" myeloma cell line specimen (± dilution in whole blood) for flow cytometric analysis, and two "dry" challenges (printouts of patient flow cytometric test results, from various flow cytometry labs of committee members).

Results: A total of 91-106 labs participated in the proficiency testing program. For the "wet" challenge, labs employed 6 different flow cytometers and 7-11 different data analysis software packages. The majority of labs gated on cells of interest using CD45 and light scatter or CD38 and/or CD138 and employed isotype controls. Almost all participants (97-100%) correctly identified the presence of neoplastic plasma cell populations based on flow cytometric analysis of myeloma cell lines, with agreement among 80% or more of participants for positive or negative staining for CD38, CD138, CD19, CD20, surface and cytoplasmic kappa and lambda light chains. Similarly, performance was excellent on "dry" challenges: 90-97% of participants were able to correctly identify the presence of small, neoplastic plasma cell populations (0.01%-5.0% clonal plasma cells), or plasma cell hyperplasia in patients with prior myeloid malignancy or HIV infection, based on printouts of flow cytometry findings. However, only 72% of participants were correctly able to identify a case of non-producer myeloma and distinguish it from non-secretory myeloma.

Conclusions: Participant performance in the new PT program was excellent overall, with the vast majority of participants able to perform flow cytometric analysis and identify neoplastic plasma cell populations, and to identify small plasma cell clones or expanded populations of reactive plasma cells in "dry" challenge flow cytometry results. The new program will allow labs to verify the accuracy of their testing

program and test interpretations for the assessment of patients suspected of having a plasma cell neoplasm. A new myeloma minimal residual disease (MRD) PT program is currently being developed and will include "wet" challenges.

1353 Primary Orbital Extranodal NK/T-cell Lymphoma, Nasal type. Clinical Pathological Study of 7 Cases from Peru

Daniela Duenas[1], Daniel Enriquez[1], Renato Luque[2], Sandro Casavilca Zambrano[1], Carlos Barrionuevo[3]
[1]Instituto Nacional de Enfermedades Neoplásicas, Lima, Peru, [2]Universidad Cientifica del Sur, Lima, Peru, [3]Instituto Nacional de Enfermedades Neoplásicas (INEN), Lima, Peru

Disclosures: Daniela Duenas: None; Renato Luque: None; Sandro Casavilca Zambrano: None; Carlos Barrionuevo: *Speaker*, ROCHE

Background: Extranodal NK/T-cell lymphoma (ENKTL) is a rare and aggressive subtype most common in Asian and Latin American populations and associated with Epstein Barr virus (EBV). While most ocular and orbital lymphomas are mainly non-Hodgkin´s B cell variety, the nasal type NK/T-cell lymphomas do occasionally invade the globe ocular adnexa and represents approximately 1%-3% of all lymphoproliferative lesions in these locations. Intraocular and orbital presentations have been confused with a range of diagnoses, including orbital cellulitis, nonspecific orbital inflammation, conjunctivitis, anterior uveitis, optic neuritis and also with aggressive solid tumors. It has been described that extranodal NK/T-cell lymphomas had worse prognosis than their B-cell counterparts.

The aim of this study was to describe the features and immunohistochemistry findings in a series of orbital primary ENKTCL cases from our institution.

Design: We evaluated seven cases diagnosed as ENKTCL with intraocular and orbital presentation during the period between 2009 to 2016 from our institution. In all cases H&E stain, CD3, CD56, CD4, CD8, GRANZYME B and EBER in situ hybridization were performed. Clinical, histopathological and immunohistochemical is described in addition to the response to treatment.

Results: Median age was 42 years (R: 25-62), 5 cases were males and 2 females. The main locations were eyelids, orbits and conjunctiva, and one case had bilateral involvement. B-symptoms were found in 1 case, and 71% had I-II clinical stage disease. 2 cases had advanced stage. All cases expressed CD3, CD56 and GRANZYME-B. Notably, 4 out of 5 cases in which CD8 was assessed were positives. All patients were in a good status performance (ECOG <2), median LDH was 1880U/dL and 57% had neutrophil-to-lymphocyte ratio (NLR) <3. Most patients received treatment based on radiotherapy, including one patient with concurrent treatment based on cisplatin and VIPD chemotherapy as consolidation. For advance disease CHOEP was used in the past as main treatment for three cases and they eventually relapsed and died. Only three patients (42.9%) achieved complete remission and are still alive. Median overall survival was 21.5 months (R: 1-89 months).

Table 1. Clinical Characteristics and Outcomes in Primary orbital extranodal NK/T-cell lymphoma

Clinical Features	Total
Patients, n (%)	7 (100)
Sex	
Male (%)	5 (71.4)
Female (%)	2 (28.6)
Median Age	42y (25-62)
Peripheral blood Infection (RT-PCR)	
Location	
Eyelid + lacrimal apparatus	3 (42.8)
Conjunctiva	1 (14.2)
Orbit	3 (42.8)
Tumor size	5.08cm (4-7)
Laterality	
Unilateral	6 (85.7)
Bilateral	1 (14.3)
Clinical Stage	
I	4 (57.1)
II	1 (14.3)
III	0 (0)
IV	2 (28.6)
B Symptoms	
Yes	1 (14.3)
No	6 (85.7)
ECOG	1.1 (0-4)
1	5 (71.4)

| 2	2 (28.6)
LDH (UI/dL)	1880.7 (429-8407)
Beta2MG (mg/dL)	2.70 (1.66-5.17)
NLR (neutrophil-to-lymphocyte ratio)	3.34 (0.75-6.84)
<3	4 (57.1)
>=3	3 (42.9)
Treatment	
Only radiotherapy	3 (42.9)
CHOEP-based	3 (42.9)
Concurrent Cisplatin-RT and VIPD	1 (14.2)
Response to First line Therapy	
Complete Response	3 (42.9)
Partial Response	3 (42.9)
Progressive Disease	1 (14.2)
Status Outcomes	
Dead	4 (57.1)
Alive	3 (42.9)
Median Overall survival (months)	21.5 (1-89)

Figure 1 - 1353
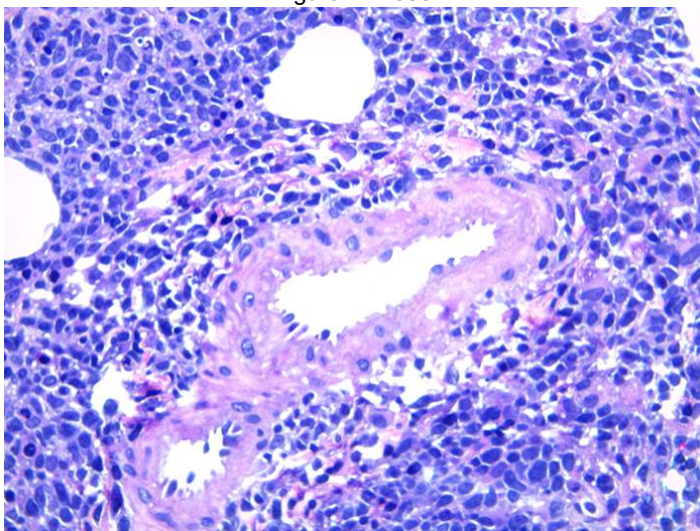
Figure 2 - 1353
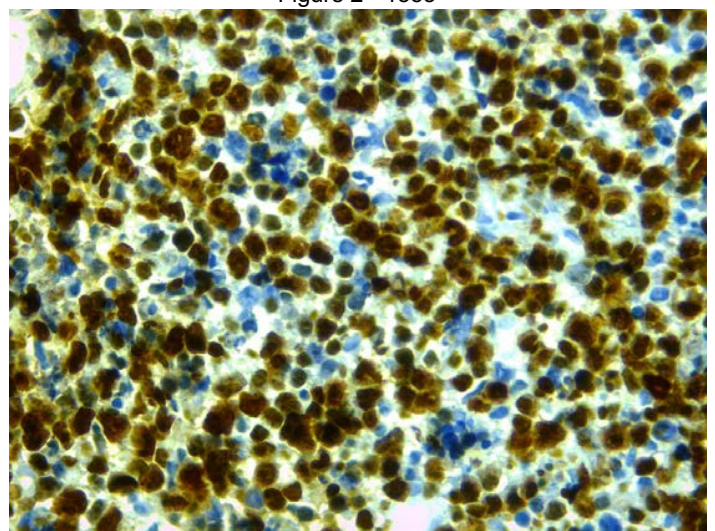
Conclusions: Extranodal NK/T-cell lymphoma (ENKTL) of the orbit is a poor prognosis entity that seems curable in localized stage. Interestingly, we found high co-expression CD56 and CD8, in the majority cases.A A study with a greater number of cases is necessary to define biological prognosis factors

1354 Hematogones with Light-Chain Restriction Detected by Flow Cytometry Immunophenotypic Analysis: A Diagnostic Pitfall in Staging Bone Marrow Evaluation
Siba El Hussein[1], Pramoda Challagundla[2], Jeff Jorgensen[1], Mahsa Khanlari[1], Mehrnoosh Tashakori[1], L. Jeffrey Medeiros[1], Wei Wang[1]
[1]The University of Texas MD Anderson Cancer Center, Houston, TX, [2]Pfizer, Groton, CT

Disclosures: Siba El Hussein: None; Pramoda Challagundla: None; Jeff Jorgensen: None; Mahsa Khanlari: None; Mehrnoosh Tashakori: None; L. Jeffrey Medeiros: None; Wei Wang: None

Background: Hematogones (HGs) are B-cell precursors of different stages of maturation. They characteristically lack surface light-chain expression in early stages and a subset of cells exhibits polytypic light-chain expression in late stages. HGs with light-chain restriction (LCR) are extremely rare. We have occasionally encountered such rare cases detected by flow cytometry analysis (FCA).The aim of this study is to describe and summarize the key features helpful in recognizing LCR- HGs, as well as features to distinguish between LCR- HGs and lymphoma cells.

Design: We collected 24 staging bone marrow (BM) cases over a 10-year interval in which FCA showed LCR-HGs. We reviewed clinical information of underlying hematologic malignancy, bone marrow status and treatment. The immunophenotype of HGs as well as their percentage and duration time were analyzed.

Results: All 24 patients had a history of hematologic neoplasm and bone marrow biopsy was performed for staging. Nine (37%) BM specimens were involved by hematologic neoplasms including 3 diffuse large B-cell lymphoma (DLBCL),2 follicular lymphoma (FL),2 multiple myeloma (MM),1 mantle cell lymphoma (MCL) and 1 hairy cell leukemia (HCL).The remaining 15 (63%) BM specimens were negative for lymphoma including 4 DLBCL,4 MCL,3 FL,1 HCL,1 MM,1 extranodal marginal zone lymphoma and 1 Hodgkin lymphoma. Eleven(46%) cases showed persistent LCR-HGs in more than 1 FCA sample, and the duration of monotypic HGs ranged from 4 months to up to 2 years. Kappa LCR was seen in 13(54%) cases, whereas lambda LCR was seen in 11(46%) cases. The percentages of LCR-HGs ranged from 1.5 % to 99%(median,51%) of B cells. HGs demonstrated a distinct location on the CD45/side Scatter(SSC) plot, with dim CD45 and a low side scatter. The HGs were consistently positive for CD10, CD19,CD38(bright),CD43,and CD200.The major challenge was distinguishing LCR-HGs from CD10-positive lymphoma cells (such as FL),which are typically located in the lymphocyte gate with brighter CD45 on CD45/SCC plots, express dimmer CD19 and CD38,and are negative for CD43.In addition, the CD10/CD20 plot in FL cases does not show the characteristic maturation pattern seen in HGs.

Figure 1 - 1354
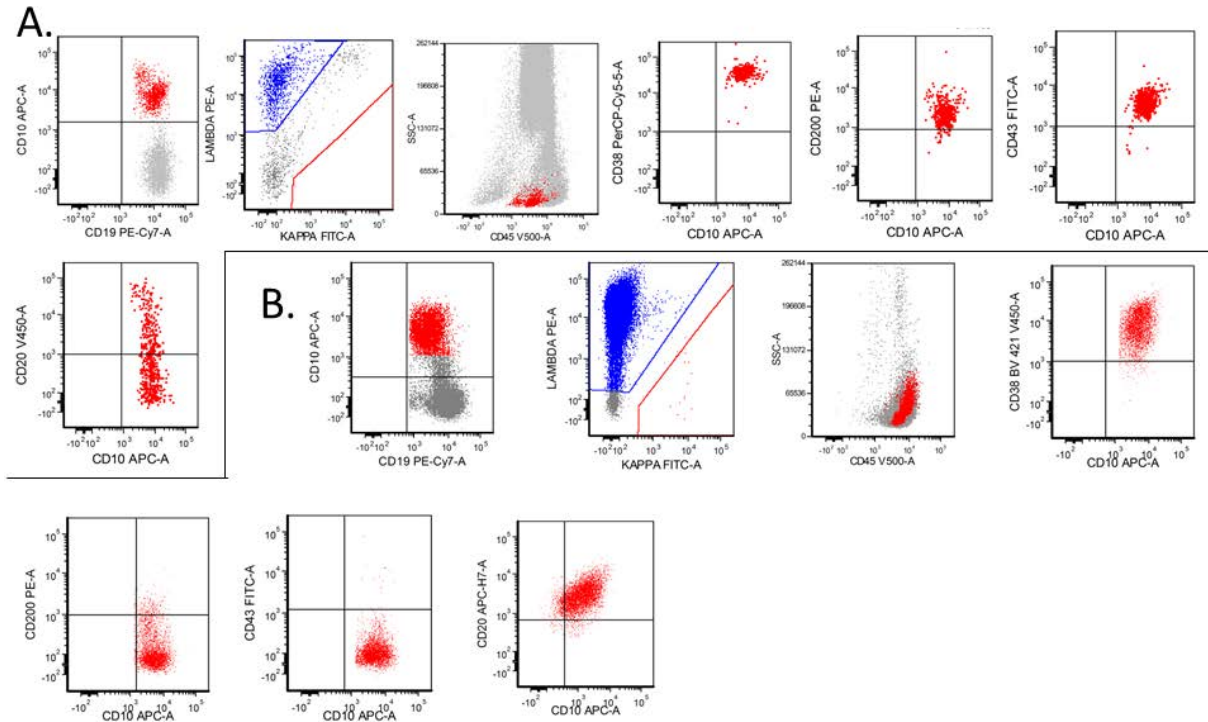
A. Light chain restricted hematogones

B. Light chain restricted follicular lymphoma

Conclusions: Recognizing basic patterns of HGs presentation on FCA is fundamental for accurate assessment of BM staging. Actively looking for a HG-like pattern on CD45/SSC, and checking the status of CD10,CD19,CD38,CD43,and CD200 are good strategies to unveil the presence of LCR-HGs and avoid misdiagnosing an LCR-population as lymphoma.

1355 Whole Exome Sequencing of Acute Leukemias with Heterogeneous Cytoplasmic CD3 Expression

Mohammad Eldomery[1], Rohit Gulati[1], Lin Wang[1], Magdalena Czader[2]
[1]Indiana University School of Medicine, Indianapolis, IN, [2]Indiana University, Indianapolis, IN

Disclosures: Mohammad Eldomery: None; Rohit Gulati: None; Lin Wang: None; Magdalena Czader: None

Background: Diagnosis of acute leukemia is straightforward in the majority of cases with flow cytometric immunophenotyping playing a pivotal role in classifying leukemias into B and T lymphoblastic, and myeloid lineages. Rare leukemias lack distinct features of one lineage and those are assigned to categories of acute undifferentiated or mixed phenotype leukemias. The majority of T lymphoblastic leukemia/lymphomas (T-LL) are defined by a strong positivity for CD3 antigen with an intensity close to that seen in normal residual T-cells. However, rare cases show a weaker expression of cytoplasmic CD3 antigen (cCD3). In this study, we investigate the

immunophenotypic and molecular characteristics of rare cases of acute leukemias with a dim and heterogeneous cytoplasmic CD3 expression.

Design: We identified 9 patients with acute leukemia displaying dim to heterogeneous cCD3 (7 T lymphoblastic leukemia/lymphoma, 1 acute myeloid leukemia, NOS, 1 mixed phenotype acute leukemia, T/myeloid; age range 2-49 years, 4 males). All patient underwent Whole Exome Sequencing (WES). Variant calling was executed by GATK MuTect2. Variant Calling File (VCF) and Mutation Annotation File (MAF) were generated by Oncotator software. Manual variant curation in accordance with American College of Medical Genetics and Genomics and Association of Molecular Pathology guidelines was followed to identify potential driver genes. Subsequent bioinformatics analysis was performed using MAF tools – R package to further characterize the frequency of the most altered genes and molecular pathways.

Results: All but one T-LL patient were classified as early T-cell precursor (ETP) lymphoblastic leukemia and 5 showed coexpression of CD56 antigen. The genetic alterations of RTK-RAS pathway were frequent (Figure. 1) and included *NRAS* G12D/G13D in 3 patients; *PTPN11* in two patients (including co-occurrence with *NRAS* in one patient*)*; *ALK, FLT3* and *KRAS*. Co-occurrence of RTK-RAS with WNT pathway mutations was seen in three patients and co-occurrence of RTK-RAS with NOTCH mutations was also observed in two other patients. *DNMT3A* with *ALK* mutations were also detected in one patient. *RUNX1 and NOTCH1* mutations each were found in separate patients.

Figure 1 - 1355
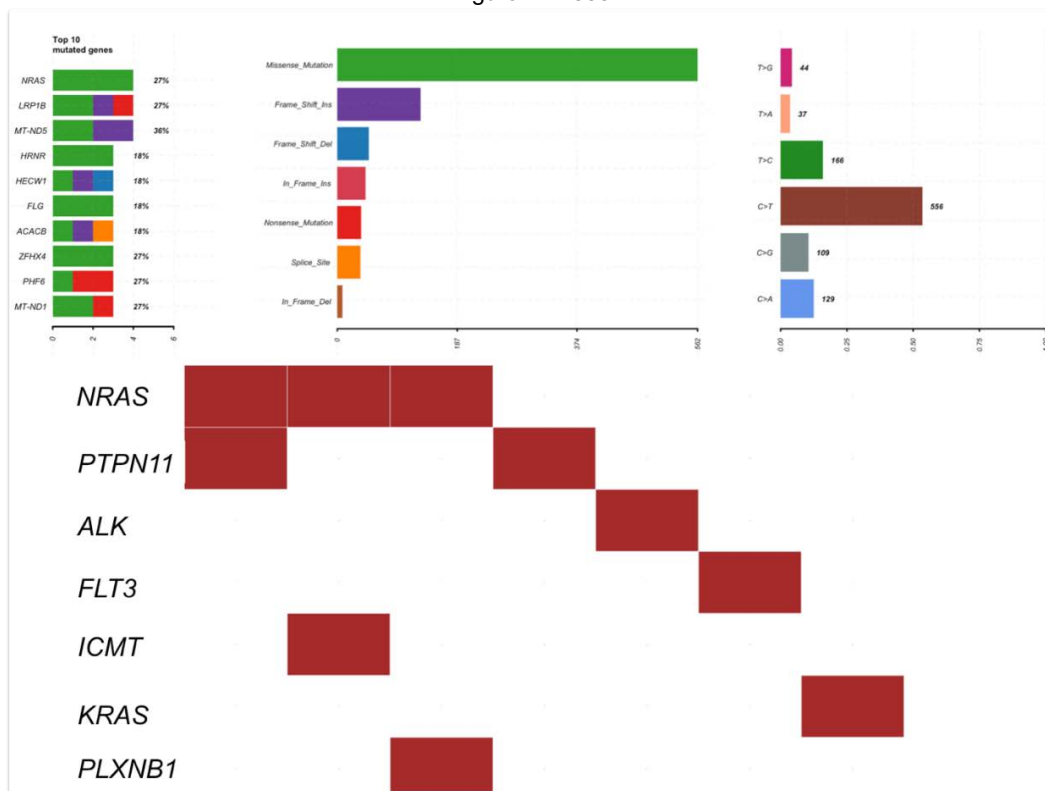
Conclusions: RTK-RAS, WNT and NOTCH pathways are most frequently involved in patients with acute leukemia displaying heterogeneous cCD3 expression. The involvement of RTK-RAS pathway has been previously reported in ETP T-LL.

1356   MDM2 and MDM4 Dual Inhibitor ALRN-6924 Upregulates p21 Expression in Myelodysplastic Syndrome and Acute Myeloid Leukemia

Mohammad Eskandari[1], John Liu[2], Yang Shi[3], Joseph Albanese[4], Swati Goel[3], Amit Verma[5], Yanhua Wang[5]
[1]Altru Health System, Grand Forks, ND, [2]Rensselaer Polytechnic Institute, Bronx, NY, [3]Montefiore Medical Center, Albert Einstein College of Medicine, Bronx, NY, [4]Montefiore Medical Center, Bronx, NY, [5]Albert Einstein College of Medicine, Bronx, NY

Disclosures: Mohammad Eskandari: None; John Liu: None; Yang Shi: None; Joseph Albanese: None; Swati Goel: None; Amit Verma: None; Yanhua Wang: None

Background: MDM2 and MDM4 (also named MDMX) are oncogenes highly expressed in many malignancies. P53 together with its downstream product p21 as tumor suppressors play an important role in tumorigenesis. MDM2 and MDM4 regulate the functions of p53 tightly by degradation via ubiquitination and direct binding. ALRN-6924 (Aileron), a stapled a-helical peptide can bind to MDM2 and MDM4 and serves as a dual inhibitor. However, its effect on p53 and p21 has not been illustrated on human acute myeloid leukemia (AML) and myelodysplastic syndrome (MDS).

Design: The expression of MDM2, MDM4, p53 and p21 in the bone marrow biopsies from 120 patients with MDS/Myeloproliferative neoplasms (MPNs) or AML, and benign bone marrow biopsies, including 18 samples before and after MDM2/MDM4 dual inhibitor ALRN-6924 (Aileron) treatment is assessed by immunohistochemistry (IHC). Double immunohistochemical stain is used to localize the expression of MDM2/p53 and MDM4/p53. TP53 mutation status is analyzed by next generation sequencing (NGS).

Results: We found that p53 expression detected by immunohistochemistry had a similar prognostic value compared to TP53 mutational status by NGS (Figure 1). Loss of p21expression is identified in almost all TP53 mutated cases. The MDM4+ hematopoietic cells were more than MDM2+ cells in benign, MDS/MPNs and AML; however, MDM2/p53 double positive cells were more than MDM4/p53 positive cells in MDS/MPNs and AML cases. P21 protein expression was up regulated after the use of MDM2/MDM4 dual inhibitor in MDS/AML cases (Table 1).

Table 1. p21 expression before and after ALRN-6924 treatment

Case #	Age	Sex	Diagnosis	Cytogenetic	Pre-p21	Post-P21
1	88	F	MDS	-7	ND	10%
2	80	F	MDS	-11q	2%	10%
3	66	M	MDS	normal	5-10%	>10%
4	68	F	MDS	-11q	1%	10%
5	45	F	AML	t(7:14)	ND	1%
6	38	M	AML	t(9;22), -11	ND	Tissue insufficient
7	65	M	MDS	-7	1%	5%
8	84	F	AML	+8	10%	10%
9	21	F	MDS	-7, complex karyotype	ND	1%

ND: not done

Figure 1 - 1356
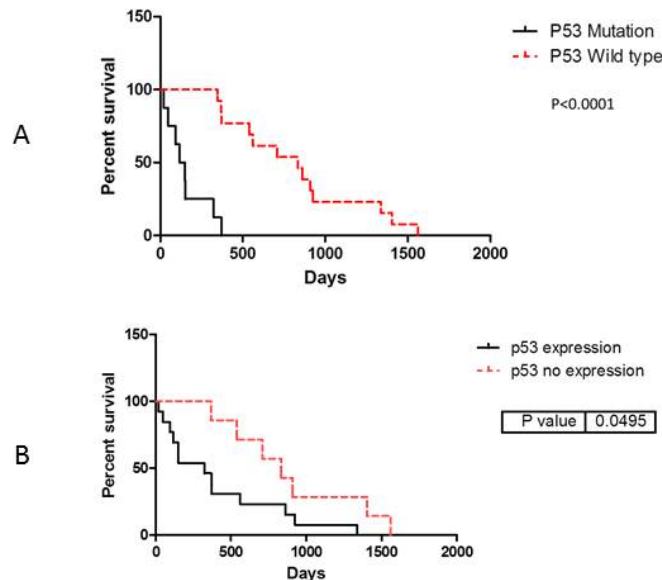
Conclusions: Our study showed that MDM2 and MDM4 were highly expressed in hematopoietic cells in both benign bone marrow biopsies and MDS/MPNs/ AML cases, with MDM4+ cells more prevalent than MDM2+ cells. Expression of p53 by IHC had a good correlation with TP53 mutation status and the high expression of P53 was associated with a poor clinical outcome. P21 expression was inversely related to the p53 expression or TP53 mutation status. The treatment effect of ALRN-6924 (Aileron) in MDS/AML was probably through up regulating p21 in p53 pathway, yet the exact mechanism needed to be elucidated.

1357 Morphologic Spectrum of Myeloid Neoplasm with t(v;11p15); NUP98 Rearrangement

Lauren Eversmeyer[1], Zhongxia Qi[1], Sonam Prakash[1], Jingwei Yu[1], Linlin Wang[1]
[1]University of California San Francisco, San Francisco, CA

Disclosures: Lauren Eversmeyer: None; Zhongxia Qi: None; Sonam Prakash: None; Jingwei Yu: None; Linlin Wang: None

Background: Chromosome rearrangements involving *NUP98* at 11p15 are rare but recurring abnormalities in AML. The *NUP98* gene, encoding a nucleoporin can be fused to a number of genes through chromosome translocation similar to those observed in *MLL*. However, t(v;11p15) with rearranged *NUP98* is not included as an entity in the 2017 WHO classification. We aimed to study morphologic, immunophenotypic, molecular and clinical features of myeloid neoplasms with t(v;11p15).

Design: Six cases of adult myeloid neoplasms with 11p15 abnormalities were identified from 2008-2019. 5/6 cases were positive for *NUP98* rearrangement by FISH. Among them, 3 cases including 2 de novo AML and 1 MDS/MPN with increased blasts showed t(7;11)(p15;p15);*NUP98-HOXA9*; 1 case of therapy related AML (t-AML) showed t(2;11)(q11;p15);*NUP98-HOXD11*; 2 cases including t-AML and CML with myeloid blast crisis showed t(9;11)(p22;p15);*NUP98-PSIP1*.

Results: The 3 cases of myeloid neoplasm with t(7;11)(p15;p15) showed similar blast morphology with Auer rods and cytoplasmic granules with or without perinuclear hoff. Flow cytometry showed high side scatter in 1/3 cases, blasts with no (2/3) or variable (1/3) HLA-DR expression, variable/weak CD34 expression (2/3), and MPO expression (3/3). These features mimic acute promyelocytic leukemia (APML). One case of t-AML with t(2;11)(q11;p15) showed cytoplasmic granules and perinuclear hoff but no Auer rods. Two cases of AML with t(9;11)(p22;p15) showed no or rare Auer rods, scant cytoplasmic granules with or without perinuclear hoff. Mutations identified in these 5 cases included *WT1*, *KRAS*, *NRAS*, *GATA2*, *CSF3R*, *TET2*, *FLT3*-ITD, *CBL* and *RUNX1*. Patient age ranged from 25-72 years and included 3 women and 2 men. The follow-up time ranged from 2-20 months. 5 cases showed persistent disease and 1 case is in remission after allogeneic-transplant.

Conclusions: Myeloid neoplasms with 11p15;*NUP98* rearrangements show a disease spectrum including de novo AML, t-AML, CML with myeloid blast crisis and MDS/MPN with increased blasts and are usually resistant to therapy. The partners of *NUP98* rearrangements may play important roles in morphology and pathogenesis of the disease. In particular, t(7;11)(p15;p15); *NUP98-HOXA9* appears to be associated with features that mimic APML. Whereas, t(2;11)(q11;p15) *NUP98-HOXD11* and t(9;11)(p22;p15) *NUP98-PSIP1* appear to be associated with therapy-related and/or progressing disease with different morphologic features.

1358 T(6;14)(q25;q32) Involves BCL11B and is Highly Associated with Mixed Phenotype Acute Leukemia, T/Myeloid

Hong Fang[1], Hannah Beird[1], Shimin Hu[1], Carlos Bueso-Ramos[1], Guilin Tang[1], Zhenya Tang[1], M. James You[2], Joseph Khoury[1], L. Jeffrey Medeiros[1], Wei Wang[1]
[1]The University of Texas MD Anderson Cancer Center, Houston, TX, [2]Houston, TX

Disclosures: Hong Fang: None; Hannah Beird: None; Shimin Hu: None; Carlos Bueso-Ramos: None; Guilin Tang: None; Zhenya Tang: None; M. James You: None; Joseph Khoury: None; L. Jeffrey Medeiros: None; Wei Wang: None

Background: T(6;14)(q25;q32) has been described in the form of rare case reports in hematopoietic malignancies and *BCL11B* on chromosome 14q32 is potentially involved. The impact of the t(6;14) on expression of *BCL11B* and the clinicopathologic features of cases carrying this translocation are not explored. In this study, we systemically characterized the hematopoietic neoplasms carrying t(6;14)(q25;q32).

Design: In total, 19 cases of hematopoietic neoplasms carrying t(6;14)(q25;q32) were collected. Whole genome sequencing and Sanger sequencing were conducted to characterize the genes involving t(6;14)(q25;q32). RNAseq analysis and immunohistochemistry were performed to measure mRNA and protein levels in these cases respectively. Their clinicopathological features are also characterized.

Results: Whole genome and Sanger sequencing demonstrated that *BCL11B* was involved in t(6;14)(q25;q32) and that the breakpoint was located in the 3'-untranslated region of the gene. We further demonstrate that *BCL11B* was integrated into an intergenic region on chromosome 6q25. The translocation was associated with increased *BCL11B* expression at both mRNA and protein levels. No fusion transcripts were detected.

Of these 19 cases, 15 (79%) had a diagnosis of mixed-phenotype acute leukemia (MPAL), T/myeloid. Four of 5 (80%) cases tested for *FLT3* mutation showed *FLT3* internal tandem duplication and/or D835 mutations. Of 3 cases with known *NRAS* and *WT1* mutation status, all (100%) showed mutations in *NRAS* and *WT1*. Finally, we measured BCL11B expression in MPAL, T/myeloid without t(6;14)(q25;q32) and the result showed that about half of MPAL, T/myeloid cases without 14q32 abnormalities overexpress BCL11B.

Conclusions: T(6;14)(q25;q32) is rare and involves *BCL11B* being translocated to a non-coding region of chromosome 6. This translocation induces BCL11B expression at both mRNA and protein levels and is highly associated with the T/myeloid subtype of MPAL.

Mutations in *FLT3*, *NRAS* and *WT1* are common in these neoplasms. BCL11B expression is not limited to cases with t(6;14)(q25;q32) and about half of MPAL, T/myeloid cases without t(6;14)(q25;q32) were positive for BCL11B, suggesting other alternative mechanisms mediating BCL11 expression in these neoplasms.

1359 Myelodysplastic Syndrome with t(6;9)(p22;q34.1) Categorized as Acute Myeloid Leukemia: A Large Multicenter Study of 105 Cases

Hong Fang[1], Mariko Yabe[2], Xiaohui Zhang[3], Young Kim[4], Yulei Shen[5], Lina Shao[6], Yuan Ji[7], Xiaojun Wu[8], Gang Zheng[9], Qi Shen[10], Yongzhong Yuan[11], Rong He[9], Dong Chen[9], L. Jeffrey Medeiros[1], Shimin Hu[1]
[1]The University of Texas MD Anderson Cancer Center, Houston, TX, [2]Memorial Sloan Kettering Cancer Center, New York, NY, [3]Moffitt Cancer Center, Tampa, FL, [4]City of Hope National Medical Center, Duarte, CA, [5]Henry Ford Hospital, Detroit, MI, [6]University of Michigan, Ann Arbor, MI, [7]University of Nebraska Medical Center, Omaha, NE, [8]Johns Hopkins School of Medicine, Baltimore, MD, [9]Mayo Clinic, Rochester, MN, [10]Winter Park, FL, [11]AmeriPath/Quest Diagnostics, Shelton, CT

Disclosures: Hong Fang: None; Mariko Yabe: None; Xiaohui Zhang: None; Young Kim: None; Yulei Shen: None; Lina Shao: None; Yuan Ji: None; Xiaojun Wu: None; Gang Zheng: None; Qi Shen: None; Qi Shen: None; Yongzhong Yuan: None; Rong He: None; Dong Chen: None; L. Jeffrey Medeiros: None; Shimin Hu: None

Background: The t(6;9)(p23;q34.1)/*DEK-NUP214* is a recurrent genetic abnormality that occurs in a subset of cases of acute myeloid subset leukemia (AML) and rarely in myelodysplastic syndrome (MDS). However, it is not known whether all cases with t(6;9) (p23;q34.1) should be categorized as AML when blast count is <20%. In this study, we characterized and compared the clinicopathologic features of patients with MDS versus AML harboring t(6;9)(p23;q34.1).

Design: Cases of AML or MDS carrying t(6;9)(p23;q34.1), diagnosed in 10 institutions, were collected and their clinicopathologic features were reviewed retrospectively.

Results: The study cohort included 105 patients with t(6;9): 75 patients with AML and 30 with MDS. In all 98 patients with available data, the t(6;9) was detected at initial diagnosis of AML or MDS. There were 53 men and 52 women with a median age of 44 years (range, 10-82) at initial diagnosis. Patients with AML were slightly younger than patients with MDS (median: 39 *vs.* 52 years) but this difference was not significant (*P*=0.08). As expected, patients with AML presented with leukocytosis and higher blast counts in peripheral blood and bone marrow (*P*=0.009, 0.004, <0.0001, respectively). However, no significant differences were observed in the hemoglobin level, platelet count, and basophil percentages in peripheral blood and bone marrow between patients with MDS versus AML.

The median follow up time was 21.8 months. Of 30 patients with MDS, 17 (57%) developed AML after a median interval of 29 months (range, 1-94). There was no difference in overall survival between patients with MDS versus AML (median: 33.9 *vs.* 23.7 months, *P*=0.45). Fifty-seven patients received stem cell transplant during their clinical course. Patients who received transplant had longer overall survival than the non-transplant group (median: not reached *vs.* 17.3 months, *P*<.0001). After stratification by status of transplant, however, there were no significant differences between patients with MDS and patients with AML.

Conclusions: Our data support the idea that myeloid neoplasms associated with t(6;9), irrespective of blast percentage, are best categorized as acute myeloid leukemia with recurrent genetic abnormalities, analogous to the WHO classification guidelines for myeloid neoplasms with t(8;21) and inv(16). Aggressive treatment strategies such as stem cell transplant might improve the survival of patients with myeloid neoplasms associated with t(6;9).

1360 Overexpression of MDM2 is Associated with Poor Prognosis and Drug Resistance in Myeloma and Inhibition of MDM2 by MX69 Leads to Apoptosis of Myeloma Cells

Omar Faruq[1], Davidson Zhao[2], Jian Wu[3], Min Zhang[3], Hong Chang[4]
[1]UHN, Toronto, ON, [2]Department of Laboratory Medicine and Pathobiology, Faculty of Medicine, University of Toronto, Toronto, ON, [3]Toronto General Hospital/University Health Network, Toronto, ON, [4]Toronto, ON

Disclosures: Omar Faruq: None; Davidson Zhao: None; Jian Wu: None; Min Zhang: None; Hong Chang: None

Background: Multiple myeloma (MM) is a plasma cell malignancy that is incurable in part due to its high resistance to drug-induced apoptosis. Mouse double minute 2 homolog *(MDM2)* and X-linked inhibitor of apoptosis protein *(XIAP)* are oncogenes that confer resistance to radio- and chemo-therapy. However, their prognostic significance is unclear, and the effect of the newly discovered dual *MDM2* plus *XIAP* inhibitor MX69, is unknown in MM.

Design: *MDM2* and *XIAP* expression were analyzed from GEO and NIH CoMMpass datasets. Western blotting and qRT PCR of MM cell lines were used to quantify gene expression. Cell proliferation and apoptosis were detected by Cell Counting Kit-8 and FACS analysis after MX69 treatment.

Results: High expression of *MDM2* and *XIAP* in the GSE9782 dataset correlates with shorter overall survival in MM patients (median 14.7 vs 24.2 months and 15.3 vs 22.5 months, P=0.0011 and P=0.0072, respectively). CoMMpass dataset analysis revealed high expressions of *MDM2* and *XIAP* are correlated with advanced stage of MM (P<0.0001 and P=0.0073, respectively) and with significantly shorter progression-free survival (median 26.3 vs 36.6 months and 26.2 vs 39.3 months, P=0.0047 and P<0.0001, respectively). Analysis of GSE2658 and GSE38627 revealed that MDM2 expression increased at MM relapse compared to their original paired diagnosis samples (P<0.0001).

We recently reported that MX69 reduces MM cell proliferation, but it remains unclear whether MX69 exerts cytotoxic effects as well. Here, we show that MX69 activates the pro-apoptotic TP53 pathway and induces cell death in MM cell lines and primary MM samples. Inhibition of *MDM2* expression, stabilization of wild-type TP53 and induction of apoptosis by MX69 involved modulation of multiple apoptotic regulatory proteins (Bcl-2/Bcl-xL) and activation of caspases through the extrinsic pathway. In MM TP53-null cells, we found that MX69 treatment induced TP53 family pro-apoptotic factors p63 and p73, reduced c-MYC oncogene expression and increased apoptotic activator BAX-3.

Conclusions: Our results indicate that *MDM2* overexpression is associated with disease progression and drug resistance in MM. Treatment with *MDM2/XIAP* dual inhibitor MX69 induced apoptosis in otherwise drug resistant MM cells by activation of extrinsic caspase pathway.

1361 Absolute Lymphocyte Count Kinetics Correlates with Response and Toxicity in CAR T Cell Therapy

Sophia Faude[1], Vinodh Pillai[2], Michele Paessler[3], Gerald Wertheim[4]
[1]Children's Hospital of Philadelphia, Philadelphia, PA, [2]The Children's Hospital of Philadelphia, Penn Valley, PA, [3]The Children's Hospital of Philadelphia, Newtown, PA, [4]Children's Hospital of Philadelphia, University of Pennsylvania, Philadelphia, PA

Disclosures: Sophia Faude: None; Vinodh Pillai: None; Michele Paessler: None; Gerald Wertheim: None

Background: Chimeric antigen receptor (CAR) modified T cell therapy is approved for treatment of B-Acute Lymphoblastic Leukemia and Diffuse Large B cell lymphoma. CAR T cell therapy is associated with adverse effects such as cytokine release syndrome (CRS) and neurotoxicity (NT) that are difficult to predict. The histomorphological, immunophenotypic and laboratory aspects of CAR T cell therapy and their correlation with toxicity and efficacy are not well understood. Here, we analyzed the laboratory aspects of CAR T cells and correlated them with outcome and toxicity.

Design: 178 patients with B-ALL who received CAR T cell therapy at our institution from 2012-2017 were identified. Complete blood counts, CSF counts and flow cytometric data from pre and post-CAR time points were analyzed. CAR T cell expansion was estimated from absolute lymphocyte counts (ALC) and CD3, CD4 and CD8 immunophenotypic data. EMR data was used to classify responses, grade CRS (grades 0-5, CTCAE guidelines) and NT (grades 0-5). Morphology of CAR T cells were reviewed from archived slides and images. Archived bone marrow (BM) biopsies, aspirate smears, and BM flow cytometry data were analyzed. Expression of CD3, CD4, CD8, and perforin were assessed using IHC on pre and post-CAR bone marrows.

Results: CAR T cell kinetics were plotted using peripheral blood ALC (n=41) and absolute CD3 counts (n=13) and showed rapid expansion between 7-14 days post infusion, contraction between 14-21 days, and then plateau. ALC expansion at day 30 was significantly greater in responders compared to non-responders (Mann-Whitney test, p=.0004*). ALC kinetics was independent of pre-treatment disease burden. Pre-CAR CD4:8 ratio was significantly greater than post-CAR CD4:8 ratio (Mann-Whitney test, p=.0004*). CSF showed a similar ALC expansion from the pre-CAR to post-CAR timepoint (n=162) that correlated with severity of NT (NT=0,1 vs NT=2,3,4,5, Mann-Whitney test, p=.049*). Immunophenotypic analysis of post-infusion BMs revealed scattered interstitial and loose aggregates of CD3+ lymphocytes with reversed CD4:CD8 ratio and prominent perinuclear granules (n=29).

Conclusions: CAR T cell kinetics differ from standard pharmacokinetics. They show expansion, contraction and plateau that can be followed by ALC and CD3 counts. Peripheral blood ALC expansion was correlated with response. CD8+ CAR cells are preferentially expanded *in vivo*. CSF ALC correlates with NT. CAR T cells resemble activated T cells during expansion and normal LGL in the quiescent phase.

1362 Human Endogenous Retrovirus Expression in HIV-associated Diffuse Large B-cell Lymphoma

Yuri Fedoriw[1], Nathan Montgomery[2], Tamiwe Tomoka[3], Maurice Mulenga[4], Satish Gopal[5], Sara Selitsky[5]
[1]University of North Carolina, Pittsboro, NC, [2]University of North Carolina, Chapel Hill, NC, [3]UNC Project Malawi, Lilongwe, Malawi, [4]Kamuzu Central Hospital, Lilongwe, Malawi, [5]University of North Carolina

Disclosures: Yuri Fedoriw: None; Tamiwe Tomoka: None; Maurice Mulenga: None

Background: Human endogenous retroviruses (ERVs) are viral elements integrated into the genome that are associated with health and disease, including autoimmunity, cancer, and chronic viral infections. ERVs are up-regulated by HIV, and some anti-retroviral therapy drugs may cause a decrease in ERV expression, specifically the in the HERV-K family. The association of ERVs, HIV, and ART has not been assessed in Diffuse Large B-cell Lymphoma (DLBCL) despite its association with HIV infection.

Design: The whole transcriptome from 36 pre-treatment cases of DLBCL (21 HIV+/15 HIV-) from the Kamuzu Central Hospital Lymphoma Study in Lilongwe, Malawi was computationally interrogated for ERV expression using a method we previously reported, hervQuant. Expression patterns were analyzed by HIV status, ART duration, and compared to clinical outcomes and other clinical and laboratory HIV-related variables, including CD4 count.

Results: Of 21 HIV+ DLBCL, 11 were ART naïve, and 10 were ART experienced (therapy >6 months at diagnosis). HIV status was not associated with overall survival differences (p=0.3803). ERV expression was identified in all cases of DLBCL. Independent of HIV status, 500 of 2,579 (19%) ERVs were associated with prognosis (p<0.05), with high expression associating with inferior overall survival. ERVs were up-regulated in HIV+ and ART-naïve patients compared to HIV- patients, and down-regulated in HIV+ and ART-experienced patients compared to those without HIV (p=0.02, ANOVA). ERV expression was not associated with CD4 count.

Conclusions: In other cancers, immune response directed against ERV epitopes has been well documented, but patterns of expression in HIV associated DLBCL have not been reported. In this study, we identify an inferior overall survival in DLBCL associated with increased ERV expression. We also show that HIV and ART status significantly impact ERV expression levels in DLBCL. Whether ERV contributes to lymphoma development or effective host response to tumor in this setting remains uncertain. However, we uniquely show that expression of ERVs in HIV+ DLBCL correlates with ART duration. These data will inform future study of endogenous retroviruses in the setting of HIV infection and lymphoma.

1363 PD-L1 and CD8 Expression Correlate with Aggressive Behavior of Breast Implant Anaplastic Large Cell Lymphoma Cells

Maria Ferrufino-Schmidt[1], Daniela Duenas[2], Edwin Parra[3], Luisa Solis Soto[3], Jiexin Zhang[3], Mark Clemens[3], L. Jeffrey Medeiros[3], Beatriz Sanchez-Espiridion[3], Moumita Chakraborty[3], Mario Marques-Piubelli[3], J. Jack Lee[3], Ignacio Wistuba[3], Roberto Miranda[3]
[1]The University of Texas MD Anderson Cancer Center, Lima, Lima, Peru, [2]Instituto Nacional de Enfermedades Neoplásicas, Lima, Peru, [3]The University of Texas MD Anderson Cancer Center, Houston, TX

Disclosures: Maria Ferrufino-Schmidt: None; Daniela Duenas: None; Edwin Parra: None; Luisa Solis Soto: None; Jiexin Zhang: None; Mark Clemens: None; L. Jeffrey Medeiros: None; Beatriz Sanchez-Espiridion: None; Moumita Chakraborty: None; Mario Marques-Piubelli: None; J. Jack Lee: None; Ignacio Wistuba: None; Roberto Miranda: None

Background: Breast implant anaplastic large cell lymphoma (BI ALCL) is a T-cell lymphoma that arises around breast implants, usually confined by a fibrous capsule. In most patients, the disease presents as an effusion, but a subset presents as a mass that can invade through the capsule into adjacent tissues and can metastasize to regional lymph nodes. The mechanisms associated with tumor progression are unknown. To better define the cellular mechanisms associated with tumor progression, we analyzed BI ALCL cases using multiplex immunofluorescence (mIF).

Design: 16 invasive and 3 superficial BI ALCL cases (Table 1) were analyzed using 2 mIF panels, both with CD30 to identify malignant cells. Panel 1: CD3, CD8, CD30, CD68, PD-1, PD-L1 and DAPI. Panel 2: CD3, CD8, CD30, CD45RO, FOXP3, granzyme B and DAPI. Slides were scanned with a multispectral microscope (Vectra™ 3.0.5, PerkinElmer). Tumor areas were analyzed using InForm2.4.4 software (PerkinElmer) (Fig. 1). Cell phenotypes were consolidated as cells/mm^2. Immunohistochemistry (IHC) was added to test other antibodies: T-bet/TBX21; OX-40/CD134 and TIA-1. Mann-Whitney U test, Spearman's correlation and Kaplan-Meir estimate were performed.

Results: 17 different cell phenotypes were identified. Total macrophages had a higher density in tumor areas than in non-tumor areas (p= 0.03), and PD-L1 expression by neoplastic cells positively correlated with the expression of PD-L1 by macrophages (r= 0.53; p=0.02).

By mIF 25% (4/16) invasive cases had PD-L1+ lymphoma cells, compared with zero superficial cases (p= 0.03). By IHC, lymphoma cells of invasive cases were positive for T-bet in 7/16 (44%); OX-40 in 7/16 (44%), and TIA-1 in 9/16 (56%). Lymphoma cells of 3 superficial cases were positive for T-bet in 1/3 (33%); TIA-1 in 2 (67%) cases, and all were negative for OX-40.

Patients with lymphoma cells expressing CD8+ had poorer OS than patients whose lymphoma cells lacked CD8 (median OS: 24 months vs undefined; p= 0.007).

Table 1. Clinical and pathologic findings of 19 patients with BI-ALCL									
#	Age	Sex	Side of tumor	Reason for implant	Clinical presentation	MDACC pathological stage at Diagnosis*	Breast capsule involvement	Follow-up (months)	Endpoint**
1	63	F	Right	Breast cancer reconstruction	Breast effusion	T4	Invasive	163	DOUD
2	41	F	Right	Cosmetic	Breast mass	T4	Invasive	20	CR
3	61	F	Left	Cosmetic	Breast mass	T4	Invasive	1	CR
4	52	F	Right	Cosmetic	Breast effusion	T4	Invasive	6	DOD
5	70	F	Left	Cosmetic	Breast mass	T4	Invasive	42	CR
6	52	F	Left	Cosmetic	Breast effusion	T4	Invasive	5	CR
7	72	F	Left	Breast cancer reconstruction	Breast mass	T4	Invasive	30	AWD
8	56	F	Left	Cosmetic	Breast effusion	T4	Invasive	7	CR
9	53	F	Right	Cosmetic	Breast mass	T4	Invasive	66	AWD
10	51	F	Right	Cosmetic	Breast mass	T4	Invasive	64	CR
11	65	F	Right	Cosmetic	Breast effusion	T4	Invasive	20	AWD
12	54	F	Right	Cosmetic	Breast effusion	T4	Invasive	12	CR
13	62	F	Left	Breast cancer reconstruction	NA	T4	Invasive	14	CR
14	45	F	Right	Cosmetic	Breast effusion	T4	Invasive	17	CR
15	47	F	Right	Breast cancer reconstruction	Breast mass	T4	Invasive	24	DOD
16	69	F	Right	Breast cancer reconstruction	NA	T4	Invasive	33	CR
18	48	F	Right	Cosmetic	Breast effusion	T2	Superficial	19	CR
19	76	F	Right	Breast cancer reconstruction	Breast effusion	T2	Superficial	55	DOUD
20	76	F	Left	Cosmetic	Breast effusion	T2	Superficial	63	DOUD
*Pathologic stage according to Clemens et al, J Clin Oncol 2016 and Quesada et al, Mod Pathol 2019.									
**Endpoint: CR: complete remission; DOD: dead of disease; DOUD: Dead of unrelated disease; AWD: alive with disease.									

Figure 1 - 1363
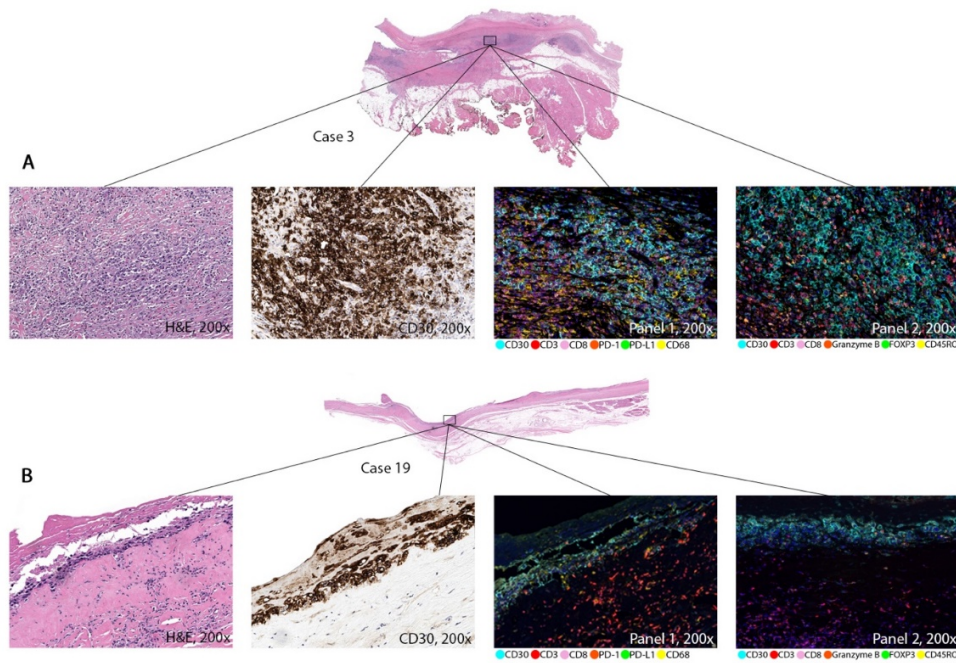
Figure 1. Microphotograph of an invasive case (A) and a superficial case (B) showing the images used for analysis

Conclusions: The mIF analysis allowed us to identify up to 17 cell phenotypes in cases of BI ALCL. The expression of PD-L1 was more frequently found in lymphoma cells and histiocytes in the invasive cases compared with the non-invasive cases, suggesting that the microenvironment of the invasive stage is mostly immunosuppressive, facilitating tumor progression. CD8 expression in BI ALCL is associated with decreased OS.

1364 Detection of Partial Tandem Duplications in KMT2A/MLL from RNA Using Next-Generation Sequencing with Anchored Multiplex PCR

Adam Fisch[1], Lucas Massoth[2], Dora Dias-Santagata[2], John Iafrate[2], Long Le[2], Jochen Lennerz[3], Valentina Nardi[2], Harrison Tsai[4]
[1]Massachusetts General Hospital, Cambridge, MA, [2]Massachusetts General Hospital, Boston, MA, [3]Massachusetts General Hospital, Harvard Medical School, Boston, MA, [4]Brigham and Women's Hospital, Boston, MA

Disclosures: Adam Fisch: None; Lucas Massoth: None; Dora Dias-Santagata: None; John Iafrate: *Stock Ownership*, ArcherDx; Long Le: *Advisory Board Member*, ArcherDx; *Stock Ownership*, ArcherDx; Jochen Lennerz: None; Valentina Nardi: None; Harrison Tsai: None

Background: The *KMT2A* gene (formerly *MLL*) on chromosome 11q23 encodes a histone H3 lysine 4 methyltransferase active in hematopoiesis. Recurrent partial tandem duplications (*KMT2A*-PTD) occur in 5-10% of patients with acute myeloid leukemia (AML), where they are associated with variably worse outcomes depending on the presence of additional cytogenetic abnormalities. *KMT2A*-PTD involves a subset of exons 2-10 or 3-11, depending on the exon numbering scheme used, and is typically detected via RT-PCR with multiple primer pairs for various potential exon boundaries. Recent next-generation sequencing (NGS) efforts have focused on *KMT2A*-PTD detection within DNA-based hematologic panels, however many laboratories do not currently test for this clinically relevant aberration. We investigated the feasibility to detect *KMT2A*-PTD within an RNA-based NGS assay routinely used in clinical laboratories to target gene fusions by anchored multiplex PCR (AMP).

Design: We examined a case series of all 38 patients at our institution in 2018, and additional patients from 2017 and 2019, who were diagnosed with AML and for whom NGS was performed to detect gene fusions by AMP. *KMT2A*-PTD was detected by a laboratory developed pipeline as an intragenic fusion of non-consecutive exons at the PTD boundaries, defined by transcript NM_005933, and by visualization of mapped reads via the Integrated Genomics Viewer (Broad Institute, Cambridge, MA).

Results: *KMT2A*-PTD was observed in 4 of the 38 patients (10.5%) in 2018 who had fusion testing on bone marrow biopsies diagnostic of AML; it was also observed in 5 patients from 2017 and 2019. There were 104-945 reads (mean = 516; SD = 261) supporting the PTD in the positive cases, which involved exons 2-8 in 5 cases, exons 2-10 in 3 cases, and exons 3-6 in 1 case.

Conclusions: Using targeted RNA sequencing via AMP to detect intergenic and intragenic gene fusions in hematopoietic malignancies, we are able to detect *KMT2A*-PTD in patients with AML, including the rarely described PTD of exons 3-6. The rate of detection via AMP was consistent with the reported prevalence in AML. The ability to diagnose *KMT2A*-PTD in AML using an NGS assay frequently performed on bone marrow specimens at many institutions eliminates the need for PTD testing through RT-PCR. Follow-up studies using DNA-based NGS are underway to assess its performance as a complementary assay, as well as for orthogonal validation.

1365 Myeloproliferative Neoplasms with Progression to Acute Myeloid Leukemia- Clonal Evolution or a Separate De Novo Myeloid Neoplasm?

Taylor Forns[1], Yue Zhao[1], Endi Wang[1]
[1]Duke University Medical Center, Durham, NC

Disclosures: Taylor Forns: None; Yue Zhao: None; Endi Wang: None

Background: Progression to acute myeloid leukemia (AML) from myeloproliferative neoplasm (MPN) has been widely debated as to whether the resulting AML is truly clonal evolution of the MPN or a therapy-related de novo myeloid neoplasm. We report a series of 13 patients with AML arising from MPN with a comprehensive analysis of cytogenetic and somatic mutation profiles to study whether AML arises from clonal evolution or a de novo clone.

Design: We identified 13 patients with MPN who later developed AML. Cytogenetic study and mutational analysis via next generation sequencing (NGS) or real-time PCR for JAK2 V617F mutation were used to compare cytogenetic and/or somatic mutation profiles between each MPN and AML to determine its evolution.

Results: Of 13 patients, 10 were male and 3 were female. Age at diagnosis of MPN ranged from 40 to 80 years with a median of 54 years. Types of MPN included 7 essential thrombocythemia, 4 polycythemia vera, 1 primary myelofibrosis, and 1 MPN-U. 10 of 12 cases tested showed JAK2 V617F mutation. 3 cases had cytogenetic analysis. Latency from MPN to AML ranged from 27 to 227 months with a median of 120 months. At diagnosis of AML, cytogenetic study showed a clonal abnormality in 9 of 10 cases tested. 10 of 12 cases tested showed JAK2 V617F mutation. Comparing cytogenetic and somatic mutation profiles between MPN and AML in each case, 11 were identified as clonal evolution owing to retention of its somatic mutation profile and/or persistence of cytogenetic abnormalities seen in MPN. The other 2 cases were thought to be de novo clonal processes due to either a much lower JAK2 mutation allele frequency than leukemic blast count or the gain of new cytogenetic abnormalities with loss of prior cytogenetic abnormalities. Kaplan survival analysis demonstrated a median survival of 4 months (CI=0-16.33) for the entire series. Of the 11 patients with clonal evolution, 8 died of disease with a median survival of 4 months (CI=0-16.75). Of the 2 patients with probable de novo AML, 1 died of disease progression 2 months after diagnosis. The other was enrolled in a clinical trial and was alive 10 months after diagnosis.

Conclusions: Transformation of MPN to AML exhibited a very poor outcome with the majority of AML being clonal evolution of the MPN. A minority of AML may arise from a de novo clone suggesting therapy may play a role in the progression of MPN. The underlying molecular mechanism and clinical significance of this distinction remain to be studied in larger cohorts.

1366 Neutrophil Extracellular Traps (NETs), Protease-Activated receptor-2 (PAR-2) and Fibrosis in Hodgkin's Lymphoma

Ivo Francischetti[1], Julie Alejo[1], Theresa Davies-Hill[1], Elaine Jaffe[1], Stefania Pittaluga[2]
[1]National Cancer Institute, National Institutes of Health, Bethesda, MD, [2]National Institutes of Health, Washington, DC

Disclosures: Ivo Francischetti: None; Julie Alejo: None; Theresa Davies-Hill: None; Elaine Jaffe: None; Stefania Pittaluga: None

Background: NETs formation is increasingly recognized as a major component promoting inflammation in numerous pathologic conditions, including cancer, autoimmunity and infectious diseases. NETs modulate inflammation by multiple mechanisms. For instance, NETs activate the coagulation cascade, leading to FXa and thrombin generation which plays a pivotal role in thrombosis. These enzymes, in addition to neutrophil elastase, activate Protease-Activated receptors (PARs) which signals through the ERK pathway. More recently, NETs have been implicated in promoting tissue fibrosis. However, whether and how NETs take part in lymphomagenesis remained elusive thus far.

Design: In classical Hodgkin`s lymphoma (cHL), Nodular Sclerosis subtype, intense neutrophilic and eosinophilic infiltrations are observed. We sought to determine whether NETs formation takes place in cHL, and whether HRS cells express PAR-2 and/or show ERK phosphorylation (p-ERK). We also interrogated whether tissue fibrosis is associated with NETs formation. Immunohistochemistry assays were employed to detected NETs (polyclonal antibody for citrullinated histones), PAR-2 (monoclonal antibody SAM11) and p-ERK (monoclonal antibody). Fibrosis was estimated with Masson`s trichome stain. We analyzed 25 cases of cHL: 14 nodular sclerosis (NS), 5 mixed cellularity (MC), 5 lymphocyte-rich (LR) and 1 lymphocyte-depleted (LD) subtypes. In addition, 4 cases of nodular lymphocyte-predominant HL (NLP HL) and 5 cases of follicular hyperplasia (FH) were analyzed.

Results: A great proportion of cHL NS cases (10/14, 72%) exhibits NETs formation. NETs were not detected in MC, LR and LD cHL subtypes, or in NLP HL, or in FH. In addition, in most cHL (22/25, 88%), at least 50% of HRS cells variably expressed PAR2 irrespective of the subtype. Moreover, in 56% of cHL (14/25), more than 50% of the HRS showed pERK nuclear staining. In contrast, most HRS in LR cHL were pERK dim or negative. Notably, all NS cHL cases that were positive for NETs showed intense fibrosis (10/10; 100%).

Conclusions: A picture emerges where the pleotropic effects of NETs may contribute to the inflammatory tumor microenvironment in cHL.

1367 Triple Positive (CD10+BCL6+MUM1+) Diffuse Large B-Cell Lymphomas Are a Heterogenous Group Enriched in Large B-Cell Lymphomas with IRF4 Rearrangement

Leonie Frauenfeld[1], Natalia Castrejón[2], Sebastian Streich[3], Annika Mayer[4], Barbara Mankel[4], Julia Steinhilber[5], Joan Enric Ramis-Zaldivar[2], Julia Salmeron-Villalobos[2], Irina Bonzheim[1], Magda Pinyol[6], Itziar Salaverria[7], Falko Fend[8], Olga Balagué[7], Elías Campo[2], Leticia Quintanilla-Fend[9]
[1]University of Tuebingen, Tübingen, Germany, [2]Hospital Clinic Barcelona, University of Barcelona, Barcelona, Spain, [3]University of Tuebingen, Tuebingen, Baden-Württemberg, Germany, [4]Institute for Pathology, Tübingen, Baden-Württember, Germany, [5]Tübingen, Baden-Württemberg, Germany, [6]IDIBAPS, Barcelona, Spain, [7]Hospital Clinic of Barcelona, Barcelona, Spain, [8]University Hospital of Tuebingen, Tuebingen, Baden-Württemberg, Germany, [9]University of Tuebingen, Tuebingen, Baden-Wuerttemberg, Germany

Disclosures: Leonie Frauenfeld: None; Natalia Castrejón: None; Sebastian Streich: None; Annika Mayer: None; Barbara Mankel: None; Julia Steinhilber: None; Joan Enric Ramis-Zaldivar: None; Julia Salmeron-Villalobos: None; Irina Bonzheim: None; Magda Pinyol: None; Itziar Salaverria: None; Falko Fend: None; Olga Balagué: None; Elías Campo: *Advisory Board Member*, Nanostring; Leticia Quintanilla-Fend: None

Background: Diffuse large B-cell lymphoma (DLBCL) is the most common NHL in adults. Gene expression profiling (GEP) divides DLBCL according to the cell of origin (COO) into three subgroups: GCB, ABC and unclassifiable (UNC), exhibiting different mutational profiles. A surrogate of GEP is the Hans algorithm (HA) based on CD10, BCL6 and MUM1 expression. This algorithm classifies cases expressing CD10, BCL6 and MUM1 as GCB but it is not clear whether all these cases correspond to GCB subtype or whether this group may be more heterogeneous. Accordingly, the recently identified LBCL with *IRF4* rearrangement usually expresses GC phenotype (CD10+, BCL6+) together with strong MUM1/IRF4. The aim of this study was to characterize the molecular heterogeneity of DLBCL triple positive (CD10+BCL6+MUM1+).

Design: Forty-seven triple positive DLBCL were investigated with FISH (*BCL2, BCL6, MYC, IRF4*, IGH), NGS targeted sequencing (covering *BCL2, CD79B, PIM1, PRDM1, IRF4, MYD88, EZH2, CARD11, TNFAIP3* genes), and GEP using Nanostring and/or HTG

molecular. Nine DLBCL, 5 GCB-type and 4 non-GCB-type were included as controls. *BCL2* and *EZH2* mutations were considered consistent with GCB COO; whereas *MYD88* and *CD79B* consistent with ABC.

Results: According to GEP, 26/41 (63%) cases were classified as GCB, 12/41 cases (29%) as ABC and 3/41 (7%) UNC. According to the mutational profile only 17/36 (47%) cases could be sub-classified; 11 cases as ABC and 6 cases as GCB. Of the latter, four cases revealed *BCL2* mutations and /or *BCL2* break by FISH. There were 4 discordant cases that were assigned by GEP to the GCB group but carried *MYD88* and/or *CD79B* mutations. Interestingly 8/43 cases revealed an *IRF4* break. One additional case presented in the tonsil and showed an IGH break but lacked a demonstrable *IRF4* break. In total 9/43 cases (21%) were considered LBCL with *IRF4* rearrangement (Table 1). GEP assigned 5 of these 9 cases as GCB, one ABC, one UNC and two were not evaluable. Five cases carried *IRF4* mutations. The 9 control DLBCL showed a perfect correlation between the HA, GEP and mutational analysis.

Case No	Age	Sex	Site	FISH *MYC*	FISH *BCL2*	FISH *BCL6*	FISH *IRF4*	FISH IGH	Mutations (NGS)	COO Mutational profile
5	37	f	LN Salivary gland	0	0	0	R	NA	*CARD11*	UNC
10	37	f	Tonsil	0	0	0	R	R	*IRF4*	UNC
11	67	f	Extra-nodal	NA	0	NA	R	NA	*IRF4/ PIM1*	UNC
16	62	m	LN inguinal	0	0	0	R	NA	*MYD88/ PIM1/ CD79B*	ABC
20	77	m	Tonsil	0	0	0	0	R	*CARD11*	UNC
26	55	m	Extra-nodal	0	R	R	R*	R	*IRF4/CREBBP/EZH2*	GCB
31	79	m	GI	0	0	G	R	R	*IRF4/MYD88/ MAP2K1*	ABC
44	38	f	GI	0	0	0	R	NA	*IRF4*	UNC

f: female; m: male; 0: no rearrangement; R: rearranged; NA: not available; G: gains; FISH: fluorescence in situ hybridization, NGS: next generation sequencing; COO: cell of origin, GEP: gene expression profile; GI: gastrointestinal tract; UNC: unclassifiable; NE: not evaluable

IRF4 rearrangement was observed in a lower number of cells than *BCL2* rearrangement suggesting that the *IRF4* alteration might be a secondary event in these DLBCL.

Conclusions: 1) Triple positive (CD10+MUM1+BCL6) DLBCL should not be sub-classified with the Hans Algorithm. 2) Triple positive DLBCL are enriched in LBCL with *IRF4* rearrangement, which are mostly of GCB-type and show frequent *IRF4* mutations. 3) Mutational analysis and GEP give complementary information and demonstrate further the heterogeneity of DLBCL triple positive.

1368 Utility of Evaluating CCR7 Expression for Differentiating Classic Hodgkin Lymphoma and Other B Cell Lymphomas by Immunohistochemistry

Jonathan Fromm[1], Xueyan Chen[1], Lorinda Soma[2]
[1]University of Washington, Seattle, WA, [2]University of Washington Medical Center, Seattle, WA

Disclosures: Jonathan Fromm: None; Xueyan Chen: None; Lorinda Soma: None

Background: Classic Hodgkin lymphoma (CHL) is a B cell neoplasm where neoplastic cells are rare. CHL can be difficult to differentiate from nodular lymphocyte predominant Hodgkin lymphoma (NLPHL), diffuse large B cell lymphoma (DLBCL), NOS, primary mediastinal large B cell lymphoma (PMLBCL), and T cell/histiocyte rich large B cell lymphoma (THLBCL). Our laboratory has demonstrated that CCR7 is useful in distinguishing these lymphomas by flow cytometry and studies in other laboratories suggest that CCR7 expression may play a role in dissemination of neoplastic cells in tissues. Thus, the utility of evaluating expression of CCR7 by immunohistochemistry (IHC) was explored.

Design: CCR7 expression of neoplastic cells (93 cases; 27 CHL, 36 DLBCL, NOS, 9 PMLBCL, 10 NLPHL, 6 THLBCL, 2 EBV+ DLBCL, 2 monomorphic (DLBCL) post transplant lymphoproliferative disorder (PTLD), and 1 DLBCL, leg type) were evaluated by IHC by 3 pathologists. Percentage of cases positive, semi-quantitative measurement of percentage of cells positive, patterns of expression, and mean of semi-quantitative evaluation of intensity of expression were measured. Reactive lymphocytes expressing CCR7 were also assessed in each subgroup.

Results: CCR7 (clone 150503) was almost uniformly expressed on neoplastic cells in CHL (25/27 cases positive; 92.6%), while neoplastic cells of only 3 DLBCL, NOS (8.3%; all ABC type), and 1 NLPHL case (10%) expressed this antigen (Table). Neoplastic cells of all PMLBCL

and THLBCL were negative. One of 2 PTLD, 1 of 2 DLBCL, EBV+, and 0 of 1 DLBCL, leg type were positive for CCR7. When positive, neoplastic cells from CHL showed greater percentage of cells positive and greater antigen intensity than the other B cell lymphomas. Pattern of reactivity were typically golgi or golgi and cytoplasmic, although 2 of the 3 positive DLBCL, NOS cases showed membranous staining. Highest percentage of cases with some CCR7+ reactive lymphocytes was seen in CHL, while the lowest was in DLBCL, NOS.

Table^

	% Positive cases^^ (positive cases/cases evaluated)	Percentage involvement mean score#	Pattern of expression@	Mean intensity score&	Reactive lymphocytes**
CHL	92.6 (25/27)	2	23 GC, 2 G, 0 M	1.5	80
DLBCL, NOS*	8.3 (3/36)	1	1 GC, 0 G, 2M	1.17	22
PMLBCL	0 (0/9)	NA	NA	NA	33
NLPHL	10 (1/10)	1	1 G	0.5	70
THLBCL	0 (0/6)	NA	NA	NA	50

^For lymphomas with 6 or more cases examined

*19 germinal center B cell type (GCB), 16 activated B cell (ABC) type, 1 unspecified type

^^A case is considered positive if any convincing staining above background is observed

scored as: 1=0-25%; 2=25%-50%; 3=50%-75%; 4=75%-100%. Value is mean of positive cases

@G=golgi, C=cytoplasmic, GC=golgi and cytoplasmic, M=membranous

&scored as: 0=negative; 1=dim; 2=moderate; 3=intense. Value is the mean of scored positive cases

**% of cases with any convincing positive reactive lymphocytes

NA, not applicable

Conclusions: Similar to prior flow cytometric studies, the current studies by IHC show CCR7 is present on neoplastic cells in the vast majority of CHL cases and rarely or never seen in DLBCL, NOS, NLPHL, PMLBCL, or THLBCL. Consequently, CCR7 is specific for CHL compared to its morphologic mimics, providing a valuable tool in differentiating these lymphomas by IHC. Building on the work of others, our studies may help to provide a rationale for dissemination of neoplastic cells in these lymphomas.

1369 Therapy-Related T-cell Acute Lymphoblastic Leukemia with Recurrent KMT2A-MAML2, Novel SLC16A3-METRNL, and Complex Genetic Profile Revealed by Whole Transcriptome Sequencing

Lucy Fu[1], Rachel Mariani[2], Dawn Kirschmann[3], Silva Mercedes[3], Pauline Chou[4], Kai Lee Yap[3], Shunyou Gong[3]
[1]Northwestern University Feinberg School of Medicine, Chicago, IL, [2]Nationwide Children's Hospital - The Ohio State University, Columbus, OH, [3]Ann and Robert H. Lurie Children's Hospital of Chicago, Chicago, IL, [4]Lurie Children's Hospital of Chicago, Chicago, IL

Disclosures: Lucy Fu: None; Rachel Mariani: None; Dawn Kirschmann: None; Silva Mercedes: None; Pauline Chou: None; Kai Lee Yap: None; Shunyou Gong: None

Background: Patients with primary malignances treated with cytotoxic chemoradiotherapy develop therapy-related myeloid neoplasms, including myelodysplastic syndrome and acute myeloid leukemia. Less commonly, therapy-related acute lymphoblastic leukemias/lymphomas (t-ALL) with either B- or T-cell lineage also occur, but are overall poorly understood. We reported the third and youngest T-t-ALL patient with inv(11)(q21q23); KMT2A-MAML2, and suggested that this is a recurrent genetic abnormality in T-t-ALL (Mariani R, et al. J. Ped Hem. Onc., in press) (Figure 1). Since we are interested in studying the overall genetics of this rare disease type, whole transcriptome mRNA sequencing (RNAseq) was performed, and revealed a complex genetic profile with total 88 gene fusion transcripts. Further characterization of these gene fusions is warranted to provide insight on the pathogenesis of T-t-ALL.

Design: The gene fusions from RNAseq were further characterized. A literature review was performed to identify potential associations with known hematologic or non-hematologic malignancies. We further confirmed the gene fusion of SLC16A3-METRNL, which had

the most junction reads on RNAseq, by reverse transcriptase polymerase chain reaction (RT-PCR). Confirmation of other potentially important gene fusions for leukemogenesis is underway.

Results: Of the total 88 gene fusion transcripts, the number of junction reads ranged from 1 to 98. Table 1 summarizes a subset of the most significant gene fusions, some associated with hematologic or non-hematologic malignancies but never described in T-ALL, and others are novel but involve genes encoding functionally important proteins in tumorigenesis. RT-PCR confirmed SLC16A3-METRNL gene fusion, which has been detected in some AMLs but not in ALLs to date (Figure 2).

| TABLE 1. Selected gene fusions identified in our case of T-t-ALL				
Fusion Name	Junction Reads	Novel gene fusion?	Reported in:	Protein functions
KMT2A--MAML2	8	No	t-MN, t-ALL	"KMT2A (MLL): Encodes a DNA-binding protein that methylates histone H3 and positively regulates expression of target genes including multiple HOX genes. MAML2: Member of the Mastermind-like family of proteins which binds the ankyrin repeat domain of intracellular domain of the Notch receptors. Positively regulates Notch signaling. "
SLC16A3--METRNL	98	No	AML	"SLC16A3: Catalyzes plasma membrane transport of moncarboxylates (e.g. lactate, pyruvate). METRNL: Secreted protein expressed in white adipose tissue and barrier tissues; plays important roles in neural development, white adipose browning, and insulin sensitization. "
CYTH1--USP36	6	No	Lung adenocarcinoma	"CYTH1: Member of the PSCD family which mediate the regulation of protein sorting and membrane trafficking. Highly expressed in natural killer and peripheral T cells. Regulates the adhesiveness of integrins at the plasma membrane of lymphocytes. USP36: Member of the ubiquitin-specific protease family of cystein proteases. This protein may deubiquitinate and stabilize the transcription factor c-Myc, an important oncoprotein upregulated in many human cancers. May also regulate the activation of autophagy. "
POLE--FBRSL1	5	No	B-ALL	"POLE: Enzyme involved in DNA repair and chromosomal DNA replication. FBRSL1: Fibrosin Like 1 is an important paralog of AUTS2 which has been implicated in neurodevelopment and as a candidate gene for numerous neurological disorders including autism spectrum disorders, intellectual disability, and developmental delay. "
NCOR2--UBC	9	No	CLL	"NCOR: Encodes a nuclear receptor co-repressor that mediates transcriptional silencing of certain target genes by using histone deacetylases to modify chromatin structure. UBC: Ubiquitin C, a polyubiquitin precursor. Conjugation of ubiquitin monomers/polymers can lead to various effects including protein degradation, DNA repair, cell cycle regulation, kinase modification, endocytosis, and regulation of other cell signaling pathways. "
CYB561A3--CXCL16	18	Yes	N.A.	"CYB561A3: Ferric-chelate reductase that reduces Fe3+ to Fe2+ before its transport from endosome to cytoplasm. CXCL16: Scavenger receptor on macrophages which specifically binds to oxidized low density lipoprotein; may be involved in atherogenesis. "
CSNK1G2--REXO1	17	Yes	N.A.	"CSNK1G2: Transferase activity (transferring phosphorus-containing groups) and protein tyrosine kinase activity. REXO1: Nucleic acid binding and exonuclease activity; ribosome biogenesis in eukaryotes. "
CSNK1G2--KLF16	12	Yes	N.A.	"CSNK1G2: Transferase activity (transferring phosphorus-containing groups) and protein tyrosine kinase activity. KLF16: DNA-binding transcription factor activity."
CHST15--FAM53B	6	Yes	N.A.	"CHST15: Type II transmembrane glycoprotein that acts as a sulfotransferase to chondroitin sulfate. Co-expressed with RAG1 in B-cells and potentially acts as a B-cell surface signaling receptor. FAM53B: Regulator of Wnt signaling pathway by regulating beta-catenin nuclear localization. "
NOTCH2--RAC2	1	Yes	N.A.	"NOTCH2: Notch receptor family member, regulating lymphocyte development. RAC2: Rho family GTPase, control of protein kinase activation. "

Figure 1 - 1369

Figure 2 - 1369
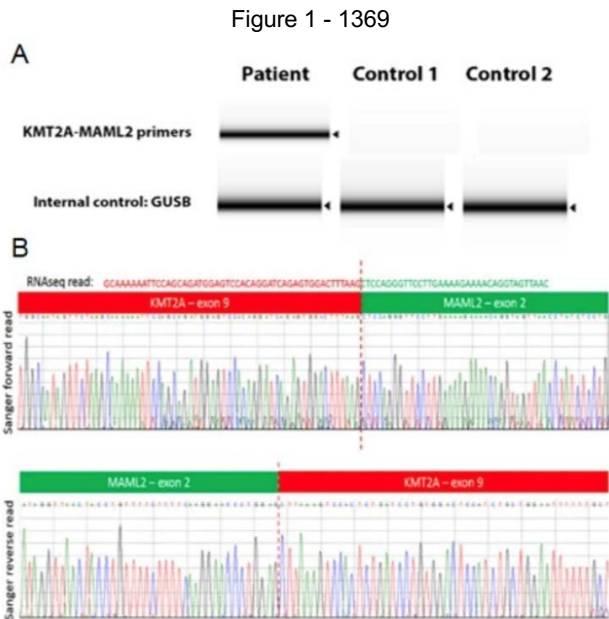
FIGURE 1. A, Polymerase chain reaction (PCR) amplification of cDNA derived from RNA of patient and two healthy controls was performed, and the PCR products were subjected to electrophoresis. Amplification of the housekeeping gene GUSB confirmed good quality of all three RNA samples.
B, Sanger sequencing of the KMT2A-MAML2 PCR product confirmed the in-frame fusion of KMT2A exon 9 (red) and MAML2 exon 2 (green). Both forward and reverse reads are shown.
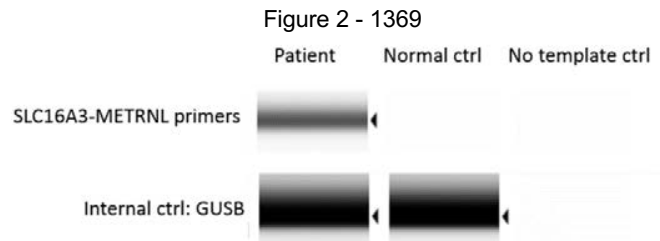

FIGURE 2. Polymerase chain reaction (PCR) amplification of cDNA derived from RNA of patient, healthy control, and a no-template control was performed, and the PCR products were subjected to electrophoresis. Amplification of the housekeeping gene GUSB confirmed good quality of all three RNA samples.

Conclusions: Our data revealed a complex genetic profile in T-t-ALL, and suggested that KMT2A-MAML2 gene fusion may be considered a recurrent genetic abnormality in T-t-ALL to the next revision of the World Health Organization (WHO) classification. Moreover, SLC16A3-METRNL fusion has been reported in AML but never in T-ALL. We are confirming the remaining gene fusions by RT-PCR and Sanger sequencing. Confirmed novel gene fusions including SLC16A3-METRNL are being tested in the other 2 T-t-ALLs and 11 de-novo T-ALLs at our institution. We expect these further investigations will shed new light on the pathogenesis of T-t-ALL and also facilitate understanding of genes involved in tumor cell biology as a whole.

1370 High MYC Protein Expression in MDS and MDS/MPN Predicts Early Disease Transformation to AML

David Gajzer[1], Pukhraz Basra[1], Yun Seongseok[2], Ling Zhang[3]
[1]H. Lee Moffitt Cancer Center & Research Institute, University of South Florida, Tampa, FL, [2]Moffitt Cancer Center, Tampa, FL, [3]Tampa, FL

Disclosures: David Gajzer: None; Pukhraz Basra: None; Yun Seongseok: None; Ling Zhang: None

Background: Acute myeloid leukemia (AML) with myelodysplasia-related changes (AML-MRC) is associated with dismal clinical outcomes, and there remains a pressing need for new therapeutic strategies. We recently reported that high MYC expression dictates inferior overall survival (OS) in AML-MRC (Yun et al, 2019). Here, we compared MYC protein expression levels in bone marrow (BM) specimens of patients with preexisting MDS or MDS/MPN and their subsequent AML-MRC specimens to determine whether increased MYC expression is associated with early progression to AML.

Design: We retrospectively identified 21 patients with histologically confirmed AML-MRC evolving from MDS or MDS/MPN and reviewed their BM biopsies from the time of MDS or MDS/MPN and AML-MRC diagnosis. Clinical data were retrieved through chart review. MYC expression was assessed by immunohistochemistry on 3 µm tissue sections with an anti-MYC antibody (clone Y69, Roche Diagnostics) using a Ventana Benchmark automated system, scored independently by two hematopathologists and categorized as low vs. high, as previously described, with high MYC expression being ≥5% positive cells among blasts counted. OS was estimated with the Kaplan-Meier method and compared using the log-rank test. All statistical analyses were performed using SPSS v24.0.

Results: The median age at MDS or MDS/MPN diagnosis was 66.5 (48.4-78.7) years and 71% (n=15) of patients were male. A total of 81% (n=17), 10% (n=2), and 10% (n=2) patients were treated with hypomethylating agents, Revlimid, and chemotherapy, respectively (Table 1). High MYC expression was identified in 19% (4/21) of patients at the time of MDS or MDS/MPN diagnosis compared with 43%

(9/21) at AML-MRC diagnosis. A total of 33% (n=7) of patients had increase of MYC levels with disease progression to AML. The median blast percentage at MDS or MDS/MPN diagnosis was higher in high MYC patients (11.5% vs. 5%, *p*=0.1932) and median time to AML progression was shorter in high MYC patients (5.9 vs. 12.4 months, *p*=0.2292). Statistical analysis for OS was attempted; however, it did not reach significance due to limited number of cases.

PARAMETER	LOW MYC (n=17)	HIGH MYC (n=4)	TOTAL (n=21)
Median age, year (range)	66.1 (48.4-78.7)	68.5 (54.6-72.4)	66.5 (48.4-78.7)
Gender (male/female)	12/5	3/1	15/6
Original diagnosis (%)	1 (6)	0 (0)	1 (5)
MDS-SLD	5 (29)	0 (0)	5 (24)
MDS-MLD	4 (24)	0 (0)	4 (19)
MDS-EB-1	4 (24)	2 (50)	6 (29)
MDS-EB-2	0 (0)	1 (25)	1 (5)
MDS-U	0 (0)	1 (25)	1 (5)
t-MDS	3 (18)	0 (0)	3 (14)
CMML-2			
Blast counts, % (range)	5.0 (0.5-15)	11.5 (2.2-15)	5.2 (0.5-15)
Median Time to AML Progression, months (range)	12.4 (0.3-99.1)	5.9 (2.5-7.1)	7.9 (0.3-99.1)
Treatment before AML-MRC (%)	1 (6)	0 (0)	1 (5)
Hydrea	1 (6)	1 (25)	2 (10)
ESAs	13 (76)	4 (100)	17 (81)
Hypomethylating agents	2 (12)	0 (0)	2 (10)
Revlimid	2 (12)	0 (0)	2 (10)
Chemotherapy	1 (6)	1 (25)	2 (10)
Others	3 (18)	0 (0)	3 (14)
Unknown	3 (18)	0 (0)	3 (14)
Allogeneic stem cell transplantation			
Abbreviations: MDS with single lineage dysplasia (MDS-SLD), MDS with multilineage dysplasia (MDS-MLD), MDS with excess blasts-1 (MDS-EB-1), MDS with excess blasts-2 (MDS-EB-2), MDS unclassifiable (MDS-U), therapy related MDS (t-MDS), chronic myelomonocytic leukemia-2 (CMML-2), acute myeloid leukemia (AML), erythropoiesis stimulating agents (ESAs).			

Conclusions: High MYC expression at the MDS or MDS/MPN stage is associated with higher blast percentages and shorter time to AML progression in our cohort. Investigation of a greater sample size and underlying molecular alterations will lead to a better understanding of the role of MYC in the progression to AML.

1371 Epstein Barr Virus Negative Marginal Zone Lymphoma (MZL): A Unique Monomorphic Post-Transplant Lymphoproliferative Disorder (PTLD)

Pallavi Galera[1], Shunyou Gong[2], Niall Swan[3], Richard Flavin[4], Natasha Savage[5], Huan-You Wang[6], Annapurna Saksena[7], Liqiang Xi[8], Mark Raffeld[9], Stefania Pittaluga[10], Elaine Jaffe[8]
[1]Memorial Sloan Kettering Cancer Center, New York, NY, [2]Ann and Robert H. Lurie Children's Hospital of Chicago, Chicago, IL, [3]St. Vincent's University Hospital, Elm Park, Dublin, Ireland, [4]St. James's Hospital, Dublin, Ireland, [5]Medical College of Georgia, Augusta, GA, [6]University of California San Diego, La Jolla, CA, [7]NIH, Bethesda, MD, [8]National Cancer Institute, National Institutes of Health, Bethesda, MD, [9]National Cancer Institute, Bethesda, MD, [10]National Institutes of Health, Washington, DC

Disclosures: Pallavi Galera: None; Shunyou Gong: None; Niall Swan: None; Richard Flavin: None; Natasha Savage: None; Huan-You Wang: None; Annapurna Saksena: None; Liqiang Xi: None; Mark Raffeld: None; Stefania Pittaluga: None; Elaine Jaffe: None

Background: Monomorphic PTLDs are defined as lymphoid or plasmacytic proliferations that fulfill the criteria for one of the B-cell or T/NK-cell neoplasms seen in immunocompetent hosts. Low grade B-cell neoplasms have historically been excluded from this category; although recently, Epstein Barr virus (EBV) positive marginal zone lymphomas (MZLs) were described in the post-transplant setting.

Design: Recently, the authors encountered a series of EBV-negative MZLs presenting following solid organ transplantation. The pathology archives of our institution were searched between 01/2005 to 03/2019 for similar cases. Appropriate immunophenotypic and molecular studies were performed.

Results: We identified 9 cases of post-transplant EBV-negative MZLs (Table 1). All patients presented more than one-year post-transplantation (median time to presentation 84 months). There were 4 females and 5 males, with a median age of 46-years at presentation. All cases occurred in solid organ transplant recipients (4 renal, 3 liver, 1 cardiac, and 1 liver, pancreas, & small bowel). Seven patients presented with extranodal MZL (ENMZL) of MALT type, all of whom had GI tract involvement (4 colon, 1 stomach, 1 duodenum, and 1 oropharynx/base of tongue). Multiple intestinal polyps were present in 2 patients post-liver transplant. Two patients had stage IV disease with both bone marrow and nodal involvement. ENMZL cases demonstrated a dense, atypical lymphoid infiltrate with

prominent plasmacytic differentiation, expanding the lamina propria and extending into the submucosa. Two cases presented with only nodal MZL.

Immunoglobulin gene rearrangement studies showed clonal peaks in 7 of the 8 cases with successful amplification. All cases demonstrated light chain restriction. One patient, with intestinal recurrence at 4 years, revealed a different light chain restriction (lambda to kappa) as well as a different clonal peak by immunoglobulin gene rearrangement studies. EBER by ISH was negative in the neoplastic cells in all cases. One case tested for rearrangements of *MALT1* was negative. Additional next generation sequencing studies are in progress.

In patients with available follow-up (5 patients; mean 33.4 months), all had an indolent course with complete remission following various therapies. A subset of cases responded to reduction in immunosuppression and anti-CD20 therapy alone.

Table 1. Clinical Features of Post-transplant EBV Negative Marginal Zone Lymphoma

	Age/Sex	Reason for Transplant (TX)	Type of TX	Immunosuppr-ession	Time from TX (mos)	Site of MZL	Diagnosis	Treatment	Outcome	Follow-up Time (mos)
1	40/F	Auto-immune hepatitis	Liver	Tacrolimus, prednisone	156, 180, 216	Colon, multiple polyps	ENMZL	RI, 6 cycles x Pentostatin	Alive, no active disease for 48 months, recurrence with different clone*	108
2	62/M	Primary sclerosing cholangitis	Liver	Tacrolimus, mycophenolate mofetil	13	Colon and small bowel, multiple polyps	ENMZL	Surgery	Alive, no active disease	7
3	44/M	ESRD secondary to FSGS	Kidney	Tacrolimus, mycophenolate mofetil, prednisone	84	Mass, left base of tongue	ENMZL	Rituximab	Alive, no active disease	6
4	70/F	NI	Liver	NI	24	Cecum, mass	ENMZL	NI	NI	Lost to follow-up
5	73/M	NI	Kidney	Tacrolimus, mycophenolate mofetil, prednisone	168	Descending colon polyp	ENMZL	NI	NI	Lost to follow-up
6	18/F	Idiopathic dilated cardiomyopathy	Heart	Tacrolimus, mycophenolate mofetil	84	Duodenum, ulcer#	ENMZL	RI, 6 cycles x Rituximab, cyclophosphamide, prednisone	Alive, no active disease	26
7	9/M	Necrotizing enterocolitis	Liver, pancreas, small bowel	Tacrolimus, mycophenolate mofetil, prednisone	84	Stomach#	ENMZL	RI, 4 doses of Rituximab	Alive, no active disease	20
8	46/M	NI	Kidney	NI	180	Groin, lymph node	Nodal MZL	NI	NI	Lost to follow-up
9	52/F	CRF	Kidney	Mycophenolate	96	Mesenteric lymph node	Nodal MZL	NI	NI	Lost to follow-up

* currently being treated with RI, 8 doses of Rituximab; # H. pylori negative

CRF, Chronic renal failure; ENMZL, Extranodal marginal zone lymphoma; ESRD, End stage renal disease; F, Female; FSGS, Focal segmental glomerulosclerosis; LAD, Lymphadenopathy; M, Male; MZL, Marginal zone lymphoma; NI, no information available; RI, reduced immunosuppression

Conclusions: The indolent course and response to immune reconstitution suggest that EBV-negative MZL may represent a form of monomorphic PTLD.

1372   Frequent RUNX1 and TP53 Mutations in Secondary Acute Myeloid Leukemia with Mixed Phenotype

Pallavi Galera[1], Jeeyeon Baik[1], Christopher Famulare[1], Allison Sigler[1], Yanming Zhang[1], Maria Arcila[1], Ahmet Dogan[1], Martin Tallman[1], Ross Levine[1], Jacob Glass[1], Mikhail Roshal[1], Wenbin Xiao[1]
[1]Memorial Sloan Kettering Cancer Center, New York, NY

Background: Mixed phenotype blasts are characteristic for *de novo* mixed phenotype acute leukemia(dMPAL) but can also be seen in blast crisis of myeloproliferative neoplasms(MPN), myeloid/lymphoid neoplasms with eosinophilia and rearrangements, AML with recurrent cytogenetic abnormalities(AML-RCA) and secondary acute myeloid leukemia(sAML; including AML with myelodysplasia-related changes [AML-MRC] and therapy-related AML[t-AML]). sAML with mixed phenotype, empirically excluded from the diagnosis of dMPAL by WHO classification, has not been studied.

Design: A cohort of patients diagnosed as AML with mixed phenotype(defined by flow cytometry per WHO criteria) from 01/2014 to 08/2019 was obtained by searching MSKCC database. Patients meeting the criteria for sAML were included. Clinical, histological, flow cytometric, cytogenetic & molecular evaluation was performed. These were compared to a cohort of 29 dMPALs, previously reported from our institution.

Results: 45 cases of sAML-mixed phenotype were retrieved(Table 1). The median age at diagnosis was 67 years which was higher than dMPALs(42 years, p=0.01). There was a slight male preponderance(M:F ratio of 1.5). Out of the 45 cases; 25, 17 and 3 revealed B/Myeloid(B/M), T/M and B/T/M phenotype, respectively. The clinical characteristics as well as the overall survival were not significantly different between the different phenotypes (Fig 2A). Per WHO classification 32 cases met criteria for AML-MRC and 13 for t-AML. The WBC, Hb, platelet count and peripheral blood blast count were all higher in the dMPAL cohort.

Molecular studies performed on 43 out of the 45 cases(Fig 1) revealed that the most commonly mutated genes were *RUNX1*(42%), *DNMT3A*(28%), *TP53*(26%), *TET2*(23%), *ASXL1*(21%), *NRAS*(19%). Mutations in *PHF6* frequently noted in dMPALs were uncommon (5% vs 23% in dMPAL), while *TP53* mutations were enriched in this cohort (26% vs 0% in dMPAL). In addition, mutations in RUNX1 and ASXL1 were also uncommon in the dMPALs. The overall survival was significantly inferior in the sAML-mixed phenotype cohort in comparison to dMPAL cohort(median survival:419 vs 1317 days, p value 0.0007; Gehan-Breslow-Wilcoxon test; Fig 2B).

Table 1. Clinical Characteristics of patients with AML- Mixed Phenotype vs De novo Mixed Phenotype Acute Leukemia					
	De novo MPAL	AML - Mixed phenotype			
		Total	B/Myeloid	T/Myeloid	B/T/Myeloid
Age, median years (Range)	42 (0-69)	67 (9-82)	65 (12-82)	72 (9-82)	52 (50-67)
Gender (M/F)	18/11	27/18	13/12	13/4	1/2
CBC prior to induction					
WBC, median X 10*9/L (Range)	19.2 (0.8-323)	2.75 (0.3-75.6)	2.75 (0.6-75.6)	6.6 (0.3-55.9)	1.4 (0.7-2.3)
Hb, median g/dL (Range)	9.4 (6-13.3)	8.55 (6.3-12.5)	8.85 (6.6-12.5)	8.5 (6.3-10.2)	8.4 (7.9-10.3)
PLT, median X 10*9/L (Range)	96 (13-403)	34 (2-298)	39 (14-298)	23 (2-285)	60 (30-109)
Blasts, median % (Range)	27 (0-94)	11.5 (0-83)	17.5 (0-83)	11 (0-81)	0 (0-14)
AML WHO classification					
MPAL with t(v;11q23.3)	4	0	0	0	0
MPAL with t(9;22)	3	0	0	0	0
MPAL, B/myeloid, NOS	7	0	0	0	0
MPAL, T/myeloid, NOS	12	0	0	0	0
MPAL, NOS	3	0	0	0	0
t-AML	0	13	8	4	1
AML-MRC	0	32	17	13	2
CG risk stratification					
Favorable	0	0	0	0	0
Intermediate	10	10	8	2	0
Normal	6	6	4	2	0
Adverse	10	21	8	10	3
Failed/ not done	3	8	5	3	0

Figure 1 - 1372

Figure 1. Mutational Landscape of Secondary Acute Myeloid Leukemia - Mixed Phenotype

Figure 2 - 1372

Figure 2A.

Figure 2B.

Conclusions: The sAML-mixed phenotype shows clinicopathological and mutational profile similar to other secondary AMLs with frequent somatic mutations in *RUNX1*, *TP53*, *ASXL1*, *TET2*, and *NRAS*, which is different from dMPAL. This study provides further rationale to exclude this entity from dMPAL studies and novel insights into its pathogenesis.

1373 Myelodysplastic/Myeloproliferative Neoplasms (MDS/MPN) in Patients with Germline GATA2 Mutations

Pallavi Galera[1], Gaurav Gupta[2], Weixin Wang[3], Deepak Salem[2], Megan Trick[2], Amy Hsu[4], Dennis Hickstein[5], Steven Holland[2], Katherine Calvo[2]

[1]Memorial Sloan Kettering Cancer Center, New York, NY, [2]National Institutes of Health, Bethesda, MD, [3]Clinical Center/NIH, Bethesda, MD, [4]NIAID/NIH, Bethesda, MD, [5]National Cancer Institute, National Institutes of Health, Bethesda, MD

Disclosures: Pallavi Galera: None; Gaurav Gupta: None; Weixin Wang: None; Deepak Salem: None; Megan Trick: None; Amy Hsu: None; Dennis Hickstein: None; Steven Holland: None; Katherine Calvo: None

Background: Germline heterozygous *GATA2* mutations are often associated with bone marrow failure, monocytopenia & immunodeficiency with high risk of transformation to MDS/AML. However, a subset of GATA2 patients(pts) present with MDS/MPN which is not well described.

Design: 6 pts were identified with germline *GATA2* mutations(Table 1) who presented with findings diagnostic of one of the WHO defined MDS/MPNs. Bone marrow(BM), peripheral blood(PB), flow cytometry & cytogenetic studies were reviewed.

Results: The age at presentation ranged from 15-79 yrs.4 pts had a family history of either atypical mycobacterial infection or MDS/AML.5 pts presented with a history of recurrent infections.3 pts had warts, 2 had severe genital HPV infection and 2 pts had atypical mycobacterial infections.2 pts were apparently healthy and were discovered secondary to family screening(case#2 & #4, grandfather of case #2).

At initial presentation all pts except one had varying degrees of anemia, 3 had leukocytosis, 3 had marked monocytopenia; in contrast 2 pts presented with monocytosis and met criteria for Chronic Myelomonocytic Leukemia (CMML).1 of the monocytopenic pts later developed monocytosis.2 pts presented with eosinophilia both in the PB and BM. The diagnostic BM biopsies of all the pts revealed hypercellular marrows with myeloid hyperplasia and megakaryocytic atypia. The blast percentage was <5% in all pts except one (case#2) who also had concurrent mild myeloid and erythroid dyspoiesis and monosomy 7.The flow cytometric analysis revealed monocytopenia(3 pts), B cell lymphopenia(5 pts), NK cell lymphopenia(5 pts) and decreased dendritic cells. 3 of the 5 pts with cytogenetic studies showed abnormal clones. Somatic mutational analysis is currently being performed. 3 pts with PB monocytosis met WHO criteria for CMML and 2 were classified as MDS/MPN, unclassifiable with eosinophilia. One pt was initially diagnosed as MDS/MPN, unclassifiable but later evolved into CMML.

Table 1. Patients with Germline GATA2 Mutations and Myelodysplastic/Myeloproliferative Neoplasms									
#	Age/Sex	Family History	Past Medical History	Presentation	*GATA2* mutation	CBC	BM	Diagnosis	Cytogenetics
1	21/F	Maternal history of asthma. Mother and Sister negative for *GATA2* mutation	AML-M2 (7 years prior), culture (-) intra abdominal abcesses, disseminated CMV, persistent genital HSV2 infection and IgM deficiency	Persistent genital HSV2 ulcerations	c.302delG	WBC:3.72 K/uL, HB:7.3 g/dL; HCT:23.5 %; MCV 81 fL; PLT: 186 K/uL; DIFF: N-36.6%, L-54.8%, M-7.5%, E-0.8%, B-0.3%; ANC: 1.36 K/uL; ALC: 2.04 K/uL; AMC: 0.28 K/uL; AEC: 0.03 K/uL	- Markedly hypercellular marrow with granulocytic hyperplasia, mild megakaryocytic atypia, fibrosis, and less than 5% blasts	MDS/ MPN --> CMML-0	-7q, +8 --> -11q
2*	15/M	Mother and Brother positive for *GATA2* mutation. Mother- h/o AML	Recurrent sinus and ear infections during his childhood, as well as warts on his feet	Recurrent infections	c. 1017+572C>T	WBC: 15.61 K/uL, HB: 12 g/dL; HCT: 36.9 %; MCV 97.1 fL; PLT: 440 K/uL; DIFF: Blasts-5.8%, N-20.6%, MM-11.1%, Mye-8%, L-42.3%, M-9%, E-0.5%, B-2.7%; ANC: 3.22 K/uL; ALC: 6.6 K/uL; AMC: 1.4 K/uL; AEC: 0.08 K/uL; ABC: 0.42 K/uL	- Markedly hypercellular bone marrow (90-100%) with markedly increased dysplastic megakaryocytes, myeloid hyperplasia, myeloid and erythroid dyspoiesis, and increased myeloblasts (6-8%). - Absent B-cell precursors and absent dendritic cells. Decreased mature B-cells and NK-cells.	CMML-1	-7 in 20 out of 20 metaphases

3	40/F	Mother and sister also had a history of disseminated Mycobacterium avium intracellulare. Sister h/o MDS/AML, positive for *GATA2* mutation	Severe Genital HPV and CIN	Fevers, dyspnea, fatigue, weight loss, diffuse cutaneous nodules (+ve for MAC)	c.1192C>T	Absence of monocytes, Marked B cell lymphopenia, NK cell lymphopenia and T cell lymphopenia with inverted CD4:CD8 ratio (0.5)	- Hypercellular marrow with mild megakaryocytic and myeloid dysplasia	CMML and R posterior orbital EBV+ leiomyosarcoma	Normal Karyotype
4*	79/M	5 children: 2 with *GATA2* mutation, 1 p/w mono-MAC and metastatic adenocarcinoma; 2nd p/w AML 5 siblings: No infections or leukemia/lymphoma/cancer in siblings.	Unremarkable	Healthy	c. 1017+572C>T	WBC:8.25 K/uL, HB:15.7 g/dL; HCT:45 %; MCV: 94.1 fL; PLT: 229 K/uL; DIFF: N-46.2%, L-24%, M-29.8%, E-0%, B-0%; ANC: 3.81 K/uL; ALC: 1.98 K/uL; AMC: 2.46 K/uL; AEC: 0 K/uL	- Hypercellular marrow for age with increased monocytes and monocytic precursors (18%); - Increased T-cell large granular lymphocytes; - Less than 5% blasts; - Absolute peripheral blood monocytosis (2.49 K/uL);	CMML-0	Normal Karyotype
5	54/F	Sister with leukemia diagnosed at age 8 years; Brother with HCV, squamous cell carcinoma of the head, neck, and tongue	Pulmonary alveolar proteinosis, disseminated mycobacterial infection	Fevers and productive cough	c.1192C>T	WBC:15.7 K/uL, HB:11.7 g/dL; HCT:35.2 %; MCV: 76.2 fL; PLT: 325 K/uL; DIFF: N-80.1%, L-11.4%, M-0.1%, E-8%, B-0.5%; ANC: 12.5 K/uL; ALC: 1.8 K/uL; AMC: 0.01 K/uL; AEC: 1.24 K/uL; ABC 0.09 K/uL	- Hypercellular marrow with myeloid hyperplasia, mild megakaryocytic atypia and eosinophilia	MDS/MPN with eosinophilia	NA
6	37/F	Severe chicken pox, shingles, and death attributed to an adrenal tumor in her mother	Shingles, severe varicella zoster pneumonia, Bell's palsy, warts on hands & feet and genital HPV infection (VIN 3)	fevers, skin abscess, and lymphadenopathy (Mycobacterium kansasii)	c.1192C>T	WBC:13.8 K/uL, HB: 7.3 g/dL; HCT: 23.2 %; MCV: 81.1 fL; PLT: 217 K/uL; DIFF: N-73.9%, MM-3%, Mye-3%, L-8.5%, M-0%, E-11.1%, B-0.5%; ANC: 10.2 K/uL; ALC: 1.17 K/uL; AMC: 0 K/uL; AEC: 1.5 K/uL	- Markedly hypercellular bone marrow with severe monocytopenia, marked eosinophilia, increased mature granulocytes and atypical appearing megakaryocytes	MDS/MPN with eosinophilia	Abnormal clones with loss of one X, trisomy 1q, and trisomy 8

* Related

Conclusions: Overt immunodeficiency often precedes onset of overt myeloid neoplasm in *GATA2* pts. However, CMML with increased blasts & monosomy 7 was diagnosed in one apparently healthy adolescent and his apparently healthy grandfather was diagnosed with CMML without a recognized preceding period of immunodeficiency (case# 2 & 4).These cases highlight the importance of screening family members of probands and close surveillance of mutation positive members. MDS/MPN diagnosis is rare in adolescence and young adulthood, raising concern for *GATA2* mutation.

1374 EBV Negative Aggressive NK-Cell Leukemia/lymphoma: An Under-Recognized Disease Characterized by Genomic Instability, Frequent TP53 Alterations and PD-L1 Overexpression

Juehua Gao[1], Qing Chen[2], Xinyan Lu[3], Madina Sukhanova[2], Nabeel Yaseen[2], Amir Behdad[2], Yanming Zhang[4], Yi-Hua Chen[1]
[1]Northwestern Memorial Hospital, Chicago, IL, [2]Northwestern University Feinberg School of Medicine, Chicago, IL, [3]Chicago, IL, [4]Memorial Sloan Kettering Cancer Center, New York, NY

Disclosures: Juehua Gao: None; Qing Chen: None; Xinyan Lu: None; Madina Sukhanova: None; Nabeel Yaseen: None; Amir Behdad: *Speaker*, Pfizer; *Consultant*, Bayer/ Loxo; *Consultant*, Thermo Fisher; Yanming Zhang: None; Yi-Hua Chen: None; Yi-Hua Chen: None

Background: EBV- aggressive NK-cell leukemia/lymphoma is a rare, highly aggressive disease recently described by us and another group. Patients often present with constitutional symptoms, hepatosplenomegaly and HLH, and follow a fulminant clinical course. In contrast to EBV+ aggressive NK-cell leukemia/lymphoma, the EBV- disease affects non-Asians. The underlying molecular pathways have not been well studied.

Design: Comprehensive genetic studies, including conventional cytogenetic analysis, SNP array and NGS, were performed on 4 patients with EBV- aggressive NK-cell leukemia/lymphoma diagnosed in our institution.

Results: Our patients included 3 males and 1 female (all non-Asian) with ages ranging from 48 to 88 years. The neoplastic cells were highly atypical and pleomorphic with an NK-cell phenotype and EBV-. All 4 patients presented at advanced stage and died in < 3 weeks (3/4) and < 3 months (1/4) of initial presentation. Cytogenetic analysis on 2 patients with available specimens revealed hyperdiploidy and highly complex karyotypes including multiple numerical and structural abnormalities and several marker chromosomes (Figure 1. SNP array whole genome view of a representative case). SNP array on 2 patients showed microdeletion at 17p13.1 (*TP53*); multiple copy number changes were also detected. NGS analysis on 3 patients identified loss of function mutations of *TP53* in 2 patients. Additional mutations in *DDX3X, LRRFIP1, FOXP1, HIST1H3J, SRSF3* and *SETBP1* were also identified. Immunohistochemistry demonstrated the vast majority of neoplastic cells were strongly positive for PD-L1 (3/4) and p53 (3/4) (Figure 2. Pathologic features of a representative case). FISH performed on a case with available material showed amplification of *PD-L1* gene. The case with negative p53 immunostaining had a nonsense mutation on one allele and deletion on the other allele, resulting in loss of p53 expression.
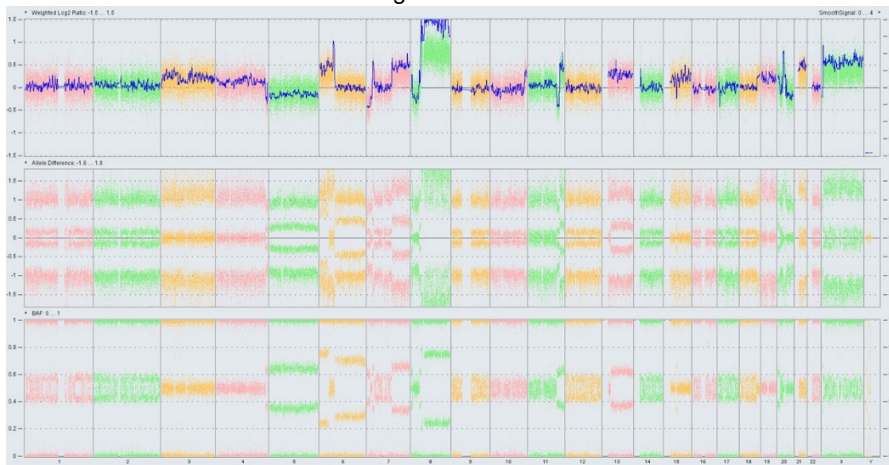
Figure 1 - 1374

Figure 1. Whole genome view of a representative case of EBV- NK-cell leukemia/lymphoma
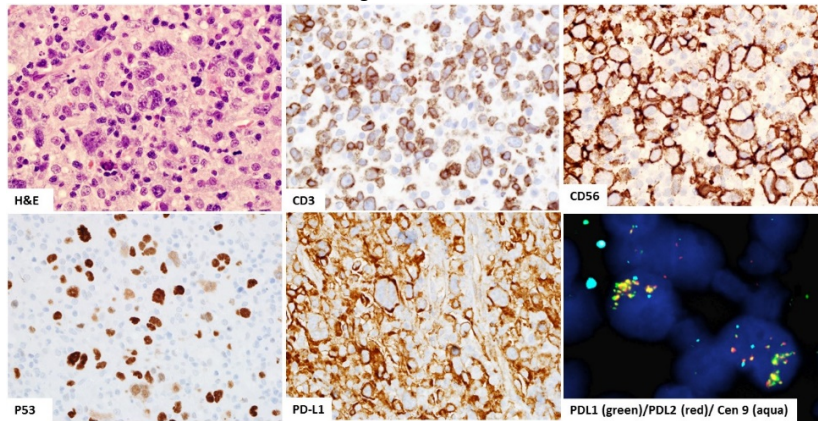
Figure 2 - 1374

Figure 2. Pathologic features of a representative case of EBV- NK-cell leukemia/lymphoma. The neoplastic cells are dim CD3+, CD56+, P53+ and strongly express PD-L1. In addition, the neoplastic cells are CD2+, CD30+, CD4-, CD5-, CD7-, CD8-, CD20-, PAX5-, TIA1-, BF1-, TCR delta- (Not shown). EBER is also negative. FISH shows amplification of PD-L1 gene.

Conclusions: This is the first comprehensive genetic study, including cytogenetics, SNP array and NGS analysis, of EBV- aggressive NK-cell leukemia/lymphoma. We found complex genetic changes, frequent *TP53* mutations/deletions, and strong p53 and PD-L1 expression. Our results suggest that loss of p53 due to *TP53* mutations and/or deletion may represent one of the molecular pathways responsible for increased genomic instability in this disease. High expression of PD-L1 suggests that checkpoint inhibitors may be beneficial to patients with this highly aggressive leukemia/lymphoma.

1375 Characterization of p53 and MYC Expression in Acute Myeloid Leukemia and Myelodysplastic Syndrome

Linlin Gao[1], Azhar Saeed[2], Shivani Golem[2], Da Zhang[3], Janet Woodroof[4], Wei Cui[5]
[1]University of Kansas Medical Center, Overland Park, KS, [2]University of Kansas Medical Center, Kansas City, KS, [3]Kansas University Medical Center, Kansas City, KS, [4]Kansas University Medical Center, Shawnee, KS, [5]University of Kansas Medical Center, Shawnee, KS

Disclosures: Linlin Gao: None; Azhar Saeed: None; Shivani Golem: None; Da Zhang: None; Janet Woodroof: None; Wei Cui: None

Background: Patients with p53 mutated and overexpressed acute myeloid leukemia (AML) and myelodysplastic syndrome (MDS) have an aggressive clinical course. Limited studies also show MYC expression has served as an adverse prognostic marker in patients with AML. However, expression of MYC in relationship to p53 status has not been evaluated in AML and MDS. To the best of our knowledge this is the first study to evaluate p53 and MYC expression simultaneously in AML and MDS.

Design: We identified 193 patients via keyword search in our electronic record system during 2017-2019. The cases included patients with newly diagnosed or residual AML (n=86), MDS (n=73), and lymphoma with negative staging bone marrow findings as negative control (n=34). We retrospectively assessed p53 and MYC expression by immunohistochemistry using a cut-off of 5% and 8% of 3+ nuclear staining, respectively and correlated MYC expression with protein expression and mutational status of p53 detected by either Next Gene Sequencing or cytogenetics, and cytogenetic risk. We also analyzed the impact of p53 and MYC expression on overall survival (OS) in AML and MDS patients.

Results: Expression of p53 and MYC was significantly higher in AML (mean: 11.0%; 13.4%) and MDS (mean: 4.9%; 5.4%) patients compared to control patients (mean: 0.18%; 2.3%) (p=0.001-0.02). In addition, p53 and MYC expression was even more elevated in AML patients than MDS patients (p<0.001). MYC expression was significantly associated with p53 expression, *TP53* mutation and high risk cytogenetic abnormalities in AML patients (p=0.02-0.001), but not in MDS patients. p53 expression was associated with *TP53* mutation in both groups. Both p53 and MYC expression showed an adverse impact on OS (p=0.0002-0.03) in AML patients while only p53 but not MYC expression showed an adverse impact on OS in MDS patients. Additionally, expression of p53 and MYC demonstrated synergistically adverse impact on OS in AML patients.

Conclusions: MYC expression is associated with p53 expression, *TP53* mutation, high risk cytogenetic abnormalities and poor OS in AML patients, but not in MDS patients. These findings may indicate that MYC expression may provide proliferative advantage for leukemic progression in p53 dependent manner.

1376 TP53 Splice-Site Mutations in Myelodysplastic Syndromes (MDS) and Acute Myeloid Leukemia (AML): A Clinicopathologic and Cytogenetic Correlation

Sofia Garces Narvaez[1], Mitul Modi[2], Jennifer Morrissette[3], Jason Rosenbaum[4], Salvatore Priore[5]
[1]The Hospital of the University of Pennsylvania, Philadelphia, PA, [2]Pennsylvania Hospital of University of Pennsylvania Health System, Philadelphia, PA, [3]Perelman School of Medicine, University of Pennsylvania, Philadelphia, PA, [4]UPenn, Center for Personalized Diagnostics, Philadelphia, PA, [5]Hospital of the University of Pennsylvania, Philadelphia, PA

Disclosures: Sofia Garces Narvaez: None; Mitul Modi: None; Jennifer Morrissette: None; Jason Rosenbaum: None; Salvatore Priore: None

Background: *TP53* mutations are seen in only 5-10% of de novo MDS/AML but are enriched in poor prognosis categories including complex karyotype and therapy-related forms. Canonical *TP53* splice-site mutations in MDS/AML have unknown prevalence and functional consequence. Moreover, there is a lack of studies that have separately analyzed the clinicopathologic and cytogenetic findings in this mutational subgroup.

Design: A retrospective analysis of massively parallel sequencing data from the past 7 years was performed for MDS/AML with *TP53* mutations. Twenty-one patients were identified with MDS/AML harboring *TP53* splice-site mutations, comprising ~7% of all *TP53*-mutated MDS/AML. The cases were subclassified by current WHO criteria. Clinicopathologic and cytogenetic data were collected. A cohort of 60 patients with MDS/AML harboring *TP53* exonic (non-splice-site) mutations was used as control.

Results: The study group included 4 women and 17 men (median age: 67 years [range, 47-75]). The diagnoses were therapy-related AML or MDS (t-MDS/AML) in 9 (43%), including t-AML (n=7) and t-MDS (n=2); AML with myelodysplasia-related changes in 9 (43%) and other in 3 (14%). *TP53* splice-site mutations were single nucleotide variants (n=18, 86%) or deletions/insertions (n=3, 14%) involving consensus intronic dinucleotide sequences at either the splice acceptor (13, 62%) or splice donor (8, 38%) sites. Affected introns were 4, 5, 6, 8 and 9. Nineteen (90%) cases had complex karyotype and 16 (76%) monosomal karyotype; 20 (95%) had deletion/monosomy of chromosome 5, and 13 (62%) of chromosome 7. In 12 (57%) patients, the splice-site mutation was the sole genetic abnormality in *TP53.* Compared to MDS/AML with exonic *TP53* mutations, MDS/AML with *TP53* splice-site mutations were significantly more often classified as t-MDS/AML (43% vs. 18%, *P*= 0.0385). No other significant differences were observed between the two groups.

Conclusions: *TP53* intronic splice-site mutations account for ~7% of *TP53* mutations in MDS/AML. Similar to exonic *TP53* mutations, splice-site mutations are enriched in high-risk disease subgroups, including MDS/AML with complex/monosomal karyotype though showing a significantly higher frequency of t-MDS/AML. Whereas functional studies are needed to elucidate the functional impact of splice-site mutations in the tumor suppressor *TP53*, our findings emphasize the importance of thorough analysis of this gene including consensus intronic splice-site sequences, as rarely, they can be the sole abnormality in *TP53.*

1377 Utility of CRLF2 Flow Cytometry to Detect CRLF2 Gene Rearrangements in Pediatric B-Cell Acute Lymphoblastic Leukemia

Annie Garcia[1], Amos Gaikwad[2], Reshma Kulkarni[3], Choladda Curry[2], Kevin Fisher[2]
[1]Baylor College of Medicine, Houston, TX, [2]Baylor College of Medicine/Texas Children's Hospital, Houston, TX, [3]Texas Children's Hospital, Houston, TX

Disclosures: Annie Garcia: None; Amos Gaikwad: None; Reshma Kulkarni: None; Choladda Curry: None; Kevin Fisher: None

Background: Risk stratification for B-cell acute lymphoblastic leukemia (B-ALL) requires integration of clinical and laboratory data. *BCR-ABL1*-like (Ph-like) B-ALLs are associated with an unfavorable prognosis and patients with Ph-like B-ALL are considered to have high risk disease. Cytokine Receptor Like Factor 2 (CRLF2) located on the pseudoautosomal region of chromosome Xp is rearranged in approximately 50% of Ph-like B-ALLs, and these rearrangements result in overexpression of CRLF2 surface protein (CRLF2-Hi). We therefore assessed the utility of CRLF2 flow cytometry to detect pediatric B-ALL patients with *CRLF2* gene rearrangements (CRLF2-R).

Design: We retrospectively reviewed flow cytometric results from 349 pediatric B-ALL patients diagnosed from 1/2013 to 3/2018 at our institution. Clinicopathologic data including age, sex, age at diagnosis, B-ALL risk stratification, conventional cytogenetics, and FISH results were obtained from the electronic medical record.

Results: We identified 28 B-ALL patients (8.0%) with CRLF2-Hi by flow cytometry. CRLF2-Hi was attributable to CRLF2-R in 11 cases (39.3%) or copy gains of the X chromosome (+X) in 6 cases (21.4%). False-positive CRLF2-Hi results were also observed in cases of intrachromosomal amplification of chromosome 21 (iAMP21, n=4, 14.3%) or no discernible HR cytogenetic abnormality (n=6, 21.4%).

Conclusions: CRLF2 flow cytometry may be used as a screening tool to identify Ph-like B-ALL with *CRLF2* rearrangement as all CRLF2-R B-ALL cases in our study expressed CRLF2-Hi. However, further studies to assess the overall sensitivity and specificity and optimal screening algorithms are needed. Nonetheless, CRLF2-Hi should prompt additional testing to assess for CRLF2-R to enable appropriate

risk stratification. Ultimately, a multimodal approach of clinical data, flow cytometry, FISH, and molecular diagnostics is needed to comprehensively risk stratify pediatric B-ALL patients.

1378 Plasmablastic Lymphoma Mutational Profile is Characterized by MYC, STAT3 and PRDM1/Blimp1 Mutations

Julia Garcia-Reyero[1], Nerea Martinez[2], Irene Hernandez-Alconchel[3], Sonia Gonzalez de Villambrosia[4], Angela Gomez Mediavilla[5], Sanam Loghavi[6], Ainara Gonzalez[7], Emanuele d'Amore[8], Carlo Visco[9], Joseph Khoury[6], Santiago Montes-Moreno[4]
[1]HUMV/IDIVAL, Santander, Spain, [2]IDIVAL, Santander, Cantabria, Spain, [3]HUMV, Santander, Cantabria, Spain, [4]Hospital Universitario Marqués De Valdecilla, Santander, Spain, [5]IDIVAL, Valladolid, Castilla y León, Spain, [6]The University of Texas MD Anderson Cancer Center, Houston, TX, [7]IDIVAL, Santander, Spain, [8]Ospedale S. Bortolo, Vicenza, VI, Italy, [9]Department of Medicine, Section of Hematology, University of Verona, Verona, Italy

Disclosures: Julia Garcia-Reyero: None; Irene Hernandez-Alconchel: None; Angela Gomez Mediavilla: None; Sanam Loghavi: None; Joseph Khoury: None; Santiago Montes-Moreno: None

Background: Plasmablastic lymphoma (PBL) is an uncommon large B-cell neoplasm. Genetic alterations in *MYC* have been described in ~60% of PBL cases, frequently in association with *PRDM1*/Blimp1 mutations. The aim of this study was to determine the mutational profile of a series of well characterized PBL cases and correlate with the tumor cells phenotype and microenvironment cell populations.

Design: Here we performed a targeted exonic NGS of 30 PBL cases with a B cell lymphoma dedicated panel for the detection of mutations in 35 genes and FISH for *MYC* translocations. IHC for the determination of oncogene expression, tumor associated macrophages (TAM), T cells and immune checkpoint markers was performed and quantified by averaging the number of positive cells within 3 representative high-power fields (40x magnification).

Results: We have identified an enrichment in recurrent genetic events in MYC (3 cases with missense point mutations, 15 cases with MYC translocation, 1 case with MYC amplification), PRDM1/Blimp1 (6 cases, with recurrent D203E variant in 4 cases) and STAT3 (5 cases with recurrent missense point mutations in SH2 domain). These mutations were more frequent in EBV positive disease. Other genetic events included mutations in BRAF (2 cases, BRAFV600E and BRAFG469A), EP300 (2 cases), BCR pathway (CD79a and CD79B, 2 cases), NOTCH pathway (NOTCH2 (1 case), NOTCH1 (1 case) and SGK1 (2 cases)), CARD11 (1 case) and MYD88L265P (1 case). Immunohistochemical analysis showed universal MYC expression, significantly higher in cases with MYC rearrangements (Mann-Whitney p value < 0,0001) together with Phospho-STAT3 (Tyr705) overexpression restricted to cases with STAT3 SH2 domain mutations. Microenvironment populations were also heterogeneous and unrelated with EBV status, with an enrichment of TAM and PD1 positive T cells. PD-L1 was expressed in all cases in the TAM population but only in 5 cases in the neoplastic cells (4 out of 14 EBV positive cases). HLA expression was absent in the majority of PBL cases.

Conclusions: Plasmablastic lymphoma mutational profile is heterogeneous and related with EBV infection in the neoplastic cells. Genetic events in MYC, STAT3 and PRDM1/Blimp1 are more frequent in EBV positive disease. Both MYC translocation/amplification and STAT3 SH2 mutations lead to overexpression of MYC and Phospho-STAT3, respectively. An enrichment in TAM and PD1 reactive T lymphocytes is found in the microenvironment of PBL, despite the very low frequency of PD-L1 expression by the neoplasia.

1379 MUC4 Protein Expression is Specific to Philadelphia Positive and Philadelphia-like B-Acute Lymphoblastic Leukemia (B-ALL) and Identifies a Subset with Worse Prognosis

Catherine Gestrich[1], Kwadwo Oduro[2]
[1]University Hospitals Cleveland Medical Center, Case Western Reserve University, Brecksville, OH, [2]University Hospitals Cleveland Medical Center, Cleveland, OH

Disclosures: Catherine Gestrich: None; Kwadwo Oduro: None

Background: Mucin 4 (MUC4) is a glycoprotein that plays a role in cell growth signaling pathways and is thought to play a role in tumor progression by halting apoptosis. It is known to be overexpressed in low-grade fibromyxoid sarcoma (LGFMS) and a subset of pancreatic ductal adenocarcinoma. MUC4 expression in hematologic malignancies has not been explored. Gene expression profiling has previously identified MUC4 overexpression at the RNA level in Philadelphia-like (Ph-like) B-ALL. We sought to determine the expression of MUC4 at the protein level in B-ALL.

Design: We identified a total of 47 B-ALL cases (22 pediatric cases, 25 adult cases; age range 1 to 82 years old) representing all genetically WHO defined subgroups of B-ALL, determined based on cytogenetics studies performed at the time of diagnosis. All Ph-like cases had a CRLF2 rearrangement and overexpressed CRLF2 by flow cytometry. Immunohistochemical staining for MUC4 was performed on archival formalin fixed paraffin embedded (FFPE) bone marrow biopsy specimens. A score of 0 (negative), 1+ (weak), or 2+ (strong) was given based on intensity of staining.

Results: A total of 4/47 (8.5%) cases demonstrated positive, cytoplasmic staining for MUC4. All cases were either Philadelphia positive (Ph+) (3/9 or 33%) or Ph-like (1/6 or 17% of cases). 3/9 (33%). All 3 Ph+ cases had strong (2+) staining while the Ph-like cases demonstrated weak (1+) staining. All 4 patients with positive MUC4 (100%) subsequently relapsed (3 cases) or had residual disease (MRD) following induction (1 case with limited follow-up). In contrast 4 out of the 10 remaining B-ALL cases with follow up subsequently relapsed or had positive post-induction MRD.

Conclusions: We conclude that MUC4 protein expression is rare in B-ALL but appears to be restricted to Ph+ and Ph-like cases. MUC4 IHC in concert with the widely available BCR-ABL1 FISH may be employed as a specific, albeit not sensitive, marker for identification of Ph-like B-ALL cases. The findings in this limited cohort also suggests that MUC4 expression may be associated with worse clinical outcomes. These conclusions will need to be validated in larger studies.

1380 GAB1 Expression in Philadelphia-like Acute Lymphoblastic Leukemia

Catherine Gestrich[1], Kwadwo Oduro[2]
[1]University Hospitals Cleveland Medical Center, Case Western Reserve University, Brecksville, OH, [2]University Hospitals Cleveland Medical Center, Cleveland, OH

Disclosures: Catherine Gestrich: None; Kwadwo Oduro: None

Background: Philadelphia chromosome-like B acute lymphoblastic leukemia (Ph-like B-ALL) is a "high-risk" (poor prognosis) B-ALL subtype comprising 10-25% of B-ALL cases. These cases lack the *BCR-ABL1* fusion and are characterized by a gene expression profile, rather than a single molecular alteration. Gene expression profiling is often a send out test, resulting in a lengthy turnaround time. One gene that is over expressed is GAB1, which is involved in morphogenesis, proliferation and cell adhesion and motility. Since an immunohistochemical (IHC) stain exists for GAB1, our goal was to investigate the staining pattern of GAB1 in Ph-like B-ALL and to assess whether it could be used as a marker to identify these patients more rapidly.

Design: We selected a total of 47 B-ALL cases representing all genetically WHO defined subgroups of B-ALL, determined based on cytogenetics studies performed at the time of diagnosis. Our patients ranged from 1 to 82 years old at the time of initial diagnosis, with an average age of 27. Immunohistochemical staining for GAB1 was performed on formalin fixed paraffin embedded (FFPE) bone marrow biopsy specimens. A score of 0 (negative), 1+ (weak), or 2+ (strong) was given based on intensity of staining.

Results: GAB1 was most strongly (2+) expressed in specific B-ALL subgroups, including Ph-like (3/6, 50%), Ph+ (5/9, 56%), and ETV6-RUNX1 (4/5, 80%). Of the remaining patients in the Ph-like group, 2/6 (40%) had weak, 1+ staining and 1/6 (20%) had negative staining. The ages of the Ph-like patients ranged from 4 to 49 at time of diagnosis, with an average of 29. 2/3 (67%) Ph-like patients with strong, 2+ staining were pediatric patients, ages 4 and 11.

	0	1+	2+
Ph-like (n = 6)	1 (20%)	2 (40%)	3 (50%)
Ph+ (n = 9)	1 (11%)	3 (33%)	5 (56%)
Hyperdiploid (n = 11)	4 (36%)	6 (55%)	1 (9%)
ETV6-RUNX1 (n = 5)	0	1 (20%)	4 (80%)
TCF3-PBX1 (n = 4)	4 (100%)	0	0
iAMP 21 (n = 1)	0	1 (100%)	0
Hypodiploid (n = 2)	0	1 (50%)	1 (50%)
NOS (n = 9)	3 (33%)	3 (33%)	3 (33%)

Conclusions: Ph-like B-ALL expresses GAB1, which can be identified using routine IHC. Although B-ALL has an overall good prognosis, certain subgroups, such as Ph-like patients, often have a poor outcome. Therefore, additional treatment options are needed. In medulloblastoma, GAB1 IHC is used to identify cases that exhibit a Sonic Hedgehog (SHH) profile. Currently, there are two FDA-approved drugs targeting the SHH pathway. One drug, glasdegib, is being evaluated in clinical trials for acute myeloid leukemia treatment. This could represent a potential therapeutic option for those Ph-like patients that express GAB1.

1381 Determining Factors Influencing White and African American Patients with Multiple Myeloma Using Demographics, Bone Marrow Morphology, and Molecular Data

Sharmila Ghosh[1], Michael Guerrero-Calderon[2], Lesly Polanco[3], Christian Salib[4], Julie Teruya-Feldstein[5], Jane Houldsworth[4]
[1]Mount Sinai West, Icahn School of Medicine, New York, NY, [2]New York Harbor Healthcare System, NYU School of Medicine, Freeport, NY, [3]Mount Sinai Hospital Icahn School of Medicine, Bronx, NY, [4]Icahn School of Medicine at Mount Sinai, New York, NY, [5]Mount Sinai Icahn School of Medicine, New York, NY

Disclosures: Sharmila Ghosh: None; Michael Guerrero-Calderon: None; Lesly Polanco: None; Christian Salib: None; Julie Teruya-Feldstein: None; Jane Houldsworth: None

Background: Risk stratification in multiple myeloma and monoclonal gammopathies incorporates molecular markers including large genomic abnormalities, mutations, and gene expression profiling. While few studies have researched differences in these features independently across different races, rarely have all been evaluated in the same cohort and included detailed pathologic features.

With a large cohort of patients, we focused on differences between self-identified white (Wh) and African American (AA) patients in terms of who is more at risk with certain characteristics.

Design: 599 patients diagnosed with monoclonal gammopathy were enrolled at a single institution in an IRB approved study over 2 years; 77 self-identified as AA and 381 WH. One specimen was selected per patient based mostly on highest percentage of monoclonal plasma cell and availability of molecular testing. Pathologic features, FISH data and mutations (Foundation Medicine Heme NGS Panel) and MyPRS gene expression profiling risk classification and molecular subtype were reviewed. Statistical correlations were assessed using 2-sided Fisher's exact test.

Results: Table 1 summarises pathologic features, MyPRS gene expression findings, and large genomic abnormalities detected by FISH. Overall pathologic features were comparable between the races and for FISH-detected genomic abnormalities. *IGH* rearrangements in AA patients was more likely to involve 11q13 rather other higher risk loci. Not unexpectedly, there was a higher proportion MyPRS CD-1 and CD-2 molecular subtypes, representing those with CCND1-IGH rearrangements. There were relatively fewer AA patients with the hyperdiplod proliferation gene expression signature (HY) than WH. For 26AA and 149 WH patients with available mutation data, AA and WH patients exhibited comparable mutations per specimen (1.69 versus 1.75, excluding detected IGH-associated rearrangements). The frequencies of occurrence of *KRAS*, *NRAS*, *TP53* mutations were similar between the races, but higher frequencies of *DNMT3A* and *CD36* mutations were found in AA patients compared with WH (27% AA versus 15%, 15% versus 0.03%), with the later reaching significance (P=0.03).

Feature	Category	WH	AA
Grade	1	38	8
	2	82	16
	3	6	2
Bartl Stage	1a	41	3
	1b	46	10
	1	58	13
	2	46	9
	3	42	13
Plasma cell %	0-25	248	49
	26-50	39	6
	51-75	27	6
	76-100	17	6
Monocyte %	<1.9	83	21
	2.0-8.0	233	42
	>8.1	16	3
Light chain restriction	K	154	35
	L	103	20
MyPRS Risk Classification	High Risk	79	15
	Low Risk	103	16
MyPRS Molecular Subtypes	CD1+CD2	61	17
	HY	39	3
	LB	16	2
	MF	20	3
	MS	24	4
	PR	20	3
FISH abnormalities	1q22/chr1 gain	85 (37%)	19 (42%)
	IGH rearrangement	124 (64%)	27 (63%)
	t(11;14)	64 (34%)	15 (55%)
	t(14,16),t(14,20)	15 (8%)	3 (7%)
	t(4;14)	25 (13%)	4 (9%)
	17p loss	27 (12%)	5 (11%)
	13q14/chr13 loss	101 (49%)	18 (38%)
	MYC rearrangement	35 (19%)	6 (15%)

Conclusions: In this study, few differences in pathologic and molecular features were identified between the two ethnic groups. Only mutations in *CD36* was significantly different between AA and WH patients. Expansion of the study to include other patient of other races is ongoing.

1382 Histopathologic, Immunophenotypic, and Mutational Landscape of Follicular Lymphomas with Plasmacytic Differentiation

Sarah Gibson[1], Yen-Chun Liu[2], Nicholas Barasch[3], Steven Swerdlow[2]
[1]Mayo Clinic Arizona, Scottsdale, AZ, [2]University of Pittsburgh School of Medicine, Pittsburgh, PA, [3]University of Pittsburgh Medical Center, Pittsburgh, PA

Disclosures: Sarah Gibson: None; Yen-Chun Liu: None; Nicholas Barasch: None; Steven Swerdlow: None

Background: Follicular lymphomas (FL) with plasmacytic differentiation (FL-PCDiff) include cases with predominantly interfollicular plasmacytic differentiation (interF-PCDiff), which often have *BCL2* rearrangements, and others with predominantly intrafollicular plasmacytic differentiation (intraF-PCDiff), which generally lack *BCL2* rearrangements (Mod Pathol 2010;23:71). We suggested these latter cases may be more like marginal zone lymphomas (MZL). 25 FL-PCDiff were studied to further evaluate our previous observations, as well as to investigate the mutational landscape of these 2 types of FL-PCDiff.

Design: 25 FL-PCDiff were assessed to determine the pattern of PCDiff, the presence of *BCL2* and *BCL6* rearrangements, and their mutational landscape using next-generation sequencing mutation analysis.

Results: The FL-PCDiff included 11 with intraF-PCDiff, 10 with interF-PCDiff, and 4 with relatively equal proportions of both. FL with intraF-PCDiff were commonly IgM+, kappa+ and CD10-, and often lacked *BCL2* rearrangements. The most common pathogenic mutations in FL-PCDiff were in *KMT2D* (52%), *TNFAIP3* (20%), *TNFRSF14* (20%), *CREBBP* (16%), and *EZH2* (16%). *KMT2D*, *CREBBP* and *TNFAIP3* mutations were more common in FL with interF-PCDiff. Compared to published FL, interF-PCDiff cases had less frequent *BCL2* mutations and more frequent *TNFAIP3* mutations (p=0.02), while intraF-PCDiff cases had less common *BCL2*, *CREBBP* and *KMT2D* mutations (p≤0.003). FL with interF-PCDiff also had more frequent *CREBBP* and *KMT2D* mutations (p≤0.04) compared to published nodal MZL (NMZL). There were no significant differences in mutation frequency between intraF-PCDiff cases and NMZL.
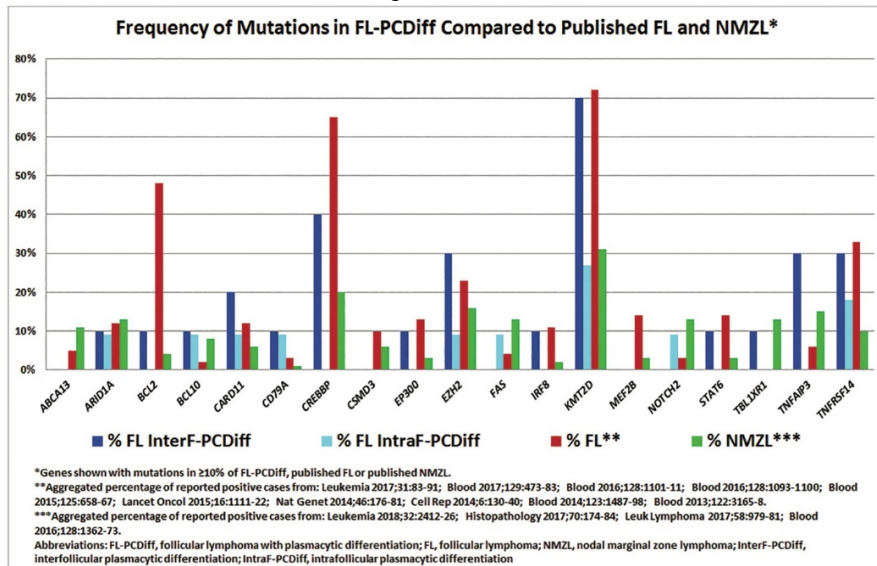
Figure 1 - 1382

Frequency of Mutations in FL-PCDiff Compared to Published FL and NMZL*

Legend: ■ % FL InterF-PCDiff ■ % FL IntraF-PCDiff ■ % FL** ■ % NMZL***

*Genes shown with mutations in ≥10% of FL-PCDiff, published FL or published NMZL.
**Aggregated percentage of reported positive cases from: Leukemia 2017;31:83-91; Blood 2017;129:473-83; Blood 2016;128:1101-11; Blood 2016;128:1093-1100; Blood 2015;125:658-67; Lancet Oncol 2015;16:1111-22; Nat Genet 2014;46:176-81; Cell Rep 2014;6:130-40; Blood 2014;123:1487-98; Blood 2013;122:3165-8.
***Aggregated percentage of reported positive cases from: Leukemia 2018;32:2412-26; Histopathology 2017;70:174-84; Leuk Lymphoma 2017;58:979-81; Blood 2016;128:1362-73.
Abbreviations: FL-PCDiff, follicular lymphoma with plasmacytic differentiation; FL, follicular lymphoma; NMZL, nodal marginal zone lymphoma; InterF-PCDiff, interfollicular plasmacytic differentiation; IntraF-PCDiff, intrafollicular plasmacytic differentiation

Figure 2 - 1382

Histologic, Immunophenotypic, and Genetic Features of 25 FL-PCDiff			
	InterF-PCDiff	IntraF-PCDiff	Mixed InterF-/IntraF-PCDiff	InterF- vs. IntraF-PCDiff (p-value)
No.	10	11	4	
Grade 1-2	7 (70%)	5 (45%)	3 (75%)	NS
IgM+	3 (30%)	8 (73%)	4 (100%)	0.09
Kappa+	3 (30%)	8 (73%)	2 (50%)	0.09
CD10+	9 (90%)	5 (45%)	1 (25%)	0.06
BCL2+	9 (90%)	10 (91%)	4 (100%)	NS
BCL2 R	10 (100%)	3 (27%)*	1 (25%)	0.001
BCL6 R	3 (30%)	3 (27%)*	1 (25%)	NS

Comparison of Pathogenic Mutations Identified in 25 FL-PCDiff to Published FL and NMZL										
Gene	InterF-PCDiff	IntraF-PCDiff	Mixed InterF-/IntraF-PCDiff	Published FL**	Published NMZL***	InterF- vs. IntraF-PCDiff (p-value)	InterF-PCDiff vs. FL (p-value)	InterF-PCDiff vs. NMZL (p-value)	IntraF-PCDiff vs. FL (p-value)	IntraF-PCDiff vs. NMZL (p-value)
ARID1A	1 (10%)	1 (9%)	0 (0%)	12%	5%	NS	NS	NS	NS	NS
BCL2	1 (10%)	0 (0%)	0 (0%)	48%	4%	NS	0.02	NS	0.001	NS
BCL10	1 (10%)	1 (9%)	1 (25%)	2%	8%	NS	NS	NS	NS	NS
CARD11	2 (20%)	1 (9%)	0 (0%)	12%	6%	NS	NS	NS	NS	NS
CD79A	1 (10%)	1 (9%)	1 (25%)	3%	1%	NS	NS	NS	NS	NS
CREBBP	4 (40%)	0 (0%)	0 (0%)	65%	12%	0.04	NS	0.04	0.0001	NS
CSMD3	0 (0%)	0 (0%)	0 (0%)	10%	6%	NS	NS	NS	NS	NS
EP300	1 (10%)	0 (0%)	2 (50%)	13%	3%	NS	NS	NS	NS	NS
EZH2	3 (30%)	1 (9%)	0 (0%)	23%	16%	NS	NS	NS	NS	NS
IRF8	1 (10%)	0 (0%)	0 (0%)	11%	2%	NS	NS	NS	NS	NS
KMT2D	7 (70%)	3 (27%)	3 (75%)	72%	32%	0.09	NS	0.03	0.003	NS
MEF2B	0 (0%)	0 (0%)	0 (0%)	14%	3%	NS	NS	NS	NS	NS
STAT6	1 (10%)	0 (0%)	0 (0%)	14%	3%	NS	NS	NS	NS	NS
TNFAIP3	3 (30%)	0 (0%)	2 (50%)	6%	15%	0.09	0.02	NS	NS	NS
TNFRSF14	3 (30%)	2 (18%)	0 (0%)	33%	10%	NS	NS	NS	NS	NS

No., number; R, rearranged; NS, not significant; vs., versus

*No IntraF-PCDiff cases contained both BCL2 and BCL6 rearrangements.

**Aggregated percentage of reported positive cases from: Leukemia 2017;31:83-91; Blood 2017;129:473-83; Blood 2016;128:1101-11; Blood 2016;128:1093-1100; Blood 2015;125:658-67; Lancet Oncol 2015;16:1111-22; Nat Genet 2014;46:176-81; Cell Rep 2014;6:130-40; Blood 2014;123:1487-98; Blood 2013;122:3165-8.

***Aggregated percentage of reported positive cases from: Leukemia 2018;32:2412-26; Histopathology 2017;70:174-84; Leuk Lymphoma 2017;58:979-81; Blood 2016;128:1362-73.

Conclusions: FL-PCDiff include 2 subsets with distinctive histologic, immunophenotypic, and genetic features, plus a small number with overlapping features. While both groups had a mutational profile distinct from other FL, only the interF-PCDiff group showed significant differences from NMZL. Furthermore, the 2 most common mutations found in FL (*CREBBP* and *KMT2D*) were the most frequent in the interF-PCDiff group, while the intraF-PCDiff group had significantly fewer. These results further support that while FL-PCDiff have some distinctive features in general, those with intraF-PCDiff appear to be more similar to NMZL and less similar to other FL. Nevertheless, the presence of *BCL2* or *BCL6* rearrangements in over 50% of intraF-PCDiff cases would not be typical for NMZL.

1383 Increased Frequency of Monoclonal B Lymphocytosis in Primary Myelofibrosis

Behiye Goksel[1], Khaled Alayed[2], Erika Moore[3], Howard Meyerson[4]
[1]Case Western Reserve University/University Hospitals Cleveland Medical Center, Shaker Heights, OH, [2]King Saud University, Case Western Reserve University, University Hospitals/Case Medical Center, Aurora, OH, [3]University of Pittsburgh, Pittsburgh, PA, [4]University Hospital Case Medical Center, Cleveland, OH

Disclosures: Behiye Goksel: None; Khaled Alayed: None; Erika Moore: None; Howard Meyerson: None

Background: Monoclonal B lymphocytosis (MBL) is defined as a clonal B-cell population in the peripheral blood with fewer than 5 × 109/L B-cells with no other clinical signs and symptoms of a lymphoproliferative disorder. The frequency of MBL in the general population increases with age; with 3.5% to 6.7% in those aged 40 to 60 years and 5% to 9% among individuals older than 60 years. In course of our practice we noted a relatively high incidence of MBL in patients with primary myelofibrosis (PMF) and wondered whether the frequency was truly higher than that seen in a comparable population. Therefore we assessed the frequency of MBL in bone marrow specimens from patients with PMF in comparison to chronic myeloid leukemia (CML).

Design: Patients with PMF (n= 45) and CML (n= 49) over the age of 60 were identified from a search of the CoPath and Genetic databases at University Hospitals Cleveland Medical Center. Patients with MBL were then identified within these groups by review of the electronic medical record. Clone size and type (CLL vs non-CLL) and bone marrow morphology were reviewed in cases with MBL. Statistical analysis was carried out use R software.

Results: MBLs were more frequent in PMF compared to CML (13/45 (28.9%) vs 5/49 (10.2%), p = 0.02). No statistical age (70.7 yrs in CML vs 72.5 yrs in PMF, p =0.3) or gender differences were noted. The size of the clones in PMF ranged from 0.01% to 22% and were

larger than that seen in CML, (*p* = 0.02). Within the PMF group there was no association with the Jak2 mutation status and the presence of MBL (p = 0.4). Of the MBLs phenotyped 5/11 PMF/MBLs had a CLL-like phenotype by flow cytometry but there was no difference in MBL type between PMF and CML (p = 0.9). Morphologically, 6 of 11 PMF/MBL cases evaluated showed characteristics of end stage disease with WHO grade MF-3 fibrosis. 4/11 cases showed lymphoid aggregates on either core biopsy or clot specimen and 2/11 demonstrated increased interstitial B lymphocytes. None of the CML/MBL cases showed morphologic evidence of a lymphoid infiltrate.

Conclusions: We show that the incidence of MBL in patients with PMF is approximately 3 times higher than the age-matched CML patients (*p* = 0.02). The incidence is also higher than that previously reported in older adults. The increased frequency was unrelated to Jak2 mutational status. The high frequency of end-stage fibrosis suggests a possible correlative link.

1384   Clinical and Pathologic Spectrum of DDX41 Mutated Hematolymphoid Neoplasms

Tanu Goyal[1], Zheng Jin Tu[2], James Cook[3]
[1]Beachwood, OH, [2]Robert J. Tomsich Pathology & Laboratory Medicine Institute, Cleveland Clinic, Cleveland, OH, [3]Cleveland Clinic, Cleveland, OH

Disclosures: Tanu Goyal: None; Zheng Jin Tu: None; James Cook: None

Background: Germline *DDX41* mutations are associated with a familial predisposition to myeloid malignancies. Most cases have been reported as AML or MDS, but the spectrum of clinical and pathologic findings in *DDX41* mutated neoplasia remains unclear. At our institution, a 62 gene NGS panel including *DDX41* is employed for evaluation of hematologic neoplasms. In this study, we review the detailed clinical and pathologic features of *DDX41* mutated neoplasms.

Design: NGS cases analyzed January 2018 through August 2019 were searched for *DDX41* mutations. *DDX41* variants were classified as germline/likely germline (G/LG) or somatic/likely somatic (S/LS) based on prior literature, variant allele fraction, and analysis of remission bone marrow (available in 1 case). The clinical history, morphology, cytogenetics and molecular results were reviewed.

Results: 24/1039 (2.3%) analyzed cases were *DDX41* mutated. 8 with likely benign/uncertain significance *DDX41* variants were excluded. 16 remaining cases contained 23 *DDX41* variants (14 missense, 6 nonsense, 1 frameshift, 1 splice site, 1 inframe del). 16/16 (100%) contained 1 G/LG *DDX41* mutation and 7 (44%) carried a second S/LS mutation. Family histories included 2 with hematologic neoplasms and 8 with solid tumors. Median age was 65 years (52-85). Diagnoses included AML (n=7), MDS (n=5), CMML (n=1), CCUS (n=1), PMF (n=1) and T-LGL (n=1). One CMML case and 2 AML cases were simultaneously involved by CLL and plasma cell neoplasms (PCN), respectively. Additional mutations were identified in 24 genes (Figure1) and 3 cases had abnormal karyotype. Morphologic review of 12 cases of AML/MDS showed a hypo- (n=8, 67%), normo- (n=3, 25%) or hyper-cellular (n=1, 8%) bone marrow for age (range 10-80%, median 20%). Overt dysplasia (>10%) was observed in erythroids (n=1, 8%), granulocytes (n=1, 8%) and megakaryocytes (n=6, 50%). 14 patients were alive at last follow up, one lost to follow up and one patient died (median follow-up 9 months).

Figure 1 - 1384
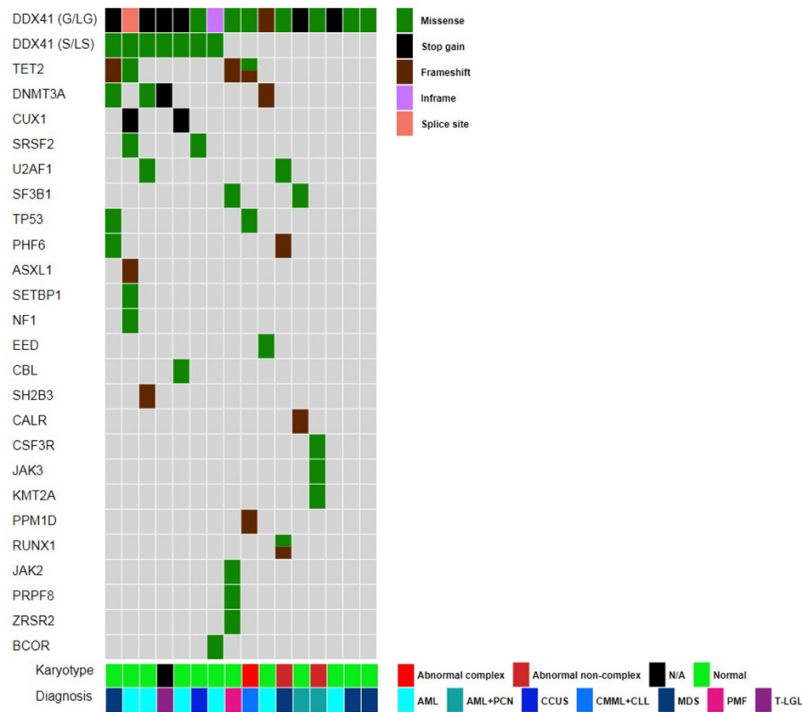
Conclusions: While *DDX41* mutated neoplasms are most commonly AML and MDS, this study identifies additional cases including CCUS, CMML and PMF. *DDX41* mutated AML/MDS is frequently hypocellular, often with megakaryocytic dysplasia. This cohort also includes lymphoid and plasma cell neoplasms, including the first reported case of *DDX41* mutated LGL leukemia, suggesting that germline *DDX41* mutations may also predispose to lymphoid malignancies.

1385 Is There Added Value to Performing Metaphase Analysis on Negative Bone Marrows?

Neha Gupta[1], Jie Li[2], John Van Arnam[3], Jihui Qiu[4], Jennifer Morrissette[5], Adam Bagg[6]
[1]Perelman School of Medicine, Hospital of the University of Pennsylvania, Philadelphia, PA, [2]University of Manitoba, Winnipeg, MB, [3]Philadelphia, PA, [4]Department of Pathology and Laboratory Medicine, Jefferson Health New Jersey, Cherry Hill, NJ, [5]Perelman School of Medicine, University of Pennsylvania, Philadelphia, PA, [6]University of Pennsylvania, Philadelphia, PA

Disclosures: Neha Gupta: None; Jie Li: None; John Van Arnam: None; Jihui Qiu: None; Jennifer Morrissette: None; Adam Bagg: None

Background: Conventional cytogenetics (CC) is an integral facet of the evaluation of hematologic neoplasms and provides essential diagnostic and prognostic data. As such, metaphase analysis is typically routinely ordered on all bone marrow (BM) studies in many institutions. We wished to determine the degree to which performing CC on negative BMs might provide additional and potentially clinically-actionable information and when CC might be unnecessary.

Design: In an IRB-approved study, we retrospectively screened our pathology and cytogenetics databases over a 2-year period to identify cases with negative BMs (NBMs) that had been submitted for CC, focusing on those revealing "clonal" CC abnormalities (CCA). Pathology reports and clinical databases were reviewed to determine the indication for performing BMs.

Results: Of a total of 3124 BMs submitted for CC, we identified 614 cases with NBMs. Of these, 48 were inadequate or cancelled, leaving 566 with analyzable metaphases. No CC abnormalities were identified in 89% (505/566). The bulk of these BMs were performed for gauging post-therapy responses, staging of lymphomas or unexplained cytopenias. Of the 61 with CC abnormalities, 10 were constitutional, including a rare balanced t(5;8), and 18 showed non-clonal (<75%) loss of sex chromosomes. The remaining 5.8% (33/566) with bona fide CCA comprised 26 cases compatible with "minimal" residual disease post therapy (19 AML, 2 CML, 2 ALL, 1 CLL, 1 MDS, 1 MM), 4 for lymphoma staging and 3 with unexplained cytopenias. Both CMLs also showed Ph- clones, while the CLL and MM cases showed "myeloid-associated" clones that were or could be harbingers of therapy-related myeloid neoplasms (TRMN). Of the 4 cases for lymphoma staging; one showed a rare t(10;18) in a patient with intravascular B-cell lymphoma while another was concerning for an evolving TRMN. None of the CCAs in the unexplained cytopenias was MDS defining.

Conclusions: Unsurprisingly, the majority (89%) of NBMs are negative for CCAs. After excluding age-related and constitutional (including rare) CCAs, only a minority (5.8%) show bona fide CCAs, not all of which are clinically actionable; some may be unrelated to the primary neoplasm and may be harbingers of TRMNs. Given the cost and labor-intensiveness of CC, it may be prudent to consider judicious formal triage of CC requests on BMs, which may lead to substantial health care savings by minimizing the number of unhelpful studies.

1386 Re-Evaluation of Monoclonal B-cell Lymphocytosis Incidentally Discovered in Soft Tissue and Lymph Node

Gabriel Habermehl[1], Eric Hsi[1]
[1]Cleveland Clinic, Cleveland, OH

Disclosures: Gabriel Habermehl: None; Eric Hsi: *Consultant*, Seattle Genetics; *Consultant*, Jazz Pharmaceuticals; *Grant or Research Support*, Eli Lilly; *Grant or Research Support*, Abbvie; *Grant or Research Support*, Cellerant

Background: Incidentally discovered B-cell clones in tissue may represent a tissue-based counterpart to blood defined MBL, herein termed tMBL. Reported cases are primarily lymph node samples, and are limited to "Chronic Lymphocytic Leukemia (CLL) type" MBL—without examination of WHO MBL subtypes such as "Atypical Chronic Lymphocytic Leukemia (ACLL)" or "Non- Chronic Lymphocytic Leukemia (NCLL)". We aimed to detail the clincopathologic characteristics of tMBL seen in our institution.

Design: We retrospectively reviewed all non-bone marrow/blood specimens over a 10 year period and identified all cases with previously unknown blood-based MBL. Specimens with a known diagnosis of CLL and a clinical history of lymphadenopathy/splenomegaly directly attributable to the MBL in question were also excluded. 54 cases were identified (35 lymph node, 3 splenic, and 16 soft tissue/other viscera). In all cases, presence of tMBL was confirmed by tissue based flow cytometry (TBFC) with a panel of antibodies directed at non-Hodgkin lymphoma.

Results: Median age at diagnosis was 65 years (range 37-88) with a male:female ratio of 1.16. The major indication for biopsy/excision was non-specific lymphadenopathy (19 cases). 48 cases were CLL-type, 2 were ACLL, and 6 were NCLL. All 16 cases of tMBL detected in non-lymphoid soft-tissue/viscera were of the CLL phenotype. Median white blood cell and absolute lymphocyte count were 7.73 k/uL (range 2.74 – 16.4) and 2.21 k/uL (range 0.3 – 7.8), respectively. In 51 cases immunohistochemistry was also performed (44 CLL-type, 2 ACLL, 5 NCLL) and an abnormal B-cell population consistent the TBFC was identified in 14 (all CLL-type)—none of which showed proliferation centers on hematoxylin & eosin. Concurrent blood flow cytometry (FC, available in 9 cases) showed low-count MBL (3 cases, all CLL), high-count MBL in (5 cases, all CLL), and was negative for a clonal population in 1 case (NCLL). With median follow-up of 46.2 mos, two patients showed "progression" of disease (CLL, 68.7 mos; and DLBCL, 6 mos), both with the same light chain and phenotype.

Conclusions: CLL-type tMBL is the most commonly detected subtype (89%), though ACLL and NCLL subtypes are uncommonly observed. Concurrent blood FC detects a *bona fide* MBL of similar phenotype in most cases. That only CLL-type MBL was detected in soft-tissue suggests that CLL MBL may be more widespread (extranodal) when compared to ACLL or NCLL MBL subtypes, though further studies are needed.

1387 Assessment of Acute Myeloid Leukemia for Expression of Tryptase and CD123 by Immunohistochemistry

Medina Hatooglu[1], Dennis O'Malley[2]
[1]NeoGenomics Laboratories, Inc., Aliso Viejo, CA, [2]NeoGenomics Laboratories, Inc., Dana Point, CA

Disclosures: Medina Hatooglu: None; Dennis O'Malley: None

Background: Myelomastocytic leukemia, that is, acute myeloid leukemia (AML) with evidence of mast cell differentiation has been described, but is quite rare, and exact criteria are not well-defined in relation to the possibly related rare entity, tryptase positive AML. CD123 is estimated to be expressed in 20-30% of AML cases and is also expressed in basophils. It is of current importance due to the development of targeted anti-CD123 therapies in AML. We evaluated 43 cases of AML with tryptase and CD123 IHC staining and correlated with flow, FISH, cytogenetic and NGS results.

Design: Cases of confirmed acute myeloid leukemia were identified from our files. Diagnoses were made according to current WHO criteria. Standard immunohistochemistry was performed for CD123 and tryptase. CD123 and tryptase were assessed by a semi-qualitative method in samples with AML. The percentage of blasts expressing was then evaluated. Positive cases were then correlated with results for: flow, FISH, cytogenetics and myeloid NGS.

Results: CD123 Immunohistochemical CD123 expression was identified in 10/43 cases (23%). In all positive cases, expression was 2-3+ intensity, with variation from 20-100% of blasts (avg. 46%). In most cases, CD123 expression of 2-3+ was identified in scattered basophils. One half of cases (5/10) had complex karyotypes. In all tested cases (8/8), three or more mutations were detected in a variety of AML related genes.

Tryptase

In most cases, variable numbers of mast cells served as an internal control. They were scattered, rare and expressed tryptase at 2-3+. Tryptase expression was identified in blasts of 3/43 cases (7%). Expression was seen in 5-20% of blasts, and in one case was in nodules. All cases expressed CD117 by flow. In two cases evaluated, no KIT mutations were identified. One case harbored a t(8;21); the others had complex, poor prognosis genetic/NGS findings.

Conclusions: We found tryptase expression in a higher than expected number of cases of AML (7%). We cannot confidently endorse a specific criteria for myelomastocytic leukemia, although more frequent evaluation of tryptase expression in AML may be warranted. In addition, we found CD123 expression in 23% of AML cases, comparable to other studies. We opine that these leukemias could represent very limited differentiation toward a basophil lineage, but additional studies are required to confirm this. We intend to test significantly more cases to further expand these findings.

1388   Primary Effusion Lymphoma: A Clinicopathological Study of 29 Cases

Zhihong Hu[1], Weina Chen[2], Wei Wang[3], Brenda Mai[4], Nghia Nguyen[4], L. Jeffrey Medeiros[3], Shimin Hu[3]
[1]The University of Texas Health Science Center at Houston, Sugar Land, TX, [2]University of Texas Southwestern Medical Center, Dallas, TX, [3]The University of Texas MD Anderson Cancer Center, Houston, TX, [4]The University of Texas Health Science Center at Houston, Houston, TX

Disclosures: Zhihong Hu: None; Weina Chen: None; Wei Wang: None; Brenda Mai: None; Nghia Nguyen: None; L. Jeffrey Medeiros: None; Shimin Hu: None

Background: Primary effusion lymphoma (PEL) is a rare aggressive large B-cell lymphoma associated with human herpesvirus 8 (HHV8) infection. PEL most often presents as an effusion without solid masses, but occasionally PEL can present as an extracavitary mass. In this study, we describe our collective experience to better characterize the clinicopathologic features of PEL.

Design: We retrospectively reviewed cases of PEL diagnosed from January 1, 2004 through June 30, 2019 from four major institutions. Patients' clinical information including demographic data, treatment regimens, and follow-up data were analyzed.

Results: The study cohort is composed of 29 patients with PEL: 22 HIV infection, 2 heart transplant and 5 without known immunodeficiency history. All patients were men with a median age of 46 years (range, 29-88). 11/22 HIV patients had Kaposi sarcoma, but none of 7 non-HIV+ patients. Sixteen patients presented with effusions only, 10 with solid masses only, and 3 with both effusion and solid masses. No bone marrow involvement was detected (0/8). The lymphoma cells were large with immunoblastic, plasmablastic or anaplastic morphology. Immunophenotypically, all 29 cases were positive for HHV8. The lymphoma cells were also positive for CD38 in 18/18 (100%), MUM1/IRF4 12/13 (92%), CD45 25/28 (89%), EMA 6/7 (85%), CD30 18/25 (72%), CD43 5/9 (56%), monotypic kappa or lambda 2/9 (22%), CD3 5/27 (19%), and weak CD20 2/28 (7%). CD19 (n=15) and ALK1 (n=13) were negative. Ki-67 showed a high proliferation rate of >90% in 8/10 (80%). ISH showed 16/25 (64%) cases positive for EBV-encoded RNA (EBER). FISH to assess MYC showed an extra copy in 3/3 (100%) cases. Treatment information was available in 16 patients; 12 (41%) received chemotherapy, including 7 DA-EPOCH and 5 CHOP. 15/27 (56%) patients died with a median follow up of 6.8 months (range, 0-80.2). The median overall survival (OS) was 38 months for the entire cohort. When compared to patients with extracavitary PEL (median OS, 45 months), patients with effusion-based PEL appeared to have a trend toward inferior OS with a median of 2 months, without significant difference (p=0.16).

Conclusions: PEL is an aggressive lymphoma with a male predominance, variable morphology, a plasmablastic immunophenotype, and a poor prognosis. Awareness of CD3 expression in a small subset of PEL is important to avoid misdiagnosis. Patients with effusion-based PEL appear to have a poorer prognosis than patients with extracavitary PEL, but currently employed therapies are not effective.

1389   Differential Expansions of Large Granular Lymphocyte Subpopulations in the Bone Marrow of Patients with Plasma Cell Myeloma are Associated with Patient Outcome

Bailey Hutchison[1], Ryan Ahern[2], Michelle DeLelys[1], Frederic Preffer[1], Robert Hasserjian[3]
[1]Massachusetts General Hospital, Boston, MA, [2]Gettysburg College, Gettysburg, PA, [3]Massachusetts General Hospital, Harvard Medical School, Boston, MA

Disclosures: Bailey Hutchison: None; Ryan Ahern: None; Michelle DeLelys: None; Frederic Preffer: None; Robert Hasserjian: None

Background: Large granular lymphocytes (LGLs) are immunophenotypically diverse cytotoxic T-cells defined by CD8/CD57 co-expression. Cytotoxic T-cells identified in the blood of plasma cell myeloma (PCM) patients are thought to have anti-myeloma specificity. This study aims to identify and determine the prognostic significance of immunophenotypic LGL subpopulations in the bone marrow (BM) of patients with plasma cell neoplasms.

Design: LGL data was gathered from all BM flow cytometry reports containing plasma cell (PC) analysis at our institution from 6/1/17-5/31/19. A total of 481 flow cytometry studies from 368 patients were retrieved. Cases included those with no clonal plasma cell population, MGUS, AL amyloidosis, previously untreated PCM, and treated PCM with or without residual disease. Patient outcome was obtained via chart review.

Results: LGLs comprised a higher proportion of BM T-cells in post-treatment PCM than untreated PCM (p<0.01). In untreated PCM (n=129), percentage of LGLs was positively correlated with percentage of marrow PCs (p=0.04). An increased proportion of CD5- LGLs was seen in treated PCMs with residual disease compared to those without residual disease (p<0.001). The proportion of CD5- LGLs was positively correlated with the percentage of PCs in untreated (p=0.025) and treated (p=0.019) PCM. The percentage of LGLs was not associated with overall survival (OS) in treated or untreated PCM, but untreated PCM patients with more than 10% CD5- LGLs had significantly shorter OS (p<0.0001). An increased proportion of CD16+ LGLs was also associated with shorter OS in untreated PCM (p=0.029). Patients with both more than 10% CD5- LGLs and more than 50% CD16+ LGLs had significantly shorter OS (median 12 months vs. undefined, p<0.0001). These effects were independent of the marrow PC percentage on multivariable analysis.

Figure 1 - 1389

Flow Cytometry Data Summary				
Clinical Groups	Number of Samples	Mean % LGLs (of all Lymphocytes)	Average % of CD5- LGLs	Average % of CD16+ LGLs
No Plasma Cell Neoplasm	51	14.2	5.3	52.4
AL Amyloidosis	7	16.7	2.8	59.0
Monoclonal Gammopathy of Unknown Significance (MGUS)	35	15.2	3.7	54.7
Untreated Plasma Cell Myeloma	129	16.3	6.8	54.9
Treated Plasma Cell Myeloma with No Residual Disease	74	25.3	3.9	54.7
Treated Plasma Cell Myeloma with Residual Disease	185	24.6	8.0	60.4

Figure 2 - 1389
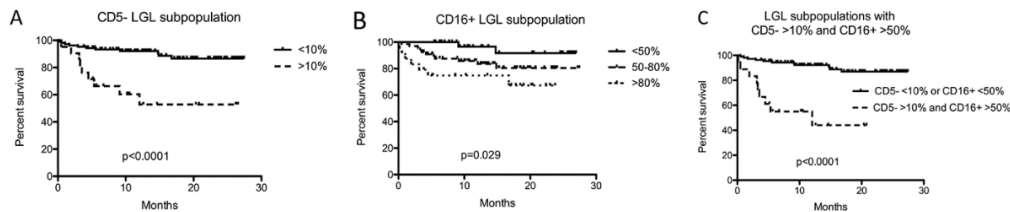
Conclusions: BM LGLs increase after treatment for PCM. In untreated PCM, increased proportions of CD5- and CD16+ LGLs are associated with shortened OS independent of disease burden. Cytotoxic T-cells in solid tumors downregulate CD5, which is a T-cell receptor signaling inhibitor. CD16+/CD8+ T-cells are thought to represent effector T-cells with NK-cell-like properties that respond to chronic antigen stimulation. Our data raise the possibility that increased cytotoxic CD5-/CD16+ LGLs in the marrow microenvironment are associated with increased disease aggression in PCM, which may have implications for immunomodulatory treatment strategies.

1390 The Diagnostic Utility of a Myeloid Mutational Panel for Myelodysplastic Syndromes and Myelodysplastic/myeloproliferative Neoplasms

Warda Ibrar[1], Jesse Cox[2], Catalina Amador[3], Hina Qureishi[2], Kai Fu[2], Timothy Greiner[2], Allison Vokoun[4], Weiwei Zhang[2], Yuan Ji[2]
[1]Department of Pathology and Microbiology, University of Nebraska Medical Center, Omaha, NE, [2]University of Nebraska Medical Center, Omaha, NE, [3]University of Nebraska, Omaha, NE, [4]Nebraska Medical Center, Omaha, NE

Disclosures: Warda Ibrar: None; Jesse Cox: None; Catalina Amador: None; Hina Qureishi: None; Kai Fu: None; Timothy Greiner: None; Allison Vokoun: None; Weiwei Zhang: None; Yuan Ji: None

Background: The diagnosis of myelodysplastic syndromes (MDS) and myelodysplastic/myeloproliferative neoplasms (MDS/MPN) is based on morphology and cytogenetics/FISH findings per 2017 WHO classification. With rare exceptions (e.g. *SF3B1* mutations), somatic mutations have not been incorporated as diagnostic criteria. In this study we analyzed the utility of mutational analysis with a targeted 54-gene or 40-gene next generation sequencing (NGS) panel in diagnosis of MDS and MDS/MPN.

Design: The clinicopathologic data and NGS results of patients with unexplained cytopenia with or without cytosis who underwent a bone marrow (BM) biopsy, and had sequencing with either a 54 gene Trusight Myeloid or a 40 gene Oncomine Myeloid NGS Assay performed at our institution from 2017 to 2019. Morphologic diagnosis of BM biopsy based on 2017 WHO classification was considered gold standard.

Results: A total 74 patients were identified, including 25 low-grade MDS (peripheral blood blasts <1% and BM blasts <5%), 16 high-grade MDS (peripheral blood blasts 2-19% and BM blasts 5-19%), 5 therapy-related MDS, 14 MDS/MPN, and 14 morphological negative ones. Of 74 patients, 158 somatic mutations involving 37 genes were detected and had variant allele frequency (VAF) ranging from 3% to 99%. 62% (23/37) genes showed recurrent mutations and 38% (14/37) genes had one mutation each. The most common mutated genes were *TET2*, *ASXL1*, *RUNX1, SF3B1* and *TP53*. Morphological negative, low-grade MDS, high-grade MDS, therapy-related MDS and MDS/MPN showed an average number of somatic mutations with a mean VAF: 1.5/20%, 2/37%, 3.1/38%, 2/33% and 4.8/41%, respectively. Mutations in *TP53*, *RUNX1, or ASXL1* were associated with high-grade and therapy-related MDS (p=0.004), while *SF3B1* mutations were associated with low-grade MDS (p=0.001). In 60 of 74 patients with a diagnosis of MDS or MDS/MPN, 32 showed abnormal cytogenetics and 28 showed normal cytogenetics. One or more mutations were detected in 25 of 28 (89%) MDS or MDS/MPN patients with normal cytogenetics. The sensitivity, specificity, and positive predictive value (PPV) and negative predictive value (NPV) of mutations for MDS and MDS/MPN with different cutoffs are summarized in Table 1*.

Table 1. Diagnostic performance of mutations for MDS and MDS/MPN with different cutoffs.

	Any mutations (VAF≥1%)	VAF≥20%	≥2 mutations	VAF≥10% and ≥2 mutations	VAF≥10% and ≥2 mutations, or abnormal cytogenetics/FISH
Sensitivity	87%	75%	58%	58%	83%
Specificity	50%	93%	93%	100%	86%
PPV	88%	98%	98%	100%	96%
NPV	47%	46%	34%	36%	54%

Conclusions: A myeloid mutational panel provides additional evidence of clonality besides cytogenetics/FISH studies in diagnosis of cytopenia with or without cytosis, and ≥ 2 mutations with ≥ 10% VAF highly predicts MDS and MDS/MPN with a PPV of 100%.

1391 Cell of Origin Studies are not Always Concordant in Relapsed or Concurrent Biopsies of Diffuse Large B-cell Lymphoma

Haaris Iqbal[1], Steven Kroft[2], Alexandra Harrington[3], John Astle[2], Ashley Cunningham[4], Vasiliki Leventaki[2], Maria Hintzke[5]
[1]Brookfield, WI, [2]Medical College of Wisconsin, Milwaukee, WI, [3]Milwaukee, WI, [4]Medical College of Wisconsin, Oconomowoc, WI, [5]Medical College of Wisconsin, New Berlin, WI

Disclosures: Haaris Iqbal: None; Steven Kroft: None; Alexandra Harrington: None; John Astle: None; Ashley Cunningham: None; Vasiliki Leventaki: None; Maria Hintzke: None

Background: Diffuse large B-cell lymphoma (DLBCL) is subclassified into germinal center (GCB) and non-germinal center (non-GCB) cell of origin (COO) most often using the Hans Algorithm (HA) to guide prognostication and potentially treatment, especially in the context of qualifying for clinical trials. While COO classification is recommended at initial diagnosis per 2016 WHO, the utility of classifying multiple, concurrently collected specimens and/or re-classification at relapse is unclear. As such, we aimed to investigate COO differences in newly diagnosed and refractory/relapsed DLBCL.

Design: Case archives were searched from 2005-2018 for non-bone marrow DLBCL patients (pts) (>18 yo) with 2 or more uniquely accessioned specimens. Clinical and laboratory data collected included pt age at diagnosis, sex, site of involvement, FISH, and treatment as available. Cases were classified as GCB vs non-GCB using HA, noting % tumor cell expression of CD10, BCL-6, and/or MUM-1 via manual count. Cases with insufficient tissue for HA classification were excluded.

Results: We identified 21 DLBCL pts (43 total specimens) meeting study inclusion criteria (13 M:8 F; 18-86 yrs; median 66 yrs). Sites of involvement included GI/liver (12), soft tissue (11), LN (4), brain (4), bone (3), skin (2), lung (1), mediastinum (1), buccal (1), nasopharynx (1), and bladder (1). Of these, 8 pts had concurrently collected specimens and 13 pts had refractory/relapsed disease sampled (0.3-5.3 yrs after initial diagnosis, mean of 1.9 yrs). At diagnosis, there were 12 GCB (57%) and 6 non-GCB (29%) pts. 3/8 pts (38%) with concurrently collected specimens had 1 GCB and 1 non-GCB site. 4/13 (31%) refractory/relapsed pts showed change in COO, with 2 GCB to non-GCB (0.5-0.7 yrs after initial diagnosis) and 2 non-GCB to GCB (5.1 and 5.3 yrs after initial diagnosis).

Conclusions: Our study serves as an initial survey of COO differences both in concurrently sampled sites as well as in refractory/relapsed DLBCL when compared to initial diagnostic HA classification. The data highlights COO tumor heterogeneity at diagnosis in over 1/3 of concurrently sampled sites. In refractory/relapsed DLBCL, nearly 1/3 pts show COO differences and may represent biologically distinct disease. Reclassification after initial diagnosis may be warranted, especially if it will impact potential therapeutic options.

1392 Overlap Between Pediatric Marginal Zone Lymphoma and Pediatric Follicular Lymphoma: Morphological and Mutational Analysis

Elaine Jaffe[1], Caoimhe Egan[1], Stefania Pittaluga[2], Julia Salmeron-Villalobos[3], Blanca Gonzalez-Farre[4], Joan Enric Ramis-Zaldivar[3], Dominik Nann[5], Falko Fend[6], Mark Raffeld[7], Elías Campo[3], Itziar Salaverria[4], Leticia Quintanilla-Fend[8]
[1]National Cancer Institute, National Institutes of Health, Bethesda, MD, [2]National Institutes of Health, Washington, DC, [3]Hospital Clinic Barcelona, University of Barcelona, Barcelona, Spain, [4]Hospital Clinic of Barcelona, Barcelona, Spain, [5]Institute of Pathology and Neuropathology, Tuebingen, Germany, [6]University Hospital of Tuebingen, Tuebingen, Baden-Württemberg, Germany, [7]National Cancer Institute, Bethesda, MD, [8]University of Tuebingen, Tuebingen, Baden-Wuerttemberg, Germany

Disclosures: Elaine Jaffe: None; Caoimhe Egan: None; Stefania Pittaluga: None; Julia Salmeron-Villalobos: None; Blanca Gonzalez-Farre: None; Joan Enric Ramis-Zaldivar: None; Dominik Nann: None; Falko Fend: None; Mark Raffeld: None; Elías Campo: None; Itziar Salaverria: None; Leticia Quintanilla-Fend: None

Background: Pediatric-type follicular lymphoma (PFL) and pediatric nodal marginal zone lymphoma (PMZL) are rare indolent B-cell lymphomas that occur predominantly in males and involve the head and neck region. The differential diagnosis is based on nodal architecture and immunophenotype of the atypical cells. In PMZL the atypical cells are interfollicular and are negative for markers of follicle center derivation such as CD10 and BCL6. In contrast, PFL is characterized by expanded and serpiginous follicles, often with blastoid cytology, with expression of CD10 and BCL6. We and others have noted cases that show intermediate features between both entities, making definitive categorization as PFL or PMZL challenging. We performed morphological review and mutational analysis to further explore the relationship and overlap between PMZL and PFL.

Design: As the mutational changes in PFL are well-described, morphologic and immunohistochemical analysis concentrated on 27 cases, most of which (n=22) were initially categorized as PMZL. The case series was restricted to patients less than 30 years of age. Following review, 21 cases were classified as showing overlapping features of PMZL and PFL and 6 cases had features that were more typical of PMZL. Targeted sequencing was performed using a FL panel that included *MAP2K1* and *TNFRSF14*, known to be frequently altered in PFL.

Results: Cases with morphologic overlap showed at least some serpiginous CD10 positive follicles as seen in PFL, but also had an increase in interfollicular B-cells beyond the follicular component. A subset exhibited PTGC-like changes, with fragmented germinal centers outlined by IgD-positive cells. Plasmacytoid differentiation was present in 10/27 cases. Frequent mutations in *MAP2K1* (10/21) were identified, predominantly in "overlap" cases (n=9/15). *TNFRSF14* mutations were detected in 5/18 cases, in both overlap (n=3/13) and PMZL (n=2/5) groups.

Conclusions: PMZL frequently shows overlapping histologic and immunophenotypic features with PFL. The presence of recurrent mutations in *MAP2K1* and *TNFRSF14* raises the question whether they represent two distinct entities or different morphological spectrum of the same disease.

1393 Clinical Utility of Targeted Next Generation Sequencing (NGS) in the Evaluation of Low-Grade Lymphoid Malignancies

Audrey Jajosky[1], Nathaniel Havens[1], Navid Sadri[2], Kwadwo Oduro[3], Erika Moore[4], Rose Beck[5], Howard Meyerson[6]
[1]Case Western Reserve University/University Hospitals Cleveland Medical Center, Cleveland, OH, [2]Cleveland, OH, [3]University Hospitals Cleveland Medical Center, Cleveland, OH, [4]University of Pittsburgh, Pittsburgh, PA, [5]University Hospitals of Cleveland, Case Western Reserve University, Cleveland, OH, [6]University Hospital Case Medical Center, Cleveland, OH

Background: High-throughput sequencing has helped to characterize the molecular features of B-, T-, & NK-cell malignancies. In the setting of difficult to classify lymphomas, molecular profiling may not only help to establish a diagnosis, but also aid in disease prognostication & predicting patient response to therapy. Therefore, we investigated the clinical utility of a custom-designed targeted NGS panel in the evaluation of patients with low-grade lymphoid neoplasms.

Design: We custom-built an NGS assay to evaluate peripheral blood (PB) & bone marrow (BM) specimens that contained >5% clonal lymphoid cells by flow cytometry &/or were highly suspicious for a lymphoproliferative disorder. The panel was designed to detect single nucleotide variants & small insertions/deletions within the hotspots of 31 genes involved in low-grade lymphoid malignancies: *ATM, BIRC3, BRAF, BTK, CARD11, CCND1, CD79B, CXCR4, EGR2, FBXW7, IKBKB, KLF2, KRAS, MAP2K1, MAP3K14, MYD88, NFKBIE, NOTCH1, NOTCH2, NRAS, PLCG2, POT1, RPS15, SF3B1, STAT3, STAT5B, TNFAIP3, TP53, TRAF2, TRAF3, & XPO1*. Over 18 months, 148 PB, BM, & lymph node (LN) specimens were sequenced. Pathology reports, including molecular addendums, & clinical notes were reviewed to determine how NGS findings were clinically utilized in each case.

Results: Of the 148 specimens tested, 86% were collected at diagnosis & 14% represented relapsed/refractory disease. Ultimately, 33% of cases were classified as CLL/SLL, 13% as LPL, 13% as MZL, 9.5% as MBL, 8% as T-LGL leukemia, 5% as MCL, 1% as B-PLL, 1% as HCL, 1% as HCL-v, 1% as CTCL, 1% as PTCL NOS, & 13.5% as other. Overall, molecular variant(s) were detected in 95/148 (64%) of cases (Table I) & 46% of mutated cases displayed ≥2 variants. Molecular features varied by disease subtype, although some genes were recurrently mutated across several disorders (Table I).

Disorder	# mutated cases/ total cases	Genes mutated (# patients with mutation)
Chronic lymphocytic leukemia/Small lymphocytic leukemia (CLL/SLL)	33/49 (67.3%)	*NOTCH1* (9), *TP53* (7), *ATM* (6), *BIRC3* (4), *EGR2* (4), *NFKBIE* (4), *SF3B1* (4), *BRAF* (3), *MYD88* (2), *POT1* (2), *XPO1* (2), *KLF2* (1), *KRAS* (1), *PLCG2* (1), *RPS15* (1), *TNFAIP3* (1)
B cell prolymphocytic leukemia (B-PLL)	1/1 (100%)	*BRAF* (1), *KLF2* (1), *NOTCH1* (1)
Lymphoplasmacytic leukemia (LPL)	18/19 (94.7%)	*MYD88* L265P (17), *CXCR4* (4), *BIRC3* (2), *ATM* (1), *TNFAIP3* (1), *TP53* (1)
Marginal zone lymphoma (MZL)	14/19 (73.7%)	*TP53* (3), *CARD11* (3), *KLF2* (3), *CXCR4* (2), *TNFAIP3* (2), *ATM* (1), *KRAS* (1), *MYD88* (1), *NFKBIE* (2), *NOTCH1* (1), *POT1* (1), *TRAF3* (1)
Mantle cell lymphoma (MCL)	6/7 (85.7%)	*ATM* (3), *CXCR4* (1), *IKBKB* (1), *NOTCH2* (1), *TP53* (2)
Hairy cell leukemia (HCL)	2/2 (100%)	*BRAF* V600E (2)
Hairy cell leukemia-variant (HCL-v)	2/2 (100%)	*BRAF* (1), *MAP2K1* (1), *NFKBIE* (1), *TP53* (1)
Follicular lymphoma (FL)	0/2 (0%)	-
Diffuse large B cell lymphoma (DLBCL)	2/5 (40%)	*TP53* (2), *CARD11* (1), *MYD88* (1), *NOTCH1* (1)
Monoclonal B-cell lymphocytosis (MBL)	4/14 (28.6%)	*ATM* (1), *BIRC3* (1), *FBXW7* (1), *MYD88* (1), *NOTCH1* (1), *TP53* (1)
T large granular lymphocytic (LGL) leukemia	10/12 (83.3%)	*STAT3* (9), *CARD11* (1), *STAT5B* (1), *TNFAIP3* (1), *TP53* (1)
Cutaneous T cell lymphoma (CTCL)	1/2 (50%)	*TP53* (1)
Peripheral T cell lymphoma (PTCL), not otherwise specified (NOS)	1/1 (100%)	*NRAS* (1), *TP53* (1)
T cell lymphocytosis	0/2 (0%)	-
Atypical T-cell population by flow cytometry	0/5 (0%)	-
Aggressive NK-cell leukemia	1/1 (100%)	*TP53* (1), *KRAS* (1)
Atypical NK-cell population by flow cytometry	0/3 (0%)	-
Plasma cell dyscrasia	0/2 (0%)	-

Conclusions: NGS helped to resolve the differential diagnosis of B-cell lymphomas with plasmacytic differentiation & of CLL vs. CD5+ MZL, among others. Therapeutically relevant *TP53* & *PLCG2* variants were identified in 10 CLL/SLL & MCL patients. Notably, NGS of a splenic MZL led to the incidental discovery of a cancer-predisposing germline *POT1* variant. Overall, NGS may aid in the diagnosis & treatment of patients with low-grade lymphoid neoplasms involving the PB or BM. Genes that are somatically mutated in lymphoid malignancies may also be mutated in familial cancer predisposition syndromes, so caution should be exercised when interpreting & reporting results

1394 Single-Cell Evaluation of Myelodysplastic Syndrome Stem Cells Identifies Determinants of Hypomethylating Agent Response and a Novel Prognostic Gene Signature

Sara Javidiparsijani[1], Igor Dolgalev[2], Priyanka Vijay[3], Monica Del Rey Gonzalez[4], Sean Devlin[5], Virginia Klimek[5], Stephen Chung[6], Christopher Mason[7], Christopher Park[8]

[1]NYU Langone Health, New York, NY, [2]New York University School of Medicine, New York, NY, [3]North Chicago, IL, [4]NYU Langone, New York, NY, [5]Memorial Sloan Kettering Cancer Center, New York, NY, [6]UT Southwestern Medical Center, Dallas, TX, [7]Weill Cornell Medicine, New York, NY, [8]NYU School of Medicine, New York, NY

Disclosures: Sara Javidiparsijani: None; Priyanka Vijay: None; Monica Del Rey Gonzalez: None; Christopher Park: None

Background: The myelodysplastic syndromes (MDS) are disorders of ineffective hematopoiesis that arise in hematopoietic stem cells (HSCs). To better understand the mechanisms underlying MDS pathogenesis and clinical responses to the hypomethylating agent decitabine (DAC), we used single-cell RNA-sequencing to evaluate HSCs from MDS patients treated with DAC as well as from normal young and old controls.

Design: HSCs (Lin-CD34+CD38-CD90+CD45RA-) were purified from low-risk MDS patients (n=6) as well as normal controls including cord blood (n=2), young adults (range 21-35; n=2), middle-age adults (range:40-50; n=2) and elderly controls (>65 years old; n=2); paired pre- and post-DAC samples from MDS patients undergoing therapy were evaluated. Using the Fluidigm C1 platform, we captured a total of 1,606 single cells from 26 samples and performed RNA-sequencing (Illumina HiSeq2500,100 bp paired-end reads)

Results: Uniform Manifold Approximation and Projection (UMAP) dimensionality reduction revealed that normal and MDS HSCs exhibit unique transactional profiles and confirmed the unique transcriptional features of each of the tested groups (Fig1). Pseudotime ordering showed that MDS HSCs express a gene signature that is independent of age. Intriguingly, mRNAs encoding genes recurrently mutated in myeloid neoplasms and associated with clonal hematopoiesis(e.g. ASXL1, TET2, DNMT3A, PP1MD) were downregulated in the elderly HSCs. HSCs from DAC responders are more similar to normal controls than non-responder HSCs, and are characterized by decreased ribosomal protein expression and increased p53 activation, particularly in non-responders. Comparison of MDS HSCs from responders to non-responder identified 455 DEGs (FDR<0.01) enriched for gene ontology (GO) terms involving "mRNA catabolic process, NMD," "protein localization to the ER," and "translational elongation," with 12 of the top 13 DEGs being ribosomal proteins (RPs). Utilizing the 491 DEGs (FDR< 0.01) in MDS HSCs compared to age-matched controls, we used LASSO regression to identify and validate a 10-gene signature that was able to stratify patients into low, intermediate, and high risk groups and predict overall survival (OS) in a large cohort of MDS patients (GSE19429)

Figure 1 - 1394
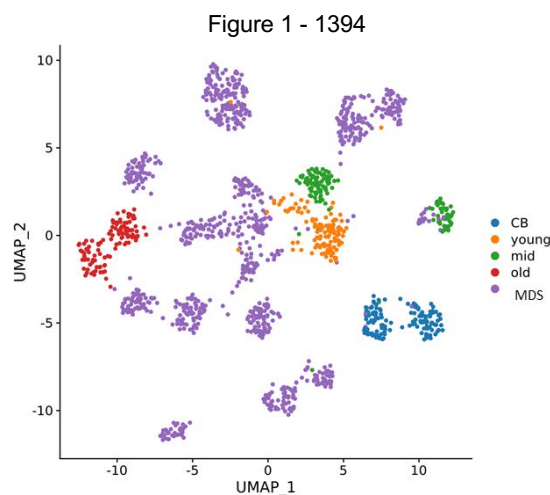
Conclusions: Single-cell RNA sequencing identifies genes that distinguish MDS from normal HSCs. MDS HSCs exhibit transcriptional changes that predict OS as well as clinical responses to DAC therapy. These studies support the importance of HSCs in determining clinical outcomes in MDS.

1395 Pathologic Findings in Patients with Refractory B-Lymphoblastic Leukemia Treated with Blinatumomab

Rajeswari Jayakumar[1], Laura Wake[2], Amy Duffield[3]
[1]Johns Hopkins Medical Institutions, Ellicott City, MD, [2]The Johns Hopkins Medical Institutions, Baltimore, MD, [3]Baltimore, MD

Background: There have been significant recent advances in the treatment of B-lymphoblastic leukemia (B-ALL), including blinatumomab, a bispecific T-cell engager that allows T-cells to specifically target CD19+ cells. Here we characterize the pathologic findings in patients treated with blinatumomab, and identify an unusual pattern of extramedullary relapse.

Design: The archives of the department of pathology were searched for cases of refractory B-ALL that were treated with standard chemotherapeutic regimens +/- blinatumomab. All relevant clinical and laboratory data were extracted and analyzed.

Results: 41 patients treated with blinatumomab with a minimum of 12 months (median=19, range=1-40) of follow up were identified. They had a median age of 43 years (range= 20-79), and included 59% men (24/41). The control group (n=46) had a median age of 54.5 years (range= 20-79), and included 54% men (25/46). In the group treated with blinatumomab, 17 patients (41%) relapsed. The relapses were identified in the bone marrow (n=9), CNS (n=3), joint space of the knee (n=1), breast (n=1), abdominal wall (leukemia cutis, n=1), stomach (n=1), and inguinal lymph node (n=1). All patients with extramedullary relapses had concurrent bone marrow biopsies that were negative for B-ALL to a level of sensitivity of 0.01%. The blasts in all cases of relapses except one, retained surface CD19 expression by flow cytometry. Two cases (2/17) showed loss of CD34. The patients with recurrent disease had genetic studies that showed abnormalities in Philadelphia chromosome (n=2), *CDKN2A* (n=5), *KMT2A* (n=4), *IGH* (n=5), *CSF3R* (n=2), *PBX1* (n=1), *CRLF2* (n=2) and *MYD88* (n=1), which was similar to the pattern seen in the control group. In the control group, treated with standard chemotherapy regimens, 19 patients (41%) relapsed. All of the relapses in the control group involved the bone marrow, with the exception of two patients who demonstrated CNS relapse only. Only one patient with bone marrow involvement showed extramedullary disease, involving the oropharynx and lymph nodes (Table 1).

	Refractory B-ALL cases treated with Standard Chemotherapy regimen and Blinatumomab (Cases)	Refractory B-ALL cases treated with Standard Chemotherapy regimen only (Controls)
No. of patients	41	46
Median age in years (Range)	43 (20-79)	54.5 (20-79)
Median months of follow up (Range)	19 (1-40)	35.5 (1-124)
Number of patients relapsed	17	19
Median months to relapse (Range)	4 (1-24)	13 (3-71)
Site of relapse		
Bone marrow	9	17
Exclusive extramedullary	8	2
CNS	3	2
Other body sites	5	None
No. of patients died	16	18
Median months to death (Range)	5 (1-23)	14.5 (1-42)
No. of relapsed patients harboring selected cytogenetic abnormalities		
t(9;22)	2	11
CDKN2A	5	4
KMT2A	4	1
IGH	5	1
CSF3R	2	None
CRLF2	2	None
MYD88	1	None
RUNX1	2	1
ETV6	2	None
TCF3	1	None
PBX1	1	None
No. of non-relapsed patients harboring selected cytogenetic abnormalities		
t(9;22)	5	15
CDKN2A	4	1
KMT2A	6	3
IGH	3	3
CSF3R	None	None
CRLF2	1	None
MYD88	None	None
RUNX1	0	1
ETV6	2	None
TCF3	1	None
PBX1	4	1

Conclusions: Patients treated with blinatumomab and with refractory B-lymphoblastic leukemia show a propensity for recurrence in unusual extramedullary sites. Interestingly, these extramedullary recurrences occur in the setting of negative bone marrow biopsies, exhibit retention of surface expression of CD19, and do not show an association with specific cytogenetic abnormalities.

1396 Clinical Sequencing of more than 2500 Patients with Myeloid Disorders using a Targeted Next Generation Sequencing Platform

Taylor Jensen[1], Heidi Hoffmann[2], Angela Leo Kenyon[2], Michael Mooney[1], Sabrina Gardner[1], Wenjie Chen[2], Narasimhan Nagan[2], Sarah Abdul-Wajid[3], Deborah Boles[4], Tamara Richman[5], Stanley Letovsky[2], Henry Dong[6], Li Cai[1], Anjen Chenn[7], Marcia Eisenberg[4]
[1]Laboratory Corporation of America, Durham, NC, [2]Laboratory Corporation of America, Westborough, MA, [3]Laboratory Corporation of America, San Diego, CA, [4]Laboratory Corporation of America, Burlington, NC, [5]Laboratory Corporation of America Holdings, Westborough, MA, [6]Laboratory Corporation of America, New York, NY, [7]Integrated Oncology, Westborough, MA

Disclosures: Taylor Jensen: *Employee*, Laboratory Corporation of America; Heidi Hoffmann: *Employee*, LabCorp; *Stock Ownership*, LabCorp; Angela Leo Kenyon: None; Sabrina Gardner: *Employee*, Labcorp; Wenjie Chen: *Employee*, Laboratory Corporation of America; Narasimhan Nagan: *Employee*, Laboratory Corporation of America; Deborah Boles: *Employee*, Laboratory Corporation of America; Henry Dong: None; Li Cai: None

Background: Conditions associated with abnormal myeloid proliferation and/or differentiation can be broadly categorized as myeloid malignancies. This group of disorders is heterogeneous and includes acute myeloid leukemia (AML), myelodysplastic syndromes (MDS), myeloproliferative neoplasms (MPN) and others. These disorders are often driven by somatic mutations in a subset of genes and the detection of these mutations can have diagnostic, prognostic, and therapeutic relevance to the patient.

Design: We designed, validated, and implemented a laboratory developed test (IntelliGEN Myeloid) based on a next generation sequencing (NGS) panel that targets mutations within 50 genes linked to myeloid malignancies. Within these genes, multiple somatic variants including single nucleotide variants, insertions, and deletions were reported. Whole blood or bone marrow samples from more than 2500 patients were submitted for testing during the evaluation period. DNA was extracted from each sample and used as the template for creating targeted NGS libraries (ArcherDx, Boulder, CO) that were subsequently sequenced on Illumina Miseq DNA sequencers (Illumina, San Diego, CA). Results were reviewed, orthogonally confirmed unless previously validated, and reported by clinical laboratory directors. Herein, we present the anonymized results from this cohort.

Results: While testing is ongoing and it is likely that additional samples will be included in the final analysis, we censored these data to include 2489 patient samples with reported results at the time of submission with the most common provided diagnoses in this cohort being AML and MDS. Actionable variants (reported as Tier-I/II) or variants of unknown significance (reported as Tier III) were identified in 98% (49/50) of the genes within the panel, consistent with a comprehensive panel being necessary to encompass the variants present in these diseases. The median number of variants per patient was 3 and ranged from 0 to 11. In total, more than 2900 unique variants were observed in this cohort. Clinically or potentially relevant variants (Tier I, II, or III) were detected in the majority of patients tested (74.1%). Moreover, 56.4% of patients were shown to harbor at least one variant classified as Tier I. The size of our cohort also enables disease specific evaluation of mutational profiles. In patients where the indication for testing included AML, the most commonly mutated genes were TET2, DNMT3A, FLT3, ASXL1, NPM1, and TP53.

1397 Prognostic Impact of FLT3-ITD Mutational Burden and NPM1 Mutation in Normal Karyotype Acute Myeloid Leukemia Patients Undergoing HSCT

Gina Jiang[1], José-Mario Capo-Chichi[2], Eshetu Atenafu[3], Mark Minden[3], Hong Chang[4]
[1]University Health Network, Markham, ON, [2]University Health Network, University of Toronto, Toronto, ON, [3]University Health Network, Toronto, ON, [4]Toronto, ON

Disclosures: Gina Jiang: None; José-Mario Capo-Chichi: None; Eshetu Atenafu: None; Mark Minden: None; Hong Chang: None

Background: Normal karyotype (NK) AML accounts for 40–50% of all cases and an emphasis has been placed on mutations in *NPM1* (*NPM1*mut) and *FLT3*-ITD to further refine disease outcome. Both mutations are routinely tested for, however, there are limited studies with controversial results on the prognostic significance of ITD mutational burden (MB) and *NPM1* mutations in patients who have received hematopoietic stem cell transplantation (HSCT).

Design: 428 patients were diagnosed with *de novo* adult NK-AML with known *NPM1* and *FLT3*-ITD mutation status at our institution. 129 (30%) received HSCT and were retrospectively analyzed. *FLT3*-ITD MB was evaluated by multiplex RTPCR and calculated from the ratio of mutant *FLT3*-ITD isoforms over the sum of *FLT3* isoforms detected (*FLT3*-ITD and *FLT3*-wt). Patients were categorized into 3 groups: (1) ITDneg (MB<5%), (2) ITDlow (MB≥5% but <50%) and (3) ITDhigh (MB≥50%). Survival outcomes were evaluated with event-free survival (EFS) and overall survival (OS).

Results: 47% of patients tested were $NPM1^{mut}$ and 40% had a $FLT3$-ITD; of these, 73% were ITD^{low} and 27% were ITD^{high}. Analysis of the 3 groups stratified by $FLT3$-ITD MB produced significant results for EFS and OS (EFS P=0.042; OS P=0.011), thus, we proceeded to pairwise comparison. ITD^{neg} patients did not significantly differ on EFS and OS with ITD^{low} patients (EFS P=0.22; OS P=0.51). In contrast, ITD^{high} patients were associated with shorter EFS and OS compared to ITD^{neg} patients (EFS P=0.03; OS P=0.002) and shorter OS compared to ITD^{low} patients (P=0.046). When analysis was restricted to $NPM1^{mut}$ cases, a significant result for OS was observed between the 3 groups (EFS P=0.052; OS P=0.013). Pairwise comparison revealed ITD^{neg} patients did not significantly differ in EFS and OS compared to ITD^{low} patients (EFS P=0.18; OS P=0.30). In contrast, ITD^{high} patients were associated with shorter OS compared to ITD^{neg} patients (OS P=0.003) and shorter EFS and OS compared to ITD^{low} patients (EFS P=0.019; OS P=0.043). Univariate analysis was performed for age ≥60 years, WBC count ≥30x10^9/L, and $NPM1^{mut}$. None were significant for EFS and only age ≥60 years was significant for OS (P=0.012). ITD^{high} was an independent predictor for shorter OS [P=0.0028, HR:3.009 (95% CI:1.46–6.19)].

Conclusions: Our study indicates that $FLT3$-ITD mutational burden is a significant factor in AML prognostication. ITD^{high} is associated with poor overall survival; while ITD^{neg} and ITD^{low} patients have similar outcome, irrespective of their $NPM1$ genotype.

1398 Diagnosis of AML-MRC Based on Multilineage Dysplasia Alone does not Show Inferior Outcome to AML-NOS

Gina Jiang[1], Maryam Pourabdollah[2], Eshetu Atenafu[3], Anne Tierens[3], Hong Chang[4]
[1]University Health Network, Markham, ON, [2]University of Toronto, Toronto, ON, [3]University Health Network, Toronto, ON, [4]Toronto, ON

Disclosures: Gina Jiang: None; Maryam Pourabdollah: None; Eshetu Atenafu: None; Anne Tierens: *Advisory Board Member*, Jazz Pharmaceutical, Astella; Hong Chang: None

Background: AML with multilineage dysplasia (MLD) was initially introduced in 1999 then revised multiple times into AML with myelodysplasia-related changes (AML-MRC) due to controversy about the clinical relevance of MLD. Diagnostic criteria in the 2016 WHO classification system now excludes patients with MLD alone in the presence of $NPM1^{mut}$. Generally, AML-MRC confers poor prognosis, however, those diagnosed according to the 2016 WHO system are still a group with heterogenous outcome. We investigated the prognostic relevance of MLD alone within AML-MRC and whether $NPM1^{mut}$ still has a significant impact on the current classification.

Design: Our retrospective study included 179 adult AML-MRC patients diagnosed according to the 2016 WHO classification at our institution. We investigated the prognostic significance of clinical and laboratory parameters including a diagnosis with MLD alone, MDS-related cytogenetic changes, previous history of MDS, $NPM1^{mut}$, $FLT3$-ITD, age ≥60 years, WBC count ≥30 10^9/L, sex, and stem cell transplantation (SCT). Furthermore, 105 adult normal karyotype AML not otherwise specified (NK AML-NOS) patients were used as a control group.

Results: 41% of patients were diagnosed with a previous history of MDS, 41% with MDS-related cytogenetics, and 26% with MLD alone. 17% of patients received SCT. $NPM1^{mut}$ was detected in 6% of patients and $FLT3$-ITD was detected in 9%. Upon univariable analysis, diagnosis with MLD alone, absence of MDS-related cytogenetics, age <60 years, and SCT were associated with longer EFS (P=0.008, P=0.021, P=0.015, P<0.0001, respectively) and OS (P=0.0024, P=0.011, P=0.013, P<0.0001, respectively). Multivariable analysis confirms SCT as an independent predictor for longer EFS and OS (P=0.0002 and P<0.0001). Diagnosis based on MLD alone was an independent predictor for longer OS (P=0.025). Furthermore, AML-MRC patients diagnosed with MLD alone had similar EFS and OS to the NK AML-NOS control group (P=0.86 and P=0.93). However, AML-MRC patients diagnosed by other criteria were associated with shorter EFS and OS (P=0.0003, P<0.0001, respectively) when compared to the control group.

Conclusions: The typical poor prognostic implication of AML-MRC is not evident in patients diagnosed with MLD alone. They have comparable outcome to NK AML-NOS patients and may be considered not to be classified in the same group as other AML-MRC patients. Additionally, patients with $NPM1^{mut}$ who still remain classified as AML-MRC show no difference in outcome from $NPM1^{wt}$ patients.

1399 ALK-positive Large B-cell Lymphoma is a Neoplasm with Terminal B-cell Differentiation Featuring Frequent Germinal Center B-cell-like Mutations and TLR-NF-κB Pathway Activation

Xiang Nan Jiang[1], Bo Hou[1], Wan-Hui Yan[1], Xiaoqiu Li[2]
[1]Fudan University Shanghai Cancer Center, Shanghai, China, [2]Shanghai Cancer Center, Shanghai, China

Disclosures: Xiang Nan Jiang: None; Bo Hou: None; Wan-Hui Yan: None; Xiaoqiu Li: None

Background: Anaplastic lymphoma kinase-positive large B-cell lymphoma (ALK+ LBCL) is a rare aggressive lymphoid malignancy that expresses a terminal B-cell differentiation program. Little is known about the molecular/genetic alterations involved in the pathogenesis of this disease except for the activation of ALK/$STAT3$ signaling pathway.

Design: Ten cases of ALK+ LBCL were studied. Molecular genetic analysis was performed by next-generation sequencing (NGS) approach on 136 genes known to be important for diffuse large B-cell lymphoma (DLBCL) tumorigenesis using formalin fixed paraffin embedded samples.

Results: Recurrent mutations of genes involved in the *TLR-NF-κB* pathway (*MFHAS1*, *CARD11*, *IRF8*, *MYD88*, and *BIRC3*) were identified in all ALK+ LBCL cases. Two of eight informative cases also demonstrated gene mutations (*SOCS1*, *JAK3*) that may result in the *JAK-STAT* activation. In addition, the DNA repair gene *ATM* and *NOTCH1/2* were mutated in 3 and 2 cases, respectively. Intriguingly, six cases of this peculiar neoplasm with terminal B-cell differentiation program had demonstrated striking genetic changes (*FOX1*, *ARID1A*, *EZH2*, *CERBBP*, and *TET2* mutations) similar to germinal center (GCB)-type DLBCL.

Conclusions: Our study disclosed for the first time the mutational landscape of ALK+ LBCL. This unusual neoplasm features frequent genetic aberrations involving the *TLR-NF-κB*, and sometimes the *JAK-STAT* and *NOTCH1/2* pathways. The GCB-like molecular changes noticed in this post-germinal center neoplasm might have suggested a more complex genetic background or pathogenesis distinct from DLBCL, NOS. These findings may provide a rational basis for targeting these pathways.

1400 Whole Genome Profiling in Plasma Cell Neoplasms with MYC and MYCN Aberrations

Yujung Jung[1], Steven Swerdlow[2], Miroslav Djokic[3], Svetlana Yatsenko[3]
[1]University of Pittsburgh Medical Center, Pittsburgh, PA, [2]University of Pittsburgh School of Medicine, Pittsburgh, PA, [3]University of Pittsburgh, Pittsburgh, PA

Disclosures: Yujung Jung: None; Steven Swerdlow: None; Miroslav Djokic: None; Svetlana Yatsenko: None

Background: *MYC* aberrations in plasma cell neoplasms (PCN) are known to be associated with adverse clinical features. In the present study, we aimed to characterize *MYC* alterations including rearrangements and amplifications, and co-existing genomic abnormalities in PCN using multiple cytogenetic techniques including array-based Comparative Genomic Hybridization (array-CGH), fluorescence in situ hybridization (FISH) analysis on CD138 positive cells, and G-banding karyotypes.

Design: Whole genome array-CGH, FISH and karyotype analyses were performed on 1176 PCN referred for genetic testing. A total of 19 PCN with *MYC* aberrations by either array-CGH or FISH were further evaluated including one patient with *MYCN* gene amplification.

Results: The 19 PCN included 14 plasma cell myelomas, 2 IgG kappa monoclonal gammopathies of undetermined significance, 2 plasma cell leukemias, and one plasmacytoma from 13 males and 6 females (ages at diagnoses: 39-83). There were 15 *MYC* rearrangements: 11 unbalanced alterations including 9 identified by both array-CGH and FISH, and 2 found only by array-CGH; and 4 balanced rearrangements detected only by FISH. There were 3 *MYC* and 1 *MYCN* amplifications. The *MYCN* amplification was observed in a plasma cell myeloma which included a subset of plasma cells with plasmablastic features, and this patient died two weeks after the diagnosis. The *IGH/MYC* and *IGL/MYC* rearrangements were detected in 6 and 2 patients, respectively. In 7 patients, *MYC* rearrangements occurred within the 8q24 chromosome region and were negative for *IGH, IGL, or IGK* rearrangements by FISH. Apart from *MYC* aberration, 5 and 2 patients showed *IGH/CCND1* and *IGH/FGFR3* fusions, respectively. All 19 cases had 3 to 22 (median = 12) genomic alterations in CD138 cells demonstrated by array-CGH, whereas only 10 patients had abnormal karyotypes. Six patients revealed *TP53* deletion as well.

Conclusions: *MYC* aberrations in PCN are associated with highly abnormal genomic profiles with multiple numerical and structural chromosome abnormalities. This study highlights the importance of array-CGH analysis in detecting *MYC* aberrations and concurrent genomic alterations in PCN. Array-CGH on CD138+ cells is a superior approach for evaluation of chromosome imbalances which otherwise might not be detectable by conventional cytogenetic studies. Also, here we present the first case of *MYCN* amplification in PCN which was associated with an aggressive course.

1401 Myeloid Neoplasms with Isolated Isochromosome 17q Represent a Distinct Subset within Myelodysplastic/Myeloproliferative Neoplasms-Unclassifiable (MDS/MPN-U) with a Significantly Worse Outcome: A Multi-Institutional Collaborative Study from the Bone Marrow Pathology Group

Rashmi Kanagal-Shamanna[1], Attilio Orazi[2], Robert Hasserjian[3], Daniel Arber[4], Kaaren Reichard[5], Eric Hsi[6], Adam Bagg[7], Heesun Rogers[6], Julia Geyer[8], Kyle Devins[9], Olga Pozdnyakova[10], Tracy George[11], Paola Dal Cin[10], Sa Wang[12], Carlos Bueso-Ramos[12]
[1]The University of Texas MD Anderson Cancer Center, Bellaire, TX, [2]Texas Tech University Health Science Center, El Paso, TX, [3]Massachusetts General Hospital, Harvard Medical School, Boston, MA, [4]The University of Chicago, Chicago, IL, [5]Mayo Clinic, Rochester, MN, [6]Cleveland Clinic, Cleveland, OH, [7]University of Pennsylvania, Philadelphia, PA, [8]Weill Cornell Medicine, New York, NY, [9]Hospital of the University of Pennsylvania, Philadelphia, PA, [10]Brigham and Women's Hospital, Boston, MA, [11]University of Utah, Salt Lake City, UT, [12]The University of Texas MD Anderson Cancer Center, Houston, TX

Disclosures: Rashmi Kanagal-Shamanna: None; Attilio Orazi: None; Robert Hasserjian: None; Daniel Arber: None; Kaaren Reichard: None; Eric Hsi: *Consultant*, Seattle Genetics; *Consultant*, Jazz Pharmaceuticals; *Grant or Research Support*, Eli Lilly; *Grant or Research*

Background: Myeloid neoplasms with isolated i(17q) show mixed myelodysplastic and myeloproliferative features, and many belong to the WHO MDS/MPN-U category. These neoplasms lack *TP53* mutations and have poor outcome with a high rate of AML transformation. It has been suggested that these neoplasms represent a unique subtype of MDS/MPN-U, but data is limited due to rarity. To address this, we undertook a multi-institutional retrospective study to review the clinicopathologic and molecular genetic characteristics.

Design: We searched for all subtypes of MDS/MPN with isolated i(17q) or with 1 additional abnormality (other than del(7q)/-7). All cases were negative for *BCR/ABL1*. A series of MDS/MPN-U without isolated i(17q) abnormality formed the control group.

Results: We identified a total of 43 MDS/MPN with i(17q) including 29 (67%) MDS/MPN-U, 9 (21%) CMML and 5 (12%) aCML. The 29 MDS/MPN-U i(17q) patients had a median age of 68 (range, 41-88), with an M:F ratio of 13:16. Twenty four (83%) had isolated i(17q), rest (n=5) had 1 additional abnormality (+13 most frequent). In the majority, i(17q) was identified at diagnosis. Control group included 51 MDS/MPN-U patients without i(17q) [M:F ratio 33:18]. Compared to controls, MDS/MPN-U with i(17q) had a lower median age (67 vs. 71 yrs; p=0.005), lower median platelet count (75 vs. 142, p=0.013), lower ANC (4.6 vs. 16, p=0.008), higher frequency of splenomegaly [(20, 69%) vs. (8, 16%); p=0.001] and higher PB blasts% (2 vs. 0, p=0.057). Morphologically, MDS/MPN-U i(17q) cases showed pseudo-Pelger Huët neutrophils (18/22, 82%), frequent micromegakaryocytes (12/18, 67%); a subset showed increased (MF 2-3) fibrosis (4/11, 36%). These findings were only rarely observed in the control group. By NGS studies, most frequent mutations included *SRSF2* (70%), *ASXL1* (50%), *SETBP1* (50%) and *NRAS* (16%) (Fig 1). With a median follow-up of 52 months, 76% of MDS/MPN-U patients with i(17q) died and 21% transformed to AML (median 7.7 months). By preliminary analysis, MDS/MPN-U with i(17q) showed a significantly shorter median OS compared to MDS/MPN-U without i(17q) [14 vs. 21.8 months; p=0.03] (Fig 2).

Figure 1 - 1401

Figure 2 - 1401

Conclusions: The majority (67%) of MDS/MPN cases with isolated i(17q) belong to the MDS/MPN-U WHO category. MDS/MPN-U with isolated i(17q) cases show characteristic morphologic, clinical and molecular features, carry a poor prognosis, and may warrant being recognized as a distinct subtype within the unclassifiable MDS/MPN category.

1402   Assessment of Comprehensive Mutational Profiling in Pediatric Acute Myeloid Leukemias: Experience of the Children's Hospital in a Large Healthcare System

Nidhi Kataria[1], Yonah Ziemba[2], Hector Chavarria Bernal[3], Sean Hacking[4], Ashwin Reddy[5], Kalpana Reddy[6]
[1]Northwell Health, Hofstra School of Medicine, Manhasset, NY, [2]Donald and Barbara Zucker School of Medicine at Hofstra/Northwell, Flushing, NY, [3]Northwell Health, New Hyde Park, NY, [4]Northwell Health, Forest Hills, NY, [5]Carnegie Mellon University, Pittsburgh, PA, [6]Northwell Health, Garden City, NY

Background: Acute myeloid leukemia (AML) is a leading cause of childhood mortality. The advent of comprehensive molecular profiling has furthered our understanding of the biology of pediatric AML and increasingly provides diagnostic, prognostic and predictive information.

Design: A total of 33 total pediatric patients (≤21 years) were diagnosed with AML from 2016-2019 at our Children's Hospital. Next-generation sequencing was performed on DNA and/or RNA extracted from fresh blood/marrow aspirates at a CLIA-certified, CAP-accredited laboratory. The hematology panel sequenced DNA of 406 genes, introns of 31 gene rearrangements and RNA of 265 genes. We reviewed the salient findings from the genomic profiles of 14 of these patients.

Results: Out of all our pediatric AML patients including both cytogenetically normal (CN-AML; 10/33) and abnormal (CAbN-AML; 23/33), 16 successfully sequenced samples from 14 patients showed that the most frequent mutations (5/14) involved the RAS pathway: *NRAS, KRAS, PTPN1, NF1* followed by *FLT3* (3/14). We uncovered 1 case of germline *RUNX1* mutation/ familial platelet disorder with associated myeloid malignancy. *NUP98-NSD1* fusion frequency is higher in children (5-7%) versus adults (1%), often co-occurs with *FLT3*-ITD, displaying an apparently normal karyotype, as in our case. Since these fusions are associated with lower complete remission rates, worse event-free and overall survival, our patient underwent a bone marrow transplant. Other mutations like *WT1* and *KIT* that are typically enriched in children were also noted in our cohort, but common adult AML mutations *DNMT3, IDH1/2* or *NPM1* were not seen, and only one child had mutated *TP53*. Of the CNAbn-AML cases, 2/3 with *RUNX1-RUNX1T1* had *KIT* mutation and 1/3 pediatric APL cases with *PML-RARA* had mutated *FLT3.* While *KMT2A-MLLT3* is found in up to 25% pediatric AML cases, it was noted only in 7% of our patient group. In addition, a child diagnosed initially as AML with aberrant CD3 was re-classified as early T-cell precursor lymphoblastic leukemia, also supported by *RELN* mutation (which can occur in ~4% ETP-ALL).

Examples of co-occurring mutations in our pediatric AML cases

Cases	Mutations			
Case 1	FLT3	NUP98	NSD1	
Case 2	FLT3	RARA		
Case 3	FLT3	KMT2A		
Case 4	NRAS	MLK1		
Case 5	NRAS	KIT	RUNX1	
Case 6	KRAS	PTPN11	MLL	PTEN
Case 7	NF1	WT1	RUNX1	

Figure 1 - 1402

Most frequent mutations in cytogenetically normal and abnormal pediatric AML cases
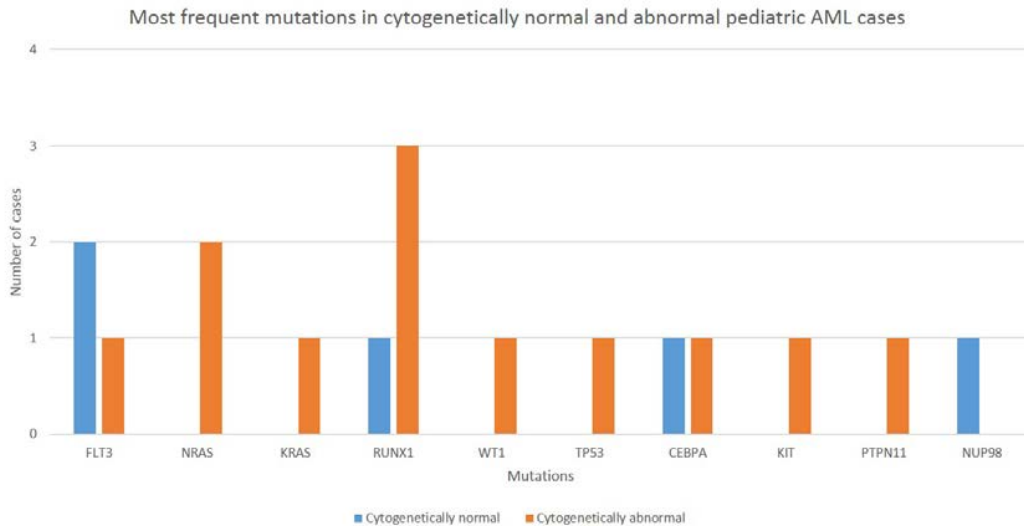
Conclusions: The pediatric-adult differences in mutational profiles underscore the need to systematically characterize heterogeneous pediatric AML by clinical molecular testing to avoid trickle-down adult therapies. Assessment of the gene alterations noted in our pediatric AML patients were useful in refining diagnosis, prognosis and development of personalized treatment regimens, particularly in our CN-AML cohort.

1403 The Abundance of PD1+ T Follicular Helper Cells in the Tumor Microenvironment Correlates with Clonal Plasma Cell Differentiation in Nodal Marginal Zone Lymphoma

Hani Katerji[1], Andrea Baran[2], Andrew Evans[3]
[1]Rochester, NY, [2]University of Rochester, Rochester, NY, [3]University of Rochester Medical Center, Rochester, NY

Disclosures: Hani Katerji: None; Andrea Baran: None; Andrew Evans: None

Background: Nodal marginal zone lymphoma (NMZL) is an indolent small B-cell lymphoma that commonly exhibits plasmacytic differentiation. Programmed death 1 (PD1) is specific marker of T-follicular helper (TFH) cells in the germinal center microenvironment, where B cell affinity maturation and early plasma cell differentiation occurs. We hypothesized that microenvironmental architecture, including the distribution of CD21+ and CD23+ follicular dendritic cells (FDC) and number of PD1+ TFH cells might contribute to neoplastic B cell survival and plasma cell differentiation. We sought to quantify how these microenvironmental cell populations correlate with plasma cell differentiation in NMZL.

Design: Excisional biopsies of NMZL were randomly selected from pathology archives. IHC staining for PD1, CD21, CD23 was performed and in-situ hybridization (ISH) used to evaluate for cases with clonal plasma cell differentiation (kappa:lambda ratio >4.0 or <1.0) versus non-clonal plasma cells (ISH kappa:lambda ratio 4.0-1.0). Separately, in a blinded fashion, the average number of PD1+ cells in 10 random (200x) fields was measured. Histomorphologic patterns were evaluated for CD21/CD23 FDC and relationship to PD1+ cells. The average number of PD1+ cells in cases with clonal versus non-clonal plasma cells was compared using the Wilcoxon rank-sum test, and the predictive value of the average number of PD1+ cells to determine the presence of clonal plasma cell differentiation was estimated using the area under the receiver operator curve (ROC).

Results: Eighteen cases of NMZL were randomly selected. Nine cases (50%) showed clonal plasma cell proliferation. The number of PD1+cells per 200x field ranged from 0-1466 (Figure-1). The expression of PD1 was markedly increased and significantly higher in NMZL cases with clonal plasma cell differentiation compared to those without, p= 0.00016. The area under the ROC was 0.975 (Figure-2), with p<0.0001 for comparing that area to 0.5 (chance). For this data set, applying a threshold of >377 PD1+ cells/200x field, on average, yielded 100% specificity and 89% sensitivity for detecting clonal plasma cell differentiation.
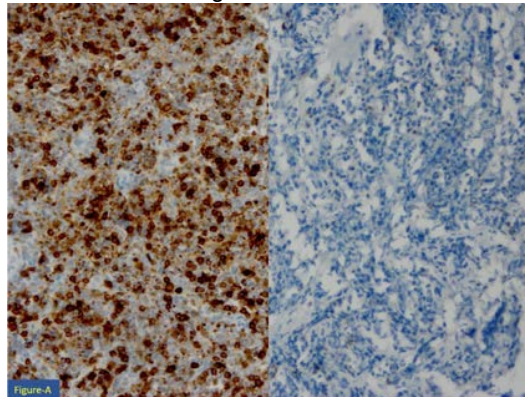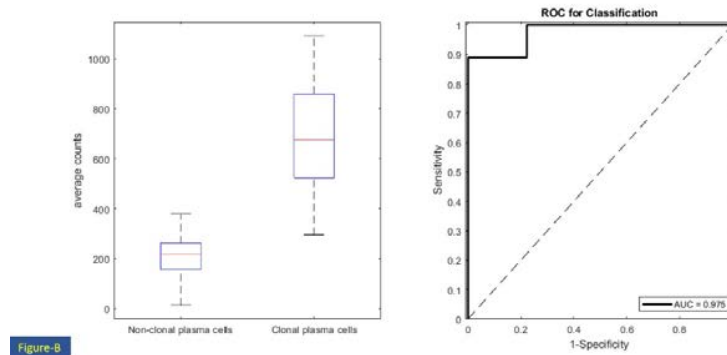
Figure 1 - 1403

Figure 2 - 1403

Conclusions: The microenvironmental abundance and distribution of PD1+ TFH cells strongly correlates with the presence of clonal plasma cell differentiation in NMZL. These data suggests neoplastic B-cells in this tumor type may depend on TFH support for survival and provide insight into novel strategies to target the tumor microenvironment.

1404 Correlation Analysis of Lymphoma–Associated Macrophages and DLBCL Cell-of-Origin Classification

Fahad Khan[1], Adnan Mubasher[2], Ali Saad[3], Shafinaz Hussein[4], Zakaria Grada[5], Adolfo Firpo-Betancourt[6], Siraj El Jamal[7]
[1]Mount Sinai St. Luke`s-West Hospital, New York, NY, [2]New York, NY, [3]University of Miami Miller School of Medicine, Miami, FL, [4]Mount Sinai Hospital, New York, NY, [5]Beth Israel Deaconess Medical Center, Boston, MA, [6]Mount Sinai Medical Center, New York, NY, [7]Icahn School of Medicine at Mount Sinai, New York, NY

Disclosures: Fahad Khan: None; Fahad Khan: None; Adnan Mubasher: None; Ali Saad: None; Shafinaz Hussein: None; Zakaria Grada: None; Adolfo Firpo-Betancourt: None; Siraj El Jamal: None

Background: Lymphoma-associated macrophages (LAM) are an important component of diffuse large B-cell lymphoma (DLBCL) microenvironment. To simplify their role in tumor progression, tumor-associated macrophages are generally subdivided into two major groups, M1 (immune activating and tumoricidial) and M2 (immunosuppressive and promote tumor progression). In this study, we investigate the relation between the LAM content in DLBCL and its correlation to the cell-of-origin (COO) classification (germinal center vs. non-germinal center) by the four major immunohistochemistry algorithms (Hans, Tally, Choi, and Visco).

Design: We used tissue microarray (TMA) for 93 primary nodal DLBCL cases. All cases were confirmed to be DLBCL according to the WHO criteria. We stained the TMA slides for CD10, GCET-1, BCL6, MUM-1, and FOXP1 to classify each case to ABC or GCB according to the four IHC algorithms. Then, using CD68 as a common marker for macrophages and CD163 as a specific marker for M2 LAMs, we classified the CD68-positive/CD163-negative cells as M1 while CD68-positive/CD163-positive cells as M2 in each core. Cases with an average of >20 CD68-positive LAMs/hpf are regarded as LAM-rich DLBCL. The number of CD163-positive cells is counted in ratio to the CD68-positive cells with >50% considered as a cut-off for cases with high in M2 macrophages. Cases with less than 50% of M2 are considered high in M1 macrophages. The correlation between each COO algorithm and LAM contents was calculated using Spearman rho test (ρ).

Results: Of the 93 cases, 50 cases (53% of total) were classified as LAM-rich DLBCL. Out of those 50 LAM-rich DLBCL case, 29 cases showed high number of M2 macrophages (31% of total cases; 54% of LMA-rich cases). We found that an increased total number of macrophages in DLBCL is positively correlated with germinal center DLBCL in all four COO IHC algorithms. However, the type of macrophages (M1 or M2) does not show any independent, statistically significant, association with the COO (table 1).

Rho (ρ) coefficient and P value	Visco	Tally	Choi	Hans
CD68	0.267 (P 0.01)	0.239 (P 0.021)	0.267 (P 0.01)	0.299 (P 0.004)
CD163	-0.189 (P 0.07)	-0.213 (P 0.06)	-0.125 (P 0.233)	-0.165 (P 0.115)

Conclusions: Increased number of total macrophages is correlated with germinal center COO in DLCBCL. Our findings highlight the importance of tumor microenvironment and the role that LMA may play in the lymphomagenesis of germinal-center DLBCL. However, the exact mechanism in which LMA interact with lymphoma cell is yet to be elucidated.

1405 Recipient Chimerism of CD34+ Cells is a Strong Predictor of Acute Myeloid Leukemia Relapse

Poonam Khan[1], Meriam Berka[2], Khadeeja Tariq[2], Gaurav Tripathi[3], Jan Storek[2], Faisal Khan[1]
[1]Cumming School of Medicine, University of Calgary and Division of Hematopathology, Alberta Public Laboratories, Calgary, AB, [2]Cumming School of Medicine, University of Calgary, Calgary, AB, [3]University of Calgary, Calgary, AB

Disclosures: Poonam Khan: None; Meriam Berka: None; Khadeeja Tariq: None; Gaurav Tripathi: None; Jan Storek: None; Faisal Khan: None

Background:
Acute Myeloid Leukemia (AML) relapse is the foremost cause of mortality after allogeneic hematopoietic cell transplantation (HCT), accounting for 20-25% of posttransplant deaths. The efficacy of therapies like donor lymphocyte infusion is limited due to delay in detection of AML relapse. Chimerism assessment using donor and recipient specific unique gene signatures to quantify donor and recipient derived myeloid cells after HCT is the gold standard for engraftment but has very limited sensitivity in predicting relapse. In the present investigation, we used a 'modified chimerism approach' of detecting recipient chimerism in AML specific target cells (CD34+ cells for CD34+ve AML) to predict AML relapse.

Design: A total of 315 cryopreserved peripheral blood mononuclear cells (PBMNCs) from 55 AML patients treated with allogeneic HCT were analyzed retrospectively. Pretransplant donor and recipient, and posttransplant recipient at relapse; and 1-2 months and 3-4 months prior to relapse were analyzed. Disease risk matched recipients with no relapse were analyzed at the same time points as relapsed

recipients. CD34+ve cells were sorted from posttransplant peripheral blood mononuclear cells (PBMNCs) using multicolor flow sorting or magnetic bead sorting. Genomic DNA extracted from sorted CD34+ve cells was PCR amplified for a panel of fluorescent-labeled 16 Short Tandem Repeat (STR) loci. Fluorochrome labeled amplicons were size fractionated by capillary electrophoresis. Pre-transplant donor and recipients STR alleles were used to identify informative markers for each donor-recipient pair. These informative markers were utilized to calculate recipient chimerism in posttransplant sorted CD34+ve cells.

Results: Recipient chimerism in CD34+ve cells was detected at least 3 months before the onset of relapse in 12 out of 14 patients with relapse. On the contrary, only 1 out of 15 patients without relapse showed detectable recipient CD34 chimerism at matched time points. Overall, recipient chimerism in CD34+ve cells showed sensitivity of 86% and 93% specificity in predicting AML relapse after allogeneic HCT with at least 3-month lead time.

Conclusions: Modified chimerism approach (recipient chimerism of CD34+cells in CD34+ AML patients) is an early, and highly sensitive and specific method for detection AML relapse after allogeneic HCT. This chimerism approach will allow hematologists to preemptively treat high risk HCT recipients, which will ultimately lead to improved survival and quality of life of HCT recipients.

1406 Importance of Bone Marrow Morphologic Features for Surveillance of Patients with Myelofibrosis Following Molecular Clearance after Stem Cell Transplant

Mahsa Khanlari[1], Sanam Loghavi[1], Sa Wang[1], Siba El Hussein[1], Mehrnoosh Tashakori[1], Carlos Bueso-Ramos[1], C. Cameron Yin[1], Rashmi Kanagal-Shamanna[2], Joseph Khoury[1], L. Jeffrey Medeiros[1], Keyur Patel[1], Uday Popat[1], Sergej Konoplev[3]
[1]The University of Texas MD Anderson Cancer Center, Houston, TX, [2]The University of Texas MD Anderson Cancer Center, Bellaire, TX, [3]Houston, TX

Background: Allogeneic stem cell transplant (allo-SCT) is considered a curative therapeutic option for eligible patients with advanced-stage myeloproliferative neoplasms (MPN). In such patients, driver mutations involving *JAK2*, *MPL* and/or *CALR* are detectable in 80-90% of cases and can serve as measurable residual disease (MRD) markers after allo-SCT. Reversal of the bone marrow (BM) morphologic features of MPN often lags behind molecular clearance following allo-SCT, thereby creating diagnostic challenges in disease surveillance in routine practice particularly in the absence of molecular data.

Design: The study group included patients with primary myelofibrosis (PMF) and advanced-stage post essential thrombocythemia (ET) and polycythemia vera (PV) myelofibrosis who underwent allo-SCT. Pre-transplant and post-transplant day +100±20 BM samples were reviewed and correlated with corresponding molecular data. Molecular MRD assessment was performed by next-generation sequencing and/or allele-specific quantitative PCR.

Results: Patients (n=24) included 11 men and 13 women with a median age of 62 years (range 44-73 years) diagnosed with PMF (n=16), and post-ET/PV MF (n=8). Driver mutations included *JAK2*p.V617F (n=16, 66%), *MPL* (n=2, 8%) and *CALR* (n=7, 30%). One patient (Post-PV-MF) had concurrent *JAK2* (VAF: 95%) and *MPL* (VAF<10%) mutations. The morphologic features of pre- and post-transplant BM biopsy samples are summarized in Table 1. Although all patients had molecular MRD-negative status by day +100±20, the most notable persistent morphologic abnormalities at this time point included megakaryocytic atypia, osteosclerosis and myelofibrosis.

Morphologic features	Pre-transplant (%) N=24	Post allo-SCT (%) N=24
Increased BM cellularity for age	14 (60%)	7 (30%)
Atypical megakaryocyte morphology (>5%)	24 (100%)	20 (83%)
Megakaryocyte clustering (>1/mm^2)	20 (83%)	5 (21%)
Erythroid islands (>1/ mm^2)	3 (12%)	17 (71%)
Bone marrow fibrosis (MF-2/MF-3)	21 (87%)	10 (42%)
Osteosclerosis (grade 2 or 3)	18 (75%)	19 (80%)
Table 1. Morphologic features of pre- and post-transplant BM biopsy samples.		

Conclusions: Reversal of bone marrow morphologic features following allo-SCT for MF lags behind molecular clearance. Some morphologic changes including BM hypercellularity, atypical megakaryopoiesis, bone marrow fibrosis, and osteosclerosis tend to persist following transplant despite mutation clearance. Re-emergence of erythroid islands and lack of tight megakaryocytic clustering are helpful features that indicate potential clearance of disease.

1407 FOXC1 and CXCL12 Expressions in Stromal Cells and their Influence on the Diffuse Large B Cell Lymphoma Tumor Microenvironment

Ji-Ye Kim[1], Sun Och Yoon[2]
[1]Ilsan Paik Hospital, Inje University, Goyang-si, Gyeonggi-do, Korea, Republic of South Korea, [2]Yonsei University College of Medicine, Yonsei University Health System, Severance Hospital, Seoul, Korea, Republic of South Korea

Disclosures: Ji-Ye Kim: None; Sun Och Yoon: None

Background: Tumor-stromal cell interactions appear to play a critical role in tumorigenesis. Stromal expressions of novel markers, FOXC1, CXCL12 have been implicated in various cancers. FOXC1, a transcription factor of the forkhead family, is associated with aggressive DLBCL phenotype with implications in tumor migration and invasion. CXCL12, a chemokine produced by stromal cells is associated with cancer proliferation and migration. ERK1-2 and p38 are intracellular kinase pathways with opposing functions in tumorigenesis; ERK1-2 stimulate proliferation and metastasis, while p38 inhibit malignant transformation by activating p53. However, stromal cells and their effects on tumor cells by activating ERK1-2 and p38 pathways has not yet been elucidated in DLBCL. This study is the first to examine stromal-expressed FOXC1 and CXCL12 to investigate their significance within the DLBCL microenvironment in terms of tumoral ERK1-2, p38 activation.

Design: FOXC1 and CXCL12 expression in stromal cells as well as p38 and ERK1-2 expression in tumor cells were semiquantitatively analyzed using immunohistochemistry for 134 DLBCL cases.

Results: Stromal CXCL12 expression had significant relationship with stromal FOXC1 ($\rho = 0.324$, $P < 0.001$) and tumoral p38, ERK1-2 expressions ($\rho = 0.220$, $P = 0.022$; $\rho = 0.306$, $P = 0.001$, each respectively). However, there was no significant relationship between stromal FOXC1 and tumoral ERK1-2, p38 expressions. High FOXC1 positive stromal cell group (> 16.375/HPF) and ERK1-2 positive tumor cell group (> 1.125%/HPF) was significantly associated with shorter overall (OS) and progression-free survival (PFS) compared to low group. In multivariate analysis, high FoxC1 stromal expression was an independent prognostic factor of inferior PFS and OS in addition to high IPI score. In contrast, low p38 positive tumor cell group (≤ 75.625%/HPF) was significantly associated with shorter OS and PFS. Stromal CXCL12 expression had no prognostic significance.

Correlation of infiltrating CXCL12-positive and FOXC1-positive reticular cell levels with clinicopathological characteristics

parameters	Total	FoxC1		CXCL12	
	N= 134 (%)	Cells/HPF (Mean ± SD)	P	Cells/HPF (Mean ± SD)	P
Age (years)*			0.836		**0.008**
≤ 60	91 (58.3)	22.1 ± 11.6		14.1 ± 6.8	
> 60	65 (41.7)	21.9 ± 9.5		18.8 ± 11.8	
ECOG performance status*			0.952		0.103
< 2	116 (83.2)	21.7 ± 11.0		20.8 ± 10.9	
≥ 2	21 (16.8)	21.8 ± 9.6		33.9 ± 45.3	
Extranodal Involvement*			0.163		0.740
< 2	79 (57.7)	21.3 ± 10.0		22.0 ±11.6	
≥ 2	58 (42.3)	22.3 ± 11.8		24.1 ± 28.8	
LDH level*a*			0.424		0.868
Normal	70 (51.1)	21.5 ± 10.3		21.61 ± 10.69	
Elevated	67 (48.9)	21.9 ± 11.3		24.12 ± 27.43	
Ann-Arbor stage*			**0.033**		0.269
I-II	60 (49.6)	14.4 ±7.3		20.64 ± 10.10	
III-IV	61 (50.4)	17.5 ± 9.5		24.89 ± 26.86	
IPI risk group*			0.293		0.501
0,1,2	78	15.3 ± 7.6		15.5 ± 8.0	
3,4,5	58	16.9 ± 9.8		16.6 ± 11.5	
Hans classification*			0.258		0.284
GCB	37 (27.6)	19.9 ± 8.8		19.8 ± 8.7	
Non-GCB	97 (72.4)	22.3 ±11.5		24.1 ± 23.5	
EBV*			0.740		0.720
Negative	119 (88.8)	21.8 ± 10.8		22.4 ± 21.6	
Positive	15 (11.2)	22.8 ± 10.1		24.4 ± 11.2	
Ki-67 *			0.526		**0.020**
< 50%	82 (61.2)	16.6 ± 9.3		14.3 ± 7.8	
≥ 50%	52 (38.8)	15.6 ± 7.3		18.2 ± 11.4	
BCL2*			0.755		0.577
Negative	83 (62.4)	16.3 ± 8.9		21.8 ± 9.4	
Positive	50 (37.6)	15.8 ± 8.1		23.4 ± 31. 7	
C-MYC*			0.779		**0.037**
Negative	91 (67.9)	16.0 ± 9.1		14.6 ± 7.9	
Positive	43 (32.1)	16.5 ± 7.5		18.3 ± 12.0	
BCL2 and C-MYC*			0.728		0.130
Negative	113 (85.0)	16.0 ± 8.7		14.8 ± 7.4	
Positive	20 (15.0)	16.75 ± 8.31		20.49 ± 15.94	

Abbreviations: HPF, High Power Field; SD, Standard Deviation; GCB, Germinal Center;

[a] LDH level at diagnosis

* Information not available in some cases. Valid percentages are presented in the parenthesis.
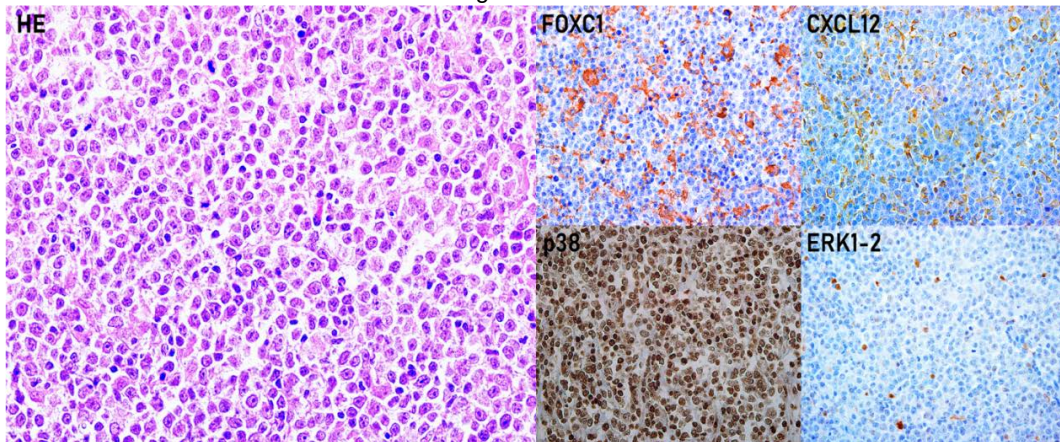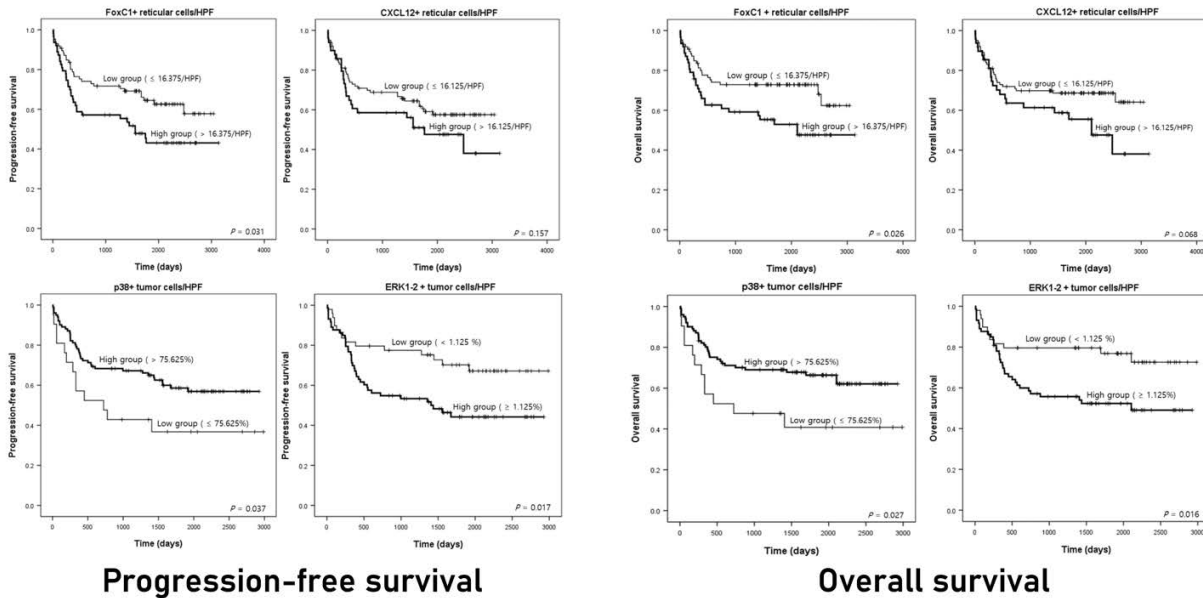
Figure 1 - 1407

Figure 2 - 1407

Progression-free survival   Overall survival

Conclusions: Stromal FOXC1 and tumoral ERK1-2, p38 expressions were important determinants of DLBCL prognosis. Stromal FOXC1 expression correlated with aggressive behavior DLBCL tumor cells, and this pathway might be through activation of stromal CCXL12 which is correlated to ERK1-2 and p38 signals.

1408 ERG Immunoreactivity is a Diagnostic Pitfall and a Promising Marker of Blastic Myelomonocytic Neoplasms

Matthew Koo[1], Yaso Natkunam[1]
[1]Stanford University Medical Center, Stanford, CA

Disclosures: Matthew Koo: None; Yaso Natkunam: None

Background: Erythroblast transformation specific regulated gene-1 (ERG) is an established marker of vascular differentiation that also stains subsets of prostatic adenocarcinoma, Ewing sarcoma, epithelioid sarcoma, and a major subset of acute myeloid leukemia / myeloid sarcoma (AML/MS). ERG may play a dual role in immunohistochemical profiling: while strong nuclear ERG immunoreactivity comparable to that of the background vascular endothelial nuclei may be supportive of vascular differentiation, weak-moderate nuclear ERG immunoreactivity may be suggestive of a blastic hematolymphoid neoplasm in the appropriate context. We explored ERG reactivity in

various hematolymphoid neoplasms to gain a better understanding of the diagnostic pitfalls and potential utility of ERG in the workup of undifferentiated and immature neoplasms.

Design: A spectrum of mature and immature hematolymphoid neoplasms from our pathology archive was selected. Unstained slides with 4-μm formalin-fixed paraffin-embedded tissue sections were stained using a Ventana BenchMark ULTRA IHC/ISH automated staining system with the rabbit anti-ERG monoclonal antibody EP111/EPR3864 (Cell Marque, 434R-16) at 1:400 dilution and CC1 retrieval. Only cases with a positive internal control (nuclear endothelial staining) were included in the study.

Results: ERG was positive (weak-moderate) in myelomonocytic blasts in 14 of 15 (93%) total AML/MS, including 4 of 5 (80%) CD34-/CD117- AML/MS. The internal positive control was weak in the sole case of CD34-/CD117-/ERG- AML/MS, which may suggest that ERG staining was adversely affected. Weak to moderate ERG staining was also seen in lesional cells in 3 cases of T-lymphoblastic leukemia, a case of hematogone hyperplasia, and all 4 cases of systemic mastocytosis. ERG was negative in all other cases as detailed in Table 1.

| CASE DIAGNOSIS	ERG +	TOTAL	%
Acute myeloid leukemia / myeloid sarcoma, Total	14	15	93
Acute myeloid leukemia / myeloid sarcoma, CD34-/CD117-	4	5	80
Acute myeloid leukemia / myeloid sarcoma, Pure erythroid leukemia (pEL)	3	3	100
Acute myeloid leukemia / myeloid sarcoma, Acute megakaryoblastic leukemia (AMkL)	2	2	100
T-lymphoblastic leukemia (T-ALL)	3	3	100
Hematogone hyperplasia (HH)	1	1	100
Systemic mastocytosis (SM)	4	4	100
Blastic plasmacytoid dendritic cell neoplasm (BPDCN)	0	2	0
Histiocytic sarcoma (HS)	0	5	0
Rosai-Dorfman disease (RDD)	0	8	0
Langerhans cell histiocytosis (LCH)	0	7	0
Erdheim-Chester disease (ECD)	0	1	0
Diffuse large B-cell lymphoma (DLBCL)	0	20	0
Primary mediastinal large B-cell lymphoma (PMLBL)	0	3	0
Post-transplant immunoproliferative disorder, DLBCL (PTLD, DLBCL)	0	1	0
Anaplastic large cell lymphoma (ALCL)	0	6	0
Peripheral T-cell lymphoma, not otherwise specified (PTCL, NOS)	0	2	0
Mantle cell lymphoma (MCL)	0	6	0
Follicular lymphoma, grade 1-2 (FL, 1-2)	0	44	0
Follicular lymphoma, grade 3 (FL, 3)	0	19	0
Chronic lymphocytic leukemia / small lymphocytic lymphoma (CLL/SLL)	0	21	0
Nodal marginal zone lymphoma (NMZL)	0	1	0
Extranodal marginal zone lymphoma (ENMZL)	0	2	0
Splenic marginal zone lymphoma (SMZL)	0	2	0
Lymphoplasmacytic lymphoma (LPL)	0	5	0
Plasma cell myeloma (PCM)	0	1	0
Gastrointestinal stromal tumor (GIST)	0	1	0
Benign thymus	0	2	0
Benign tonsil	0	3	0
Benign lymph node	0	1	0
Benign spleen	0	7	0

Figure 1 - 1408
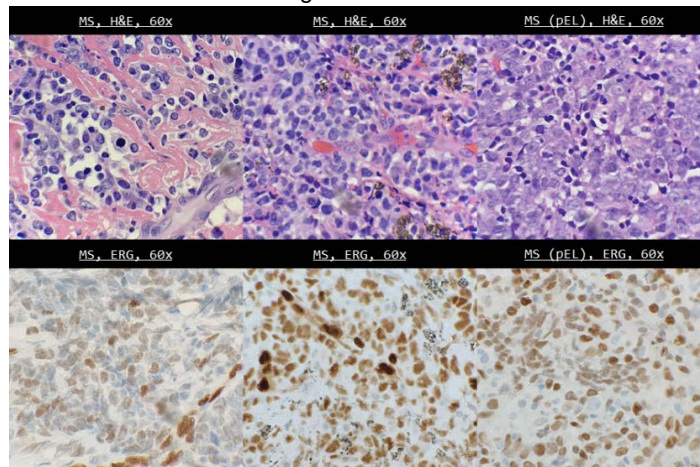
Figure 2 - 1408
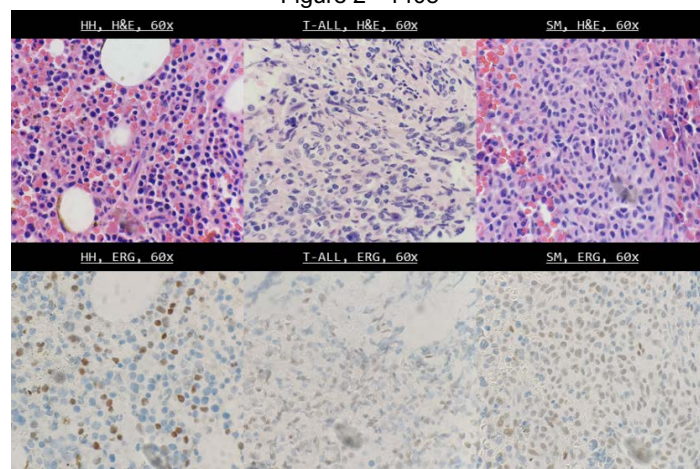
Conclusions: ERG may have a dual role in immunohistochemistry. While strong nuclear ERG immunoreactivity is suggestive of vascular differentiation, weak-moderate nuclear ERG immunoreactivity (relative to the positive internal control) is a promising marker in the diagnosis of AML/MS, especially in CD34-/CD117- cases. Awareness of this staining pattern is important to avoid diagnostic errors, particularly in the workup of undifferentiated neoplasms presenting in extramedullary sites. It is also important to note the intensity of ERG staining in vascular endothelial nuclei, which benchmarks strong intensity of ERG staining within the tissue.

1409 HGAL and LMO2: Potential Markers of T Follicular Helper (TFH) Phenotype

Matthew Koo[1], Yaso Natkunam[1]
[1]Stanford University Medical Center, Stanford, CA

Disclosures: Matthew Koo: None; Yaso Natkunam: None

Background: To establish a TFH phenotype in a T-cell lymphoma, the World Health Organization classification update of 2016 recommends positivity of at least two markers of TFH derivation (e.g. PD-1, CXCL13, CD10, BCL6, ICOS, and SAP); however, these established markers show varying degrees of sensitivity for T-cell lymphomas with TFH phenotype. Therefore, additional markers of greater sensitivity are needed in the workup of TFH lymphomas. We observed that HGAL and LMO2, two markers of germinal center B-cells, also stained TFH cells. To systematically address their efficacy as TFH markers, a comparative staining profile of HGAL and LMO2 in various T-cell lymphomas of TFH phenotype is characterized and described herein.

Design: T-cell lymphomas of TFH phenotype that were diagnosed in the last 5 years were selected from our pathology archive with the following inclusion criteria: 1) nodal involvement by a lymphoma of TFH phenotype, characterized by positivity for at least 2 well-established TFH markers: PD-1, CXCL13, CD10, and BCL6; and 2) sufficient diagnostic tissue to perform HGAL and LMO2 staining. Unstained 4-μm formalin-fixed paraffin-embedded tissue sections from 16 specimens were stained with HGAL and LMO2, as detailed in Table 1. Details of other routine stains are not provided. An H-score was calculated for each marker and averaged (Figure 1). The average

net difference in case-matched H-score between HGAL and each of the other TFH markers used in this study was calculated; the same analysis was performed for LMO2 (Figure 1).

Results: The average H-scores for PD-1, CXCL13, CD10, BCL6, HGAL, and LMO2 are as follows, respectively: 133.812, 69.375, 69.364, 120, 104.062, and 33.833. The average net difference in case-matched H-score within a given biopsy between HGAL and PD-1, HGAL and CXCL13, HGAL and CD10, and HGAL and BCL6 are as follows, respectively: -29.75, +34.688, +47, and +6.667. Six of 16 biopsies show an H-score value for HGAL that is greater than that of PD-1. The average net difference in case-matched H-score between LMO2 and PD-1, LMO2 and CXCL13, LMO2 and CD10, and LMO2 and BCL6 are as follows, respectively: -98.75, -46.583, -39.625, and -98.625.

ANTIBODY	CLONE	INSTRUMENT	DILUTION	RETRIEVAL	SPECIES	VENDOR	CATALOG
HGAL	MRQ-49	Leica	1:100	ER2	Mouse	Cell Marque	375M-96
LMO2	1A9-1	Leica	1:4	ER2	Mouse	Ventana	790-4368

Figure 1 - 1409
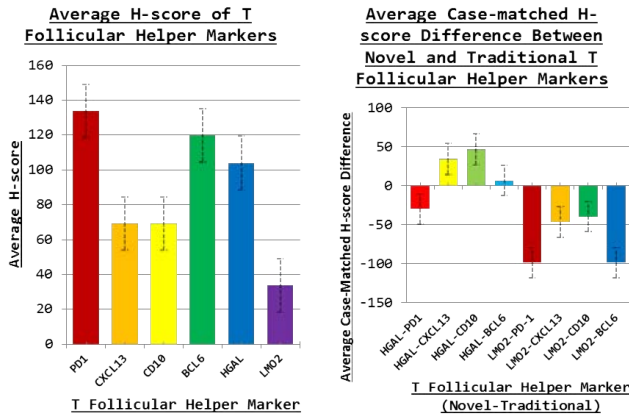
Figure 2 - 1409
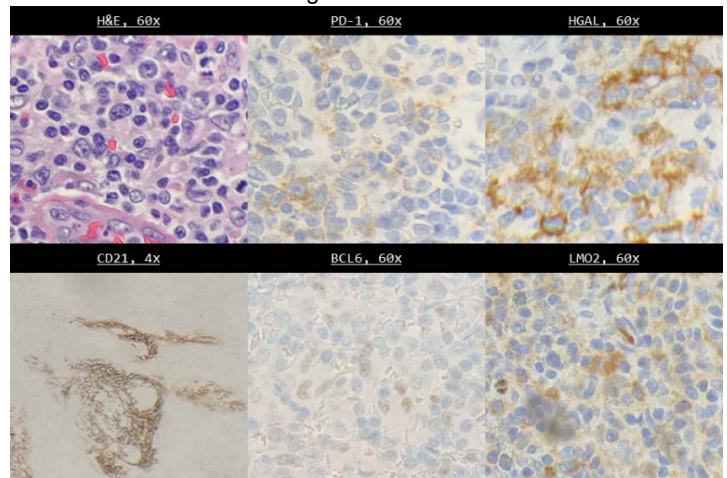
Conclusions: HGAL is a promising marker of TFH phenotype, showing comparable (and sometimes even more robust) staining compared to that of well-established markers. LMO2 is a less robust marker of TFH phenotype, showing weak to moderate staining intensity relative to that of the background vascular endothelial cell nuclei.

1410 Post-Treatment Bone Marrow Findings in Acute Myeloid Leukemia Patients with FLT3-ITD Mutations Treated with Midostaurin

Habibe Kurt[1], Pamela Egan[2], Christopher Elco[3], Mark Legolvan[4], Dariusz Stachurski[5], John Reagan[3], Diana Treaba[6]
[1]Alpert Medical School of Brown University, Providence, RI, [2]Rhode Island Hospital, Providence, RI, [3]Brown University, Alpert Medical School, Lifespan Cancer Institute, Providence, RI, [4]Lifespan, Providence, RI, [5]Newport Hospital, Newport, RI, [6]Brown University Lifespan Academic Medical Center, Providence, RI

Disclosures: Habibe Kurt: None; Christopher Elco: None; Mark Legolvan: None; Dariusz Stachurski: None; Diana Treaba: None

Background: *FLT3*-internal tandem duplication (ITD) mutation occur commonly (~25%) in de-novo acute myeloid leukemia (AML). Because patients with *FLT3*-ITD AML present with more aggressive disease and higher relapse rate after remission, FLT3 tyrosine kinase inhibitors (TKIs) have been investigated as a potential targeted therapy for this disease. The role of supplementing midostaurin with standard induction chemotherapy conferred a survival benefit to a population presented with *FLT3*-ITD mutations.

Design: Patients with a diagnosis of de-novo AML with *FLT3*-ITD mutations who received midostaurin in addition to conventional chemotherapy between 1/2017 and 9/2019 were identified. Post-treatment bone marrow (BM) biopsies were reviewed.

Results: We identified 6 patients [male (n=3), female (n=3), ages of 56-70 years old with a median age of 62] with a diagnosis of AML with *FLT3*-ITD mutations who received midostaurin during induction chemotherapy. They underwent BM biopsies between days 20 to 27. Residual disease was initially detected in 3 of the patients based on either aspirate morphology, flow cytometry, or *FLT3*-ITD mutation analysis; however repeat biopsies performed at the end of the induction therapy showed complete remission. Overall bone marrow cellularity ranged from normocellular (n=4) to hypercellular (n=5). Myeloid series were hyperplastic(n=4), adequate (n=2), or hypoplastic (n=3), and showed left-shifted maturation in the majority of the cases. Megakaryocytic hyperplasia was noted in all cases. Megakaryocytes

showed atypical features including tight (n=2) or loose clusters (n=5), deeply lobulated nuclei (n=3), and paratrabecular localization(n=1). Reticulin stain was performed in 1 case, and it showed mild to moderate reticulin fibrosis. Due to unusual findings seen in post-induction settings, there was concern for an underlying myeloproliferative neoplasm (n=2) or myelodysplastic/myeloproliferative neoplasm (n=1) in 3 patients.

Conclusions: In the era of midostaurin treatment, post-induction BM biopsies may show unusual findings including hypercellularity, left-shifted myeloid hyperplasia and atypical megakaryocytic hyperplasia instead of the typical rapid loss of cellularity seen after conventional chemotherapy. These unusual findings may cause a diagnostic challenge. Although myeloid differentiation effect of FLT3 TKIs and marrow hypercellularity in the post-induction marrows have been reported, to our knowledge, megakaryocytic hyperplasia has not been reported.

1411 Clinical and Genomic Characterization of Myeloproliferative Neoplasms Harboring PHF6 Mutations

Jason Kurzer[1], Valentina Nardi[2], Madhu Ouseph[3], Olga Weinberg[4]
[1]Stanford University School of Medicine, Mountain View, CA, [2]Massachusetts General Hospital, Boston, MA, [3]Brigham and Women's Hospital, Harvard Medical School, Dedham, MA, [4]Children's Hospital Boston, Boston, MA

Disclosures: Jason Kurzer: None; Valentina Nardi: None; Madhu Ouseph: None; Olga Weinberg: None

Background: Plant homeodomain finger 6 (*PHF6*) is a PHD-like zinc-finger containing protein that binds subsets of transcriptional regulatory machinery. Mutations in *PHF6* have been reported in multiple hematopoietic neoplasms, including myelodysplastic syndrome, acute myeloid leukemia, mixed myelodysplastic syndrome/myeloproliferative neoplasms, but only rarely (<3%) in pure myeloproliferative neoplasms (MPN). The goal of this study was to characterize cases of myeloproliferative neoplasms that harbor *PHF6* mutations and assess for its clinical significance.

Design: We searched 3 academic institutions' next generation sequencing data to identify cases carrying a diagnosis of myeloproliferative neoplasm that possessed *PHF6* mutations. Among 12,758 cases reviewed, 433 harbored mutations within *PHF6.*

Results: We identified 21 patients with a diagnosis of MPN and one with clinical suspicion for a MPN. Patient ages ranged from 55 to 81 years old (mean 71), with 12 men and 10 women. The MPN diagnoses included polycythemia vera (9), essential thrombocytosis (4), MPN unclassifiable due to moderate to advanced fibrosis (4), primary myelofibrosis (2), and MPN unclassifiable for non-fibrosis reasons (2). For cases with bone marrow biopsies, 12 of 21 (57%) cases showed MF-3 fibrosis and 16 of 21 (76%) cases showed at least MF-2 fibrosis. 16 (76%) showed <5% blasts, 3 (14%) showed accelerated phase (10% -19% blasts), and 3 (14%) cases showed transformation to blast crisis.

19 patients had cytogenetic results. 10 patients showed a normal karyotype (53%) and the most common cytogenetic abnormality was del(20q) (37%). 2 of 3 patients with blast crisis had complex karyotypes. Non-*JAK2* and *PHF6,* mutations were identified in 24 other genes, with *ASXL1* (57%) and *TET2* (33%) being the most frequent, with an average of 2.5 additional mutated genes identified per patient (see table).

Clinically, 72% of patients were managed with hydroxyurea and/or Jakifi, while 14% underwent a bone marrow transplant. 2 of 3 blast crisis patients are deceased with 1 transitioning to hospice care.

Gene	Patient 1 (VAF)	Patient 2 (VAF)	Patient 3 (VAF)	Patient 4 (VAF)	Patient 5 (VAF)	Patient 6 (VAF)	Patient 7 (VAF)	Patient 8 (VAF)	Patient 9 (VAF)	Patient 10 (VAF)	Patient 11 (VAF)	Patient 12 (VAF)	Patient 13 (VAF)	Patient 14 (VAF)	Patient 15 (VAF)	Patient 16 (VAF)	Patient 17 (VAF)	Patient 18 (VAF)	Patient 19 (VAF)	Patient 20 (VAF)	Patient 21 (VAF)	Patient 22 (VAF)
JAK2		47.6%	84.7%	96.7%		82%	13.3%	80.3%	40.2%	61%	86.4%	95.2%	22.4%		83.7%	86.0%		88.0%	83%		93.2%	54%
PHF6	36.4%	72.7%	77.8%	69.8%	8%	29.1%	35.6%	33.7%	10.8%	40%	47.6%	85.6%	7.5%	36%	88%	21.3%	15.3%	85.1%	59%	15%	51.2%	18%
																			9%		32.7%	9%
																					3.1%	8%
																						12%
TET2	62.9%										40.1%			42%	45.1%	47.9%			32%	44%		
	42.6%																			41%		
U2AF1	37.5%						34.2%		21.0%								12.2%					
MPL				52%																		
CBL						31.6%								35%								
IDH2								30.8%										47.4%				
NOTCH2									15.8%													
KMT2A										46%												
SF3B1												57.7%										
PTPN11												23.9%										
SRSF2													25.0%							21%	5.6%	
BRAF													46.8%									
ZRSR2															92.0%							95%
TP53													12.3%									
PPM1D													22.2%									
CEBPA													47.1%									
CUX1																	10.5%					
RUNX1																	8.9%					
NRAS																5.5%						
NF1																			46%			
SH2B3																				24%		
																				13%		
RB1																					9.1%	
CREBBP																						49%
JAK3																						50%
ASXL1	39.1%				31%					45%	50.1%			33%	40.5%	27.2%	30.6%	47.5%	30%		23.8%	42%

Conclusions: This is the first clinical and pathologic study of patients with MPN harboring *PHF6* mutations and reveals an enrichment for advanced stage disease, including increased fibrosis and transformation to blast crisis. The most common co-occuring mutations include *ASXL1* and *TET2* with a median of 2.5 co-mutated genes other than JAK2. These data implicate *PHF6* mutations as likely helping to promote disease progression.

1412 Pathologic and Molecular Spectrum of SETBP1 Mutations in Myeloid Neoplasms

Daniel Larson[1], Dong Chen[1], Phuong Nguyen[1], Jennifer Oliveira[1], Kaaren Reichard[1], James Hoyer[1], Nikita Mehta[2], David Viswanatha[1], Rong He[1]
[1]Mayo Clinic, Rochester, MN, [2]Division of Hematopathology, Mayo Clinic, Rochester, MN

Disclosures: Daniel Larson: None; Dong Chen: None; Phuong Nguyen: None; Jennifer Oliveira: None; Kaaren Reichard: None; James Hoyer: None; Nikita Mehta: None; David Viswanatha: None; Rong He: None

Background: *SETBP1* encodes the poorly characterized SET binding 1 protein, which has been shown to bind and stabilize SET, a negative regulator of the tumor suppressor protein phosphatase 2A. The incidence and pathologic/molecular spectrum of *SETBP1* mutations in myeloid neoplasms (MN) has not been well-documented. We aimed to better delineate the clinicopathological and mutational spectrum of *SETBP1* in MN.

Design: After approval from our institutional review board, results from a 35-gene next generation sequencing (NGS) panel were retrospectively reviewed. Patients harboring a pathogenic/likely pathogenic (P/LP) mutation were included. Medical records were reviewed for collection of patients' demographics, pathologic and pertinent laboratory and clinical findings. Pathologic diagnoses were classified using the 2016 WHO criteria.

Results: Among 1907 patients who had NGS performed between 7/2015 and 12/2018, 51 (2.7%) had *SETBP1* mutations. The diagnosis encompassed 14(27%) myelodysplastic syndrome/myeloproliferative neoplasm (MDS/MPN), 14(27%) MDS, 12(24%) acute myeloid leukemia (AML, 11 with myelodysplasia-related changes [AML-MRC], 1 AML-NOS), 6(12%) MPN, 2(4%) chronic MN and 3(6%) clonal cytopenia of undetermined significance (CCUS). *SETBP1* mutations identified were all missense mutations in the highly-conserved region of the SKI homologous domain, including D868N (55%), G870S (27%), I871T (6%), S867R (4%), D868T/G870D/E858K/G870R/T873R (2% each). Mean variant allele fraction (VAF) was 32.8% (5.2-56%). Concurrent mutations of other genes were seen in 49 cases (96.1%), including *ASXL1* (78%), *SRSF2* (59%), *CBL* (12%), *NRAS* (15%), *JAK2*/*TET2*/*EZH2* (12% each), *RUNX1*/*ETV6* (10% each), *U2AF1*/*FLT3* (8% each), *TP53*/*KRAS*/*PTPN11* (6% each), *DNMT3A*/*GATA2*/*SF3B1* (4% each),

and *ZRSR2/ WT1/IDH2/BRAF/CSF3R/BCOR/PHF6* (2% each). The mean number of concurrent mutations was 3.0 (0-6). Morphologically, 38 (75%) cases showed dysplasia in at least one lineage, including 14 MDS, 14 MDS/MPN and 10 AML-MRC.

Conclusions: *SETBP1* mutations rarely occur in a broad array of myeloid disorders ranging from CCUS to AML. The P/LP mutations are enriched for missense mutations in the SKI homologous domain. They are associated with morphologic dysplasia and the high frequency of AML-MRC cases in the AML group suggests *SETBP1*'s association with secondary AML and suggests probable clonal evolution from a myelodysplastic process to AML in these cases.

1413 Sizable Indolent B-Lymphoblastic Expansions in Reactive Pediatric Lymph Nodes

Won Lee[1], Siddharth Bhattacharyya[2], Jonathan Lake[3], Guang Yang[4], Vinodh Pillai[5], Adam Bagg[6]
[1]Evanston, IL, [2]Hospital of the University of Pennsylvania, Edison, NJ, [3]University of Pennsylvania Health System, Philadelphia, PA, [4]The Hospital of the University of Pennsylvania, Philadelphia, PA, [5]The Children's Hospital of Philadelphia, Penn Valley, PA, [6]University of Pennsylvania, Philadelphia, PA

Disclosures: Won Lee: None; Siddharth Bhattacharyya: None; Jonathan Lake: None; Guang Yang: None; Vinodh Pillai: None; Adam Bagg: None

Background: Physiologic B-cell precursor (hematogone) hyperplasia can be seen in the bone marrow or blood in a variety of reactive conditions, particularly in the pediatric setting. However, while nodal expansions of non-clonal T-cell precursors are well described (indolent T-lymphoblastic proliferations or iT-LBL), similar nodal expansions of B-cell precursors are not well characterized, other than in a publication from nearly 20 years ago (PMID: 12162686). That study revealed low numbers of non-clonal hematogones in negative staging lymph nodes from children with solid malignancies. Sizeable expansions (as seen in iT-LBP) were not seen in that study and not been described since.

Design: We analyzed excisional lymph node specimens from a spectrum of deep and superficial anatomic sites in 34 pediatric patients (ages: 5 mo-18 yrs), of which 19 were reactive lymphadenopathies and 15 were negative staging nodes for a variety of solid tumors. The lymph node specimens were stained for TdT, CD10, PAX5 and/or CD20, CD34, and CD3. A select case was also stained for BCL6 and analyzed by IGH PCR for clonality. Given the focal distribution of percentage positive staining, this was scored both globally (whole node) and regionally (1 or more HPFs).

Results: A variety of histologic patterns was seen, with reactive cases showing mostly follicular hyperplasia and sinus histiocytosis dominating staging lymph nodes. A sizable expansion (10-20% globally, 30-70% regionally) of CD10+ PAX5+ CD20(occasionally dim)+ B-cells was detected in 8 cases; lesser expression of TdT and CD34 was seen. [Figures 1 and 2]. All were located in a perisinusoidal distribution. The only significant difference between these 8 cases and the 26 without such expansions was a higher female:male ratio. There was no difference with regard to age, indication for excision and anatomic site. Neither BCL6 expression nor IGH monoclonality was evident in the case with the greatest degree of expansion (20% globally, 70% regionally). No patients were known to develop B-lymphoblastic neoplasms on follow-up.

Figure 1 - 1413

Figure 2 - 1413
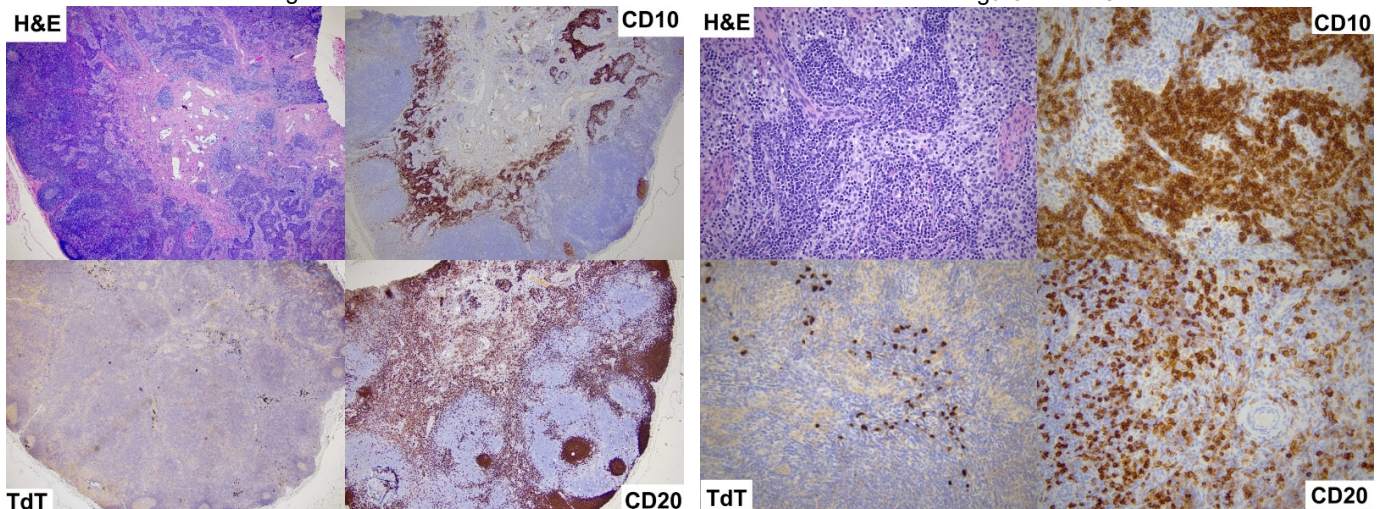
Conclusions: This study highlights the presence of robust expansions of CD10-positive B-cell precursors in lymph nodes from pediatric patients, in both reactive and staging cases. Recognizing the existence of such benign populations is paramount in differentiating these

from B-lymphoblastic leukemia/lymphoma, the most common pediatric hematolymphoid neoplasm. Further study is required to determine if similar expansions are also seen in adult populations.

1414 Clonal Hematopoiesis (CH) in Angioimmunoblastic T-Cell Lymphoma (AITL) with Divergent Evolution to Myeloid Neoplasms (MNs)

Natasha Lewis[1], Kseniya Petrova-Drus[1], Zachary Epstein-Peterson[1], Sarah Huet[2], Qi Gao[1], Allison Sigler[1], Jeeyeon Baik[1], Anita Kumar[3], Steven Horwitz[1], Yanming Zhang[1], Maria Arcila[1], Ross Levine[1], Mikhail Roshal[1], Ahmet Dogan[1], Wenbin Xiao[1]
[1]Memorial Sloan Kettering Cancer Center, New York, NY, [2]Laboratory of Haematology, CHU Lyon-Sud, Hospices Civils de Lyon, Pierre-Bénite, Auvergne-Rhône-Alpes, France, [3]Memorial Sloan Kettering Cancer Center, Short Hills, NJ

Background: *TET2* and *DNMT3A* mutations are common in AITL, CH and MNs. The relationship between CH, AITL and MNs is not well studied. Here we show that CH is common in AITL patients and can divergently evolve to AITL and MNs.

Design: Pathology database search identified patients with *TET2*-mutated AITL and tissue and bone marrow (BM) available for targeted next-generation sequencing (NGS). BM cytogenetic, flow cytometry (FC) and T-cell receptor gene rearrangement (TCR) studies were performed during clinical work-up. FC sorting was performed on selected BMs (n=4). NGS was performed on tissue, BM and FC-sorted cells. In non-FC-sorted samples, we used allele frequency and tumor content to identify the compartment in which a mutation was present (AITL or non-AITL BM). Clinical data was obtained from electronic medical records.

Results: 17 patients were identified (11 male, 6 female; median age 69 [range 53-93] years) (Table 1). No patient had a prior MN diagnosis. AITLs harbored *TET2* (17/17, 100%), *DNMT3A* (8/17, 47%), *RHOA* G17A (6/17, 35%) and *IDH2* R172 (2/17, 12%) mutations. BMs were involved by AITL by morphology (range <5-50%) in 9 patients; minimal involvement was detected by FC +/- TCR (0.0079%, 0.036%) in 2 additional patients. BMs from the remaining 6 patients were negative for AITL by FC and TCR (TCR performed in 3/6). Identical mutations were detected in the AITL and non-AITL BM compartments of 10 patients, including *TET2* (10/10) and *DNMT3A* (5/5 with *DNMT3A*+ AITLs) (Figures 1, 2). MNs were diagnosed in BMs of 4 patients based on 2017 World Health Organization morphologic, cytogenetic and molecular criteria (see Table 1 for patients and MN types), 3 of which shared CH mutations in their AITL and MN (pts 9, 10, 16; *TET2* in 3/3, *DNMT3A* in 1/1 with *DNMT3A*+ AITL). Genomic alterations unique to the MNs included del(7q) and *RUNX1* mutation (pt 9), inv(3) and *WT1* mutation (pt 10), *DNMT3A* mutations (pts 9, 10) and *SRSF2* mutation (pt 16). Mutations unique to AITL (among entire cohort) included *IDH2*, *RHOA* and *TET3*.

Patient	Sex	Age (y)	Prior cancer history (treatment, dates)	Date of AITL diagnosis	Tissue used for NGS	BM bx date	Indication for BM bx	Indication for NGS on BM	Myeloid neoplasm diagnosed on BM bx (type)	AITL-directed therapy prior to BM bx	Outcome	Overall survival (mo)
1	M	67	None	7/12/17	LN	8/8/17	Initial staging	Ordered by pathologist to work-up small abnormal B-cell population detected by flow cytometry only	No	None	DOD	7
2*	M	53	None	11/20/14	Skin	10/5/16	Persistent TCP 17 mo. after completion of chemo	Work-up for lymphoma and/or myeloid neoplasm	No	Chemo	DOD	41
3*	F	82	None	8/8/14	LN	12/18/15	Acutely worsening pancytopenia 12 mo. after completion of chemo	Work-up for lymphoma and/or myeloid neoplasm	No	Chemo	A w/o active D	57
4*	M	93	Melanoma (Excision, 2016)	11/30/17	LN	12/22/17	Initial staging	Ordered by pathologist for full work-up and evaluate the T-cell infiltrate	No	None	AWD	5
5	F	68	Breast ca (Chemo, XRT, hormonal therapy, 1997 & 2000)	12/23/15	Mesenteric mass	5/15/17	Evaluate disease status at relapse	Assess potential therapeutic targets (likely ordered on	No	Chemo	AWD	41

Table 1. Clinical characteristics of 17 patients with angioimmunoblastic T-cell lymphoma.

#	Sex	Age	History	Date	Site	Date	Reason	Purpose	Myeloid	Treatment	Status	OS (mo.)
								incorrect specimen)				
6*	F	73	None	3/4/15	LN	3/20/15	Initial staging	Identify potentially actionable mutations	No	None	DOD	37
7	M	73	Prostate ca (Active surveillance then resection in 2017)	2/19/15	LN	3/4/15	Initial staging	Identify potentially actionable mutations	No	None	A w/o D	51
8*	M	66	Bladder ca (Excision, date unknown)	12/19/14	Spleen	1/8/18	Required for clinical trial enrollment	Ordered by pathologist to evaluate for myeloid neoplasm due to peripheral cytoses	No	Chemo, TT	AWD	53
9*	F	63	None	4/20/16	LN	12/10/18	Persistent pancytopenia 6 mo. after ASCT	Ordered by pathologist due to concern for myeloid neoplasm	Yes (AML)	Chemo, ASCT	DOD	33
10*	M	71	None	3/23/15	LN	12/10/18	Worsening pancytopenia on clinical trial that persisted 1.75 mo. after therapy cessation	Work-up for lymphoma and/or myeloid neoplasm	Yes (MDS-EB-1)	Chemo	A w/o D; Progressed to AML	50
11	M	61	None	11/12/15	LN	8/29/17	Worsening anemia, TCP on chemo that persisted 2 mo. after completion	Work-up for lymphoma and/or myeloid neoplasm	No	Chemo, ASCT, localized XRT	DOD	22
12	M	69	None	8/7/18	LN	11/2/18	Repeat after possibility of myeloid neoplasm raised on outside initial staging BM bx	Work-up for myeloid neoplasm	Yes (MDS-U)	Chemo	A w/o active D; Del(7q) disappeared on follow-up BM bxs	8
13*	F	69	None	8/11/11	Skin	3/16/18	Persistent cytopenias 18 mo. post relapse (on therapy) and assess disease status at first visit to our institution	Work-up for lymphoma and/or myeloid neoplasm	No	Chemo, ASCT	A w/o D	91
14	M	71	Clear cell RCC (Excision, 2004; recurrence/metastasis, observed since 2012)	3/5/15	LN	3/2/18	Staging of newly diagnosed laryngeal plasmacytoma	Routine diagnostic work-up	No	Chemo	A w/o D	50
15	F	61	Classical Hodgkin lymphoma (Chemo, XRT, 2007)	12/7/11	LN	1/5/18	Confirm relapse	Identify potentially actionable mutations	No	Chemo, ASCT, TT	A w/o D	90
16*	M	73	None	9/30/16	LN	7/11/19	Required for clinical trial enrollment at time of relapse	Ordered by pathologist due to concern for myeloid neoplasm	Yes (CMML-0)	Chemo, ASCT	A w/o active D; Persistent CMML	34
17*	M	74	None	7/16/19	LN	7/30/19	Initial staging	Routine diagnostic work-up	No	None	AWD	2

Overall survival indicates the time from diagnosis to date of death or last follow-up. Y indicates years; AITL, angioimmunoblastic T-cell lymphoma; NGS, next-generation sequencing; BM, bone marrow; bx, biopsy; mo., months; M, male; F, female; Ca, cancer; XRT, radiation; RCC, renal cell carcinoma; LN, lymph node; TCP, thrombocytopenia; ASCT, autologous stem cell transplant; AML, acute myeloid leukemia; MDS-EB-1, myelodysplastic syndrome with excess blasts 1; MDS-U, myelodysplastic syndrome, unclassifiable; CMML-0, chronic myelomonocytic leukemia 0; TT, targeted therapy; DOD, dead of disease; A w/o D, alive without evidence of disease (AITL); AWD, alive with disease (AITL). *=Patients with evidence of shared mutations in their AITL and non-AITL bone marrow compartment.
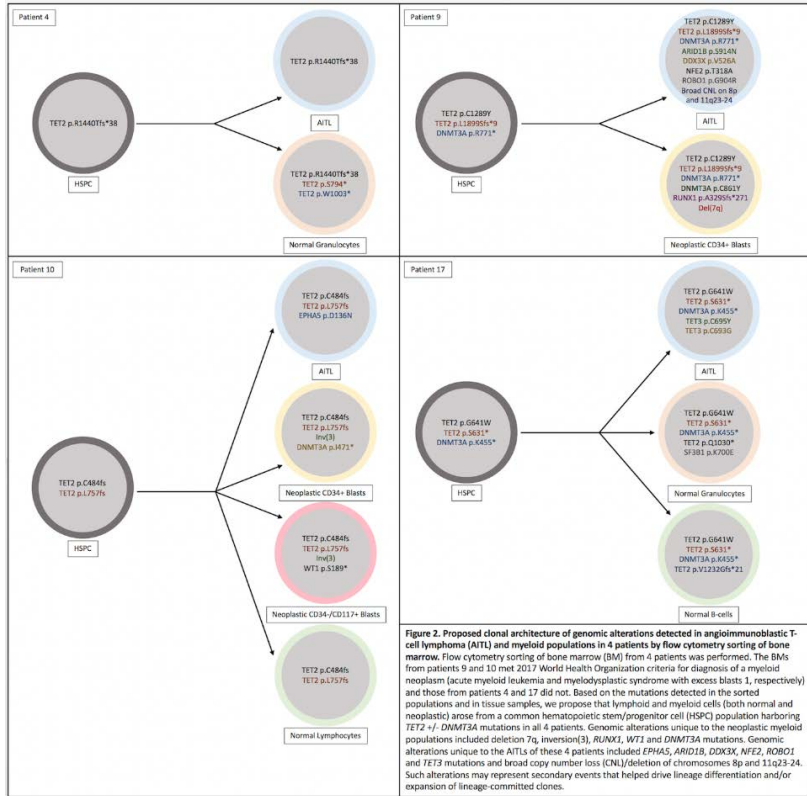
Figure 1 - 1414

Figure 1. Next-generation sequencing results from paired angioimmunoblastic T-cell lymphoma (AITL) and bone marrow samples from 17 patients. Mutations and their variant allele frequencies (VAFs) were identified by next-generation sequencing (NGS) in paired tissue samples involved by AITL and bone marrow biopsies from each of 17 patients. NGS was performed on flow cytometry (FC)-sorted populations from bone marrow in selected cases (n=4). Based on comparison of tumor content and VAFs by NGS results from FC-sorted populations, the cellular compartments in which each mutation was present (within the AITL or non-AITL hematopoietic cells) was determined. Each cell represents a single mutation, the status of that mutation and its VAF (%) in each patient's AITL ("T" column) and non-AITL bone marrow compartment ("BM" column). The extent of involvement of each bone marrow by AITL is provided (values indicate the percentage of bone marrow cellularity comprised by AITL as determined by morphology, FC and T-cell receptor gene rearrangement studies (TCR); "FC" indicates the AITL was detected by FC +/- TCR only (% is based on FC analysis); "S" indicates NGS was performed on FC-sorted cells). T*=Sequencing performed and VAFs obtained from FC-sorted abnormal T-cells from bone marrow. BM^= Sequencing performed and VAFs obtained from FC-sorted granulocytes from bone marrow. BM#= Sequencing performed and VAFs obtained from FC-sorted abnormal myeloid blasts from bone marrow.

- Mutation and its VAF identified in neoplastic T-cells or non-AITL bone marrow compartment (one cell per mutation)
- Mutation not definitively identified within neoplastic T-cells and/or non-AITL bone marrow compartment
- Gene not evaluated by sequencing analysis performed

Figure 2 - 1414

Figure 2. Proposed clonal architecture of genomic alterations detected in angioimmunoblastic T-cell lymphoma (AITL) and myeloid populations in 4 patients by flow cytometry sorting of bone marrow. Flow cytometry sorting of bone marrow (BM) from 4 patients was performed. The BMs from patients 9 and 10 met 2017 World Health Organization criteria for diagnosis of a myeloid neoplasm (acute myeloid leukemia and myelodysplastic syndrome with excess blasts 1, respectively) and those from patients 4 and 17 did not. Based on the mutations detected in the sorted populations and in tissue samples, we propose that lymphoid and myeloid cells (both normal and neoplastic) arose from a common hematopoietic stem/progenitor cell (HSPC) population harboring TET2 +/- DNMT3A mutations in all 4 patients. Genomic alterations unique to the neoplastic myeloid populations included deletion 7q, inversion(3), RUNX1, WT1 and DNMT3A mutations. Genomic alterations unique to the AITLs of these 4 patients included EPHA5, ARID1B, DDX3X, NFE2, ROBO1 and TET3 mutations and broad copy number loss (CNL)/deletion of chromosomes 8p and 11q23-24. Such alterations may represent secondary events that helped drive lineage differentiation and/or expansion of lineage-committed clones.

Conclusions: CH-type mutations are common in AITL patients. We show evidence that AITLs and MNs in 3 patients arose from common TET2+, DNMT3A+/- CH clones, suggesting TET2 and DNMT3A mutations occur in hematopoietic stem/progenitor cells with the potential to clonally evolve along T-cell and myeloid lineages with evolution to AITL and MN driven by additional and divergent genetic events. Such pathobiology may place AITL patients at higher risk of MN, especially post-therapy.


1415 High Counts of CD68+ and CD163+ Macrophages in Mantle Cell Lymphoma are Associated with Inferior Prognosis

Philippa Li[1], Yuan Ji[2], Fahad Ahmed[3], Kai Fu[2], Guohua Yu[4], Hongxia Cheng[5], Mina Xu[1], David Rimm[6], Zenggang Pan[6]
[1]Yale University, New Haven, CT, [2]University of Nebraska Medical Center, Omaha, NE, [3]Yale School of Medicine, New Haven, CT, [4]Yantai Yuhuangding Hospital, Yantai, Shandong, China, [5]Provincial Hospital Affiliated to Shandong University, Jinan, Shandong Province, China, [6]Yale University School of Medicine, New Haven, CT

Background: Lymphoma-associated macrophages (LAMs) are key components in the lymphoma microenvironment, which may impact disease progression and response to therapy. There are two major types of LAMs: CD68+ M1 and CD163+ M2. M2 LAMs can be polarized from M1 LAMs, particularly in large B-cell lymphomas which often have a much higher M2 density. Mantle cell lymphoma (MCL) is typically aggressive and has a median overall survival (OS) of 3-5 years. MCL is well-known to contain frequent epithelioid macrophages with pink cytoplasm and limited phagocytic activities (so-called "pink" histiocytes) (Figures 1A and 1B). The macrophages (LAMs) in MCL have not been fully characterized. Herein we evaluate the relative ratio of LAM subtypes and assess the prognostic impact of these macrophages in MCL.

Design: A total of 73 MCLs were collected from two institutions. All cases were further reviewed to confirm the diagnosis and to select those with sufficient tissue and clinical data. A tissue microarray (TMA) block was constructed with two 1.0 mm cores for each case (Figure 1A). Immunohistochemical stains were performed using CD68 (Clone PG-M1, DAKO) and CD163 (Clone 10D6, Abcam), and the positive cells were recorded manually in 4 representative 400x fields (Figures 1C and 1D). The cut-off points of optimal separation of OS were analyzed using the X-Tile software (Camp et al, CCR 2004), the SPSS version 26 was used to construct survival curves, and the log rank test was performed to calculate the p-values.

Results: The 73 MCL patients consisted of 56 males and 17 females with a median age of 67 years. All cases were obtained through excisional biopsies prior to therapy. The average counts for CD68+ cells and CD163+ cells were 170 (range 29-493) and 57 (range 0-519), respectively, with a CD68:CD163 ratio of 3:1 (Figures 2A and 2B). For CD68+ macrophage counts, the cut-off was set to the median (50%), and the 50% patients with lower CD68+ counts had a significantly better OS than those 50% with higher counts (p-value = 0.039; Figure 2C). The X-Tile defined the optimal cut-off of CD163+ at 90%, and the 90% cases with lower CD163+ counts were associated with an improved OS (p-value=0.012; Figure 2D).

Figure 1 - 1415

Figure 2 - 1415
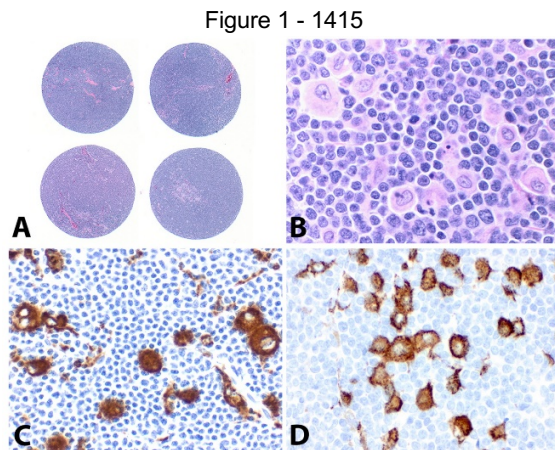
Figure 1. (**A**) Tissue microaray of mantle cell lymphoma (MCL) cases. (**B**) Scattered epitheloid histiocytes in MCL. (**C**) CD68. (**D**) CD163.
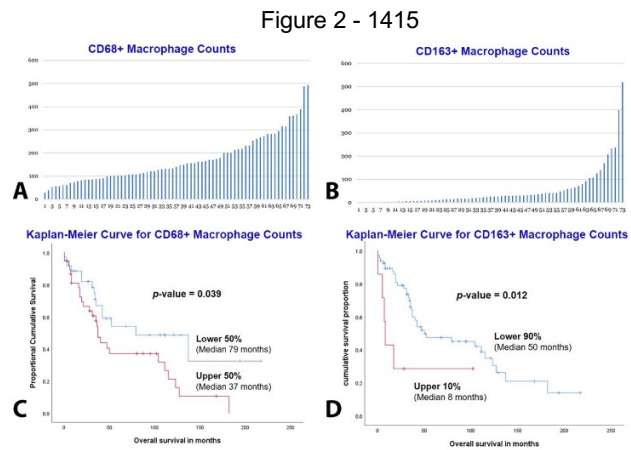
Figure 2. Macrophage counts of all 73 cases based on CD68+ (**A**) and CD163+ (**B**). Overall survivals according to the CD68+ (**C**) and CD163+ (**D**) counts.

Conclusions: In contrast to large B-cell lymphoma, MCL had a significantly lower rate of M1 to M2 polarization, and the high levels of CD68+ and CD168+ LAMs were associated with poor OS. Further studies will be performed with larger cohorts and multiplexed immunofluorescence quantitative assays.

1416 Diffuse Large B-cell Lymphoma Stromal Tumor Microenvironment Differs Based on HIV and Antiretroviral Therapy Status

Amy Lilly[1], Sara Selitsky[2], Cara Randall[3], Tamiwe Tomoka[4], Maurice Mulenga[5], Satish Gopal[2], Yuri Fedoriw[6]
[1]University of North Carolina at Chapel Hill, Chapel Hill, NC, [2]University of North Carolina, [3]UNC Chapel Hill Department of Pathology, Chapel Hill, NC, [4]UNC Project Malawi, Lilongwe, Malawi, [5]Kamuzu Central Hospital, Lilongwe, Malawi, [6]University of North Carolina, Pittsboro, NC

Disclosures: Amy Lilly: None; Cara Randall: None; Tamiwe Tomoka: None; Maurice Mulenga: None; Yuri Fedoriw: None

Background: Diffuse Large B-cell Lymphoma (DLBCL) is not only the most common lymphoma subtype but also the most common cause of cancer death among HIV-positive individuals in high-income countries. Despite histologically similar appearances, HIV-associated DLBCL differs biologically from DLBCL in immunocompetent populations. Lymphomagenesis is driven both by genetic changes within the malignant cells but also by selective pressures in the local tumor microenvironment (TME), including angiogenesis, an essential driver of tumor development and progression. We aimed to compare the transcription-level differences related to the stromal TME of DLBCL, based on HIV status.

Design: 36 DLBCL cases from the ongoing Kamuzu Central Hospital Lymphoma Study in Malawi were analyzed: whole transcriptome sequencing was performed on all cases (22 HIV+/14 HIV-) and CD34 immunohistochemistry (IHC) was performed on 34 cases (21 HIV+/13 HIV). Lymphoma-related clinical and laboratory data were collected for all patients, along with HIV RNA, CD4, and ART status for the HIV-infected cohort. We determined enriched gene sets using Gene Set Variation Analysis to compute a module score and then used linear regression to test associations of the Hallmark gene set and immune gene modules. To determine microvessel density (MVD), we enumerated CD34 IHC staining and averaged the number of vessels counted over 10 high-power fields (hpf).

Results: Of the 36 cases, 10 were female and average age was 49 years. Compared to HIV- DLBCL, HIV+ cases were enriched in hypoxia-related genes and modules related to oxidative stress (q-values < 0.05 by linear regression, FDR adjustment). Vascular Endothelial Growth Factor (VEGF) and VEGF-receptor (VEGFR) showed graded expression, lowest in the HIV- cases, and highest in the ART-naïve DLBCL (ANOVA p=0.0002 and p=0.0119, respectively). Compared to HIV- DLBCL, HIV+ DLBCL cases had a higher MVD (27.1 vs 22.0 vessels per hpf, p=0.160)

Conclusions: Although lymphomas in HIV patients arise in a TME distinct from immunocompetent hosts, few studies have examined whether specific microenvironmental patterns are associated with HIV+ DLBCL. Our data demonstrate HIV+ DLBCL have a differential angiogenic and stromal expression signature when compared to HIV- DLBCL. This transcriptional difference is not definitively supported by our initial IHC assessment. Further studies to elucidate the morphologic correlates of these transcriptional differences are required.

1417   Down Syndrome (DS) with B-Cell Acute Lymphoblastic Leukemia (B-ALL) versus Non-DS B-ALL in Children and Young Adults: Pathogenetic Differences

Kaleigh Lindholm[1], Liming Bao[2], Billie Carstens[3], Xiayuan Liang[4]
[1]University of Colorado Anschutz Medical Campus, Denver, CO, [2]Colorado Cytogenetics Laboratory, Aurora, CO, [3]University of Colorado Anschutz Medical Campus, Aurora, CO, [4]Children's Hospital Colorado, Aurora, CO

Disclosures: Kaleigh Lindholm: None; Liming Bao: None; Billie Carstens: None; Xiayuan Liang: None

Background: Down Syndrome (DS) is characterized by a constitutional extra copy of chromosome 21. Children with DS have an increased incidence of acute leukemia, most commonly B-cell acute lymphoblastic leukemia (B-ALL). DS B-ALL is a distinct category and are treated with a chemotherapy regimen different from non-DS B-ALL based on Children's Oncology Group. The 2016 WHO Classification of Hematologic Malignancies categorizes B-ALL into those with and without recurrent genetic abnormalities, many of which show significant prognostic indications. However, whether DS B-ALL patients and non-DS B-ALL share pathogenetic features has not been well studied. We examined the pathogenetic landscape of both patient populations to assess differences between DS B-ALL and non-DS B-ALL.

Design: Between 2001 and 2019, 31 cases of newly diagnosed DS B-ALL were identified at our institution. We compared this group to newly diagnosed non-DS B-ALL in 2015 and 2016 (87 cases). We analyzed age at diagnosis, M:F ratio, WBC (≥50k), CSF+, mean S-phase, recurrent cytogenetic abnormalities (*ETV6-RUNX1*, *BCR-ABL1*, *KMT2A*-rearranged, *TCF3-PBX1*, *IgH/IL3*, iAMP21, hyperdiploidy, and hyodiploidy), and other cytogenetic abnormalities. A p-value was calculated with a value of <0.05 considered statistically significant.

Results:

	B-ALL DS	B-ALL Non-DS	*p* value
Case #	31	87	
Mean age	6.00 (1-21 y)	5.64 (10 d – 18 y)	0.7410
Male:Female	21:10	35:42	0.0546
WBC (>=50k)	3/31 (9.68%)	13/87 (14.92%)	0.5560
CSF+	3/29 (10.34%)	26/84 (30.95%)	0.0832
Mean S-phase	10.10 (1.60-22.40)	6.99 (0.40-20.00)	0.0194
ETV6-RUNX1	3/28 (10.71%)	12/84 (14.29%)	0.7577
BCR-ABL1	1/28 (3.57%)	4/84 (4.76%)	1.0000
Other recurrent cytogenetic abnormalities	0/28 (0%)	24/84 (28.57%)	0.0004
Miscellaneous cytogenetic abnormalities	16/28 (57.14%)	37/84 (44.05 %)	0.2771

Conclusions: 1. Patients with DS have higher S-phase in their blasts than patients without DS suggesting that constitutional trisomy 21 may promote leukemic cell proliferation. 2. *ETV6-RUNX1* and *BCR-ABL1* fusions were seen equally in those with and without DS, but all other recurrent cytogenetic alterations are absent in DS patients. These findings suggest that constitutional trisomy 21 may selectively suppress certain recurrent cytogenetic abnormalities.

1418 Decreased CD58 Expression in B-ALL is Associated with Higher Rate of Minimal Residual Disease at Day 29 After Induction Therapy and May Indicate an Immune Escape Phenotype

Yevgeniy Linnik[1], Bruce Greig[2], Ridas Juskevicius[1]
[1]Vanderbilt University Medical Center, Nashville, TN, [2]Vanderbilt University, Nashville, TN

Disclosures: Yevgeniy Linnik: None; Bruce Greig: None; Ridas Juskevicius: None

Background: Minimal residual disease (MRD) monitoring by flow cytometry (FC) after therapy to guide further treatment is standard of care in the management of patients with B lymphoblastic leukemia/ lymphoma (B-ALL). Given the strong expression in many B-ALLs, CD58 is included in FC MRD panels. CD58 is a ligand of CD2 which is expressed on most cytotoxic T lymphocytes (CTLs) and NK cells. CD58 expression on target cells is important for the adhesion and activation of CTLs and NK cells. Although many patients achieve MRD negativity by day 29 of therapy, some show persistent disease at low-levels. The biologic reasons for this are not clear. Disruption of CD2/CD58 interactions result in diminished recognition of tumor cells by CTLs and NK cells and may contribute to immune escape. We have noted decreased expression of CD58 in some cases of B-ALL and asked a question if this may be associated with increased rate of MRD positivity.

Design: 47 consecutive patients diagnosed with B-ALL from 2016 to 2017 at our medical center were included in this study. FC with validate panel of antibodies (CD9, CD10, CD19, CD20, CD34, CD38, CD45, CD58) for the detection of MRD was performed on the diagnostic and post therapy day 29 bone marrow (BM) samples. The lower limit of detection for this assay is validated at 0.01% of total events. List mode files were analyzed with WinList3D program to determine mean fluorescent intensity (MFI) of CD58 expression on B lymphoblasts in the diagnostic BM samples. BM MRD status at day 29 was recorded. MRD positivity was defined by a population of B lymphoblasts with similar phenotype to the diagnostic BM detected above the validate lower limit of detection. Clinical data with up to 3 years of follow up were recorded. CD58 MFI of B lymphoblasts in the diagnostic BMs was compared between patient groups with negative and positive MRD at day 29. The data analysis was performed with Excel using *t*-test.

Results: Out of 47 patients, 13 were found to have MRD positivity at day 29. 11 of MRD positive patients had CD58 MFI which was lower than mean and median for all cases. In patients with MRD positivity mean and median of CD58 MFI was significantly lower as compares with MRD negative patients (85.5 and 76.9 vs 136.5 and 115.6 respectively, p= 0.005, two tailed) (figure 1 and 2).
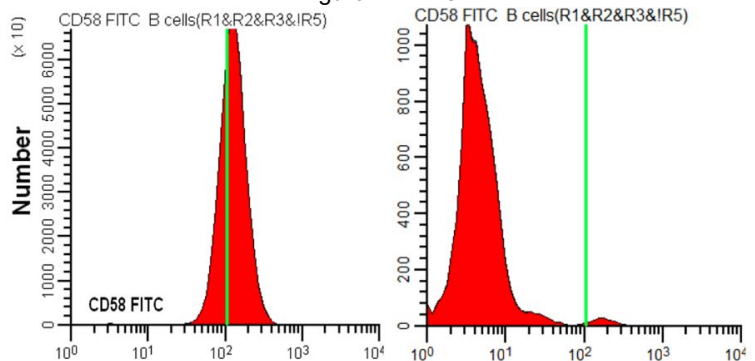

Figure 1 - 1418
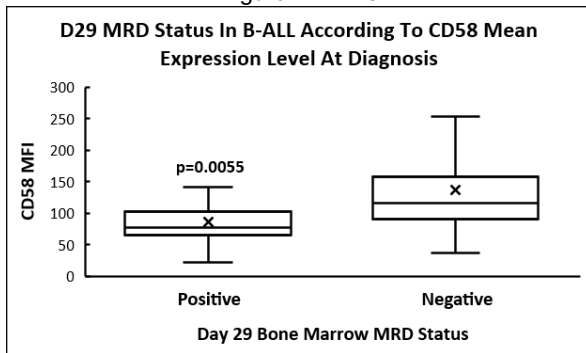
Figure 2 - 1418

Conclusions: Decrease CD58 expression in B lymphoblasts as determined using FC at the time of diagnosis of B-ALL is associated with increased rate of MRD positivity at day 29. Study is ongoing with additional data.

1419 Lipoprotein Lipase Deletion: a Potential Biomarker to Further Stratify Patients with 17p-deleted Chronic Lymphocytic Leukemia (CLL)

Wei Liu[1], Jie Xu[2], L. Jeffrey Medeiros[1], Guilin Tang[1]
[1]The University of Texas MD Anderson Cancer Center, Houston, TX, [2]Houston, TX

Disclosures: Wei Liu: None; Jie Xu: None; L. Jeffrey Medeiros: None; Guilin Tang: None

Background: Deletion (del) of chromosome 17p/*TP53* in CLL is associated with poorer prognosis and resistance to conventional chemotherapies. Although targeted therapy using ibrutinib has significantly improved the clinical outcome of CLL patients with del (17p), the prognosis of patients in this subgroup is heterogeneous. Deletion of lipoprotein lipase (LPL) has been shown to be a negative predictor of prognosis in CLL patients and ibrutinib has been postulated to enable its anti-tumor effect through inhibiting LPL-mediated free fatty acid (FFA) metabolism in CLL. The aim of this study is to explore the potential of LPL deletion as a new marker to further stratify 17p-deleted CLL patients in terms of biological behavior and treatment response to ibrutinib.

Design: 179 CLL patients with del (17p) were tested for LPL deletion by FISH from 1/1/2017 to 7/1/2019. Within this group, 52 patients had complete clinical data to be included in this study. Patients were treated with ibrutinib alone or as part of other therapies. Also analyzed are expression of CD38 and ZAP70, somatic hypermutation of IGHV (SH-IGHV) and mutational profile by NGS. Treatment response and overall survival were analyzed for clinical outcomes.

Results: LPL deletion was detected in 37 of 179 (20.7%) patients. Among the 52 patients included for further analysis, 33 had LPL deletion (LPL-del) and 19 had normal LPL (LPL-nml). LPL-del cases showed a higher frequency of being CD38 positive than LPL-nml cases (68.4% vs. 35.3%, p<0.05). Neither ZAP70 expression nor SH-IGHV showed a significant difference between the two groups. Mutational profile by NGS was available for 25 LPL-del and 12 LPL-nml cases and showed 18 mutated genes, with *TP53* mutation being most common (68% in LPL-del vs. 83% in LPL-nml), followed by SF3B1 (32% vs. 17%). The numbers of mutated genes were not significantly different between the two groups (1.96+/-0.73 vs. 2.08+/-0.99). In response to ibrutinib-based therapy, survival analysis showed that patients with LPL-nml had better overall survival (OS) than LPL-del patients (median OS: undefined vs. 212.8 months), although there was no significant difference between two groups in terms of response to ibrutinib treatment and disease status.

Conclusions: LPL deletion is a common genetic abnormality occurring in about 20% of patients with CLL associated with del (17p). LPL deletion is associated with a higher frequency of CD38 expression and poorer overall survival following ibrutinib-based therapy.

1420 Clinicopathologic Characterization of A Multi-Institutional Cohort of Therapy-related Myeloid Neoplasms with Different Latencies

Yen-Chun Liu[1], Gwendolyn Illar[2], Briana Canady[2], Julia Geyer[3]
[1]University of Pittsburgh School of Medicine, Pittsburgh, PA, [2]University of Pittsburgh, Pittsburgh, PA, [3]Weill Cornell Medicine, New York, NY

Disclosures: Yen-Chun Liu: None; Gwendolyn Illar: None; Briana Canady: None; Julia Geyer: None

Background: Therapy-related myeloid neoplasm (t-MN) has long been considered as a complication of chemotherapy (CT) and radiation therapy (RT) causing DNA damage. Advances in molecular technology and the recognition of germline predisposition in leukemogenesis prompt the re-evaluation of the concept. t-MN diagnosis is rendered in patients receiving CT and/or RT but the entity may not be as homogenous as previously speculated. Prior studies suggest t-MNs ordinarily occur 1-10 years after the treatment. We aim to further understand this heterogeneous category by characterizing a t-MN cohort from 2 large tertiary medical centers with different latencies.

Design: Review of the records and pathology material (including cytogenetic and next-generation sequencing studies) identified 134 t-MNs (56 AMLs and 78 non-AMLs). 19/134 patients received RT only, 61 received CT only while 54 got both. 21/134 patients had ≥2 malignancies besides t-MN. 70 cases had complex karyotypes. 20 cases with normal karyotypes had 0-6 mutations by sequencing. 39 cases showed a latency >10 years after initial treatment (t-MN-long); 88 cases had a latency of 1-10 years (t-MN-ord), and 7 cases showed a latency of <1 year.

Results: The median survival in t-MN is 10.3 months. There is no significant survival difference among cases based on treatment (CT or RT), marrow cellularity, abnormal karyotype, different latencies or multiple malignancies. t-MN-long cases are older than t-MN-ord (median 73 vs 68; p=0.02). Complex karyotype (70/120), del(5q) and/or del(7q)/-7 (58/121) and *TP53* aberrations (45/87) were seen in high percentages of t-MNs with different latencies with no significant differences among groups. A significantly higher portion of t-MN-long cases had multiple malignancies (including carcinoma, lymphoma, myeloma, melanoma and sarcoma)(12/39) when compared to t-MN-ord (p=0.01). t-MN-long cases were exposed to CT/RT at a younger age when compared to t-MN-ord (median 54 vs 63 years; p<0.01).

Conclusions: We didn't identify survival difference between groups receiving CT or RT, supporting the inclusion of RT-related MN cases in the t-MN group. The lack of survival difference in cases with different latencies may result from similarities in the cytogenetic/molecular profiling, suggesting t-MN-long cases still share features with ordinary t-MNs. However, the high percentage of multiple malignancies in t-MN-long group suggests a potential distinctive combination of genetic and environmental risk factors in this unusual group.

1421 Minimal Residual Disease Detection in B-ALL: Comparison of a High-Sensitivity, Single-Tube, 13-Color Flow Cytometry Assay and an NGS-Based Assay

Ying Liu[1], Qi Gao[1], Douglas Mata[1], Wayne Yu[1], Maria Arcila[1], Khedoudja Nafa[1], Jessica Wardrope[1], Ahmet Dogan[1], Caleb Ho[1], Mikhail Roshal[1]
[1]Memorial Sloan Kettering Cancer Center, New York, NY

Disclosures: Ying Liu: None; Qi Gao: None; Douglas Mata: None; Wayne Yu: None; Maria Arcila: *Speaker*, Invivoscribe; *Speaker*, Biocartis; Khedoudja Nafa: *Speaker*, Biocartis; Jessica Wardrope: None; Ahmet Dogan: *Consultant*, Roche, Corvus Pharmaceuticals, Seattle Genetics, Oncology Specialty Group, Pharmacyclics, Celgene, Novartis, Takeda; *Primary Investigator*, Roche/Genentech; Caleb Ho: *Speaker*, Invivoscribe, Inc.; Mikhail Roshal: None

Background: Detection of minimal residual disease (MRD) is a powerful predictor of outcome in B-lymphoblastic leukemia (B-ALL). Recent data show improvement of risk stratification with a more sensitive NGS-based assay with a technical sensitivity of 10^{-5} to 10^{-6}. We recently developed and validated a single-tube, 13-color, 15-antigen high-sensitivity FC (hsFC) assay for MRD detection. In this study, we compared the performance of our hsFC-based assay with NGS for B-ALL MRD detection.

Design: Bone marrow (n = 93) and peripheral blood (n = 1) samples from 54 post-treatment B-ALL patients with no morphologic evidence of disease and <5% abnormal blasts by traditional FC were obtained between May 2018 and August 2019. For this study, the samples were processed with an NGS-based assay (an in-house implementation of LymphoTrack®) and an hsFC assay in parallel. All samples had prior disease-specific clonal sequences characterized by NGS using primers to the *IGHV* FR1/FR2 and VH conserved regions or primers to the *TRG* Vγ and Jγ conserved regions. The LOD/LOQ of the hsFC assay was 0.001% of WBC or 20 events, whichever was greater, in 4×10^6 cells acquired.

Results: The results of the hsFC and NGS assays were concordant in 95.7% (90/94) of samples, including 74 MRD-negative and 16 MRD-positive cases (Table). There were 4 discordant samples from 3 patients with MRD negativity by hsFC but MRD positivity by NGS. This yielded a Cohen's kappa of 0.86 (95% CI: 0.73 to 0.99, *p* < 0.001).

	hsFC MRD−	hsFC MRD+ (<1% abnormal immature B cells)	hsFC MRD+ (1-5% abnormal immature B cells)
NGS−	74	0	0
NGS+	4	12	4

Conclusions: The hsFC and NGS assays performed similarly for B-ALL MRD detection. Both achieved a higher sensitivity (~10^{-5} to 10^{-6}) than standard FC (10^{-4}). Analysis by hsFC offers a shorter turn around time and permits samples without previously characterized clones to be analyzed. However, NGS may be useful in cases that are MRD negative by hsFC. The clinical significance of the discrepancies between the two assays merits further study.

1422 **Erythroid/Megakaryoblastic Leukemia with TP53 and RUNX1 Mutations Frequently Occurs in Blast Transformation of Philadelphia Chromosome-Negative Myeloproliferative Neoplasms: A Single-Institution Experience with 56 Cases**

Ying Liu[1], Douglas Mata[1], Jeeyeon Baik[1], Christopher Famulare[1], Allison Sigler[1], Maria Arcila[1], Yanming Zhang[1], Ahmet Dogan[1], Martin Tallman[1], Ross Levine[1], Kamal Menghrajani[1], Raajit Rampal[1], Mikhail Roshal[1], Wenbin Xiao[1]
[1]Memorial Sloan Kettering Cancer Center, New York, NY

Disclosures: Ying Liu: None; Douglas Mata: None; Jeeyeon Baik: None; Christopher Famulare: None; Allison Sigler: None; Maria Arcila: *Speaker*, Biocartis; *Speaker*, Invivoscribe; Yanming Zhang: None; Ahmet Dogan: *Consultant*, Roche, Corvus Pharmaceuticals, Seattle Genetics, Oncology Specialty Group, Pharmacyclics, Celgene, Novartis, Takeda; *Primary Investigator*, Roche/Genentech; Martin Tallman: None; Martin Tallman: None; Martin Tallman: None; Ross Levine: None; Kamal Menghrajani: None; Raajit Rampal: None; Mikhail Roshal: None; Wenbin Xiao: *Primary Investigator*, Stemline therapeutics

Background: Blast transformation (BT) is a late complication of Philadelphia chromosome-negative (Ph-negative) myeloproliferative neoplasms (MPNs) that is refractory to treatment and confers a dismal prognosis. Most published reports have focused on the clinical features and prognostic factors of MPN-BT. In this report, we examined the immunophenotype and mutational profiles of 56 MPN-BT cases diagnosed at our institution.

Design: All Ph-negative MPNs that had undergone BT at our institution between January 2008 and September 2018 were identified. The H&E morphology, IHC, flow cytometry (FC), and cytogenetic and molecular results of the bone marrow (BM) core biopsies, aspirates, and peripheral blood (PB) smears were reviewed. Cases with available FFPE material were further tested with an IHC panel consisting of CD34, CD117, MPO, CD61, CD71, E-cadherin, spectrin, LMO2, ERG, FLI-1, c-MYC, and P53.

Results: In all, 56 patients with MPN-BT were identified. The median interval between MPN diagnosis and BT was 5 years (range, 0.1-19.5) and the median age at BT was 66 years (range, 49-83). The MPN diagnoses included PV (n=15, 27%), ET (n=15, 27%), PMF (n=9, 16%), and MPN, unclassifiable (n=17, 30%). *JAK2*, *CALR*, and *MPL* mutated and triple-negative cases accounted for 64%, 4%, 5%, and 27% of cases, respectively. BT was diagnosed on either the bone marrow aspirate (n=40, 71%) or by peripheral blood blasts counts (n=16, 29%). Moderate to marked myelofibrosis was present in 75% (42/56) of cases at the time of BT. Necrosis was present in 13% (7/56) of cases. Cytogenetic studies detected complex, simple, and normal karyotypes in 38%, 28%, and 33% of cases, respectively. Essentially all cases exhibited clonal evolution by having acquired other genetic alternations in addition to those in *JAK2*, *CALR*, and *MPL*. The most common were in *TP53* (27%), *RUNX1* (27%), *ASXL1* (25%), and *TET2* (23%). For the 28 cases with available material for further testing, based on morphology, IHC, and FC, 29% (8/28) were classified as acute erythroid/megakaryoblastic leukemia, 7% (2/28) as acute erythroid leukemia (FAB M6), and 21% (6/28) as acute megakaryoblastic leukemia (FAB M7). A slightly higher frequency of *TP53* (50%

[4/8] vs. 15% [3/20], *p* = 0.14) and *RUNX1* (38% [3/8] vs. 30% [6/20], *p* = 1.0) alterations was observed in M6/M7 vs. non-M6/M7 leukemias.

	PV (n=15)	ET (n=15)	PMF (n=9)	MPN-U (n=17)	Total (n=56)
Sex (M/F)	10/5	7/8	8/1	7/10	32/24
Age at BT, years, median (range)	64 (52-79)	67 (56-84)	72 (58-82)	65 (46-80)	66 (49-83)
Time to BT, years, median (range)	9.7 (1-19.5)	8.8 (0.1-12.5)	1.6 (0.3-9.5)	2.9 (0.3-10.3)	5.0 (0.1-19.5)
Overall survival after BT, months, median (range)	16 (6-32)	5.3 (0.5-47)	11 (0-32)	11.7 (1.6-96)	7.6 (0-96)
Blasts >20%, BM/PB, n	10/5	12/3	6/3	12/5	40/16
% BM cellularity, median (range)	85 (25-100)	80 (10-100)	85 (70-100)	93 (20-100)	78 (10-100)
BM reticulin fibrosis					
MF-1, n (%)	3 (20%)	5 (33%)	1 (11%)	5 (30%)	14 (25%)
MF-2, n (%)	5 (33%)	3 (20%)	3 (33%)	6 (35%)	17 (30%)
MF-3, n (%)	7 (47%)	7 (47%)	5 (56%)	6 (35%)	25 (45%)
BM osteosclerosis, n (%)	6 (40%)	8 (53%)	4 (44%)	6 (35%)	24 (43%)
BM necrosis, n (%)	3 (20%)	1 (7%)	2 (22%)	1 (6%)	7 (13%)
FAB classification, n (%)					
Non-M6/7	4 (50%)	8 (80%)	6 (86%)	2 (67%)	20 (71%)
M6	1 (12.5%)	1 (10%)	0 (0%)	0 (0%)	2 (7%)
M7	3 (37.5%)	1 (10%)	1 (14%)	1 (23%)	6 (22%)

Figure 1 - 1422
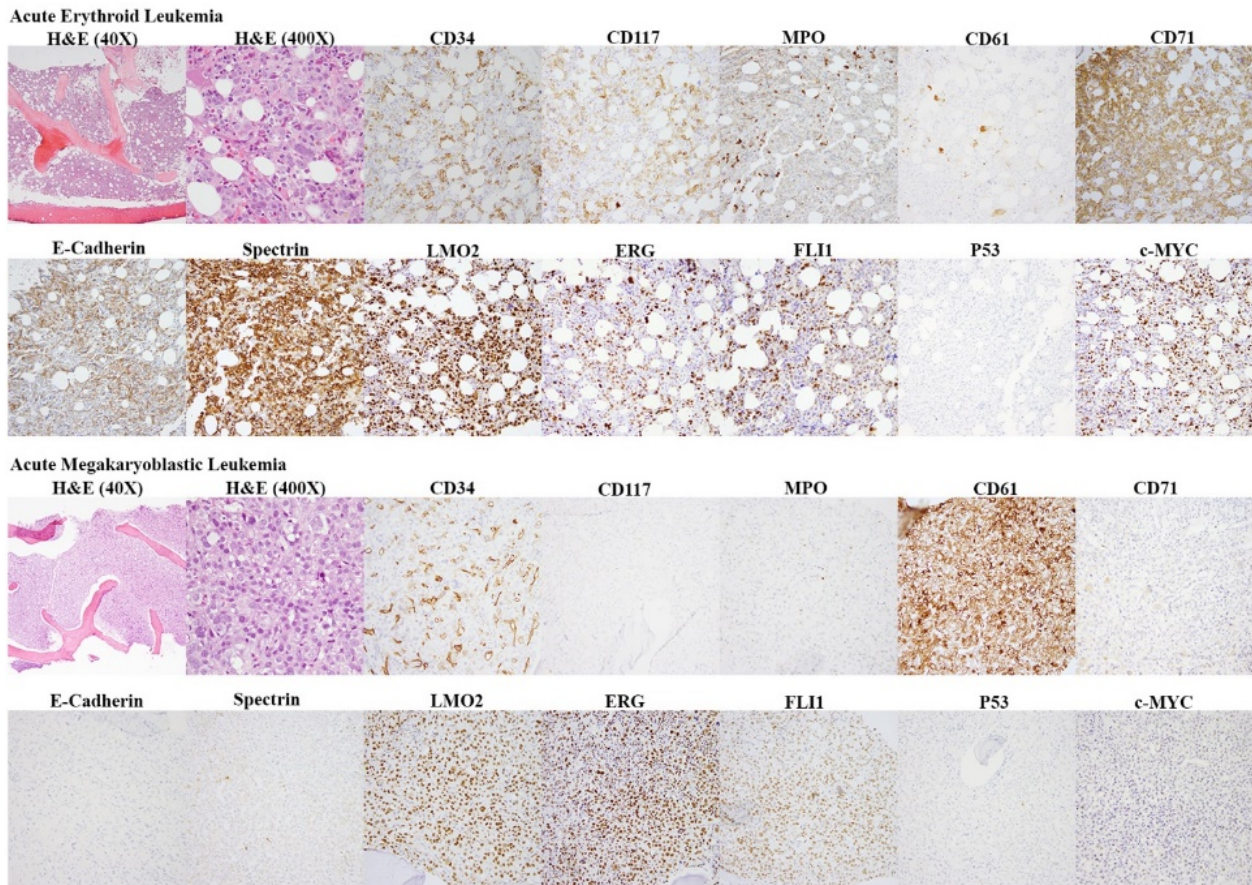
Figure 2 - 1422
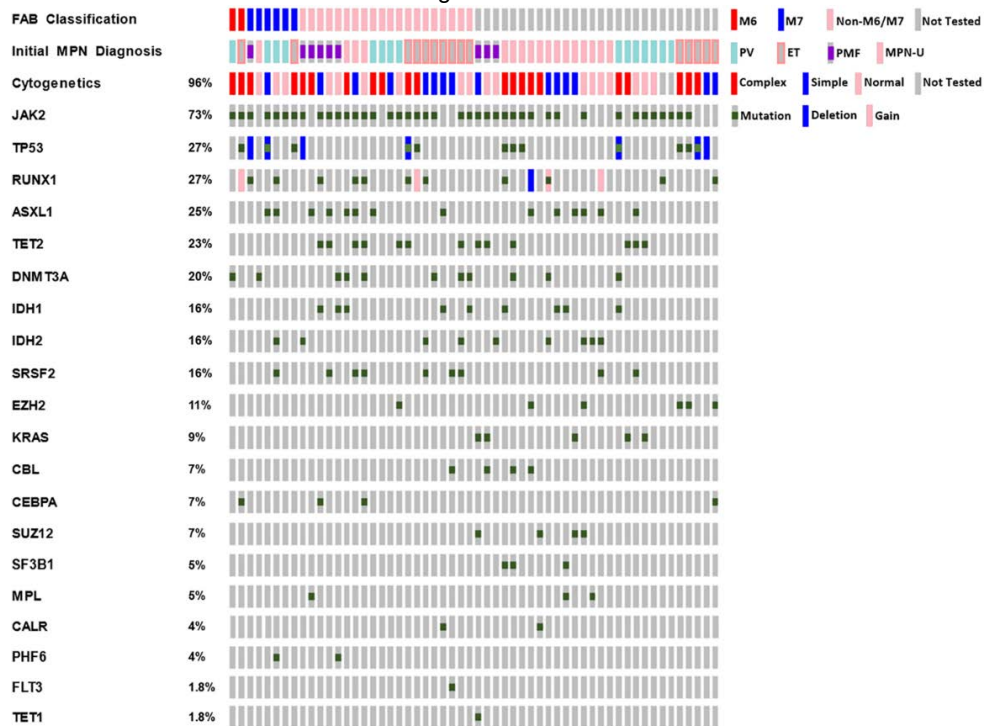
Conclusions: Erythroid/megakaryoblastic leukemia frequently occurs in the setting of MPN-BT and may be associated with an elevated frequency of *TP53* and *RUNX1* mutations.

1423 Frequent TET2 Mutations in Histiocytic Neoplasms

Ying Liu[1], Kseniya Petrova-Drus[1], Benjamin Durham[1], Jeeyeon Baik[1], Allison Sigler[1], Raajit Rampal[1], Omar Abdel-Wahab[1], Eli Diamond[1], Ahmet Dogan[1], Mariko Yabe[1]
[1]Memorial Sloan Kettering Cancer Center, New York, NY

Background: Histiocytic neoplasms are rare and heterogeneous disorders derived from mononuclear phagocytes or histiocytes, accounting for <1% of tumors presenting in the lymph nodes or soft tissue. Among them, Langerhans cell histiocytosis (LCH) and Erdheim-Chester disease (ECD) are known to have recurrent mutations activating MAPK signaling, including *BRAF, NRAS, KRAS, ARAF*, and *MAP2K1*. High prevalence of myeloid neoplasms has been reported in association with ECD and/or LCH (Papo M, et al. Blood 2017; 130(8):1007-13), and bone marrow myeloid stem cells are reported to contain *BRAF* V600E alleles in patients with LCH and ECD (Milne P, et al. Blood 2017; 130(2):167-175). These findings support the hematopoietic stem cells as a cell-of-origin of LCH and ECD. However, whether histiocytic neoplasms harbor genetic alterations commonly seen in myeloid neoplasm such as *TET2* has not been thoroughly studied.

Design: Cases with histiocytic neoplasms diagnosed at our institution by tissue biopsy between April 2017 and September 2018 were reviewed. Genomic analysis was performed by a capture based 400-gene NGS-assay alongside a matched normal sample, RNA sequencing to detect fusion genes (Archer FusionPlex Heme panel,), or DNA coding sequence for 406 genes, noncoding sequence for 31 genes, and RNA coding sequence for 265 genes (FoundationOne-Heme).

Results: 5 patients with histiocytic neoplasms diagnosed with tissue biopsy were found to have myeloid neoplasm-associated genetic alterations (Table 1). Among these, 4 patients (case 1, 2, 3, 5) had *TET2* mutations. Case 2 presented with LCH in lymph node and non-LCH (ECD) in skin, and these two lesions shared the same *TET2* mutations. Case 3 and Case 5 harbored *BRAF* mutation and presented with additional *TET2* and *ASXL* mutations and *TET2* and *CBL* mutations, respectively. The *KIF5B-ALK* fusion, which has been reported in ECD, was detected in Case 4, and additional *DNMT3A* mutation was found in this case. Variant allele frequencies (VAFs) were much higher than those of these genes in the setting of clonal hematopoiesis of indeterminate potential (CHIP), supporting that peripheral blood contamination is unlike cause of these findings (Arends CM, et al. Leukemia 2018; 32 (9): 1908-1919).

Case #	Gender	Age	Specimen	Diagnosis	Immunohistochemistry						Corresponding molecular results (VAF)
					CD14	CD68	CD163	CD1a	S100	Langerin	
1	M	59	Left neck mass	monocytic/histiocytic neoplasm	Pos	Pos	Neg	Neg	Neg	Neg	TET2 p.C1289Y (19.1%), TET2 p.C1221S (11.8%)
2	F	53	Skin, left upper back	non-LCH (ECD)	ND	ND	ND	Neg	Neg	Neg	TET2 p.N1774Qfs*15 (5.7%), TET2 p.N442Kfs*5 (6.5%), TET2 p.R1216G (9.2%)
			Lymph node, axilla	LCH	ND	ND	ND	Pos	Pos	Pos	TET2 p.N1774Qfs*15 (NA), TET2 p.N442Kfs*5 (NA), CTNNB1 p.T41A (NA)
3	M	68	Lung	LCH	Neg	Neg	ND	Pos	Pos	ND	TET2 p.C1133Y (17.4%), ASXL1 p.Q925* (22.5%), BRAF p.V600E (14.8%)
4	F	43	Skin, upper back	non-LCH (ECD)	ND	Pos	Pos	Neg	Neg	Neg	DNMT3A p.R882H (33.9%), KIF5B-ALK fusion
5	F	55	Spleen	LCH	Pos	Pos	Pos	Pos	Pos	Pos	TET2 p.S890* (NA), BRAF V600E (NA), CBL R420Q (NA)
				non-LCH (ECD)	Pos	Pos	Pos	Neg	Neg	Neg	

Figure 1 - 1423

Case 3. 68 year-old man, Lung.
LCH with *BRAF, TET2, ASXL1* mutations

Figure 2 - 1423

Case 5. 55 year-old woman, Spleen.
Mixed LCH/ non-LCH (ECD) with *BRAF, TET2, CBL* mutations
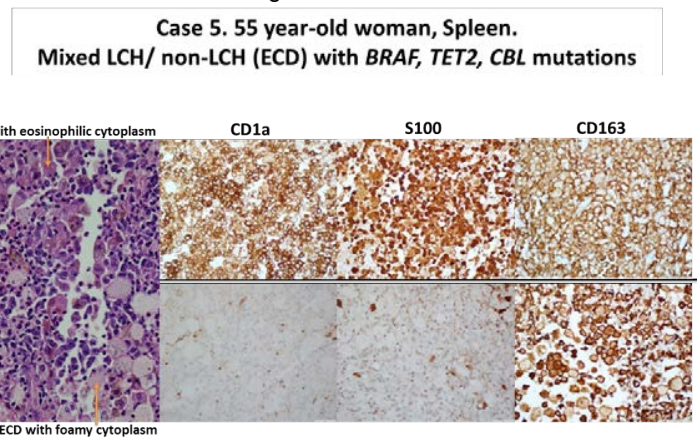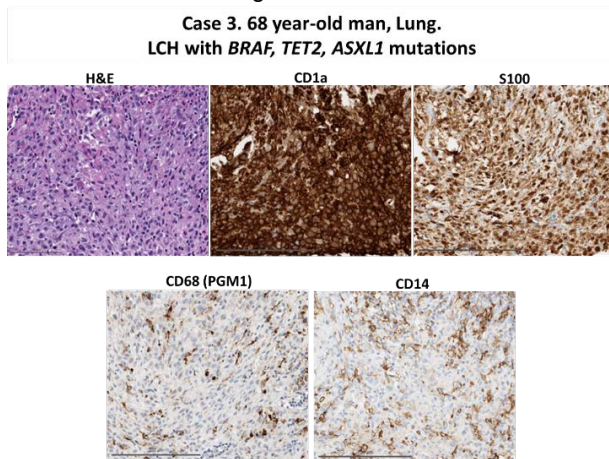
Conclusions: Our study confirmed that myeloid neoplasm-associated genetic alterations, such as *TET2, ASXL1, DNMT3A* are seen in histiocytic neoplasm. These findings give further support for a hematopoietic stem cell as an origin of histiocytic neoplasms.

1424   Improved Blood Staging of Mycosis Fungoides/Sezary Syndrome (MF/SS) via the Use of ICCS Immunophenotyping Method for Aberrant T-cell Quantitation

Kirill Lyapichev[1], Ismael Bah[1], Mark Routbort[1], Jeff Jorgensen[1], Francisco Vega[1], L. Jeffrey Medeiros[1], Sa Wang[1]
[1]The University of Texas MD Anderson Cancer Center, Houston, TX

Disclosures: Kirill Lyapichev: None; Ismael Bah: None; Mark Routbort: None; Jeff Jorgensen: None; Francisco Vega: None; L. Jeffrey Medeiros: None; Sa Wang: None

Background: Blood involvement by MF/SS influences prognosis and therapeutic decisions. EORTC defines blood stages by enumerating absolute CD4+CD26- or CD4+CD7- cells, with <250 cells/μL as stage B0, 250–1000 cells/μL as B1 and ≥1000 cells/μL as B2 . However, it is known that normal CD4+ T-cell subsets include CD26- or CD7- T-cells. ICCS recommends the enumeration of MF/SS cells based on identification of immunophenotypically aberrant CD4+ T-cells. We conducted the study to compare the accuracy of these 2 quantification methods and the downstream clinical impact of favoring one method over the other.

Design: We reviewed MF/SS cases sent for FCI. Blood from 54 normal adult donors were also tested. The FCI panel was composed of 6 Abs (CD45, CD3, CD4, CD8, CD7, CD26). WBC was generated from the same blood draw by an automatic hematology analyzer. T-cell Vβ chain analysis by FCI was performed in + or equivocal cases to confirm clonality. Validated sensitivity amounted to 1% of the lymphocyte gate.

Results: 54 normal donors had a median absolute CD4+CD26- count of 159(46-1121) cells/µL, and CD4+CD7- count of 78(28-761)cells/µL. 7 donors had CD26- or CD7- T-cell counts that would fall in the range of EORTC B1 stage, and 1 in EORTC stage B2. All of these samples were negative for aberrant T-cells by ICCS. A total of 309 MF/SS patients(160 men and 149 women), had blood samples sent for FCI. The median number of CD4+CD26- cells was 170(0-47205)cells/µL, whereas of CD4+CD7- cells was 108(1-46002)cells/µL. Per EORTC, 222(71.8%) patients had B0, 56(18.2%) B1, and 31(10.0%) B2. As per ICCS, 52 patients were found to have blood involvement with a median of 1553(42-46976)cells/µL. Among patients with EORTC B0, 2/222 (0.9%) were found to be + for MF/SS per ICCS, confirmed by Vβ chain analysis. And among 56 EORTC B1 patients, 21 showed no aberrant T-cells per ICCS, yielding a false + rate of 37.5% for EORTC. Regarding EORTC B2 cases, all 31(100%) patients showed immunophenotypic abnormalities, but the median for CD26- or CD7- (3927, 994-47205) cells/µL per EORTC was borderline lower than that detected by ICCS of 4692 (1045-46976) cells/µL(p=0.079).

Conclusions: MF/SS cell quantification based on CD26 or CD7 loss, by EORTC is helpful in defining B0 and B2. However, among B1 stage cases per EORTC, >1/3 were in fact false + cases, shown to be - for MF/SS involvement. These findings explain the inconsistent data observed among EORTC stage B1 patients with regard to prognosis and treatment response.

1425 Clinicopathological and Genetic Characterization of Acute Myeloid Leukemia with t(8;16)(p11;p13)/KAT6A-CREBBP: Single Institution Experience

Malary Mani[1], Prasad Koduru[1], Jeffrey Gagan[2], Franklin Fuda[1], Yuannyu Zhang[1], Giovanni Botten[1], Jian Xu[1], Hung Luu[1], James Malter[2], Weina Chen[1]
[1]University of Texas Southwestern Medical Center, Dallas, TX, [2]University of Texas Southwestern, Dallas, TX

Disclosures: Malary Mani: None; Prasad Koduru: None; Jeffrey Gagan: None; Franklin Fuda: None; Yuannyu Zhang: None; Giovanni Botten: None; Jian Xu: None; Hung Luu: None; James Malter: None; Weina Chen: None

Background: Acute myeloid leukemia (AML) with a t(8;16)(p11;p13)/*KAT6A-CREBBP*, presumably altering histone acetyltransferase activity, is a rare type of AML. While a few studies illustrated the characteristics of clinicopathologic features, molecular studies on the mutational profile are largely absent.

Design: A search of an institutional database identified 8 cases of AML with t(8;16)(p11;p13) between 2000-2019 (< 0.5% of AML): 3 pediatric and 5 adult patients (3 M and 5 F, median age 55 years). Clinical, morphological, immunophenotypic, and cytogenetic studies were assessed in all cases, next generation sequencing (NGS of 1,385 known cancer-related genes or FoundationOne Heme panel) in 4 cases, and RNA-seq in 1 case.

Results: The clinicopathological and genetic features are shown in Table 1. All cases were classified as either acute monoblastic leukemia or acute myelomonocytic leukemia with immunophenotypically aberrant immature monocytes that variably expressed myelomonocytic markers (in 8/8) including downregulation of CD14 (in 6/8), and expressed novel monocytic markers (LILRB1 and LILRB4 in 2/2). Erythophagocytosis by leukemia cells was present in 2/8 (Figure 1). *KAT6A-CREBBP* fusion transcript was detected in 5/5 by NGS or RNA-seq. NGS showed mutations in genes encoding chromatin modifiers (*ASXL1* in 2/4), DNA hydroxymethylation (*TET2* in 1/4), tumor suppressors (*TP53* in 1/4, *EPHA7* in 1/4], spliceosome (*SRSF2* in 1/4), telomeres (*POT1* in 1/4), and activating signaling (*FLT3*-D835 in 2/6). Adult cases were mostly therapy-related AML (t-AML, in 4/5) with a short overall survival (OS) (median survival of 6.4 months), while pediatric cases were *de novo* with variable OS (undefined median survival).

Table 1: Clinical, Immunophenptypic and Genetic Findings of AML with t(8;16)/ *KAT6A-CREBBP*

No	Sex	Age (year)	Diagnosis (FAB/WHO)	History	CD14	Molecular*	F/u months (D or A)
1	F	69	M4/t-AML	breast cancer & lymphoma	-	*ASXL1, TET2* *KAT6A-CREBBP*	4.1 (D)
2	F	67	M5a/t-AML	liver cancer	+	*FLT3* D835 *KAT6A-CREBBP*	0.7 (D)
3	M	70	M5a/t-AML	prostate cancer	pt+	*ASXL1, SRSF2* *KAT6A-CREBBP*	3.0 (A)
4	M	55	M4/AML-MRC	MDS	pt+	ND	21 (D)
5	F	56	M5a/t-AML	breast cancer	pt+	*FLT3* D835	6.4 (D)
6	F	8	M5a/M5a	*de novo*	-	ND	148 (A)

| 7 | F | 7 | M5a/M5a | *de novo* | + | *TP53, POT1, EPHA7,* *KAT6A-CREBBP* | 6.5 (D) |
| 8 | M | 0.3 | M5a/M5a | *de novo* | pt + | *KAT6A-CREBBP* | 13.5 (A) |

Abbreviations: F/u, follow-up; MDS, myelodysplastic syndrome; MRC, myelodysplasia related changes;
D/A, Dead/Alive; ND, not done; pt, partial;
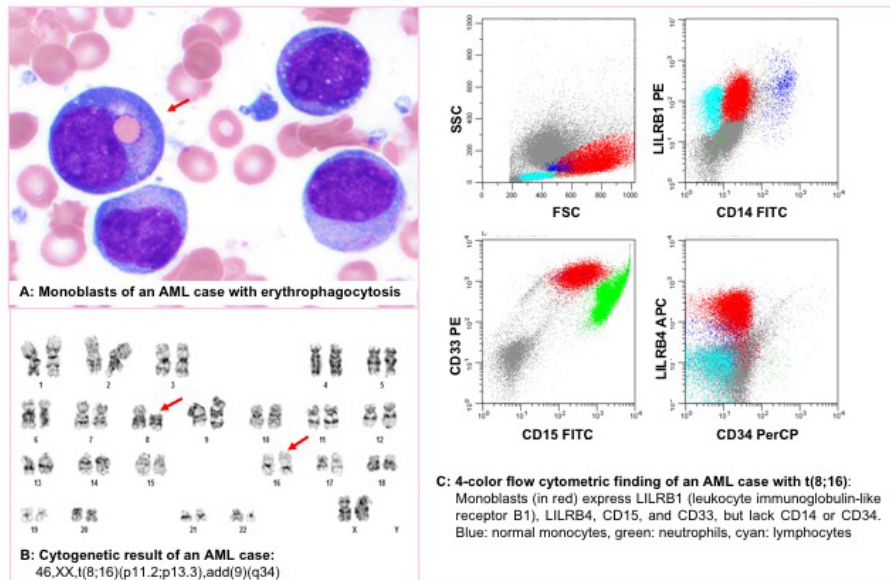*: Cases 2, 4, 5, and 6: no NGS studies

Figure 1 - 1425

A: Monoblasts of an AML case with erythrophagocytosis

B: Cytogenetic result of an AML case:
46,XX,t(8;16)(p11.2;p13.3),add(9)(q34)

C: 4-color flow cytometric finding of an AML case with t(8;16):
Monoblasts (in red) express LILRB1 (leukocyte immunoglobulin-like receptor B1), LILRB4, CD15, and CD33, but lack CD14 or CD34.
Blue: normal monocytes, green: neutrophils, cyan: lymphocytes

Figure 1: AML with t(8;16): monoblasts (A), cytogenetics (B), and immunophenotype of monocytic differentiation (C)

Conclusions: This is the first report comprehensively describing molecular genetic abnormalities in AML with t(8;16)(p11;p13)/*KAT6A-CREBBP* in addition to substantiating the reported clinicopathological features of this rare entity, including monocytic differentiation and poor prognosis in adults. While further studies on a larger cohort are needed, the identified co-operative mutations among the various genes/pathways may provide new insights into leukemogenesis and novel therapeutic targets, such as histone deacetylase and DNA methyltransferase inhibitors.

1426 Increased Incidence of KIT M541L Variant in Pediatric Systemic Mastocytosis

Irina Maric[1], Xiaoping Sun[2], Dean Metcalfe[3], Melody Carter[4]
[1]National Institutes of Health, Bethesda, MD, [2]Bethesda, MD, [3]National Institute of Allergy and Infectious Diseases, Bethesda, MD, [4]LAD/NIAID/NIH, Bethesda, MD

Disclosures: Irina Maric: None; Dean Metcalfe: None

Background: Mastocytosis is a clonal disease characterized by the presence of excessive numbers of mast cells in the skin and internal organs. Mastocytosis may present with varied clinical manifestations depending on the mast cell burden and the extent of tissue involvement. Children are primarily represented on the benign end of the disease spectrum, with disease limited to the skin. However, children may also have systemic mast cell disease, most often associated with the somatic mutations in *KIT D816V*, presenting as early as infancy.

Design: We studied 33 patients with cutaneous and systemic variants of pediatric-onset mastocytosis enrolled into the NIH clinical protocols. Patients underwent bone marrow biopsy for evaluation of systemic disease, mast cell flow cytometric analysis and KIT gene molecular analysis by allele-specific KIT D816V qPCR, by qBiomarker somatic mutation PCR array human KIT pathway (Qiagen) and/or targeted NGS Human Myeloid Neoplasms Panel (Qiagen).

Results: 13 pediatric patients were diagnosed with urticaria pigmentosa (UP), 5 with diffuse cutaneous mastocytosis (DCM) and 15 with indolent systemic mastocytosis (ISM). All patients with ISM carried somatic *KIT D816V* mutation in the peripheral blood and/or bone marrow, while no patients with cutaneous variants of mastocytosis were *KIT D816V* positive in the peripheral blood and/or bone marrow. *KIT D816V* variant allelic frequency (VAF) ranged from 0.03% - 18.7%. In addition, molecular results revealed that 5/15 (33%) of ISM patients also carried *KIT M541L* variant, while none (0/18) of the cutaneous (UP and DCM) mastocytosis patients were positive for *KIT*

M541L. In 4/5 *KIT M541L* positive patients, VAF was 50%, and in one *KIT M541L* positive patient VAF was 100%, consistent with germline variant.

Conclusions: Our data suggest that the single nucleotide polymorphism resulting in the substitution M541L in the transmembrane domain of c-KIT may predispose to the pediatric indolent systemic mastocytosis.

1427 Incidence and Spectrum of CEBPA Mutations in Myeloid Neoplasms

Daniel Martig[1], Rong He[1], Dong Chen[1], Phuong Nguyen[1], Jennifer Oliveira[1], Kaaren Reichard[1], James Hoyer[1], Nikita Mehta[2], David Viswanatha[1]
[1]Mayo Clinic, Rochester, MN, [2]Division of Hematopathology, Mayo Clinic, Rochester, MN

Disclosures: Daniel Martig: None; Rong He: None; Dong Chen: None; Phuong Nguyen: None; Jennifer Oliveira: None; Kaaren Reichard: None; James Hoyer: None; Nikita Mehta: None; David Viswanatha: None

Background: Biallelic *CEBPA* mutations are associated with a favorable prognosis in acute myeloid leukemia (AML). The classic biallelic pattern is comprised of a frameshift or nonsense (FS/NS) variant in the N-terminus (NT, p.1-120), and an in-frame indel (IFindel) or missense (MS) variant in the C-terminus (CT, p.278-358). However, the frequency and spectrum of *CEBPA* mutations have not been thoroughly examined across other myeloid neoplasms (MN). In this study, we investigate the incidence, type, and pattern of *CEBPA* mutations in MN.

Design: Following institutional review board approval, results from a MN-targeted next generation sequencing (NGS) panel were retrospectively reviewed. Patients with *CEBPA* variant(s) were included. Patient demographics, pathology, and pertinent laboratory and clinical findings were collected from medical records. Pathologic diagnoses were classified according to the 2016 WHO criteria.

Results: Of 2174 samples that had NGS performed for diagnosed/suspected MN between 7/2015 and 8/2018, 67 (3%) harbored *CEBPA* genetic variants, including 43 (64%) AML, 17 (25%) non-AML MN [9 myelodysplastic syndromes (MDS), 2 myeloproliferative neoplasms (MPN), 2 MDS/MPN, 1 chronic MN, 1 indolent systemic mastocytosis, 1 chronic eosinophilic leukemia, 1 mixed phenotype acute leukemia-T/myeloid], and 7 (11%) others [1 each of T-lymphoblastic leukemia/lymphoma, aplastic anemia, clonal cytopenia of uncertain significance (CCUS), and 4 without features of MN]. In AML, 12/43 (28%) harbored ≥2 *CEBPA* variants (11 cases with 2 variants and 1 case with 3 variants). Among the 12, 50% exhibited the classical biallelic pattern of NT-FS/NS and CT-MS/IFindel. The other 31 (72%) AMLs showed 1 *CEBPA* variant: 12 (39%) with NT-FS, 10 with CT variants (4 FS, 6 MS), and 9 with middle (M) variants (5 FS/NS, 2 MS, and 2 IFindel). In non-AML MN, none showed the classical biallelic pattern and all had 1 *CEBPA* variant, with 3 in NT (2 FS, 1 MS), 4 in CT (1 NS, 3 MS), and 10 in the middle (5 FS/NS, 4 MS, and 1 IFindel). Similar to the non-AML MN, the "others" group showed absence of biallelic *CEBPA* variants with all having 1 variant (6 MS in NT, CT and M regions and 1 IFindel in the M region).

Conclusions: *CEBPA* genetic variants are rare in MN and predominantly occur in AML. They can occur in a wide spectrum of myeloid disorders with variable patterns. The classical biallelic pattern of NT-FS/NS and CT-MS/IFindel is characteristic of AML and absent in non-AML MN or cases without features of MN.

1428 Mast Cell Sarcoma: Report of 5 Cases with Review of the Literature

Nana Matsumoto[1], Jun Wang[2], Qi Shen[3], Xueyan Chen[4], Young Kim[5], Craig Zuppan[2], Chung-Che (Jeff) Chang[6], Mina Xu[7], Zenggang Pan[8]
[1]Yale New Haven Hospital, New Haven, CT, [2]Loma Linda University Medical Center, Loma Linda, CA, [3]Central Florida Pathology Associates, Winter Park, FL, [4]University of Washington, Seattle, WA, [5]City of Hope National Medical Center, Duarte, CA, [6]Florida Hospital, Orlando, FL, [7]Yale University, New Haven, CT, [8]Yale University School of Medicine, New Haven, CT

Disclosures: Nana Matsumoto: None; Jun Wang: None; Qi Shen: None; Xueyan Chen: None; Young Kim: None; Craig Zuppan: None; Chung-Che (Jeff) Chang: None; Mina Xu: None; Zenggang Pan: None

Background: The diagnosis of mast cell sarcoma (MCS) is challenging due to its extraordinary scarcity and lack of the typical morphology found in systemic mastocytosis. Therefore, MCS is likely underdiagnosed. We undertook this study to better clarify the clinicopathologic and molecular features of MCS.

Design: Five cases of MCS were collected from multiple institutions. The clinical, radiologic, morphologic, and immunophenotypic features were assessed. *CKIT* D816V mutations were tested by allele-specific PCR assays. In addition, next generation sequencing (NGS) analyses with a 200-gene panel were carried out in 2 cases and will be performed in 2 more cases. Additional 22 cases were retrieved from the English literature for review.

Results: Our 5 patients included 2 males and 3 females with a median age of 53 years (Table 1). Four patients had bone involvement initially. Serum tryptase levels were elevated in 4/4 patients (up to 1,034 ng/ml). In 3 cases, the tumor cells were mostly medium-sized with

mild to moderate pleomorphism, whereas the remaining 2 cases contained highly pleomorphic cells with frequent bizarre nuclei. Moreover, significant heterogeneity was noted in one case (Figs 1A to 1C). The tumor cells expressed CD43 (5/5), CD117 (5/5), mast cell tryptase (MCT; 5/5), and CD25 (4/4) (Table 1; Figs 2A-2C). *CKIT* D816V mutation was not detected (0/5). NGS detected the following somatic mutations; case #1 *RB1* R73fs, *TP53* H179R, and *NF1* R1337W; case #2 *TP53* L330R, *MLH1* L259S, and *NOTCH1* D1185N.

Review of the 27 cases (Table 1), including our 5 cases, showed that MCS nearly equally affected the male and female with a median age of 40.5 years. Most cases involved the bone (16/27, 60%) and bone marrow (11/19, 58%). Serum tryptase was elevated in 86% (12/14) of patients. The prognosis was poor with a median survival of 12 months. In most (17/23, 74%) cases, MCS displayed a highly pleomorphic cytology. The positive immunostains included CD43 (100%), CD117 (96%) and MCT (96%), with variable expressions of CD2 (31%) and CD25 (75%). Only 14% (3/22) of cases had *CKIT* D815V mutations.

	Our Study (n=5)	Literature (n=22)	Combined (n=27)
Age (years)	Median 53 (range 1-59)	Median 39 (range 4-77)	Median 40.5 (range 1-77)
Gender	2M, 3F	11M, 11F	13M, 14F
Locations*	Bone 4, soft tissue 3, brain 1, lung 1	Bone 12, GI 5, soft tissue 4, lymph node 3, brain 2, lung 1, skin 2, larynx 1, kidneys 1, heart 1, testis 1, uterus 1, ear 1, spleen 1, lip 1, liver 1	Bone 16, GI 5, soft tissue 7, lymph node 3, brain 3, lung 2, skin 2, larynx 1, kidneys 1, heart 1, testis 1, uterus 1, ear 1, spleen 1, lip 1, liver 1
Bone Marrow Involvement	1 of 5	10 of 14	11 of 19
Serum Tryptase (ng/mL)	Median 31 (range 13-1034; n=4)	Median 172 (range <1 to 386; n=10)	Median 212 (range <1 to 1034; n=14)
Median Overall Survival (months)	Median 4 (range 3-35; n=3)	Median 12.5 (range 1.3-48; n=20)	Median 12 (range 1.3-48; n=23)
Cytology (mild-moderate /marked pleomorphism)	3/2	3/15	6/17
CD2	0/4 (0%)	5/12 (42%)	5/16 (31%)
CD25	4/4 (100%)	8/12 (67%)	12/16 (75%)
CD43	5/5 (100%)	6/6 (100%)	11/11 (100%)
CD68	3/4 (75%)	13/13 (100%)	16/17 (94%)
CD117	5/5 (100%)	19/20 (95%)	24/25 (96%)
Mast Cell Tryptase	5/5 (100%)	20/21 (95%)	25/26 (96%)
CKIT D816V Mutation	0/5 (0%)	3/17 (18%)	3/22 (14%)

* Some patients had tumor involvement of multiple locations.

Figure 1 - 1428
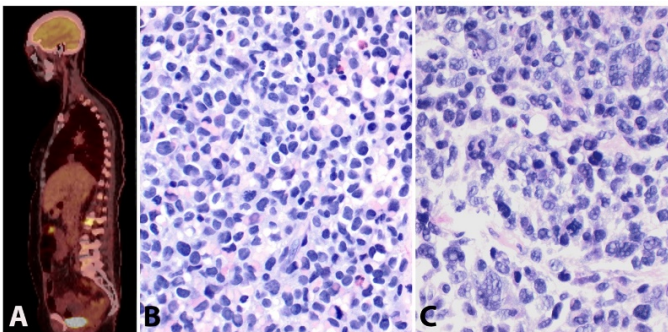
Figure 1. A 56-year-old female had a L2 vetebral lesion (**A**) and an elevated serum tryptase level at 1,034 ng/ml. Biopsies from the same lesion showed heterogenous morphologic features with medium-sized cells (**B**, 400x) and highly pleomorphic sacomatous cells (**C**, 400x).

Figure 2 - 1428
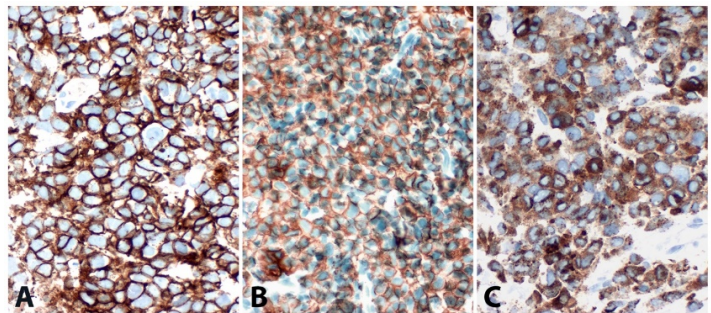
Figure 2. The tumor cells in mast cell sarcoma were positive for CD43 (**A**), CD117 (**B**), and mast cell tryptase (**C**).

Conclusions: After excluding the common hematologic and non-hematologic neoplasms during initial workup for a high-grade sarcoma, mast cell sarcoma may be considered in the differential diagnosis, particularly in the case with bone involvement and expression of CD43 and CD117. Further immunostains (MCT, CD2, and CD25) and serum tryptase levels are useful in establishing the diagnosis.

1429 Detection of MYC Rearrangement is Useful in Distinguishing Plasmablastic Lymphoma from Plasmablastic Variant of Plasma Cell Myeloma

Nathan McCammon[1], Prasad Koduru[2], Aliyah Sohani[3], Weina Chen[2], Mingyi Chen[2], Flavia Rosado[2]
[1]University of Texas Southwestern Medical Center, Norman, OK, [2]University of Texas Southwestern Medical Center, Dallas, TX, [3]Massachusetts General Hospital, Boston, MA

Disclosures: Nathan McCammon: None; Prasad Koduru: None; Aliyah Sohani: None; Weina Chen: None; Mingyi Chen: None; Flavia Rosado: None

Background: Plasmablastic lymphoma (PBL) is a rare type of large B-cell lymphoma seen in immunosuppressed patients and characterized by sheets of plasmablasts. Plasmablastic myeloma (PBM) is a variant of plasma cell myeloma (PCM) morphologically and immunophenotypically indistinguishable from PBL. Previous studies have shown that while *MYC* rearrangements are frequent in PBL and less common in PCM overall, they may be more prevalent in PCM with plasmablastic morphology. We assessed the diagnostic utility of *MYC* rearrangement detected by fluorescence in situ hybridization (FISH) in differentiating PBL from PBM.

Design: We conducted a retrospective search for tissue and bone marrow reports containing the word "plasmablastic" in 2 large academic institutions. Only well-characterized cases of PBL and PBM with at least 50% plasmablasts, as defined by nuclear size and nucleolar prominence, and sufficient medical records and/or paraffin tissue blocks were included. In the PBM group, only clots sections containing at least 90% tumor cells were sent for FISH. Cases of PBL known to be EBV-negative or HHV8+ and cases without suitable material for FISH were excluded.

Results: Of 14 PBL cases, 11 were HIV+, and 12 were male (median age 52, range 24-74). There were 10 extranodal masses, 2 lymph nodes, and 2 fluids (confirmed HHV8-negative). All PBL were EBV+ by EBER ISH. The 12 PBM included 5 males (median age 65, range 29-71). Abnormal cytogenetics were detected in 10; all showed findings typical of PCM. 12/14 PBL (86%) and 0/12 (0%) PBM showed a *MYC* rearrangement (P<0.0001). 4 PBM showed extra copies of *MYC*.

Conclusions: These findings support the diagnostic utility of *MYC* FISH in differentiating PBL from PBM, although larger studies are needed for confirmation.

1430 Accurate Mitotic Counts in Mantle Cell Lymphoma Using Phosphohistone H3 (PHH3) Immunohistochemistry

Hanine Medani[1], Mohamed Elshiekh[1], Kikkeri Naresh[2]
[1]Imperial College London, London, United Kingdom, [2]Department of Cellular pathology, Imperial College London, London, United Kingdom

Disclosures: Hanine Medani: None; Mohamed Elshiekh: None; Kikkeri Naresh: None

Background: Mantle cell lymphoma (MCL) patients have a heterogeneous clinical course ranging from indolent to an aggressive rapidly progressive disease. Proliferation is an important predictor for poor prognosis, contributing to the Mantle cell international prognostic index score (MIPI). High proliferation would necessitate aggressive and tailored therapy. Contrary to solid tumours, accurate manual counts in small cell lymphomas are difficult due to the small cellular size making it prone to a high degree of inter-observer variability. Furthermore, cases with a high mitotic count were often documented as >20/10-HPF or >30/10-HPF and not as precise counts. Immunohistochemical staining of Phospho-histone H3 (PHH3) has emerged as a more accurate mitosis marker and is exclusively expressed on condensing chromatin of mitotic nuclei. The aim of the study is to compare manual counts of PHH3 stained mitotic cells with reported manual counts from H&E sections and Ki-67 proliferation indices (Ki-67%).

Design: 24 MCL cases were identified (2018-2019). The morphological patterns included nodular (9), mantle zone (3,) diffuse (6), blastoid (5) and pleomorphic (2) morphologies. With approval from the institution's tissue bank, slides were stained with Phosphohistone H3 rabbit polyclonal primary antibody. Dark and coarsely clumped staining of cells was considered as mitosis, which included cells in prophase and metaphase stages (PHH3 MC) and separating daughter cells (PHH3 A-T). Speckled and intranuclear staining was considered as late G2 phase (PHH3 G2) of the cell cycle and not mitosis. PHH3 stained cell counts per 10 high power fields, reported H&E mitotic counts and Ki-67 proliferation indices were compiled. Whole slide images will be captured for automated digital counts and compared with the manual scoring, exploring the ease, accuracy and rapidity of using automated digital analysis.

Results: 24 cases was analysed using PRISM 5.01. PHH3 MC was consistently higher than HE MC with a mean of 614.2 compared with 85.7. There was a strong linear relationship between Ki-67% and PHH3 MC (r^2= 0.7731, P< 0.0001). PHH3 MC showed a strong correlation with Ki-67% (r= 0.879, P<0.0001) compared with HE MC (r= 0.4375, P= 0.0325). A linear relationship was identified between the PHH3 MC and PHH3 G2 nuclei (r^2= 0.5633, P< 0.0001). No relationship was found between PHH3 A-T and HE MC.

Pattern of Mantle cell lymphoma	Number of cases	Mean HE mitotic count/10HPF	Mean PHH3 mitotic count/10HPF

|	(N= 24)		
Blastoid	5	33	138.8
Pleomorphic	2	42	225
Diffuse	6	5.5	99
Mantle	2	2.5	75.5
Nodular	9	5.7	75.7
Low grade (nodular, mantle, and diffuse)	17	5.3	83.9
High grade (blastoid and pleomorphic)	7	36	167.5

Figure 1 - 1430

Figure 1a. Mantle cell lymphoma with PHH3 stain. The dark, clumped staining shows mitoses (long arrow) and the speckled pattern indicates G2 phase (short arrow).

Figure 1b. Mantle cell lymphoma with PHH3 stain on a mitotic figure in anaphase (long arrow) and speckled pattern showing G2 phase (short arrow).

Figure 1c: Ki-67 % compared with PHH3 MC/10HPF and HE MC/10HPF

Figure 1d : Ki-67 % compared with PHH3 MC/10HPF and G2 MC/10HPF

Figure 2 - 1430

Conclusions: The study proposes PHH3 MC to be a valuable and a more specific reproducible method to quantify mitoses in mantle cell lymphoma.

1431 Bone Marrow Trephine Biopsy in Patients of Primary Immune Thrombocytopenia on Treatment with Thrombopoietin Receptor Agonists

Hanine Medani[1], Anwar Sayed[1], Nichola Cooper[2], Kikkeri Naresh[3]
[1]Imperial College London, London, United Kingdom, [2]Clinical Haematology Department, Imperial College Healthcare London, London, United Kingdom, [3]Department of Cellular Pathology, Imperial College London, London, United Kingdom

Background: Thrombopoietin is a cytokine which acts as the main regulator of megakaryopoiesis differentiation and platelet production. It does so by binding to the receptor c-MPL which triggers downstream pathways involving *JAK-2*, *IP3* and *RAS*. This results in megakaryocyte differentiation and maturation and platelet production. In addition, c-MPL receptor is also found on haemopoietic stem cells. Thrombopoietin receptor agonists (TPO-A) have been extensively tested and found to provide elevation of platelet counts in patients with primary immune thrombocytopaenia (PIM). Treatment with TPO-A has been associated with a mild increase in reticulin fibres. Previous studies have shown that PIM patients treated with TPO-A show changes in the bone marrow trephine biopsies (BMTB) similar to myeloproliferative disorders but with no subsequent transformation to clonal myeloproliferative disease.

Design: We studied 20 BMTB samples from 12 patients during January 2006 and May 2019 for primary PIM treated with TPO-A eltrombopag and/or romiplostin. Five of 12 patients had pre- and post-treatment biopsies, and the rest had one or more post-treatment samples. Nine patients had only one drug and 3 had both drugs. Information from histology reports about megakaryocyte morphology, cellularity and clustering; any changes in erythroid and myeloid lineages; and bone marrow reticulin was noted. Corresponding and subsequent platelet counts were also recorded. Molecular and cytogenetic results were reviewed to exclude secondary thrombocytopenia from MDS, myeloproliferative diseases or aplastic anaemia.

- 5 of 12 patients were <12 years old.
- Eight of 12 patients showed megakaryocyte enlargement and hyper-lobation.
- In the one-drug subgroup; 4 BMTB (44%) had enlarged and hyper-lobated megakaryocytes and 5 (56%) had either small and/or hypo-lobated megakaryocytes.
- In the two-drug subgroup, all 4 (100%) had enlarged and hyper-lobated megakaryocytes.
- One of the post-treatment samples showed dyserythropoiesis, and post-treatment samples in 7 patients show shift to left in the myeloid lineage cells.
- In 4 patients, post-treatment samples showed increased marrow reticulin (grades 1 or 2).

Figure 1 - 1431
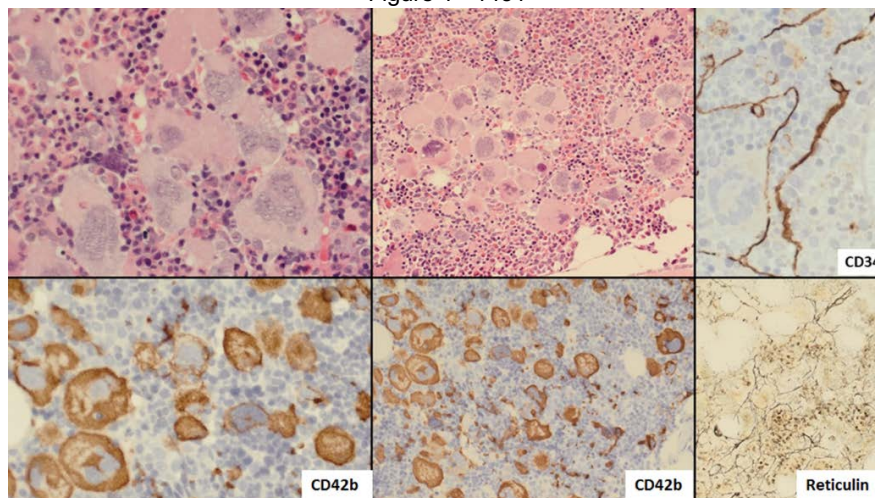
Conclusions: The study showed morphological changes of BMTB in patients with PIM. Megakaryocyte changes consisted of increase in megakaryocyte number, size and hyperlobation mimicking those seen in a myeloproliferative neoplasm.

1432 Targeting Bcl-XL in Anaplastic Large Cell Lymphoma Using the Synthetic Proteolytic DT2216

Edward Medina[1], Daohong Zhou[2], Guangrong Zheng[3], Robert Hromas[4], Marsha Kinney[5], Javier Esparza[1]
[1]Division of Hematopathology, Department of Pathology and Laboratory Medicine, University of Texas Health Science Center at San Antonio, San Antonio, TX, [2]Department of Pharmacodynamics, College of Pharmacy, University of Florida, Gainesville, FL, [3]University of Florida, Gainesville, FL, [4]Department of Medicine, University of Texas Health Science Center at San Antonio, San Antonio, TX, [5]The University of Texas Health Science Center at San Antonio, San Antonio, TX

Disclosures: Edward Medina: None; Daohong Zhou: *Stock Ownership*, Dialectic Therapeutic; Guangrong Zheng: *Stock Ownership*, Dialectic Therapeutics, Inc; Robert Hromas: *Advisory Board Member*, Dialectic Therapeutics; Marsha Kinney: None; Javier Esparza: None

Background: Systemic anaplastic large cell lymphoma (ALCL) is an aggressive CD30+ T-cell lymphoma with two subtypes: anaplastic lymphoma kinase-positive (ALK+), which is associated with the *NPM-ALK* t(2;5) translocation, and ALK-negative (ALK-). While ALK+ ALCL is treated favorably with anthracycline-based regimens, they are ineffective for many patients with ALK- ALCL which necessitates consolidative autologous stem cell transplantation. Progress in understanding the pathogenesis of ALCL is enabling the development of targeted therapies. Therapeutic ALK inhibition induces long-lasting complete remissions (CRs), although ALK inhibitor resistance inevitably occurs. Drug combination therapy targeting the kinase as well as pathways downstream of NPM-ALK may necessary to achieve durable CRs or cures. There is some evidence that Bcl-XL, a member of the Bcl-2 family of anti-apoptotic proteins (e.g., Bcl-XL, Bcl-2 and Mcl-1), plays a critical role in NPM-ALK-mediated ALCL cell survival.

Design: We evaluated the activity of DT2216, a synthetic proteolytic that targets Bcl-XL for degradation by the ubiquitin-proteasome system, against the ALK+ ALCL cell lines JB6, SU-DHL-1 and Karpas-299.

Results: JB6 robustly expressed Bcl-XL and Mcl-1, and expressed low levels of Bcl-2. SU-DHL-1 and Karpas-299 expressed low levels of Bcl-XL and Mcl-1, and expressed no detectable Bcl-2. DT2216 potently killed JB6 and SU-DHL-1 cells (LD50 of 200 nM for both) while it only mildly affected the survival of Karpas-299 cells. Western analysis showed that DT2216, in all of the cell lines at all concentrations (50-1000nM), induced the complete degradation of Bcl-XL, and decreased PARP expression and increased the levels of cleaved PARP. The agent dose-dependently downregulated the expression of full-length Mcl-1 in JB6 cells and induced the generation of cleaved Mcl-1, and it stimulated a mild increase in Bcl-2. DT2216 dose-dependently increased the expression of Mcl-1 in the Karpas-299 cells, which may have compensated for the loss of Bcl-XL and mediated the dampened anti-lymphoma effect of the agent.

Conclusions: Taken together, our findings demonstrate the potential of targeting Bcl-XL in ALCL using low doses of the Bcl-XL synthetic proteolytic DT2216. We plan to test the agent's effect on the survival of ALK+ ALCL cell lines when combined with an ALK inhibitor, and evaluate its activity against ALK- ALCL cell lines and tumor growth in a xenograft ALCL mouse model.

1433 Safety Measures in Platelet Transfusion in Thrombocytopenic Patients with Hematological Malignancies

Tanushri Mukherjee, Command Hospital, Panchkula, Haryana, India

Disclosures: Tanushri Mukherjee: None

Background: The transfusion of platelets if often an imperative, if not dire requirement, in oncological centers treating patients with hematological malignancies. Thrombocytopenia is a common complication of most chemotherapeutic regimens. Additional causes of significant thrombocytopenia in patients of cancer include myelopthisis (tumor involvement of bone marrow), disseminated intravascular coagulation or thrombotic thrombocytopenic purpura . Lymphoproliferative malignancies may also cause thrombocytopenia by an immune mediated process.

The risk of bleeding in patients with thrombocytopenia is inversely related to the platelet count, and risk of spontaneous bleeding is highest in patients with counts of less than 20 x 10^3 / microL. The American Association of Blood Banking recommends a single apheresis unit of platletes (single donor platelets or SDP) to hospitalized adult patients with a platelet count of 10 × 10^9 cells/micro Lor less. This significantly reduces the risk of spontaneous bleeding. Random donor platelets (RDP) are not recommended due to their low yield, chances of infections and alloimmunisation. Apheresis platelet have become the standard of care in platelet transfusions.

However, the transfusion of apheresis platelets is not without risk. Febrile non hemolytic transfusion reactions (FNHTR) and allergic reactions occur in upto 30% of transfusions.Rare complications include the potentially fatal Transfusion related acute lung injury (TRALI). In ABO incompatible platelet transfusions, acute (AHTR) and delayed (DHTR) transfusion reactions may also occur.

We conducted a retrospective study to determine the rate of transfusion reactions after platelet transfusions in this facility, and whether adherence to stringent transfusion guidelines has any effect on reducing risk of such complications

Design: We defined strict criteria regarding indications of platelet transfusion as follows

1. patients having platelet counts less than 10 x 10^3 / microL, with or without active bleeding

2. patients having platelets counts less than 50 x 10^3 / microL, with active bleeding

Platelet counts were carried out using a Beckman Coulter LH750 5 part cell counter, and verified by manual method (in a Neubauer's chamber). Only patients of diagnosed cancer (including leukemias) and immune thrombocytopenic pupura were included in this study. The two other common patient cohort, traumatic and post partum hemorrhage, were excluded from the study.

A total of 750 platelet transfusions were carried out in the three years. Table 1 shows the indications of platelet counts in these 750 cases

Platelet count < 10 x 10^3/ microL

Results: We then compared the incidence of any one of the aforementioned complications across two groups depending on whether strict criteria of platelet transfusion were adhered to (Table 3).

	Criteria adhered	Criteria not adhered	Total
Complications present	09	30	39
Complications absent	466	245	711
Total	475	275	750

3: Incidence of complications in transfusions depending on whether strict criteria were met. A test of independence (Chi-Square) with alpha 0.05 produced chi-square = 28.70 (p=8.49E-08) which is statistically significant. We then made a similar comparison between transfusions following ABO cross match, and those not following ABO cross match (i.e. done in a dire urgency in severely bleeding patients).

	ABO match done	ABO match not done	Total
TRALI		01	
TACO		02	
FNHTR		30	
DHTR		01	
AHTR		02	
Unclassified		03	
Total		39	

Conclusions: The appropriateness of demand for platelet transfusion should always be audited and be justifiable and the follow up count post transfusion 1 unit is mandatory. The compatibility of the platelet count should also be appropriate as per the guidelines to minimize platelet refractoriness.

1434 Clinicopathologic Analysis of Myeloid Sarcoma with Megakaryocytic Differentiation: Case Series and Review of the Literature

Michiko Nagamine[1], Hiroaki Miyoshi[2], Koichi Ohshima[3]
[1]Kumamoto Red Cross Hospital, Kumamoto, Kumamoto, Japan, [2]Kurume University School of Medicine, Kurume, Japan, [3]Kurume University, Kurume, Japan

Disclosures: Michiko Nagamine: None

Background: Myeloid sarcoma (MS) is defined as a tumor mass consisting of myeloid blasts occurring at an anatomical site other than bone marrow according to WHO Classification of Tumours of Haematopoietic and Lymphoid Tissues, revised fourth edition. It includes both de novo lesions and cases with concurrent leukemia, myeloproliferative neoplasm (MPN), or myelodysplastic syndrome (MDS) as long as the tumor mass effaces the tissue architecture. MS with megakaryocytic differentiation is extremely rare, but case reports have been accumulating over the years.

Design: We searched the authors' consultation file between 2006 and 2016 and identified 11 cases of extramedullary mass-forming malignant tumor composed of immature non-lymphoid hematopoietic cells expressing CD41 with or without bone marrow lesions. Clinical information, including patients' age, sex, medical history, and follow-up data, was obtained from the submitting clinicians or the pathologists. The clinicopathological analysis was performed on these 11 cases. Previous case reports were also reviewed and 17 cases were identified.

Results: The patients consist of 8 males and 3 females, with a male-to-female ratio of 2.7:1. The mean age of the patients at the diagnosis was 45.9 years old, ranging from 2 to 78. Extramedullary mass lesions were solitary in 5 cases (45%) and multiple in 6 cases (55%). Tumor locations were lymph nodes (6 cases), subcutaneous tissue (3 cases), bone (1 case), and intramuscular (1 case). Ten of 11 cases (91%)

presented with past histories of or concurrent bone marrow pathology including leukemia (4 cases), myelofibrosis (3 cases), essential thrombocythemia (2 cases), and MDS (1 case). Only 1 case seemed to be de novo case. In 5 cases, patients had undergone allogenic transplantation (stem cell transplant in 3 cases and bone marrow transplant in 2 cases). Follow-up data were available on 2 cases, and the mean survival after the diagnosis was 10 months. Tumor cells positive for CD41, CD33, CD34, MPO, and CD68 (KP1 or PGM1) were observed in 11 (100%), 4 (36%), 7 (64%), 4 (36%), and 7 (64%) cases, respectively. Cytogenetic analysis was successfully done in 4 cases, which often show complex, but inconsistent abnormalities.

Conclusions: Comparing to MS without megakaryocytic differentiation as described in the WHO Classification, MS with megakaryocytic differentiation tends to present with multiple lesions, is more often associated with MPN, and shows much worse prognosis.

1435 Correlation between p16 Overexpression and Grading in Follicular Lymphoma
Shachar Naor, Tel Aviv Medical Center, Givataim, Israel

Disclosures: Shachar Naor: None

Background: The p16 (INK4A) protein, a product of the CDKN2A gene, is a Tumor suppressor gene that inhibits several Cyclin Dependent Kinases in the cell cycle (e.g. CDK4, CDK6). Overexpression of p16 (by immunohistochemistry or mRNA expression) is seen in several cancer types, especially those associated with Human Papilloma Virus 16, 18 (e.g. Cervical cancer, some types of oral squamous cell carcinoma). In our routine work, we observed a case of head and neck lymphoma that was positive for p16. In order to investigate this further, the immunohistochemical staining pattern of p16 in cases of follicular lymphoma was determined.

Design: Cases of adult follicular lymphoma were culled from our pathology archive (2012-2018). A formalin fixed paraffin embedded tissue microarray was created, and p16 immunohistochemistry staining was performed. We determined p16 overexpression cut off as a positive (>+2 intensity on a scale of 1-3) staining of both the nuclear and the cytoplasmic compartments, in >50% of the cells. The association between p16 overexpression and the grade (grade <3 low, $\geq$3a high), Ki-67 (<60% low, $\geq$60% high), age and sex was analyzed by the Fisher exact's test for categorical variables or the Mann Whitney test for non-categorical variables (SPSS).

Results: Twenty-one cases of Follicular lymphoma were examined. Ten cases were of low grade (grade 1-2) and eleven cases were of high grade (3a or 3b). There were 12 females and 9 males, with an age range of 29-86 (Mean 66). See Table. There was no statistical difference between the two groups by age or sex. As a baseline control we performed p16 staining on 5 reactive tonsillar tissue. No lymphocyte staining was observed, compatible with what is described previously. Overexpression of p16 was seen only in the high grade follicular lymphoma cases (7/11, 67%) and none in the low grade (0/10, 0%) (p= 0.004). Example in Figure 1. There was no statistical significant difference in Ki67, age or sex between the two lymphoma groups.

| Patient	Grade	Age	Sex	p16	Ki67
1	1	60	Female	Negative	Low
2	3a	69	Female	Positive	Low
3	1	69	Female	Negative	Low
4	2	82	Male	Negative	Low
5	1	54	Male	Negative	Low
6	3a	72	Male	Positive	Low
7	3a	72	Female	Positive	High
8	1	62	Female	Negative	Low
9	3b	73	Male	Negative	High
10	1	64	Male	Negative	Low
11	3b	57	Female	Positive	Low
12	3a	46	Female	Positive	Low
13	3b	86	Male	Positive	High
14	1	58	Male	Negative	Low
15	3b	29	Male	Negative	High
16	1	66	Female	Negative	Low
17	3a	76	Female	Negative	Low
18	3a	72	Male	Negative	Low
19	2	71	Female	Negative	Low
20	1	74	Female	Negative	Low
21	3a	63	Female	Positive	High

Figure 1 - 1435
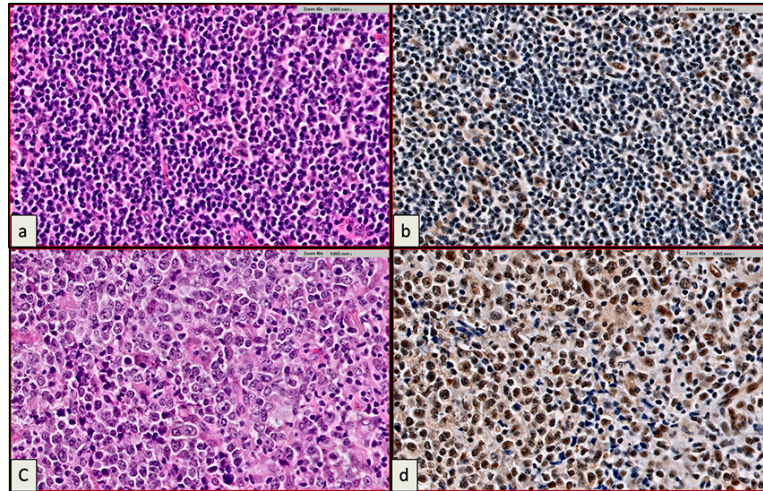
Fig 1:
Grade 1 follicular lymphoma (a. H&E, High power x40 b. p16 immunostaining, High power x40) and Grade 3a follicular lymphoma (c. H&E, High power x40. d. p16 immunostaining, High power x40).

Conclusions: In twenty-one patients with follicular lymphoma we found a statistically significant association between the grade and overexpression of p16, such that only high grade follicular lymphoma showed an overexpression of the protein. These results suggest that p16 immunostaining may aid in the grading of follicular lymphomas.

1436 High Variant Allele Frequency of DNMT3A Mutation is Associated with Granulocytic Dysplasia, High White Blood Cell Count, and Predicts Unfavorable Outcome in De Novo AML

Damodaran Narayanan[1], Olga Pozdnyakova[2], Sanjay Patel[3], Robert Hasserjian[4], Olga Weinberg[5]
[1]University of Wisconsin Hospital and Clinics, Madison, WI, [2]Brigham and Women's Hospital, Boston, MA, [3]Weill Cornell Medical College, New York, NY, [4]Massachusetts General Hospital, Harvard Medical School, Boston, MA, [5]Children's Hospital Boston, Boston, MA

Disclosures: Damodaran Narayanan: None; Olga Pozdnyakova: *Grant or Research Support*, Sysmex Corporation of America; *Consultant*, Promedior; Sanjay Patel: None; Robert Hasserjian: None; Olga Weinberg: None

Background: DNA methyl transferase 3 alpha (*DNMT3A*) is one of the most frequently mutated genes in *de novo* AML, but controversy surrounds its clinical significance. We have recently shown that a high *NPM1* variant allele fraction (VAF) is associated with adverse outcome in AML, especially in patients with *DNMT3A* commutation. Since *DNMT3A* mutation is often age-related, the goal of this study is to evaluate the association of *DNMT3A* VAF on clinical and morphologic parameters and outcome in *de novo* AML.

Design: 168 cases of *de novo* AML cases lacking cytogenetic abnormalities defining AML with myelodysplasia-related changes and recurrent cytogenetic abnormalities were identified from two institutions. All patients were treated with standard induction chemotherapy, with or without subsequent allogeneic stem-cell transplant (SCT). Each case was reviewed in a blinded fashion by three hematopathologists and dysplastic features in each lineage were scored. Event-free survival (EFS) was evaluated by univariate and multivariable analyses.

Results: Among the 68 AML cases with *DNMT3A* mutation with median VAF of 44% (range 2-96%), 55 (81%) had a normal karyotype and co-occurring mutations are listed in Table 1. A high *DNMT3A* VAF (≥44%) correlated with higher WBC count (38 vs 5.3x10^9/L; p=0.0006) and peripheral blasts (27% vs 13%; p=0.03), but not with age, abnormal cytogenetics, hemoglobin level, platelet count or marrow blasts, or co-mutational pattern (Table 1). High *DNMT3A* VAF cases were also associated with greater granulocytic dysplasia (35% vs 18%; p=0.02), including cells with abnormal nuclear shape (p=0.008) and hypogranulation (p=0.02), but with no difference in erythroid or megakaryocytic dysplasia. High *DNMT3A* VAF correlated with shorter EFS (9.7 months vs not reached; p=0.002) (Figure 1); similar findings were seen in subgroups with normal karyotype and with and without *NPM1* mutations (p<0.05). Multivariable analysis identified high *DNMT3A* VAF (hazard ratio (HR)=2.586; p=0.011) and higher peripheral blasts (HR=1.017; p=0.001) as significantly associated with shorter EFS while SCT (HR=0.328; p=0.01) and *NPM1* mutation (HR=0.271; p=0.002) associated with longer EFS.

Table 1. Characteristics of patients with *de novo* AML with mutated *DNMT3A* (N=68)

	Mutated *DNMT3A* (N=68)	*DNMT3A* VAF ≤43 (N=33)	*DNMT3A* VAF ≥44 (N=35)	p-value: *DNMT3A* VAF ≤43 vs *DNMT3A* VAF ≥44
Patient characteristics				
Median age (range), y	61 (23-83)	57 (23-82)	62 (30-83)	>0.05
Male/female ratio	0.8	0.9	0.7	>0.05
Clinical parameters				
Median WBC (range), x 10^9/L	15 (0.6-220)	5.3 (0.96-140)	38 (0.6-220)	0.0006
Median PB blasts (range), %	21 (0-98)	13 (0-87)	27 (0-98)	0.0281
Median BM blasts (range), %	67 (17-96)	60 (17-90)	70 (22-96)	>0.05
Median Hb (range), g/dL	9 (3.7-15)	9 (5.7-12.5)	9 (3.7-15)	>0.05
Median platelets (range), x 10^{12}/L	92 (12-342)	111 (19-342)	66 (12-271)	>0.05
Abnormal cytogenetics, N (%)	13 (19)	5 (15)	8 (23)	>0.05
Morphologic parameters				
Erythroid dysplasia				
Mean dysplasia, %	28	25	33	>0.05
Mean megaloblastic change, score 0-4	0.9	0.9	1.0	>0.05
Mean multinucleation, score 0-4	0.7	0.6	0.8	>0.05
Mean nuclear irregularities, score 0-4	1.5	1.3	1.7	>0.05
Granulocytic dysplasia				
Mean dysplasia, %	27	18	35	0.0177
Mean abnormal nuclear shape, score 0-4	1.0	0.7	1.3	0.0082
Mean hypogranulation, score 0-4	1.2	0.9	1.5	0.0201
Megakaryocytic dysplasia				
Mean dysplasia, %	44	38	49	>0.05
Mean micromegakaryocytes, score 0-4	1.2	1.0	1.4	>0.05
Mean separated nuclear lobes, score 0-4	1.2	1.2	1.2	>0.05
Mean hypolobated nuclei, score 0-4	1.4	1.4	1.4	>0.05
WHO classification, N (%)				
AML, NOS	17 (25)	11 (33)	6 (17)	>0.05
AML-MRC	7 (10)	4 (12)	3 (9)	>0.05
Comutations				
Median number per case (range)	4 (1-7)	4 (1-7)	5 (1-6)	>0.05
Individual comutations, N (%)				
IDH1	17 (25)	5 (15)	12 (34)	>0.05
IDH2	13 (19)	4 (12)	9 (26)	>0.05
TET2	15 (22)	8 (24)	7 (20)	>0.05
ASXL1	8 (12)	4 (12)	4 (11)	>0.05
BCOR	7 (10)	6 (18)	1 (3)	0.0381
RUNX1	8 (12)	3 (9)	5 (14)	>0.05
NPM1	38 (56)	15 (45)	23 (66)	>0.05
NRAS	14 (21)	4 (12)	10 (29)	>0.05
FLT3-TKD	15 (22)	7 (21)	8 (23)	>0.05
FLT3-ITD	20 (29)	12 (36)	8 (23)	>0.05
PTPN11	13 (19)	4 (12)	9 (26)	>0.05

AML, NOS, AML, not otherwise specified; AML-MRC, AML with myelodysplasia-related changes; BM, bone marrow; Hb, hemoglobin; PB, peripheral blood; WBC, white blood cell; WHO, World Health Organization

Figure 1 - 1436

Figure 1. Kaplan-Meier curve showing effect of *DNMT3A* VAF on event-free survival
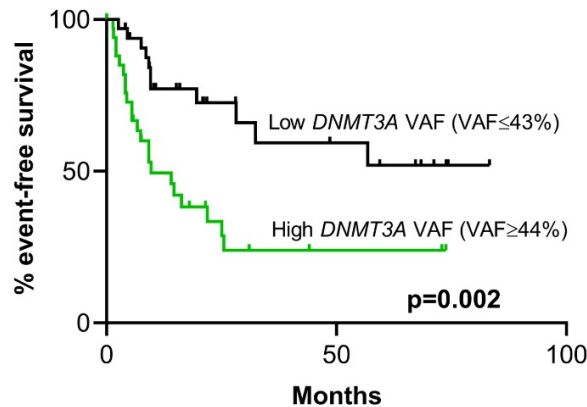
Conclusions: In *de novo* AML, presence of high *DNMT3A* VAF (≥44%) is associated with a more proliferative presentation, granulocytic dysplasia, and unfavorable clinical outcome. Our findings indicate that the prognostic effect of *DNMT3A* mutation in AML may be influenced by the relative abundance of the mutated allele.

1437   Characterization of Plasmacytoid Dendritic Cells, Microbial Sequences, and Identification of a Candidate Public T-cell Clone in Kikuchi-Fujimoto Lymphadenitis

Nya Nelson[1], Wenzhao Meng[2], Aaron Rosenfeld Rosenfeld[1], Susan Bullman[3], Chandra Sekhar Pedamallu[4], Jason Nomburg[5], Gerald Wertheim[6], Michele Paessler[7], Geraldine Pinkus[8], Jason Hornick[9], Matthew Meyerson[10], Eline Luning Prak[2], Vinodh Pillai[11]
[1]Hospital of the University of Pennsylvania, Philadelphia, PA, [2]University of Pennsylvania, Philadelphia, PA, [3]Dana-Farber Cancer Institute, Boston, MA, [4]The Broad Institute, Cambridge, MA, [5]Harvard Medical School, Boston, MA, [6]Children's Hospital of Philadelphia, University of Pennsylvania, Philadelphia, PA, [7]The Children's Hospital of Philadelphia, Newtown, PA, [8]Brigham and Women's Hospital, Boston, MA, [9]Brigham and Women's Hospital, Harvard Medical School, Boston, MA, [10]Boston, MA, [11]The Children's Hospital of Philadelphia, Penn Valley, PA

Disclosures: Nya Nelson: None; Chandra Sekhar Pedamallu: None; Jason Nomburg: None; Gerald Wertheim: None; Michele Paessler: None; Geraldine Pinkus: None; Jason Hornick: *Consultant*, Eli Lilly; *Consultant*, Epizyme; Eline Luning Prak: None; Vinodh Pillai: None

Background: Kikuchi-Fujimoto disease (KFD) is a histiocytic necrotizing lymphadenitis of unclear etiology that occurs in adolescents and young adults. Infectious and autoimmune etiologies have been proposed but no definitive link has been established. Features of KFD overlap with infectious and autoimmune disorders and the distinction can be difficult on histology alone. CD123-positive clusters of plasmacytoid dendritic cells are increased in KFD but can also be seen in many reactive lymphadenitides. The etiology of KFD remains unclear, and genetic, viral, and autoimmune etiologies have been proposed.

Design: KFD cases and controls (reactive lymphadenitis with necrosis) were identified. Clinical notes, laboratory studies, hematoxylin and eosin stained slides, and immunohistochemical stains (IHC) were reviewed to confirm the diagnosis. CD123 antibody was used to stain FFPE tissue slides and staining was quantified using Aperio Image Scope. Next generation sequencing (NGS) and detailed analysis of the B and T cell immune repertoire was performed, and RNAseq was used for microbial detection.

Results: Lymph nodes (LN) with >0.85% CD123+ cells by IHC had the highest likelihood of having a diagnosis of KFD (OR 6.0, sensitivity 75%, specificity 87.5%). NGS and detailed analysis of the B and T cell immune repertoire of nine KFD LN and six reactive LN was performed. Profiling analysis revealed a candidate public T cell clone with a shared CDR3 sequence, CASRGEDSVMETQYF, as well as shared use of the same Vβ family (Vβ6). No epitope matches to this CDR3 sequence or similar Vβ rearrangements were found in public immune repertoire databases. RNAseq based comparative microbial analysis of 5 KFD and 4 control samples did not detect novel or known pathogen sequences unique to KFD.

Conclusions: We utilized digital imaging for an unbiased analysis of CD123 expression in KFD and controls, which revealed an overall increase in total percentage of CD123+ cells in KFD. The presence of an unusual clone in multiple KFD subjects, but not control subjects, suggests that a shared but thus far undefined antigen or set of antigens is associated with KFD. The undefined target antigen could be of self or viral origin given the T cell predominance of immune response in KFD. Our analysis of KFD cases failed to reveal any definitive association of KFD with known or novel pathogens.

1438 Validation of the Double-Hit Gene Expression Signature (DLBCL90) in an Independent Cohort Diffuse Large B-cell Lymphoma of Germinal Center B-cell Origin

Ha Nguyen[1], Minlin Xu[2], Anamarija Perry[3], Pamela Skrabek[4], Michel Nasr[5], Victoria Bedell[6], Joyce Murata-Collins[7], Alex Herrera[7], Wing Chung Chan[8], Dennis Weisenburger[6], David Scott[9], Joo Song[10]
[1]City of Hope National Medical Center, Glendale, CA, [2]LLUMC, Loma Linda, CA, [3]University of Michigan, Ann Arbor, MI, [4]CancerCare Manitoba, Winnipeg, MB, [5]SUNY Upstate Medical University, Syracuse, NY, [6]City of Hope National Medical Center, Duarte, CA, [7]City of Hope, Duarte, CA, [8]City of Hope National Medical Center, Pasadena, CA, [9]BC Cancer Agency and University of British Columbia, Vancouver, BC, [10]City of Hope Medical Center, Duarte, CA

Disclosures: Ha Nguyen: None; Anamarija Perry: None; Pamela Skrabek: None; Michel Nasr: None; Victoria Bedell: None; Joyce Murata-Collins: None; Alex Herrera: *Grant or Research Support*, Bristol-Myers Squibb, Genentech, Immune Design, AstraZeneca, Merck, Seattle Genetics and Kite Pharma, Gilead Sciences; *Consultant*, Bristol-Myers Squibb, Genentech, Merck, Adaptive Biotechnologies Kite Pharma and Gilead; Wing Chung Chan: None; Dennis Weisenburger: None; David Scott: *Grant or Research Support*, NanoString Technologies; Joo Song: None

Background: Diffuse large B-cell lymphoma (DLBCL) is a biologically heterogeneous disease that is characterized by recurrent translocations and somatic mutations. Prognosis has been associated with clinical parameters, cell-of-origin, and genetic aberrations. Recently, Ennishi et al developed a gene expression assay (DLBCL90) to identify cases with outcome similar to high-grade B-cell lymphoma with concurrent *MYC* and *BCL2* translocation (double-hit lymphoma) or *MYC*, *BCL2*, and *BCL6* translocations (triple-hit lymphoma). The aim of this study was to validate the predictive power of the DLBCL90 assay in an independent cohort of germinal center B-cell (GCB) DLBCL.

Design: We identified 253 patients with a diagnosis of *de novo* DLBCL between 2000-2016 at two cancer centers who were treated with R-CHOP therapy. RNA was extracted from the formalin-fixed paraffin-embedded tissue (FFPET). Immunostaining (Hans algorithm, MYC, BCL2), FISH analysis (*MYC*, *BCL2*, and *BCL6*), and a NanoString-based gene expression assay (DLBCL90) were performed to determine the cell-of-origin and "double-hit signature" status (DHITsig-pos, DHITsig-neg, and an indeterminate group DHITsig-ind). Only 81 cases had adequate RNA for Nanostring and determined to have a GCB phenotype (GCB DLBCL). Overall survival (OS) was estimated using Kaplan-Meier method. Receiver operating characteristics (ROC) curve were determined using the FISH results and the DHITsig scores.

Results: Of the 81 cases of GCB DLBCL, there were 4 cases of double-hit lymphoma with translocations of *MYC* and *BCL2*, 2 cases of double-hit with *MYC* and *BCL6*, and 5 triple-hit lymphomas (*MYC*, *BCL2*, and *BCL6*). The DLBCL90 identified 15 cases that were DHITsig-pos, 7 cases of DHITsig-ind, and 59 cases of DHITsig-neg. The *MYC/BCL6* double-hit lymphomas were negative for the DHITsig, whereas the assay was positive in 8/9 *MYC/BCL2* and triple-hit lymphomas. There were 7 cases that were DHITsig-pos that lacked a genetic double- or triple-hit (3 of the cases had *MYC* rearrangement). The ROC curve had an area under the curve of 0.901 (95% CI: 0.76-1.00). The 5-year OS for the DHITsig-neg patients was 84% versus only 53% for the DHITsig-pos patients (p=0.0221).

Figure 1 - 1438
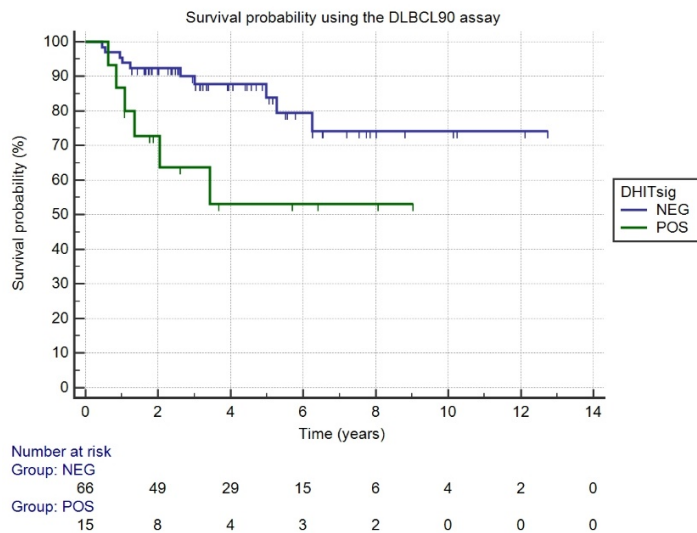
Conclusions: We have validated the DLBCL90 assay in an independent cohort of GCB DLBCL, confirmed the results described by Ennishi et al. This assay identifies the double- and triple-hit lymphomas as well as a poor prognostic group with the gene expression signature that would have been missed by conventional FISH analysis.

1439 Morphologic Changes Associated with BTK Inhibitor Treatment Failure in CLL

Mushal Noor[1], Joel Kruger[1], Philip Meacham[1], Clive Zent[1], Andrew Evans[1]
[1]University of Rochester Medical Center, Rochester, NY

Disclosures: Mushal Noor: None; Joel Kruger: None; Philip Meacham: None; Clive Zent: *Grant or Research Support*, Acerta/AstraZeneca; Andrew Evans: None

Background: Chronic lymphocytic leukemia/small lymphocytic lymphoma (CLL/SLL) may exhibit morphologically aggressive features that fall short of Richter transformation (RT). Cases of "accelerated" CLL (aCLL) exhibit increased prolymphocytes, enlarged proliferation centers, and elevated Ki67, and are associated with inferior clinical outcome. Targeted treatment of CLL with Bruton's tyrosine kinase inhibitors (BTKi) also causes dramatic morphologic changes, at least transiently, but these may be seen in patients even with good clinical response. We sought to determine if treatment failure (TF) to BTKi therapy is associated with prolymphocytic changes or otherwise aggressive morphologic features in CLL.

Design: All CLL patients treated with BTKi from our cancer research database were identified. Patients with treatment failure (TF) were selected based on following criteria 1) disease progression warranting BTKi discontinuation, 2) Richter transformation to large/aggressive B cell lymphoma, or 3) death. Available diagnostic CLL/SLL specimens corresponding to time of treatment initiation and/or TF for each patient were re-reviewed by 2 pathologists and scored for morphologic features of aCLL. Morphologic and molecular findings (*BTK* and phospholipase C gamma2 (*PLCg2*) resistance mutations) were correlated with demographic, clinical, treatment, and outcome data.

Results: We identified 221 BTKi treated CLL patients, with TF occurring in 16 patients (7.2%) after median follow-up of 2.3 years (range 0-8). Three (3) cases were excluded from further morphologic analysis due to overt RT. Among remaining cases, aggressive morphologic features were common, with positive findings in 7/13 patients (54%) overall, including 2 patients biopsies demonstrating aggressive features even prior to treatment initiation. Common histologic findings included: increased number of large cells/prolymphocytes in 7/13 (54%; Fig A), diffusely expanded and/or coalescent proliferation centers in 3/11 (27%; Fig B and C), and Ki67 index ≥40 % in 2 of 13 cases (15%, Fig D). In total, 3/12 patients tested positive for BTKi resistance mutations after TF (all C481S mutation in *BTK,* including one case of RT).

Figure 1 - 1439
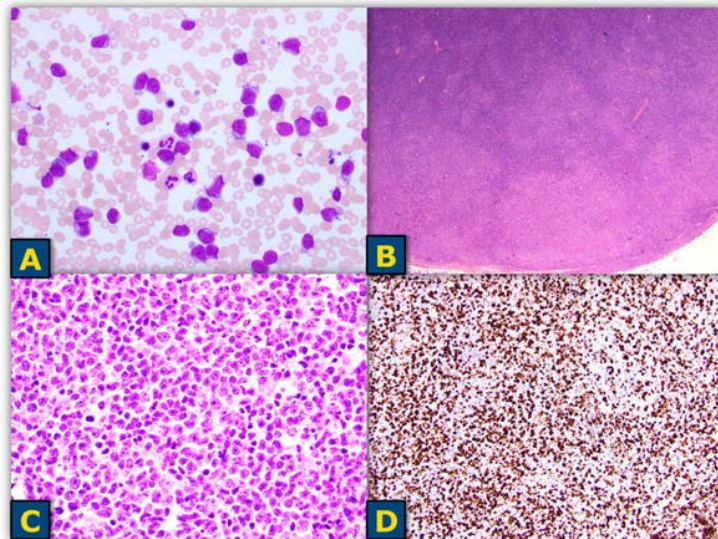
Conclusions: CLL patients with treatment failure on BTKi therapy frequently demonstrate histologically aggressive features, including prolymphocytic changes and aCLL. How these changes should be classified in the setting of BTKi therapy warrants further investigation to better inform prognosis and clinical management decisions.

1440 LEF-1 Negativity in Atypical Chronic Lymphocytic Leukemia a Potential Diagnostic Pitfall

Fernando Alekos Ocampo Gonzalez[1], Nicholas Ward[1]
[1]Rush University Medical Center, Chicago, IL

Disclosures: Fernando Alekos Ocampo Gonzalez: None; Nicholas Ward: None

Background: The term "atypical chronic lymphocytic leukemia" (atypical-CLL) has been used colloquially for cases that exhibit some, but not all features of classic chronic lymphocytic leukemia, which includes differences in cytologic and immunophenotypic features. Atypical CLL cases often are enriched in unique cytogenetic and molecular features. Overexpression of nuclear lymphoid enhancer-binding factor 1 (LEF-1) is highly associated with chronic lymphocytic leukemia/small lymphocytic lymphoma, and its use has shown to be a suitable marker for differential diagnosis of small B-cell lymphomas. We evaluated the clinical and pathologic characteristics as well as the utility of LEF-1 staining in atypical CLL.

Design: We conducted a search of our institutional records (2000-2019) for any cases of chronic lymphocytic leukemia with atypical features, as defined by morphological (greater nuclear irregularity, increased cells with prominent nucleoli or have plasmacytoid features) and immunophenotypical characteristics (bright CD20 expression, FMC7 positivity, strong surface immunoglobulin, CD5 and/or CD23 negativity). For all verified cases, an immunohistochemical stain for LEF-1 was evaluated. The threshold for positivity as reported in the literature, was set at >10% of tumor cells. For all negative cases we opted for a dual stain of CD20 (membranous) and LEF-1 (nuclear) for confirmation (figure 1).

Results: A total of 12 cases of a-CLL were identified with LEF-1 being negative (<10%) in 5/12 cases. LEF-1 negative cases demonstrated atypical immunophenotypic findings in all cases (5/5) which commonly included CD20bright+ (5/5 cases), FMC7+ (5/5 cases), CD23- (1/5 cases) and bright light chain expression (3/5 cases). Of note no CD10, cyclinD-1 or SOX-11 expression was seen in any cases. The LEF-1 negative cases were enriched in the cytogenetic finding (Table-1) of trisomy 12 (4/5 cases) and atypical morphologic features were present in 3/5 cases.

Case #	LEF-1	Immunophenotype	Morphology	Cytogenetics	FISH	Site	Extent Involvement / Pattern	Absolute Lymphocyte (K/uL)
1	LEF-1 (80%+)	CD19(+)CD5(+)CD10(-)CD23(dim+)CD38(+)CD79a(+)CyclinD-1(-)SOX-11(-)lambda(dim+)	Typical CLL morphology	46,XX [20]	Del13q14.3 (81%)	BM	5% / Nodular	137.7
2	LEF-1 (-)	CD19(+)CD20(bright+)CD5(+)CD10(-)FMC7(+)CD23(-)CD38(-)lambda(dim+)	Typical CLL morphology	46, XY [20]	Negative CLL FISH Panel	BM	90% / Dense Interstitial	81.1
3	LEF-1 (90%+)	CD19(+)CD20(dim+)CD5(dim+)CD10(-)CD23(+)FMC7(-)CD38(-)kappa(+)	Typical CLL morphology	47,XY,+12[5]	Trisomy 12 (82%)	BM	>95% / Dense Interstitial	59.8
4	LEF-1 (80%+)	CD19(+)CD20(dim+)CD5(+)CD10(-)CD23(partial+)FMC7(-)CD38(+)lambda(dim+)	Nuclear irregularity/prominent nucleoli	46,XY[19] 47,XY,+12[1]	Del11q22.3(ATM)(34%) and Trisomy 12 (76%)	BM	70% / Dense Interstitial	106.4
5	LEF-1 (-)	CD19(+)CD20(bright+)CD5(+)CD10(-)CD23(dim+)FMC7(+)CD38(-)lambda(+)	Nuclear irregularity/prominent nucleoli	Not available	Trisomy 12 (58%)	BM	>95% / Diffuse Effacement	151.0
6	LEF-1 (-)	CD19(+)CD20(bright+)CD10(-)CD23(partial+)FMC7(partial+)CD38(-)lambda(+)	Typical CLL morphology	46,XY[20]	Del13q14.3 (30%) and Trisomy 12 (3.8%)	BM	40% /Interstitial-nodular	15.3
7	LEF-1(80%+)	CD19(+)CD20(+)CD5(+)CD10(-)CD23(+)FMC7(-)CD38(-)kappa(+)	Nuclear irregularity/prominent nucleoli	42,XX-3+6der(6;8)(p10;q10)-9der(13)t(13;15)(q34;p11.2)-15del(17)(p13)add(21)(p11.1)[11]	Del 17p13.1(p53)(93%) and Trisomy 12 (53%)	BM	30% / Interstitial-nodular	30.1
8	LEF-1 (-)	CD19(+)CD20(bright+)CD5(+)CD10(-)FMC7(+)CD23(+)CD38(-)lambda(dim+)	Nuclear irregularity/prominent nucleoli	46, XY [20]	Trisomy 12 (31%)	BM	70% / Dense Interstitial	46.1
9	LEF-1 (70%+)	CD19(+)CD20(+)CD5(+)CD10(-)CD23(dim+)CD38(-)FMC7(partial+)kappa(+)	Typical CLL morphology (20% prolymphocytes noted)	46XXinv(11)(p11.2q23)[15]/46XX[5]	Del 17p13.1(p53)(64%) and Trisomy 12 (83%)	BM	90% / Dense Interstitial	21.1
10	LEF-1(90%+)	CD19(+)CD20(+)CD5(+)CD10(-)CD23(+)CD38(-)FMC7(-)lambda(+)	Nuclear irregularity/prominent nucleoli	46,XY[20]	Del11q22.3 (ATM)(15%), del13q14.3(17%) and trisomy 12 (13%)	BM	20% / Interstitial-nodular	2.0
11	LEF-1(60%+)	CD19(+)CD20(+)CD5(+)CD10(-)CD23(+)CD38(+)kappa(+)	Typical CLL morphology	46, XX[20]	Trisomy 12 (21%)	LN	20% / Interstitial-nodular	3.2

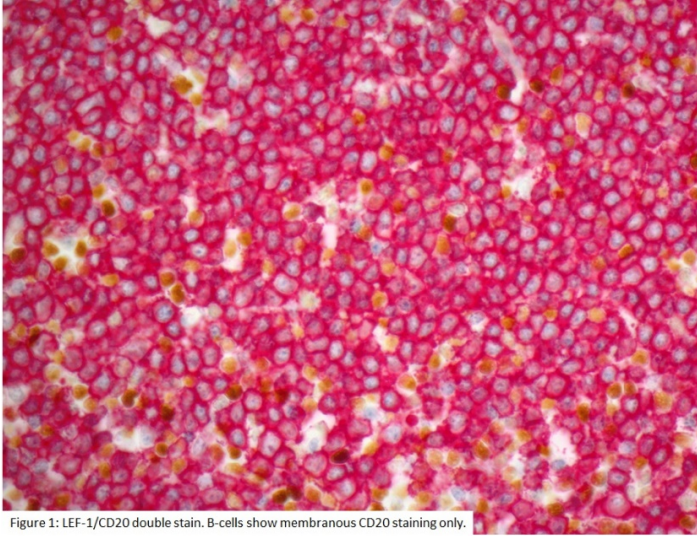| 12 | LEF-1(-) | CD19(+)CD20(bright+)CD5(dim+)CD10(-)CD23(+)CD38(+)FMC7(+)kappa(+) | Nuclear irregularity/prominent nucleoli | 47,XX,+12[4]/46,XX[10] | Del11q22.3 (ATM)(46%) and trisomy 12 (74%) | BM | 20% / Interstitial-nodular | 99.6 |

Figure 1 - 1440

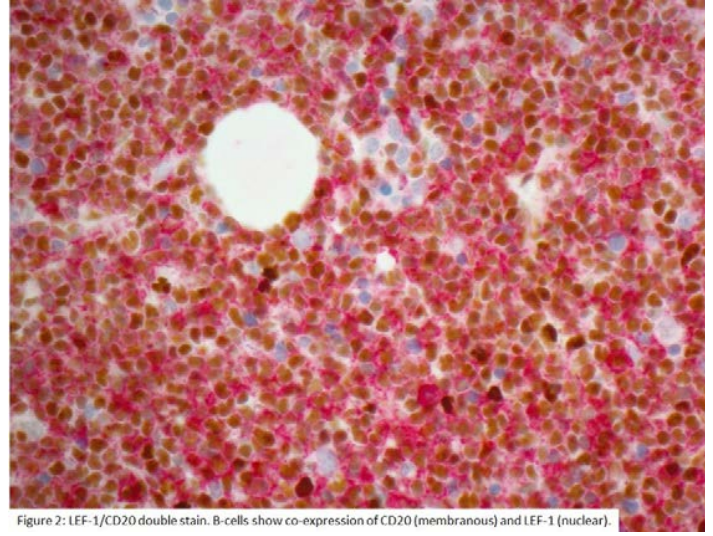Figure 1: LEF-1/CD20 double stain. B-cells show membranous CD20 staining only.

Figure 2 - 1440

Figure 2: LEF-1/CD20 double stain. B-cells show co-expression of CD20 (membranous) and LEF-1 (nuclear).

Conclusions: Our results show that 42% of atypical-CLL patients were negative for LEF-1 (5/12 cases). After correlation with clinical and radiographic features no distinct alternative lymphoproliferative disorder was clearly evident. It is unclear if these atypical-CLL cases with LEF-1 negativity represent a unique biologic subset of CLL cases that lack expression or if these results suggest an alternative diagnosis. Our results provide evidence that in the interpretation of LEF-1 negativity caution be advised before excluding a-CLL in the differential diagnosis.

1441 Clinico-Pathologic Features of Post-Transplant Plasma Cell Myeloma: A Single Institutional Retrospective Analysis

Kenneth Ofori[1], Murty Vundavalli[1], Craig Soderquist[2], Rebecca Leeman-Neill[3], Bachir Alobeid[2], Govind Bhagat[1]
[1]Columbia University Medical Center, New York, NY, [2]New York, NY, [3]Columbia Medical Center, New York, NY

Disclosures: Kenneth Ofori: None; Murty Vundavalli: None; Craig Soderquist: None; Rebecca Leeman-Neill: None; Bachir Alobeid: None; Govind Bhagat: None

Background: Multiple myeloma occurring in recipients of solid organ allografts, referred to as post-transplant plasma cell myeloma (PT-PCM), constitutes a rare subtype of monomorphic post-transplant lymphoproliferative disorder (PTLD), with a reported prevalence of approximately 1/1000 organ transplant patients. Limited epidemiologic studies suggest that PT-PCM occurs later after transplantation and in older individuals (median age, 60 yrs), compared to other PTLD subtypes. However, due to its rarity, the biology of PT-PCM is not well understood. Hence, we sought to assess the pathologic features, underlying cytogenetic abnormalities and the clinical presentation and outcomes of PT-PCM patients diagnosed and treated at our institution.

Design: We searched our pathology department database to identify cases of PT-PCM over a 15 year period (2004-2019). Histopathologic and immunophenotypic features, results of laboratory tests and cytogenetic analysis and imaging findings were reviewed. Demographic and clinical data were obtained from the electronic medical records.

Results: Fourteen cases of PT-PCM (M:F - 3.6:1) were identified, which occurred at a median age of 57yrs (15-79 yrs) post kidney (n=6), heart (n=4), liver (3) and lung (1) transplantation. PT-PCM constituted 11% of all B-cell PTLDs diagnosed within the study period. All cases represented multiple myelomas, including 2 cases of smoldering myeloma. The time from transplant to development of PCM ranged from 0.6-24.7 years (median 11 yrs). The immunosuppressive regimens consisted of mycophenolate (n=6) and/or a calcineurin inhibitors (n=10). The most frequent paraprotein was IgG (50%) followed by IgA (21.4%), light chain only (21.4%) and IgD (7%). Plasma cell burden ranged from 10 to 90% (median 20%); 3 cases (21.4%) also had amyloidosis. The proportion of kappa and lambda chain restriction was similar (50%). EBER ISH was negative in all cases evaluated (n=9). Karyotype and myeloma-specific FISH probes identified cytogenetic abnormalities in 50% of cases, which were similar to conventional multiple myeloma. Eight patients had chemotherapy and one patient had a stem cell transplant. The 5-year survival was 55.4%.

Conclusions: PT-PCM appears more common than previously reported and has similar biologic features as myeloma occurring in immunocompetent individuals, with comparable clinical outcomes in the current era. However, the age of onset is shorter than reported for immunocompetent myeloma (median 68-70 yrs) and a higher male predominance.

1442 Anaplastic Large Cell Lymphoma Involving Body Cavities: Comparison to Breast Implant-Associated ALCL

Naoki Oishi[1], Fabio Facchetti[2], Kennosuke Karube[3], Akira Satou[4], Surendra Dasari[5], Jianping Kong[5], Nada Ahmed[5], Andrew Feldman[5]
[1]University of Yamanashi, Chuo, Yamanashi, Japan, [2]University of Brescia, Brescia, Italy, [3]University of the Ryukyus Graduate School of Medicine, Nakagami-gun, Japan, [4]Aichi Medical University Hospital, Nagakute, Japan, [5]Mayo Clinic, Rochester, MN

Disclosures: Naoki Oishi: None; Fabio Facchetti: None; Kennosuke Karube: None; Akira Satou: None; Surendra Dasari: None; Jianping Kong: None; Nada Ahmed: None; Andrew Feldman: None

Background: Anaplastic large cell lymphomas (ALCLs) represent a clinically and genetically heterogeneous group of CD30-positive T-cell lymphomas. Breast implant-associated (BIA-) ALCL is a new provisional WHO subtype arising in peri-prosthetic effusions. We and others have found that, in contrast to ALCLs as a whole, BIA-ALCL has more uniform molecular features, including absence of *ALK*, *DUSP22*, and *TP63* gene rearrangements ("triple-negative"), consistent JAK-STAT3 activation, and a hypoxic signature with carbonic anhydrase-9 (CA9) expression. It is not known whether these molecular features are common to ALCLs occurring in body cavities or are specific to BIA-ALCL.

Design: We identified ALCLs involving body cavities (not implant-associated) from our archives and reviewed available pathologic and clinical data. Primary involvement was defined as pathologically confirmed involvement of a body cavity within 30 days of initial ALCL diagnosis. When tissue was available immunohistochemistry for pSTAT3 and CA9 expression and fluorescence in situ hybridization (FISH) for *DUSP22* and *TP63* were performed.

Results: Thirty-two patients with ALCL involving body cavities were included (16M:16F, mean age, 58 years; range, 19-87 years). Sites included pleura/pleural fluid (n=23), peritoneum/peritoneal fluid (n=8), and pericardial fluid (n=1). Eleven were primary, five were secondary, and sixteen were undetermined. By WHO criteria, 7 were ALK-positive ALCLs and 25 were ALK-negative ALCLs. Of 14 ALK-negative ALCLs tested, 4 had *DUSP22* rearrangements, 2 had *TP63* rearrangements, and 8 were triple-negative. Tumors were positive for pSTAT3 (≥30% of cells) in 11/14 cases and were positive for CA9 in 2/12.

Conclusions: In contrast to the uniform features identified in BIA-ALCL, body cavity-based ALCLs show a heterogeneous spectrum of clinicopathologic and molecular features similar to ALCLs seen in more typical anatomic sites. These findings suggest that body cavity-based ALCLs and BIA-ALCLs have distinct underlying pathogenesis, and that the unique molecular characteristics of BIA-ALCL are specific to its association with breast implants rather its origin in an effusion-filled cavity.

1443 Pathologic Spectrum of Chronic Myeloid Neoplasms Harboring Concomitant Mutations in Myeloproliferative Neoplasm Driver Genes and SF3B1

Chi Young Ok[1], Kevin Trowell[2], Kyle Parker[3], Karen Moser[4], Olga Weinberg[5], Heesun Rogers[6], Kaaren Reichard[7], Tracy George[4], Eric Hsi[6], Carlos Bueso-Ramos[1], Wayne Tam[8], Attilio Orazi[9], Adam Bagg[10], Daniel Arber[11], Robert Hasserjian[12], Sa Wang[1]
[1]The University of Texas MD Anderson Cancer Center, Houston, TX, [2]Hospital of the University of Pennsylvania, Philadelphia, PA, [3]University of Chicago Medicine, Chicago, IL, [4]University of Utah, Salt Lake City, UT, [5]Children's Hospital Boston, Boston, MA, [6]Cleveland Clinic, Cleveland, OH, [7]Mayo Clinic, Rochester, MN, [8]Weill Cornell Medicine, New York, NY, [9]Texas Tech University Health Science Center, El Paso, TX, [10]University of Pennsylvania, Philadelphia, PA, [11]The University of Chicago, Chicago, IL, [12]Massachusetts General Hospital, Harvard Medical School, Boston, MA

Disclosures: Chi Young Ok: None; Kevin Trowell: None; Karen Moser: None; Olga Weinberg: None; Heesun Rogers: None; Kaaren Reichard: None; Tracy George: None; Eric Hsi: *Consultant*, Seattle Genetics; *Consultant*, Jazz Pharmaceuticals; *Grant or Research Support*, Eli Lilly; *Grant or Research Support*, Abbvie; *Grant or Research Support*, Cellerant; Carlos Bueso-Ramos: None; Attilio Orazi: None; Adam Bagg: None; Daniel Arber: None; Robert Hasserjian: None; Sa Wang: None

Background: *JAK2*, *CALR* and *MPL* are MPN driver mutations, whereas *SF3B1* is strongly associated with ring sideroblasts (RS) in myelodysplastic syndrome (MDS). Concomitant mutations of *SF3B1* and *JAK2* are pathognomonic of MDS/MPN with RS and thrombocytosis (MDS/MPN-RS-T). This study is to review all cases of chronic myeloid neoplasms (CMN) with *SF3B1* and one of the MPN driver mutations, to better define the spectrum of these diseases, amid the recent debate if diseases should be defined genetically or phenotypically.

Design: We searched all CMN cases tested by NGS panels interrogating at least 42 myeloid neoplasm-related genes between 2016-2019 in 9 different institutions. MDS/MPN-RS-T cases were included as a separated co

Results: In addition to 17 MDS/MPN-RS-T, we found other 68 patients, with a median age of 69 years (35-95), 56 with *JAK2*, 4 with *MPL* and 8 with *CALR*, and 42 (62%) with additional mutations. NGS was performed at diagnosis in 27 cases, and at various times during disease course (67.9 months, 12.3-1407) in 41 patients. Anemia was frequent (80%), with Hb≤10g/dL in 44 patients (65%) and transfusion dependency in 30 (44%), whereas thrombocytopenia (<100x10^9/L) was uncommon (14/68, 21%). MF2-3 myelofibrosis was seen in 35/60 patients (58%) and ≥15% RS in 23/52 (44%). These features were overlapping among WHO defined MPN (n=46), MDS (n=14) and MDS/MPN (n=8) (p >0.05), but organomegaly was more common in MPN (32/46, 70%) than MDS (2/14, 14%)(p=0.001). As a group, *JAK2/MPL/CALR* had a median VAF of 41.8% (0.6-98.6%) and *SF3B1* of 38.9% (1.7-48.0%). A >20% difference in *JAK2/MPL/CALR* vs *SF3B1* VAF was more frequent in MPN than MDS (20/43 vs 2/14, p=0.056), while the reverse VAF hierarchy was more common in MDS than MPN (7/14 vs 2/43, p<0.001). The MDS/MPN-RS-T patients had less frequent karyotypic abnormalities compared to other CMN (2/15 vs 26/64, p=0.038). Within a median follow-up of 45.7 months from diagnosis, the median overall survival (OS) was not reached in all WHO subgroups of patients.

Conclusions: Myeloid neoplasms with concomitant MPN driver mutations and *SF3B1* mutation can be observed in CMN other than MDS/MPN-RS-T. These CMNs share some clinicopathological features, but also demonstrate clinical and genetic differences among the WHO defined MDS, MPN and MDS/MPN groups. Differences in VAFs of the two mutations among the disease subtypes suggests that the mutation hierarchy influences the type of disease presentation. The findings support a combination of phenotype and genotype

1444 T-Cell Receptor Rearrangement by Whole-Genome Sequencing and Copy Number Variation Analysis – A Novel Marker of T cell Clonality

Ming Liang Oon[1], Sai Mun Leong[2], Jing Quan Lim[3], Bernett Lee[4], Olaf Rotzschke[5], Choon Kiat Ong[3], Wee-Joo Chng[6], Siok-Bian Ng[2]

[1]National University Hospital, Singapore, Singapore, [2]National University of Singapore, Singapore, Singapore, [3]National Cancer Centre Singapore, Singapore, Singapore, [4]Singapore Immunology Network (SIgN), Agency for Science, Technology and Research (A*STAR), Singapore, Singapore, [5]Singapore Immunology Network, Agency for Science, Technology and Research (A*STAR), Singapore, Singapore, [6]National University Cancer Institute of Singapore, Singapore, Singapore

Disclosures: Ming Liang Oon: None; Jing Quan Lim: None; Bernett Lee: None; Choon Kiat Ong: None

Background: Generation of diversity in T-cell receptor (TCR) genes is a critical component of adaptive immunity, achieved through somatic recombination of multiple variable (V), diversity (D) and joining (J) regions. Rearrangement occurs within the thymus in a sequential fashion, beginning with TCR delta (TCRD), followed by gamma (TCRG), beta (TCRB), and finally alpha- (TCRA). Recognition of this unique molecular hallmark has been exploited by hematolymphoid pathologists in the diagnosis of T-cell lymphomas (TCL). The aim of this study is to perform whole-genome sequencing (WGS) and copy number variation (CNV) analysis of TCR loci in TCL specimens, identify monoclonal deletions in these loci and study the dynamics of TCR rearrangement.

Design: WGS was performed on frozen tissues from 44 pairs of TCL with matched controls , and 10 cases of extranodal NK/T-cell lymphoma, nasal-type (ENKTL). The TCL selected included angioimmunoblastic TCL (AITL, n=20), anaplastic large cell lymphoma (ALCL, n=6), monomorphic epitheliotropic intestinal TCL (MEITL, n=5), peripheral TCL NOS (PTCL, n=12) and hepatosplenic gamma-delta TCL (HSTL, n=1). CNV were predicted by CNVkit and sequencing reads aligned to the TCRD/G/B/A regions were extracted for visual confirmation for the presence or absence of monoclonal losses in each TCR loci.

Results: 39 (89%) of cases showed monoclonal pattern of deletions of one or more TCR loci, indicating monoclonal TCR rearrangements. 17 cases (39%) showed monoclonal rearrangement of TCRG, TCRB and TCRA, indicating that malignant transformation originated from mature T-cells that have completed all TCR rearrangements. 9 cases (20%) showed rearrangement of TCRG only. 5 cases (11%) showed no deletion of any TCR loci. Interestingly, 11 cases (25%) showed monoclonal rearrangements of TCRG and TCRA, but not TCRB, indicating the existence of an aberrant sequence of rearrangement of TCR genes. No TCR deletions were identified in all ENKTL cases, compatible with NK-cell origin.
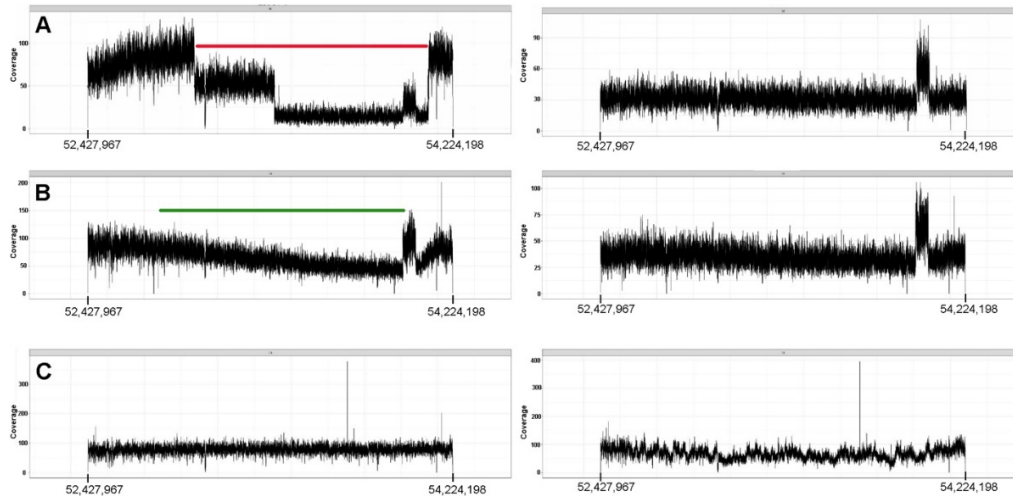
Figure 1 - 1444

Figure 1 A-C. Copy number loss of TCRA locus in T- and NK-cell lymphomas. The copy number profile of TCRA locus of paired tumor (left) and matched controls (right) are illustrated. Y-axis represents number of reads and X-axis represents TCRA gene location. A) A case of peripheral T-cell lymphoma showing a monoclonal pattern of loss with sharply demarcated broad segment deletions (highlighted in red) compared to matched control, indicating a clonal population with an identical copy number loss. B) A case of angioimmunoblastic T-cell lymphoma showing a polyclonal pattern with a 'gradient' loss (highlighted in green), likely due to presence of background reactive T cells with diverse copy number loss across the gene.C) A case of extranodal NK/T cell lymphoma, nasal-type, showing no copy number loss over the entire gene, compatible with an NK cell origin.

Conclusions: We demonstrate that it is feasible to identify monoclonal rearrangements of TCR loci in TCL using a combination of WGS and CNV analysis. Our method represents a novel and specific platform for the detection of T-cell clonality. We further identified a subset of TCL with deviant sequence of TCR loci rearrangement, which we postulate might arise from expansion of a T-cell clone with atypical or dysregulated TCR rearrangement. Our study may shed new light on the ontogeny of malignant T-cell populations.

1445 Peripheral T-Cell Lymphomas are Characterized by Transcriptionally Active FOXO3

Megan Parilla[1], Michael Leukam[2], Sabah Kadri[1], Lauren Ritterhouse[3], Jeremy Segal[4], Jennifer Jacobsen[1], Maria Krunic[1], Sandeep Gurbuxani[1]
[1]The University of Chicago, Chicago, IL, [2]University of Chicago Medical Center, Chicago, IL, [3]Massachusetts General Hospital, Harvard Medical School, Boston, MA, [4]The University of Chicago, Riverside, IL

Background: FOXO3, a member of the family of forkhead box transcription factors, plays a critical role in T-cell development in immature thymocytes. The functional activity of FOXO3 is controlled by post translational modifications of the protein that determine its subcellular localization. Because of the critical role of FOXO3 in normal T-cell development we wanted to investigate its role in mature T-cell lymphomas such as peripheral T-cell lymphomas (PTCL). We have previously demonstrated frequent nuclear expression of FOXO3 in PTCL by immunohistochemistry compared with normal T-cell controls (https://doi.org/ 10.1093/ajcp/140.suppl1.212). The current study was undertaken to determine the functional consequences of nuclear FOXO3 expression in mature T-cell lymphomas.

Design: A composite data set was created from publicly available gene-expression data (GSE6338, GSE14879 and GSE19069). Raw microarray data were imported, normalized and log transformed for variance stabilization using the *affy* R package. Gene set variation analysis was used to score the expression in each sample of four previously published gene sets of FOXO3 targets. Mean gene set expression was compared between PTCL and controls with the Mann-Whitney U-test. P-values < 0.05 were considered statistically significant. Separately, three PTCL samples (2 PTCL-NOS; 1 ALK-negative ALCL) were run on the UCM-OncoPlus 1,213 gene targeted hybrid capture NGS panel with DNA prepared from FFPE tissue.

Results: Within the compiled data set 78 samples were subclassified as PTCL-NOS and 72 as controls. The mean GSVA enrichment score in each of the three experimentally-derived and one computationally predicted set of FOXO3 targets was higher in PTCL than controls, indicating increased FOXO3 activity in the PTCL samples. No mutations were found in *FOXO3* in three patient samples by NGS.

Figure 1 - 1445

Gene Set Expression in Individual Samples per Disease Group
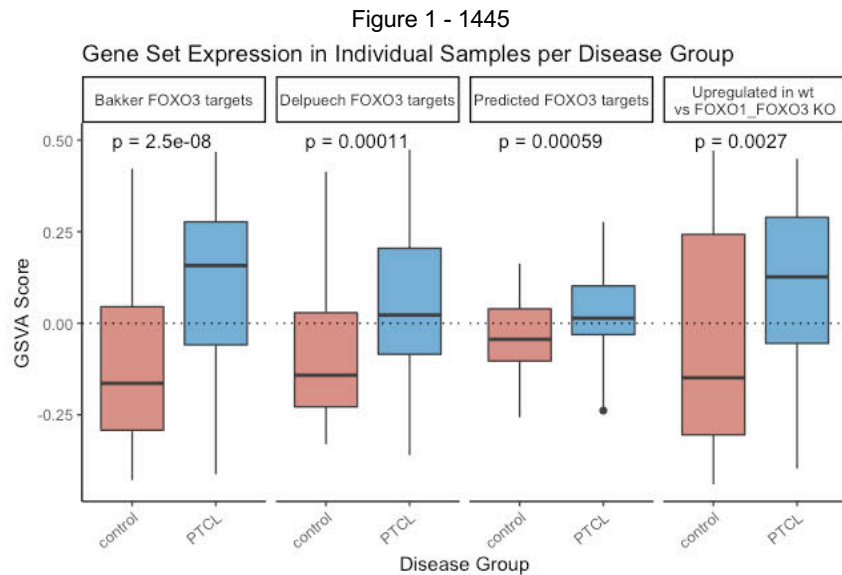
Conclusions: We do not find evidence of a mutation in the *FOXO3* gene in a small series of PTCL cases indicating nuclear localization is not driven by mutations in nuclear localization domains of the protein. Furthermore, gene set variation analysis suggests that the FOXO3 nuclear localization seen by immunohistochemical stains in PTCL is functional; FOXO3 downstream targets are activated preferentially in T-cell lymphomas compared to controls. Ongoing analysis of the composite expression data is focused on identifying pathways involved in FOXO3 nuclear localization as well as identifying specific FOXO3 targets that might contribute to lymphomagenesis.

1446 Utility of FISH Analysis on CD19-Positive Selected Cells for Detecting Cytogenetic Aberrations in Samples with Low Level Involvement by B-cell Neoplasms

Andrew Parrott[1], Murty Vundavalli[2], Caitlin Walsh[3], Alecia Christiano[3], Govind Bhagat[2], Bachir Alobeid[4]
[1]New York-Presbyterian/Columbia University, New York, NY, [2]Columbia University Medical Center, New York, NY, [3]New York-Presbyterian/Columbia University Medical Center, New York, NY, [4]New York, NY

Disclosures: Andrew Parrott: None; Murty Vundavalli: None; Caitlin Walsh: None; Alecia Christiano: None; Govind Bhagat: None; Bachir Alobeid: None

Background: Detection of low-level disease in B-cell neoplasms can be challenging. However, technologies are available to enrich cells of interest and improve the rate of detection. One of these technologies is immune-magnetic cell sorting using the B-cell marker CD19. To test the utility of CD19-positive selection (CD19S), we performed Fluorescence in situ hybridization (FISH) cytogenetic analysis on both non-selected (NS) and CD19S cells in a series of B-cell neoplasms using a variety of FISH probes.

Design: CD19 magnetic bead-based selection (RoboSep, Stemcell Technologies Inc, Vancouver) was performed in all cases with a history of B-cell neoplasm and recurrent chromosome aberrations. FISH using probes targeting the aberrations (Table 1) was performed on CD19S and NS samples. The findings were compared with concurrent flow cytometry (FC) analysis, which was performed routinely.

Results: CD19S FISH was performed in a cohort of 93 cases from 69 patients (M:F – 2.2:1, ages 2-89 yrs, median 60 yrs) over a period of 14 months (88% bone marrow and 12% peripheral blood samples). The cohort comprised B-ALL (43%), CLL (38%), and other B-cell NHL (19%), of these 71 representing post-therapy follow up (PT), 20 untreated disease (UD), and 2 primary diagnostic (PD) samples (Table 1). Disease was detected by FC and/or FISH in 62% of cases, while 38% had no detectable disease by either FISH or FC (Fig 1). CD19S FISH was positive in 81% of all positive cases. NS FISH was performed in 61% of the positive cases and detected disease in only 42% of them. FC was performed in 95% of the entire cohort and was positive in 97% of all positive cases (Fig 1). NS FISH did not detect disease in any cases negative by either FC or CD19S FISH. When direct comparison was possible, a highly significantly increased rate of detection of percent positive cells was observed with CD19S FISH compared to NS FISH (P<0.001) (Fig 2). Of note, CD19S FISH was able to detect disease in 5 of 8 B-ALL cases and 2 of 6 NHL cases that were negative by NS FISH (Fig 2).

Table 1: Summary of B-cell neoplasms and FISH analysis probes.		
Diagnosis	Number of cases (PT/UD/PD)	FISH Probes
B-ALL	40 (40/0/0)	BCR/ABL, D7S486/CEP 7, TEL/AML1, CEP 4, CEP 10, CEP 17, XY, TCF3/PBX1
CLL	35 (22/13/0)	D13S319/CEP 12, TP53/ATM, p16/CEP 9, IGH
MZL	7 (3/3/1)	PRDM1, TNFIAP3, CEP 6, D7S486/CEP 7, IGH, BCL2
MCL	5 (3/1/1)	IGH/CCND1
FL	3 (2/1/0)	IGH/BCL2
LPL/WM	2 (1/1/0)	PRDM1, TNFIAP3, CEP 6
PTLD	1 (0/1/0)	MYC

Figure 1 - 1446
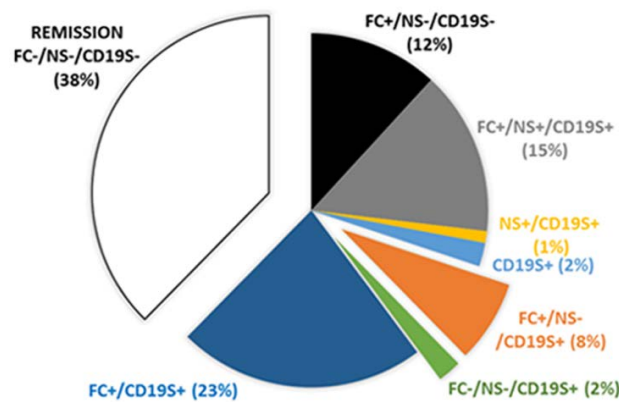
Figure 1. Relative proportion of cases assayed by NS and CD19S FISH, and FC. Positive (+) or negative (-) detection by a testing modality is denoted.

Figure 2 - 1446
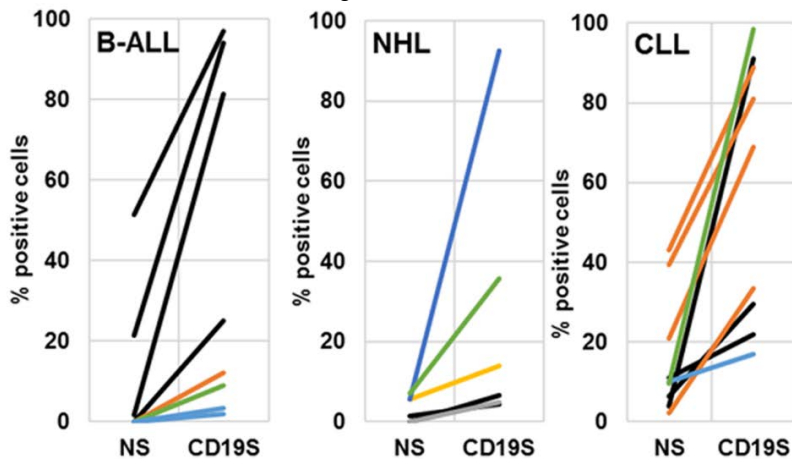
Figure 2. Relative percentage of cells with chromosomal aberrancies detected by NS and CD19S FISH.

Conclusions: The present study clearly establishes the utility of CD19-positive selection in detection of recurrent genetic aberrations in a wide-variety of B-cell neoplasms. CD19S FISH highly significantly improves the rate of disease detection when compared to NS FISH, at a level comparable to that of FC. CD19S FISH can complement FC in disease detection and contribute additional cytogenetic information important for risk stratification and further management.

1447 Genetic Alterations and Immunohistochemical Expression of Program Death Ligand 1 and 2 (PD-L1/2) in Intravascular Large B-cell Lymphoma

Nisha Patel[1], Lisa Durkin[2], Hisae Nakamura[3], Susana Ben-Neriah[4], Juraj Bodo[2], Graham Slack[5], Daniel Socha[6], Christian Steidl[3], Eric Hsi[2]

[1]Cleveland Clinic, Bethesda, MD, [2]Cleveland Clinic, Cleveland, OH, [3]British Columbia Cancer Agency, Vancouver, BC, [4]British Columbia Cancer Agency, Vancouver, BC, [5]Vancouver, BC, [6]Cleveland Clinic, Westlake, OH

Background: Intravascular Large B-cell Lymphoma (IVL) represents a distinct extranodal large B-cell lymphoma with aggressive clinical behavior. A subset of IVLs have recently been reported to express PD-L1, a potential target for checkpoint inhibition therapy. Characterization of PD-L2 expression and genetic alterations in the PD-L1/2 loci have not been evaluated. We investigate the expression and genetic features of PD-L1/2 in a series of IVL cases.

Design: 16 IVL cases were retrospectively collected over a 29-year period from 4 autopsy, 11 biopsy, and 1 native liver resection specimens. Immunohistochemical stains for PD-L1 (clone 22C3; Agilent) and PD-L2 (clone D7U8C; Cell Signaling) were performed on formalin fixed paraffin-embedded (FFPE) tissue. Cases were considered positive for PD-L1 or PD-L2 expression when greater than 5% of tumor cells had moderate or strong membranous staining. Fluorescence in-situ hybridization (FISH) was performed on available FFPE sections (n=15) using a custom 9p24 dual-color break-apart probe. Amplification was defined as more than 4 fused signals whereas copy number gain was classified as 3-4 fused signals.

Results: Overall, 38% (6/16) of IVLs expressed either PD-L1 (5/16, 31%) or PD-L2 (1/16, 6%) by IHC. None of the cases coexpressed PD-L1 and PD-L2. PD-L1 staining varied in intensity (moderate to strong) and percent tumor cellularity (40-90%). The sole PD-L2 positive case showed strong staining in 90% of tumor cells.

Five of 15 (33%) cases demonstrated at least one chromosomal alteration (CA) by FISH including copy number gains (2/15, 13%), amplifications (3/15, 20%), and rearrangements (2/15, 13%). Three cases with CAs displayed PD-L1/2 expression. All three cases had strong IHC staining in more than 90% of tumor cells.

Among PD-L1 IHC positive cases, one case showed both rearrangement and copy number gains, while another case contained amplification only. The three remaining PD-L1 IHC positive cases lacked FISH alterations. The sole PD-L2 IHC positive case showed both amplification and rearrangement. Two IHC negative cases harbored amplification and copy number gains without rearrangement.

TABLE 1: PD-L1 and PD-L2 Immunohistochemical and Fluorescence in-situ Hybridization Findings						
Case Number	Tissue Site	Specimen Type	IHC PD-L1	IHC PD-L2	FISH Break-apart	FISH Copy Number
Case 1	Kidney/Adrenal Gland	Autopsy	**90% strong**	0%	**Positive**	**Gain**
Case 2	Muscle	Biopsy	**40%, strong**	0%	Negative	Normal
Case 3	Brain	Biopsy	**90%, moderate**	0%	Negative	**Amplification**
Case 4	Kidney	Biopsy	0%	**90%, strong**	**Positive**	**Amplification**
Case 5	Brain	Biopsy	**80% strong**	0%	Negative	Normal
Case 6	Liver	Native Liver Explant	**80%, strong**	0%	Negative	Normal
Case 7	Left Lung	Autopsy	0%	0%	Negative	Normal
Case 8	Skin	Biopsy	0%	0%	Negative	Normal
Case 9	Muscle/Nerve	Biopsy	0%	0%	*Failed*	*Failed*
Case 10	Brain	Biopsy	0%	0%	Negative	Normal
Case 11	Adrenal gland	Biopsy	0%	0%	Negative	Normal
Case 12	Kidney/Adrenal Gland	Autopsy	0%	0%	Negative	Normal
Case 13	Skin	Biopsy	0%	0%	Negative	**Amplification**
Case 14	Skin	Biopsy	0%	0%	Negative	Normal
Case 15	Adrenal Gland	Autopsy	0%	0%	Negative	**Gain**
Case 16	Lung	Biopsy	0%	0%	Negative	Normal

Conclusions: Approximately 40% of IVLs express PD-L1/2 by IHC, half of which harbored a CA by FISH. One third of total IVLs had a CA, including two IHC negative cases. These data suggest rearrangement of PDL1/PDL2 as one mechanism for PD-L1/2 overexpression; however, involvement of other regulatory mechanisms appears likely.

1448 Multiparametric In Situ Imaging of NPM1-Mutated Acute Myeloid Leukemia Reveals Prognostically-Relevant Features of the Marrow Microenvironment

Sanjay Patel[1], Mikel Lipschitz[2], Geraldine Pinkus[3], Jason Weirather[2], Olga Pozdnyakova[3], Emily Mason[4], Giorgio Inghirami[5], Robert Hasserjian[6], Scott Rodig[3], Olga Weinberg[7]

[1]Weill Cornell Medical College, New York, NY, [2]Dana-Farber Cancer Institute, Boston, MA, [3]Brigham and Women's Hospital, Boston, MA, [4]Vanderbilt University Medical Center, Nashville, TN, [5]New York-Presbyterian/Weill Cornell Medical Center, New York, NY, [6]Massachusetts General Hospital, Harvard Medical School, Boston, MA, [7]Children's Hospital Boston, Boston, MA

Background: Acute myeloid leukemia (AML) with mutated *NPM1* is the most common WHO subtype of AML associated with a single pathogenic somatic mutation. Previous data have identified two different populations in *NPM1*-AML of potential prognostic relevance: 1) CD34+ leukemic stem cells and 2) anti-leukemic T-cells; however, ancillary techniques utilized to study these populations have largely been performed using aspirated material. In this study, we performed multiparametric *in situ* imaging to evaluate the *NPM1*-AML microenvironment.

Design: Multiparametric immunofluorescence (MIF) staining was performed on 17 formalin-fixed paraffin-embedded (FFPE) diagnostic *NPM1*-AML core biopsy specimens using DAPI plus a panel of six primary antibodies (mutant NPM1-specific antibody, CD3, CD4, CD8, CD34, Granzyme B). Three to six regions of interest were imaged at 20x and subsequently annotated using InForm software. Data outputs were parsed using custom R algorithms to acquire counts (cells/mm2) and percentages of specific cell types. Diagnostic NGS (n=17), flow cytometry (FC, n=14), and CR1 *NPM1*-specific molecular MRD (n=16) data were also available.

Results: The total nucleated cell count obtained ranged from 6,914-23,041 (n=17, median 13,176). The %CD3+ T-cells correlated positively between FC and MIF (r=0.53, p=0.05), but was significantly lower by MIF (1.62% vs. 3.4%, p=0.009). The percentage of mutant NPM1-positive (NPM1c+) cells ranged from 9.7-90.8% (median 45.4%) and did not correlate with the *NPM1* mutant allele fraction (p>0.05). The %CD34+/NPM1c+ cells ranged from 0-1.8% (median 0.07%). There was no difference between MRD+ (n=8) and MRD- (n=8) cases with respect to the %CD3+ T-cells or %CD34+/NPM1c+ cells (p>0.05); however, the %NPM1c+ cells correlated inversely (34% vs. 62%, p=0.03) with the presence of MRD, while the percentages of CD3-/NPM1c- cells (64% vs. 35%, p=0.03), and specifically CD3-/CD4-/NPM1c- cells (26% vs. 13%, p=0.04), correlated positively with MRD.

Figure 1 - 1448
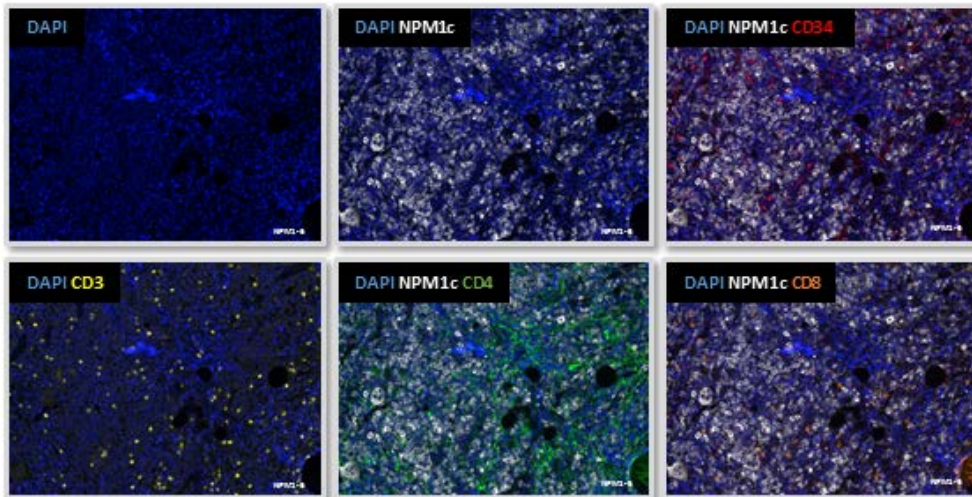
Conclusions: We find that the quantitation of specific bone marrow populations in *NPM1*-AML by MIF, and by orthogonal methodologies (FC, NGS), is not absolutely concordant, suggesting that aspirate materials are likely an imperfect reflection of the core biopsy tissue. *In situ* analyses further reveal that additional *NPM1* wild-type cells within the microenvironment may support leukemia cell survival and be of prognostic significance. Additional multiparametric *in situ* analyses will be necessary to better define these populations.

1449 Quantitative Microvascular Phenotyping of Human B-Cell Lymphomas

Nathan Paulson[1], Jordan Pober[2], Mina Xu[2]
[1]Yale School of Medicine, New Haven, CT, [2]Yale University, New Haven, CT

Disclosures: Nathan Paulson: None; Jordan Pober: None; Mina Xu: None

Background: Human lymphomas vary in the extent to which they are infiltrated by cytotoxic T-lymphocytes (CTLs), a variable which may correlate with responsiveness to immunotherapies. The principal mechanism governing T-cell recruitment to inflammatory sites is the activation state of the local microvasculature. We hypothesize that the same will apply to recruitment of CTLs into human lymphomas. Here we describe a test of this hypothesis using quantitative immunofluorescence microscopy to compare different B-cell lymphomas, correlating infiltrating immune cells with microvascular endothelial expression of leukocyte adhesion molecules.

B-cell lymphomas show broad heterogeneity, ranging from Diffuse Large B-Cell Lymphoma (DLBCL) with minimal infiltrating inflammatory cells to Classic Hodgkin Lymphoma (CHL) and T-Cell/Histiocyte Rich Large B-Cell Lymphoma (TCHRLBL) with extensive background inflammatory cells. Immune checkpoint inhibitors have had more encouraging responses in patients with CHL than in patients with DLBCL, which may be associated with the relative permissiveness of the tumor microenvironments.

Design: Cases of formalin-fixed, paraffin-embedded DLBCL, CHL, and TCHRLBL with sufficient tissue for staining were pulled from the pathology archives and reviewed. Unstained slides were cut for three-marker multiplex immunofluorescence studies using Ulex, CD45, and one of three vascular adhesion markers (VCAM-1, E-selectin, P-selectin). Three stained slides were generated for each case. Images were captured for the entire section using the EVOS FL Auto 2 imaging system with image tiling. Quantitative analysis of staining intensity was performed in ImageJ and MATLAB.

Results: Twenty-eight cases were stained: 10 each of DLBCL and CHL, and 8 TCHRLBL. For all vascular adhesion markers tested, there were statistically significant differences between the fluorescence intensity in the 3 groups of lymphomas ($p < 0.05$). Cases of DLBCL had the lowest mean fluorescence intensity for VCAM-1, E-selectin and P-selectin. CHL had the highest mean fluorescence intensity for VCAM-1, whereas TCHRLBL had the highest for both E-selectin and P-selectin.

Conclusions: B-cell lymphomas are a heterogenous group with different morphologic features and different responses to immunotherapies. The phenotype of the microvasculature using VCAM-1, E-selectin, and P-selectin is significantly different between DLBCL, CHL, and TCHRLBL. These differences may be a key determinant of infiltration by T cells in these tumor types.

1450 Research CBC Parameters Predict Cytopenias Associated with Active Myelodysplastic Syndromes and Underlying Mutations

Olga Pozdnyakova[1], Radu Niculescu[2], Tracey Kroll[3], Lisa Golemme[4], Nolan Raymond[5], Debra Briggs[6], Annette Kim[1]
[1]Brigham and Women's Hospital, Boston, MA, [2]PTC, Wayne, PA, [3]Analytics Center of Excellence, PTC, Wayne, PA, [4]Brigham and Women's Hospital, Harvard Medical School, Boston, MA, [5]Brigham and Women's Hospital and Harvard Medical, Boston, MA, [6]Dana Farber Cancer Institute, Boston, MA

Disclosures: Olga Pozdnyakova: *Grant or Research Support*, Sysmex Corporation of America; *Consultant*, Promedior; Radu Niculescu: *Consultant*, Sysmex America, Inc.; Tracey Kroll: *Consultant*, Sysmex America, Inc.; Lisa Golemme: None; Nolan Raymond: None; Debra Briggs: None; Annette Kim: None

Background: Given the time, expense, and clinical expertise required for the diagnosis of myelodysplastic syndromes (MDS), there is a need for cost-effective laboratory screening that can rapidly and accurately identify cytopenic patients that require more extensive workup. Since conventional CBC parameters alone cannot distinguish reactive cytopenias from MDS, we examined the combination of all conventional and research automated CBC parameters, in addition to mutational data, as a potential screening tool in patients presenting with abnormal CBC.

Design: We measured 92 CBC parameters using the Sysmex XN hematology analyzer in 592 consecutive patients (pts): 221 pts with abnormal CBC due to underlying myeloid neoplasms and 371 age-matched controls with normal CBC. The MDS group had 59 pts with active disease and 24 pts in remission. We developed models to predict the presence of active MDS using CBC and molecular data, as well as CBC data alone. Correlation matrix analysis was used to establish relationships between MDS-associated mutations and CBC parameters; relevant association was considered at the levels of above 0.25 or below -0.25.

Results: Table 1 lists the performance of the champion predictive models for the presence of active MDS. The most discriminatory research CBC parameters in MDS reflect dysplastic changes in neutrophil morphology (NE-SFL, NE-WY, NE-WX, NE-FSC, NE-SSC) and degrees of cytopenia (increased IPF and decreased TNC). Figure 1 shows separation of active MDS from MDS in remission and controls using NE-SSC and NE-FSC. *ASXL1* is associated with changes in WBC [higher LY-X (0.38), TNC (0.28), WBC (0.28) and neutrophil (0.27)] and RBC [IRF (-0.67), RBC (-0.30) and reticulocyte (-0.31)] parameters. *DNMT3A* and *SF3B1* mutations show higher platelet
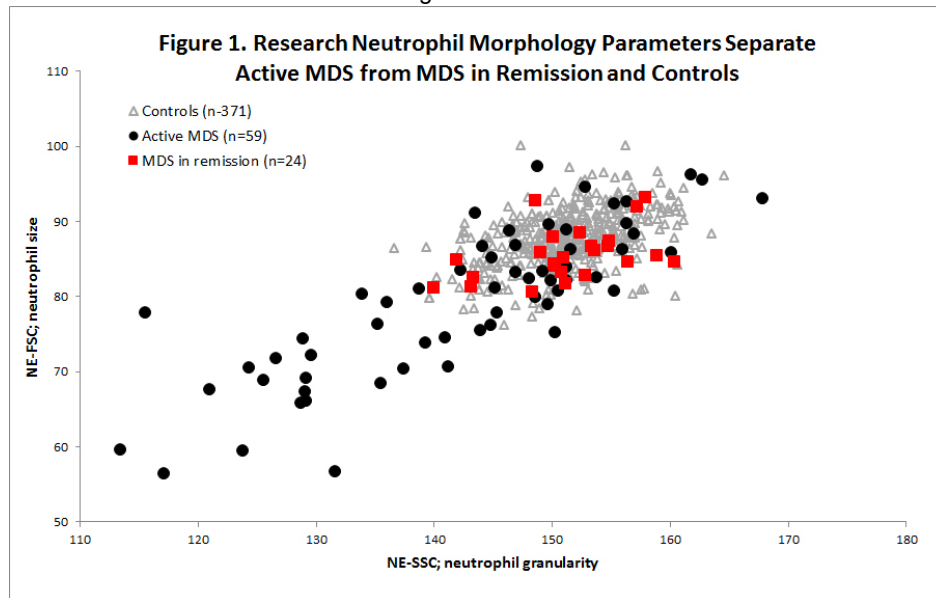
correlations (0.32). *SF3B1* is associated with lower neutrophil granularity (-0.32), cell size (-0.32) and nuclear complexity (-0.39). *TP53* shows positive association with neutrophil and lymphocyte parameters reflecting population heterogeneity (0.26-0.40).

Table 1. The leave one out performance of the champion predictive models* for active MDS based on different variables (all clinical and research CBC [CRCBC] parameters, mutations, age and gender).

Variables	ROC	Sensitivity	Specificity	PPV	NPV
CRCBC	0.86	0.75	0.92	0.96	0.60
CRCBC+Mutations	0.91	0.81	0.96	0.98	0.67
CRCBC+MUtaitons+Age+Gender	0.91	0.81	0.92	0.96	0.66

*Predictive models tested: Linear and Logistic Regression, Decision Trees, Random Forests, Neural Networks, Support Vector Machines, Gradient Boosting.

Figure 1 - 1450

Figure 1. Research Neutrophil Morphology Parameters Separate Active MDS from MDS in Remission and Controls

Conclusions: Our exploratory study shows: 1.Sysmex XN research parameters, measured with all routine CBCs, may be used in patients with cytopenias to build a predictive model to screen for active MDS, which improves when the molecular status is added. 2.Most relevant research parameters are reflective of dysplastic neutrophil morphology and very specific for MDS; the parameters normalize in remission. 3.There may be unique CBC parameter signatures depending on underlying mutations.

1451 Quality Parameters for Flow Cytometric Minimal Residual Disease (MRD) Assessment in Plasma Cell Neoplasms

Rashid Qureshi[1], Gregory Otteson[2], Michael Timm[2], Min Shi[2], Horatiu Olteanu[2], Shaji Kumar[2], Dragan Jevremovic[2]
[1]Division of Hematology, Mayo Clinic, Rochester, MN, [2]Mayo Clinic, Rochester, MN

Disclosures: Rashid Qureshi: None; Gregory Otteson: None; Michael Timm: None; Min Shi: None; Horatiu Olteanu: None; Shaji Kumar: None; Dragan Jevremovic: None

Background: MRD assessment, by either flow cytometry (FC) or DNA analysis, in treated plasma cell neoplasms is an excellent prognostic factor, and possibly will be a therapy-guiding test. One of the advantages of the FC method is the ability to assess the quality of the specimen (i.e. hemodilution). In this study we reviewed quality parameters - counts of hematogones (HG), mast cells (MC), and total plasma cells (PC) in 724 consecutive cases of MRD testing by FC.

Design: 724 consecutive bone marrow studies were performed on patients with the previous diagnosis of multiple myeloma or light chain amyloidosis. PCs were detected by FC using Euroflow method with antibodies to CD19, CD27, CD38, CD45, CD56, CD81, CD117, CD138, and cytoplasmic kappa and lambda (two 8-color tubes). Quality parameters (hematogones (HG): $CD19^+CD38^{bright}CD45^{dim}cIg^-$ FSC/SSC^{low}; mast cells (MC): $CD117^{bright}CD45^+CD38^+SSC/FSC^{high}$; and total plasma cells $CD38^{bright}CD138^+$) were defined during gating for identification of clonal plasma cells.

Results: Median collected event number was 8.6x10^{6} (range 1.4x10^{6}-9.9x10^{6}). Out of 724 specimens, there were 210 MRD[+] and 514 MRD[-]. 148 (20%) had total HG below 0.05% and 136 (19%) had MC below 0.002%., which have previously been proposed as adequate cutoffs for hemodilution. There was only 41 (6%) specimen in which both hematogones and mast cells were below the proposed cutoffs. Within these 41, there were 12 MRD[+] and 29 MRD[-] cases, with the distribution similar to the total cohort (p=1.00; Fisher's exact test). Interestingly, when the combined counts of HG, MC, and PC was used as a quality parameter, instead of the percentages of HG and MC, the patients with less than 1500 collected events were less likely to be MRD[+] (4/39 vs. 206/704; p=0.0096; Fisher's exact test).

Conclusions: Quality assessment of the bone marrow specimen is necessary for adequate interpretation of negative MRD results. Based solely on the frequency of MRD positivity, the previously proposed cutoffs were not informative. Combined counts of hematogones, mast cells and total PCs of less than 1500 could be a useful parameter for this determination, despite inherent bias in using the number of PC in calculations. Longer clinical follow-up, with progression-free survival analysis, to determine clinical validity of this approach is pending.

1452 Copy Number Differences in Diffuse Large B-cell Lymphoma with a Germinal Center B-cell Phenotype versus an Activated B-cell Phenotype

Nina Rahimi[1], Anamarija Perry[2], Pamela Skrabek[3], Michel Nasr[4], Victoria Bedell[5], Maria Valle-Catuna[6], Joyce Murata-Collins[6], Alex Herrera[6], Wing Chung Chan[7], Joo Song[8], Dennis Weisenburger[5]
[1]Duarte, CA, [2]University of Michigan, Ann Arbor, MI, [3]CancerCare Manitoba, Winnipeg, MB, [4]SUNY Upstate Medical University, Syracuse, NY, [5]City of Hope National Medical Center, Duarte, CA, [6]City of Hope, Duarte, CA, [7]City of Hope National Medical Center, Pasadena, CA, [8]City of Hope Medical Center, Duarte, CA

Disclosures: Nina Rahimi: None; Anamarija Perry: None; Pamela Skrabek: None; Michel Nasr: None; Victoria Bedell: None; Maria Valle-Catuna: None; Joyce Murata-Collins: None; Alex Herrera: *Grant or Research Support*, Bristol-Myers Squibb, Genentech, Immune Design, AstraZeneca, Merck, Seattle Genetics and Kite Pharma, Gilead Sciences; *Consultant*, Bristol-Myers Squibb, Genentech, Merck, Adaptive Biotechnologies Kite Pharma and Gilead; Wing Chung Chan: None; Joo Song: None; Dennis Weisenburger: None

Background: Diffuse large B-cell lymphoma (DLBCL) is a heterogeneous disease with recurrent genomic abnormalities. There are distinct biological differences between DLBCL with a germinal center B-cell phenotype (GCB) and those with an activated B-cell phenotype (ABC). The purpose of this study was to determine the copy number variation (CNV) differences between these two distinct subtypes of DLBCL, which may elucidate the distinct biological subtypes.

Design: We identified 253 patients with a diagnosis of *de novo* DLBCL between 2000-2016 at two major cancer centers and who were treated with R-CHOP therapy. DNA and RNA was extracted from the formalin-fixed paraffin-embedded tissue (FFPET). Immunostaining (Hans algorithm, MYC, BCL2), and the Lymph2Cx assay (Nanostring) were performed to determine the cell-of-origin. Oncoscan (Thermo Fisher) was performed to determine the CNV of the cases and analysis was performed using Nexus 10.0 (Biodiscovery). Regions of interest were explored using the Cancer Gene Census (COSMIC) database.

Results: There were 136 cases of DLBCL that had adequate material for Onoscan analysis. There were 96 cases (71%) of GCB DLBCL and 40 cases (29%) of ABC DLBCL. Copy number (CN) differences were seen between the two groups with frequent gains of chr 18 (q21.33) (*BCL2*) in ABC DLBCL as compared to GCB DLBCL (50% versus 20%, p=0.00073). In contrast, there were frequent CN gains seen in chr 2 (p16.1) (*REL*) in GCB DLBCL as compared to ABC DLBCL (53% versus 27.5%, p=0.008). CN loss of chr 9 (p21.3) (*CDKN2A, CDKN2B*) was frequently seen in ABC DLBCL versus GCB DLBCL (48% versus 17%, p=0.0004). No significant differences were seen between GCB DLBCL and ABC DLBCL in chromosome regions of chr 17p13.1 (*TP53*, 16% vs 8%), chr 8q24.21 (*MYC*, 30% vs 23%), and chr 9p24.1 (*PDL1/PDL2*, 19% vs 38%).

Figure 1 - 1452
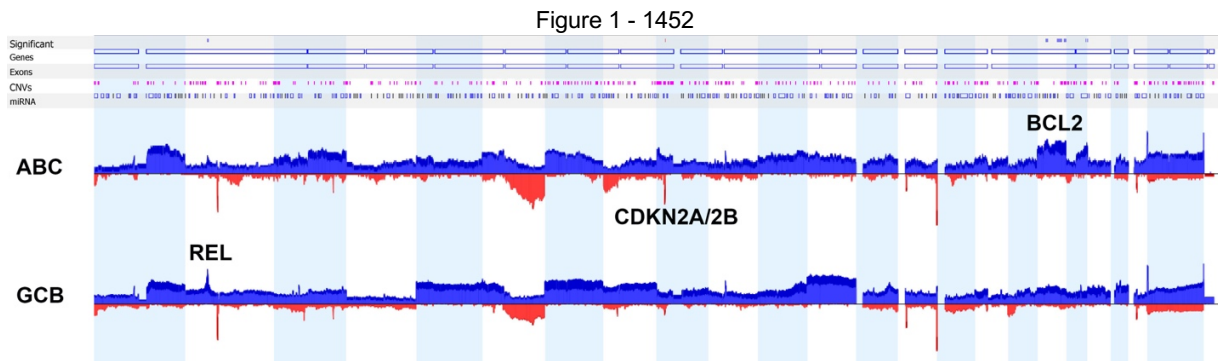
Conclusions: This study further confirms the biologic differences from the genetic standpoint of CNV between GCB DLBCL and ABC DLBCL. While GCB DLBCL has more frequent translocations of *BCL2*, ABC DLBCL have more frequent gains of this gene. We also

found significant differences in the *REL* and *CDKN2A/2B* genes but saw no significant differences in *TP53*, *MYC*, or *PDL1/L2* between the two subtypes.

1453 Utility of Core-Needle Biopsy (CNB) as Initial Diagnostic Sampling Procedure in Patients with Suspected Lymphoma

Solomon Raphael[1], Sridhar Chaganti[2], Bindu Vydianath[3]
[1]University of Abuja, Abuja, Nigeria, [2]Queen Elizabeth Hospital Birmingham, Edgbaston, Birmingham, United Kingdom, [3]University Hospitals Birmingham NHS Foundation Trust Queen Elizabeth Hospital Birmingham, Harborne, Birmingham, United Kingdom

Disclosures: Solomon Raphael: None; Sridhar Chaganti: None

Background: Tissue diagnosis of lymphoma is traditionally made on surgically excised lymph nodes. This diagnosis is to be reached by morphology, immunophenotypic and molecular studies performed on sample, according to the recent WHO classification scheme. CNB which is a cheaper, faster, less invasive and well tolerated procedure relative to surgery, has been shown to be an effective sampling procedure, especially when guided by imaging modality. Consequently, it is increasingly the preferred procedure for obtaining tissue for the diagnostic investigation of patients with suspected lymphoma. We evaluated the diagnostic quality of CNB in patients investigated for suspected lymphoma and examined factors which impact its diagnostic yield in this patients' group.

Design: All suspected lymphoma cases initially investigated by CNB over a 7-years (2012-2018) were studied retrospectively. Pathology and clinical data were collated. The diagnostic adequacy of CNB specimens for lymphoma typing was categorized as fully diagnostic (WHO subtyping/grading with treatment instigated), not fully diagnostic or inadequate (further biopsy requested). The effects of biopsy depth, core diameter, number of cores, total length of cores and histology of the lymphoma on the diagnostic adequacy of the specimens were analyzed.

Results: The study included 501 patients [male: female ratio of 1.2:1, age range (16-96 years), mean (±SD) of 54.9±19.9 years]. Lymphoma was diagnosed in 325 (65%) patients. CNB specimens were fully diagnostic for lymphoma in 263/325, i.e. the diagnostic yield of CNB for lymphoma typing was 81% according to WHO classification. In 38 patients, additional excision biopsy was required to reach a full diagnosis. The length of core tissue and lymphoma subtypes significantly affected the adequacy of CNB acquired specimens. Diagnosing Hodgkin and T-cell lymphoma, and grading follicular lymphoma on CNB specimens was a recurring challenge. Small specimen size and poor sample quality were the main reasons for diagnostic difficulties in the use of CNB specimens in the evaluation of lymphoma.

Conclusions: Our data showed that core needle biopsy has a high diagnostic yield for complete lymphoma subtyping/grading, providing the basis upon which therapeutic decision was taken for a majority of patients. This yield can be optimized through close collaboration between clinicians, radiologists and pathologists.

1454 Utility of Lymphoid Enhancer-Binding Factor -1 (LEF-1) Expression by Immunohistochemistry in Hodgkin Lymphoma and Anaplastic Large Cell Lymphoma

Aishwarya Ravindran[1], Karen Rech[1], Ellen Mcphail[1], Andrew Feldman[1], Paul Kurtin[1], Min Shi[1]
[1]Mayo Clinic, Rochester, MN

Disclosures: Aishwarya Ravindran: None; Karen Rech: None; Ellen Mcphail: None; Andrew Feldman: None; Paul Kurtin: None; Min Shi: None

Background: Hodgkin lymphoma (HL), a B cell-derived neoplasm shows morphologic and phenotypic overlap with anaplastic large cell lymphoma (ALCL), which is T-cell derived. Although there is CD30 expression in both, HL expresses B-lineage specific transcription factor PAX-5 and ALCL is commonly positive for T-lineage associated markers, including cytotoxic markers such as perforin, granzyme and T-cell intracellular antigen 1. However, a few cases of ALCL expressing PAX-5 and HL expressing cytotoxic markers have been reported. Lymphoid enhancer-binding factor (LEF-1) is normally expressed in T-cells and pro-B cells, but absent in mature B-cells. In this study, we explored the utility of LEF-1 expression by immunohistochemistry to distinguish HL and ALCL.

Design: On review of the institutional database, we randomly selected cases with HL and ALCL, confirmed by a combination of morphologic and immunophenotypic criteria. Immunohistochemical studies were performed on paraffin-embedded sections of fresh frozen tissue using antibodies against LEF-1 antigen. LEF-1 nuclear expression in the neoplastic cells was graded as negative, weak (1+), intermediate (2+) or strong (3+) in at least 20% tumor cells. This study was approved by the institutional review board.

Results: Twenty HL cases (16 classic HL and 4 nodular lymphocyte predominant HL) with a median age of 50 years (range: 19-82; 13 male and 7 female) were analyzed. Sixteen (80%) of 20 showed LEF-1 expression (Figure 1 and Table), of which 11 had >75% tumor cells expressing LEF-1 (2+ to 3+), 4 had 51-75% tumor cells expressing LEF-1 (1+ to 3+), and 1 had 20-50% tumor cells expressing LEF-1 (2+). On comparison, 16 ALCL cases (4 ALK+ and 12 ALK-) with a median age of 67 years (range: 13-88; 11 male, 5 female) were analyzed.

Eleven (68.8%) of 16 ALCL cases showed no LEF-1 expression (Figure 2 and Table). The remaining 5 ALCL cases demonstrated LEF-1 expression, of which 1 had >75% tumor cells expressing LEF-1 (3+), 2 had 51-75% tumor cells expressing LEF-1 (1+ to 3+), and 2 had 20-50% tumor cells expressing LEF-1 (2+). Statistical analysis demonstrated significantly increased LEF-1 expression in HL compared to ALCL (P = 0.006).

Table				
Diagnosis	Negative LEF-1 (<20%)	Positive LEF-1 (20-50%)	Positive LEF-1 (51-75%)	Positive LEF-1 (>75%)
HL (N=20)	4	1	4	11
ALCL (N=16)	11	2	2	1

Figure 1 - 1454
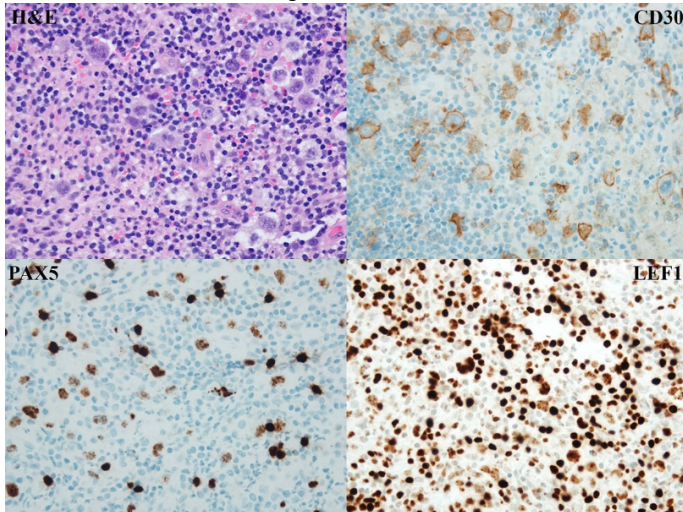
Figure 2 - 1454
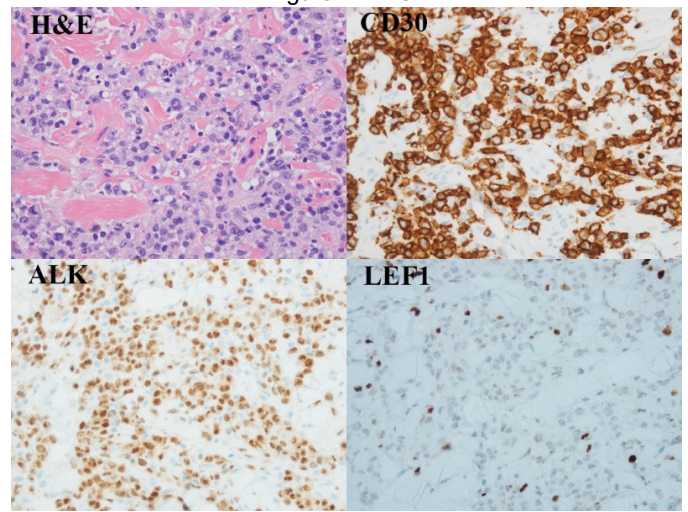
Conclusions: Our study demonstrated increased LEF-1 expression in HL and decreased LEF-1 expression in ALCL. Hence, LEF-1 could possibly serve as an additional marker in distinguishing HL and ALCL with equivocal morphologic and immunophenotypic features.

1455   The Phenotypic Spectrum in Histiocytic Sarcoma and Langerhans Cell Sarcoma Parallels the Developmental Relationships between Monocytes, Macrophages and Dendritic Cells

Aishwarya Ravindran[1], Gaurav Goyal[2], Jithma Abeykoon[1], Gordon Ruan[1], Ronald Go[1], Karen Rech[1]
[1]Mayo Clinic, Rochester, MN, [2]The University of Alabama at Birmingham, Birmingham, AL

Disclosures: Aishwarya Ravindran: None; Gaurav Goyal: None; Jithma Abeykoon: None; Gordon Ruan: None; Ronald Go: None; Karen Rech: None

Background: Histiocytic sarcoma (HS) and Langerhans cell sarcoma (LCS) are rare, aggressive neoplasms of histiocytic or dendritic cell lineage. Their variable and overlapping cytologic and phenotypic features reflect the heterogeneous nature of these diagnostic categories. We aim to expand on the phenotypic characterization of these cases to provide insight into their ontogeny in light of modern understanding of the derivation of these myeloid mononuclear cell populations.
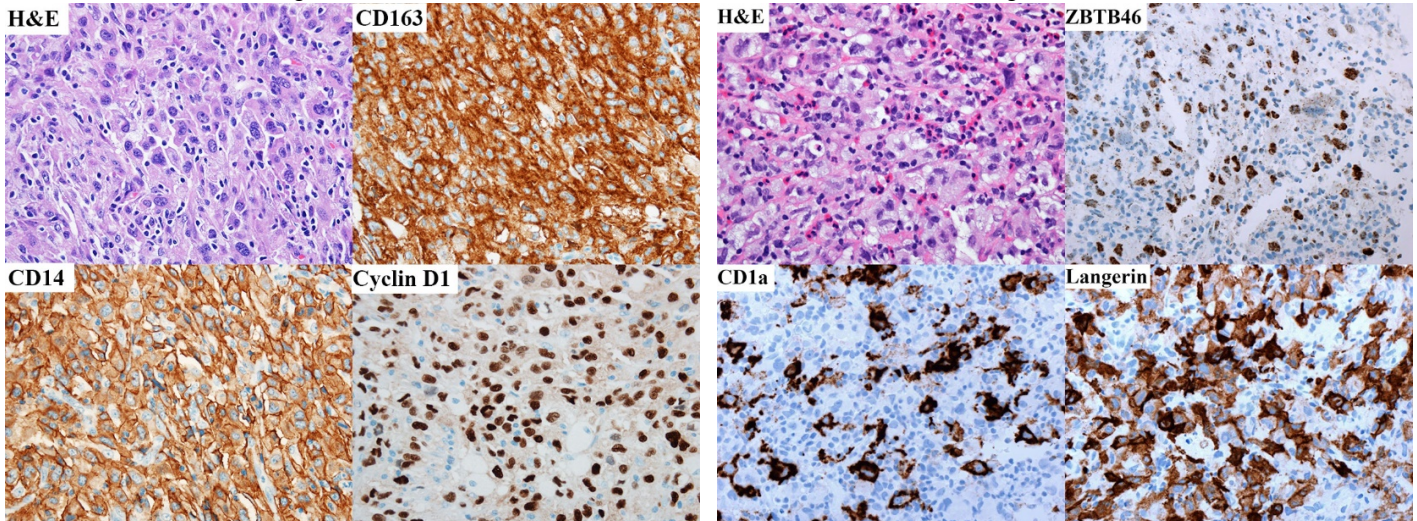
Design: In our institutional database (2002-2018), 10 (HS, LCS) cases had formalin-fixed paraffin embedded tissue for immunohistochemical (IHC) studies. IHC was scored as positive if staining was present in at least 30% of neoplastic cells, unless noted.

Results: Ten patients (5 Male, 5 Female) with median age of 65 years at diagnosis (range: 34-84) were analyzed. Morphologically, both HS (Figure 1) and LCS (Figure 2) cells appear pleomorphic with occasionally oval/folded nuclei, vesicular chromatin with abundant cytoplasm admixed with spindled forms. The cases were categorized into 3 groups based on phenotype (table): monocyte-macrophage (mo-mac; N=5), monocyte-dendritic cell (mo-DC; N=2), and dendritic/Langerhans cell (LCS; N=3). All 10 cases were positive for CD68 and cyclin D1. The mo-mac category included 5 cases with expression of CD163 (100%), CD14 (80%), CD11c (40%), OCT2 (40%), S100 (40%), and were negative for CD1a, Langerin and ZBTB46. The mo-DC category included two cases with expression of CD11c, S100, ZBTB46 and were negative for CD14, CD163, OCT2, CD1a and Langerin. All 3 LCS cases expressed CD11c, S100, CD1a, Langerin, ZBTB46, and were negative for OCT2. One of these LCS cases showed CD1a and Langerin expression in a minor subset (5% of cells). Further, all 3 LCS cases expressed CD14 and CD163, two antigens that are not expressed in benign Langerhans cells or cells of Langerhans cell histiocytosis (LCH). Of the ten cases, one LCS case was positive for *BRAF* V600E by IHC.

	Monocyte-Macrophage lineage; N=5	Monocyte-dendritic cell lineage; N=2	Dendritic/Langerhans cell lineage; N=3
Sites involved (n)	Supraclavicular lymph node (1)	Axillary lymph node (1)	Mesenteric lymph node (1)
	Bone marrow (1)	Soft tissue, chest wall (1)	Bone marrow (1)
	Brain (1)		Soft tissue, groin (1)
	Small bowel (1)		
	Multifocal (1) including small bowel/omentum/ovary		
IHC (n)			
CD68	5/5	2/2	3/3
CD163	5/5	0	3/3
Cyclin D1	5/5	2/2	3/3
CD11c	2/5	2/2	3/3
CD14	4/5	0	3/3
OCT2	2/5	0	0
S100	2/5	2/2	3/3
ZBTB46	0	2/2	3/3
CD1a	0	0	3/3
Langerin	0	0	3/3
BRAF V600E	0	0	1/3

Figure 1 - 1455

Figure 2 - 1455

Conclusions: HS and LCS represent a heterogeneous group of diseases as reflected by the variable phenotype with expression of antigens associated with monocytes, macrophages and dendritic cells. All HS and LCS cases were positive for CD68 and cyclin D1. Useful markers for macrophage lineage include CD163, CD14 and OCT2, whereas dendritic cell lineages can be identified by CD11c, ZBTB46, CD1a and Langerin. Aberrant expression of CD14 and CD163 in Langerhans cell neoplasms may be useful in distinguishing LCS from LCH.

1456 Pathologic Spectrum and Molecular Landscape of Myeloid Neoplasms with FLT3 Mutations

Aishwarya Ravindran[1], Dong Chen[1], Phuong Nguyen[1], Jennifer Oliveira[1], Kaaren Reichard[1], James Hoyer[1], Nikita Mehta[2], Kebede Begna[1], Mark Litzow[1], Aref Al-Kali[1], David Viswanatha[1], Rong He[1]
[1]Mayo Clinic, Rochester, MN, [2]Division of Hematopathology, Mayo Clinic, Rochester, MN

Disclosures: Aishwarya Ravindran: None; Dong Chen: None; Phuong Nguyen: None; Jennifer Oliveira: None; Kaaren Reichard: None; James Hoyer: None; Nikita Mehta: None; Kebede Begna: None; Mark Litzow: None; Aref Al-Kali: None; David Viswanatha: None; Rong He: None

Background: FMS-like tyrosine kinase III (FLT3) mutations are some of the most common mutations seen in acute myeloid leukemia (AML) and portend a poor clinical outcome, particularly in the intermediate cytogenetic risk group. However, the incidence and impact

of *FLT3* mutations in non-AML myeloid neoplasms have not been clearly defined. In this study, we aimed to investigate the pathologic spectrum and molecular landscape of myeloid neoplasms harboring *FLT3* mutations.

Design: Following institutional review board approval, our internal database was screened for cases that had *FLT3* mutations identified using a 35-gene targeted next generation sequencing (NGS) panel. Relevant clinical, laboratory and pathological findings were recorded by medical chart review. Pathologic diagnoses were confirmed based on the 2016 WHO criteria. Survival comparison was performed using Kaplan-Meier survival analysis and log-rank test.

Results: A total of 130 patients harboring *FLT3* mutations were identified from 7/2015-8/2018, with 111 (85%) AML, 14 (11%) myelodysplastic/myeloproliferative neoplasm (MDS/MPN), 4 (3%) T or B-lymphoblastic leukemia/lymphoma, and 1 (0.8%) myelodysplastic syndrome. Of the 14 MDS/MPN patients [9/5, male (M)/female (F), median age 71 years, range 42-90], 12 had internal tandem duplication and 2 had D835 tyrosine kinase domain mutations, respectively. All showed co-occurrence of other mutations (median 4, range 3-8), including *ASXL1, SRSF2, TET2/CBL/RUNX1/SETBP1, GATA2/BCOR/U2AF1, EZH2/IDH1/NRAS/CSF3R* in 11 (79%), 9 (64%), 3 (21%), 2 (14%), and 1 (7%) cases, respectively. Karyotyping was normal in 11/14 with the remaining 3 patients showing del(3)(q21) in 6/20, +13 in 15/20, and del(20q) in 16/16 metaphases. Three of 14 (21%) patients progressed to AML during the course of follow-up. In comparison, 11(13%) of 84 MDS/MPN patients without *FLT3* mutations (54/30, M/F; median age 72 years, range 42-89) progressed to AML. MDS/MPN patients with *FLT3* mutations showed inferior progression-free survival (median 8.4 months, 95% CI: 0.5-26.9 versus 19.2 months, 95% CI: 11.3-30.8, *P*=0.015) and overall survival (median 20 months, 95% CI: 1.2-30.9 versus 34 months, 95% CI: 30.4-36.2, *P*=0.039).

Conclusions: *FLT3* mutations occur predominantly in AML and infrequently in MDS/MPN or MDS. In MDS/MPN, they commonly coexist with normal karyotype and *ASXL1* and *SRSF2* mutations. *FLT3* mutations in MDS/MPN are associated with inferior clinical outcomes and the findings warrant confirmation in larger cohort studies.

1457 Clinicopathologic Characteristics of Hyperhaploid Plasma Cell Neoplasms Identified by CGH Microarray

Bryan Rea[1], Svetlana Yatsenko[2]
[1]University of Pittsburgh School of Medicine, Pittsburgh, PA, [2]University of Pittsburgh Medical Center, Pittsburgh, PA

Disclosures: Bryan Rea: None; Svetlana Yatsenko: None

Background: Plasma cell neoplasms (PCN) can be divided into two subgroups based on chromosomal numerical abnormalities: hyperdiploid and non-hyperdiploid. Among the non-hyperdiploid PCN, the hypodiploid subtype has been associated with a particularly poor prognosis. Hyperhaploid clones are characterized by a catastrophic loss of nearly a haploid set of chromosomes (24-34 chromosomes) followed by a doubling of such chromosome complement, resulting in a karyotype with monosomy, disomy, trisomy, and tetrasomy for various chromosomes. Doubling of near diploid or hyperdiploid clones, resulting in a near tetraploid complement, is associated with an aggressive and treatment resistant PCN. These cases are difficult to identify through locus-targeted FISH studies, and we sought to assess the utility of whole genome microarray analysis to identify and characterize these rare neoplasms.

Design: CGH microarray (Agilent 60K CGH platform) was performed on CD138+ sorted cells in 1176 cases of plasma cell neoplasms as part of routine clinical care in our institution from 2017-2019. Twelve patients with hyperhaploid/near tetraploid clones were identified by a combined evaluation of results of microarray, FISH, and conventional karyotyping. Chart review was completed to identify relevant clinical, laboratory, and survival characteristics.

Results: The 12 cases had a median age of 70.5 years, and the male to female ratio was 7:5. Bone marrow plasma cell count was high, averaging 66%. All cases had additional genetic aberrations. Four cases had IGH rearrangements, with one example each of t(4;14)(IGH/FGFR3), t(14;16)(IGH/MAF), and t(8;14)(IGH/MYC), and with an undetermined partner. Other common abnormalities included 17p deletion (4), 1q duplication (4), and 13q deletion/monosomy 13 (7). 9/12 cases had ISS stage III disease at presentation. Even in the relatively short follow-up period of this study, 7 of 12 patients had died of disease, 4 had persistent disease, and only one patient went into clinical remission. The median survival was 9.2 months.

Case	Age	Gender	Isotype	Light chain	BM PC %	Other abnormalities	ISS stage	Disease Status	Follow-up (months)
1	73	F	IgG	kappa	76	IGH rearrangement; unknown partner, hyperdiploidy 3, 4, 9, monosomy 13, 1q duplication, complex structural abnormalities	III	DOD	2.6
2	62	M	IgA	kappa	97	IGH/FGFR, monosomy 13, 17p deletion, monosomy 12, trisomy 15, complex structural abnormalities	II	DOD	9.2
3	86	M	IgG	kappa	71	trisomy 5,15,21; complex structural abnormalities	III	DOD	1.7
4	58	M	IgG	kappa	28	13q deletion, 1p deletion, monosmy 4, complex structural abnormalities	II	AWD	24.4
5	59	F	IgG	lambda	21	hyperdiploidy, complex structural abnormalities	II	ANED	23.6
6	73	F	IgG	kappa	95	IGH/MAF, 13q deletion, 1p deletion, monosomy 13, complex structural abnormalities	III	DOD	10.4
7	69	M	IgG	kappa	90	complex structural abnormalities	III	DOD	0.9
8	63	F	Free light chain	lambda	86	1q duplication, 13q deletion, 17p deletion, complex structural abnormalities	III	DOD	0.7
9	72	M	Free light chain	lambda	85	IGH/MYC , 17p deletion, 1q duplication, monosomy 13, complex structural abnormalities	III	AWD	12.0
10	79	F	IgG	lambda	45	Hyperdiploidy, complex structural abnormalities	III	AWD	13.3
11	61	M	IgG	kappa	30	Trisomy 5,15,21, monosomy 13, monosomy 17, complex structural abnormalities	III	DOD	7.8
12	72	M	IgG	lambda	65	1q duplication, 16q deletion	III	AWD	7.7

Clinicopathologic Characteristics of 12 Hyperhaploid Plasma Cell Neoplasm Patients

BM PC: Bone marrow plasma cell; DOD: Died of disease; AWD: Alive with disease; ANED: Alive no evidence of disease

Conclusions: Hyperhaploid and near tetraploid clones demonstrate distinct abnormal genomic profiles revealed via microarray testing, enabling a successful diagnosis of these rare PCN entities. Hyperhaploid PCNs are associated with multiple additional poor prognostic cytogenetic abnormalities, leading to a very poor (9.2 months) median survival. Further studies may provide new insights into biology, clinical prognosis, and treatment approaches of hyperhaploid PCNs.

1458   Clinicopathologic Characteristics of Myeloid/Lymphoid Neoplasms with PDGFRB Rearrangement: A Bone Marrow Pathology Group (BMPG) Study

Heesun Rogers[1], Caroline Astbury[2], Farah El-Sharkawy Navarro[3], Sam Sadigh[4], Jennifer Morrissette[5], Megan Parilla[6], Angela Lager[6], Kristin Karner[7], Daniel Babu[8], Olga Weinberg[9], Adam Bagg[3], Daniel Arber[6], Tracy George[7], M. Kathryn Foucar[8], Robert Hasserjian[10], Eric Hsi[1]

[1]Cleveland Clinic, Cleveland, OH, [2]Cleveland Clinic, Westlake, OH, [3]University of Pennsylvania, Philadelphia, PA, [4]MGH, Boston, MA, [5]Perelman School of Medicine, University of Pennsylvania, Philadelphia, PA, [6]The University of Chicago, Chicago, IL, [7]University of Utah, Salt Lake City, UT, [8]University of New Mexico, Albuquerque, NM, [9]Children's Hospital Boston, Boston, MA, [10]Massachusetts General Hospital, Harvard Medical School, Boston, MA

Background: Myeloid/lymphoid neoplasms (M/LN) with *PDGFRB* rearrangement (R), located in chromosome 5q32, are very rare disorders and a new diagnostic category in WHO classification. Various myeloid neoplasms including myeloproliferative neoplasm (MPN), myelodysplastic syndrome (MDS)/MPN, and acute leukemia, and B or T lymphoblastic leukemia (LL)/lymphoma have been reported with *PDGFRB-R* but most are reported as case reports or very small series. We aimed to better describe the clinicopathologic features of patients with *PDGFRB*-R in a multi-institutional study.

Design: Pathologic and clinical characteristics of archival patients from BMPG institutions were collected and described herein.

Results: 17 patients with *PDGFRB* rearrangement (11 myeloid neoplasm (MN) and 6 LL) were included. The patients were male dominant and often present with leukocytosis, anemia and thrombocytopenia. MN patients presented with a median age of 52 years, often with eosinophilia (54%; median 2590/uL) and monocytosis (45%; median 1200/uL). MN patients comprised 7 MPN, 2 MDS and 2 MDS/MPN. Bone marrows (BM) showed hypercellularity, eosinophilia, abnormal eosinophils (27%), mildly increased blasts (median 2.8%) and dysplasia (36%). Myelofibrosis and extramedullary hematopoiesis were noted in 33% of MN patients.

In comparison, LL patients (4 B-LL and 2 T-LL) were young (median 22 years), had increased BM blasts (median 74%) and lacked eosinophilia and monocytosis. 16 M/LN patients were positive by *PDGFRB* FISH. 1 MN patient was negative by FISH but positive in *G3BP1-PDGFRB* by RNA fusion assay. 2 patients showed fusion partners with *RABEP1* and *ETV6*. All 8 patients who performed sequencing had additional mutations. Karyotype showed various translocations with breakpoints 5q31-5q33 including 5q abnormalities, t(5;12), t(5;16), t(5;17) and t(5;16;17) in 13 M/LN patients. 2 patients had both MN and T-lymphoblastic lymphoma either at the same time or later. 94% of M/LN patients received various therapies. 72% of MN and 50% of LL patients received TK inhibitors (TKI). Among them, 87% of MN and 66% of LL patients showed responses. Overall, 72% of MN and 83% of LL patients were alive with median followup of 18 and 35 months, respectively.

Conclusions: M/LN with *PDGFRB* rearrangement have heterogeneous clinicopathologic features. LL patients present in younger patients while MN patients are older. Only rare patients manifest with both myeloid and lymphoid components. Clinical outcomes appear favorable in patients receiving TKIs.

1459 Role of Chromosomal Microarrays in the Evaluation of Myelodysplastic Syndromes: A Single Institution Experience

Vinay Sakaleshpura Mallikarjuna[1], Sahar Matloob[2], Jianming Pei[2], Jacqueline Talarchek[2], Sahar Poureghbali[3], Essel Dulaimi Al-Saleem[4], Henry Fung[2], Mariusz Wasik[2], Joseph Testa[2], Reza Nejati[5]
[1]Fox Chase Cancer Center, Bensalem, PA, [2]Fox Chase Cancer Center, Philadelphia, PA, [3]Norfolk, VA, [4]Fox Chase Cancer Center, Plymoth Meeting, PA, [5]TUHS-Fox Chase Cancer Center, Philadelphia, PA

Background: Morphological and cytogenetic studies are currently used as standard methods to diagnose and genetically subclassify Myelodysplastic syndromes (MDS). Notably, MDS can also be identified in the presence of a defining cytogenetic abnormality without any morphological evidence of dysplasia. High-resolution single-nucleotide polymorphism (SNP)-based chromosome microarrays (CMA) permit the precise identification of clinically significant submicroscopic copy number alterations (CNAs) and copy neutral Loss of Heterozygosity (cnLOH) that cannot be detected by standard methods including conventional cytogenetics and fluorescence-in-situ (FISH) analysis. However, the guidelines for using CMA as a diagnostic tool in evaluating MDS are not well defined. In this study, we assessed the frequency of CNAs and cnLOH by SNP-based CMA in patients with MDS and correlated these findings with clinicopathological features and results of karyotyping and FISH.

Design: The pathology case database was searched for bone marrow biopsies diagnosed as MDS that had SNP-based CMA performed between 2014 and 2018. All cases were re-reviewed by a hematopathologist, and 86 cases were selected for the study. The patients' clinicopathological data were reviewed and correlated with CMA data.

Results: Chromosomal alterations were identified in 32 out of 86 cases (38%) by conventional cytogenetics, whereas CMA demonstrated chromosomal aberrations in 54 cases (63%). Furthermore, CMA demonstrated additional subtle abnormalities in 19 out of the 32 patients (59%) with abnormal karyotypes. Unexpectedly, cnLOH was the most common recurrent alteration (24%), followed by complex chromosomal abnormalities (21%) (Table 1). Standard FISH panel detected abnormalities in 6 of 13 cases (46%) in which FISH analysis was performed. CMA identified all of the abnormalities detected by FISH, but also additional abnormalities in all 6 patients. In addition, molecular profiling, which was done in 40 cases, showed mutations in *SFRB1*(13%), *TET2* (10%), *ASXL1* (10%), *TP53* (10%), *SRSF2* (7%), *IDH1/IDH2* (7%), *U2AF1* (7%), *EZH2* (5%), *NRAS* (5%) and *RUNX1* (3%).

Abnormalities detected by CMA	del (5q)	-7 or del(7q)	+ 8	del(20q)	-Y	Complex abnormalities (> 3)	cnLOH
No. of patients (%)	12 (14%)	10 (12%)	10 (12%)	8 (9%)	7 (8%)	18 (21%)	21 (24%)

Conclusions: Our data demonstrate the high diagnostic yield of CMA in MDS, as it uncovered chromosomal abnormalities in a significant number of karyotypically normal cases. In particular, cnLOH frequency is high in MDS and can be missed by conventional karyotyping and FISH studies. Additional aberrations detected by CMA may add to prognostication and have potential implications in precision medicine.

1460 Peripheral T cell Lymphoma (PTCL)-NOS with T Follicular Helper (TFH)-cell Phenotype Tends to Behave Better than Their Non-TFH Counterpart

Ali Sakhdari[1], Narittee Sukswai[2], L. Jeffrey Medeiros[2]
[1]University Health Network, University of Toronto, Toronto, ON, [2]The University of Texas MD Anderson Cancer Center, Houston, TX

Disclosures: Ali Sakhdari: None; Narittee Sukswai: None; L. Jeffrey Medeiros: None

Background: PTCL comprises less than 15% of non-Hodgkin lymphomas in the United States. The recent WHO classification has proposed a new category of nodal lymphoma with TFH-cell phenotype, which is further subclassified into three main entities: angioimmunoblastic T cell lymphoma (AITL), follicular T-cell lymphoma (T-FL) and TFH-PTCL-NOS. Although these lymphomas arise from lymph-node resident TFH cells, little is known about prognosis of patients with different types of TFH-PTCL or if it is different from other non-TFH-PTCL. In this study, we evaluated the probability of survival among different types of TFH-PTCL and compared it with non-TFH-PTCL.

Design: We identified a total of 54 patients with treatment-naive PTCL (AITL, n=21; PTCL-TFH, n=8; non-TFH-PTCL-NOS, n=25). ALCL (both ALK-positive and ALK-negative) patients were excluded from PTCL-NOS group. The overall survival was assessed among the cases of the cohort.

Results: The study cohort included 36 men (m) and 18 women (w) [AITL, m=10, w=11; PTCL-TFH, m=3, w=5; PTCL-NOS, m=23, w=2; p=0.0004]. The median (med) age at diagnosis was 59 years (range: 24 to 87) [AITL, med=60 (40-81); PTCL-TFH, med=70 (36-87); PTCL-NOS, med=57 (24-85); p=ns]. Median follow-up for the entire cohort was 12.2 months (range: 0.2 to 80). The median survival for PTCL-TFH patient did not reach while this was 47 and 17 months for AITL and PTCL-NOS respectively (p=0.07). (Figure 1)

Figure 1 - 1460
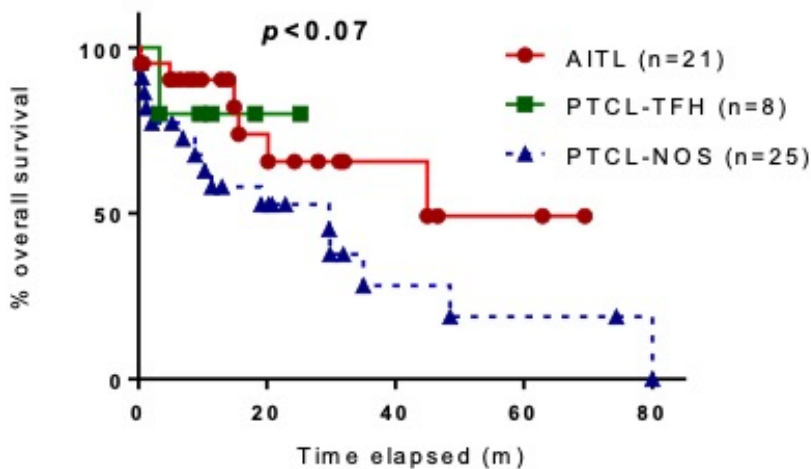
Conclusions: PTCL-NOS with TFH phenotype shows a better prognosis than the non-TFH counterpart. The latter show a dramatic predilection for male. Among PTCL with TFH phenotype, it seems that bona fide AITL histology tends to behave more aggressively.

1461   9p24.1/PDL1 Amplification and Checkpoint Molecule Expression in T-Cell Lymphomas

Sajad Salehi[1], Yi-Hua Chen[1], Xinyan Lu[2], Juehua Gao[1], Andrew Alexander[3], Amir Behdad[3], Qing Chen[3]
[1]Northwestern Memorial Hospital, Chicago, IL, [2]Chicago, IL, [3]Northwestern University Feinberg School of Medicine, Chicago, IL

Disclosures: Sajad Salehi: None; Yi-Hua Chen: None; Xinyan Lu: None; Juehua Gao: None; Andrew Alexander: None; Amir Behdad: *Speaker*, Pfizer; *Consultant*, Bayer/Loxo; *Consultant*, Thermo Fisher; Qing Chen: None

Background: T-cell lymphomas encompass a heterogeneous group of lymphoid malignancies. Patients with T-cell lymphomas have variable clinical outcome and response to therapy. Antibodies targeting PD1 and its ligands PDL1 have shown remarkable clinical efficacy in a wide range of malignancies, but its efficacy in T-cell lymphomas has not been fully explored. Reliable biomarkers for predicting anti-PD1 response are needed. Recent studies have found 9p24.1/*PDL1* amplification as a promising biomarker. Here we examine the prevalence of *PDL1* amplification in a group of T and NK-cell lymphomas, and explore the rationale and mechanisms for targeting the PD1/PDL1 pathway in the treatment of T-cell lymphomas.

Design: We studied 39 patients, 14 with peripheral T-cell lymphoma (PTCL), 12 with ALK- anaplastic large cell lymphoma (ALCL), 7 with ALK+ ALCL, and 6 with NK/T-cell lymphoma (NKTCL, 3 EBV+ and 3 EBV-). 9p24.1/*PDL1* amplification was evaluated by FISH analysis using probes targeting PDL1 and a region centromeric to PD-L2. Expression of PD1, PDL1 and LAG3 was studied by immunohistochemistry.

Results: 9p24.1/*PDL1* amplification was identified in 9 of 39 cases (23%), including 5/14 (36%) PTCL, 3/12 (25%) ALK- ALCL, and 1 EBV-NKTCL. 8/9 cases with *PDL1* amplification had strong PDL1 expression by IHC; but most of the strong PDL1+ cases, including all the ALK+ ALCL and EBV+ NKTCL, lacked *PDL1* amplification, indicating other mechanisms are involved in PDL1 upregulation in these tumors. PD1 was expressed by a subset of PTCL, but not by ALCL or NKTCL. LAG3 is another important checkpoint molecule and a new target for immunotherapy. We found high level LAG3 expression in 4/14 PTCL tumor cells, 3 of which had *PDL1* amplification. LAG3+ background T-cells were found in most of the cases, some quite numerous.

Conclusions: A significant subset of T-cell lymphomas harbor 9p24.1/*PDL1* amplification, with the highest prevalence in PTCL. Our data suggest that *PDL1* amplification is a major genetic mechanism for PDL1 expression and evasion of anti-tumor immunity in a subset of T-cell lymphomas. Additionally LAG3 is strongly expressed in some of the *PDL1* amplified PTCL. It is conceivable that PD1 or combined PD1/LAG3 blockade may be particularly effective in this subset of T-cell lymphomas. Given the recent evidence indicating a positive correlation between *PDL1* amplification and durable response to PD1 blockade, it may be imperative to examine 9p24.1/*PDL1* amplification in patients who may benefit from checkpoint inhibitors.

1462   SETD8 Staining in Plasma Cell Myeloma is Associated with Tumor Aggressiveness

Christian Salib[1], Samir Parekh[1], Julie Teruya-Feldstein[2]
[1]Icahn School of Medicine at Mount Sinai, New York, NY, [2]Mount Sinai Icahn School of Medicine, New York, NY

Disclosures: Christian Salib: None; Samir Parekh: None; Julie Teruya-Feldstein: None

Background: Plasma cell myeloma (PCM) is a malignant neoplasm of clonal plasma cells with clinical and genetic heterogeneity. While prognosis is favorable in most cases, 10-15% of patients face dismal survival rates while on intensive chemotherapeutic regiments. Current guidelines recommend FISH-based testing for chromosomal aberrations to assess risk status, though FISH for PCM may have 20-30% QNS rates. In such cases, a substitute method must utilized for risk stratification.

One alternative is the *SETD8* gene, which encodes a histone-lysine N-methyltransferase responsible for mono-methylation of histone H4, as well as non-histone proteins, such as P53. *SETD8* mRNA over-expression correlated with worse prognosis in >700 newly diagnosed PCM patients analyzed in CoMMpass, a longitudinal genomic study. RNA-seq also elucidated an association between *SETD8* RNA expression and CCND1 or MAF translocated patients.

To date, there are currently no studies evaluating correlation between SETD8 protein expression level in primary PCM, underlying genetic composition and outcomes.

Design: FFPE bone marrow biopsies from 60 in-house PCM cases were evaluated for SETD8 protein expression by IHC (Table 1). SETD8 optimal antibody titration was determined by assessing thyroid and tonsil tissue controls, including a positive cell line control (OPM2). Stained slides were evaluated by 2 blinded hematopathologists for staining pattern (nuclear, cytoplasmic, both or neither) and compared with translocation t(11;14), t(14;14), 17P loss and P53 mutation data obtained from targeted NGS studies.

Results: 1.56 out of 60 cases (93%) are SETD8 positive, with various staining patterns (Fig. 1) 2. SETD8 protein expression is higher in cases with TP53 and 17p alterations than those without (82.5% vs. 62.5%)

3. Presence of t(11;14) translocation shows preferential SETD8 nuclear staining (68%) than those cases without the translocation (8%) (Fig. 2)

Table 1. Result summary of SETD8 IHC staining of 60 plasma cell myeloma cases with their corresponding genetic alterations								
		Molecular				**FISH**		
		TP53	17p	TP53+17p	None	t(14;16/20)	t(11;14)	None
	AVERAGE	10	13	6	31	11	25	25
SETD8	67.3	56.5	69	82.5	62.5	70.5	60	73
%N (n)	57.4 (35)	5 (5)	50 (7)	66.7 (4)	58.1 (18)	72.7 (8)	68 (17)	40 (10)
%C (n)	4.9 (3)	0 (0)	7.1 (1)	0 (0)	6.5 (2)	0 (0)	8 (2)	4 (1)
%N+C (n)	31.1 (19)	3 (3)	28.6 (4)	33.3 (2)	32.3 (10)	27.3 (3)	16 (4)	48 (12)
%Negative (n)	6.6 (4)	2 (2)	7.1 (1)	0 (0)	3.2 (1)	0 (0)	8 (2)	8 (2)
%BM Cellularity	48.8	46.3	53.2	53.8	46.7	62.1	50	48.8
%BM Plasma	39.3	34	41.5	63.8	24.4	31.2	23.5	39.4
Age (y)	66.2	74.9	65.1	56.7	56.6	66.3	67.1	65.4
Gender (M/F)	32/29	4/6	8/6	4/2	16/15	4/7	15/10	13/12

Figure 1 - 1462
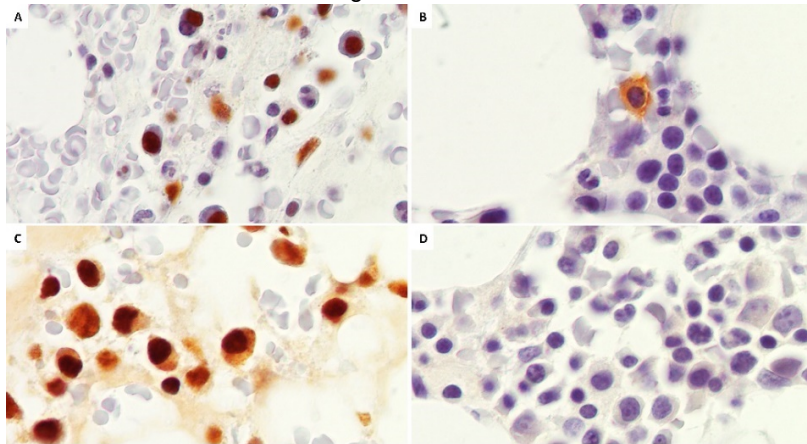
Figure 1. Immunohistochemical staining pattern of SETD8 showing (A) nuclear, (B) cytoplasmic, (C) nuclear & cytoplasmic and (D) negative staining.

Figure 2 - 1462
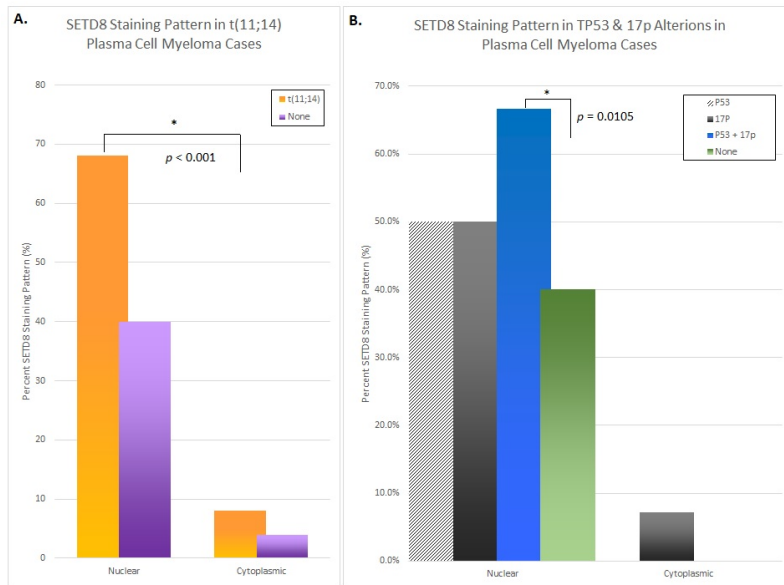
Figure 2. A. Comparison of SETD8 staining pattern shows preferential nuclear staining in cases with t(11;14) translocation than those cases without the alteration. B) Similar SETD8 preferential nuclear staining pattern is seen in cases with TP53 or 17p alterations, with significantly higher staining in cases with *concurrent* P53 & 17p alterations.

Conclusions: SETD8 is overexpressed in PCM and shows staining pattern differences. SETD8 (nuclear) IHC staining pattern correlates with t(11;14) translocation. SETD8 protein expression is significantly higher in cases with TP53 and 17p aberrations. Small molecule inhibitors are being evaluated to overcome the aberrant epigenetic regulation of histone and non-histone (ie. TP53) proteins by SETD8.

1463 Comparison of SPE, IFE, and FLC in Monitoring Patients with Multiple Myeloma after Autologous Stem Cell Transplantation: A Review of 105 Cases

Sandra Sanchez[1], Marines Faya[2], Humberto Torres[3], Nicole Osorio[4], Lazaros Lekakis[5], Taban Ghaffaripour[6], Jennifer Chapman[7], Julio Poveda[8], Yi Zhou[9], Chris Wunsch[2]

[1]University of Miami/Sylvester Cancer Center, Miami, FL, [2]Miami, FL, [3]Hialeah, FL, [4]University of Miami, Davie, FL, [5]University of Miami Miller School of Medicine, Sylvester Cancer Center, Miami, FL, [6]University of Miami Health System, Miami, FL, [7]University of Miami, Miller School of Medicine, North Miami, FL, [8]University of Miami, Miller School of Medicine, Miami, FL, [9]University of Miami, Miami, FL

Disclosures: Sandra Sanchez: None; Marines Faya: None; Humberto Torres: None; Nicole Osorio: None; Lazaros Lekakis: None; Taban Ghaffaripour: None; Jennifer Chapman: None; Julio Poveda: None; Yi Zhou: None; Chris Wunsch: None

Background: Conventionally, serum protein electrophoresis (SPE) and serum immunofixation electrophoresis (IFE) are used as primary methods to diagnose and monitor multiple myeloma (MM). Recently, serum-free light chain (FLC) assay has been incorporated into hematological screening programs for myeloma. The purpose of this study is to compare the performance of the three methods in monitoring MM patients after autologous stem cell transplantation (ASCT).

Design: We studied a well-characterized cohort of 105 patients with MM who underwent ASCT. As a part of disease's monitoring process, we reviewed and analyzed the available results of SPE, serum IFE and serum FLC assay to compare which of the three methods is more sensitive in the detection of relapse of the disease.

Results: Of the 105 patients median age 61 (35-77), and with a male to female ratio 63:42 who had undergone ASCT, ninety-four (90%) had relapsed. At relapse onset, mean of 3.6 months (0.5-57). IFE test was positive in all patients (100%), SPE was positive in seventy-two patients (76.6%), and the FLC assay was abnormal in sixty-six patients (70.2%). Among the ninety-four patients who had relapsed, eighty-four patients (89.4%) showed a constant isotype, three patients (3.2%) showed a changed isotype, and seven patients (7.4%) showed a second isotype; out of those three had a second clonality that was most probably induced by Daratumumab therapy and the four patients showed a biclonal gammopathy.

Table 1: Characteristics and performance of SPE, IFE and FLC assay in MM patients who relapsed after ASCT

Total cases=105	
Group 1	**N=32**
IFE positive	30.5%
SPE (peak present)	0.40(0.05-2.15)g/dL
NORMAL FLC ratio 0.26 - 1.65	0.91(0.08-1.60)
Group 2	**N=40**
IFE positive	38%
SPE (peak present)	0.69(0.04-3.06) g/dL
FLC ratio(<0.26)	N=10(25%) 0.04(0.00-0.11)
FLC ratio(>1.65)	N=30(75%)
Group 3	**N=11**
IFE negative	10.5%
SPE negative	PEAK NOT PRESENT
FLC ratio(<0.26)	1(9%) 0.14
FLC ratio(>1.65)	10(91%) 8.74(2.02-40.58)
Group 4	**N=15**
IFE positive	14.3%
SPE (negative)	PEAK NOT PRESENT
FLC ratio(<0.26)	4(27%) 0.05(0.00-0.17)
FLC ratio(>1.65)	11(73%) 15.07(1.84-58.01)
Group 5	**N=7**
IFE positive	7%
SPE (negative)	PEAK NOT PRESENT
NORMAL FLC ratio 0.26 - 1.65	0.92(0.38-1.37)

Conclusions: Our results indicate that the sensitivity of IFE is much higher than SPE and FLC assay in detection of relapse. The positivity of IFE is independent of a normal or abnormal FLC ratio, since some of the patients with normal FLC ratio showed a positive IFE. Additionally, the changed isotypes that we found in some patients are probably not recurrence but rather oligoclonal reconstitution, a positive prognostic finding in this group.

1464 A Population-Based Study Identifies Novel Variants for Myelodysplastic Syndrome Associated Genes

Iman Sarami[1], Diane Smelser[1], Adam Cook[1], Jeremy Haley[1], Joseph Vadakara[1], Yi Ding[1], David Carey[2]
[1]Geisinger Medical Center, Danville, PA, [2]Geisinger, Danville, PA

Disclosures: Iman Sarami: None; Diane Smelser: None; Adam Cook: None; Jeremy Haley: None; Joseph Vadakara: None; Yi Ding: None; David Carey: None

Background: Large-scale genetic analyses linked to electronic health records (EHRs) have the potential to provide insight into gene-disease associations. MyCode biobank has generated a database of >92,000 whole-exome sequences linked to clinical phenotypes derived from EHR data. In this study, we investigated genetic variants and related phenotypes for genes associated with myelodysplastic syndrome (MDS).

Design: We identified MDS patients and control population using accepted clinical criteria and EHR data. Rare coding variants (minor allele frequency < 0.0005) in *ASLX1*, *DNM3A*, *TET2*, *SF3B1*, *RUNX1*, and *SRSF2* were identified using exome sequence data from 92,450 adult MyCode participants.

Results: Ninety-three rare variants (46 predicted loss of function [pLOF] and 47 missense) were identified in at least one individual with MDS. Of 347 MDS cases, 96 (28%) harbored a rare coding variant in one of these genes (Table 1). The most common was *TET2* (36 cases) and the least common was *SRSF2* (1 case). The types of MDS-associated variants varied among the genes: of 28 *ASXL1* variants 24 were pLOFs; of 17 DNMT3A variants only 2 were pLOFs; of 6 *SF3B1* variants all were missense. Twenty percent of carriers of variants identified in MDS cases had a diagnosis of MDS. This also varied by gene, from 50% for *SRSF2* (1 of 2 carriers) to 9% for *RUNX1* (6 of 68 carriers). Carriers of these variants with an MDS diagnosis were older than those without a diagnosis (means of 73 years for cases and 59 years for non-cases, $P < 0.0001$), and more likely to be male (57% of cases vs. 39% in the study cohort, $p < 0.0001$). Mean hemoglobin levels of variant carriers without an MDS diagnosis were lower than non-carriers (13.2 g/dl vs 13.4 g/dl, $p = 0.02$). This effect was more pronounced in males (13.4 g/dl vs 14.1 g/dl, $p = 0.0003$).

Gene	Variant Carriers		Sex		Mean Age*		p
	Total # MDS Cases (n=358) (% of total cases)	Total # Control population (n=89710) (% of total controls)	Total # MDS Cases - Male (% of cases with variant)	Total # Control population - Male (% of controls with variant)	Cases (sd)	Controls (sd)	
ASXL1	30(8.4)	100(0.11)	21(70)	56(56)	74.4(±10.5)	65.1(±19.1)	0.001
DNMT3A	17(4.7)	88(0.1)	7(41.2)	32(36.4)	75.7(±10.1)	71.7(±17.1)	0.2083
TET2	36(10.0)	104(0.12)	19(52.8)	40(38.5)	76.7(±9.1)	63.7(±20.9)	<0.0001
SF3B1	6(1.7)	24(0.03)	6(100)	15(62.5)	82.2(±6.5)	82.5(±9.7)	0.9422
RUNX1	6(1.7)	62(0.07)	4(66.7)	19(30.6)	82.5(±7.6)	55.5(±19.7)	<0.0001
SRSF2	1(0.3)	1(0.001)	0(0)	1(100)	56.2(N/A)	73.2 (N/A)	(N/A)
Total	96(26.8)	379(0.4)	57(59.4)	163 (43.0)	74.6(±8.8)	68.6(±8.5)	<0.0001
*Current age or age at death							

Conclusions: This study identifies potential pathogenic variants in genes previously associated with MDS in a clinical population that was not selected for cancer or hematologic traits. These findings can provide estimates of the prevalence and disease penetrance of clinically relevant variants. Several of the variants observed in MDS cases were novel, and most were not previously reported in clinical databases as pathogenic for MDS. In this clinical population, we observed a greater genetic risk of MDS in males. Our results also suggest that some carriers of these variants might develop MDS in the future and could benefit from enhanced monitoring for early-stage disease.

1465 Primary Cutaneous Methotrexate-Associated B-cell Lymphoproliferative Disorders Other Than EBV-Positive Mucocutaneous Ulcer: Clinical, Pathological, and Immunophenotypic Features

Akira Satou[1], Shogo Banno[2], Kei Kohno[3], Taishi Takahara[1], Emiko Takahashi[4], Shigeo Nakamura[5], Toyonori Tsuzuki[2]
[1]Aichi Medical University Hospital, Nagakute, Japan, [2]Aichi Medical University Hospital, Nagakute, Aichi, Japan, [3]Nagoya University Hospital, Nagoya, Japan, [4]Nagakute, Aichi, Japan, [5]Nagoya University Hospital, Nagoya-shi, Japan

Disclosures: Akira Satou: None; Shogo Banno: None; Kei Kohno: None; Taishi Takahara: None; Emiko Takahashi: None; Shigeo Nakamura: None; Toyonori Tsuzuki: None

Background: Methotrexate (MTX)-associated B-cell lymphoproliferative disorders (B-LPD) may first present in the skin. EBV+ mucocutaneous ulcer (EMCU) is now a well-known disease listed in the 2017 WHO classification; however, only a small number of cases of primary cutaneous MTX (pcMTX) B-LPD of non-EMCU type has been reported, and the clinicopathological characteristics remain unknown. Here, we retrospectively analyzed eight cases of pcMTX B-LPD of non-EMCU type.

Design: A total of 75 patients with MTX B-LPD were retrieved. Among them, cases presenting with only skin (epidermis, dermis, and subcutis) lesion were considered primary cutaneous lesions. Based on clinical and pathological findings, eight cases were classified as pcMTX B-LPD of non-EMCU type, and were retrospectively investigated for this study.

Results: The clinical and pathological features of the eight cases are summarized in Table 1. The three men and five women had a median age of 76 years (range, 54-83). One patient had B symptoms, and none had bulky masses. Information on macroscopic findings was available in six cases; five and one had nodules and plaque, respectively. Histologically, three cases showed a polymorphic pattern, and five showed a monomorphic pattern. Immunohistochemically, all eight cases were consistently positive for CD20, and one case with monomorphic pattern showed positivity for CD5. Only three of the eight cases expressed EBERs on the tumor cells. Tumor cells of the other five cases were negative for EBER, but scattered EBV-infected B-cells were detected in one case. After the diagnosis of pcMTX B-LPD, MTX was immediately withdrawn in seven cases (3 EBV+ and 4 EBV- cases). All seven showed spontaneous regression (SR), and none experienced relapse. The patient with CD5 positivity received R-CHOP chemotherapy as the initial treatment. This patient achieved a CR after the initial treatment, but eventually experienced disease relapse resulting in death.

Case No.	Sex/Age	Subtype	EBV status (tumor cells)	Skin Lesions	Treatment	Response	Recurrence	Status (months)
				Table 1. Clinical and Pathological Features of pcMTX B-LPD				
1	M/78	poly	pos	Multiple nodules on lower leg	MTX off	CR	No	D- 32
2	M/74	mono	pos	Solitary tumor on buttock	MTX off	CR	No	A- 16
3	F/72	poly	pos	Solitary nodule on thigh	MTX off	CR	No	A- 64
4	F/79	poly	neg	Two nodules on lower leg	MTX off	CR	No	A- 93
5	M/77	mono	neg	Multiple nodules on lower leg	MTX off	CR	No	A- 50
6	F/74	mono	neg	Solitary plaque on lower leg	MTX off	CR	No	A- 34
7	F/83	mono	neg	Multiple tumor on arm, chest	MTX off	CR	No	A- 101
8	F/54	mono (CD5+)	neg	Multiple nodules on chest, thigh	R-CHOP	CR	Yes	D+ 129

A-, alive without disease; CR, complete response; D-, died of causes unrelated to lymphoma, D+, died of lymphoma; F, female; M, male; mono, monomorphic; MTX, methotrexate; neg, negative; poly, polymorphic; pos, positive

Conclusions: The results showed that, with the exception of the patient with CD5 positivity, all patients with pcMTX B-LPD of non-EMCU type showed SR regardless of EBV positivity and had an excellent clinical course without relapse. Therefore, we conclude that most cases of pcMTX B-LPD of non-EMCU type can be treated simply by cessation of MTX similar to EMCU, and cytotoxic therapies are not needed.

1466 The Use of Multiparametric Flow Cytometry to Measure Residual Neoplastic Plasma Cells in Harvested Products Collected with and without Bortezomib Prior to Autologous Stem Cell Harvest for Multiple Myeloma

Venkata Sethapati[1], Alec Britt[2], Joseph McGuirk[2], Sunil Abhyankar[2], Leyla Shune[2], Tara Lin[2], Milind Phadnis[2], Mark Cunningham[2], Wei Cui[3], Janet Woodroof[4], Siddhartha Ganguly[5]

[1]KUMC, Kansas City, KS, [2]University of Kansas Health System, Kansas City, KS, [3]University of Kansas Medical Center, Shawnee, KS, [4]Kansas University Medical Center, Shawnee, KS, [5]University of Kansas Health System, Westwood, KS

Disclosures: Venkata Sethapati: None; Alec Britt: None; Leyla Shune: None; Milind Phadnis: None; Mark Cunningham: None; Wei Cui: None; Janet Woodroof: None; Siddhartha Ganguly: *Speaker*, Seattle Genetics

Background: Multiparametric Flow Cytometry (MFC) has been used in bone marrow samples to determine minimal residual disease (MRD) status with a high sensitivity. High dose chemotherapy followed by autologous stem cell transplant (ASCT) is the standard of care for patients with newly diagnosed transplant eligible patients with multiple myeloma (MM). Residual neoplastic plasma cells in the harvested stem cell product may lead to poor disease-free survival. Various techniques have been used to measure contaminating plasma cells in the graft including PCR based techniques which requires the knowledge of the original IgH chain gene rearrangement sequencing. We used MFC as a means to assess tumor cell contamination with or without Bortezomib prior to stem cell collection.

Design: 101 patients with MM treated with novel therapy prior to ASCT were randomly assigned to a control or treatment cohorts. The control group underwent standard of care stem cell collection. The treatment group received bortezomib injections for attempted in vivo purging on days -11 and -8, and G-CSF on days -4 through -1. Patients underwent stem cell harvest on day 0, and MFC was used to measure MRD in the harvested products.

Results: 101 patients with MM were included. There were 51 patients in the control arm and 50 patients in the treatment arm. Of the 101 patients, 24 (23.7%) had residual neoplastic multiple myeloma cells in the harvested products detected by MFC (MRD+). Eleven (22%) of the control group and 13 (26%) of the treatment group were MRD+, showing no significant difference in contamination rates in between the groups (p=0.6) (table 1). International Myeloma Working Group (IMWG) response criteria was used to determine status at ASCT: Complete remission (CR), very good partial remission (VGPR), partial remission(PR) and progressive disease(PD). MRD+ cases in combined CR

and VGPPR was 12% and combined PR and PD was 60% showing correlation between disease status at transplant and contamination rate (p=0.002) (Fig 1). The mean number of CD34+ stem cells and time to engraftment did not significantly differ between the two groups.

Table 1 - treatment arm vs control arm			
	treatment arm	control arm	total
positive contamination on flow cytometry	13	11	24
negative contamination on flow cytometry	37	40	77
	50	51	101

Conclusions: MFC is a sensitive and novel tool to measure MRD in harvested products of patients with MM. Neoplastic plasma cells in the harvested products correlated with the disease status at the time of ASCT In our study, in vivo purging with bortezomib did not alter tumor contamination rates in the harvested product and may not be necessary in the era of novel therapy.

1467 Unconjugated Hyperbilirubinemia and Gilbert Syndrome in Transfusion-Dependent β-Thalassemia: An Indian Experience

Prashant Sharma[1], Oshan Shrestha[2], Reena Das[1], Alka Khadwal[2], Jasbir Hira[2], Amita Trehan[1], Manphool Singhal[2], Arnab Pal[1]
[1]Postgraduate Institute of Medical Education & Research, Chandigarh, India, [2]PGIMER, Chandigarh, India

Disclosures: Prashant Sharma: None; Oshan Shrestha: None; Reena Das: None; Alka Khadwal: None; Jasbir Hira: None; Amita Trehan: None; Manphool Singhal: None; Arnab Pal: None

Background: Frequencies of cholelithiasis and unconjugated hyperbilirubinemia (UCHB) in transfusion-dependent β-thalassemia (TDBT) vary from 15-28%. Gilbert syndrome (GS), resulting from a TA-repeat in the *UGT1A1* gene promoter, is associated with jaundice and gallstones.

Design: We studied the prevalence of GS and its relationship with UCHB and cholelithiasis in 102 TDBT patients. Demographic and clinical data were recorded. Liver function tests and upper abdominal ultrasound were done. Gilbert genotyping was done by Sanger sequencing.

Results: Median age was 26 years with 66% males. The 5 commonest Indian thalassemic mutations i.e. IVS-1 position-5 (G>C), 619-bp deletion, IVS-1 position-1 (G>T), Fr 41/42 (-TCTT) and Fr 8/9 (+G) together comprised 87.3% of alleles. Twenty-three (22.5%) patients were previously splenectomised; 49 had variable degrees of splenomegaly while 58 had hepatomegaly. Serum total and unconjugated bilirubin were elevated (>1.0 and >0.7 mg/dl) in 83/102 and 86/102 patients respectively. Serum aspartate aminotransferase was elevated in 30 patients (29.4%), alanine aminotransferase in 48 (47.1%), and alkaline phosphatase in 22 patients (21.6%). Recent viral serology (HIV, HBSAg, HCV) available in 92 patients showed 19 (18.6%) positive for at least 1 infection.

Eighteen patients (17.7%) had the Gilbert genotype (TA)7/7, 48 (47.1%) were heterozygous (TA)6/7 and the remaining 36 (35.3%) were wild-type (TA)6/6 homozygotes (Figure 1). GS patients (TA7/7) had significantly higher total as-well-as unconjugated bilirubin than heterozygotes (TA6/7), who in turn had higher levels than wild-type homozygotes (TA6/6). Gallstones were found in 13.7% patients (n=14), as shown in Table 1. Total or unconjugated bilirubin levels in patients with-versus-without gallstones were not statistically significant different. Nor were there any significant differences in the frequencies of gallstones between patients with the 6/6, 6/7 or 7/7 genotypes.

Table 1. Unconjugated bilirubin levels and gallstones in 102 TDBT patients with various *UGT1A1* promoter genotypes.

UGT1A1 promoter genotype	Unconjugated bilirubin level (mg %)			Gallstones present n (%)
	Mean ± S.D.	Median	Range	
(TA)7/7, *n=18*	3.24±2.07	3.54	0.6 - 7.76	3 (16.7)
(TA)6/7, *n=48*	1.5±0.74	1.38	0.54 - 3.27	8 (16.7)
(TA)6/6, *n=36*	1.4±0.87	1.15	0.37 -4.69	3 (8.3)

Figure 1 - 1467

Sanger sequencing chromatograms showing the *UGT1A1* gene promoter

A.   (TA)6/6

B.   (TA)6/7

C.   (TA)7/7
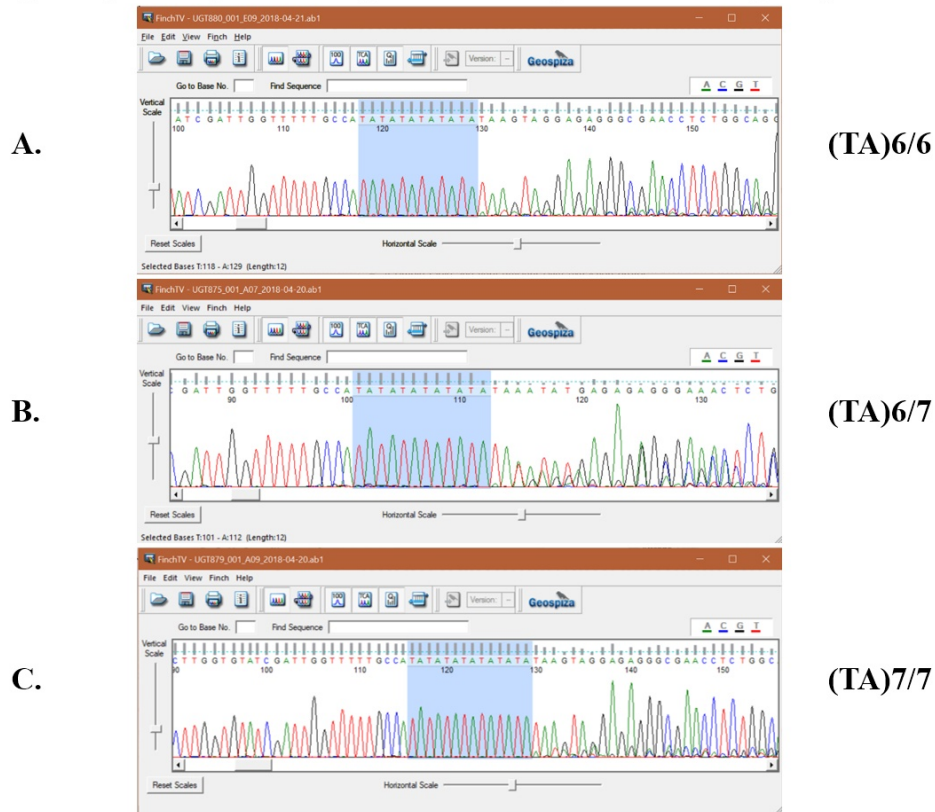
Conclusions: High frequency of GS and its significant association with UCHB suggest that *UGT1A1* promoter sequencing should be considered in TDBT patients whose jaundice remains unexplained after treatable causes like viral infections, chelator toxicity or transfusion-related hemolytic reactions are excluded. GS not being significantly associated with cholelithiasis could be due to a lower incidence of cholelithiasis overall (14/102) in our patients, our younger cohort or, a truly weaker association of GS with gallstones than is currently suspected.

1468 Chronic Lymphocytic Leukemia/Small Lymphocytic Lymphoma Involving Cerebrospinal Fluid (CSF) Shows Pathogenic TP53 Mutations

Anna Shestakova[1], Nahideh Haghighu[2], Sami Souccar, Xiaohui Zhao[1], Jefferson Chan[3], Sherif Rezk[4]
[1]University of California Irvine, Orange, CA, [2]University of California Irvine, Mission Viejo, CA, [3]UC Irvine Medical Center, Orange, CA, [4]Orange, CA

Disclosures: Anna Shestakova: None; Sami Souccar: None; Sherif Rezk: None

Background: Chronic lymphocytic leukemia (CLL)/small lymphocytic lymphoma (SLL) is characterized by proliferation of clonal mature small lymphocytes in peripheral blood, bone marrow and lymphoid tissue. Rarely, CLL involves the extramedullary sites, including central nervous system (CNS). CNS involvement by CLL is considered a disease progression that requires aggressive treatment. TP53 genetic aberrations are the key biomarkers to predict clinical course and response to chemotherapy. Pathogenic TP53 clones might drive involvement of CNS by CLL. Aim of this study is to utilize targeted next generation sequencing of TP53 to estimate clonal evolution in patients with CLL/SLL involving CNS.

Design: Retrospective analysis identified four patients with clinically significant persistent involvement of CNS that were treated at our institution from 01-2018 to 09-2019. CSF involvement with CLL was confirmed by flow cytometry. There was no large cell transformation. For each patient samples were collected at/before and after CLL/SLL involvement of CNS. Samples included CSF, peripheral blood, bone marrow aspirate, bone marrow cores, lymph nodes and brain biopsy. Next generation sequencing using DNA and TP53-specific primers was performed (VariantPlex TP53 Assay, Archer). Only pathogenic mutations in TP53 were reported.

Results: Patient 1: SLL presented in 2018 with CNS involvement. Brain biopsy showed c.814G>A (2.3%). CSF showed c.920-2A>G (7%), c.949del (2.3%) and c.574C>T (2.8%). Patient 2: CLL diagnosed in 2008. At the time of CSF involvement in 2018 a homozygous c.782+1G>T (70%) mutation was identified in bone marrow. As disease progressed, bone marrow showed additional c.739A>G (6%) and c.951_952delinsAA (5%). Patient 3: SLL diagnosed in 1999, pre-CNS involvement lymph node had c.68G>A (1%). At the time of CNS involvement in 2018, brain biopsy showed increase in c.68G>A (5%). Patient 4: CLL was diagnosed in 2006. Pre-CNS involvement bone marrow had c.880del (4%). CSF was involved in 2018 and showed c.880del (1%).

Conclusions: CLL clones that involve CSF and/or brain parenchyma invariably showed pathogenic TP53 mutations (patient1, 3 and 4). We were able to identify similar pathogenic TP53 clones that were present in the pre- and post-CNS involvement brain biopsy and CSF samples (patient 3 and 4). Patient 2 had a persistent single pathogenic homozygous TP53 mutation in bone marrow. Further studies are necessary to correlate TP53 mutational landscape with the course of the disease.

1469   Clinical Utility of T-cell Receptor Constant β Chain-1 Staining in the Diagnosis of T-cell Large Granular Lymphocytic Leukemia by Flow Cytometry

Min Shi[1], Horatiu Olteanu[1], Dragan Jevremovic[1], Rong He[1], David Viswanatha[1], Heidi Corley[1], Pedro Horna[1]
[1]Mayo Clinic, Rochester, MN

Background: T-cell large granular lymphocytic leukemia (T-LGLL) is a clonal proliferation of large granular lymphocytes associated with cytopenias. Distinction from reactive large granular lymphocytes is challenging. Available T-cell clonality assays are limited by suboptimal sensitivity and specificity, and/or high complexity. We recently reported a T-cell clonality assay by flow cytometry, based on the expression of one of two mutually exclusive T-cell receptor constant β chains (TRBC1). We now demonstrate the utility of this approach in the diagnosis of T-LGLL.

Design: Peripheral blood (55) or bone marrow (15) specimens from 23 patients with T-LGLL, and 47 patients with no T-cell neoplasm, were studied by flow cytometry using an anti-TRBC1 antibody on a T-cell panel. TRBC1 expression was analyzed on all immunophenotypically distinct T-cell subsets. Clonality was defined as >85% TRBC1-positive or TRBC1-negative events, or monophasic TRBC1-dim expression. Killer immunoglobulin-like receptor expression by flow cytometry (KIR analysis) and T-cell receptor gene rearrangement studies (TCGR) were performed on selected cases.

Results: TRBC1 staining showed a clonal CD8-positive (87%), CD4-positive (4%) or CD4/CD8-negative (9%) T-cell population in all T-LGLL cases, accounting for 60% of lymphocytes on average (range: 14% to 95%). The neoplastic cells were TRBC1-positive (39%), TRBC1-negative (52%) or TRBC1-dim (9%). Clonal CD8 T-cell subsets were also identified in 11 of 47 patients with no T-cell malignancy (23%), accounting for less than 10% of lymphocytes, except for 2 patients with clinically silent clonal CD8 T-cell expansions (46% and 50% of lymphocytes). TCGR studies were positive (17 of 19 cases tested, 90%) or equivocal (2) in patients with T-LGLL; and negative (17 of 21, 81%) or equivocal (4) in patients with no T-cell malignancy. KIR analysis was positive in 5 of 22 cases of T-LGLL tested (23%), and negative in 17 tested patients with no T-cell malignancy. Using a threshold of 10% clonal CD8 T-cells (of lymphocytes), TRBC1 staining showed superior sensitivity and specificity in identifying T-LGLL (100% and 96%, respectively), compared to TCGR (90% and 81%) and KIR analysis (23% and 100%).

Figure 1 - 1469
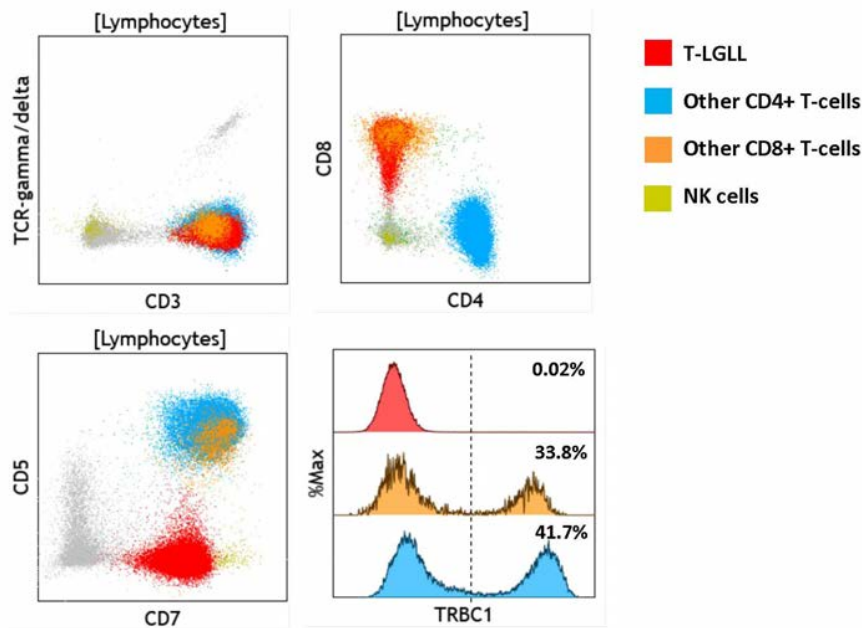
Conclusions: Assessment of T-cell clonality by TRBC1 staining provides a rapid and low-cost approach for the diagnosis of T-LGLL, superior to KIR analysis and TCGR. A threshold of 10% clonal CD8 T-cells (of lymphocytes) distinguishes T-LGLL from most clonal CD8 T-cell populations of uncertain significance.

1470 PRDM1 is an Important Tumor Suppressor of NK-cell Lymphoma and Regulator of NK Cell Homeostasis

Yunfei Shi[1], Xuxiang Liu[1], Yuping Li[2], Bouska Alyssa[3], Gehong Dong[4], Qiang Gong[5], Javeed Iqbal[6], Haiqing Li[7], Jinhui Wang[8], Shuhua Yi[5], Timothy W. McKeithan[9], Wing Chung Chan[10]
[1]City of Hope National Medical Center, Duarte, CA, [2]City of Hope, Duarte, CA, [3]University of Nebraska Medical Center, [4]Beijing, China, [5]City of Hope National Medical Center, [6]University of Nebraska Medical Center and on behalf of the LLMPP and I-PTCL Consortium, Omaha, NE, [7]Department of Computational and Quantitative Medicine, City of Hope National Medical Center, Duarte, CA, [8]City of Hope, [9]Department of Pathology, City of Hope National Medical Center, Duarte, CA, [10]City of Hope National Medical Center, Pasadena, CA

Disclosures: Yunfei Shi: None; Yuping Li: None; Haiqing Li: None; Wing Chung Chan: None

Background: Human PRDM1(also known as Blimp-1) is an important transcription factor for plasma cell differentiation and T cell homeostasis. It has been found to be inactivated in multiple types of lymphomas, including ABC-DLBCL, ALCL, PTCL-GATA3 and ENK/TCL, suggesting PRDM1 is an important tumor suppressor gene (TSG) in lymphoma. PRDM1 inactivation is particularly frequent in ENK/TCL through a combination of deletion, mutation or promoter hypermethylation. How PRDM1 loss promotes NKCL development is still poorly defined. To clarify this, we investigated how PRDM1 regulates NK cell homeostasis.

Design: We employed established NKCL cell lines and a culture system with engineered K562-Cl9-mb21 feeder cells that enables normal NK cells to expand for months and allows various in vitro manipulations. Re-introduction of PRDM1 into NKCL lines with inactivated PRDM1 caused growth arrest and apoptosis of the cells. When we deleted PRDM1 in normal NK cells using the CRISPR/CAS9 system, the deleted cells showed a marked increase in cloning efficiency, increased proliferation and cell cycle progression. To understand how PRDM1 regulates these functions, we identified the genomic targets it regulates using assays on genome-wide binding (ChIP-seq), DNA accessibility (ATAC-seq) and mRNA expression profiling on NK cells grown with or without feeder cells.

Results: PRDM1 bound many more target genes (2880) in NK cells without feeder than in NK with feeder (802, with 98.5% overlap) while PRDM1 consensus binding motifs were almost identical in both. PRDM1 repressed many pathways and genes associated with T and NK cell activation, function and growth(MYC, TOX2, TLR4, CCR4, VEGF, IRF4, BCAT1, FGFR1, and MYB etc). Many of the target genes were validated based our GEP analysis on PRDM1 knockout NK cells. Interesting, PRDM1 also acted as an activator for some genes including the immune checkpoint genes, TIGIT, LAG3, CTLA4, and TIM-3.

Figure 1 - 1470

Fig.1 ChIP-seq and ATAC analysis detected MYC as target genes of PRDM1 in human NK cells with or without feeder
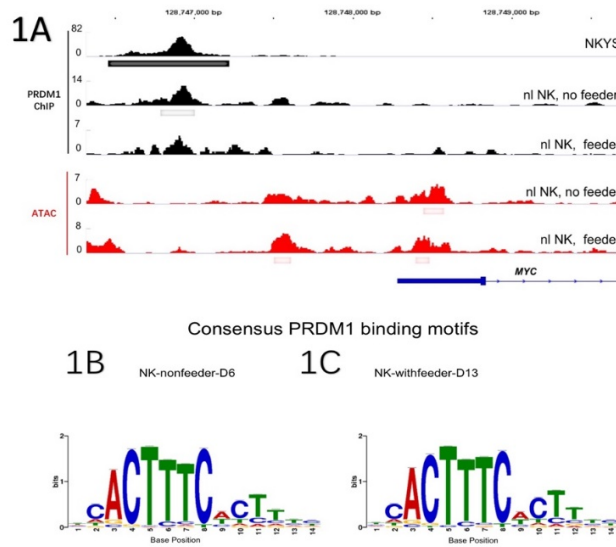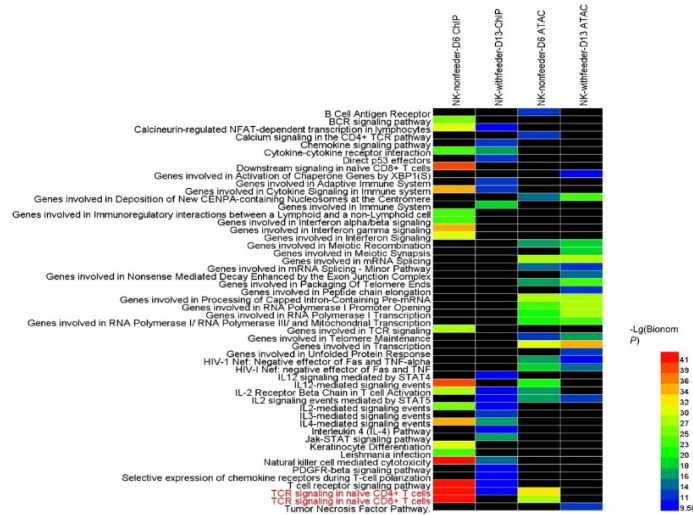

Figure 2 - 1470

Fig. 2 Pathway analyses of functional significance for both PRDM1-ChIP-seq and ATAC-seq

Conclusions: In summary, our study demonstrated that PRDM1 repressed many pathways and genes important in NK cell homeostasis that could partially explain the TSG function of PRDM1. Culturing with feeder cells could modify PRDM1 DNA-binding, preventing repression of most of the target genes and the activation of immune checkpoint molecules, thus allowing normal NK-cells to continue to proliferate. We have elucidated the mechanisms of PRDM1 as a TSG and suggested the possibility of inactivating PRDM1 to augment NK cell function in immunotherapy for cancers.

1471 Targetable Markers May Be Differentially Expressed by Flow Cytometry in Peripheral Blood and Bone Marrow Blasts in Acute Leukemias

Volodymyr Shponka[1], Steven Kroft[2], Maria Hintzke[3], Ashley Cunningham[4], John Astle[2], Vasiliki Leventaki[2], Laura Michaelis[2], Alexandra Harrington[5]
[1]Medical College of Wisconsin, Brookfield, WI, [2]Medical College of Wisconsin, Milwaukee, WI, [3]Medical College of Wisconsin, New Berlin, WI, [4]Medical College of Wisconsin, Oconomowoc, WI, [5]Milwaukee, WI

Background: Bone marrow (BM) evaluation, consisting of morphologic, flow cytometric (FC), cytogenetic, and molecular studies, is the gold standard for acute leukemia (AL) diagnosis. However, the preliminary diagnosis is often rendered based on peripheral blood (PB) FC. At some institutions this leads to cancellation of BM FC, with the assumption that the immunophenotype (IP) of the leukemic blasts is identical in PB and BM. Likewise, PB FC may be cancelled if a concomitant BM sample is obtained. As immunophenotypic differences across sample types are well-described in chronic lymphoid leukemias and lymphomas, we hypothesized that there may be differences in blast IPs across specimen types in AL and sought to study this rigorously in new ALs, concentrating on immunotherapy-targetable markers.

Design: We reviewed all new AL patients (pts), who had both concurrent PB and BM FC and compared blast IPs. 8-color FC was performed with surface and cytoplasmic antibodies, including myeloid and lymphoid markers, and targetable markers (CD19, CD20, CD22, CD33, and CD123). Positive antigen (Ag) expression was defined as >20% as compared to an isotype control. Expression patterns and % blasts exceeding the isotype control were recorded. Differences were defined as qualitative expression pattern variability (dim, partial, variable) and changes from (+) to (-) or vice versa.

Results: We identified 18 pts (8M: 10F, 40-75yrs) with new acute myeloid (n=12; AML), mixed-phenotype (4; MPAL), B-lymphoblastic (1; ALL), and undifferentiated (1) leukemia. In all cases, the immunophenotypic concordance between PB and BM was sufficient for accurate diagnosis. Differences in blast expression patterns across PB and BM were present in 13/18 ALs (72%) for a total of 34 differences (0-10, median 1.5), including 10 pts (56%) with 16 (+/-) Ag changes (Table 1). Pts without differences included 4 AMLs and 1 MPAL. Eight pts (44%) had differences in CD123, 5 with (+) PB and (-) BM expression and 2 with (-) PB and (+) BM expression; 2 pts (11%; 17% of AMLs) had differences in CD33, with (-) PB and partial(+) BM expression; and other (+/-) Ag differences are shown in Table 1.

Case	Acute leukemia	Antigen	Qualitative PB	Qualitative BM	% expression* PB	% expression* BM
1	AML	CD33	(-)	Partial(+)	12	22
		TDT	Dim(+)	(-)	36	18
2	AML	CD33	(-)	Partial(+)	19	57
		CD123	(-)	Dim(+)	8	57
4	AML	CD123	Dim(+)	(-)	28	3
5	AML	MPO	(-)	Dim(+)	3	26
		CD11b	(-)	Partial(+)	15	23
6	AML	CD123	Dim(+)	(-)	22	2
10	AML	CD123	Partial(+)	(-)	31	7
11	AML	CD15	(-)	Variably(+)	17	65
12	MPAL	CD22	(-)	Partial dim(+)	10	22
		CD123	(-)	Partial(+)	19	24
		CD79a	(-)	Partial(+)	7	33
15	B-ALL	CD20	Partial(+)	(-)	46	17
		CD123	Partial(+)	(-)	20	11
18	AUL	CD123	Partial(+)	(-)	44	19
* As compared to an isotype control (positive antigen expression defined as >20%) PB- peripheral blood; BM- bone marrow; AML- acute myeloid leukemia; MPAL- mixed phenotype acute leukemia; B-ALL- B-lymphoblastic leukemia/lymphoma; AUL- acute undifferentiated leukemia; MPO- myeloperoxidase; TDT- terminal deoxynucleotidyl transferase						

Conclusions: Our data shows that over 50% of ALs show differences in blast IPs by FC across PB and BM analyses. Most commonly, this occurred with CD123 but was observed in other Ags such as CD20, CD22, and CD33. Our data support analyses across specimens for ALs and may be particularly critical in an era of targeted therapy for ALs.

1472 Diminished Expression of 5hmC in Reed-Sternberg Cells in Classical Hodgkin Lymphoma is a Common Epigenetic Marker

Andrew Siref[1], Colin McCormack[2], Washington Lim[3], Serhan Alkan[4]
[1]Cedars-Sinai, Los Angeles, CA, [2]Baylor Scott & White Health, Temple, TX, [3]Cedars-Sinai Medical Center, Los Angeles, CA, [4]Cedars-Sinai Medical Center, Beverly Hills, CA

Background: Loss of the epigenetic marker 5-hydroxymethylcytosine (5hmC) has been demonstrated in a variety of neoplasms. Several recent studies have shown epigenetic alteration in Classical Hodgkin lymphoma (CHL), contributing to the silencing of B-cell-specific genes. Evaluation of DNA modification, and in particular DNA methylation analysis, of CHL has been limited. Vitamin C - a cofactor for the ten-eleven translocation (TET) enzymes which oxidize 5-methylcytosine (5mC) to 5hmC - may replenish levels of 5hmC.

Design: 49 cases of classical Hodgkin lymphomas, including 21 whole tissue sections retrieved from our surgical pathology archive and 28 cases derived from small tissue arrays were analyzed. All cases were reviewed and the diagnosis confirmed. Cases included all subtypes of CHL, including: 34 nodular sclerosing, 12 mixed cellularity, 2 lymphocyte rich, and 1 lymphocyte depleted. Multiplex immunohistochemical detection of 5hmC and CD30 was performed using 5hmC rabbit monoclonal antibody (clone RM236) from RevMAB Biosciences (San Francisco, CA) at 1:10,000 dilution and CD30 mouse monoclonal antibody from Dako (Glostrup, Denmark) at 1:25 dilution. CHL L428 cell line grown in optimal conditions was then subjected to vitamin C treatment for 24 hours at 0mM, 1mM, 5mM, 10mM, and 20mM concentrations. Cells were then assessed for viability by 7-AAD flow cytometry and morphologic review, as well as 5hmC concentration by flow cytometry.

Results: We demonstrate near universal depletion of 5hmC in the neoplastic Hodgkin Reed-Sternberg (H/RS) cells in all cases of CHL (49/49). Only a handful of cases (12%) contained rare H/RS cells (≤ 20%) with weak, blush-like staining. Background stromal cells show strong and diffuse 5hmC staining, functioning as an internal control. A dose-dependent response to vitamin C treatment was observed, with maximal cytotoxicity seen at concentrations ≥ 5 mM. Incubation of the cell line with vitamin C at 20mM showed increased 5hmC expression by flow cytometry compared to control (untreated) cells.

Conclusions: We have demonstrated the novel observation that 5hmC is almost universally depleted in the H/RS cells of CHL. 5hmC can be repleted in H/RS cells following pharmacologic treatment with vitamin C - presumably through increased TET enzymatic activity, leading to cell death. Irrespective of the underlying molecular events in CHL, altered DNA methylation and in particular mechanisms that govern 5hmC appear to be critical for cellular survival.

1473 BIM Expression is Low in BCL2-negative Follicular Lymphoma

Daniel Socha[1], Xiaoxian Zhao[2], Lisa Durkin[2], Juraj Bodo[2], Eric Hsi[2]
[1]Cleveland Clinic, Westlake, OH, [2]Cleveland Clinic, Cleveland, OH

Background: Follicular lymphoma (FL) is characterized by the t(14;18)(q32;q21) or variant translocations leading to overexpression of the anti-apoptotic molecule BCL2. However, a subset of FLs lack *BCL2* rearrangement and do not express BCL2 by IHC. The aim of our study was to evaluate expression of anti-apoptotic (MCL-1 and BCL-xL) and pro-apoptotic proteins (BIM) by IHC in both BCL2(-) and BCL2(+) FLs.

Design: Cases of FL diagnosed between 2009-2019 were reviewed to identify BCL2(-) cases by IHC (assessed by clone 124). Grade matched BCL2(+) FLs were identified for the control group. Cases were re-reviewed to confirm the diagnosis and clinical data was collected by chart review. IHC stains for BCL2 (EP36), Ki-67, MCL-1, BIM, and BCL-xl were performed on TMAs or whole slides. BCL2 (EP36) was interpreted as positive or negative. Ki-67 was interpreted on tumor cells in 10% increments. The remaining stains were scored on tumor cells at 10% increments and intensity was interpreted as weak, moderate, or strong to derive an H-score.

Results: 24 BCL2(-) FLs were identified with sufficient tissue for additional IHC. On repeat testing with BCL2(EP36) IHC, 5/24 were reclassified as BCL2(+) leaving 19 BCL2(-) FLs. 33 BCL2(+) FLs were selected with sufficient tissue for additional IHC. Mean ages were 64.7 years and 63.9 years (BCL2(-) and BCL2(+), respectively). The male/female ratio was 0.8 and 0.9 (BCL2(-) and BCL2(+), respectively). There was no significant difference in expression of anti-apoptotic BCL-xl or MCL-1 between BCL2(-) and BCL2(+) FLs. However, pro-apoptotic BIM was significantly lower in BCL2(-) cases compared to BCL2(+) cases (**Table 1**). Representative examples of IHC expression in BCL2(-) and BCL2(+) FLs are shown in **Figure 1.**

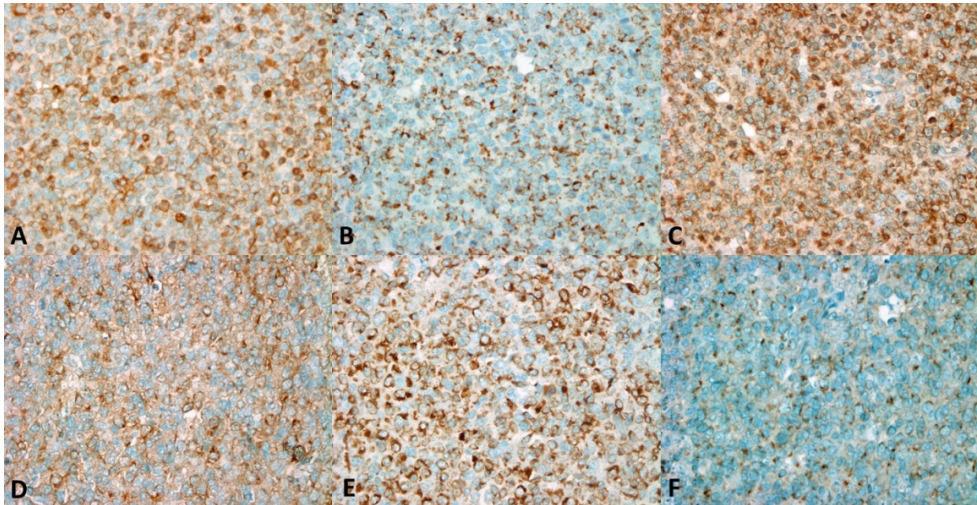| Mean Scores +/- 1 SD			
	BCL2-negative	BCL2-positive	P-value
BCL-xl (H-score)	60.9 +/- 52.0	66.6 +/- 40.8	0.59
BIM (H-score)	50.6 +/- 38.8	87.7 +/- 56.8	0.002
MCL-1 (H-score)	50.9 +/- 53.0	34.1 +/- 38.1	0.11
Ki-67 (%)	37.0 +/- 27.7	43.2 +/- 21.0	0.21

Figure 1 - 1473

Figure 1: BCL2(-) FL (A-C) and BCL2(+) FL (D-F). Immunohistochemical stains for BCL-xl (A & D), BIM (B & E), and MCL-1 (C &F).

Conclusions: 21% of putative BCL2(-) FLs are BCL2(+) when tested with alternative clones, supporting the practice of having more than one BCL2 clone in IHC labs. The anti-apoptotic proteins BCL-xl and MCL-1 are expressed at similar levels in BCL2(+) and BCL2(-) FLs. However, the pro-apoptotic protein BIM is expressed at lower levels in BCL2(-) FLs. Decreased BIM could have an overall anti-apoptotic effect and could represent an alternate mechanism for cell survival in BCL2(-) FLs. This is supported by the phenotype of *BCL2L11* (*BIM*) knockout mice which show similar lymphadenopathy and autoimmune disease as seen in *BCL2* knockout mice.

1474 Computer-Assisted Grading of Follicular Lymphoma Using Convolutional Neural Networks

Lauren Stanoszek[1], Jerome Cheng[2], Sarah Choi[2]
[1]Toledo, OH, [2]University of Michigan, Ann Arbor, MI

Disclosures: Lauren Stanoszek: None; Jerome Cheng: None; Sarah Choi: None

Background: Diagnosis and grading of follicular lymphoma (FL) typically occurs using histopathologic evaluation of slides by light microscopy. While morphologic features are essential for guiding appropriate patient management, accurate interpretation can be affected by factors such as sampling bias or interobserver variation. Emerging technologies in machine learning can potentially assist pathologists with their morphologic evaluation, however their utilization has not been comprehensively explored in the realm of hematolymphoid neoplasia.

Design: Three images at 20X magnification were taken using PicPick of hematoxylin and eosin stained normal germinal centers of benign lymph nodes (n=8) and neoplastic follicles of cases of both follicular lymphoma grade 1-2 (n=11) and follicular lymphoma grade 3A (n=11), (Graph 1, A. benign lymph nodes, B. FL grade 1-2, C. FL grade 3). Two 224x224 pixel images of the germinal center or neoplastic follicle regions were handpicked from each of these three images, with a total of six 224x224 pixel images of each case. A pre-trained CNN (convolutional neural network) model ResNeXt-101 was applied on images belonging to the three categories, generating 4096 feature values for each image. Dimensional reduction was performed on the 4096 features obtained from each image by way of t-SNE (T-distributed Stochastic Neighbor Embedding) to emphasize differences in feature values among each image in a two-dimensional graph.

Results: The three groups formed unique clustering in the t-SNE plot (Graph 2). While cases of benign lymph nodes and FL grade 1-2 showed primarily single clusters, the FL grade 3A cases demonstrated less distinctive, multiple, smaller subclusters. Preliminarily, the CNN model was able to extract features from each image that could be used to classify each image into the appropriate category.
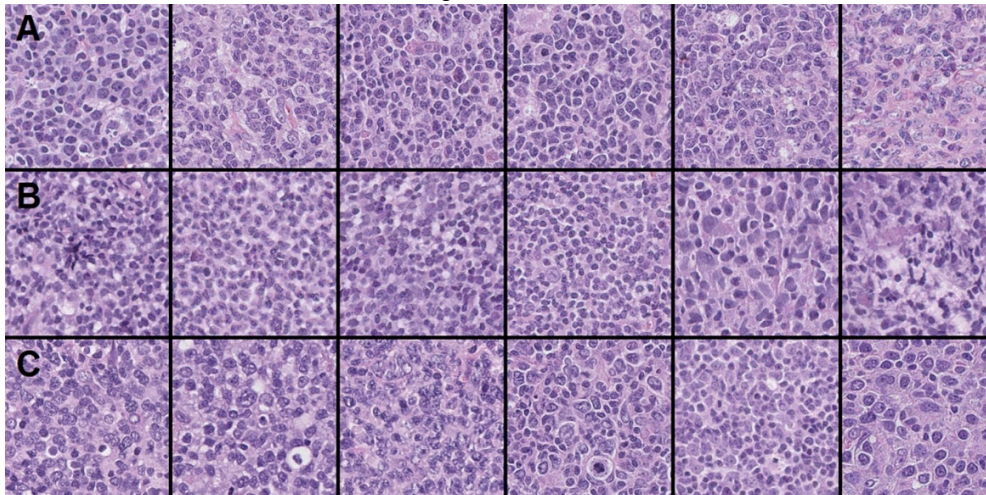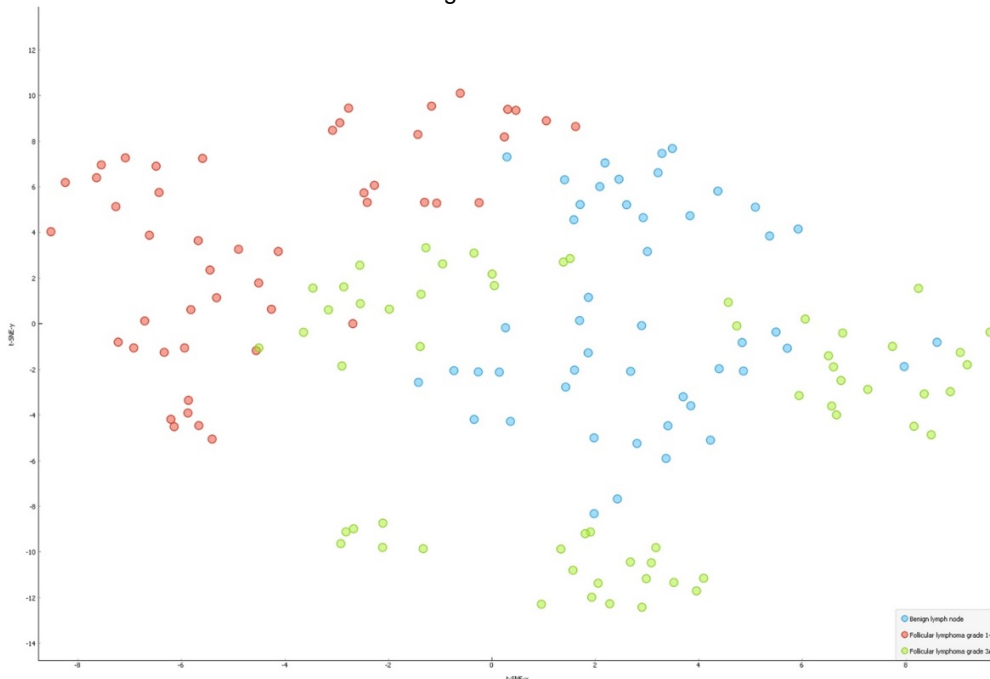
Figure 1 - 1474

Figure 2 - 1474

Conclusions: Although further analysis of larger cohorts is needed, these results suggest that the CNN model has the potential to distinguish benign versus neoplastic follicles and also assist with grading in FL. It will be important to assess how this methodology compares to conventional histologic analysis in the prediction of clinical course and identification of patients at higher risk of disease relapse or transformation.

1475 Treatment-Associated Monocytosis and Eosinophilia in Plasma Cell Myeloma: A 10-Year Retrospective Study of a Single Tertiary Care System

Aryeh Stock[1], Julie Teruya-Feldstein[2]
[1]Icahn School of Medicine at Mount Sinai, New York, NY, [2]Mount Sinai Icahn School of Medicine, New York, NY

Disclosures: Aryeh Stock: None; Julie Teruya-Feldstein: None

Background: Plasma cell myeloma (PCM) constitutes approximately 15% of hematopoietic neoplasms in the United States. The prognosis of PCM is highly variable and dependent upon numerous factors including biologic features of the plasma cell clone as well as patient-specific factors such as age, performance status, and comorbidities. In the last decade, several new classes of drugs, including proteasome inhibitors and immunomodulators have proven useful in achieving improved clinical response. However, the mechanisms by

which these drugs act are not fully defined. Use of these drugs may have unanticipated effects on the immune system, some of which we describe in this study.

Design: 2,853 patients with a diagnosis of plasma cell myeloma treated with one or more of lenalidomide, pomalidomide, thalidomide, daratumumab, venetoclax, bortezomib, carmustine, carfilzomib, and elotuzumab who were seen at the Mount Sinai Medical System from 9/26/2009 to 9/25/2019 were identified. Patients were stratified by age, race, and sex. Time from initiation of treatment to development of monocytosis and eosinophilia was measured. Demographic data was collected from all patients and compared to those who developed monocytosis within 1 month of initiating therapy. Data was collected using Epic SlicerDicer and analyzed with R Studio (R 3.6.1, tidyverse 1.2.1).

Results: 2,853 patients with plasma cell myeloma treated were treated with one or more of the above medications. Of these, 1,865 (65.4%) developed monocytosis and 1,243 (43.3%) developed eosinophilia within 1 month of initiation of treatment. Time to onset of monocytosis (figure 1) and eosinophilia (figure 2) are shown. Demographic data demonstrate a relatively increased rate of monocytosis in minority groups as compared with caucasians (table 1). Preliminary mortality data suggests that mortality may be 3% higher among those patients who develop monocytosis.

CHARACTERISTIC		NO. OF PATIENTS ON DRUG	%	NO. WITH MONOCYTOSIS AT 1 MONTH	%
SEX					
	Female	1,240	43.5%	830	43.3%
	Male	1,613	56.5%	1,085	56.7%
AGE, YEARS					
	21 years or less	0	0.0%	0	0.0%
	22 to 43 years	53	1.9%	42	2.2%
	44 to 65 years	1,151	40.4%	818	42.7%
	66 to 87 years	1,555	54.5%	1,004	52.4%
	88 years or more	94	3.3%	51	2.7%
DRUGS					
	bortezomib	1,947	68.3%	1,495	78.1%
	carfilzomib	792	27.8%	692	36.1%
	carmustine	171	6.0%	168	8.8%
	daratumumab	966	33.9%	841	43.9%
	elotuzumab	236	8.3%	208	10.9%
	lenalidomide	2,083	73.1%	1,439	75.1%
	pomalidomide	826	29.0%	696	36.3%
	thalidomide	489	17.1%	405	21.1%
	venetoclax	288	10.1%	246	12.8%
RACE					
	Asian (Pacific Islander)	19	0.7%	15	0.8%
	Asian Indian	19	0.7%	13	0.7%
	Black or African American	508	17.8%	383	20%
	Caucasian	1,409	49.4%	919	48.0%
	Chinese	29	1.0%	26	1.4%
	Other	869	22.9%	559	29.2%

Figure 1 - 1475

Monocytosis in Plasma Cell Myeloma by Drug

Figure 2 - 1475

Eosinophilia in Plasma Cell Myeloma by Drug
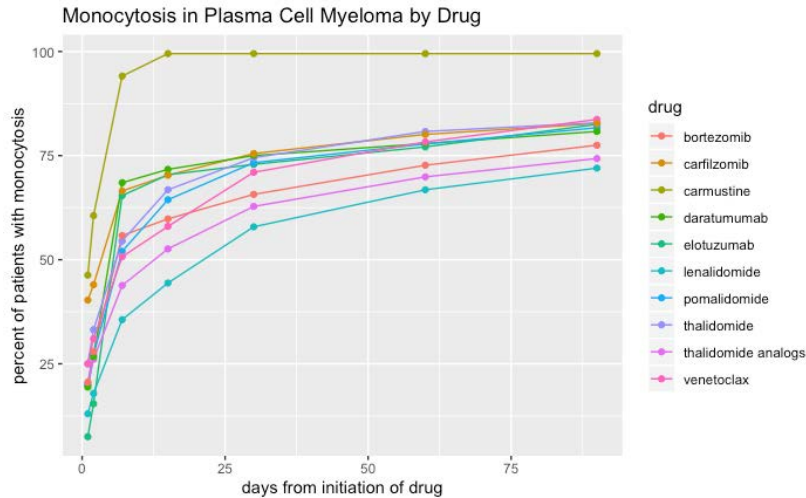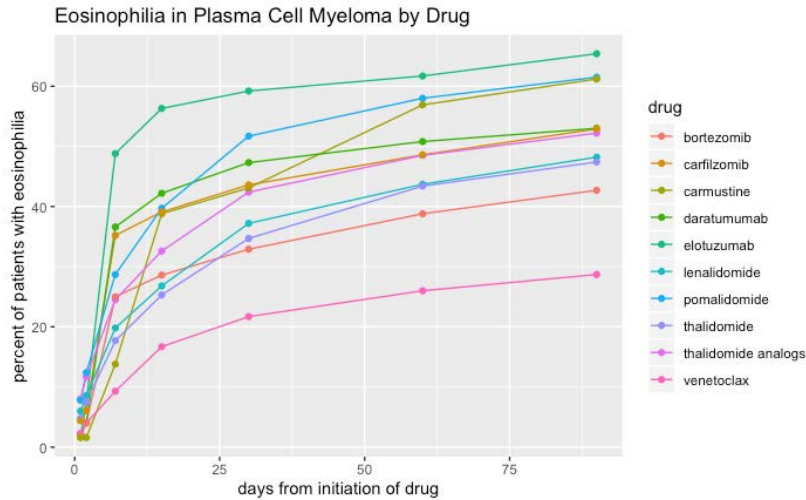
Conclusions: Monocytosis and eosinophilia occur relatively commonly in the setting of PCM therapy. The role played by monocytosis and eosinophilia in the setting of PCM treatment and response is poorly understood. Further understanding of the patterns of these phenomena may provide insight into the significance of these findings and how they may be leveraged to improve treatment response. To our knowledge this study of monocytosis and eosinophilia associated with plasma cell myeloma immunotherapies is the first of its kind. It is our hope that this study will serve as a platform for future investigations.

1476 Aggressive Morphologic Variants of Mantle Cell Lymphoma Demonstrate Frequent Mutations of TP53, Loss of CDKN2A/B and Chromothripsis

Lukas Streich[1], Amir Behdad[2], Yi-Hua Chen[3], Qing Chen[2], Juehua Gao[3], Girish Venkataraman[4], Madina Sukhanova[5], Xinyan Lu[6], Stephanie Mathews[7], Shanxiang Zhang[8], Katalin Kelemen[9], Jeremy Segal[10]
[1]Northwestern University, Chicago, IL, [2]Northwestern University Feinberg School of Medicine, Chicago, IL, [3]Northwestern Memorial Hospital, Chicago, IL, [4]University of Chicago Medical Center, Chicago, IL, [5]University of Chicago Medicine, [6]Chicago, IL, [7]Pittsboro, NC, [8]Indiana University School of Medicine, Indianapolis, IN, [9]Mayo Clinic, Phoenix, AZ, [10]The University of Chicago, Riverside, IL

Disclosures: Lukas Streich: None; Amir Behdad: *Speaker*, Pfizer; *Consultant*, Loxo/Bayer; *Consultant*, Thermo fisher; Yi-Hua Chen: None; Qing Chen: None; Juehua Gao: None; Girish Venkataraman: *Speaker*, Sylvant; Xinyan Lu: None; Stephanie Mathews: None; Shanxiang Zhang: None

Background: The aggressive variants of mantle cell lymphoma (MCL), blastoid (B-MCL) and pleomorphic (P-MCL), are defined by high proliferation index and eponymous morphology, and are associated with poor clinical outcomes. Here, we describe the genomic landscape of B/P-MCL, including novel chromosomal aberrations and high prevalence mutations.

Design: Twenty-four cases with diagnoses of P-MCL or conventional MCL were identified and reviewed; eighteen cases met inclusion criteria. Nine cases of conventional MCL (C-MCL) were selected as controls. Immunohistochemical stains were performed on, and genomic DNA was extracted from, formalin-fixed paraffin-embedded (FFPE) tissue. Comprehensive next generation sequencing (NGS) and SNP-array were performed on 13 B/P MCL cases with adequate DNA, and SNP-array on 9 cases of C-MCL.

Results: Our cohort included 18 patients, half of whom had a prior history of C-MCL. In 14 patients with available follow up data, the median survival was 318 days from diagnosis, and nine were deceased. Two cases (11%) cases were cyclin D1 negative but SOX-11 positive. SOX-11 was negative in 2 cases (11%) including 2 P-MCLs progressed from leukemic, non-nodal MCL. The median proliferative index was 85% as measured by ki-67 expression.

Chromothripsis was identified in 8 of 13 (62%) B/P MCL cases, along with a high degree of genomic complexity; in contrast, the C-MCL cases showed no chromothripsis and less genomic complexity (Figure 1). Twelve of 13 (92%) B/P-MCL cases showed loss of *CDKN2A/B* (6 bi-, 7 mono-allelic); only one C-MCL showed mono-allelic *CDKN2A/B* loss. In B/P-MCL, *TP53* was mutated in 8 cases (62%), 6 of which showed associated loss of chromosome 17. All mutated cases also showed overexpression of p53. Of the 8 cases with chromothripsis, 6 (85%) harbored *TP53* mutations. Other recurrent mutations in B/P-MCL included *ATM* (7, 53%), *CCND1* (5, 38%), *NOTCH1* (2, 18%), *NOTCH2* and *BIRC3* (each in 3, 23%). Four of 5 *TP53* non-mutated B/P-MCL cases harbored *ATM* mutations.

Figure 1 - 1476
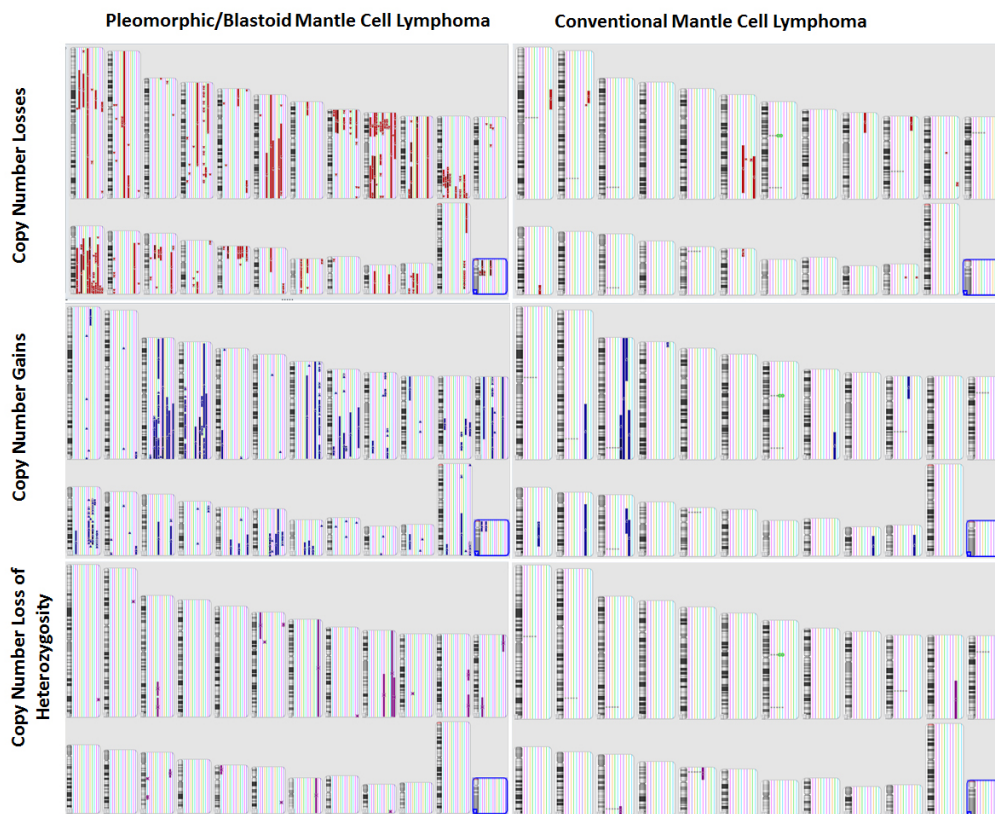
Conclusions: We report an in-depth analysis of the genomic landscape of aggressive variants of MCL, demonstrating chromothripsis and a high frequency of *CDKN2A/B* and *TP53* alterations. This is the first identification of chromothripsis in MCL; this catastrophic genetic event may play a critical role in disease progression and possibly portends a poor prognosis.

1477 Characterization of Bone Marrow Morphologic and Genetic Features of Myeloid Neoplasms with Germline DDX41 Mutation in 10 Distinct Pedigrees

Narittee Sukswai[1], Joseph Khoury[1], Keyur Patel[1], Mark Routbort[1], Rajyalakshmi Luthra[1], Carlos Bueso-Ramos[1], Sanam Loghavi[1], L. Jeffrey Medeiros[1], Rashmi Kanagal-Shamanna[2]
[1]The University of Texas MD Anderson Cancer Center, Houston, TX, [2]The University of Texas MD Anderson Cancer Center, Bellaire, TX

Background: Myeloid neoplasms with germline *DDX41* mutation occur in the elderly without a pre-existing disorder or organ dysfunction, and are often underdiagnosed. In this study, we characterized the clinicopathologic and genetic features of this entity with emphasis on bone marrow (BM) features.

Design: We selected all AML and MDS patients with confirmed germline DDX41 mutation. We reviewed the BM morphologic, flow, cytogenetic and NGS findings.

Results: Study group comprised 10 patients (9 male; 1 female) from 10 distinct pedigrees: median age of 71 yrs (57-85). Six patients had AML, 4 had MDS. None had prior bleeding disorder or organ dysfunction. All but 1 patient had a strong family history of cancer. Germline *DDX41* mutations included p.D140fs (n=5, 50%), p.M1I (n=2), p.E426Afs (n=1), p.Q41* (n=1) and c.572-1G>A (n=1).

All patients had pancytopenia. BM cellularity was variable. Notable features in both MDS and AML included erythroid predominance, moderate-severe megakaryocytic dysplasia (66%) and mild-moderate erythroid dysplasia (77%). Granulocytic dysplasia was minimal. All AML patients showed dysplasia in at least 50% cells in ≥2 lineages. All had prominent background immune cells: plasma cells (CD138 IHC: average 5-10% of cells), T-cells (interstitial and within aggregates, n=2). One AML patient had concurrent plasma cell myeloma and another had a small lambda-monotypic B-cell population that disappeared with decitabine therapy. All patients had at least 1 additional somatic genetic aberration: 7 had a second *DDX41* mutation, 5 had mutations in *DNMT3A, TP53, JAK2, KMT2A, SRSF2, ASXL1, TET2* and 3 had karyotype abnormalities: trisomy 8; der(1;14) and concurrent del(5q)/del(7q).

Six patients (3 MDS, 3 AML) had repeat mutation profiling at remission. 4 patients [all 3 MDS, 1 AML: received either lenalidomide or azacitidine +/- PD1 inhibitor) achieved full somatic mutation clearance. Two AML patients did not achieve molecular remission: 1 with mutated *TP53* and JAK2; the other with mutated *ASXL1* and *DDX41*. *The latter underwent* clonal evolution to MDS with additional somatic mutations. Over the follow-up period, 3 AML patients died (2 of disease; 1 with transplant complications).

Conclusions: Despite some distinctive morphologic BM features, routine sequencing is essential for identification of myeloid neoplasms with germline *DDX41* mutation. Prominent background inflammation may suggest potential responsiveness to immune modulatory drugs such as lenalidomide and immune check point inhibitors.

1478 Diagnostic Utility of CRLF2 Immunohistochemistry in BCR/ABL-Like B-Lymphoblastic Leukemia

Moe Takeda[1], Zhengshan Chen[2], Imran Siddiqi[3], Maria Vergara-Lluri[4]
[1]University of Southern California, Los Angeles, CA, [2]LAC + USC Medical Center, Los Angeles, CA, [3]University of Southern California Keck School of Medicine, Los Angeles, CA, [4]Keck School of Medicine of University of Southern California, Los Angeles, CA

Background: B-lymphoblastic leukemia, *BCR-ABL1*-like (Ph-like ALL) is a provisional entity in the 2016 WHO classification and consists of a heterogenous group of cases with genetic alterations leading to a gene-expression profile akin to that of *BCR-ABL1* (Ph+) B-ALLs. The genetic aberrations of Ph-like ALLs can be categorized into the following: translocations involving *CRLF2* (which comprise 50% of Ph-like ALLs) and kinase alterations involving one of the following: *ABL* class fusions, *EPOR* or *JAK2* rearrangements, other *JAK-STAT* sequence mutations, *Ras* pathway alterations, and other kinase alterations. The aim of this study is to investigate the CRLF2 immunohistochemical (IHC) staining pattern in several types of B-ALLs, with particular focus in *CRLF2*-rearranged Ph-like ALLs.

Design: Bone marrow core biopsies of 34 B-ALL patients were collected from our institutions and immunostained with CRLF2 (TSLP-receptor polyclonal; Invitrogen). Among these, 19 were Ph-like ALLs, including 16 *CRLF2*-rearranged (10 fused with *IGH,* 3 fused with *P2RY8,* and 3 whose fusion partners were not further characterized); 9 Ph+ ALLs; 2 with *ETV6-RUNX1;* and 4 B-ALLs with hyperdiploidy (HD). Lymphoblasts were scored for staining intensity (0-3+) and percentage of positive blasts evaluated. Cases were considered positive when blasts had 2+ or 3+ membranous staining, and when >5% of blasts were positive. Cases with 0-1+ staining or granular cytoplasmic staining were scored as negative.

Results: Overall, 14 of 34 cases were scored as positive for CRLF2 by IHC. Of the 16 *CRLF2*-rearranged cases, 12 were positive for CRLF2 (75%), including 100% of *CRLF2-IGH* cases (10/10), 33% of *CRLF2-P2RY8* (1/3), and 33% of *CRLF2*-rearranged cases with unknown fusion partner (1/3). The *CRLF2-P2RY8* CRLF2 IHC positive case had a complex karyotype, including additional rearrangements of *MYC* and *KMT2A-ATP5L*. Additionally, 1 case of Ph+ ALL and 1 HD were scored as positive (2 of 18 non-*CRLF2* cases, 11%); however, both cases were confirmed to lack *CRLF2* rearrangements by FISH studies.

Conclusions: Our study demonstrated high concordance of CRLF2 IHC staining in *CRLF2*-rearranged cases, particularly in *CRLF2-IGH* cases, though a minor subset of non-*CRLF2* rearranged cases appeared to show that not all CRLF2 positivity by IHC are predictive of *CRLF2* rearrangement. CRLF2 IHC staining shows potential in rapidly identifying cases and decreasing turnaround time. Future studies with expanded cohorts to confirm these findings are warranted.

1479 Exploring the Molecular Grey Zone of Myeloid Neoplasms: Concurrent SRSF2 and Classic MPN Driver Mutations

Mehrnoosh Tashakori[1], Joseph Khoury[1], Mark Routbort[1], Keyur Patel[1], Sa Wang[1], Chi Young Ok[1], Rashmi Kanagal-Shamanna[2], Rajyalakshmi Luthra[1], Shimin Hu[1], Mahsa Khanlari[1], Siba El Hussein[1], Pei Lin[1], Carlos Bueso-Ramos[1], L. Jeffrey Medeiros[1], Sanam Loghavi[1]
[1]The University of Texas MD Anderson Cancer Center, Houston, TX, [2]The University of Texas MD Anderson Cancer Center, Bellaire, TX

Background: Myeloproliferative neoplasms (MPNs) are clonal myeloid neoplasms frequently associated with classic driver mutations in *JAK2, MPL* or *CALR. SRSF2* is among the most frequently mutated splicing genes in myeloid neoplasms and is known to confer a poor prognosis in patients with MPNs (N Engl J Med 2018; 379:1416-1430). We sought to explore the phenotypic features of myeloid neoplasms harboring concurrent *SRSF2* and classic MPN driver mutations.

Design: We searched our archives for myeloid neoplasms harboring concurrent mutations in *SRSF2* and MPN-associated driver genes. Cases were classified using the WHO 2017 diagnostic criteria. Mutation analysis was performed using next generation sequencing (Illumina Inc., San Diego, California). Clinical and laboratory data were obtained from the electronic medical records.

Results: The study group included 24 men and 5 women with a median age at diagnosis was 71 years (range, 51-84). The median interval between initial diagnosis and molecular characterization was 18.9 months (range, 0-293). BM fibrosis was present in all cases assessed [n=22]. Organomegaly was present in 15 patients. Relative and absolute monocytosis were present 38% of cases. Morphologic dysplasia was present in 15 (53.6%) cases (table 1). Megakaryocytic hyperplasia and/or clustering was seen in 13 cases. Twelve cases had an abnormal karyotype (Table 1). The cases were classified as: primary myelofibrosis (13), acute myeloid leukemia (5), chronic myelomonocytic leukemia (3), polycythemia vera (PV;3), post-ET/PV myelofibrosis (2), MPN-unclassifiable, MDS-unclassifiable and MDS/MPN-unclassifiable (1 each). (Table 1)

SRSF2 variants included P95H (67%), P95R (20%), P95L (6.5%), p.P95_R102del (6.5%) with median variant allelic frequency (VAF) of 44% (range, 2 to 65). MPN driver mutations included *JAK2* [n=20; median VAF 36% (range, 2 to 73)]; *MPL* [n=8; W515L (4), S493A (1), 1 L629Q (1), Y591N (1), V501M (1)]; median VAF 24% (range, 5.54 to 88.31)]; and *CALR* [n=2; E396del (1), K385fs(1)]; VAF 51.34 and 57.5, respectively]. Other recurrent co-mutations included *ASXL1* (n=20), *TET2* (n=11), *NRAS/KRAS* (n=8

Table 1. Diagnostic classification of cases (WHO 2017).

Patient	Initial diagnosis WHO 2017	Diagnosis at time of molecular profiling	Karyotype	Dysplasia (G, E, M)
1	PV	PV	46,XY	
2	PMF	PMF	46,XY	
3	PMF	PMF	46,XX,del(20)(q11.2q13.3)[17]/47,XX,+13,del(13)(q12q14)x2[1]/46,XX[2]	G, E
4	PV	PV	46,XY	
5	MDS, unclassifiable	MDS, unclassifiable	46,XY	G,E,M
6	PMF	PMF	46,XY	G, E
7	PV	Post PV- MF	46,XY	0
8	CMML-2	CMML-2	46,XX	
9	PMF	PMF	46,XY	
10	N/A	AML-MRC	47,XY,+8,inv(9)(p12q13),i(17)(q10)[1]/48,idem,+13[19]	
11	N/A	Therapy related AML	46,XY	M
12	CMML-1	AML arising from CMML	47,XY,+8[20]	M
13	PV	PV	46,XY	G, M
14	N/A	PMF	46,XY	
15	PMF	MPN, unclassifiable	46,XX	
16	PMF	PMF	46,XY,del(20)(q11.2q13.3)[1]/44,XY,-6,del(13)(q12q14),-20[1]/46,XY[18]	G, M
17	PMF	PMF	46,XY	
18	PMF	PMF	46,XY,inv(9)(p12q13)[20], FISH: Positive for -5/del(5q)	
19	ET	Post ET-MF	46,XY	
20	PMF	AML evolving from PMF	47,XY,+8[19]/47,XY,+8,add(17)(p13)[1]	E, M
21	PMF	PMF	47,XY,+8,i(17)(q10)[19]/46,XY,del(20)(q11.2q13.3)[1]	
22	PMF	PMF	46,XY,del(13)(q12q22)[5]/46,XY[15]	G, E
23	CMML-1	CMML	46,XY	G
24	PMF	PMF	46,XY	
25	PMF	PMF	46,XX	M
26	MDS	MDS/MPN-unclassifiable	46,XY,r(7)[9]/46,XY[11]	G,E,M
27	N/A	Therapy related AML	46,XY,del(20)(q11.2q13.3)[2]/46,XY[18]	E
28	PMF	PMF	47,XY,+13[1]/46,XY[19]	G
29	CMML-1	CMML-1	47,XY,+21[5]/46,XY[15]	G, E, M

AML: acute myeloid leukemia; ET: essential thrombocythemia; CMML; chronic myelomonocytic leukemia; E: erythroid; G: granulocytic; M: megakaryocytic; MDS: myelodysplastic syndrome; MPN; myeloproliferative neoplasm; MRC: myelodysplasia-related changes; PMF: primary myelofibrosis; PV: polycythemia vera.

Conclusions: Most neoplasms with concurrent *SRSF2* and MPN-associated mutations have classic MPN-like phenotypes, but a subset of cases present as AML and MDS/MPN. BM fibrosis, morphologic dysplasia, monocytosis, organomegaly and progression to AML are common and overall prognosis is poor. Allogeneic HSCT stem cell transplant may be of value in the treatment of these neoplasms.

1480 CD123 Overexpression Significantly Varies in Different Subtypes of Adult Acute Myeloid Leukemia

Mehrnoosh Tashakori[1], Sanam Loghavi[1], Jie Xu[2], Sherry Pierce[3], Jeff Jorgensen[1], Marina Konopleva[1], Naveen Pemmaraju[3], Naval Daver[3], Joseph Khoury[1], L. Jeffrey Medeiros[1], Sa Wang[1], Sergej Konoplev[2]
[1]The University of Texas MD Anderson Cancer Center, Houston, TX, [2]Houston, TX, [3]Department of Leukemia, UT MD Anderson Cancer Center, Houston, TX

Background: Several new drugs targeting the alpha-chain of the interleukin-3 receptor (CD123) have been shown to have efficacy in patients (pts) with acute myeloid leukemia (AML), but the degree of CD123 expression in leukemic cells and its comparison to normal hematopoietic precursors remain unclear. We investigated the expression of CD123 in newly diagnosed adult pts with different subtypes of AML and compared expression to normal myeloid precursors.

Design: Initially we identified pts with AML who received allogeneic stem transplantation and remained in complete remission for at least 3 years with 100% donor chimerism and analyzed CD123 expression in yearly bone marrow aspiration samples. We then retrospectively analyzed CD123 expression in adult pts with untreated AML between January 1, 2018 and June 30, 2019. CD123 expression was assessed by flow cytometry with APC-conjugated anti-CD123 antibody (BD Pharmigen Bioscience; clone 7G3); median fluorescence intensity (MFI), and MFI ratio over negative control were calculated. In the control group and in CD34+ AML cases CD123 expression was analyzed on CD34+ cells; in CD34-negative AML, CD123 expression was analyzed on cells in the CD45 dim blast gate.

Results: The control group included 8 men and 8 women with a median age of 54 years (range, 32-69). The mean value of CD123 MFI was 528(+/-55); the range was 232-845. The study group included 49 men and 79 women with a median age of 68 years (range, 22-89) diagnosed with AML NOS (n=42), AML-MRC (n=33), therapy-related AML (n=17), AML with *NPM1* mutation (n=9), acute promyelocytic leukemia (n=9) AML with CBFB rearrangement (n=9), AML with t(9;11) (n=3), and AML with t(6;9) (n=1) CD123 expression was significantly more intense in the study group compared with the control group (mean MFI 2016+/-147 vs 528+/-55, p<0.001), but did show significant variation among individual pts ranging from 20 to 12113. Of interest, 34 cases had CD123 MFI below 1000, the level often considered as an upper limit of normal. Among different pt groups, CD123 expression was the highest in *NPM1*-mutated patients and lowest in therapy-related AML, p<0.05 (table 1).

Type	Median MFI	MFI ratio
AML *NPM1*	3575+/-1127	64.7+/-16.5
APL *PML-RARA*	3147+/-2079	25.0+/-8.8
AML MRC	2071+/-179	40.9+/-7.1
AML NOS	1789+/-1764	79.5+/-40.0
AML with CBFB rearrangement	1467+/-252	26.3+/-4.7
Therapy-related AML	1311+/-151	32.5+/-5.6

Conclusions: CD123 is expressed in most AML cases, but shows significant variation in its intensity. This observation makes the use of anti-CD123 targeted therapy promising in adult AML patients, but warrants pre-clinical testing.

1481 Microsatellite Instability and its Associations with the Clinicopathologic Characteristics of Diffuse Large B-cell Lymphoma

Tian Tian[1], Jiwei Li[2], Tian Xue[3], Bao-Hua Yu[1], Xiaoyan Zhou[1]
[1]Fudan University Shanghai Cancer Center, Shanghai, China, [2]Fudan University Shanghai Cancer Center; Shanghai Medical College, Fudan University, Shanghai; Institute of Pathology, Fudan University, Shanghai, Shanghai, China, [3]Shanghai, China

Disclosures: Tian Tian: None; Jiwei Li: None; Tian Xue: None; Bao-Hua Yu: None

Background: Microsatellite instability (MSI) has been investigated as a prognostic and predictive factor for chemotherapy in colorectal cancer and has recently been demonstrated to be predictive of the PD-1/PD-L1 checkpoint blockade response in various solid tumors. However, MSI status in diffuse large B-cell lymphomas (DLBCLs) has not been thoroughly explored.

Design: This study investigated MSI status in DLBCLs and analyzed the associations between MSI and clinicopathologic characteristics and clinical outcomes. Ninety-two cases of primary DLBCLs treated with R-CHOP/CHOP chemotherapy between 2009 and 2017 were collected. MSI detection was performed by the Promega MSI Analysis System. The expression of *MLH1*, *MSH2*, *MSH6* and *PMS2* was detected by immunohistochemistry. The associations between MSI and progression-free survival (PFS) and overall survival (OS) were evaluated with Kaplan-Meier curves. The correlations between complete response (CR) after R-CHOP/CHOP chemotherapy and MSI were analyzed by univariate and multivariate logistic regression analyses.

Results: Three of 92 cases (3.2%) were high MSI (MSI-H), 9 cases (9/92, 9.8%) exhibited low MSI (MSI-L). One case with MSI-H showed loss of expression of MSH2 and MSH6. Univariate analysis indicated that MSI was associated with poor response to R-CHOP/CHOP chemotherapy in DLBCLs (OR, 0.178; 95% CI, 0.049-0.653; P = 0.009). Multivariate analysis showed that MSI was an independent factor for predicting non-CR to R-CHOP/CHOP chemotherapy (OR, 0.175; 95% CI, 0.045-0.672; P = 0.011). Kaplan-Meier curves showed that there was a trend that MSI patients had favorable PFS, which did not have statistical significance (P = 0.27) and MSI was not significantly associated with OS (P = 0.60).

Conclusions: Our study indicated that there existed MSI-H and MSI-L in DLBCLs. MSI could be an independent predictive factor for the chemotherapy response in DLBCLs. The mechanisms were partially due to the loss of MMR proteins expression and needed to be further investigated

1482   Canadian Harmonization of Hans' Algorithm for Diffuse Large B-Cell Lymphoma (DLBCL); Aligning Analytical Sensitivity with Pathologist's Readout Significantly Improves Diagnostic Accuracy

Emina Torlakovic[1], Ariz Akhter[2], Muhamad Sadek Almiski[3], Philip Berardi[4], Carol Cheung[5], Jean Deschênes[6], Rasha ElGamal[7], Pedro Farinha[8], Antonio Maietta[9], Brian Olsen[10], Catherine Ross[11], H. Rommel Seno[12], Allam Shawwa[13], Monalisa Sur[14], Adnan Mansoor[2]

[1]University of Saskatchewan and Saskatchewan Health Authority, Saskatoon, SK, [2]University of Calgary, Calgary, AB, [3]Winnipeg, MB, [4]The Ottawa Hospital - University of Ottawa, Ottawa, ON, [5]University of Toronto, Toronto, ON, [6]University of Alberta, Edmonton, AB, [7]Calgary, AB, [8]British Columbia Cancer Agency, Vancouver, BC, [9]Montreal University Health Center, Montreal, QC, [10]William Osler Health System, Brampton, ON, [11]McMaster University Medical Centre, Hamilton, ON, [12]Pasqua Hospital, Regina, SK, [13]QEII Cancer Centre/Capital Health, Dalhousie University, Halifax, NS, [14]McMaster University, Burlington, ON

Background: Hans' Algorithm (HA) is the most frequently used surrogate biomarker scheme for subtyping Diffuse Large B-cell Lymphoma (DLBCL) by the cell-of-origin (COO) into GCB and non-GCB subtypes. The originally published positive and negative predictive value (PPV and NPV) were not always reproduced in published literature and very little is known about how the HA performs in clinical practice. Canadian Association of Pathologists National Standard Committee for High Complexity Testing (CAP-ACP NSCHCT) initiated a QA project to assess current diagnostic accuracy of the HA in clinical practice, harmonize IHC protocols, IHC readout, and reporting to improve HA diagnostic accuracy.

Design: DLBCL cohort (n=84), where COO was defined by GEP (Lymph2CX, NanoString technologies) was divided into Training (TC, n=48) and validation cohort (VC, n=36). TMAtc and TMAvc were constructed. Ten Canadian laboratories applied their routine CD10, Bcl-6, and MUM1 IHC protocols and submitted the stained slides and their readouts (self-assessment) using Original HA Redout (OHAR) to the central laboratory. The stained slides were assessed for analytical sensitivity(AS) and designated as "Low AS" (1/10), "Moderate AS" (4/10), and "High AS" (5/10). In TC, the readout was adjusted for the level of IHC protocol AS; for Modified HA Readout (MHAR) we kept 30% cut-off, but only for >1+ intensity as positive for each marker and for Qualitative HA Readout (QHAR), we compared overall positivity for Bcl-6 against MUM1. All 3 readout schemes were applied to all stained slides and compared to the GEP results.

Results: The results are outlined in Table1 and Figure 1 and 2. Variation in AS with fixed readout impacted diagnostic accuracy. OHAR showed best performance in Low AS IHC protocol. MHAR improved diagnostic accuracy mostly in Moderate AS protocols, was less effective in High AS and made Low AS protocol results worse. QHAR improved diagnostic accuracy of High AS protocols, but made Low AS and Moderate AS protocols worse. MHAR and QHAR showed same effectiveness in VC cases when used for Moderate and High AS protocols respectively.

			Test Cohort				
	OHAR (range)		MHAR (range)		QHAR (range)		
	GCB	ABC	GCB	ABC	GCB	ABC	UNCL
Sensitivity	0.76-0.88	0.59-1.00	0.84-0.92	0.82-1.00	0.92-0.96	0.89-1.00	0.67-1.00
Specificity	0.58-0.95	0.71-0.85	0.81-1.00	0.79-0.93	1.00-1.00	0.93-0.96	0.93-0.98
PPV	0.70-0.96	0.68-0.80	0.82-1.00	0.73-0.88	1.00-1.00	0.90-0.95	0.50-0.75
NPV	0.70-0.83	0.76-0.95	0.83-0.91	0.89-1.00	0.91-0.95	0.93-1.00	0.98-1.00
Validation Cohort							
			MHAR		QHAR		
			GCB	ABC	GCB	ABC	GCG
Sensitivity			0.94	1.00	1.00	1.00	0.67
Specificity			1.00	0.80	1.00	0.95	1.00
PPV			1.00	0.79	1.00	0.94	1.00
NPV			0.95	1.00	1.00	1.00	0.97

OHAR= Original HA Readout; MHAR= Modified HA Readout; QHAR= Qualitative HA Readout; UNCL=Unclassified
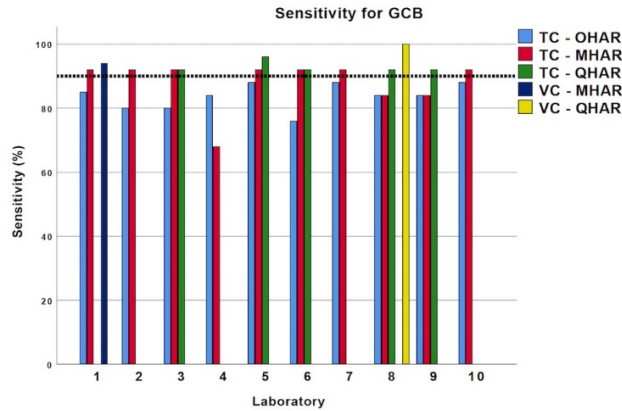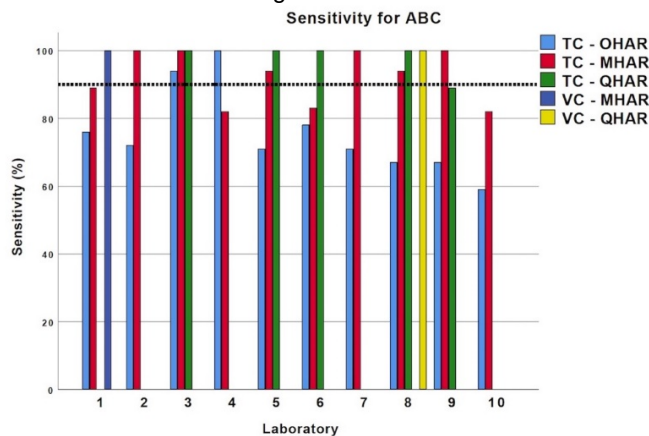
Figure 1 - 1482

Figure 2 - 1482

Conclusions: HA IHC biomarkers can be highly accurate and harmonized across different laboratories for clinical application if the pathologist's readout is adjusted to overall IHC protocol analytical sensitivity. OHAR had best performance for weak protocols, MHAR shows the best improvement for moderately sensitive protocols, and QHAR worked best overall, but only with highly sensitive IHC protocols.

1483 Somatic Mutational Spectrum of Cytogenetically Normal Myelodysplastic Syndromes

Francisco Tria[1], Phil Raess[1], Jennifer Dunlap[2], Ngoc Tran[1], Richard Press[3], Guang Fan[3]
[1]Oregon Health & Science University, Portland, OR, [2]Portland, OR, [3]OHSU, Portland, OR

Disclosures: Francisco Tria: None; Phil Raess: None; Jennifer Dunlap: None; Ngoc Tran: None; Richard Press: None; Guang Fan: None

Background: Cytogenetically normal myelodysplastic syndromes (CN-MDS) is challenging to diagnose, since cytopenia and dysplasia are not specific to MDS. Many conditions could mimic MDS. Approximately 50% of MDS are CN-MDS. However little is known about mutational spectrum of CN-MDS. We thought that next-generation sequencing (NGS) could provide comprehensive mutational profile to determine clonal abnormality in CN-MDS. We herein report NGS mutation analysis findings of CN-MDS and further compare their mutational spectrum from cytogenetically abnormal MDS (CA-MDS).

Design: The LIS was searched for MDS cases during 2018-2019 with their concurrent cytogenetics and NGS mutational testing. Bone marrow biopsy results, cytogenetic reports, and clinical history were analyzed with targeted NGS results from a panel of 220 genes associated with hematologic malignancies.

Results: Among total 105 MDS patients, 39 (37.1%) had CN-MDS and 66 (62.9%) had CA-MDS. The median age at diagnosis of CN-MDS and CA-MDS were 69 and 65 years old respectively. Total 92% of CN-MDS showed at least one mutation, comparing to 79% of CA-MDS showing a trend towards increased frequency of mutations (p=0.1). Figure 1 summarized frequencies of mutated genes in CN-MDS and CA-MDS. The most common mutations in CN-MDS include TET2 (33%), ASXL1 (31%), RUNX1 (28%), SF3B1 (23%), and SRSF2 (23%). Noticeably, TET2 mutation in CN-MDS was significantly higher than CA-MDS (33% vs 6%, p<0.001). Conversely, TP53 mutations were

significantly higher in CA-MDS than CN-MDS (18% vs. 3%, p=0.02). There was a trend towards increased frequency of mutations in SETBP1 in CA-MDS (p=0.2). Seventy-four percent (74%) of CN-MDS had 2 or more co-mutations, comparing to 58% in CA-MDS. Figure 2 displayed multi-mutational frequencies in CN-MDS and CA-MDS, up to 9 multi-mutations in both groups.
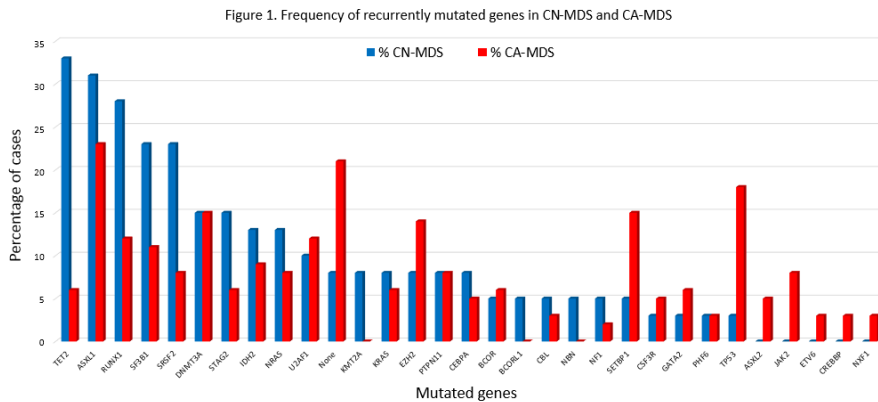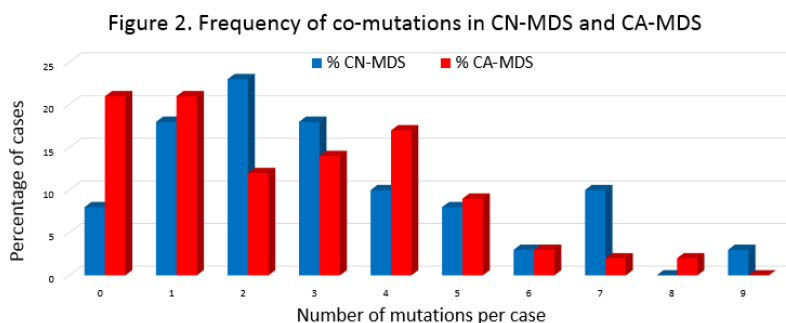
Figure 1 - 1483

Figure 1. Frequency of recurrently mutated genes in CN-MDS and CA-MDS

Figure 2 - 1483

Figure 2. Frequency of co-mutations in CN-MDS and CA-MDS

Conclusions: NGS analysis revealed that 92% of CN-MDS demonstrated somatic mutations using targeted panel of genes associated with hematologic malignancies. This study results indicated that NGS mutation analysis can provide information of the clonal abnormality in most of CN-MDS, which could assist in their diagnosis. Interestingly, CN-MDS also showed more frequent TET2 mutations, whereas there was an increasing frequency of SETBP1 mutations in CA-MDS, suggesting differing pathogenic pathways in these two entities. In addition, frequent TP53 mutations in CA-MDS support the role of TP53 in maintaining genomic integrity.

1484 BCR-ABL1-like B-Lymphoblastic Leukemia/Lymphoma Diagnostic Testing Algorithm in a Resource-Limited Setting

Maria Vergara-Lluri[1], Moe Takeda[2], Matthew Oberley[3], Le Aye[4], Imran Siddiqi[5], Ashley Hagiya[6], Stephen Dong[7], George Yaghmour[8], Russell Brynes[9]
[1]Keck School of Medicine of University of Southern California, Los Angeles, CA, [2]University of Southern California, Los Angeles, CA, [3]Children's Hospital Los Angeles, Los Angeles, CA, [4]University of Southern California, Alhambra, CA, [5]University of Southern California Keck School of Medicine, Los Angeles, CA, [6]Keck School of Medicine of University of Southern California, Pasadena, CA, [7]Keck Hospital of USC and LAC-USC Medical Center, Los Angeles, CA, [8]USC Norris Cancer Hospital Keck School of Medicine of USC University of Southern California- Jane Anne Nohl Division of Hematology and Center for the study of Blood disease, Los Angeles, CA, [9]University of Southern California, Arcadia, CA

Disclosures: Maria Vergara-Lluri: None; Moe Takeda: None; Matthew Oberley: *Speaker*, American Society for Pediatric Hematology and Oncology; *Consultant*, AMGEN; *Stock Ownership*, Caris Life Sciences; Le Aye: None; Imran Siddiqi: None; Ashley Hagiya: None; Stephen Dong: None; George Yaghmour: None; Russell Brynes: None

Background: *BCR-ABL1*-like B-lymphoblastic leukemia (Ph-like ALL) is a heterogenous group of cases with genetic alterations leading to a gene-expression profile similar to *BCR-ABL1* (Ph+) B-ALL. Among the myriad aberrations of Ph-like ALLs, cases with *CRLF2* rearrangements (*CRLF2*-R) are reported to comprise about 50%, and are associated with Hispanic ethnicity and inferior prognosis. Diagnosis of Ph-like ALL remains challenging due to disease heterogeneity, and due to expensive and complex testing

(including next-generation sequencing and multiplex RT-PCR). Recognizing that our resource-limited institution serves a diverse group of patients, including many of Hispanic origin, we devised and implemented a testing algorithm that would uncover many Ph-like ALLs.

Commencing in June 2016: all newly diagnosed or relapsed B-ALL specimens were sent to commercial labs for (1) CRLF2 flow cytometry (FC), (2) routine cytogenetics; and (3) initial B-ALL FISH panel. If karyotype and initial FISH results detected *BCR-ABL1, MLL*-R, *ETV6-RUNX1,* or *TCF3-PBX1,* no further testing was indicated. If the above were not detected and/or if lymphoblasts were positive for CRLF2 by FC, follow-up FISH testing was pursued [details in FIGURE]. The aim of this study was to evaluate the utility of the testing ialgorithm to identify Ph-like ALLs in a resource-limited setting.
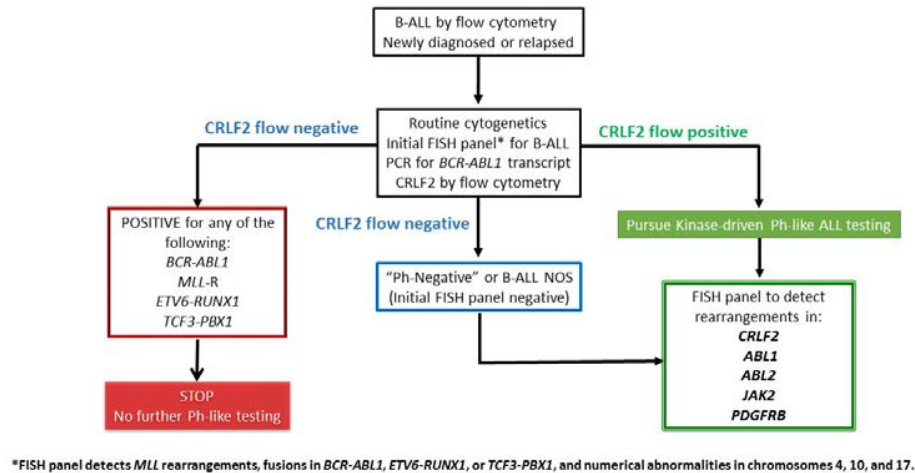
Design: B-ALLs diagnosed with a Ph-like testing algorithm between 2016-2019 (31-month period; n=80) were compared to B-ALLs diagnosed pre-algorithm between 2012-2015 (40-month period; n = 101). Characteristics of patients diagnosed as Ph-like ALL are listed in the TABLE.

Results: With the Ph-like testing algorithm, we identified 15 Ph-like ALLs of 80 total B-ALLs (19%): 1 *JAK2*-R (7%) and 14 *CRLF2*-R cases (93%) [including 10 cases with *IGH* (71%) and 2 with *P2RY8* (14%) as fusion partners]. All 8 Ph-like ALLs with positive CRLF2 FC were found to be *CRLF2*-R on follow-up FISH. CRLF2 FC-negative cases were negative for *CRLF2*-R (data not shown). B-ALL not otherwise specified (NOS) cases constituted 68% vs. 49% of B-ALLs diagnosed pre- vs. post-algorithm, respectively, following classification of NOS cases as Ph-like ALLs.

Case	Age at Dx	Ethnicity	De Novo (N) vs relapsed (R) disease	CRLF2 flow cytometry	Cytogenetics	Initial B-ALL FISH (*MLL/KMT2ABCR-ABL1, ETV6-RUNX1, TCF3-PBX1*)	Follow-up FISH studies (*CRLF2, ABL1, ABL2, JAK2, PDGFRB*)
1	60/F	Hispanic	R	POSITIVE	46,XX[20]	Normal	*CRLF2*-R
2	23/M	Hispanic	R	N/P	46,XY[7]	Normal	*CRLF2-IGH*
3	14/F	Hispanic	N	N/P	46,XX[5]	Normal	*CRLF2-IGH*
4	25/M	Hispanic	N	POSITIVE	46,XY[20]	Normal	*CRLF2-P2RY8*
5	61/M	Hispanic	N	Negative	47,XY,add(9)(p21),+21[12]/46,XY[8]	Normal	*JAK2*-R (9p24.1)
6	3/M	Jamaican	R	POSITIVE	49-51,XY,+X,+14,+17,+21,+21[cp7]/46,XY[13]	Suggestive of hyperdiploidy (9/9q,17, 21)	*CRLF2-P2RY8*
7	14/F	Hispanic	N	POSITIVE	46,XX[20]	Normal	*CRLF2-IGH* (initial called NORMAL)
8	40/M	Hispanic	N	N/P	47,XY,+X[6]/47,idem,i(7)(q10)[4]/46,XY[10]	Normal	*CRLF2-IGH*
9	54/F	Armenian	N	POSITIVE	46,XX[18]	IgH (14q32)-R	*CRLF2-IGH*
10	39/M	Hispanic	N	POSITIVE	46,XY[20]	Normal	*CRLF2-IGH*
11	39/F	Hispanic	N	N/P	46,XX[20]	Normal	*CRLF2-IGH*
12	63/F	Hispanic	R	N/P	46,XX,-18,+21[7]/46,XX[13]	Normal	*CRLF2-IGH*
13	57/F	Hispanic	N	POSITIVE	46,XX[10]	Normal	*CRLF2-IGH*
14	35/M	Hispanic	R	N/P	46,XY[20]	Normal	*CRLF2-IGH*
15	53/F	Hispanic	N	POSITIVE	46,XX[20]	Normal	*CRLF2*-R

Dx = diagnosis; N/P = not performed; R = rearranged, as in *CRLF2*-rearranged; R/R = relapsed/refractory; MRD = measurable residual disease; (-) = MRD negative

Figure 1 - 1484

*FISH panel detects *MLL* rearrangements, fusions in *BCR-ABL1*, *ETV6-RUNX1*, or *TCF3-PBX1*, and numerical abnormalities in chromosomes 4, 10, and 17.

Conclusions: This abridged algorithm allows for identification of Ph-like ALLs, primarily those with *CRLF2*-R. Although a significant subset of Ph-like cases has yet to be uncovered, this testing strategy represents a fairly high-yield approach in resource-limited settings, given that Ph-like ALLs in adults have been reported in the literature to represent 24%

1485   The Need for Rapid Cytogenetics in the Era of Vyxeos Therapy for Acute Myeloid Leukemia with Myelodysplasia Related Changes (AML-MRC)
Anjanaa Vijayanarayanan[1], Brandon Shaw[1], Kathryn Hogan[1], Kedar Inamdar[1], Madhu Menon[1]
[1]Henry Ford Health System, Detroit, MI

Disclosures: Anjanaa Vijayanarayanan: None; Brandon Shaw: None; Kathryn Hogan: None; Kedar Inamdar: None; Madhu Menon: None

Background: AML-MRC criteria includes i) history of Myelodysplastic syndrome (MDS) or Myelodysplastic syndrome/Myeloproliferative neoplasm (MDS/MPN) or ii) MDS- related cytogenetic abnormality or iii) Multilineage dysplasia (>50 % dysplasia in at least 2 lineages). Recently, the drug Vyxeos was approved for the treatment of adults with newly diagnosed therapy related AML or AML-MRC and confers a significantly better survival than standard therapy. We aimed to identify the proportion of cases diagnosed as AML-MRC solely based on MDS associated cytogenetic abnormality (i.e. not meeting the morphologic criteria and/or not having history of MDS or MDS/MPN).

Design: A cohort of 64 AML-MRC cases were re-examined morphologically to assess for and exactly quantify the degree of dysplasia. We examined bone marrow aspirate smears, touch preps, bone marrow biopsy and clot sections to assess for dysplasia. We categorized dysplasia into three categories; less than 10%, 10-50% and >50%. The other categories were normal/no dysplasia and not enough non-blast cells to accurately assess for dysplasia.

Results: Out of 64 cases of AML- MRC, 53 had complex cytogenetics (83%), 5 had del (5q) or t (5q) (8%), 4 cases had -7 or del (7q) (6%) and 2 had other MDS associated abnormalities (3%). Only 30% of cases had more than 50% dysplasia in two or more lineages. 70% of cases required either a relevant clinical history (MDS or MDS/MPN) or MDS associated cytogenetic abnormalities for AML-MRC diagnosis. More than 50% dysplasia in two lineages was seen in 34% of cases with complex cytogenetics, 20% of del (5q)/ t(5q) cases and 0% of -7/ del (7q) cases. Most frequently reported dysplastic cell line was myeloid (45%) followed by megakaryocytic (38%) followed by erythroid (16%). 22% of cases had cytogenetic abnormalities other than those tested on a routine MDS or AML FISH panel.

Conclusions: 63% of our cases needed an MDS associated cytogenetic abnormality to render a diagnosis of AML-MRC. 22% of cases had cytogenetic abnormalities which would have been missed on a routine MDS or AML FISH panel. In the absence of an AML-MRC diagnosis, patients are put on the standard 7+3 chemotherapy regimen and cannot be generally switched to Vyxeos at a later time. Considering the routine turnaround time of 7-21 days for conventional chromosomal analysis, it is imperative to have a preliminary cytogenetic result (generally 5 cell based) or a rapid chromosomal microarray analysis within 2-3 days of AML diagnosis to enable Vyxeos therapy.

1486 The Clinical, Cytogenetic and Risk Features of Myelodysplastic Syndromes with no Detectable Somatic Mutations

Sa Wang[1], Beenu Thakral[1], Elizabeth Morgan[2], Sanjay Patel[3], Valentina Nardi[4], Keyur Patel[1], Olga Weinberg[5], Robert Hasserjian[6]
[1]The University of Texas MD Anderson Cancer Center, Houston, TX, [2]Brigham and Women's Hospital, Boston, MA, [3]Weill Cornell Medical College, New York, NY, [4]Massachusetts General Hospital, Boston, MA, [5]Children's Hospital Boston, Boston, MA, [6]Massachusetts General Hospital, Harvard Medical School, Boston, MA

Disclosures: Sa Wang: None; Beenu Thakral: None; Beenu Thakral: None; Elizabeth Morgan: None; Sanjay Patel: None; Valentina Nardi: None; Keyur Patel: None; Olga Weinberg: None; Robert Hasserjian: None

Background: Using next-generation sequencing (NGS) panels covering frequently mutated genes in myeloid neoplasms, mutations are reported in about 90% of myelodysplastic syndromes (MDS). A typical MDS case often harbors 2 to 3 driver mutations, increasing in high risk MDS. While mutations in MDS are well studied, the clinicopathologic and cytogenetic features of MDS with no somatic mutations (MDS-N) is largely unknown.

Design: We searched primary MDS cases at three academic centers that NGS panels interrogating at least 50 myeloid-associated genes with a sensitivity of 1% were routinely performed between 2016-2019. The diagnosis of MDS was based on morphology and a rigorous exclusion of non-neoplastic causes of cytopenia. The MDS-N cases were compared to MDS with at least one pathogenic mutation (MDS-M).

Results: Of 304 primary MDS patients, 36(11.8%) had no pathogenic mutations detected. The MDS-N cases were composed of MDS-SLD (n=1), MDS-MLD (n=15), MDS-MLD-RS (n=3), MDS-EB-1 (n=7) and MDS-EB-2 (n=10), showing borderline fewer MDS with RS than that of MDS-M (3/36 vs 63/268, p=0.051). Clonal cytogenetic abnormalities were identified in 18/36 cases (50%), of which 12 (33%) were MDS-defining. The IPSS-R in MDS-N was very low (4, 11%), Low (11, 31%), intermediate (11, 31%), high (5, 14%), and very high (5, 14%). The cytogenetic and IPSS-R risk distributions were similar to MDS-M. 5/36 (14%) MDS-N showed progression to AML with a median of follow-up of 12.9 months. The median overall survival (OS) was not reached in patients with very low/low/intermediate IPSS-R, but only 10.4 months with high/very high groups (p=0.003). Among MDS-EB cases with a normal karyotype or –Y, MDS-N patients had significantly longer OS than MDS-M patients (not reached vs 25.8 months, p=0.012).

Conclusions: Using large-scale clinical NGS panels, about 10% of bona fide MDS lack detectable pathogenic mutations. These cases have less MDS-RS as expected due to a strong correlation of RS with SF3B1 mutation, but otherwise resemble MDS-M in cytogenetic and IPSS-R risk distributions. MDS-EB lack of detectable genetic lesions may have a better prognosis than other MDS-EB despite of similarly increased blasts. Our results suggest that MDS can be diagnosed even in the absence of genetic evidence of clonality; conversely, a simple use of NGS for peripheral blood screening of MDS should be discouraged. Whole exome/genome, methylation sequencing and RNA expression may uncover additional recurrent genetic lesions in these cases.

1487 Features of Hepatic Lymphoma: A 16-Year Retrospective Study on 90 Patients from a Single Center

Xintong Wang[1], Qian Wang[2], Yougen Zhan[3], Julie Teruya-Feldstein[4]
[1]Icahn School of Medicine at Mount Sinai, New York, NY, [2]The Icahn School of Medicine at Mount Sinai, New York, NY, [3]Trinity Health of New England, Saint Francis Hospital and Medical Center, Hartford, CT, [4]Mount Sinai Icahn School of Medicine, New York, NY

Disclosures: Xintong Wang: None; Qian Wang: None; Yougen Zhan: None; Julie Teruya-Feldstein: None

Background: Hepatic involvement by systemic lymphoma is common, but primary hepatic lymphoma (PHL) is rare. This study was designed to assess hepatic lymphomas and especially PHL at one medical center, for clinical and histopathological features, potential risk factors and outcomes. The main criteria used for PHL include primary liver involvement under pathology, absence of distant lymphadenopathy and absence of leukemic cells in the peripheral blood.

Design: This retrospective study included patients who underwent liver biopsies at Mount Sinai Hospital from 2003 to 2019. The diagnoses of hepatic lymphomas were ascertained via histology and immunohistochemistry. Our study described the characteristics of hepatic lymphoma including PHL, evaluated the distributions of age, sex, race, viral infections and transplant history. T-test was used to assess statistical differences between secondary hepatic lymphomas and PHL for continuous variables, and chi-square test was used for categorical variables.

Results: A retrospective analysis of 90 patients with hepatic lymphomas was performed, with a median age of 63.5 years, male-to-female ratio of 1.5/1.0, and the most common diagnosis of diffuse large B-cell lymphoma (n=40). Among patients with hepatic lymphomas, 13 patients met criteria for PHL. The median age of patients with PHL was 56 years, and male-to-female ratio was 0.44/1.0. There were 5 cases associated with viral infections, including HCV (n=2), EBV (n=2) and CMV (n=1). None was associated with HBV or HIV. In addition, 4 patients developed PHL on transplanted liver and 3 patients had history of autoimmune hepatitis. The diagnoses of PHL included diffuse

large B-cell lymphoma (n=5), marginal zone lymphoma (n=3), post-transplant lymphoproliferative disorder (n=3), peripheral T cell lymphoma (n=1) and mucosa-associated lymphoid tissue lymphoma (n=1). 76.9% PHL patients were still alive after 3-year follow up. In comparison with secondary hepatic lymphoma, PHL was more likely to be associated with autoimmune hepatitis, 23.1% vs. 2.6% (p=0.02) and liver transplant, 30.8% vs. 3.9% (p=0.01), and patients with PHL are more likely to be alive at 3-year follow-up, 76.9% vs. 40.3% (p=0.01).Table

Table. Patients' characteristics and hepatic lymphomas		Secondary (N=77)	Primary (N=13)	P-value
Age		61.9 (16.3)	59.8 (19.8)	0.68
Gender				0.02
	Female	27 (35.1)	9 (69.2)	
	Male	50 (64.9)	4 (30.8)	
Race				0.50
	Non-White	34 (48.6)	5 (38.5)	
	White	36 (51.4)	8 (61.5)	
Diagnosis				0.01
	Hodgkin's lymphoma	8 (10.4)	0	
	Post-transplant lymphoproliferative disorder	2 (2.6)	3 (23.1)	
	Aggressive Non-Hodgkin's lymphoma	54 (70.1)	6 (46.2)	
	Indolent Non-Hodgkin's lymphoma	13 (16.9)	4 (30.8)	
Liver involvement				0.90
	Mass	63 (81.8)	10 (76.9)	
	Sinusoid	4 (5.2)	1 (7.7)	
	No	10 (13.0)	2 (15.4)	
Hepatitis B virus				0.60
	Negative	59 (76.6)	12 (92.3)	
	Positive	2 (2.6)	0	
	Unknown	16 (20.8)	1 (7.7)	
Hepatitis C virus				0.57
	Negative	53 (68.8)	10 (76.9)	
	Positive	8 (10.4)	2 (15.4)	
	Unknown	16 (20.8)	1 (7.7)	
Epstein-Barr virus				0.07
	Negative	23 (29.9)	6 (46.2)	
	Positive	3 (3.9)	2 (15.4)	
	Unknown	51 (66.2)	5 (38.5)	
Cytomegalovirus				0.28
	Negative	26 (33.8)	7 (53.9)	
	Positive	4 (5.2)	1 (7.7)	
	Unknown	47 (61.0)	5 (38.5)	
Human immunodeficiency virus				0.22
	Negative	33 (42.9)	9 (69.2)	
	Positive	7 (9.1)	0	
	Unknown	37 (48.1)	4 (30.8)	
Liver transplant				0.01
	No	74 (96.1)	9 (69.2)	
	Yes	3 (3.9)	4 (30.8)	
Autoimmune hepatitis				0.02
	No	75 (97.4)	10 (76.9)	
	Yes	2 (2.6)	3 (23.1)	
Vital status at 3-year follow up				0.01
	Alive	31 (40.3)	10 (76.9)	
	Deceased	17 (22.1)	3 (23.1)	
	Unknown	29 (37.7)	0	

Conclusions: Our retrospective single-center study suggests that, compared to secondary hepatic lymphoma, PHL is more commonly seen in females, is more likely to have prior autoimmune hepatitis and liver transplant, and patients with PHL are more likely to remain alive at 3-year after diagnosis.

1488 Clinical, Immunophenotypic and Genomic Findings of NK-lymphoblastic Leukemia

Olga Weinberg[1], Karen Chisholm[2], Chi Young Ok[3], Yuri Fedoriw[4], Emily Mason[5], Karen Moser[6], Siddharth Bhattacharyya[7], Mina Xu[8], Adam Bagg[9], Tracy George[6], Sa Wang[3], Daniel Arber[10], Robert Hasserjian[11]
[1]Children's Hospital Boston, Boston, MA, [2]Seattle Children's Hospital, Seattle, WA, [3]The University of Texas MD Anderson Cancer Center, Houston, TX, [4]University of North Carolina, Pittsboro, NC, [5]Vanderbilt University Medical Center, Nashville, TN, [6]University of Utah, Salt Lake City, UT, [7]Hospital of the University of Pennsylvania, Edison, NJ, [8]Yale University, New Haven, CT, [9]University of Pennsylvania, Philadelphia, PA, [10]The University of Chicago, Chicago, IL, [11]Massachusetts General Hospital, Harvard Medical School, Boston, MA

Background: Natural killer (NK) cells are lymphocytes of the native immune system that play a pivotal role in host defense and immune surveillance. NK-cell development remains source of debate and the conceptual view of NK-neoplasms is evolving, with little is known about the rare NK-lymphoblastic leukemia (NK-LL), which remains as a provisional entity in the 2017 WHO Classification. The goal of this study is to characterize NK-LL cases and compare with other CD56 co-expressing acute leukemias, including acute undifferentiated leukemia (AUL) and T-lymphoblastic leukemia (T-LL).

Design: We identified 19 cases of CD56 positive acute leukemia diagnosed as NK-LL (5), AUL (6) or T-LL (8), based on current WHO diagnostic criteria, from pathology databases of nine academic institutions with available flow cytometric data, cytogenetic findings, next generation sequencing and clinical data.

Results: Compared with CD56 positive AUL, NK-LL cases showed higher expression of cytoplasmic CD3 (p=0.008), CD5 (p=0.04) and CD33 (p=0.04) and presented with higher white blood cell count (23.4 vs 4.23 x 10^9/L p=0.018). All NK-LL patients were treated with ALL-type regimens and fewer received bone marrow transplant (2/5 vs 4/6) as compared with AUL patients (5/6 being treated with AML-type regimens). As compared with CD56+ T-LL, patients with NK-LL were older (34 vs 23, p=0.051), presented with brighter CD56 intensity expression (p=0.047), decreased cytoplasmic CD3 (p=0.0087) and TdT (p=0.047) and lower white blood cell count (23.4 vs 178 x 10^9/L, p=0.031). No difference in overall survival, event free survival or complete remission rates (p>0.05) are seen when comparing NK-LL with T-LL and AUL patients. Cytogenetic analysis showed an abnormal karyotype in 3/5 NK-ALL, 4/7 T-LL and 2/6 AUL with frequent deletion of 9p21 in T-LL (4/7). The mutational profile differed in 3 groups with loss of *IKZF1* and *ETV6* in 2/3 in NK-LL, *NOTCH1* and *WT1*(3/8) and *PHF6* mutations (2/8) in T-LL and frequent *RUNX1* mutations (3/5) in AUL.

Conclusions: In this largest study to date of this poorly defined entity, we find that that NK-LL shows distinct characteristics from AUL and T-ALL, including differences in CD3, CD5, CD33, CD56 and TdT expression. We also found *IKZF1* deletions and *ETV6* mutations in NK-LL, which has not been previously reported. *RUNX1*, *NOTCH1* and *WT1* mutations, which are seen in our cases of T-LL and AUL, were not seen in our NK-LL cases. Overall, our findings validate NK-LL as a distinct acute leukemia entity.

1489 Donor-Derived Clonal Hematopoiesis After Allogeneic Hematopoietic Stem Cell Transplant: Impact on Hematologic Recovery and Evaluation of Clonal Expansion

Todd Williams[1], Ying Wang[2], James Liu[3], Laura Newell[3], Rachel Cook[3], Richard Press[4], Guang Fan[4], Phil Raess[3], Jennifer Dunlap[1]
[1]Portland, OR, [2]Aliso Viejo, CA, [3]Oregon Health & Science University, Portland, OR, [4]OHSU, Portland, OR

Background: Clonal hematopoiesis of indeterminate potential (CHIP) is defined as the presence of a leukemia driver mutation in individuals with no significant cytopenias or evidence of hematologic malignancy. CHIP mutations may be undetected in healthy donors and transferred to recipients of allogeneic hematopoietic stem cell transplant (allo-HSCT). We sought to determine if donor-derived CHIP impairs hematologic recovery and to evaluate for clonal expansion of CHIP mutations after allo-HSCT.

Design: A retrospective review to identify patients treated with allo-HSCT with NGS performed on bone marrow aspirates from the diagnostic specimen (pre-transplant) and after transplant. Donor-derived mutations were present in the first post-transplant NGS study and not in pre-transplant specimens (LOD of 0.5% VAF). Confirmation of donor origin was confirmed by sequencing donor specimens. Time to neutrophil and platelet recovery (# days from allo-HSCT to day when absolute neutrophil count and platelet count were ≥0.5 x 10^9/L and ≥50 x 10^9/L, respectively) were compared between patients with and without donor-derived CHIP, matched for donor age (>55 yr). Count recovery curves were constructed using Kaplan-Meier method. Statistical significance was calculated using log-rank test. *P* < 0.05 was considered significant.

Results: We identified donor-derived CHIP mutations in 15/290 (5.2%) patients after allo-HSCT: 10 *DNMT3A*, 1 *SF3B1*, 1 *ASXL1*, 1 *STAT3*, 1 *CSF3R*, 1 *CBLB* and 1 *TET2* (Table 1). NGS was performed on 14/15 donor specimens and identified the same CHIP

mutation. There was no significant difference between platelet recovery (median: 23 days and 20 days, HR = 0.74 [0.43-1.29], P = 0.68) or neutrophil recovery (median: 15 days and 13.5 days, HR = 0.66 [0.39-1.48], P = 0.85) in patients with and without donor-derived CHIP (Figure 1). Serial NGS was performed after transplant in 12/15 patients; only DNMT3A mutations showed increasing VAF over time (5/12, Figure 2). Three patients died from graft versus host disease and one patient developed erythroid hypoplasia of uncertain etiology; the remaining patients are alive with no significant marrow or peripheral blood abnormalities. Average follow up was 829 days post-transplant.

Recipient	Diagnosis	Donor Source	Recipient age, y	Donor age, y	Donor-engrafted mutation	Donor VAF, %	VAF at detection, %
1	aCML	Sibling	55	56	*DNMT3A* R882H	5.4	6.6
2	PMF	Sibling	48	56	*DNMT3A* Q692fs*21	40.8	42.4
					SF3B1 K700E	2.5	1.0
3	BL	Sibling	55	57	*DNMT3A* E667*	24.9	26.2
4	AML	Sibling	55	63	*DNMT3A* P777S	5.4	5.5
5	AML	Sibling	63	65	*DNMT3A* splice site	1.0	3.1
6	AMML	Sibling	55	61	*DNMT3A* C497W	7.7	5.9
7	ALL	MUD	61	55	*DNMT3A* F7341I	5.7	0.5
8	AML	Sibling	37	43	*DNMT3A* N797K	4.1	4.7
9	AML	Sibling	55	59	*DNMT3A* R882H	5.5	6
10	CML	Sibling	64	69	*DNMT3A* V339fs*7	20.7	28.9
11	MDS	MUD	66	67	*CSF3R* I720T	1.9	2.0
12	MDS	Sibling	67	69	*STAT3* P714L	5.3	7.0
13	AML	Sibling	53	57	*CBLB* R18*	2.0	2.4
14	B-ALL	Sibling	51	55	*TET2* N752fs*59	n/a	2.0
15	PMF	MUD	68	68	*ASXL1* N986fs*7	3.6	2.0

Figure 1 - 1489

Figure 1

ANC ≥0.5 x 10^9/L

PLT >50 x 10^9/L

Figure 2 - 1489

VAF in Sequential Marrows Post Transplant
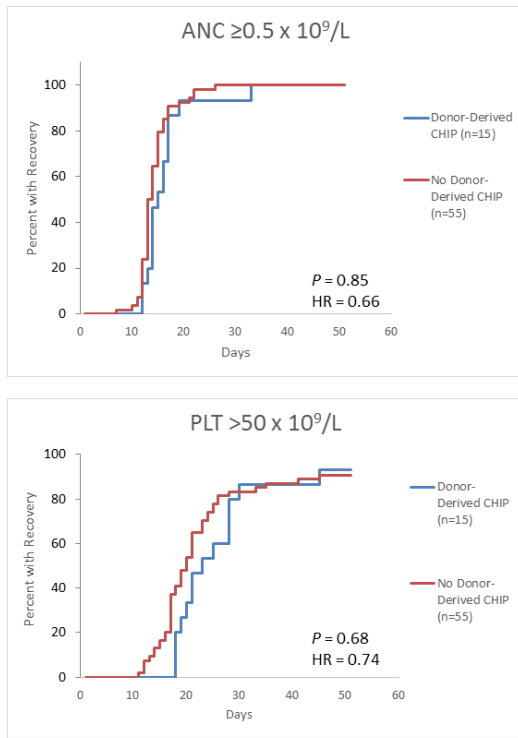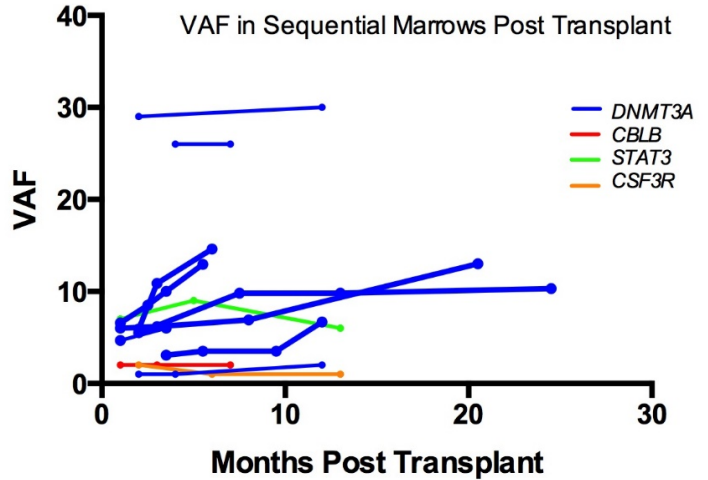
Conclusions: No significant difference in hematologic recovery was identified in patients with donor derived CHIP. Only DNMT3A CHIP mutations showed increasing VAF after transplant. Further studies are necessary to determine the clinical impact of donor derived CHIP.

1490 Utility of Flow Cytometry (FC) in Identifying Genomic Complexity in Chronic Lymphocytic Leukemia (CLL)

Jacob Wooldridge[1], Murty Vundavalli[2], Rebecca Leeman-Neill[3], Craig Soderquist[4], Govind Bhagat[2], Bachir Alobeid[4], David Park[2]
[1]New York-Presbyterian/Columbia University Medical Center, New York, NY, [2]Columbia University Medical Center, New York, NY, [3]Columbia Medical Center, New York, NY, [4]New York, NY

Disclosures: Jacob Wooldridge: None; Murty Vundavalli: None; Rebecca Leeman-Neill: None; Craig Soderquist: None; Govind Bhagat: None; Bachir Alobeid: None; David Park: None

Background: Genomic heterogeneity, as determined through chromosome banding analysis (CBA) and FISH, represents a poor prognostic indicator in chronic lymphocytic leukemia (CLL). Clonal evolution of CLL can sometimes result in alterations in the cellular expression of disease-related markers detected by flow cytometry (FC). The diagnostic utility of FC in CLL is well established; however, the ability of FC to predict genetic complexity is not. The aim of this study is to determine whether flow cytometric detection of multiple aberrant B cell populations within CLL can be used to predict the presence of multiple genomic subclones.

Design: The pathology database was searched for cases with a final diagnosis of CLL over a 36 month period. CBA, FISH and FC data were reviewed for each case. FISH analysis was performed using the following CLL probes: D13S319, CEP 12, TP53, ATM, and IGH break apart. The number of clones or subclones were determined either by CBA or FISH. Routine 4-color FC studies were performed in our lab. All flow data was analyzed using FCS express 6 software. Examples of plots with multiple populations are shown in figure 1. Clinical and laboratory data were reviewed in all cases.

Results: Our study identified 102 cases with both CBA and FC data. The average patient age was 67.8 (range 41-91) with a male to female ratio of approximately 2:1. Average absolute CLL clone size was 25K cells/μL of blood (range 5-150 K cells/μL). Frequency of CLL-associated cytogenetic abnormalities detected by FISH were similar to those previously reported. Of the 102 cases, 60 had multiple populations detected; 51 cases by FC and 35 cases by CBA and/or FISH. FC showed multiple populations in 69% of the cases that had multiple clones or subclones by CBA/FISH (24/35). Only a single population/clone was detected by both studies in 42 cases.
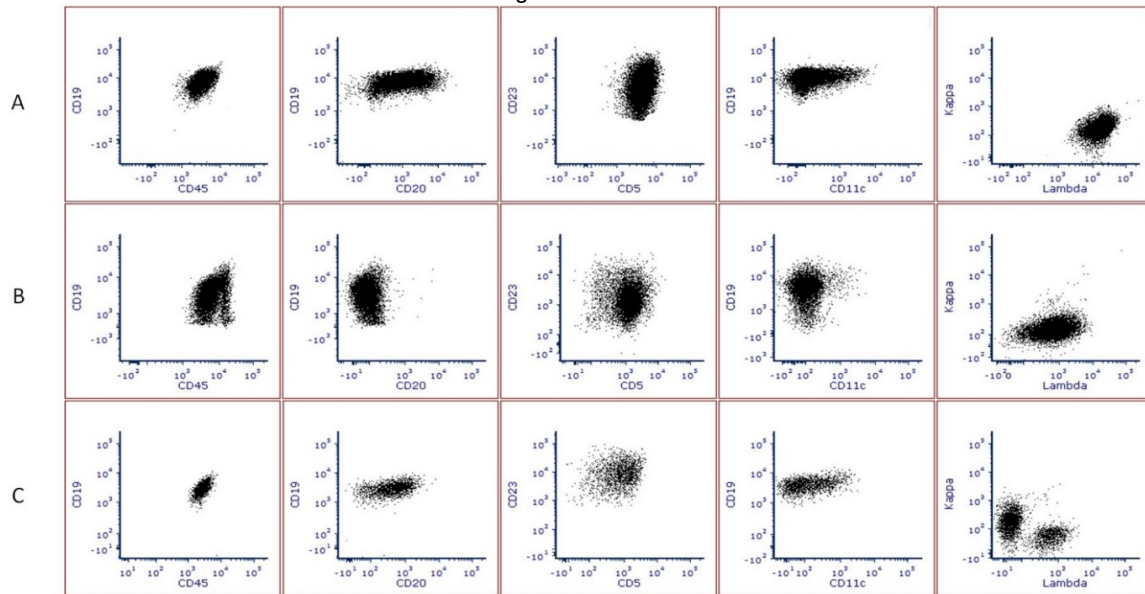
Figure 1 - 1490

Figure 1. Selectively gated plots from three representative CLL cases. Row A appears to show only one population by FC. This case had only one clone by CGA. Row B shows at least 2 populations with two visible on CD19 vs CD45, and likely 3 (1 main and 2 smaller orthogonal) populations seen on CD19 vs CD11c. This case had 6 clones on CGA. Row C appears to show only 1 population, but shows two populations that were only differentiated by the kappa vs lambda plot. This case had two unrelated CLL clones by CGA representing a biclonal CLL.

Conclusions: FC can identify multiple distinct populations in the majority of cases that harbored multiple clones or subclones by CBA or FISH. Despite CBA and FISH being the most common methods for evaluating genomic heterogeneity, they have inherent limitations which may underestimate the true degree of clonal variation. While FC is not a substitute for CBA or FISH, detection of multiple FC populations can suggest presence of genomic heterogeneity and could serve as a trigger for additional studies, including higher resolution molecular genetic analysis. Further investigation into this possible relationship are warranted.

1491 B-Cell Specific Activator Protein (BSAP)/CD5 Duplex Immunohistochemistry (IHC) in Tandem with Conventional Multiparametric Flow Cytometry (MFC) Improves Detection Rates of CD5+ B-Cell Lymphoproliferative Disorder (LPDs) Minimal Residual Disease (MRD)

Kyle Wright[1], David Dorfman[1]
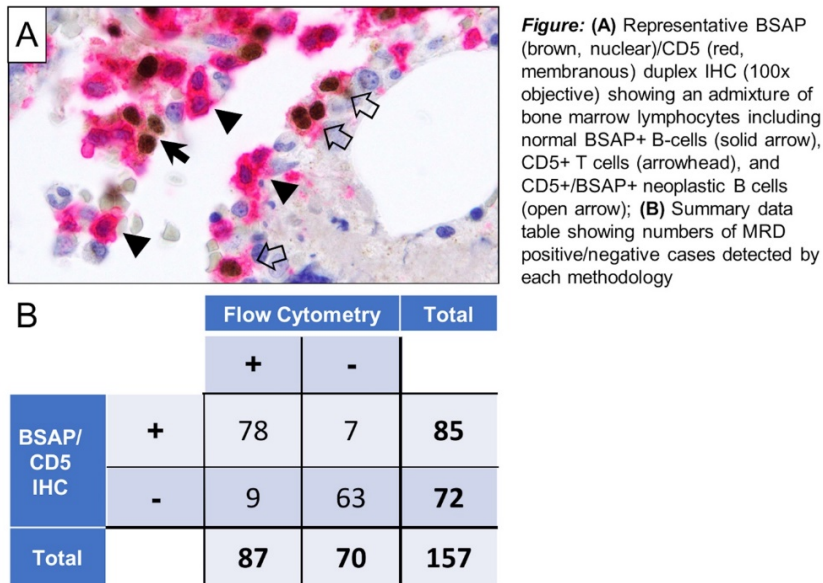[1]Brigham and Women's Hospital, Boston, MA

Disclosures: Kyle Wright: None; David Dorfman: None

Background: MRD status after treatment is predictive of overall and progression free survival in CD5+ B-cell LPDs, so adequate MRD assessment during bone marrow evaluation is of increasing prognostic importance. MFC is considered the gold standard for MRD assessment but suffers from underestimation of populations of interest as a result of specimen processing and aspirate sampling. BSAP/CD5 duplex IHC can be performed on bone marrow biopsy specimens to identify the presence of CD5+ neoplastic B cells for MRD assessment; however, comparison of this technique to conventional MFC has not been tested.

Design: Cases of CD5+ B-cell LPDs undergoing bone marrow evaluation for MRD from 4/2018-8/2019 (N= 157 total cases) were selected, including CLL/SLL (140 cases), mantle cell lymphoma (10 cases), and other CD5+ B-cell LPDs (7 cases), and evaluated by MFC of the bone marrow aspiration and BSAP/CD5 duplex IHC of the bone marrow biopsy. MRD was assessed by quantitative (MFC) or semi-quantitative (IHC) measures, and concordance rates between the two modalities were recorded. Discordant cases were independently re-reviewed and reclassified.

Results: MFC and BSAP/CD5 duplex IHC showed similar detection rates of bone marrow MRD (92.6% vs. 90.4%), generalizable to all CD5+ B-cell LPDs examined. Rates of MRD positive concordance (83.0%) and MRD negative concordance (79.7%) were high, and the overall discordance rate between the two modalities was 10.1%. Cases that were negative by IHC (but positive by MFC) showed an average involvement by a CD5+ B-cell LPD of 0.09% of total viable cells, which establishes a lower limit of detection of MRD by BSAP/CD5 IHC. When BSAP/CD5 duplex IHC was used in tandem with MFC, the overall MRD detection rate improved by 7.4% (7 additional cases in this cohort).

Figure 1 - 1491

Figure: (A) Representative BSAP (brown, nuclear)/CD5 (red, membranous) duplex IHC (100x objective) showing an admixture of bone marrow lymphocytes including normal BSAP+ B-cells (solid arrow), CD5+ T cells (arrowhead), and CD5+/BSAP+ neoplastic B cells (open arrow); (B) Summary data table showing numbers of MRD positive/negative cases detected by each methodology

		Flow Cytometry		Total
		+	-	
BSAP/ CD5 IHC	+	78	7	85
	-	9	63	72
Total		87	70	157

Conclusions: BSAP/CD5 duplex IHC of the bone marrow biopsy and MFC of the bone marrow aspiration have similar rates of detection of MRD in patients with CD5+ B-cell LPDs (92.6% vs. 90.4%). However, a reflex, tandem testing approach (BSAP/CD5 duplex IHC performed on all cases that are negative by MFC) can improve the detection rate of MRD for CD5+ B-cell LPDs during bone marrow evaluation by 7.4%.

1492 Secondary-Type Mutations Do Not Impact Prognosis in AML with Mutated NPM1

Martha Wright[1], Olga Pozdnyakova[2], Robert Hasserjian[3], Nidhi Aggarwal[4], Aaron Shaver[1], Olga Weinberg[5], Adam Seegmiller[1], Emily Mason[1]

[1]Vanderbilt University Medical Center, Nashville, TN, [2]Brigham and Women's Hospital, Boston, MA, [3]Massachusetts General Hospital, Harvard Medical School, Boston, MA, [4]University of Pittsburgh, School of Medicine, Pittsburgh, PA, [5]Children's Hospital Boston, Boston, MA

Disclosures: Martha Wright: None; Olga Pozdnyakova: *Grant or Research Support*, Sysmex Corporatin of America; *Consultant*, Promedior; Robert Hasserjian: None; Nidhi Aggarwal: None; Aaron Shaver: None; Olga Weinberg: None; Adam Seegmiller: None; Emily Mason: None

Background: AML with mutated *NPM1* (NPM1+ AML) is a genetically-defined category of AML associated with *de novo* disease and favorable prognosis. In contrast, AML with myelodysplasia-related changes (AML-MRC), defined by a prior history of MDS, multilineage dysplasia (MLD), or MDS-related cytogenetic abnormalities, is associated with poor outcomes. So-called 'secondary-type' mutations (STM) in *ASXL1*, *SRSF2*, *SF3B1*, *U2AF1*, *ZRSR2*, *BCOR*, *STAG2*, and *EZH2* are highly specific for MDS-related AML and are associated with poor outcomes. STM occur in a subset of patients with NPM1+ AML; while the presence of MLD appears to have no impact on outcomes in NPM1+ AML, the prognostic impact of STM is unknown.

Design: 240 sequential cases of *de novo* NPM1+ AML were collected from multiple institutions; patients with a known history of any myeloid neoplasm or AML-MRC-defining cytogenetics were excluded. A separate cohort of 84 patients with AML-MRC, with a history of MDS or AML-MRC-defining cytogenetics, was also examined. Clinicopathologic and next generation sequencing data were correlated with patient outcomes.

Results: Of 240 patients with NPM1+ AML, 40 (17%) harbored STM. Patients with STM were more commonly male (68% *vs.* 42%), were older (67.7 *vs.* 63.3 yrs), and showed lower platelet counts (median 38 *vs.* 65 K/mL) compared to patients without STM (p<0.01 for all). There was no significant difference in the frequency of MLD between cases with (23%) and without (19%) STM. Patients with STM showed a significantly higher frequency of *TET2* and/or *IDH1/2* mutations (78% *vs.* 57%, p=0.02) and a significantly lower frequency of *DNMT3A* mutations (13% *vs.* 49%, p<0.001) compared to patients without STM. For patients receiving induction therapy, there was no significant difference in primary induction failure rate, relapse-free (RFS) or overall survival (OS) between patients with and without STM (17%; 15.4 mos; 22.9 mos *vs.* 8%; 15.5 mos; 30.1 mos, respectively) (Figure 1a-b). Among patients treated with induction therapy, NPM1+ AML patients with STM showed significantly longer OS compared to patients with AML-MRC (8.2 mos; p=0.04) (Figure 1c).

Figure 1 - 1492

Figure 1. Secondary-type mutations (STM) do not impact outcomes in *NPM1*-mutated AML
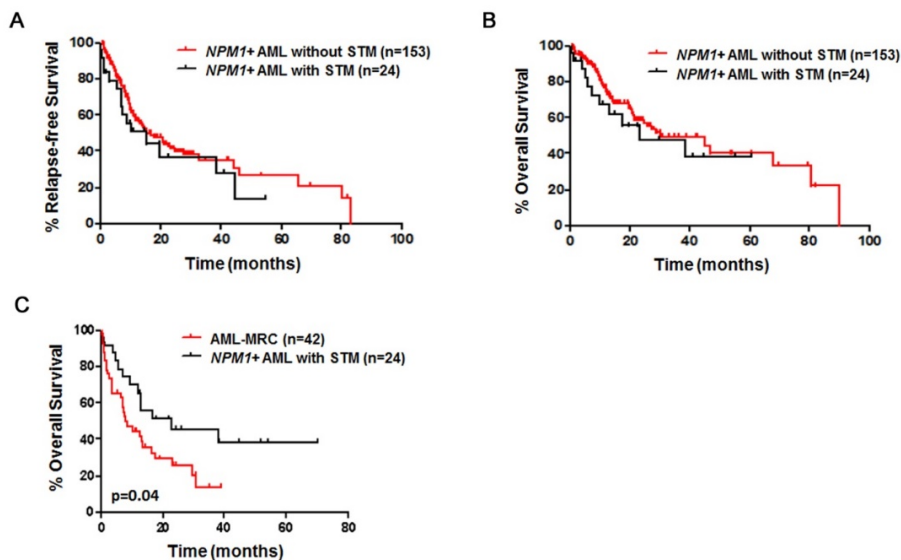
Conclusions: STM are present in 17% of patients with *de novo* NPM1+ AML and are associated with older age but have no impact on outcome in patients treated with induction therapy. Patients with *NPM1* mutations and STM should be categorized as NPM1+ AML for the purposes of prognostication and therapy, despite the presence of mutations typically associated with AML-MRC.

1493 t(11;16)(q23;p13) and t(2;11)(p21;q23) in Hematologic Neoplasms: Presumptive Evidence of Myelodysplasia Revisited

Wei Xie[1], Guilin Tang[2], Endi Wang[3], Young Kim[4], Qi Shen[5], Yi Zhou[6], Sanam Loghavi[2], Sa Wang[2], Carlos Bueso-Ramos[2], L. Jeffrey Medeiros[2], Shimin Hu[2]
[1]Baylor College of Medicine, Houston, TX, [2]The University of Texas MD Anderson Cancer Center, Houston, TX, [3]Duke University Medical Center, Durham, NC, [4]City of Hope National Medical Center, Duarte, CA, [5]Winter Park, FL, [6]University of Miami, Miami, FL

Disclosures: Wei Xie: None; Guilin Tang: None; Endi Wang: None; Young Kim: None; Qi Shen: None; Yi Zhou: None; Sanam Loghavi: None; Sa Wang: None; Carlos Bueso-Ramos: None; L. Jeffrey Medeiros: None; Shimin Hu: None

Background: t(11;16)(q23;p13) and t(2;11)(p21;q23) are rare translocations involving the 11q23 locus and are considered presumptive evidence of myelodysplastic syndromes (MDS) and acute myeloid leukemia with myelodysplasia-related changes (AML-MRC) in the current WHO classification. In this study, we re-examined the potential utility of these two translocations in defining MDS and AML.

Design: Cases of myeloid and lymphoid neoplasms harboring these two translocations diagnosed at our institution during past 20 years were reviewed retrospectively. Seven additional cases with t(11;16)(q23;p13) were obtained from four outside institutions.

Results: The study group included 18 patients with t(11;16) and 16 patients with t(2;11). Of 17 patients with known emerging time of t(11;16), 15 were diagnosed with therapy-related neoplasms (t-MN), 1 with *de novo* AML, and 1 with secondary AML. In contrast, of 16 patients with t(2;11), only 1 was diagnosed with therapy-related AML, and 15 were diagnosed with *de novo* myeloid neoplasms (7 MDS, 6 AML, 1 CMML, and 1 polycythemia vera). The median age at initial diagnosis of hematologic neoplasms with t(11;16) was 51.9 years (range, 3.4 to 84.9), and t(2;11) was 63.8 years (range: 41.7-83.3). In all cases (8/8) of AML with t(11;16), blasts showed monocytic or myelomonocytic morphology and immunophenotype. In contrast, none of the AML cases (0/9) with t(2;11) showed blasts with such features. Dysplasia, usually mild, was observed in 7/17 cases with t(11;16) while in 15/16 cases with t(2;11), often being marked in megakaryocytes in the latter. Del(5q) was observed only in 1/18 case with t(11;16) but in 9/16 cases with t(2;11). By fluorescence *in situ* hybridization analysis, *KMT2A* rearrangement was present in all tested cases (11/11) with t(11;16) but negative in all tested cases (9/9) with t(2;11). The median survival of patients from the detection of t(11;16) was 15.4 months, and the median survival of patients from detection of t(2;11) was 27.3 months.

Conclusions: t(2;11) is frequently associated with del(5q) and dysplasia, thus appears to represent genuine presumptive evidence of MDS and AML-MRC. In contrast, t(11;16) is commonly associated with t-MN. t(11;16), but not t(2;11), involves *KMT2A* rearrangement, which contributes to the morphologic and phenotypic differences of blasts in diseases with two different types of translocations. Despite lack of del(5q), the prognosis of patients with t(11;16) is poorer, in line with that of patients with t-MN.

1494 CD19-Negative B-ALL Relapses after CAR T Cell Therapy are Associated with a Hypermutator Phenotype

Guang Yang[1], Sophia Faude[2], Michele Paessler[3], Gerald Wertheim[4], Vinodh Pillai[5]
[1]The Hospital of the University of Pennsylvania, Philadelphia, PA, [2]Children's Hospital of Philadelphia, Philadelphia, PA, [3]The Children's Hospital of Philadelphia, Newtown, PA, [4]Children's Hospital of Philadelphia, University of Pennsylvania, Philadelphia, PA, [5]The Children's Hospital of Philadelphia, Penn Valley, PA

Disclosures: Guang Yang: None; Sophia Faude: None; Michele Paessler: None; Gerald Wertheim: None; Vinodh Pillai: None

Background: Chimeric antigen receptor (CAR) modified T cell therapy induce response rates of 60-90% in relapsed/refractory B-ALL when compared to standard chemotherapy. Although initial response rates of CAR T cell therapy are high, long term responses are impacted by occurrence of CD19-negative relapses in about 30% of cases. While we understand how CD19-negative relapses occur, it is not clear why they occur. In this study, we explored the hypothesis that B-ALL with a hypermutator phenotype are susceptible to a CD19-negative relapse after CAR T cell therapy.

Design: A total of 181 patients with B-ALL who received CAR T cell therapy were identified from our archives. CD19 expression by flow cytometry and/or immunohistochemistry at first recurrence was used to classify leukemia as CD19-negative or CD19-positive. Relapsed/refractory B-ALL cases were identified and divided into three groups: CD19-negative relapses (CD19-neg), CD19-positive relapses (CD19-pos), and non-responders (NR). The expression of mismatch repair (MMR) proteins (MSH2, MSH6, MLH1 and PMS2), cell cycle protein p53, and proliferation index protein Ki67, were assessed using immunohistochemistry (IHC) from both pre- and post-CAR T cell therapy time points. Concurrent cytogenetic and molecular studies of each case were also reviewed. Data analysis was performed using Chi-Square test.

Results: A representative cohort of 29 relapsed CAR treated B-ALL cases were identified. Pre-CAR diagnostic and post-CAR relapse biopsies with at least 10% blasts were analyzed. In total, hypermutator phenotype, showing aberrations in DNA repair genes/ MMR protein, and/or *TP53* alterations, was present in 57.6% of total biopsies (19/33) or 73.6% of total cases (14/19) in the CD19-neg group; in contrast,

hypermutator phenotype was only identified in 7.14% of total biopsies (1/14) or 11.1% of total cases (1/9) in the CD19-pos and NR groups (Chi-Square test, p=001384). In the 7 cases with MMR protein loss, 5 cases (71.4%) showed this finding in the pre-CAR biopsies.

Conclusions: Hypermutator phenotype is significantly higher in the CD19-neg group than in the CD19-pos and NR groups. These findings suggest a hypermutator phenotype may be cause of CD19-negative B-ALL relapse after CAR T cell therapy. In addition, the majority of the MMR protein loss cases in the CD19-neg group show the loss in the pre-CAR bone marrow biopsies. Hence, p53 and MMR immunostaining can be used to predict the risk of CD19-negative relapse before the patients receive CAR T cell therapy.

1495 Flow Cytometry is Superior to Conventional Cytology in the Evaluation of Paucicellular Surveillance Cerebrospinal Fluid Specimens for Involvement by Leukemia or Non-Hodgkin Lymphoma

Yu Yang[1], Amanda Calleroz[1], Domos Kellermayer[2], Natalia Golardi[3], Christie Finch[1], Vijayalakshmi Padmanabhan[4], Marwan Yared[1], Reka Szigeti[1]
[1]Baylor College of Medicine, Houston, TX, [2]Fordham University, Houston, TX, [3]Baylor College of Medicine, Humble, TX, [4]Baylor College of Medicine, Bellaire, TX

Disclosures: Yu Yang: None; Amanda Calleroz: None; Domos Kellermayer: None; Natalia Golardi: None; Christie Finch: None; Vijayalakshmi Padmanabhan: None; Marwan Yared: None; Reka Szigeti: None

Background: CNS involvement by B lymphoblastic leukemia/lymphoma (B-ALL) or high grade B-cell non-Hodgkin lymphomas (HGBLs) is usually associated with poor prognosis in adult patients. Incorporation of CNS surveillance and prophylaxis into treatment regimens significantly improves outcome. Early detection of leukemic involvement is extremely important for better survival and to minimize neurologic deficits. Several studies showed the superior sensitivity of flow cytometry (FC) over conventional cytology (CC) in the evaluation of cerebrospinal fluid (CSF) specimens for leukemic involvement. Most of the surveillance specimens are markedly paucicellular, which likely increases the gap in sensitivity between the two methodologies. Our goal was to compare the efficiency of FC and CC in the evaluation of paucicellular CSF specimens for leukemic involvement in patients with prior diagnosis of B-ALL or HGBCL and to examine the inter- and intra-observer reliability of these two methods.

Design: We retrospectively identified 23 patients with prior diagnosis of B-ALL or HGBL who underwent surveillance CSF examination between 2015 and 2017. All the included CSF specimens were paucicellular. Corresponding, de-identified, routinely stained cytospin preparations and FC dot plots were reviewed independently by 3 experienced cytopathologists and 3 experienced hematopathologists, respectively. The observations were performed twice to evaluate intra-, and inter-observer consistency. There was a minimal of 2-week interval between the two assessments by the same pathologist. A free diagnostic test evaluation calculator (https://www.medcalc.org/calc/diagnostic_test.php) was used to examine various test efficiency values. Interclass correlation coefficient (ICC, two-way random effects, absolute agreement, single rater) was used to assess inter-observer and intra-observer agreement

Results: FC was superior to CC in all diagnostic test measures, except for specificity (Table 1). Inter-observer reliability was good for FC (ICC 0.870-0.891), but poor for CC (ICC 0.394-0.463). Intra-observer agreement was excellent-to-perfect in FC (ICC 0.914-1.00) and poor-to-moderate with CC (ICC 0.307-0.554).

Statistics	FC Value	CC Value
Sensitivity	88.00%	7.14%
Specificity	85.71 %	96.30 %
Positive Likelihood Ratio	6.16	1.93
Negative Likelihood Ratio	0.14	0.96
Positive Predictive Value	88.00%	75.00%
Negative Predictive Value	85.71 %	40.00 %
Accuracy	86.96%	42.03%

Conclusions: FC is superior to CC in the evaluation of paucicellular CSF specimens for leukemic involvement in patients with prior diagnosis of B-ALL or HGBCL. We argue that FC should be considered the test of choice over CC in this very specific clinical setting.

1496 Primary CNS Lymphoma of Peripheral T-cell Lineage: Clinicopathological Analysis of 10 Cases from a Single Institute

Diana Yim[1], Seung Geun Song[1], Sehui Kim[2], Sun Young Park[2], Tae Min Kim[1], Sung-Hye Park[1], Yoon Kyung Jeon[1]
[1]Seoul National University College of Medicine/Hospital, Seoul, Korea, Republic of South Korea, [2]Seoul, Korea, Republic of South Korea

Disclosures: Diana Yim: None; Seung Geun Song: None; Sehui Kim: None; Sun Young Park: None; Tae Min Kim: None; Sung-Hye Park: None; Yoon Kyung Jeon: None

Background: Primary central nervous system lymphoma (PCNSL) accounts for 2-6% of primary brain malignancies and 1-2% of non-Hodgkin lymphoma. The majority of PCNSL is diffuse large B-cell lymphoma (DLBCL). Primary central nervous system lymphoma of peripheral T-cell lineage (T-PCNSL) is very rare and its clinicopathological features remain unclear. Previous reports have suggested that patients with T-PCNSL exhibit different clinical features from those with B-cell lineage (B-PCNSL) but there have been few studies on the pathologic features of T-PCNSL. Here we present 10 cases of T-PCNSL in non-immunocompromised host from a single institute.

Design: Ten cases of T-PCNSL were retrieved from the pathology database of our institution from 2005 to 2018 and their clinical and pathological characteristics were analyzed. The tumors were classified according to the World Health Organization (WHO) classification of neoplastic diseases of the hematopoietic and lymphoid tissue. Microscopically, we determined the size of tumor cells and perivascular lymphocyte degree. To confirm the T-cell lineage, TCR-γ gene rearrangement were examined by PCR analysis and tumors were stained for CD4 and CD8 to examine tumor infiltrating lymphocytes.

Results: Nine cases were classified as peripheral T-cell lymphoma, not otherwise specified (PTCL, NOS), one of which was of γδT-cell derivation. One patient (16 year-old male) was diagnosed with ALK-positive anaplastic large cell lymphoma (ALCL). Median age of patients was 61.5 years (range, 3 to 69 years) with a male:female ratio of 3:2. Most patients presented with neurologic deficit (n=7), multifocal lesions (n=6), and involvement of deep brain structures (n=7). Tumor cell size was small in five patients, small to medium in two patients, medium to large in one patient, and large in one (ALCL) patient of the nine evaluable cases. Perivascular lymphocytic infiltration was observed in all cases with prominent degree in three cases. Of the eight evaluable patients with PTCL, NOS, four cases were CD8-positive and three cases were CD4-positive, while one case (γδT-cell type) was CD4/CD8-double negative. T-cell monoclonality was observed in all eight cases evaluated by multiplex-PCR assay for TCRγ gene rearrangement.

Conclusions: T-PCNSL has heterogeneous clinical and morphological features, and the diagnosis is challenging. Immunophenotypical and molecular studies in addition to clinico-radiological and morphological evaluation may be helpful in establishing the diagnosis.

1497 High Ki67 Proliferation Index but not Cell Of Origin Subtypes is Associated with Inferior Survival in Diffuse Large B Cell Lymphoma

Feras Zaiem[1], Rada Gerbi[2], Omar Albanyan[3], Jordyn Puccio[1], Zyad Kafri[4], Jay Yang[5], Ali M. Gabali[1]
[1]Division of Hematopathology, Barbara Ann Karmanos Center and Wayne State University School of Medicine, Detroit, MI, [2]Pathology department, Christ Hospital, Cincinnati, OH, [3]Division of Hematology/Oncology, Barbara Ann Karmanos Center and Wayne State University School of Medicine, Detroit, MI, [4]St. John Hospital and Medical Center, Detroit, MI, [5]Wayne State University/Karmanos Cancer Center, Detroit, MI

Disclosures: Feras Zaiem: None; Rada Gerbi: None; Omar Albanyan: None; Jordyn Puccio: None; Jay Yang: None; Ali M. Gabali: None

Background: CD10, BCL6 and MUM1 are commonly used immunohistochemical (IHC) stains for classifying diffuse large B-cell lymphoma (DLBCL), which is useful in predicting outcome. Conflicting reports of the prognostic value of other markers such as BCL2, CD23 and Ki67 proliferation index have been reported. Our objective is to correlate the response to therapy and overall survival with the expression of these immunostains and cell of origin (COO) subtype.

Design: A retrospective study of patients diagnosed with DLBCL from 2008-2014 at an academic tertiary-care cancer hospital. The slides with the IHC stains were reviewed by two independent pathologists. The clinical outcomes - assessed by a different blinded reviewer - were response to therapy and overall survival. Complete response (CR) includes patients who achieved CR with the first line therapy, and no response to any therapy (NR) includes patients who failed to achieve CR with the first therapy line, relapsed after CR, developed therapy-related complications, were sent to hospice or died due to DLBCL. Fisher's exact test employed to detect statistical significance association (p<0.05).

Results: 41 patients were included in the study with a known COO subtype, available clinical data and at least 5 years follow up. CD10 immunostain was reported in all patients followed by Ki67 in 38 patients and CD23 was the least in only 4 patients. CD10, BCL6, MUM1 and BCL2 expression showed nonstatistically significant association with poor therapy response and inferior survival. Owing to few CD23 immunostaining cases, further analysis of association is not reported owing to lack of statistical relevance. High Ki67 expression (>80%) was associated with statistically significant inferior survival (p<0.03). However, high Ki67 expression (>80%) was associated with no response to therapy but not statistically significant. COO subtypes were not predictive in both outcomes.
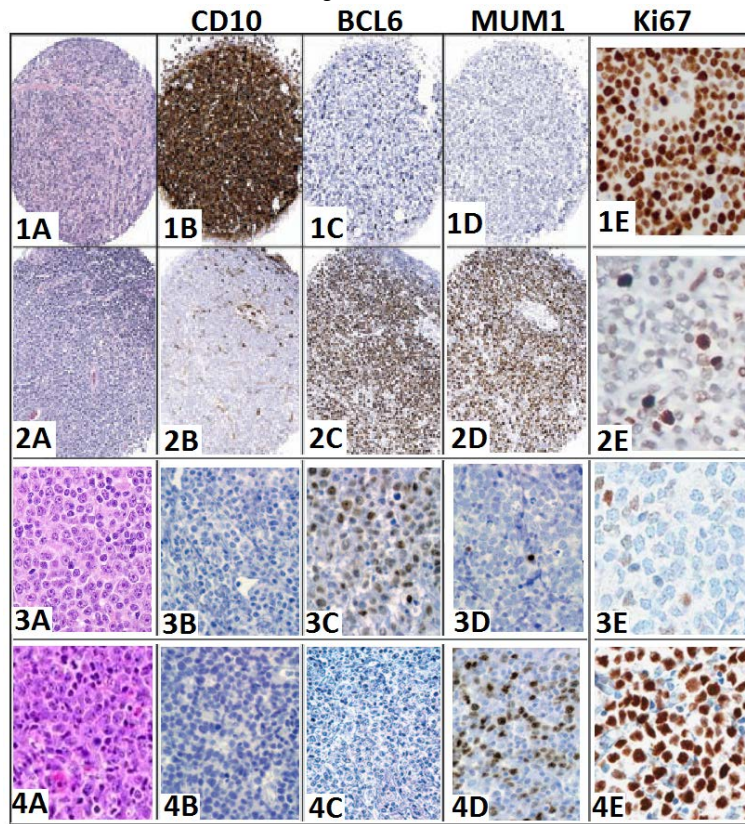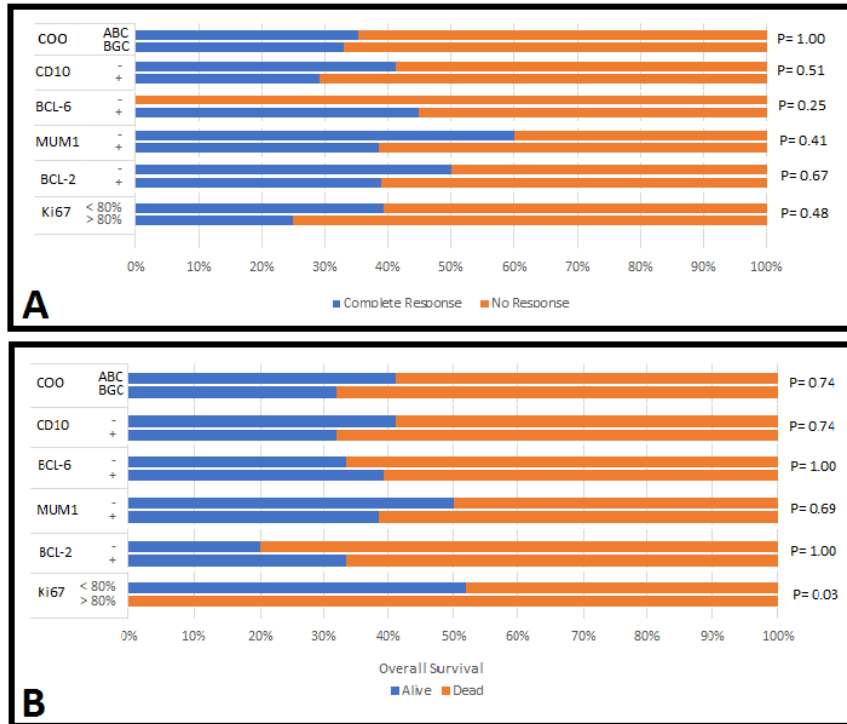
Figure 1 - 1497

Figure 2 - 1497

Conclusions: On this study, high Ki67 expression (>80%) was associated with inferior survival in patients with DLBCL. COO subtypes were not predictive.

1498 Primary Skeletal Muscle Diffuse Large B-Cell Lymphoma: A Single Institutional Experience and Literature Review

Xi Zhang[1], Kevin Kuan[2], Yanhua Wang[3], Yang Shi[2]
[1]Montefiore Medical Center, Bronx, NY, [2]Montefiore Medical Center, Albert Einstein College of Medicine, Bronx, NY, [3]Albert Einstein College of Medicine, Bronx, NY

Background: Diffuse Large B-Cell Lymphoma (DLBCL) is the most common type of non-Hodgkin lymphoma in the United States. DLBCL usually presents as lymphadenopathy and is more prevalent in elderly patients with a slight male predominance. Approximately 40% of patients present with extranodal disease that involve sites like gastrointestinal tract, bone, testis and spleen. However, DLBCL with initial presentation in skeletal muscles is very rare and usually shows poor prognosis.

Design: We systemically analyzed the clinical and pathological features of 25 cases of primary skeletal muscle DLBCL without nodal involvement from our institute (9 cases) and from previous published reports (16 cases).

Results: The average age of patients with skeletal muscle DLBCL is 58.6 years, which is lower than the median age of reported DLBCL cases (70 years old). There is no male or female predominance (male: female = 10:11), as compared to male predominance in nodal disease. The most commonly involved site is leg (36%, 9/25), followed by arm (16%, 4/25), pelvic muscles (16%, 4/25), neck (12%, 3/25), buttock (12%, 3/25) and buccal muscles (8%, 2/25) (Figure 1). Of the cases with immunohistochemical profiles available, 64% of cases are Germinal Center B-cell (GCB) type (7/11), whereas 36% of cases are non-GCB type (4/11), according to the Hans Algorithm. BCL2 expression is found in 70% of cases (7/10). BCL6 expression is found in 80% of cases (8/10). C-MYC expression is found in 71% of cases (5/7). Co-expression of BCL2 and C-MYC (Double Expressor Lymphoma) is identified in 50% of the cases in which both immunohistochemical studies are available (3/6). The three Double Expressor Lymphomas all have co-expression of BCL6 (Figure 2). The average Ki-67 proliferation index is 70-80%.
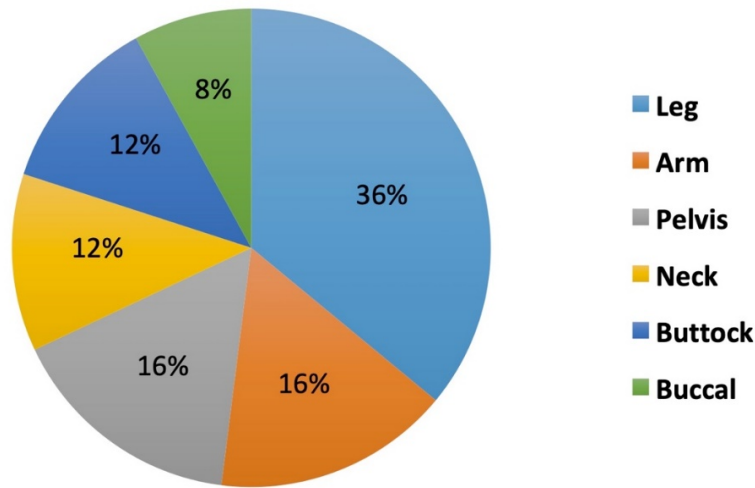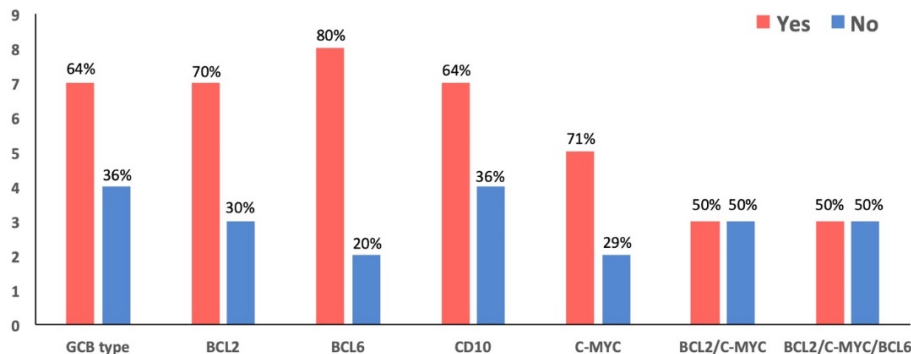
Figure 1 - 1498

Figure 2 - 1498

Conclusions: Primary skeletal muscle DLBCL occurs at a relatively younger age without gender difference compared to DLBCL, Not Otherwise Specified (DLBCL, NOS). The percentage of Double Expressor Lymphomas and the proliferation index are both high, indicating poor prognosis. However, interestingly, approximately two thirds of the cases are GCB type, which is thought to be generally associated with a favorable prognosis compared to Activated B-Cell (ABC) type. Further molecular and cytogenetic studies are needed to improve our understanding of the biology and aggressive behavior of these rare lymphomas.

1499 Evaluation of CD123 as a Potential Biomarker and Therapeutic Target in Patients with B-ALL

Davidson Zhao[1], Gina Jiang[2], Eshetu Atenafu[3], Hong Chang[4]
[1]Department of Laboratory Medicine and Pathobiology, University of Toronto, Toronto, ON, [2]University Health Network, Markham, ON, [3]University Health Network, Toronto, ON, [4]Toronto, ON

Disclosures: Davidson Zhao: None; Gina Jiang: None; Eshetu Atenafu: None; Hong Chang: None

Background: Interleukin-3 receptor alpha chain (IL-3Rα), more commonly referred to as CD123, is a cytokine receptor normally expressed on early hematopoietic cells. Upon heterodimerization with IL-3Rß, CD123 gains high-affinity binding activity to interleukin-3. This interaction promotes interleukin-3 signaling, which activates the STAT5/JAK pathway leading to cell cycle progression, cell proliferation and inhibition of apoptosis. Recent studies have shown that CD123 is frequently overexpressed in hematological malignancies, including acute myeloid leukemia and hairy cell leukemia. Thus, CD123 is an attractive target of immunotherapy, and CD123-targeted immunotherapies have already shown high potency in clinical studies. However, the frequency of CD123 expression and its prognostic implication have not been systematically studied in patients with B-cell acute lymphoblastic leukemia (B-ALL).

Design: 137 *de novo* B-ALL patients from our institution were retrospectively analyzed for clinical laboratory features, remission rates, overall survival (OS) and event-free survival (EFS). Antigens expressed by ≥20% of leukemic blasts in the sample were considered positive.

Results: There were 77 males and 60 females with median age of 51 years (range, 17–90 years) and median white blood cell (WBC) count of 14×10^9/L (range, 0.0–658.0×10^9/L). Of the 137 patients, 36 (26%) had CD123 expression in their leukemic blasts (range, 20–100%). CD123 expression was not associated with older age (≥60 years), sex, presence of Philadelphia chromosome, cytogenetic risk classification, co-expression of CD34, or remission rate. Univariate analysis showed only age ≥60 years was associated with poor OS (median 21.7 months vs 76.8 months, P=0.0016) and EFS (21.3 months vs 52.9 months, P=0.0025). There was no significant difference in OS and EFS between patients with or without CD123 expression.

Conclusions: CD123 is frequently expressed in B-ALL, thus a suitable immunotherapeutic target. However, its expression does not confer adverse outcome in B-ALL.

1500 Evaluation of Novel T-follicular Helper Cell Associated Genes as Biomarkers in T-cell Neoplasms

Xiaomin Zheng[1], Sohini Chakraborty[1], Sara Javidiparsijani[2], Arnaldo Arbini[1], Cynthia Liu[3], Paolo Cotzia[4], Christopher Park[1]
[1]NYU School of Medicine, New York, NY, [2]NYU Langone Health, New York, NY, [3]New York University, New York, NY, [4]New York University Langone Medical Center, New York, NY

Disclosures: Xiaomin Zheng: None; Sohini Chakraborty: None; Sara Javidiparsijani: None; Arnaldo Arbini: None; Cynthia Liu: None; Paolo Cotzia: None; Christopher Park: None

Background: The 2017 WHO update on hematological malignancies recognizes lymphomas of follicular helper T-cell (TFH) origin which include angioimmunoblastic T-cell lymphoma (AITL) as well as the provisional entities follicular peripheral T-cell lymphoma (F-PTCL) and nodal PTCL with TFH phenotype (PTCL-TFH). Demonstration of TFH derivation requires expression of at least 2 or 3 antigens among CD279/PD1, CD10, BCL6, CXCL13, ICOS, SAP, and CCR5, but these markers are frequently not co-expressed. We hypothesized that evaluation of normal TFH cells may identify novel markers that may aid in identifying TFH-derived neoplasms as well as resolve potential biological heterogeneity amongst them.

Design: In order to identify potential novel TFH markers, we evaluated RNA-sequencing data generated from human TFH cells, T-effector (Teff), and naïve T-cells available from the GEO database (GSE58596). Among differentially expressed genes (DEGs), a subset was assessed for their ability to stain a tissue microarray representing a variety of T-cell neoplasms using commercially available antibodies (TIM1, HES6, HDAC9, TGFBR3). Each marker was scored by at least two pathologists for staining intensity and frequency of neoplastic T-cells in two separate cores to obtain an H-score; an H-score > 5 was defined as positive.

Results: We identified 132 genes (p value <0.05) highly expressed in TFH cells compared to both Teff and naïve T-cells; these genes did not include CD279/PD1, CD10, BCL6, CXCL13, ICOS, SAP, or CCR5. While HES6 and TIM1 immunostains highlighted cells similar in number and distribution to established TFH markers such as PD1, ICOS, and CXCL13 in normal lymphoid tissue, HDAC9 and TGFBR3 were more broadly expressed. TGFBR3 was frequently expressed in AITL, MF, and ALK- ALCL, but was expressed in a smaller frequency of PTCL, NOS cases. While TIM1 and TGFBR3 highlighted the majority of AITL and PTCL, NOS cases, small subsets of AITL and PTCL,

NOS cases expressed only TIM1 or TGFBR3. A summary of staining frequencies for each candidate TFH marker is shown in the table below.

Figure 1 - 1500

	HDAC9	HES6	TGFBR3	TIM1
AITL (n=12)	12/12 (100)	3/12 (25)	8/12 (67)	11/12 (92)
PTCL, NOS (n=12)	11/12 (92)	2/12 (17)	3/12 (25)	6/12 (50)
HSTCL (n=4)	4/4 (100)	0/4 (0)	0/4 (0)	1/4 (25)
T-ALL (n=5)	3/5 (60)	0/5 (0)	1/5 (20)	2/5 (40)
MF (n=4)	4/4 (100)	0/4 (0)	3/4 (75)	2/4 (50)
NK/TCL (n=2)	2/2 (100)	0/2 (0)	0/2 (0)	0/2 (0)
ATLL (n=1)	1/1 (100)	0/1 (0)	0/1 (0)	1/1 (100)
ALCL, ALK- (n=11)	10/11 (91)	2/11 (18)	8/11 (73)	8/11 (73)
ALCL, ALK+ (n=1)	1/1 (100)	0/1 (0)	1/1 (100)	1/1 (100)
Atypical T-cell prolif (n=4)	2/4 (50)	2/4 (50)	2/4 (50)	0/4 (0)

Conclusions: Overall, these findings suggest that TGFBR3 and TIM1 may be used as TFH markers and also suggest that presumed TFH-derived neoplasms exhibit additional biological heterogeneity with respect to TFH marker expression. A more detailed comparison of TIM1 and TGFBR3 to commonly used TFH markers will be required to confirm the utility of these markers in the clinical diagnostic setting.

1501   Molecular and Cytogenetic Profiling of Therapy-Related Myeloid Neoplasms (t-MN) versus Primary Myelodysplastic Syndromes (MDS) or Acute Myeloid Leukemia (AML)
Yi Yuan Zhou[1], Audrey Jajosky[2], Navid Sadri[3], Rose Beck[1]
[1]University Hospitals of Cleveland, Case Western Reserve University, Cleveland, OH, [2]Case Western Reserve University/University Hospitals Cleveland Medical Center, Cleveland, OH, [3]Cleveland, OH

Disclosures: Yi Yuan Zhou: None; Audrey Jajosky: None; Navid Sadri: None; Rose Beck: None

Background: Therapy related myeloid neoplasms (t-MN) are aggressive malignancies that arise secondary to chemo- or radiotherapy, with survival often measured in months and overall 5-year survival of 10%. We compared the mutational profile and cytogenetic findings of 40 newly diagnosed t-MN patients with those of 50 MDS and 10 AML patients.

Design: Over a 32-month period, we identified consecutive bone marrow biopsies diagnostic of t-MN (40) or primary MN (p-MN; 50 pMDS and 10 AML). MDS cases were further divided by MDS subclassification. All cases had next generation sequencing using a custom panel of 30 myeloid-related genes. Presence of mutation, variant allele frequency (VAF), and FISH/karyotype data were collected from chart review. Based on overall frequency, mutations were divided into those related to aging (TET2, DNMT3A, ASXL1), splicesome (SF3B1, SRSF2, U2AF1, ZRSR2), TP53, IDH1/2, RUNX1, and Other. Karyotype abnormality was defined as any aberration from normal and complex karyotype defined as 3 or more separate abnormalities. Statistical comparison used 2 tailed chi-squared test or 2 tailed-Fisher exact test as appropriate with significance defined at $p<0.05$.

Results: The 40 t-MN cases included 14 low-grade MDS, 11 MDS with excess blasts (EB), and 15 AML. Compared to all 60 p-MN, t-MN cases demonstrated the same frequency of detected mutations (93%), same mean number of mutations/case (1.8), and similar mean highest VAF (46% versus 41% in p-MN). However t-MN had predominance of TP53 mutations: 50% vs. 15% of p-MN (p = 0.0004), with 35% of t-MN having TP53 as the only detectable mutation compared to 12% of p-MN (Table 1). In contrast, p-MN had predominance of spliceosome gene mutations. Presence of age-related mutations was not significantly different nor were mutations in other genes. Cases of t-MN were associated with significantly higher frequency of abnormal or complex karyotype. Differences between t-MN and p-MN were most prominent in low grade MDS and less so in MDS-EB and AML subgroups, possibly due to low numbers in subgroups.

Table 1. Molecular and genetic findings in t-MN versus p-MN.

Molecular/genetic finding	t-MN (%)	p-MN (%)	P
All cases (n)	40	60	
DNMT3A, TET2, ASXL1	15 (38)	22 (37)	0.933
SF3B1, SRSF2, U2AF1, ZRSR2	6 (15)	29 (48)	**0.001**
TP53	20 (50)	9 (15)	**<0.001**
TP53 only	14 (35)	7 (12)	**0.011**
Abnormal karyotype	36 (92)	16 (29)	**<0.001**
Complex karyotype	26 967)	12 (22)	**<0.001**
Low grade MDS (n)	14	29	
DNMT3A, TET2, ASXL1	6 (43)	13 (45)	0.903
SF3B1, SRSF2, U2AF1, ZRSR2	2 (14)	19 (66)	**0.003**
TP53	7 (50)	3 (10)	**0.003**
Abnormal karyotype	12 (86)	6 (23)	**<0.001**
Complex karyotype	7 (50)	3 (12)	**0.003**
MDS-EB (n)	11	21	
DNMT3A, TET2, ASXL1	1 (9)	4 (19)	0.637
SF3B1, SRSF2, U2AF1, ZRSR2	0 (0)	6 (29)	0.071
TP53	9 (82)	2 (10)	**0.008**
Abnormal karyotype	9 (82)	10 (53)	0.128
Complex karyotype	9 (82)	9 (47)	0.061
AML (n)	15	10	
DNMT3A, TET2, ASXL1	8 (53)	5 (50)	1
SF3B1, SRSF2, U2AF1, ZRSR2	4 (27)	4 (40)	0.667
TP53	4 (27)	0 (0)	0.125
Abnormal karyotype	9 (60)	0 (0)	**0.003**
Complex karyotype	4 (27)	0 (0)	0.125

Conclusions: Although associated with aggressive course, t-MN shares similar mutation burden and VAFs compared to p-MN. However t-MNs are predominated by mutated TP53, often as the only detectable mutation using a 30-gene myeloid panel, indicating that pre-existing age-related or other common myeloid-associated mutations are not necessary for development of t-MN. These findings reiterate the importance of mutated TP53 in the pathophysiology of t-MN.

1502 Comparison of the Clinical Microscopy Laboratory with the Cytopathology Laboratory in the Detection of Malignant Cells in Body Fluids

Patricija Zot[1], Kaitlyn Wieditz[1], Roger Riley[2]
[1]Virginia Commonwealth University Health System, Richmond, VA, [2]Virginia Commonwealth University Health System, Mechanicsville, VA

Disclosures: Patricija Zot: None; Kaitlyn Wieditz: None; Roger Riley: None

Background: Body fluid specimens are concurrently sent to the clinical hematology laboratory for cell count and differentiation and to the cytopathology laboratory for examination of malignancy. The hematology laboratory operates 24 hours a day and is often the first laboratory to receive and analyze fluids, and has the potential for the initial detection of malignant cells. The objective of this study is to assess the performance and utility of the hematology laboratory in the detection of malignant cells in body fluids.

Design: This study retrospectively analyzed reports on 4346 body fluid specimens (pleural, peritoneal, bronchoalveolar lavage, cerebrospinal and pericardial fluid) that were concurrently submitted over a 3 year period (2016-2018) to both cytopathology and hematology laboratories. The proficiency of the hematology laboratory was compared to two previous studies done at our institution in 1991-1992 and 2009-2011.

Results: There were 281 (6.5%) malignant cases overall. The hematology laboratory identified 238 of these giving a sensitivity of 85%. No false-positive results were rendered by the hematology laboratory giving a specificity of 100%. 55 (1.3%) discrepant cases were identified (Table 1). In 43 (15.3%) specimens, the cytopathology laboratory identified malignant cells not detected by the hematology laboratory and the hematology laboratory identified malignant cells in 12 (4.3%) specimens that were not detected by the cytopathology laboratory. Factors contributing to the inability of the hematology laboratory to identify malignant cells included differences in sampling, the presence of degenerating cells, and failure to recognize malignant cells. A previous study of 928 cases from 1991 and 1992 showed a sensitivity of detection of malignant cells of 24%, while a similar study of 3032 cases from 2009 to 2011 showed a sensitivity of 58%.

Table 1: Cytologic diagnoses by body fluid in cases with discrepant diagnoses.

	Bronchoalveolar Lavage	Cerebrospinal Fluid	Pleural Fluid	Peritoneal Fluid
Atypical cells	3 (50%)	5 (50%)	7 (28%)	1 (7.1%)
Epithelial malignancy	1 (16.7%)	0	17 (68%)	13 (92.9%)
Hematolymphoid malignancy	2 (33.3%)	5 (50%)	1 (4%)	0
Totals	6 (10.9%)	10 (18.2%)	25 (45.5%)	14 (25.4%)

Conclusions: The primary purpose of body fluid evaluation in the hematology laboratory is to perform cell counts and differential counts. However, technologists are also expected to identify malignant cells, since evaluation in the hematology laboratory may be the first line of detection, especially in specimens from patients with a low clinical suspicion of malignancy. In our hematology laboratory, the sensitivity increased from previous studies with the implementation of fellow review of discrepant cases and continuing education of the laboratory technical staff.